

A description of LATTE outputs

Tiago A. Marques & Len Thomas

Centre for Research into Ecological and Environmental Modelling
The Observatory, University of St Andrews, St Andrews, KY16 9LZ, Scotland

Version's date: October 30, 2015

Contents

1	Introduction	1
2	Authorship and acknowledgements	2
3	LATTE outputs	2
3.1	Standard papers in peer review journals	3
3.2	Technical Reports	4
3.2.1	Stand alone reports	4
3.2.2	Key reports	5
3.2.3	Peripheral support reports	5
3.2.4	Exploratory or incomplete reports	6
	References	7

1 Introduction

Within the LATTE project a large number of different research questions were pursued. Some of these were quite successful, while others revealed to be dead ends or were peripheral to LATTE but might be worth to revisit some time in the future.

As part of these research efforts there are a number of internal reports which were produced and which would most likely became lost forever after LATTE's completion unless there was an easy way to access them.

Therefore, in this document we present an exhaustive list of the reports available in LATTE with a direct link to each one of these. This document is intended to be distributed digitally in one of two ways:

1. as an 8 page pdf "A description of LATTE outputs.pdf" with the associated mentioned documents archived in a couple of companion sub-folders for papers and reports, such that links can be easily followed.
2. as a single 480 page pdf "A description of LATTE outputs (with appendices).pdf" which corresponds to a single file in which all the reports mentioned in section 3.2 are included as appendices. The order by which the reports appear as appendices is the same order as they are presented in section 3.2, where following the information on page size there is the indication of the page number where they start in the appendices version. If a printed version is required this would be the obvious version to print from.

Hopefully this will mean that if at some point someone comes along and decides to pick up on some thread started within LATTE, there is at least a place to begin to address the problem in an efficient way.

We note upfront that this is really a window into material which by its own nature might be incomplete and/or deprecated, hence readers are warned that they use it at their own risk. The material which we thought was complete in any sense of the word should be present in papers published in peer reviewed journals. Where relevant the link to papers in which some of the material described below is presented in a polished version are provided, and for completeness a list of such papers is presented upfront in section 3.1.

2 Authorship and acknowledgements

All documents referred to below were authored by at least TAM and LT, but many others have contributed for different documents. The due authorship and acknowledgements are present in each one of the mentioned documents.

3 LATTE outputs

We separate documents into different types, listed below in a decreasing order of completeness and relevance.

3.1 Standard papers in peer review journals

A few standard papers were published, and for easier reading, we provide the corresponding abstracts verbatim in a smaller font below:

- Langrock *et al.* (2013): Recent years have seen a fast-growing body of literature concerned with the statistical modeling of animal movement in the two horizontal dimensions. On the other hand, there is very little statistical work that deals with animal movement in the vertical dimension. We present an approach that provides an important step in analyzing such data. In particular, we introduce a hidden Markov-type modeling approach for time series comprising the depths of a diving marine mammal, thus modeling movement in the water column. We first develop a baseline Markov-switching model, which is then extended to incorporate feedback and semi-Markovian components, motivated by the observations made for a particular species, Blainville's beaked whale (*Mesoplodon densirostris*). The application of the proposed model to the beaked whale data reveals both strengths and weaknesses of the suggested modeling framework. The framework is general enough that we anticipate that it can be used for many other species given minor changes in the model structure. PDF DOI
- Moretti *et al.* (2014): There is increasing concern about the potential effects of noise pollution on marine life in the world's oceans. For marine mammals, anthropogenic sounds may cause behavioral disruption, and this can be quantified using a risk function that relates sound exposure to a measured behavioral response. Beaked whales are a taxon of deep diving whales that may be particularly susceptible to naval sonar as the species has been associated with sonar-related mass stranding events. Here we derive the first empirical risk function for Blainville's beaked whales (*Mesoplodon densirostris*) by combining in situ data from passive acoustic monitoring of animal vocalizations and navy sonar operations with precise ship tracks and sound field modeling. The hydrophone array at the Atlantic Undersea Test and Evaluation Center, Bahamas, was used to locate vocalizing groups of Blainville's beaked whales and identify sonar transmissions before, during, and after Mid-Frequency Active (MFA) sonar operations. Sonar transmission times and source levels were combined with ship tracks using a sound propagation model to estimate the received level (RL) at each hydrophone. A generalized additive model was fitted to data to model the presence or absence of the start of foraging dives in 30-minute periods as a function of the corresponding sonar RL at the hydrophone closest to the center of each group. This model was then used to construct a risk

function that can be used to estimate the probability of a behavioral change (cessation of foraging) the individual members of a Blainville's beaked whale population might experience as a function of sonar RL. The function predicts a 0.5 probability of disturbance at a RL of 150dBrms re μPa (CI: 144 to 155) This is 15dB lower than the level used historically by the US Navy in their risk assessments but 10 dB higher than the current 140 dB step-function. PDF DOI

- Laplanche *et al.* (2015): 1. Information about at depth behaviour of marine mammals is fundamental yet very hard to obtain from direct visual observation. Animal borne multi-sensor electronic tags provide a unique window of observation into such behaviours. 2. Electronic tag sensors allow the estimation of the animal's 3-dimensional (3D) orientation, depth, and speed. Using tag flow noise level to provide an estimate of animal speed we extend existing approaches of 3D track reconstruction by allowing the direction of movement to differ from that of the animal's longitudinal axis. 3. Data are processed by a hierarchical Bayesian model that allows processing of multi-source data, accounting for measurement errors, and testing hypotheses about animal movement by comparing models. 4. We illustrate the approach by reconstructing the 3D track of a 52- minute deep dive of a Blainville's beaked whale *Mesoplodon densirostris* adult male fit with a digital tag (DTAG) in the Bahamas. At depth, the whale alternated regular movements at large speed (> 1.5 m/s) and more complex movements at lower speed (< 1.5 m/s) with differences between movement and longitudinal axis directions of up to 28° . The reconstructed 3D track agrees closely with independent acoustic-based localizations. PDF DOI

3.2 Technical Reports

3.2.1 Stand alone reports

A report was fully functional but technical in nature, and so published as an internal CREEM report:

- "Procedure description: using AUTECH's hydrophones surrounding a DTAGed whale to obtain localizations.pdf" presents the description of the procedure used to localize animals on the AUTECH range, covering the aspects of detection, TDOA interpolation and localization. (10 pages; appendices version page 9, also available at "Online version")

3.2.2 Key reports

The report that essentially glues everything together and describes the simulation procedure used within LATTE is "Combining building blocks for simulating beaked whales at AUTECH". (34 pages; appendices version page 19)

There are a number of additional key reports that support this main report directly, namely:

- "Modelling beaked whales movement, sound production and detection at AUTECH" which does not contain analysis but describes the conceptual approach used. (45 pages; ; appendices version page 54)
- "Implementing a SSM to obtain pseudo-tracks and georeferenced track from DTAG data an application to Md248b" which describes the bulk of what was produced in terms of georeferencing dives. (38 pages; appendices version page 82)
- A key document related to the above is "Using animal-borne tags to estimate whale tracks in 3-dimensional space using state space models", a talk presented at ISEC 2012. (18 slides; appendices version page 120)
- "Modeling beaked whale DTag data and simulating 3D movement via a latent-variable approach with feedback and semi-Markovian components" describes many of the intermediate steps and dead end exploring of the analysis which led to Langrock *et al.* (2013). (47 pages; appendices version page 138)
- "Analysis of the 2009 Submarine Commander Course data.pdf" describes the exploratory data analysis of the data collected around the 2009 Submarine Commander Course. This was part of the data later used in Moretti *et al.* (2014). (31 pages; appendices version page 185)

3.2.3 Peripheral support reports

A number of reports describe some particular details that were not addressed fully in the above documents. These include:

- "Exploratory analysis of available DTAG data" presents an initial look at the DTAG data that was available to LATTE. (12 pages; appendices version page 216)
- "Obtaining pseudo-tracks and georeferenced locations from DTAG data" presents the initial stabs at georeferencing DTAG tracks including exploratory use of MATLAB code by Mark Johnson code later translated in to R as the basis of our georeferencing implementation of a Kalman filter. (20 pages; appendices version page 228)
- "Explaining the code for the simulation of click count vectors.pdf" is essentially an update and reproduction to a report produced in DECAF where there was a precursor of a simulator of click counts per hydrophone at AUTECH. While many of the specific implementation details were abandoned in LATTE, it presents also the initial thoughts for much of the simulation of beaked whale data within AUTECH used in LATTE. (69 pages; appendices version page 248)
- "Modelling group size as a function of autogrouper outputs.pdf" presents a simple model relating visually estimated group sizes with statistics derived by autogrouper. (13 pages; appendices version page 317)
- "*Mesoplodon densirostris* cluster sizes in the Bahamas.pdf" presents an exploratory analysis of Diane Claridge's data on group sizes in the Bahamas. (13 pages; appendices version page 330)
- "Modeling the number of clicks as a function of depth.pdf" presents a simple analysis modelling the number of clicks as a function of depth using DTAG data from AUTECH; this is the base for simulating click production conditional on simulated depth profiles. (16 pages; appendices version page 343)
- "An exploratory look over John Durban's satellite tag.pdf" presents an exploratory analysis of the available satellite Tags; this is the base for embedding the notion of home range / site fidelity in the animal movement simulation. (17 pages; appendices version page 359)

3.2.4 Exploratory or incomplete reports

- "Exploratory analysis of a simultaneous multi animal DTAG data" presents an incomplete analysis of a data set containing 3 sperm whale

simultaneously tagged with DTAG's. This was part of looking at synchrony and at depth behaviour in deep diving cetaceans. (6 pages; appendices version page 377)

- "Modeling beaked whale density in the Bahamas.pdf" presents an analysis of a visual survey data set facilitated by Diane Claridge which was supposed to lead to a spatial model of density in the Bahamas. However this analysis was halted after a number of problems were detected in the data. (19 pages; appendices version page 383)
- "Using dedicated Kalman Filter R packages to fit the georeferencing SSM.pdf" describes the attempts to implement the Kalman Filter approach used for georeferencing using a couple of existing R packages, namely KFAS (Helske, 2012) and MARSS Holmes *et al.* (2012). The hope was that these would allow to generalize the methods in a straightforward way, but that proved not to be the case. (13 pages; appendices version page 402)
- "A note about the modelling and simulation of step lengths and turning angles.pdf" presents an exploratory analysis of step length data showing that in fact it might contain more correlation structure than turning angle (which is the usual quantity people look at when dealing with correlation in movement). (15 pages; appendices version page 415)
- "A tutorial on simulated annealing.pdf" represents an exploration of what simulated annealing (SA) is and how it works. This was part of understanding the initial georeferencing procedure developed by Charlie White which used SA. (16 pages; appendices version page 430)
- "A maximum likelihood localization procedure based on arrival times at multiple sensors.pdf" includes a first stab at localization of animals based on time of arrival (TOA). This is extremely unpolished material and does not make the direct link with SECR (which is a way to do localization using also the information on missed sensors - note this is typically ignored in acoustic localization). (9 pages; appendices version page 446)

References

- Helske, J. (2012). *KFAS: Kalman Filter and Smoother for Exponential Family State Space Models*. R package version 0.9.11.
- Holmes, E. E., Ward, E. J., and Scheuerell, M. D. (2012). *Analysis of multivariate timeseries using the MARSS package - version 3.0*.
- Langrock, R., Marques, T. A., Thomas, L., and Baird, R. W. (2013). Modeling the diving behavior of whales: a latent-variable approach with feedback and semi-Markovian components. *Journal of Agricultural, Biological, and Environmental Statistics*, **19**, 82–100.
- Laplanche, C., Marques, T. A., and Thomas, L. (2015). Tracking marine mammals in 3D using electronic tag data. *Methods in Ecology and Evolution*, **6**, 987–996.
- Moretti, D., Thomas, L., Marques, T. A., Harwood, J., Dilley, A., Neales, B., Shaeffer, J., McCarthy, E., L, N., Jarvis, S., and Morrissey, R. (2014). A risk function for behavioral disruption of Blainville’s beaked whales (*Mesoplodon densirostris*) from mid-frequency active sonar. *PLOS One*, **9**, e85064.

Procedure description: using AUTECH's hydrophones surrounding a DTAGed whale to obtain localizations

Tiago A. Marques¹, Jessica Shaeffer², David Moretti² & Len Thomas¹

¹ Centre for Research into Ecological and Environmental Modelling, The Observatory, University of St Andrews, St Andrews, KY16 9LZ, Scotland.

² Naval Undersea Warfare Center Division, 1176 Howell Street, Newport, Rhode Island 02841, U.S.A.

Contents

1	Introduction	1
2	Overview of localization algorithm	3
3	Zooming in on key algorithm steps	5
3.1	Creating TDOA's	5
3.2	TDOA plots	6
3.3	Cleaning TDOA data	6
3.4	Interpolation	7
3.5	Localization of clicks	7
4	Conclusions and potential work ahead	9
	References	9

1 Introduction

One of the possible uses of DTAG (Johnson and Tyack, 2003) data is to estimate the actual track of an animal based on the measurements made on the DTAG. This is referred to as obtaining a “pseudo-track”. The reason this is called a pseudo-track is because the procedure involved is prone to errors. However, if one combines the

DTAG information with independent localizations of the animal, the procedure can become much more robust. This is referred to as “georeferencing” the track.

As part of the process of georeferencing a dive track using DTAG data, AUTECH hydrophones provide localizations of the tagged animal that are used to “adjust” a pseudo-track derived from DTAG data alone. In this report we describe how the AUTECH data is used jointly with the DTAG data to arrive at animal localizations, which can then be used as inputs into the procedure of obtaining a track from DTAG data. The georeferencing itself is elsewhere described (Marques and Thomas, 2012a) and implemented (Marques and Thomas, 2012b). Here we look in detail to the “localization” procedure. This goes from the underlying raw acoustic data, i.e. actual time of arrival (TOA) of clicks at AUTECH hydrophones surrounding the tagged whale, plus the acoustical DTAG data, all the way up to localizations of the animal at each click detected on surrounding hydrophones.

In most of the process described in this report, the only data that gets used from the DTAG is the acoustic data, that is, the time of emission of the clicks from the tagged whale. The exception is the last step, the localization algorithm itself, where as described in section 3.5, data from the pressure sensors, namely depth, is also used.

We explicitly ignore here all the processing of DTAG data that goes on “up-stream” to obtain the pitch, heading and roll data, required for the pseudotracking / georeferencing itself. Readers are referred to Johnson and Tyack (2003) for details on this, including an example on how to use the DTAG data to obtain a pseudotrack. We note however that errors introduced by said process might propagate upwards and, hence, be responsible for a large proportion of the measurement error in the georeferenced localizations, and would probably deserve to be looked at in close detail. That is not attempted here, and (despite knowing that they are not!) we take those measurements to be error free.

The pre-processing of data required to obtain the inputs into the localization algorithm is a relatively complex procedure. Due to its complexity it is hard to quantify the uncertainty present in a given click localization (x_n, y_n) estimated for the n^{th} click, $n = 1, 2, \dots, N$. Because the acoustic-based localizations are one of the inputs in the current procedure used for georeferencing (see e.g. ISEC 2012 talk), it is important to understand this process thoroughly. In particular, it would be interesting to build on it to come up with an integrated inferential framework which would then allow for estimation of the track given DTAG data and AUTECH hydrophones TOA’s. This would in turn allow to propagate the uncertainty in the acoustic localizations into the final track estimate (i.e. incorporating both DTAG data and acoustic localizations).

We note upfront that, to some extent, this might be an overkill: while accounting for the uncertainty in the AUTECH’s acoustic localizations is elegant and

conceptually appealing, it might be the case that these are very precise when compared to the DTAG data alone, and so, the variance will be nonetheless dominated by the latter.

In the next section we briefly describe the several steps involved, providing an overview of the entire process. This is then followed by a separate section, in which the procedure steps which require further clarification are expanded in separate sub-sections.

2 Overview of localization algorithm

We have a “template” sound file from the DTAG, with clicks time-of-emission (TOE). We assume that all sounds not representing clicks from the tagged whale have been identified and removed, and hence, that we have an error free record of all clicks TOE.

As stated above, the raw data corresponds to the TOA of clicks at each hydrophone. These TOA’s could, a priori, correspond to one of 3 categories:

1. TOA actually corresponds to a click emitted by the tagged animal;
2. TOA actually corresponds to a click emitted by any other animal;
3. TOA actually corresponds to a false positive (i.e. not corresponding to a beaked whale click at all).

For our analysis, we hope to identify which belong to the tagged animal (1) vs those who do not (2 and 3).

The hydrophones are assumed to be perfectly synchronized, so that hydrophone’s time-difference-of-arrival (TDOA) can be calculated from TOAs. On the contrary, note that the DTAG is not perfectly time synchronized with hydrophones and that the DTAG likely suffers from clock drift. However, the recorded “DTAG time-on” is used to time align the sound records from the DTAG and the hydrophones. More than once this created problems, because it was later confirmed that the “DTAG time-on” was incorrect. Usually, an up to 2 seconds difference shows up, which is of little consequence. That difference might be up to say 5 seconds in ‘bad’ cases, but still not an issue. For really “pathological” cases it could be much more than this, and such cases require identification as they could, otherwise, mess up the entire procedure. An obvious example of problems would be when the TOA at the hydrophone is before the TOE at the DATG. However, we note that perfect synchronicity is not required because it is the TDOA between pairs of hydrophones that gets used in the end for localization, and any time misalignment between

DTAG and hydrophones gets canceled out because the hydrophones themselves are perfectly synchronous.

Naturally, the time resolution is much higher on the DTAG, sampling at a very high frequency, compared to the hydrophones. After processing the data through the detector, Morrissey *et al.* (2006) refers the use of a 10.7 ms window, which stems from the FFT time resolution being 10.67 ms. Further, the FFT uses 50% overlap. This should also be considered a quantifiable error associated with detection time, which is then propagated into localization error.

A number of parameters need to be set before implementing the procedure:

- DTAG time window of 6 seconds; this corresponds to the “chunk” of time on the DTAG that gets processed: for each click considered we use as data for cross-correlation the recording time from TOE and TOE + 6 s;
- Hydrophone time window, Morrissey *et al.* (2006) refers the use of a 10 s window. We consider the current click TOA at the DTAG to be time 0. Then clicks before and after 10 seconds in the hydrophone are searched for. This value was considered to make sure that the click in question would be, if detected, present in this interval on all surrounding hydrophones;
- the bin width over which one considers whether there is a click or not. Note there are two different “units” to be considered here:
 1. the bin that gets slid each time, to get the TDOA, referred to as the comb sieve bin width. This is set to 5 ms.
 2. the bin over which a click is considered to be present if it is in the same time bin in the DTAG and the hydrophone data. This is set, in practice, to 10 ms

This is a consequence of how the algorithm is coded. The construct sieve function (“con_sieve.m”) automatically adds an additional 5ms bin subsequent to the detection bin, e.g. a “fudge factor”, which means that a click is considered to be present if it is in the same 10 ms bin in the DTAG and the hydrophone data. JW found that using a 10 ms comb sieve bin width to begin with, which would lead to effectively 20 seconds bin for matching, resulted in many instances where more than one time delay would have the same number of “matches” due to the presence of noise, conspecific clicks, and steady click repetition rate.

Using the data and the above parameters, for each of the K hydrophones surrounding the DTAGed whale, the following procedure is then repeated for all the N clicks present in the DTAG record.

For each hydrophone ($k, k = 1, 2, \dots, K$):

For each click ($n, n = 1, 2, \dots, N$):

1. time align DTAG and hydrophone data using the “DTAG time-on” and the AUTECH’s hydrophone clock time; For each possible time alignment over the 20 seconds window (i.e. sliding the hydrophone sound file 5 ms at the time):
 - (a) calculate and store the number of bins (of 10 ms) which simultaneously have clicks on them
 - (b) go to the next TDOA; if it is the last within the 20 second window go to next step
2. assign a TDOA to the n^{th} click, corresponding to the time difference that results in the largest correlation between the DTAG data and the current hydrophone data (further details on section 3.1);
3. go to the next click; if it is the N^{th} click, go to the next step, else go back to point 1 above
4. go to the next hydrophone; if it is the last hydrophone, procedure ends.

Then, using all the hydrophone-DTAG TDOA’s for all the click and hydrophone combinations obtained as described above:

1. plot the resulting TDOA data, with time along the dive in the x axis and TDOA on the y axis, which results in a “TDOA plot” (further details on section 3.2);
2. “clean up the TDOA plot” from clearly inconsistent TDOAs, resulting from spurious correlations (further details on section 3.3);
3. Interpolate the available TDOA measurements to obtain a TDOA for (essentially) every click and every hydrophone (further details on section 3.4);
4. transform these TDOA’s between DTAG and hydrophone into hydrophone TOA and feed the resulting TOA data into a localization algorithm, finally obtaining each click’s localization (further details on section 3.5).

3 Zooming in on key algorithm steps

3.1 Creating TDOA’s

Note at this stage TDOA’s are between the hydrophone and the DTAG, not between pairs of hydrophones, although one can get the later from the former.

For hydrophone k , the outcome of this previous step can be seen as a vector of 0's and TDOA's, represented by $TDOA_{k.}$, where say

$$TDOA_{k.} = (0, TDOA_{k2}, TDOA_{k3}, 0, 0, TDOA_{k6}, \dots)$$

means that of the first 6 clicks, only the 2nd, 3rd and 6th clicks were detected in that hydrophone, and so only for these TDOA's are available.

Note that in practice there is a very small number of 0's (if any), because there is no “correlation quality” check in this step. Even if all correlations are really low, there is always one which is the highest. This contributes for adding noise (i.e. spurious correlations) to TDOA plots (see below).

However, in the MATLAB code, several quality variables are created and outputted as part of the process, and hence could be used in the future to provide some validation. These quality check quantities include variables like number of TOAs in window, number of TOEs in window, number of matches and number of similar matches (i.e. 2, 3 or more different TDOA's could all produce the same number of matches; in particular, the code defaults to use the first one if that is the case).

3.2 TDOA plots

These present conspicuously to the naked eye a set of “TDOA lines”, which would be horizontal lines if the animal was stationary, but have slopes depending on how fast the animal is approaching or moving away from the hydrophone involved in a particular TDOA.

At this stage the plots are cluttered with TDOA's, many (if not most) of which are necessarily spurious, and hence a cleaning step is implemented, as described next.

3.3 Cleaning TDOA data

While we tend to refer to this as cleaning TDOA plots, strictly, one is cleaning the data, not the plot.

Spurious correlations, resulting from a multitude of reasons, will contribute with considerable noise to the TDOA plots. As mentioned before, there are no checks for the quality of the called TDOA, so the largest correlation wins, but actually that could correspond in the limit to a single click being in the right time bin, which could be caused by false positives (say false association of clicks).

For each hydrophone, the TDOA data is filtered by thresholding the histogram of TDOAs in sequential blocks of time and then manually selecting whether to include the selected points in the final TDOA output. The procedure involved is:

For each 1 minute period in the DTAG:

- create an histogram from the minimum TDOA to the maximum TDOA, with bins with a width of 0.01 seconds
- find the bin with the maximum number of TDOA's (the "maximum class")
- select all the TDOA's within 0.05 seconds of that bin and discard all others
- (a manual check of whether this was a reasonable thing to do, using a plot with different colors for the removed and kept TDOA's, was routinely implemented)

The rationale behind this procedure is that given the hydrophones are fixed and the animal moves slowly, TDOA cannot change abruptly over a short time period. This step depends, to some extent, on an arbitrary threshold, namely the bin width used and the range of TDOA's considered, and these values were obtained based on a trial and error empirical process, ending up with values that lead to reasonable tracks.

An additional check that might be (but was not) implemented would be to check that successive "maximum class" values were close, as these should not vary abruptly either.

3.4 Interpolation

Due to the clicks narrow beam pattern, usually each click is at best only detected at one or two, maximum 3, hydrophones. Using interpolation one can obtain a TDOA for the clicks which were not detected at a given hydrophone, provided clicks (not much) before and/or after were detected. This corresponds to interpolating the clearly visible TDOA lines in the plots for times of clicks not detected. Therefore, after the cleaning up step, the resulting TDOA is interpolated using a piecewise method that preserves the original data. A binary matrix also records which TDOAs are real versus interpolated.

For the conspecific analysis, the TDOA data was interpolated in sections, so that a pause of 20 s or greater with no data would result in a new section being created for interpolation. No interpolation was attempted during those longer gaps with no measurements. This was not what was done for the georeferentiation used in Marques *et al.* (2009), when the start and end times for interpolation were manually chosen.

3.5 Localization of clicks

Finally, the (hydrophone-DTAG) TDOA sets are converted to hydrophone TOAs by adding the DTAG TOE to the TDOA vector. The TOA vectors are indepen-

dently solved by the localization algorithm using the depth of the tagged whale for each click.

These position estimation problems typically utilize an hyperbolic model¹. The model generates a system of non-linear equations which must be solved to estimate the object's position. Additionally, a number of localization algorithm "flavours" are possible: as an example, one might choose between considering the propagation velocity sensor dependent versus constant across sensors. We do not dwell into the details of the actual algorithm here. The reader is referred to Vincent II (2001) for further details on localization algorithms and many additional references on the subject.

The localization algorithm not only produces an estimate for the animal position when the click was emitted, as it also produces an estimate of the TOE of the click. Checking this TOE against what it was supposed to be given the initial time alignment was always done, as it allows an additional check for problems.

Note localization works even if the DTAG and the hydrophones are not perfectly synchronous, because what gets used are the between hydrophone TDOA's, and any asynchronous behavior cancels out when making the differences between the TOA's for pairs of hydrophones, as hydrophones are perfectly synchronous.

At this point there is a choice to be made about the quality of the TOA's used for localization. One could consider localizing the animal only for:

- all clicks for which there are at least 3 interpolated values (this actually means you have sections of the localizations considered which are really smooth, because they are based on smoothed TDOA's), or
- for clicks for which there are at least two actual measured TDOA's + 1 interpolated TDOA (this was what actually was used for the georeferencing prior to the analysis reported by Marques *et al.* (2009), and leads to more noisy localizations).

The TOA vectors are independently solved by the localization algorithm for each click. It is important to state explicitly that the actual depth, as measured from the DTAG (remember the pressure sensors from which depth is derived are very accurate) is used as an input in the localization algorithm, hence significantly improving the ability to localize in the (x, y) plane. Note this also means you only need 3 TDOA's (for an exactly determined solution, from 4 onwards on gets an over-determined solution), rather than 4 required if depth was not used as an input, for the localization algorithm to work.

¹This is a consequence of the fact that the TOE is unknown. If it were known, we could use a spherical model. Note that had the DTAG and hydrophones been perfectly synchronized, that would be the case.

Because localization is done independently on a click by click basis, it might be inefficient, but on the other hand, it actually means once we plot all the localizations in 3D space if they do not look like a track, something went wrong: so there is some internal consistency check that is automatically implemented. On the other hand, if the process was not independently done click by click, the output might look like a reasonable track just because the way it was built successively using prior results.

4 Conclusions and potential work ahead

It is our hope that this report can serve as a record of what was done to obtain localizations based on data collected at AUTECH hydrophones combined with the DTAG data.

A number of areas that could benefit from further work include:

1. look closer to the procedure that occurs prior to obtaining the pitch and heading from the DTAG accelerometer and magnetometer data. While this data was not used here, because it is then combined with the locations obtained here, it could have a major impact in the final output;
2. quantify uncertainty/precision for the x, y coordinates obtained through localization. These might presumably be obtained as a by-product from the optimization algorithm (this is possible especially when one has more than 3 TDOA's for the localization algorithm);
3. Understand the sensitivity of the procedure to a number of ad hoc settings, including:
 - bin width for the comb sieve
 - adjustment for bin width for a match to be called
 - time over which correlation is computed (in both DTAG and hydrophone records)
 - histogram settings for TDOA clean up
4. develop a one-stop-shop procedure that takes as inputs the heading, pitch, depth and speed (strictly required to get pseudo-tracks) and the DTAG TOE's and hydrophone TOA's. This would allow at once to obtain the localizations that both best fit the acoustic data and the DTag data, and that included error in the hydrophone TDOA's in an appropriate way.

References

- Johnson, M. P. and Tyack, P. L. (2003). A digital acoustic recording tag for measuring the response of wild marine mammals to sound. *IEEE Journal Of Oceanic Engineering*, **28**, 3–12.
- Marques, T. A. and Thomas, L. (2012a). Obtaining pseudo-tracks and georeferenced locations from DTAG data. Technical report, LATTE WORKING DOCUMENT.
- Marques, T. A. and Thomas, L. (2012b). Using dedicated kalman filter r packages to fit the georeferencing ssm. Technical report, LATTE WORKING DOCUMENT.
- Marques, T. A., Thomas, L., Ward, J., DiMarzio, N., and Tyack, P. L. (2009). Estimating cetacean population density using fixed passive acoustic sensors: an example with Blainville’s beaked whales. *The Journal of the Acoustical Society of America*, **125**, 1982–1994.
- Morrissey, R. P., Ward, J., DiMarzio, N., Jarvis, S., and Moretti, D. J. (2006). Passive acoustic detection and localization of sperm whales (*Physeter macrocephalus*) in the tongue of the ocean. *Applied Acoustics*, **67**, 1091–1105.
- Vincent II, H. T. (2001). *Models, algorithms, and measurements for underwater acoustic positioning*. Ph.D. thesis, University Of Rhode Island.

Combining building blocks for simulating beaked whales at AUTECH

Tiago A. Marques & Len Thomas

Centre for Research into Ecological and Environmental Modelling
The Observatory, University of St Andrews, St Andrews, KY16 9LZ, Scotland

Version's date: September 22, 2015

Contents

1	Introduction	3
1.1	Previous reports	5
1.2	Overview of the simulation process	6
2	Preliminaries about the simulation region	9
2.1	Hydrophone location	9
2.2	Bottom depth	10
2.2.1	Etopo1 data - deprecated	10
2.2.2	NUWC data	10
2.3	Initial group locations and group sizes	16
3	Animal movement	18
3.1	General ideas	18
3.2	A 2D movement model	22
3.2.1	Simulation implementation	26
3.2.2	Some notes about this 2D movement model	28
3.2.3	A remark on pragmatism	29
4	Ideas to keep in mind	29
	References	31
	Appendix	34

1 Introduction

In this document we describe the building blocks required to create a simulation engine within LATTE. We consider an agent based modelling framework, in which whales with realistic behaviour will be used to populate AUTECH. The goal is to simulate beaked whale movement, sound production and sound detection at AUTECH. Figure 1 presents AUTECH within the wider region of the Bahamas.

The key species studied under LATTE is Blainville’s beaked whale (BBW) *Mesoplodon densirostris*. This species has been shown to be sensitive to navy exercises on the AUTECH range, likely due to SONAR use (McCarthy *et al.*, 2011; Tyack *et al.*, 2011). BBW behavior is characterized by frequent long deep dives to forage at depth interspersed with periods of shallow diving. During each deep dive the animals typically produce thousands of echolocation clicks (Tyack *et al.*, 2006). BBW echolocation clicks¹ are commonly detected year round at the AUTECH range.

In LATTE we propose to develop methods which combine different types of data, with different spatio-temporal resolution:

1. AUTECH range data: cheap, easily available, in almost continuous time, low resolution data, namely counts per hydrophone (and unit time) of detected beaked whale cues;
2. DTAG data: provides high resolution in both space (meters) and time (Hz), but expensive and with very restrict temporal coverage (hours);
3. satellite tag data: with an intermediate temporal (weeks) and spatial (kilometers) resolution.

The idea is fit a joint Movement, Sound Production, and Sound Detection (MSPSD) model that links these three data sources. This model will then be used to make inferences about possible impacts of human generated sounds on beaked whales. Such inferences would be obtained by comparing relevant model parameter estimates (e.g. a group’s vocal period length) from data collected in ‘baseline’ periods of potentially disturbing sounds absence, with data collected at ‘impacted’ periods, in which potentially disturbing sounds are being produced.

¹In this report we often refer to these simply as “clicks” or “cues”.



Figure 1: The AUTECH range location within the Bahamas region, with key islands and regions.

We note that within the realms of DECAF, we produced a simulation engine which meant to reproduce click counts on the AUTECH hydrophones, and hence many ideas on simulating these animal dives are taken from that effort (see Marques and Thomas, 2008, for further details). This exercise failed at the time to reproduce the observed click counts at AUTECH. This was mostly due to the fact that, back then:

- the detection process was not yet well characterized;
- there was a large amount of false positives, which is now lower by over an order of magnitude;
- apparent differences in hydrophone performance were present (which we still have no good handle on, but this might be a minor problem in practice).

An additional key problem is related to the fact that we only have access to data to characterize individual animal movement, while these animals happen to occur in groups. This problem persists as we write the current report. Understanding within-group-at-depth-behaviour of these animals is the focus of a recently funded ONR project (GROUPAM - Beaked whale group deep dive behaviour from passive acoustic monitoring).

1.1 Previous reports

This work was built over a report produced within the realms of DECAF. Therefore, in the corresponding DECAF folder there might be additional useful information to understand this document. However, we have tried to make this report self contained. Additionally, this work builds on ideas scattered along several other internal DECAF/LATTE reports. We try to provide such references in the appropriate sections, but we also list here key sources, which have self explanatory names:

1. Explaining the code for the simulation of click count vectors 4 LATTE (Marques and Thomas, 2012a)
2. Modeling beaked whales movement, sound production and detection at AUTECH (Marques and Thomas, 2012c)

3. Modeling beaked whale DTag data and simulating 3D movement via a latent-variable approach with feedback and semi-Markovian components Marques *et al.* (2013a)

1.2 Overview of the simulation process

The simulation process requires a number of components/modules which we list below. A qualitative assessment of each of the components current development and implementation status is also provided:

1. definition of the simulation region - conceptually straightforward; actual physical boundaries defined based on (1) depth constraints and (2) some (essentially arbitrary) decisions for the northern boundary. The actual way to keep animals within these boundaries over the course of a simulation run is embedded in the process of movement simulation itself (see component 4 below);
2. initial group location - conceptually straightforward, currently implemented using a simple uniform density in space with mean intensity following Marques *et al.* (2009); Moretti *et al.* (2010). We note that an actual density surface could be obtained, by combining data from (1) D. Claridge visual surveys and (2) AUTECH hydrophones. However this was not pursued within the realms of LATTE because: (1) it was unlikely to lead to considerable changes in any of the outcomes ; (2) any such pattern would be easily incorporated in the simulation without changing any of its underlying features; (3) Diane's data was not formatted to allow easy use for this purpose; (4) using only data from AUTECH would be a possibility, but it would be too much work without a sensible objective, since it covers only the AUTECH range while we simulate over a much wider area;
3. group size - conceptually straightforward, currently using data from D. Claridge as cited in Marques *et al.* (2009); data from group sizes obtained by modeling Autogrouper outputs might also be used (see Marques *et al.*, 2013b, for details), but then again these would probably represent an overkill for the AUTECH range while unavailable everywhere else;

4. movement of animal over space and time - conceptually (and also implementation wise) is the hardest component. There are several sub-stages involved. See section 3 for further details, but in short it consists of
 - (a) depth profiles simulated over time using models as in Langrock *et al.* (2013)
 - (b) 2D displacement conditional on a depth derived behavioural state (based on DTag data)
 - (c) constraints to avoid stranding. These are implemented via a biased random walk, conditional on distance to closest “shallow” point. These are informed by DTAG data, satellite tag data, and Diane Claridge’s personal communications.
 - (d) notion of home range, implemented via a biased random walk, conditional on distance to home range center; informed by satellite tags.
5. movement of animal(s) within a group - this is the component over which we have the least information. Gathering data about at depth behaviour of multiple animals is hindered by the fact that multiple DTAGs on the animals of a single group are extremely rare. To the best of our knowledge the only instance where this is available for beaked whales was for a pair of *Ziphius cavirostris* as described in Zimmer *et al.* (2005). Therefore, while we have a good knowledge of what an animal does at depth, we do not know how animals behave with respect to each other. The actual interaction and coordination between animals will have a strong influence in the perceived acoustic footprint of a group. We choose to consider that the above movement corresponds to a focal animal - note that this is simply conceptual and pragmatic, and no animal need to actually have said role. Defining it like this means that for a group of size one, we already have simulated the movement of the entire group. For a group of individuals we will only keep track of the individual animals positions for the periods when the group is vocally active. This is justified because (1) when the group is silent it cannot be detected acoustically and (2) at the surface groups seem to be very cohesive, with members in close vicinity, so keeping track of the position of the “focal” animal is enough; there is essentially no

data available to parameterize this component ². Currently we are considering a biased random walk with the focal animal being a 3D center of attraction, representing a 3D extension of ideas proposed by Langrock *et al.* (2014); ready to be implemented.

6. sound production - conceptually straightforward, we have opted to consider a model of sound production conditional on depth, informed by DTAG data; this could be instead based on literature, but a link to existing simulated depth profiles would then be required; ready to be implemented
7. sound detection - well characterized at AUTECH, as in Marques *et al.* (2009); ready to be implemented
8. gathering data as would be observed at AUTECH is computational intensive but nonetheless conceptually straightforward given all the above is in place

A practical problem is that all these components were separately dealt with, so the spatial and temporal scales of analysis differ and hence glueing them together is not as simple as one might hope for. As an example, sound production and detection is essentially a continuous process but movement modelling has been discretized, with 1 position per “time step”, but actual “time steps” being different depending on the analysis (e.g. 10 seconds for the fHSM component, 0.2 seconds for the georeferencing component). We have attempted to use a pragmatic approach to arrive at a full MSPSD simulator, respecting the following three properties:

1. that the approach is modular, i.e. if an improved solution is found for one of its components that component can be easily updated
2. that whenever arbitrary (in the sense of not being directly estimated from data) parameters / decisions were necessary these were chosen such that their impact would be negligible (or otherwise a remark on sensitivity made)

²We note that, as mentined above, collecting information about this component is the main objective of ONR’s project GROUPAM, and therefore we might later be able to replace this module

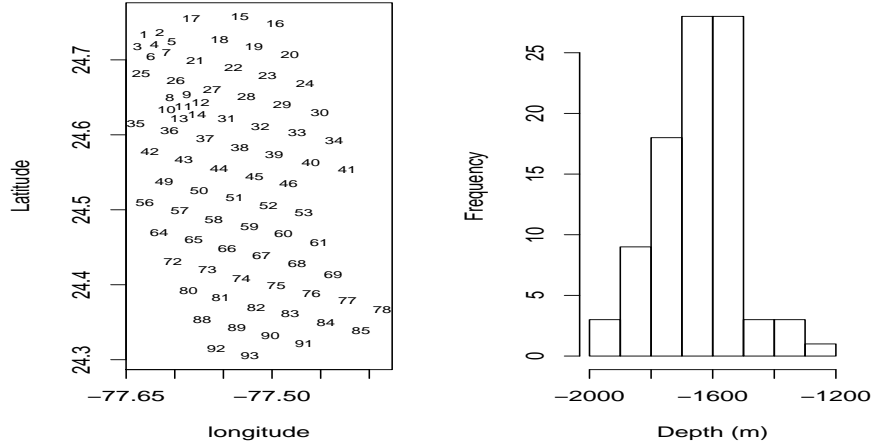


Figure 2: The AUTECH range hydrophones location (left) and an histogram of hydrophone depths (right).

3. that realism is respected, except in situations where the burden of doing so was considered too high, given the negligible impact on the results considering the spatio-temporal scale of analysis expected to occur downstream.

2 Preliminaries about the simulation region

2.1 Hydrophone location

We begin by reading in the hydrophone data from a file obtained during project DECAF. Note that in this file the locations are provided in an arbitrary coordinate system, and here it might be better to have them in latitude and longitude, despite these having been shifted and jittered for security reasons. For that reason, we considered using the information archived on OBIS Seemap (available within the DECAF case studies data sets), as that has already been approved for public release. We consider here the data in file “seamap678.csv”, which had to be tweaked to filter the adequate information. Details are given in the .Rnw file. In figure 2 we present the relative

location of the hydrophones and the distribution of the hydrophone's depths. We see these range between 1200 to 2000 meters, with a mean depth of -1652 m.

2.2 Bottom depth

We know these animals tend to avoid shallow areas. This simulation exercise will have an intrinsic spatial component, and hence we need to harvest the required information to be able to, at the very least, contain the animals within some reasonable longitude (x), latitude (y) and depth (z) boundaries. In practice, we will only explicitly constrain z , and this will then be used to define the appropriate x, y boundaries.

2.2.1 Etopo1 data - deprecated

The depth data, “etopo1.xyz”, was downloaded from NOAA’s website <http://www.ngdc.noaa.gov/mgg/global/global.html>, and presents a resolution of 1 arc-minute. This resolution is presumably too coarse for our objectives, given that a whale’s entire dive could be considered to occur at constant depth, but we will use it for the time being.

We can plot the depth contours and add AUTECH’s hydrophones (Figure 3). This figure hints for a clear mismatch between the depths and the hydrophone coordinates. As an example, hydrophone 56, the shallowest, seems to be less than 500m deep, yet we know that it is at about 1300 m. This seems to hint for a mismatch or severe inaccuracy in the depth data and/or in the hydrophone location data. Inaccuracies of this type, with areas known to be deeper appearing to be shallower, have been reported elsewhere (Amante and Eakins, 2009). The depth contours in say Ward *et al.* (2012) are closer to Andros Island (cf. Figure 4). No idea what might be the cause of this, but it could actually be that Ward *et al.* (2012) contours were based on old data, just for illustration purposes.

2.2.2 NUWC data

Motivated by the issues described in the previous section, a new source for depth data was deemed necessary. A second data set containing depths was provided by Jessica Shaffer (file : “Autec_Weapons.Range.0.2min.bathy.txt”). We read that file into R.

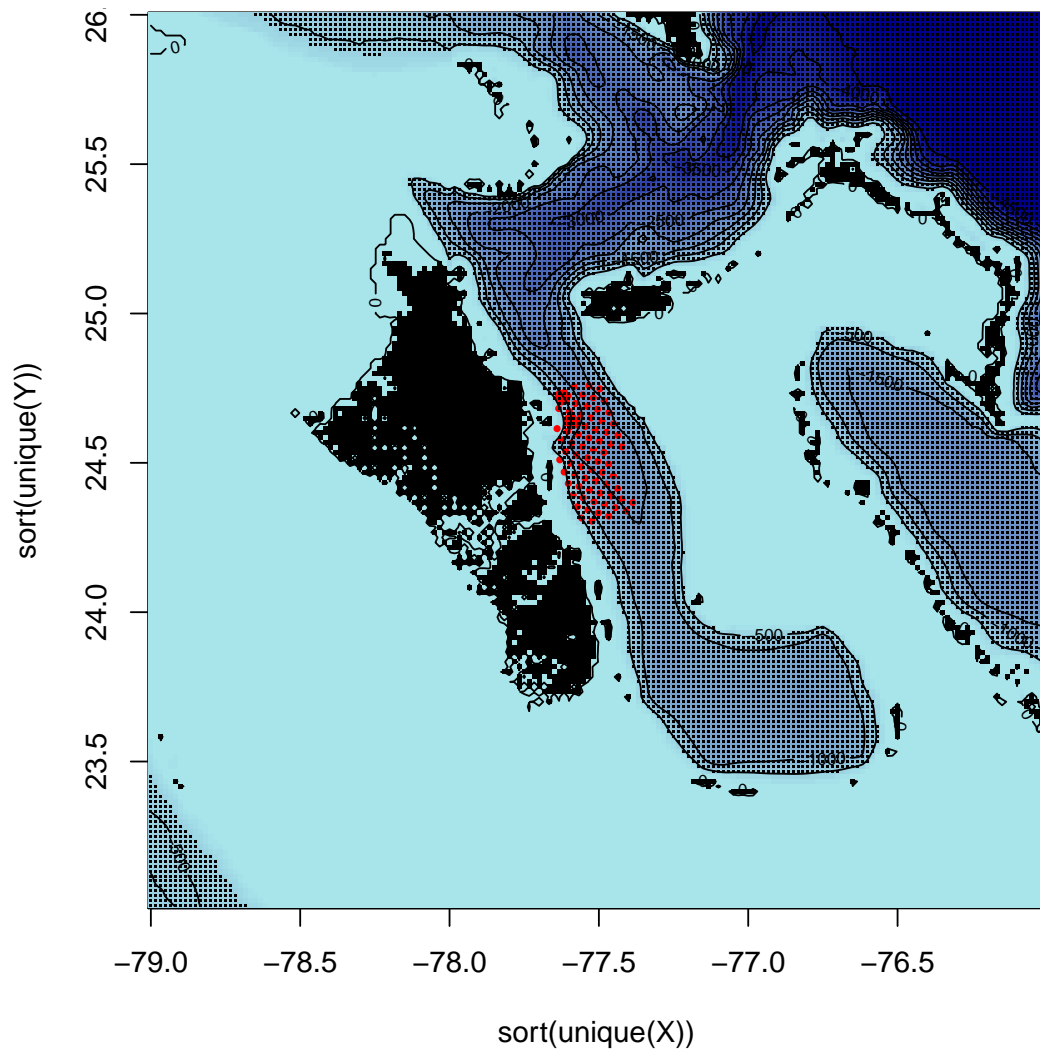


Figure 3: The AUTEK range within the Tongue of the Ocean. Red dots represent approximate hydrophone locations, and small black dots represent areas where bottom depth is below 400 meters.

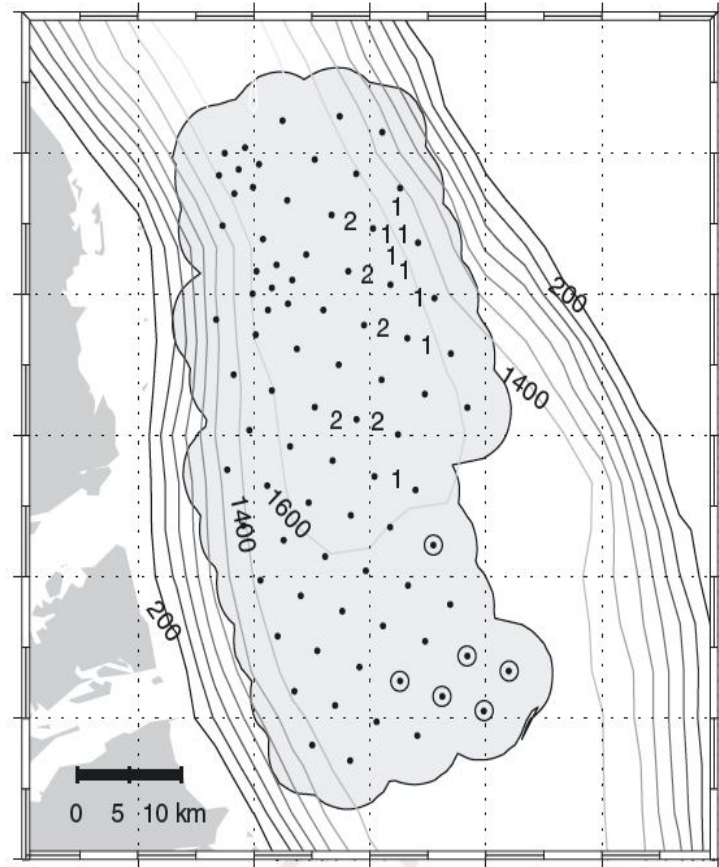


Figure 1. Atlantic Undersea Test and Evaluation Center (AUTECH) hydrophones with area of certain detection (A) indicated in gray. Numbers indicate how many simultaneous sperm whale click trains observed per sample at each location. Circles outlining hydrophones indicate sperm whales detected outside the certain detection area. Depth contours at 200 m intervals.

Figure 4: The AUTECH range within the Tongue of the Ocean, taken from Ward et al. (2012)

The difference between the depths we have for each hydrophone and the depth that it gets associated with once overlaid to the new AUTECH depth data are much smaller than before, as evidenced in figure 5 (top row).

Because we know that the hydrophone's true locations were shifted and jittered, we would not expect a perfect match regardless of the depth data quality. Assuming that the hydrophone positions were mostly shifted (i.e. relative positions kept approximately constant, just moved in latitude and longitude), one could estimate the true hydrophone locations. We coded a simple function which evaluates the discrepancy between known hydrophone depths and hydrophone depths as a function of shift. Correcting the available hydrophone positions by the shift that minimizes that function probably places the hydrophones closer to their true position.

We can plot the new depth data, with the AUTECH hydrophones locations, to see that these now make much more sense than what we previously observed (Figure 6). We also show in the same figure, in green, the position of the hydrophones which is obtained by minimizing differences in depth given what we know to be true and that obtained by overlaying hydrophone locations with AUTECH depth data. Assuming the bathymetry is correct, it seems like the true positions are about a baseline (i.e. $\approx 4\text{km}$) south of what we have been provided.

```
FALSE [1] -77.7866 -77.2400
FALSE [1] 24.155 24.905
FALSE [1] -77.63994 -77.38663
FALSE [1] 24.30488 24.75803

FALSE Warning in nlm(f = getsum, p = c(0.01749869, -0.0505816)):
NA/Inf replaced by maximum positive value
FALSE Warning in nlm(f = getsum, p = c(0.01749869, -0.0505816)):
NA/Inf replaced by maximum positive value
FALSE Warning in nlm(f = getsum, p = c(0.01749869, -0.0505816)):
NA/Inf replaced by maximum positive value
FALSE Warning in nlm(f = getsum, p = c(0.01749869, -0.0505816)):
NA/Inf replaced by maximum positive value
```

In the following we will use as hydrophone positions those which are internally most consistent with the new depth data, based on the assumption that depth data provided by NUWC are reliable and that original positions

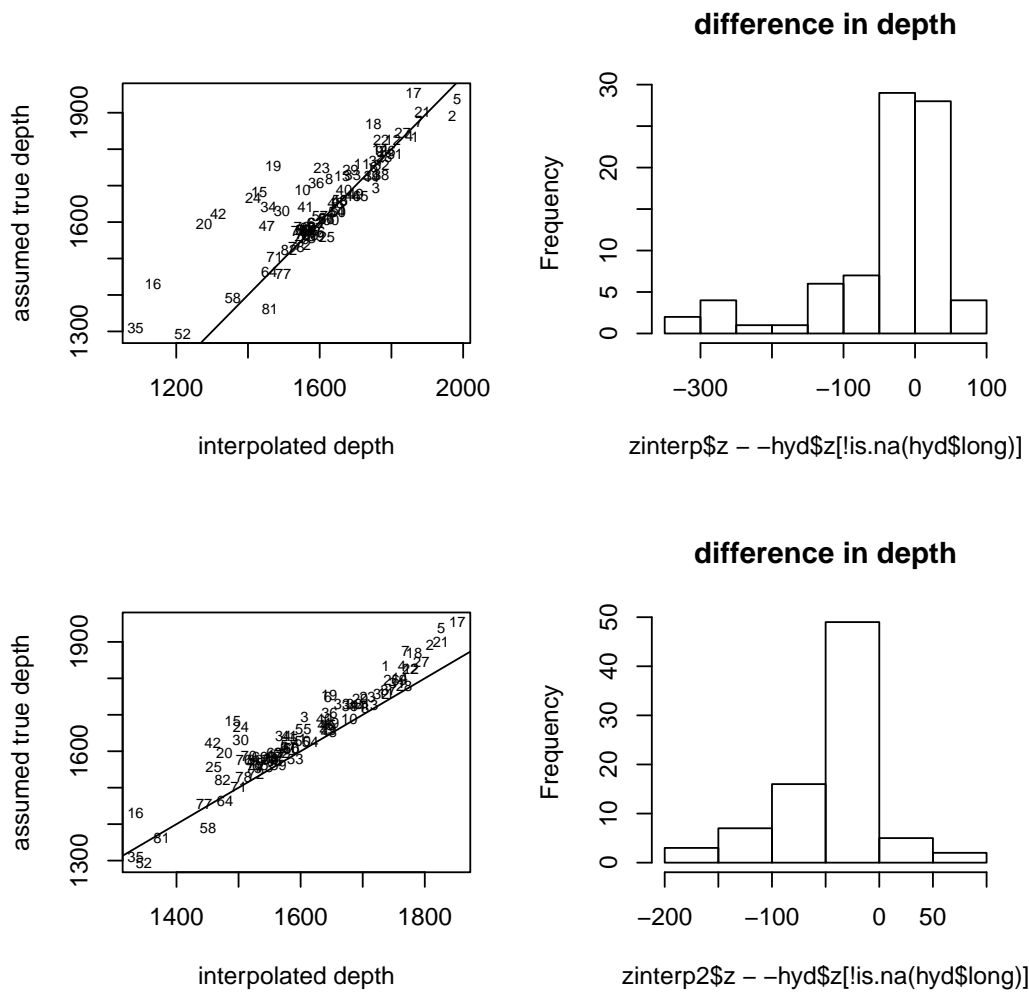


Figure 5: Relation between depths as provided with depths obtained from the depth data at the assumed coordinates. On the bottom row the same relation is shown, but from the depth data taken at the coordinates such that the difference between the provided depths and corresponding depths given the depth data is minimized.

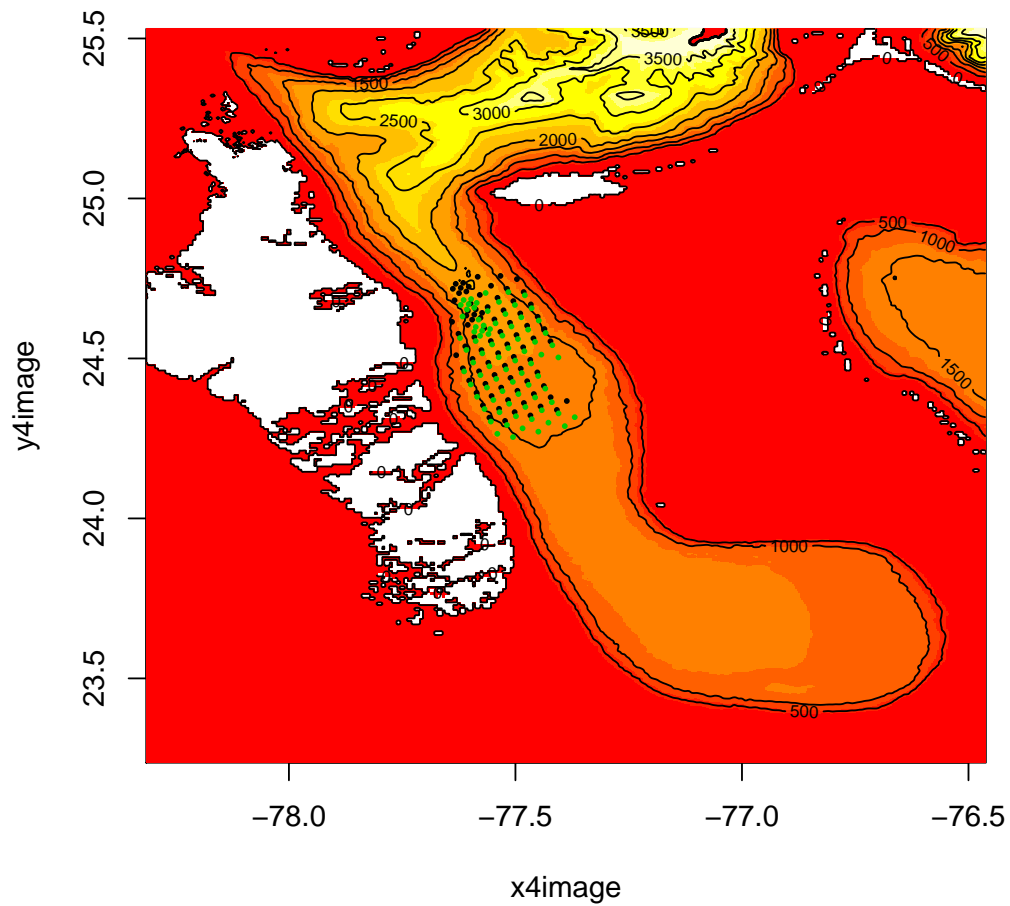


Figure 6: The AUTEc range within the Tongue of the Ocean. Black dots represent hydrophone locations provided to us, and green dots the most likely true locations obtained by minimizing the sum of the squared depth differences. White, yellow and red represent land, deep water and shallow water, respectively.

were shifted north for security reasons.

2.3 Initial group locations and group sizes

Assuming that there are no whales present at shallower waters than those above say 500 m depth, we can define the area over which we will want simulations to occur. We leverage on the ability of R's package `spatstat` to define windows over which points might be created, using function `owin`.

Note that the area covered is approximately 3 degrees of latitude and 3 degrees of longitude, and that a degree is about 111 kilometers. The area of our simulation window is about $5.2198 \times 10^4 \text{ km}^2$, which is conveniently obtained using function `area.owin`. But actually only 27.14 % of the 3 degrees side square is below 500 m, so we have an area of about $1.4168 \times 10^4 \text{ km}^2$. Given an estimate of approximately 25 whales per 1000 km^2 (Marques *et al.*, 2009) would mean that in this area we should have 354 whales. An average group size of 4.1 (Claridge (2006)) would actually mean that about 86 groups of whales would have to be generated in the area.

Beaked whales are known to exist in groups of animals. We assume for the time being that density and group size are independent, and hence, for each group that needs to be generated, we just simulate a random deviate from the relevant distribution for group sizes. As mentioned above, Claridge (2006) reported for the Bahamas an average group size of 4.1 animals, with the standard deviation (SD) being 1.9. Based on this information, a tentative model for the group sizes is $Y = X + 1$, where X is a Poisson with mean 3.1. This distribution has a SD of 1.76, which is a reasonable approximation given the 1.9 SD referred above. In figure 7 we present the hypothetical initial location of 86 groups in areas deeper than 400m. This was obtained as a realization of a marked Poisson process, with marks representing group sizes with distribution Y as defined above.

Note that a dedicated analysis based on Diane Claridge's data provided evidence that the value might be lower at AUTECH and surrounding areas Marques and Thomas (2013), around 2.82 animals per group. Therefore, the data presented in figure 7 are just for illustration.

Claridge (2013), reporting a 6 year mark-recapture study, presents no recaptures of animals from her AUTECH site at the south Abaco Island site, and vice versa. These sites are only separated by about 170 km, which seems to strongly support the notion of two distinct (sub-)populations. For this reason, in our simulation we will consider a boundary between New

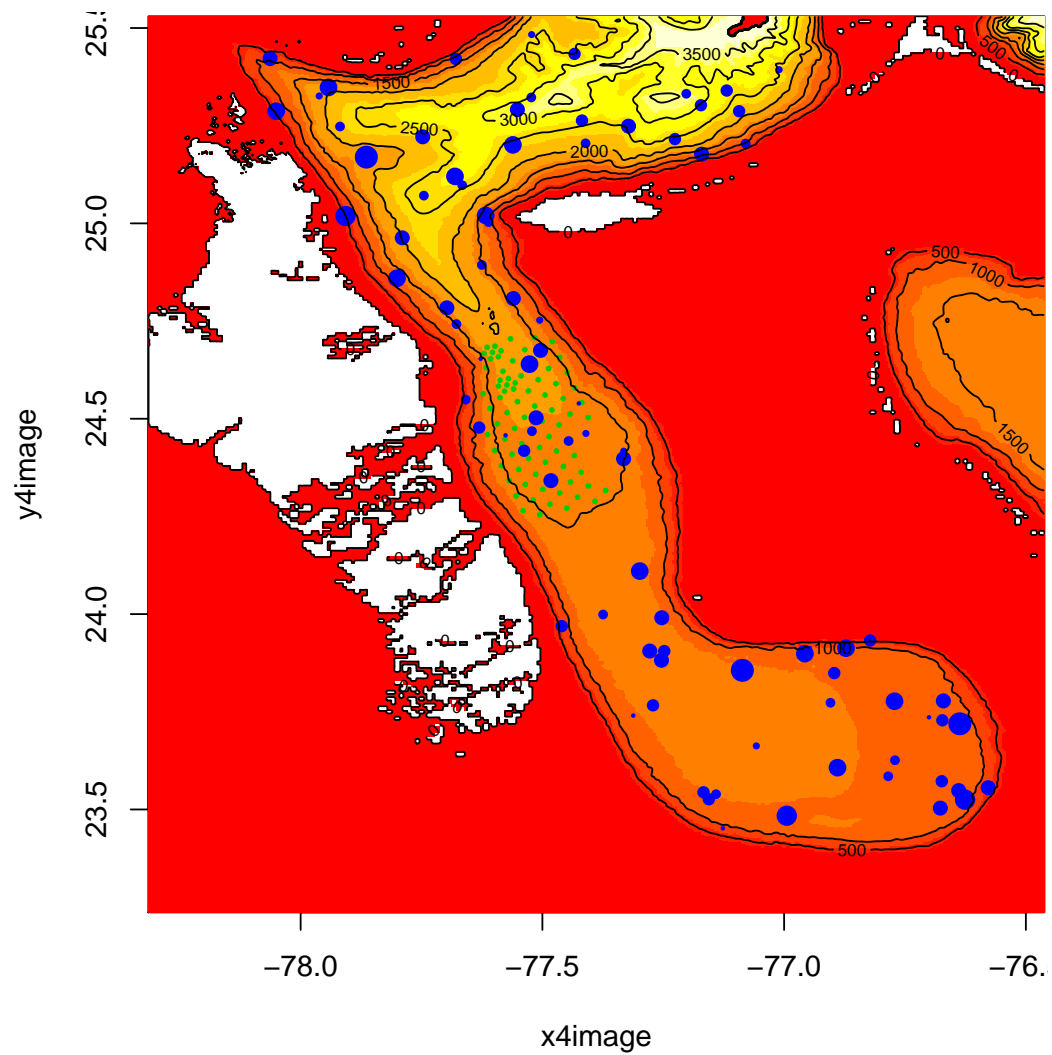


Figure 7: Location and group size representation (group size is proportional to the size of the blue dots) of 86 groups of animals present in the TOTO and surroundings.

Providence Island and the Berry Islands, over which, for the time being at least, we consider that, at the time scale our simulations occur, the animals do not cross. The way to implement this in the simulation exercise might be either via

- a simple, yet unrealistic, reflection of animals at a clearly defined boundary, or
- by adding a probabilistic repulsion effect of said boundary that makes it effectively impossible to cross by the animals, or
- by embedding animal movement behaviour with the notion of an home range center to which animals are attracted to, effectively keeping them local (this was the approach actually implemented, see details in section 3)

Further, Diane Claridge (pers. comm., 26 April 2013) noted that no beaked whales have been detected in areas shallower than 50 meters, although most are actually deeper than 500 m. Additionally, no whales have been found closer than 300 meters to shore.

Considering this information, and the fact these animals forage typically at considerable depths, we will assume in the following that animals strongly avoid shallow areas, such that most frequently they occur in areas deeper than 500m. This will be embedded by biased random walks avoiding shallow depths when required. Additional details are provided in section 3.

3 Animal movement

3.1 General ideas

Considering the material in the previous section, it seems plausible to conceptualize a movement model such that orientation would be independent of the actual location, except if near the defined boundaries (e.g 500 m depth isoline around TOTO + a boundary line between New Providence Island and the Berry Islands), where the animal will have a mean direction that somehow points away from the boundary.

On the other hand, it would seem also desirable that animals present some kind of residency. This is perhaps something that can be implemented

by assuming that the initial location represents the group home range center around which the group moves freely based on parameters for movement estimated from DTag data. However, when the animals move “far” beyond their home range center their movement becomes constrained. This could be enforced using a biased random walk, biased back towards the home range center. The strength of attraction could depend on the distance from the home range center as described by McClintock *et al.* (2012). This feature will allow groups to maintain a density pattern on average equal to what they were simulated from, rather than moving towards infinity as time goes by, which would be the case if simple random or correlated random walks were considered.

The exact way to implement this will require some additional thought; this is an extensive and certainly one of the most complex components of the simulation exercise. For the sake of this document readability and organization, a separate document Marques *et al.* (2013a) presents the analysis of DTag data integrated with a modelling framework based on HMM and extensions in order to arrive at a plausible model for animal movement that can be used for simulation. Adequate modeling of the animal movement will be one of the key aspects of this simulation exercise. Fundamental points to note from the onset include:

- movement models have almost exclusively been applied to a 2-dimensional (2D) context, and here we require a 3-dimensional (3D) models;
- a state dependent mixture of biased and correlated random walks (BRW, CRW and BCRW) seems like an adequate way to move forward, possibly based on feedback hidden semi Markov models (fHSMM) (e.g. Morales *et al.*, 2004; McClintock *et al.*, 2012; Langrock *et al.*, 2013);
- Note that fitting these to actual data from DTag’s requires that first we obtain (x, y, z) coordinates from DTag data. While z =depth is measured directly with presumably very low measurement error, (x, y) coordinates need to be obtained by some form of dead reckoning (or georeferencing of tracks). This is described in detail in Marques and Thomas (2012d) and implemented in Marques and Thomas (2012b).
- Here we assume that the process involved in the georeferencing provides 3D tracks which can be used reliably as data with no error, to fit fHSMM to. However, it would be desirable if an integrated method

was used, allowing to incorporate the uncertainty in position estimates into the state assignments and corresponding simulations. However we note that this might be more of an analytical beautifulness than of practical consequence, given that the fHSMM used is based on depth alone, and hence the data is really very accurate;

- To begin with, we assume that the animals have different behavioral states as in Langrock *et al.* (2013), corresponding to:
 1. at the surface
 2. deep diving
 - descending
 - at depth (essentially, this is the foraging stage, and hence acoustically detectable)
 - ascending
 3. shallow diving
 - descending
 - at depth
 - ascending
- For the movement in 2D horizontal plane (x, y) we can leverage the Hidden semi Markov (fHsMM) models methods developed in Langrock *et al.* (2012).
- For depth displacements we can follow the approach presented in Langrock *et al.* (2013), using feedback Hidden semi Markov (fHsMM) models
- We will need to extend the independent 2D (horizontal movement, x, y) + 1D (depth, z) approach to 3D. A first approximation is to assume that the distributions for 2D displacement (step length and turning angle) are, conditional on the state, independent of the depth displacements. This means that we can simulate independently horizontal and depth displacements.
- we only have DTAG information about individual animal movement, but these animals move in groups; a model for behaviour within group

like that of Langrock *et al.* (2014) seems a good first approach, even if at the moment we do not have much information to parameterize it

- given simulations occur over reasonable amounts of time (e.g. a week), the unconstrained animal movement that one might assume given only temporally restricted DTAG data will have to be combined with some additional constraints (say via mechanisms similar to the feedback mentioned above) such that, at least during an undisturbed scenario:
 - animals do not strand
 - animals do not hit the ocean floor
 - animals do not move away from AUTECH
 - the animal density surface is kept approximately constant
- it might make sense at a first iteration to disregard pitch, heading and roll. Another option would be to use positions at t , (x_t, y_t, z_t) , and $t + 1$ $(x_{t+1}, y_{t+1}, z_{t+1})$, to derive heading and pitch (ignoring roll, which was not used any way to characterize the detection function), therefore avoiding the need to track (and model) heading and pitch over time. We can look at DTAG data to see to what extent there is a strong correlation between heading and pitch derived in this way and observed from DTag processing (but this was not implemented).

Additionally, given that via AUTECH we only have data for the acoustic part of the deep dives, the following simplifying assumptions and model choices might make sense here:

- when animals are not vocalizing, i.e. for all behavioural states except a foraging state, model (and hence simulate) only the group center location over time; therefore we keep track of the approximate position of each animal (approximated by the group center) but we do not really need to track all animals at all times
- assume that Blainville’s beaked whale group’s behave, in some sense, by following a leader (*as described in* Langrock *et al.*, 2014); this means that we can use DTAG data to inform directly about the model for the group center, and only need to find a way to parameterize the biased or correlated or biased and correlated random walk model

that keeps the groups cohesive over time, with respect to the focal animal. A possible alternative would be modelling the center of the group instead of a focal animal; this seems less sensible from a biological point of view, but since this is mostly a conceptual difference the final choice is certainly pragmatic and should be driven by implementation simplicity. The only key advantage in modeling the leader than the group center is that DTAG data provides direct information about a given animal and not a group center. A group center will, due to the fact that it represents an average of coordinates across animals, tend to have different properties, e.g. it will typically move slower than individual animals, so the DTAG data will not typically be representative of such center. The distinction would be inexistent if we all the animals within each group were tagged.

Note that we do not expect any of the above considerations to exactly mimic reality, but we expect the difference between these and reality to be negligible for the purpose of our simulation exercise, while considerably simplifying the simulation itself.

3.2 A 2D movement model

Addressing the characteristics required in the previous section, here we describe a plausible model for 2D movement with a few basic features:

- it uses DTAG data to parametrize movement in an “unconstrained” state
- it uses satellite tag to parametrize movement respecting home ranges and avoiding shallow depths, via 2 additional constrained states (essentially “home ranging” and “avoiding stranding” states)
- respecting the initial animal distribution over the long run (as a consequence of the “home ranging” state)

We consider movement defined as a succession of step lengths (τ) and turning angles (ϕ). We consider a couple of simplifying assumptions:

1. step length distributions are derived from DTAG data only, i.e., conditional on a depth derived state a la Langrock *et al.* (2013), a step length distribution is determined based on DTAG data.

2. the same happens for the turning angle variance.

Hence, most of the 2D movement “structure” will be associated with the heading (rather than step length), which will be a function of additional features conditional on a 2D movement state, as defined below.

Ignoring a possible time index t for simplicity, at each time step t we require a number of quantities to be available (see figure 8):

- $(x_z, y_z, z_z) = p_z$, the closest point where depth is above a certain threshold z considered incompatible with beaked whale movement (i.e. shallow depths)
- d_z : the distance between the animal position and p_z
- $(x_h, y_h, z_h) = p_h$, the home range center
- d_h : the distance between the animal position and p_h
- Φ : the heading of the animal ($\Phi=0$ means the animal points north)
- Φ_h : the heading of the animal to move towards its home range center
- Φ_{z*} : the heading of the animal to move away from p_z (i.e. shallow depths)

Heading at time t (Φ_t) will be potentially a function of heading at the previous time $t - 1$ (Φ_{t-1}), or will be a function of the required heading to avoid/approach a given feature (e.g. shallow depths or home range center). In particular, the heading will be a function of where the animal is in space, defining a set of 3 movement states (in 2D), with decreasing levels of strength and complexity:

1. If the animal is closer to p_z than k_1 (i.e. $d_z < k_1$) then the dominant feature of the heading is the need to avoid shallow depths, and so heading will tend to be around Φ_{z*} , else
2. If the animal is unusually far from to p_h (i.e. $d_h > k_2$), where k_2 represents a point beyond which the need to tend to the home range center is triggered, then the dominant feature of the heading is the need to move closer to p_h , and so heading will tend to be around Φ_h , else

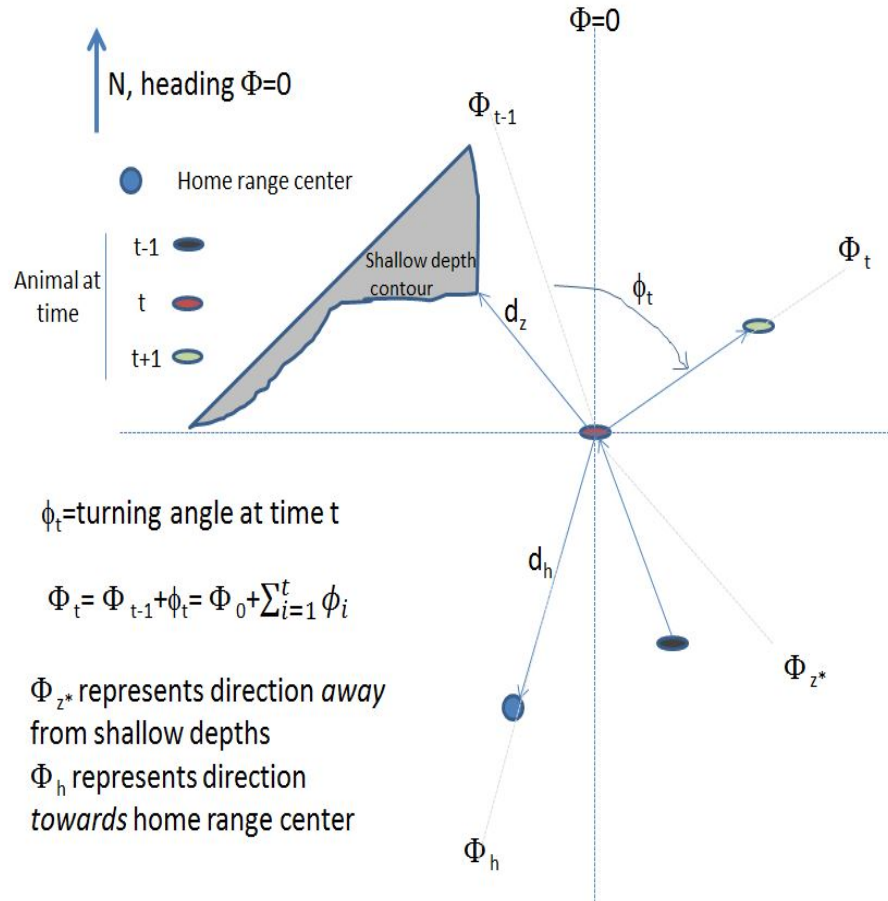


Figure 8: Quantities and notation required for the 2D movement model.

3. the animal is not far from its home range center nor risking stranding, and hence movement is simply dictated by DTAG data, which for simplicity we also refer to as the “unconstrained” state.

For simplicity, while in the “unconstrained” state the animal moves according to an uncorrelated and unbiased random walk³, in the other two constrained states the mean heading is a function of the previous heading and the directional heading required to avoid or go towards a feature (so essentially a biased and correlated random walk). The variance in turning angle will be taken from the DTag data, conditional on the depth derived state, irrespectively of the whether the whale is in an “unconstrained” mode or not.

In terms of implementing the actual simulation, the required computations at time t are:

1. obtain (x,y,z) and depth derived state $S = s$ at $t - 1$, as well as Φ_{t-1}
2. get τ_t and ϕ_t from the relevant $\tau_t|S = s$ and $\phi_t|S = s$ distributions, and then Φ_t as $\Phi_{t-1} + \phi_t$; these will be kept unless one of the two following if statements is true
3. get p_z and d_z
4. if $d_z < k_1$ (i.e. animal in avoid shallow depth mode)
 - get Φ_{z*}
 - and $\Phi_t = a\Phi_{z*} + (1 - a)\Phi_{t-1}$. The function defining a should be bounded by 0 and 1, where a tends to 1 as d_z tends to 0, and a tends to 0 as d_z tends to k_1 . A logistic or an hyperbolic tangent function were used in a similar context by McClintock *et al.* (2012). Figure 9 presents an hypothetical general form for such a function.
5. else get d_h , and if $d_h > k_2$ (i.e. animal in return to home range center mode)
 - get Φ_h

³Note that uncorrelated at the turning angle scale can be correlated at the heading scale, so strictly this wording is not correct.

- and $\Phi_t = b\Phi_h + (1 - b)\Phi_{t-1}$. The function defining b should be bounded by 0 and 1, where b tends to 1 as d_h tends to ∞ , and b tends to 0 as d_h tends to k_2 . Figure 9 presents an hypothetical general form for such a function.

Note therefore that k_1 , and the parameters of the function defining a , as well as k_2 , and the parameters of the function defining b , must to be estimated from data. We will use the available satellite tag data for that purpose.

Note also that while for the “unconstrained” state we simulate turning angles (ϕ) and from these we obtain headings (Φ), in constrained states we embed a notion of mean heading from which one can derive the required mean turning angle. Note also this means that while tuning angles are independent, the actual headings are correlated.

3.2.1 Simulation implementation

Here we describe the required steps in terms of simulation, which somewhat depart from the previous thoughts in terms of implementation. This is because it would be prohibitively slow to implement a check on the two required conditions at each time step: a) Is the animal in shallow depths? b) Is the animal away from the home range center? The simulation currently occurs at time steps of 1 second, i.e. 86400 time points per day per whale, and the triggering of a constraint is intrinsically correlated (since it depends on the animal’s position, which varies slowly and continuously over time), so occasional checking is likely enough.

A possible pragmatic approach is:

1. Simulate full track from DTAG based distributions
2. For each deep dive start point (i.e. first time step in deep diving descent mode) check
3. whether $d_z < k_1$ and $d_h < k_2$
4. If $d_z < k_1$
 - redo previous deep dive with correlated and biased random walk avoiding shallow depths
5. else if $d_h < k_2$

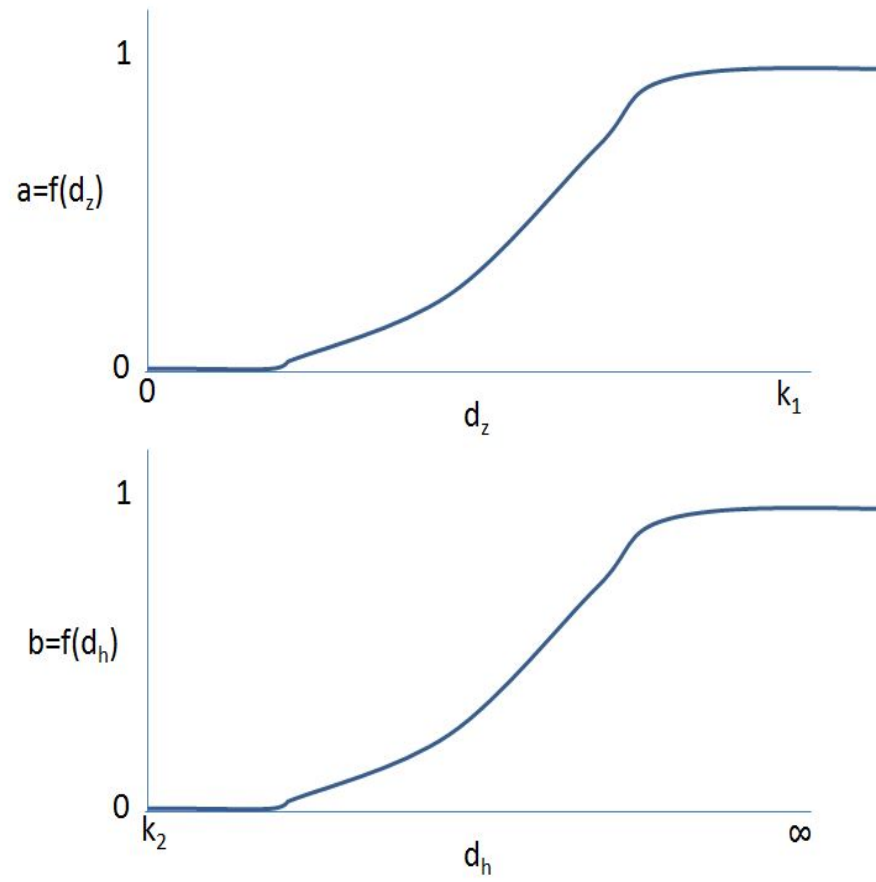


Figure 9: Hypothetical general form for functions defining a and b . See text for details.

- redo previous deep dive with correlated and biased random walk towards home range center
6. reposition track from next deep dive onwards at the last simulated position
 7. go to next deep dive (i.e. return to step 3)

However, we further simplified the process. When one of the two conditions is triggered we replace the steps 3-6 by a “rotation” of the simulated track, such that the mean direction (currently as evaluated by the direction of the first to last point in the dive) is opposite to that necessary to avoid shallow depths / stay in the “vicinity” of the home range center.

This procedure is repeated until all deep dives starts respect the 2 constraints.

This is perhaps a cumbersome approach taken for the sake of pragmatism. It is not necessarily the case that a rotation at the dive scale can achieve the desired results. As an example, depending on the specific geometrical configuration there might be no single rotation of a full dive that allows to avoid a shallow area, say. Therefore, this is a component that could definitely be improved upon.

3.2.2 Some notes about this 2D movement model

It might be the case that pairs (a, k_1) and (b, k_2) have large within-parameter-correlation, i.e. it might be difficult to estimate say a and k_1 independently, or in other words, the way in which the function increases might be dependent on the distance chosen, and so given a k_1 the estimate of a might be constrained.

Another option might be to consider that heading at time t (Φ_t) is always obtained via the same mechanism. A way to do so would be to consider that

$$\Phi_t = (\Phi_{t-1} + \phi_{z,t}) \times M_1 + \Phi_{z*} \times M_2 + \Phi_h \times M_3 \quad (1)$$

where the following conditions are enforced

- $M_1 + M_2 + M_3 = 1$
- as d_z tends to 0 M_2 tends to 1

- as d_h tends to infinity M_3 tends to 1
- if $d_z > k_1$ then $M_2 = 0$
- if $d_h < k_2$ then $M_3 = 0$
- $M_2 \gg M_3$ if both $d_z < k_1$ and $d_h > k_2$

This corresponds to generating a turning angle with mean given by

$$\phi_t = \frac{\Phi_t - \Phi_{z*} \times M_2 - \Phi_h \times M_3}{M_1} - \Phi_{t-1} \quad (2)$$

3.2.3 A remark on pragmatism

This specific conceptual approach was taken but several others would be possible, as there are a number of questions and features which could be addressed differently. A couple of examples would be:

- the two initial simplifying assumptions about step length and turning angle variance dependent on depth state alone might be relaxed and the model become more complex. The turning angle variance might be a function of the current distance to some features (e.g. home range center, shallow depths) rather than DTAG derived conditional on the depth state. This would certainly have the knock-on effect of changing the relationship between the previous heading and the current heading, say at the level of the weighted mean parameter relationship.
- while we assume in the “unconstrained state” (i.e. purely DTAG based) the animal moves according to an uncorrelated and unbiased random walk, it seems likely that this could be actually a correlated random walk to include persistence in both step length and turning angles (see Marques and Thomas (2014) for details).

4 Ideas to keep in mind

There are some ideas relevant to this simulation exercise that we keep here for reference and further discussion:

- We will want to keep animals from diving into the sea floor and moving into shore. It would be desirable to set these up using some feedback mechanism that keeps them from moving to these areas in some stochastic way, rather than setting hard boundaries.
- Consider a single animal to begin with. Having movement such that a target density surface is preserved is similar to an MCMC in which a stationary distribution is obtained via a series of steps in a Markov Chain. Therefore ideas from implementation of Bayesian samplers might be useful here. It does seem however unlikely that one is able to preserve both the density surface and the fine scale movements as we might estimate from data obtained say from georeferenced DTag data then modelled using fHsMM approaches. There must be a compromise in the realism that one can preserve in fine scale movement and the ability to preserve a constant density surface.
- All the methods mentioned above for individual animal movement have typically been fitted to single animal data. Langrock *et al.* (2012) do address the problem of fitting to multiple animals via the inclusion of a random effect in the model, i.e., by considering that some parameters are common across animals but some others (typically very few for practical implementation reasons) can vary according to some distributional form. In practice here the georeferentiation methods have only been fitted to a single animal, the same happening to the fHsMM approach for depth profiles, applied to a satellite time-depth tag, and considerable problems were found when we tried to fit this approach to DTag depth data. This means that in terms of actually simulating from these we are not adequately representing the possible range of variability in observed movements. This is a point which to address properly would require extensive work in fitting similar models to data sets from several animals. Given the work required to fit these to single animals it seems like a pragmatic approach at this point is to develop a simulation tool which ignores this underestimation of variability, providing a way to glue all these components together.

References

- Amante, C. and Eakins, B. (2009). Etopo1 1 arc-minute global relief model: procedures, data sources and analysis. Technical report, NOAA Technical Memorandum NESDIS NGDC-24.
- Claridge, D. (2013). Population ecology of Blainville’s beaked whales (*Mesoplodon densirostris*).
- Claridge, D. E. (2006). *Fine-scale distribution and habitat selection of beaked whales*. Master’s thesis, University of Aberdeen, Scotland, U.K.
- Langrock, R., King, R., Matthiopoulos, J., Thomas, L., Fortin, D., and Morales, J. M. (2012). Flexible and practical modeling of animal telemetry data: hidden Markov models and extensions. *Ecology*, **93**, 2336–2342.
- Langrock, R., Marques, T. A., Thomas, L., and Baird, R. W. (2013). Modeling the diving behavior of whales: a latent-variable approach with feedback and semi-Markovian components. *Journal of Agricultural, Biological, and Environmental Statistics*, **19**, 82–100.
- Langrock, R., Hopcraft, J. G. C., Blackwell, P. G., Goodall, V., King, R., Niu, M., Patterson, T. A., Pedersen, M. W., Skarin, A., and Schick, R. S. (2014). A model for group dynamic animal movement. *Methods in Ecology & Evolution*, **5**, 190–199.
- Marques, T. A. and Thomas, L. (2008). Explaining the code for the simulation of click count vectors. Technical report, DECAF internal report.
- Marques, T. A. and Thomas, L. (2012a). Explaining the code for the simulation of click count vectors 4 LATTE. Technical report, LATTE WORKING DOCUMENT.
- Marques, T. A. and Thomas, L. (2012b). Implementing a SSM to obtain pseudo-tracks and georeferenced track from DTAG data: an application to Md248b. Technical report, LATTE WORKING DOCUMENT.
- Marques, T. A. and Thomas, L. (2012c). Modeling beaked whales movement, sound production and detection at AUTEK. Technical report, LATTE WORKING DOCUMENT.

- Marques, T. A. and Thomas, L. (2012d). Obtaining pseudo-tracks and georeferenced locations from DTAG data. Technical report, LATTE WORKING DOCUMENT.
- Marques, T. A. and Thomas, L. (2013). *Mesoplodon densirostris* cluster sizes in the bahamas. Technical report, LATTE WORKING DOCUMENT.
- Marques, T. A. and Thomas, L. (2014). A note about the modelling and simulation of step lengths. Technical report, CREEM: LATTE WORKING DOCUMENT.
- Marques, T. A., Thomas, L., Ward, J., DiMarzio, N., and Tyack, P. L. (2009). Estimating cetacean population density using fixed passive acoustic sensors: an example with Blainville’s beaked whales. *The Journal of the Acoustical Society of America*, **125**, 1982–1994.
- Marques, T. A., Langrock, R., and Thomas, L. (2013a). Modeling beaked whale dtag data and simulating 3d movement via a latent-variable approach with feedback and semi-markovian components. Technical report, LATTE WORKING DOCUMENT.
- Marques, T. A., Shaffer, J., and Thomas, L. (2013b). Modelling group size as a function of autogrouper outputs. Technical report, LATTE internal report.
- McCarthy, E., Moretti, D., Thomas, L., DiMarzio, N., Morrissey, R., Jarvis, S., Ward, J., Izzi, A., and Dilley, A. (2011). Changes in spatial and temporal distribution and vocal behavior of Blainville’s beaked whales (*Mesoplodon densirostris*) during multiship exercises with mid-frequency sonar. *Marine Mammal Science*, **27**, E206–E226.
- McClintock, B. T., King, R., Thomas, L., Matthiopoulos, J., McConnell, B. J., and Morales, J. M. (2012). A general modeling framework for animal movement and migration using multi-state random walks. *Ecological Monographs*, **82**, 335–349.
- Morales, J. M., Haydon, D. T., Frair, J., Holsinger, K. E., and Fryxell, J. M. (2004). Extracting more out of relocation data: building movement models as mixtures of random walks. *Ecology*, **85**, 2436–2445.

- Moretti, D., Marques, T., Thomas, L., DiMarzio, N., Dilley, A., Morrissey, R., McCarthy, E., Ward, J., and Jarvis, S. (2010). A dive counting density estimation method for blainville's beaked whale (*Mesoplodon densirostris*) using a bottom-mounted hydrophone field as applied to a mid-frequency active (mfa) sonar operation. *Applied Acoustics*, **71**, 1036–1042.
- Tyack, P. L., Johnson, M., Soto, N. A., Sturlese, A., and Madsen, P. T. (2006). Extreme diving of beaked whales. *Journal of Experimental Biology*, **209**(21), 4238–4253.
- Tyack, P. L., Zimmer, W. M. X., Moretti, D., Southall, B. L., Claridge, D. E., Durban, J. W., Clark, C. W., D'Amico, A., DiMarzio, N., Jarvis, S., McCarthy, E., Morrissey, R., Ward, J., and Boyd, I. L. (2011). Beaked whales respond to simulated and actual navy sonar. *PLoS ONE*, **6**, e17009.
- Ward, J. A., Thomas, L., Jarvis, S., DiMarzio, N., Moretti, D., Marques, T. A., Dunn, C., Claridge, D., Hartvig, E., and Tyack, P. (2012). Passive acoustic density estimation of sperm whales in the Tongue of the Ocean, Bahamas. *Marine Mammal Science*, **28**, E444–E455.
- Zimmer, W. M. X., Johnson, M. P., Madsen, P. T., and Tyack, P. L. (2005). Echolocation clicks of free-ranging Cuvier's beaked whales (*Ziphius cavirostris*). *The Journal of the Acoustical Society of America*, **117**, 3919–3927.

A Some useful spatstat functions

There are a number of functions and classes in library **spatstat** which can be useful for our simulation exercise. We have mentioned a few in the text, but here we also present a list that might be useful. These include:

- classes
 - **owin** - area over which a point process occurs
 - **ppp** - point process
 - **im** - a pixel image, with values associated to each pixel. This can be useful to represent e.g. a density surface
- functions
 - **bdist.points** - check whether a given group is or not in the vicinity of the boundary, although the coordinates to be checked need to be converted to class **ppp** (point process) before.
 - **bdist.pixels** to obtain for each pixel in a **owin** the distance said pixel is from the boundary
 - **border**, which computes the border region of a window, that is, the region lying within a specified distance of the boundary of a window.
 - **rpoint** generates a random (use **rmpoint** if multitype if needed) point pattern with a fixed number of points (or a fixed number of points of each type in **rmpoint**). Note types could be used for marks, as long as mark is finite and discrete. The way to define the spatial distribution could be via a function f or a pixel image, in which case the unnormalised density at a location (x, y) for points of any type is equal to the pixel value of f for the pixel nearest to (x, y)

In figure A.1, left plot, we present the simulation area with shading proportional to the distance to the edge, obtained via **bdist.pixels**. Note that at this point the units for distance are degrees, which do not necessarily have a precise meaning. Using the ability to format the output of **bdist.pixels** as an **im** object, in figure A.1, left plot, we present the simulation of a realization of a point process which density is proportional to distance from the edge of the simulation area.

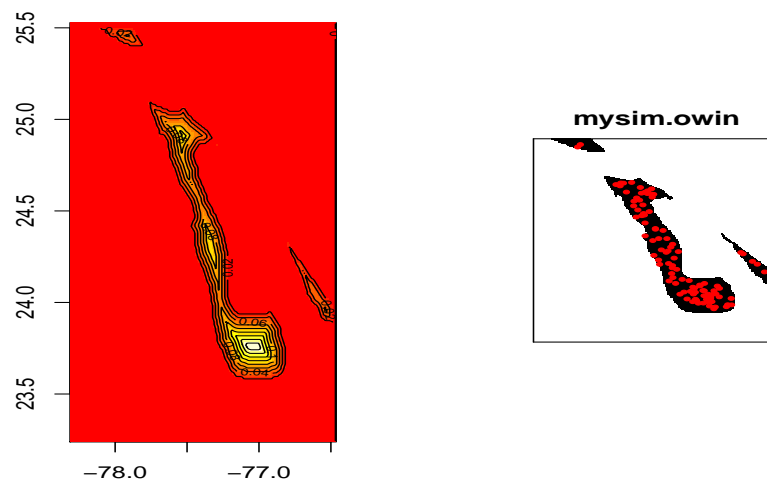


Figure A.1: Obtaining and using the distance to the edge of simulation area. Left plot: representation of distance to the boundary of simulation window. Right plot: simulation of a point process with distribution proportional to distance to the edge.

Modeling beaked whales movement, sound production and detection at AUTECH

Tiago A. Marques & Len Thomas

Centre for Research into Ecological and Environmental Modelling
The Observatory, University of St Andrews, St Andrews, KY16 9LZ, Scotland

Version's date: February 21, 2013

Contents

1	Introduction	2
2	A review about animal movement models	3
2.1	Modeling 2D movement	5
2.2	Available work describing dive data	6
2.2.1	One dimensional data: dive profiles	6
2.2.2	Two dimensional data: movement projected on the sea surface	7
2.2.3	Three dimensional data: true dive data	8
2.2.4	Dive related data	9
2.3	About Houser (2006)	9
2.3.1	Model Overview	9
2.3.2	Species definition	10
2.3.3	Distribution model types	11
2.3.4	Concluding remarks	12
3	Model components	12
3.1	Introduction, data available and random comments	12
3.2	Beaked whale movement	14
3.2.1	Behavioral state	14
3.2.2	Individual animal movement	19
3.2.3	Group movement	20
3.3	Sound production and detection	21

1 Introduction

The key species in LATTE is *Mesoplodon densirostris*, Blainville’s beaked whale (BBW). This species has been shown to be sensitive to navy exercises on the AUTECH range (McCarthy *et al.*, 2011; Tyack *et al.*, 2011), likely due to SONAR use. BBW behavior is characterized by frequent long deep dives to forage at depth. During each deep dive the animals typically produce thousands of echolocation clicks (Tyack *et al.*, 2006b). BBW echolocation clicks¹ are commonly detected year round at the AUTECH range.

In LATTE we propose to develop methods which combine (at least) 2 types of data:

1. cheap, easily available, in almost continuous time, low resolution data from the AUTECH range, namely counts per hydrophone (and unit time) of detected beaked whale cues
2. DTAG data which provides high resolution in both space and time, but expensive and with very restrict temporal coverage

The idea is to use these data to fit a Movement, Sound Production, and Sound Detection (MSPSD) model that links the two data sources. This model might, at a later stage, be used to make inferences about possible impacts of human generated sounds on beaked whales, say by comparing relevant model parameter estimates (e.g. a group’s vocal period length) from data collected at baseline periods (that is, in the absence of potentially disturbing sounds) with data collected at impacted periods (that is, in which such sounds are being produced).

Here we start addressing some of the components needed for this far from straightforward task. This report will act both as a working document and as a place to record ideas which might, along the way, end up not being used but still deserve to be put down somewhere. It will also contain some

¹In this report we often refer to these simply as “clicks” or “cues”.

background material that is useful for context and for building up the models involved.

We note that within the realms of DECAF, we produced a simulation engine which meant to reproduce click counts on the AUTECH hydrophones, and hence many ideas on simulating these animal dives are taken from that effort (see Marques and Thomas, 2008a, for further details). This exercise failed at the time to reproduce the observed click counts. This was most likely the case because when it was produced, the detection process was not yet well characterized, but also due to the large amount of false positives and apparent differences in hydrophone performance which we have no good handle on. An additional problem related to the fact that we only had data to characterize individual animal movement, and that these animals occur most often in clusters.

We start with a brief review of relevant work on animal movement models (section 2). This is followed by details on the different components of our MSPSD model (section 3), plausible model components, and available sources of data to parameterize them.

2 A review about animal movement models

In this section we present the current state of the art regarding models of animal diving. Beaked whales are essentially “occasional surfacers”, hence the aspect of diving is fundamental.

While animal diving is a process which occurs in 3 dimensions (3D), there are not many studies which consider 3D data. Here we refer to an animal location at time t as $l_t = (x_t, y_t, z_t)$, referring respectively to longitude, latitude and depth. While there is a growing literature about animal movement and its modeling, this is usually conceptually implemented in two dimensions, namely (x, y) . On the other hand, diving itself has been often treated as a 1D problem, in which depth z is recorded as a function of time (such data are often referred to as dive profiles), while discarding the x, y coordinates.

Understanding and quantitatively describing (i.e. modeling) the way animals dive is important for many reasons. For example characterizing via a statistical model the movement process of diving animals in the absence of a disturbance, and measuring the change in the model parameters in the presence of disturbance, might be a way to quantify impacts. There is considerable work comparing predictions from optimal dive models and empirical

dive observations (e.g. Heath *et al.*, 2007). Diving and surfacing patterns can inclusively have direct influence in the performance of methods used to estimate animal abundance, because they govern the availability for detection (e.g. Okamura *et al.*, 2006). Individual animal movement potentially plays an important role in the understanding of population dynamics (Morales *et al.*, 2010).

There are two different aspects about models, namely models for dive data. One can think about models which are used to simulate diving, or models fit to diving data. To the best of our knowledge there have been no attempts to fit models to 3D dive data, and there have been only a few attempts to simulate dive data from simple models, namely Houser (2006) (see section 2.3 for additional details about this paper). Within the DECAF effort there was also an attempt to simulate beaked whale dives, as stated above. A record of such effort can be found in Marques and Thomas (2008a) and Marques and Thomas (2008b).

It is interesting to note that while in terms of movement models animals are virtually always considered as independent units, in many cases animals move in groups in which movement is highly correlated across individuals. Lett and Mirabet (2008) present a review on modelling dynamics of animal groups in motion. Lukeman (2009) presents some ideas about models regarding group movement, but at a scale unlikely to be useful for LATTE purposes. There are not many instances in which data is simultaneously available for multiple animals. Zimmer *et al.* (2005) presents an exception where two Cuvier's beaked whales (*Ziphius cavirostris*) were simultaneously tagged. Mark Johnson (2010, pers. comm.) has also a couple of interesting data sets with multiple simultaneous tags on sperm whales and pilot whales, which might at the very least serve as a source of inspiration.

One of the key characteristics of movement data is the strong autocorrelation observed. See Dray *et al.* (2010) for a discussion of the implications of this feature.

As stated above, we could not find any references fitting models to true 3D dive data. Nonetheless, some references dealing with work that might be relevant include:

- Higgs and Ver Hoef (2012), which deals with drawing inferences on covariates influencing depths of dives based on categorical dive data;
- Bailleul *et al.* (2008) apply a first-passage time analysis in the depth

dimension to detect behavioral changes of southern elephant seals, noting several (hardly surprising!) differences in inferences compared to using only x, y data;

- Walker *et al.* (2011) use a SALSA smoother (spline-based) to classify dive shapes, but without ever modeling the dives themselves in a way that might be used for later general purposes;
- Dowd and Joy (2011) use a 2nd order autoregressive process to model vertical velocity and depth data collected on seals. They do not address the x, y component of the data, nor do they take into account the bounding nature of the sea surface, such that simulations from their model would lead to unrealistic movement patterns.
- Photopoulou (2012) has used sparse depth data to model dive profiles (1D)

It is interesting to quote directly from Houser (2006) here: “Implementation of analytical results into models of marine mammal movement and behavior is also a critical issue in need of addressing - whereas movement and behavior models for terrestrial mammals enjoy a rich history of development and application, similar models for marine mammals are all but nonexistent”. Because one can think of the 3D case as a generalization of the 2D case, and hence some of the 2D approaches might be extended to the 3D case, in section 2.1 we present a short number of references which review ways to fit models to 2D (x, y) data. In section 2.2 we present some of the work which describes marine animal movement data. This kind of data will inevitably be necessary to implement any model fitting exercises.

2.1 Modeling 2D movement

In recent years there has been a growing body of literature devoted to fitting models to, and drawing relevant ecological inferences from, animal movement data. We do not attempt a review of the area here, because a number of related review papers have been recently published. Hence, the reader is referred to the appropriate sources for further detail:

- Schick *et al.* (2008) present a review on understanding movement data and processes.

- Patterson *et al.* (2008) present an overview of the use of state space models applied to animal movement.
- Smouse *et al.* (2010) present a review on stochastic modeling of animal movement.
- Tomkiewicz *et al.* (2010) review the use of GPS data in animal behavior and ecological research.
- Struve *et al.* (2010) describes current views as the outcome of a recent workshop held at Silwood Park (UK, 9-11 March 2010), "Spatial models in animal ecology, management and conservation", and due to the intrinsic spatial nature of movement data, is also relevant source of material.

Morales *et al.* (2004) presented the concept of using mixtures of random walks to model movement data with different behavioral states. Jonsen *et al.* (2007) report the use of switching state space models to identify behavior states using such data, a procedure which might be interesting to use under LATTE. Note that some details of their model are only given in Jonsen *et al.* (2005). McClintock *et al.* (2012) extended that method, including the ability to use reversible jump MCMC to sample across a model space in which different models correspond to a different number of states and state-dependent behaviors. Tremblay *et al.* (2009) describe an alternative way, based on forward particle sampling, to fit models to movement data.

2.2 Available work describing dive data

Because the ultimate goal is on modeling dives, we concentrate our focus on work developed for marine animals. We note however that similar models might be applied in the modeling of movements of flying animals (e.g. birds of prey), in which the earth surface acts as a boundary in the same way that the sea surface does for diving animals.

In the following sections we list references which have dealt with different kinds of marine movement and dive data.

2.2.1 One dimensional data: dive profiles

The development of tags capable of recording animal position under water has allowed researchers to investigate dive patterns. However, we are unaware

of attempts to model the actual dive data. Usually such data has been used to test hypothesis about optimal dive models (e.g. Halsey *et al.*, 2003).

There are a number of papers reporting dive profiles, i.e. animal depth as a function of time, for considerably different species, but none of them attempting to fit models to movement data. These include:

1. Watkins *et al.* (2002) provide dive depth information on a single sperm whale
2. Hays *et al.* (2004) provide dive profiles on 4 leatherback turtles using Satellite Relay Data Loggers (SRDL). In total a few thousands of dives were available. Each SRDL included a pressure sensor, which was used to measure the depth to an accuracy of 0.33 m every 4 s, but there is actually quite a lot of “on-board” data processing involved, and only 5 points per dive are transmitted via the satellite, and hence that is the only information available for each dive. Validating dive profiles obtained from this process was described by Myers *et al.* (2006);
3. Baird *et al.* (2008) analyze diel patterns of beaked whale diving;
4. Baird *et al.* (2006) present analysis of time-depth data for beaked whales;
5. Chilvers *et al.* (2004) present data on the diving behaviour of 15 dugongs (*Dugong dugon*), documented using time-depth recorders (TDRs), which logged a total of 39,507 dives.

2.2.2 Two dimensional data: movement projected on the sea surface

As stated above, the interest on animal movement has led to a myriad of work about the fitting of models to movement data. Often papers report movement data, but make no attempt at modeling the data. One example is Schorr *et al.* (2009) who present data for Blainville’s beaked whales off the island of Hawai’i, based on satellite tags (8 individual whales tagged, 15 to 71 days of data, mean 48 days). In particular, these authors mentioned that this “population is island associated and that individuals exhibit strong site fidelity, both of which increase the susceptibility of this small population to local perturbations”. The extent to which such conclusions might also extend

to the whales which occupy the AUTECH range, in a different archipelago (and Ocean), is unknown.

2.2.3 Three dimensional data: true dive data

Only with recent technology it has been possible to obtain 3D data on animal dives. This kind of data is currently still quite expensive to obtain, and is likely to remain so for a number of years to come. The process involves several stages, from going to sea, locating the animal of interest, tagging the animal, retrieving the data and processing the data. Much of this data, especially the data with good resolution, is obtained from DTAG's (Johnson and Tyack, 2003). We will use extensively DTAG data in LATTE. The sensor suite comprises acceleration, magnetic field, and pressure sensors and is tailored to measuring information on location, orientation and sound production at sampling rates of up to 50 Hz, much higher than traditional time-depth recorders. These measures are convertible to fine resolution information on location (x, y, z) and relative animal position (heading, pitch and roll) over time (see Johnson and Tyack, 2003, for details), for usually a small number of hours. Available DTAG data sets include those described in:

1. Zimmer *et al.* (2003), for a single sperm whale
2. Johnson *et al.* (2004), for 4 beaked whales (2 *Mesoplodon densirostris* and 2 *Ziphius cavirostris*)
3. Zimmer *et al.* (2005), for 2 simultaneously tagged *Ziphius cavirostris*
4. Tyack *et al.* (2006b), for 10 beaked whales (3 *Mesoplodon densirostris* and 7 *Ziphius cavirostris*)
5. Watwood *et al.* (2006), analyzing data for 49 DTAG deployments on sperm whales
6. Ward *et al.* (2008), for a single beaked whale (the key interest here being that emitted clicks were also detected on AUTECH hydrophones)

There are instances in which one has data about (x, y, z) but not at the same time nor with good resolution (e.g. Kuhn *et al.*, 2010).

2.2.4 Dive related data

There are some examples of how one might obtain relevant dive information using bottom mounted sensors in the absence of tagged animals (e.g. Di-Marzio *et al.*, 2008). Further, development of effective and efficient detection and localization algorithms from such systems (see e.g. Adam *et al.*, 2006) might lead to additional ways to collect information on dive patterns. While this happens naturally only for sound producing species, and directly during the vocal parts of the dives, one might be able to develop models to fit to this kind of data which eventually might allow inferences about non vocal parts of the dives.

This is in fact one of the goals of LATTE, to obtain a modelling framework which allows the integration of data with different levels of resolution, from DTAG data to data collected on navy acoustic ranges.

2.3 About Houser (2006)

Being the only paper that we are aware which has explicitly described a model for 3D dives, Houser (2006) is described in additional detail here (see also Frankel *et al.* (2002), where what seems a very similar preliminary approach is taken, also involving Monte Carlo simulation of dives). Note that these concepts have been used to develop a piece of software, 3MB, to simulate the movement of marine mammals (Houser and Cross, 2009). This software documentation contains detailed information about the use of the software and reviews most of the concepts involved. The software is open source and available at http://members.cox.net/biomimetica/download_page.htm.

IMPORTANT NOTE: The following text is for most parts taken verbatim or only slightly modified from Houser (2006).

2.3.1 Model Overview

The 3MB software was specifically designed to assess the impact of sound sources on marine mammals. Hence a scenario can be chosen, animats² and sound sources distributed in space, and then exposure quantified for each animal as it moves around. The user may specify the behavior of a

²This is the name given to simulated animals within the software.

particular marine mammal species based upon current available knowledge of that species' oceanic activity.

In 3MB, movement and behavior is stochastically determined by sampling from distributions describing:

1. rates of movement in the horizontal and vertical planes
2. direction of travel
3. time at the surface between dives
4. time at depth
5. time in and transition between behavioral states³

Hence, the way a species behavior is defined is by choosing specific statistical distributions (and their respective parameters). Then one samples from these distributions to obtain parameter values used in simulation, and associated with each parameter there is also the need to define when should the parameter be “terminated” (i.e., when a new value gets sampled from the original distribution and the simulation proceeds).

Once created, species definitions are used to control a predetermined number of individuals. The location of each individual at the start of a simulation can be chosen from a random distribution (e.g. uniform in space) or user-defined. This latter approach allows expert knowledge of species distribution to be incorporated.

2.3.2 Species definition

A species is defined by distributions controlling the following processes (details regarding these can be found in the original source, but most names are self explanatory):

1. Behavioral State

³The fact that one can separately define transition probabilities and time in state puts this into the realms of semi-Markov chains. A continuous-time stochastic process is called a semi-Markov process or “Markov renewal process” if the embedded jump chain (the discrete process registering what values the process takes) is a Markov chain, and where the holding times (time between jumps) are random variables with any distribution, whose distribution function may depend on the two states between which the move is made. Verbatim from Wikipedia at http://en.wikipedia.org/wiki/Semi-Markov_process.

2. Directional Movement
3. Horizontal Speed
4. Vertical Speed
5. Diving depth
6. Reversals
7. Surface Interval

In the context of sound exposure, one can also define distributions which change once the animal is subjected to sound exposure (e.g. random movement changes to say avoidance movement once a sound is emitted).

2.3.3 Distribution model types

The way one controls the above processes is via distributions, which in 3MB can be of two types:

1. Vector Distribution Models - these models allow one to very precisely define the distributions one is sampling from, including as much detailed information as one wants. These include for example transition matrices between behavioral states (and states can in turn influence which distribution you sample from, say, values for speed).⁴
2. Alternative Distribution Models - these are essentially Uniform (one just defines the minimum and maximum) or Gaussian distributions (one just defines the mean and variance), and are used mostly when there is not enough information to parameterize vector models. In particular for bearing there are available special cases of random walks, correlated random walks and biased correlated random walks.

⁴It is not clear at this point if these do not correspond to sampling values directly from actual vectors of data, hence the name “Vector distribution models”.

2.3.4 Concluding remarks

It is recommended that the software should be used to simulate only data from relatively small periods of time, because interactions with the environment are not embedded in the models used, and hence the animals are bound to drift away. In AUTEC that would mean for example animals ending up on land. This is a general problem for simulations of animals over space, which might work relatively well in the short term, but which lead to unrealistic behavior over the long term for species with some kind of residency if there is nothing in the movement that allows the simulated animals to respect said residency.

One thing that might be interesting is, whenever we get a tentative model for movement in 3D, try to fit that model to simulated data from 3MB and see how it manages to capture the structure of the underlying models which originated the data.

As an aside, so far, our attempts to implement simulations in M3B were unsuccessful (even if just following the quick start guide). This is something that we hope to solve in the future.

3 Model components

3.1 Introduction, data available and random comments

We envisage that models will be fitted in a state-space framework, and hence it is relevant to start defining model components for the state and observation process. The DTAG data is essentially continuous in the time dimension, and at this stage it is unclear if we might want to use a “continuous-time and continuous-space” or a “discrete-time and continuous-space” framework (see McClintock *et al.*, 2012, for examples and details), although for now we assume the latter.

It is probably easier to discretize the data further than using the frequency at which we have it on DTAG’s, to avoid small scale variance which gets averaged out over longer time periods, e.g. difference between 100 data points per second to 1 data point every 10 seconds, as well as to reduce the amount of data we have to deal with, which might have a considerable influence on algorithm performance/computer efficiency. Hence, while DTAG data is collected many times per second, if movement is all we are interested in, we could probably discretize time into larger periods (e.g. 1 position every 2

minutes say, as an example, McClintock *et al.* (2012) consider time intervals of 120 minutes (with data from a single animal), so one might wonder how ambitious 2 minutes actually is!).

As stated in the introduction, the available data to fit the model to will be

- click counts at given hydrophones over time (complex data, considerably noisy due to say hydrophone specific differences⁵, and with potentially a fair proportion of false positives - if we can not reduce these to a residual amount then the observation model might have to include this component; given the recent detection and classification results presented at DCL 2010 (DiMarzio, pers. comm.), with false positives at around 3%, this might be ignored to begin with.
- DTAG data, which gives us a good handle on the diving state, providing information on time of clicks produced, depth (z), pitch (p), heading (h) and roll (r) over time, multiple times per second; note from this one might try to derive to latitude (y) and longitude (x). This data provides also information about how to connect acoustic data on the range with animals diving when there are tagged animals tracked simultaneously using range hydrophones.

We note upfront that the key lack of knowledge regarding BBW seems to be related to the way animals behave in a group, regarding a number of different components:

- within groups, fundamental to define a group acoustical footprint;
- between groups, fundamental to define animal distribution over space;
- group stability, which might be a second order problem for now (although this might deserve further thought). Some group rigidity is a

⁵I used to think that some of the observed counts differences in neighbor hydrophones were nonsense, virtually impossible given the system at hand, and hence probably hardware related. While recently reading Arranz *et al.* (2011) it became apparent that context, in particular depth and slope, might be very important, and say a hydrophone at the bottom of a suitable slope along which whales might feed could be much more insonified than another one in a less adequate-for-feeding site. It does not necessarily mean that the data must be right, but it at least provides an explanation for why it might not be wrong.

desirable working assumption, and a likely to hold assumption in particular for *Mesoplodon*, but the extent to which it might hold is not known at present.

Beaked whales seem to have distinct group behavior, and most likely dive with some type of synchronism, but hard evidence of diving synchrony is anecdotal, and in particular there is only a single instance in which two animals were simultaneously fitted with DTAG's (Zimmer *et al.*, 2005) (this was for *Ziphius*, not *Mesoplodon*). Mark Johnson provided access to a data set in which 3 sperm whales were simultaneously fitted with DTAG's, and their diving is clearly non-independent, even if not all whales participated in all deep dives (Figure 1). However, there is only so much one can say based on a sample size of 1 event for a different species. In particular the distance between these sperm whales probably means that they would be considered (visually and/or acoustically) to be individual animals (that would certainly be the case if they were to be beaked whales). Mark Johnson has some additional data sets, in particular from pilot whales, but it is hard to know what might be gained from considering these here.

3.2 Beaked whale movement

The next subsection is outdated, and in terms of behaviour states we are currently working with a system as described in Langrock *et al.* (tted). Nonetheless the material below is kept in for historical/archival reasons.

3.2.1 Behavioral state

We can consider that a single BBW might be, at any point in time, in one of two states (deep diving, or not deep diving). The transition between these occurs at any x, y location in 2D space, but at depths close to 0 by definition. The movement of BBW will likely be different in each state. Therefore we start by defining these states, which might be further divided in (sub-)states as:

1. At the surface (between the end of a deep foraging dive and the start of the next dive)

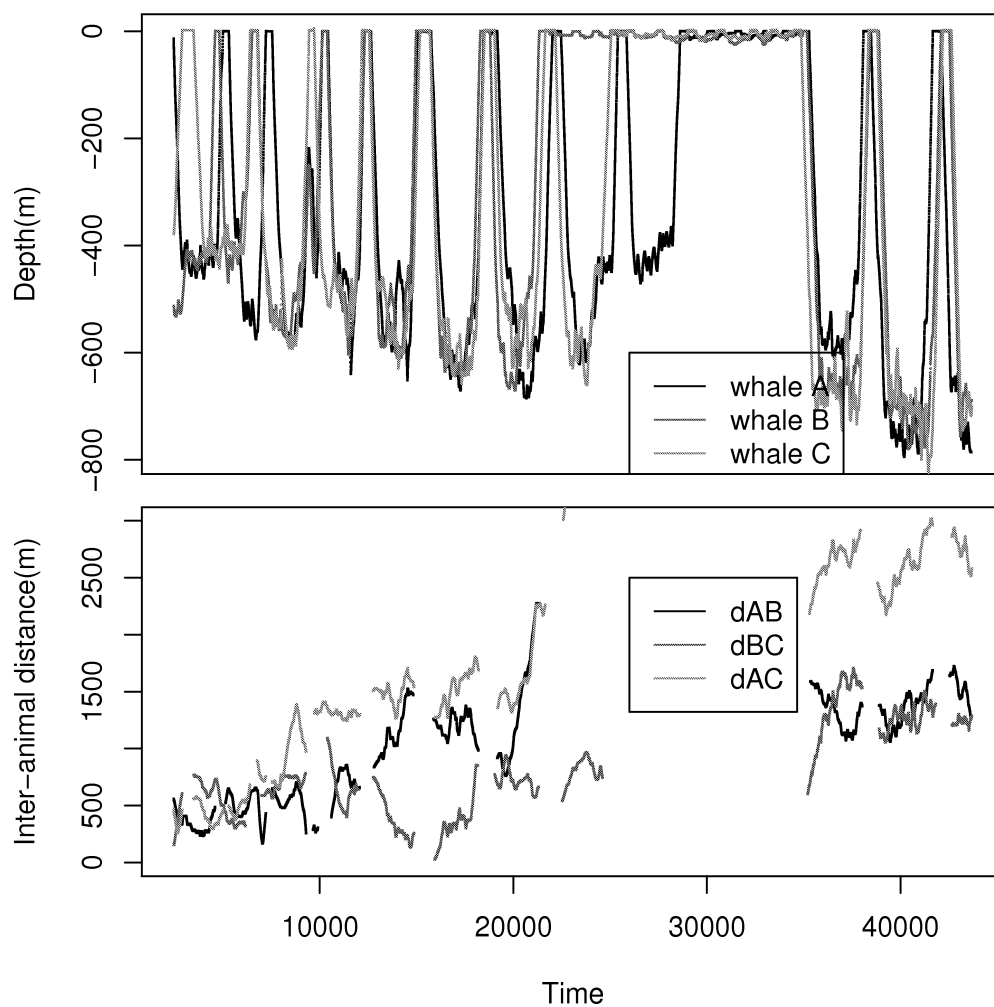


Figure 1: The depth profiles of 3 simultaneously tagged sperm whales. Some sort of dive synchrony seems clear.

- a resting
 - b performing shallow dives (we assume this ends when the animal is at the surface for the last time before reaching the point where it starts clicking)
- 2. Deep diving (from the start to the end of a deep foraging dive)
 - a descent (we assume this ends when the animal first moves up after it produced the first click)
 - b foraging (we assume this ends when the animal produced last click in a deep dive)
 - c ascent (we assume this ends when the animal reaches the surface after a deep dive)

We have relatively good knowledge from DTAGs regarding these. However, any acoustical data are only relevant for the foraging phase (2b), as that is the only time when the animals produce the echolocation clicks. This might require some additional thought, because strictly the animals might produce some clicks during the descent (2a) and ascent (2c) phases. Given that these are only conceptual states, one might alternatively define the states as

- 1. At the surface
 - a resting
 - b performing shallow dives
- 2. Deep diving
 - a silent descent
 - b vocal
 - i descent-vocal
 - ii foraging
 - iii ascent-vocal
 - c silent ascent

and then animals only produce sounds, by definition, during phase 2b. A number of points regarding these formulations are worth noting:

- irrespectively of the formulation, for the purpose of our current modeling, it might be wise to ignore (at least) what happens within stage 1 (i.e. lump 1a and 1b);
- regarding the second formulation, it is clear that DTAG acoustic data provides direct information exclusively about 2b (it might be informative about other components of the model given the links between parameters enforced by the model itself). The rest of the process could be thought about almost like a black-box, and one would only need to have a distribution to link the point in time and space where an animal stops clicking to the point where and when the animals starts clicking again;
- the distributions of variables within state 2b is less simple for the second formulation, as say the change in depth in the later state 2b is much more variable than in the previous state 2d. Hence the division presented above in additional sub-states within 2b;
- it does not make much sense to have the observation process controlling the definition of the states of the model. Hence, we might prefer to stick to the first formulation above.

The state at time t , \mathbf{S}_t , can be represented by a vector with length equal to the number of states, a 1 in the current state, and 0's in all other entries. As examples, an animal in the descent phase at time t would have $\mathbf{S}_t=(0,0,1,0,0)$, and if the animal was performing shallow dives, $\mathbf{S}_t=(0,1,0,0,0)$. The state at time t is a function of the previous state $t - 1$ according to

$$\mathbf{S}_t = \mathbf{P} \mathbf{S}_{t-1} \quad (1)$$

considering a probability transition matrix \mathbf{P} like:

$$\mathbf{P} = \begin{pmatrix} P_{1a} & P_{1b,1a} & 0 & 0 & P_{2c,2a} \\ P_{1a,1b} & P_{1b} & P_{2a,1b} & 0 & P_{2c,2b} \\ 0 & P_{1b,2a} & P_{2a} & 0 & 0 \\ 0 & 0 & P_{2a,2b} & P_{2b} & 0 \\ 0 & 0 & P_{2a,2c} & P_{2b,2c} & P_{2c} \end{pmatrix}$$

This already incorporates some logical constraints, like the fact that an animal can't go from foraging to resting or shallow diving without going

through the ascent phase. Some additional constraints might still be added, say e.g. if we assume an animal can not cancel a dive once the descent phase has started, then $P_{2a,2c} = P_{2a,1b} = 0$, or if the animal can not go back in the phase order, then,

$$\mathbf{P} = \begin{pmatrix} P_{1a} & 0 & 0 & 0 & P_{2c,2a} \\ P_{1a,1b} & P_{1b} & 0 & 0 & 0 \\ 0 & P_{1b,2a} & P_{2a} & 0 & 0 \\ 0 & 0 & P_{2a,2b} & P_{2b} & 0 \\ 0 & 0 & 0 & P_{2b,2c} & P_{2c} \end{pmatrix}$$

It seems more intuitive to model changes between states as a function of the expected time (and variance) needed to change between different states, rather than the probability of changing state at any time step. Using these, one can consider different distributions for the times in each state, while the time in a given state is an exponential random variable if all you can control is the probability of changing state at any time step. The need to relax that distributional constraint puts us into the realms of semi-Markov models (e.g. Barbu and Limnios, 2008). These are related to Markov models but for which the transition between states is not dependent on a fixed probability at every time point. Instead, the time between transition events is governed by some stochastic process which can have a variety of distributions.

Considering the latter transition matrix, we might instead consider a matrix of times within each state:

$$\mathbf{T} = \begin{pmatrix} T_{1a} & 0 & 0 & 0 & 0 \\ 0 & T_{1b} & 0 & 0 & 0 \\ 0 & 0 & T_{2a} & 0 & 0 \\ 0 & 0 & 0 & T_{2b} & 0 \\ 0 & 0 & 0 & 0 & T_{2c} \end{pmatrix}$$

and so the animal remains in a state for a period of time governed by these distributions, and then changes state using a transition matrix \mathbf{T} similar to the one we had before, but where now the probability of remaining in the same state (given a state jump is about to happen) is 0, i.e., something like

$$\mathbf{P} = \begin{pmatrix} 0 & 0 & 0 & 0 & 1 \\ 1 & 0 & 0 & 0 & 0 \\ 0 & 1 & 0 & 0 & 0 \\ 0 & 0 & 1 & 0 & 0 \\ 0 & 0 & 0 & 1 & 0 \end{pmatrix}$$

so that $S_t = \mathbf{P}S_{t-1}$ still holds.

In the above setting this makes no sense, but presumably the distribution of time in the current state could depend on the previous state.

3.2.2 Individual animal movement

Movement in 2D (x, y) is often modeled as the outcome of displacement and direction, given an initial location. Morales *et al.* (2004) used distributions for step length and turning angles. These distributions were dependent on the behavioral state, i.e., the parameter values might change for each state (state at time $t = z_t$). In Morales *et al.* (2004) the direction (turning angle ϕ) usually comes from a circular distribution, like the wrapped cauchy:

$$f(\phi|z, \mu_z, \rho_z) = \frac{1}{2\pi} \frac{1 - \rho_z^2}{1 + \rho_z^2 - 2\rho_z \cos(\phi - \mu_z)} \quad (2)$$

where μ_z represents the mean direction of movement, and ρ_z represents the variance with respect to the mean, while displacement (d) is modeled considering an heavy tail Weibull distribution

$$f(d|z, a_z, b_z) = \frac{b_z}{a_z} \left\{ \frac{s}{a_z} \right\}^{b_z-1} \exp\left\{ -\left(\frac{s}{a_z} \right)^{b_z} \right\} \quad (3)$$

where $a_z, b_z > 0$, $0 < \phi_z < 2\pi$ (an angle) and $0 < \rho < 1$ (a correlation).

Here we might do something similar, but in which the direction comes from a spherical distribution. The displacement in the horizontal plane x, y and displacement in depth z might be quite different, so we could consider different simulation approaches to move from $l_t = (x_t, y_t, z_t)$ to $l_{t+1} = (x_{t+1}, y_{t+1}, z_{t+1})$. As examples one might:

- sample to deal with the displacement in x, y only, using models like those of Morales *et al.* (2004), and then sample a change in depth from

a suitable distribution (say a gamma)⁶, or

- sample a 3D direction from a spherical distribution (or in practice a circular distribution for “longitude” and a suitable distribution (say a re-scaled beta) for “latitude”) and then sample (from say a Gamma or Weibull) either:

- the displacement in 3D

$$\Delta(x, y, z) = \sqrt{(x_{t+1} - x_t)^2 + (y_{t+1} - y_t)^2 + (z_{t+1} - z_t)^2}$$

- displacement in 2D

$$\Delta(x, y) = \sqrt{(x_{t+1} - x_t)^2 + (y_{t+1} - y_t)^2}$$

- change in depth

$$\Delta(z) = (z_{t+1} - z_t)$$

The angular central Gaussian distribution might be a suitable candidate for the 3D direction, although it has symmetry assumptions which might not hold here (see e.g. Tyler, 1987, for details).

3.2.3 Group movement

As stated above, a key issue relates to the fact that the DTAG data available gives us a reasonable handle on individual animal movement, but not on the correlation between the movement of animals in the same group over time.

In Marques and Thomas (2008a) we considered two random walks, one for the center of the group (with some variance σ_g), the other for the individual animals given its location with respect to the center of the group (with some variance $\sigma_i \ll \sigma_g$), but really one might want some attraction/repulsion effect rather than random walk movement. As an example, one might start a dive close to the position defining the center of the group, be on a random walk while in the descent and foraging phase, and then do the ascending in a biased random walk, biased towards the center of the group. Structure in the descent and foraging phases is also more likely than simple random

⁶But note that in fact the change in depth is likely correlated with displacement, in the sense that a large displacement in x,y is likely associated with a small displacement in depth, and vice versa.

movement. Something that requires some thought is that the position of the group (which is just an abstract construct, but probably useful for simulation) changes over time, and so the attraction/repulsion behaviors would have to be occurring towards points changing over time.

The formulation in McClintock *et al.* (2012), namely regarding the way to parameterize biased random walks, might be useful here, as one might imagine the center of the group as the “center of attraction” (using the wording of McClintock *et al.* (2012)) in the end of a foraging period (2b), and the “center of repulsion” at the beginning of the foraging period (2b), although as stated above, these centers of attraction/repulsion might change over time. This will mean that instead of having one potentially latent variable for the location of the “center”, there might be as many latent variables as time periods, which seems a complication to avoid. On the other hand that if movement of the animals is independent of movement of the group one can conceptually consider the movement of the animals with respect to the center of the group as being referenced to a fixed center of a group, which is then displaced according to the individual animal movement model.

3.3 Sound production and detection

Compared with the status of the knowledge about movement, individual BBW sound production and sound detection, in particular at AUTECH, are relatively well known. Regarding sound characteristics and sound production, a number of references provide useful information:

- Johnson *et al.* (2004), showing that *Z. cavirostris* and *M. densirostris* are highly vocal, producing high-frequency echolocation clicks above the range of human hearing
- Madsen *et al.* (2005), which describe the way in which the clicks are used for echolocation
- Zimmer *et al.* (2005), reporting “...source characteristics of *Ziphius* echolocation clicks using the novel approach of two tagged whales recording each other...” and “...the first estimates of the source level, directivity index, and spectral properties of *Ziphius* clicks, which are shown to differ significantly from those produced by non-ziphiid toothed whales described so far, suggesting a strong potential for passive acoustic monitoring...”

- Johnson *et al.* (2006) look at characteristics of *Mesoplodon* clicks, reporting that “...Blainville’s beaked whales produce two distinct click types associated with different phases of echolocation-mediated foraging”, and that “the unusual properties of FM search clicks may facilitate passive acoustic detection of *Mesoplodon*...”.
- Tyack *et al.* (2006a) deals with “Acoustic behavior of beaked whales, with implications for acoustic monitoring”, a self explanatory name.

Regarding click detection, there have been a number of references characterizing this process:

- Zimmer *et al.* (2008) looks at dive detection, building on individual click detection. The setting is not AUTECH, dealing with detections at hydrophones close to the surface in an environment noisier than AUTECH;
- in the process of estimating whale density, Marques *et al.* (2009) estimated the probability of detecting BBW clicks at AUTECH hydrophones as a function of distance (and off axis angles), using sounds produced at known locations (via DTAG’s) and subsequently detected or not at surrounding hydrophones to estimate a detection function via a GAM based logistic regression approach;
- Kusel *et al.* (2011) considered a single hydrophone and sound propagation models to estimate the same detection function. Some differences exist between these two and this later reference presents possible explanations for this.

References

- Adam, O., Motsch, J.-F., Desharnais, F., DiMarzio, N., Gillespie, D., and Gisiner, R. C. (2006). Overview of the 2005 workshop on detection and localization of marine mammals using passive acoustics. *Applied Acoustics*, **67**, 1061–1070.
- Arranz, P., de Soto, N. A., Madsen, P. T., Brito, A., Bordes, F., and Johnson, M. P. (2011). Following a foraging fish-finder: Diel habitat use of blainville’s beaked whales revealed by echolocation. *PLoS ONE*, **6**, e28353.

- Bailleul, F., Pinaud, D., Hindell, M., Charrassin, J.-B., and Guinet, C. (2008). Assessment of scale-dependent foraging behaviour in southern elephant seals incorporating the vertical dimension: a development of the first passage time method. *Journal of Animal Ecology*, **77**, 948–957.
- Baird, R. W., Webster, D. L., McSweeney, D. J., Ligon, A. D., Schorr, G. S., and Barlow, J. (2006). Diving behavior of Cuvier’s (*Ziphius cavirostris*) and Blainville’s beaked whales (*Mesoplodon densirostris*) in Hawai’i. *Canadian Journal of Zoology*, **84**, 1220–1228.
- Baird, R. W., Webster, D. L., Schorr, G. S., Mcsweeney, D. J., and Barlow, J. (2008). Diel variation in beaked whale diving behavior. *Marine Mammal Science*, **24**, 630–642.
- Barbu, V. S. and Limnios, N. (2008). *Semi-Markov Chains and Hidden Semi-Markov Models toward Applications: Their Use in Reliability and DNA Analysis*. Springer.
- Chilvers, B. L., Delean, S., Gales, N. J., Holley, D. K., Lawler, I. R., Marsh, H., and Preen, A. R. (2004). Diving behaviour of dugongs, *Dugong dugon*. *Journal of Experimental Marine Biology and Ecology*, **304**(2), 203 – 224.
- DiMarzio, N., Moretti, D., Ward, J., Morrissey, R., Jarvis, S., Izzi, A. M., Johnson, M., Tyack, P., and Hansen, A. (2008). Passive acoustic measurement of dive vocal behavior and group size of Blainville’s beaked whale (*Mesoplodon densirostris*) in the Tongue of the Ocean (TOTO). *Canadian Acoustics*, **36**, 166–173.
- Dowd, M. and Joy, R. (2011). Estimating behavioral parameters in animal movement models using a state-augmented particle filter. *Ecology*, **92**, 568–575.
- Dray, S., Royer-Carenzi, M., and Calenge, C. (2010). The exploratory analysis of autocorrelation in animal-movement studies. *Ecological Research*, **25**, 673–681. 10.1007/s11284-010-0701-7.
- Frankel, A. S., Ellison, W. T., and J. Buchanan, J. (2002). Application of the acoustic integration model (aim) to predict and minimize environmental impacts. In *Proc. Oceans 2002*, pages 1438–1443.

- Halsey, L., Woakes, A., and Butler, P. (2003). Testing optimal foraging models for air-breathing divers. *Animal Behaviour*, **65**, 641 – 653.
- Hays, G. C., Houghton, J. D. R., Isaacs, C., King, R. S., Lloyd, C., and Lovell, P. (2004). First records of oceanic dive profiles for leatherback turtles, *dermochelys coriacea*, indicate behavioural plasticity associated with long-distance migration. *Animal Behaviour*, **67**(4), 733 – 743.
- Heath, J. P., Gilchrist, H. G., and Ydenberg, R. C. (2007). Can dive cycle models predict patterns of foraging behaviour? diving by common eiders in an arctic polynya. *Animal Behaviour*, **73**(5), 877 – 884.
- Higgs, M. D. and Ver Hoef, J. M. (2012). Discretized and aggregated: Modeling dive depth of harbor seals from ordered categorical data with temporal autocorrelation. *Biometrics*, **68**, 965–974.
- Houser, D. S. (2006). A method for modeling marine mammal movement and behavior for environmental impact assessment. *IEEE Journal Of Oceanic Engineering*, **31**, 76–81.
- Houser, D. S. and Cross, M. J. (2009). *Marine Mammal Movement and Behavior (3MB) - A Component of the Effects of Sound on the Marine Environment (ESME) Distributed Model*. BIOMIMETICA.
- Johnson, M., Madsen, P. T., Zimmer, W. M. X., de Soto, N. A., and Tyack, P. L. (2004). Beaked whales echolocate on prey. *Proc. R. Soc. Lond. B (Suppl.)*, **271**, S383–S386.
- Johnson, M., Madsen, P. T., Zimmer, W. M. X., de Soto, N. A., and Tyack, P. L. (2006). Foraging Blainville’s beaked whales (*Mesoplodon densirostris*) produce distinct click types matched to different phases of echolocation. *The Journal of Experimental Biology*, **209**, 5038–5050.
- Johnson, M. P. and Tyack, P. L. (2003). A digital acoustic recording tag for measuring the response of wild marine mammals to sound. *IEEE Journal Of Oceanic Engineering*, **28**, 3–12.
- Jonsen, I. D., Flemming, J. M., and Myers, R. A. (2005). Robust state-space modeling of animal movement data. *Ecology*, **86**, 2874–2880.

- Jonsen, I. D., Myers, R. A., and James, M. C. (2007). Identifying leatherback turtle foraging behaviour from satellite telemetry using a switching state-space model. *Marine Ecology Progress Series*, **337**, 255–264.
- Kuhn, C. E., Tremblay, Y., Ream, R. R., and Gelatt, T. S. (2010). Coupling gps tracking with dive behavior to examine the relationship between foraging strategy and fine-scale movements of northern fur seals. *Endangered Species Research*, **12**, 125–139.
- Kusel, E. T., Mellinger, D. K., Thomas, L., Marques, T. A., Moretti, D., and Ward, J. (2011). Cetacean population density estimation from single fixed sensors using passive acoustics. *The Journal of the Acoustical Society of America*, **129**, 3610–3622.
- Langrock, R., Marques, T. A., Thomas, L., and Baird, R. (submitted). Modeling the diving behavior of whales: a latent-variable approach with feedback and semi-markovian components. *Journal of Agricultural, Biological, and Environmental Statistics*.
- Lett, C. and Mirabet, V. (2008). Modelling the dynamics of animal groups in motion. *South African Journal of Science*, **104**, 192–198.
- Lukeman, R. J. (2009). *Modeling Collective Motion in Animal Groups: from Mathematical Analysis to Field Data*. Ph.D. thesis, The University Of British Columbia.
- Madsen, P. T., Johnson, M., de Soto, N. A., Zimmer, W. M. X., and Tyack, P. (2005). Biosonar performance of foraging beaked whales (*Mesoplodon densirostris*). *The Journal of Experimental Biology*, **208**, 181–194.
- Marques, T. A. and Thomas, L. (2008a). Explaining the code for the simulation of click count vectors. Technical report, DECAF internal report.
- Marques, T. A. and Thomas, L. (2008b). Some ideas about simulating beaked whale dives. Technical report, DECAF internal report.
- Marques, T. A., Thomas, L., Ward, J., DiMarzio, N., and Tyack, P. L. (2009). Estimating cetacean population density using fixed passive acoustic sensors: an example with Blainville’s beaked whales. *The Journal of the Acoustical Society of America*, **125**, 1982–1994.

- McCarthy, E., Moretti, D., Thomas, L., DiMarzio, N., Morrissey, R., Jarvis, S., Ward, J., Izzi, A., and Dilley, A. (2011). Changes in spatial and temporal distribution and vocal behavior of blainville's beaked whales (*Mesoplodon densirostris*) during multiship exercises with mid-frequency sonar. *Marine Mammal Science*, **27**, E206–E226.
- McClintock, B. T., King, R., Thomas, L., Matthiopoulos, J., McConnell, B. J., and Morales, J. M. (2012). A general modeling framework for animal movement and migration using multi-state random walks. *Ecological Monographs*, **82**, 335–349.
- Morales, J. M., Haydon, D. T., Frair, J., Holsinger, K. E., and Fryxell, J. M. (2004). Extracting more out of relocation data: building movement models as mixtures of random walks. *Ecology*, **85**, 2436–2445.
- Morales, J. M., Moorcroft, P. R., Matthiopoulos, J., Frair, J. L., Kie, J. G., Powell, R. A., Merrill, E. H., and Haydon, D. T. (2010). Building the bridge between animal movement and population dynamics. *Philosophical Transactions of the Royal Society B: Biological Sciences*, **365**(1550), 2289–2301.
- Myers, A. E., Lovell, P., and Hays, G. C. (2006). Tools for studying animal behaviour: validation of dive profiles relayed via the argos satellite system. *Animal Behaviour*, **71**, 989–993.
- Okamura, H., Minamikawa, S., and Kitakado, T. (2006). Effect of surfacing patterns on abundance estimates of long-diving animals. *Fisheries Science*, **72**, 631–638.
- Patterson, T. A., Thomas, L., Wilcox, C., Ovaskainen, O., and Matthiopoulos, J. (2008). State-space models of individual animal movement. *Trends in Ecology and Evolution*, **23**, 87–94.
- Photopoulou, T. (2012). *Diving and depth use in seals inferences from telemetry data using regression and random walk movement models*. Ph.D. thesis, University of St Andrews.
- Schick, R. S., Loarie, S. R., Colchero, F., Best, B. D., Boustany, A., Conde, D. A., Halpin, P. N., Joppa, L. N., McClellan, C. M., and Clark, J. S. (2008). Understanding movement data and movement processes: current and emerging directions. *Ecology Letters*, **11**, 1338–1350.

- Schorr, G. S., Baird, R. W., Hanson, M. B., Webster, D. L., McSweeney, D. J., and Andrews, R. D. (2009). Movements of satellite-tagged blainville's beaked whales off the island of hawai'i. *Endangered Species Research*, **10**, 203–213.
- Smouse, P. E., Focardi, S., Moorcroft, P. R., Kie, J. G., Forester, J. D., and Morales, J. M. (2010). Stochastic modelling of animal movement. *Philosophical Transactions of the Royal Society B: Biological Sciences*, **365**(1550), 2201–2211.
- Struve, J., Lorenzen, K., Blanchard, J., Borger, L., Bunnefeld, N., Edwards, C., Hortal, J., MacCall, A., Matthiopoulos, J., Van Moorter, B., Ozgul, A., Royer, F., Singh, N., Yesson, C., and Bernard, R. (2010). Lost in space? Searching for directions in the spatial modelling of individuals, populations and species ranges. *Biology Letters*.
- Tomkiewicz, S. M., Fuller, M. R., Kie, J. G., and Bates, K. K. (2010). Global positioning system and associated technologies in animal behaviour and ecological research. *Philosophical Transactions of the Royal Society B: Biological Sciences*, **365**(1550), 2163–2176.
- Tremblay, Y., Robinson, P. W., and Costa, D. P. (2009). A parsimonious approach to modeling animal movement data. *PLoS ONE*, **4**(3), e4711.
- Tyack, P. L., Johnson, P., Zimmer, W. M., Aguilar de Soto, N., and Madsen, P. T. (2006a). Acoustic behavior of beaked whales, with implications for acoustic monitoring. *IEEE Oceans Conference Proceedings*, pages 1–6.
- Tyack, P. L., Johnson, M., Soto, N. A., Sturlese, A., and Madsen, P. T. (2006b). Extreme diving of beaked whales. *Journal of Experimental Biology*, **209**(21), 4238–4253.
- Tyack, P. L., Zimmer, W. M. X., Moretti, D., Southall, B. L., Claridge, D. E., Durban, J. W., Clark, C. W., D'Amico, A., DiMarzio, N., Jarvis, S., McCarthy, E., Morrissey, R., Ward, J., and Boyd, I. L. (2011). Beaked whales respond to simulated and actual navy sonar. *PLoS ONE*, **6**, e17009.
- Tyler, D. E. (1987). Statistical analysis for the angular central gaussian distribution on the sphere. *Biometrika*, **74**, 579–589.

- Walker, C. G., MacKenzie, M. L., Donovan, C. R., Kidney, D., Quick, N. J., and Hastie, G. D. (2011). Classification of animal dive tracks via automatic landmarking, principal components analysis and clustering. *Ecosphere*, **2**, art92.
- Ward, J., Morrissey, R., Moretti, D., DiMarzio, N., Jarvis, S., Johnson, M., Tyack, P., and White, C. (2008). Passive acoustic detection and localization of *Mesoplodon densirostris* (Blainville's beaked whale) vocalizations using distributed bottom-mounted hydrophones in conjunction with a digital tag (DTag) recording. *Canadian Acoustics*, **36**, 60–66.
- Watkins, W. A., Daher, M. A., Dimarzio, N. A., Samuels, A., Wartzok, D., Fristrup, K. M., Howey, P. W., and Maiefski, R. R. (2002). Sperm whale dives tracked by radio tag telemetry. *Marine Mammal Science*, **18**(1), 55–68.
- Watwood, S. L., Miller, P. J. O., Johnson, M., Madsen, P. T., and Tyack, P. L. (2006). Deep-diving foraging behaviour of sperm whales (*Physeter macrocephalus*). *Journal of Animal Ecology*, **75**(3), 814–825.
- Zimmer, W. M., Harwood, J., Tyack, P. L., Johnson, M. P., and Madsen, P. T. (2008). Passive acoustic detection of deep diving beaked whales. *The Journal of the Acoustical Society of America*, **124**, 2823–2832.
- Zimmer, W. M. X., Johnson, M. P., D'Amico, A., and Tyack, P. L. (2003). Combining data from a multisensor tag and passive sonar to determine the diving behavior of a sperm whale (*Physeter macrocephalus*). *IEEE Journal Of Oceanic Engineering*, **28**, 13–28.
- Zimmer, W. M. X., Johnson, M. P., Madsen, P. T., and Tyack, P. L. (2005). Echolocation clicks of free-ranging Cuvier's beaked whales (*Ziphius cavirostris*). *The Journal of the Acoustical Society of America*, **117**, 3919–3927.

Implementing a SSM to obtain pseudo-tracks and georeferenced track from DTAG data: an application to Md248b

LATTE WORKING DOCUMENT

Tiago A. Marques & Len Thomas

Centre for Research into Ecological and Environmental Modelling
The Observatory, University of St Andrews, St Andrews, KY16 9LZ, Scotland

Version's date: 14 de Novembro de 2013

Conteúdo

1	Introduction	2
2	Data details	3
3	Exploratory Data analysis	4
3.1	Characterizing distributions within states	7
4	Dead-reckoning	11
4.1	Dead-reckoning using a naive speed estimate	11
4.2	Dead-reckoning using Kalman filter speed estimates	16
4.2.1	Using MJ code	16
4.2.2	Migrating MJ code to R	19
4.3	Including latitude and longitude as states	22
5	Georeferentiation of dives	23
6	Improving the entire process	24
	References	25

1 Introduction

This document contains the analysis of the data from the whale md07_248b, with the end game being obtaining the best possible track reconstruction from all the available information.

Another objective of this exercise is to explore and get familiar with all the data sets that correspond to a single whale, namely

- the click time data
- the prh data
- the tag-on data (time and location)
- the TDOA interpolation locations ¹
- the georeferenced track locations

Additional details about the data sets are presented in section 2. We then proceed with an exploratory data analysis (section 3), which has a dedicated subsection to look at the distributions of different relevant variables in the different behavioral modes (see Marques and Thomas (2012a) for details about these behavioral modes).

Once that is accomplished, we will try to recreate what was done before by others, namely Jessica Ward, Charlie White and Mark Johnson, in terms of estimating pseudo-tracks (section 4).

Finally, we will address the georeferencing stage, by developing and fit a simple state space model to this data to obtain a track in an alternative framework (section 5).

We wrap up in section 6 by listing a number of possible extensions to the work presented.

The document Marques and Thomas (2012b) constitutes mandatory reading to fully understand what is being implemented here, and includes detailed descriptions of:

- the movement model considered and the state space model formulation used;

¹Note that here we could go one step before and work directly with the times of arrival (TOA), then building a likelihood for the location of the animal given the TOA's

- the Kalman Filter code that was developed by MJ and which we leverage extensively here;
- the existing procedure to georeference tracks prior to this effort.

2 Data details

A number of data sets need to be combined and cross-referenced. These include:

- *Md248b_Dive2_xygeoref.mat*, *Md248b_Dive3_xygeoref.mat* and *Md248b_Dive4_xygeoref.mat*: georeferenced locations. These were exported as txt and then read into R. Note that I also had georeferenced locations used in Marques *et al.* (2009), and I exported these from workspace *gxestimate2.RData* to use here, as files *geomd248b2.txt*, *geomd248b3.txt*, *geomd248b4.txt*.
- *Md248b_Dive2_localize_interp.mat*, *Md248b_Dive3_localize_interp.mat* and *Md248b_Dive4_localize_interp.mat*: localization files based on TDOA analysis.
- *Md248btagonXY*: the location at which the tag started recording. This matches up with the first record in the prh files
- *md07_248b_click_data.txt*: times of each click produced by the tagged whale
- *md07_248bprh.mat*: these files contain 4 columns², pitch heading roll and depth files sampled at 5 Hz. I also have a separate old *md07_248b_click_data.txt* which has data at a 1 Hz.
- *HYDtable.txt* - relevant hydrophone information

Note some of these might not be currently used, and so they can either be in this report subfolder “datfiles” or in a separate mother folder “georeferencing DTAG tracks”.

² Actually more, including accelerometer and magnetometer data, but we ignore these here

3 Exploratory Data analysis

All relevant data files were initially read into R. We begin by reading in the hydrophone data.

The click times and positional prh data (1 Hz) were stored in objects `cli248b` and `sec248b`, respectively.

```
> cli248b<-read.table("datfiles/md07_248b_click_data.txt")
> sec248b<-read.table("datfiles/md07_248b_sec_data.txt")
> #note this code chunk is not evaluated to speed up report generation
> #adding appropriate headings
> names(cli248b)<-c("cli", "z", "h", "p")
> names(sec248b)<-c("sec", "z", "h", "p")
```

To get a first feel for the data we plotted the dive profiles (with click events), the heading and pitch through time (Figure 1). The first thing worth noting is that the sound data is not as long as the positional data ³, which covers more dives than the sound data. This is clear from the presence of deep dives for which click events are not available. For md248b, while we have click data for 4 dives there are 5 full deep dives with positional data. Note that for some reason only dives 2 to 4 were georeferenced.

There was also some positional prh data available at a finer sampling scale (5 Hz), which was separately read in and stored in object `md07_248b`. Note however that this file includes more data than what was present in the previous files. From the previous file, we know that the tag only worked for about 63396 seconds, and so we remove from these data sets all records after that time point. I seem to remember that Jessica Ward told me that there were issues with the data after that period.

We can obtain the geo-referenced files as were used in the Marques *et al.* (2009). Additionally, we can use the geo-referenced files sent by JW. Note in particular that for whale mdd07_248b the first dive was not used in Marques *et al.* (2009), because the raw sound files were not available. Nonetheless, JW sent us a geo-referenced file for that dive based on FFT archived detections.

We can take a look at the location of the hydrophones within the AUTECH range as well as the location of the tracks for our whale (Figure 3).

³ Presumably due to lack of memory on the DTag

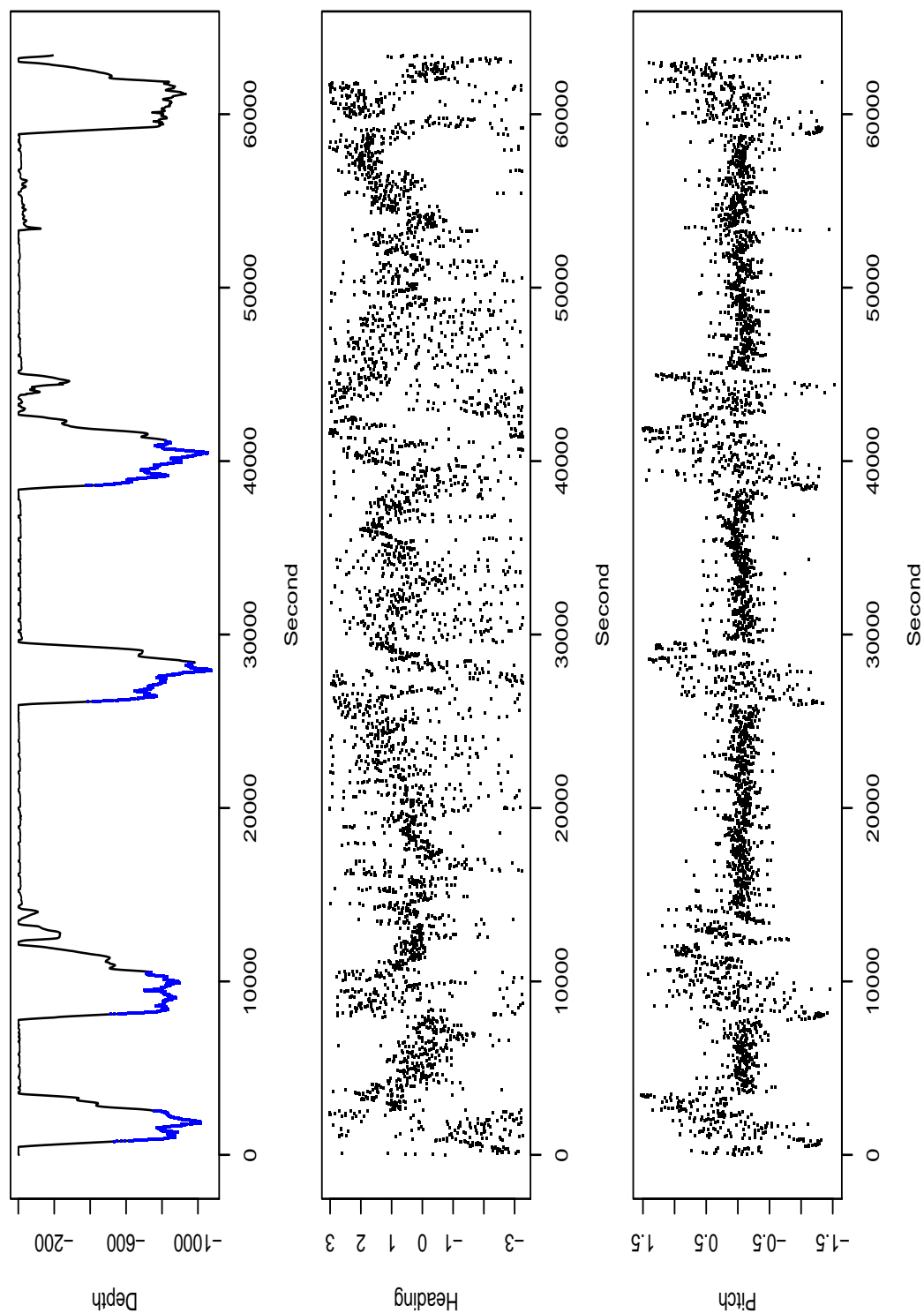


Figure 1: The dive profile (top), heading per second (center) and pitch per second (bottom) for whale 248b. On the top panel blue indicates depth at click event. Note that sound recording is only available for part of the total DTag period. Data is subsampled for keeping figure size low.

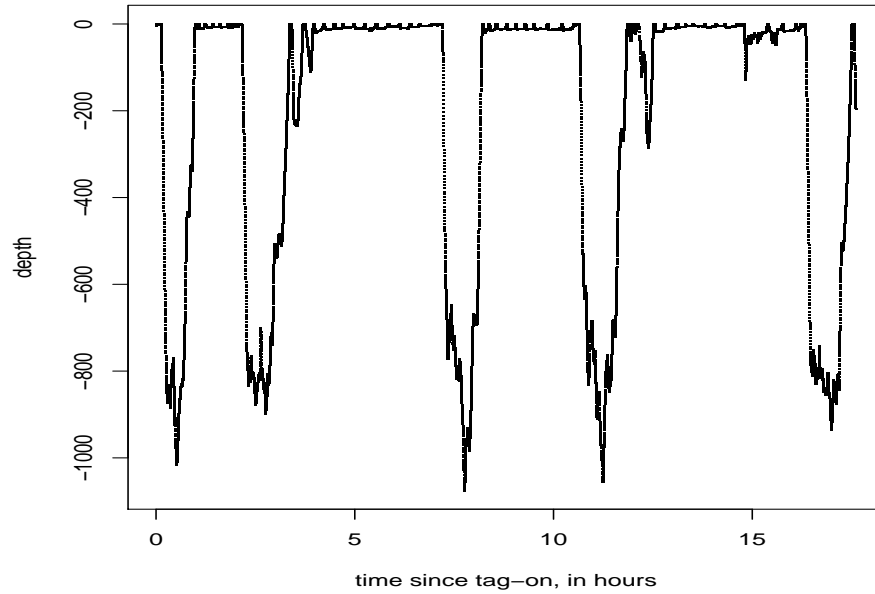


Figure 2: Depth profile for data recorded at 5 Hz.

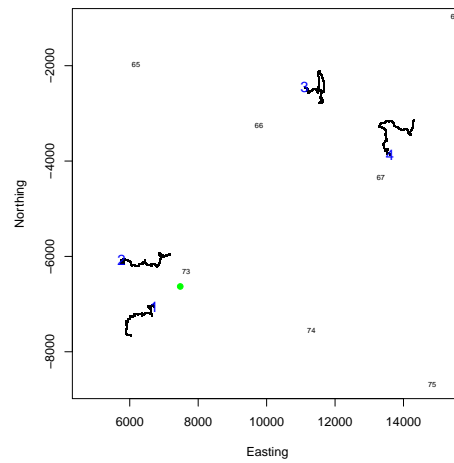


Figure 3: The AUTECH range, focussing on the hydrophones locations for which we have data, each represented by its number. The dive locations (after geo-referencing) are shown. The beginning of the dive is indicated by with the corresponding dive number. The solid green dot represents the the tag on location.

3.1 Characterizing distributions within states

We consider here the states described in Marques and Thomas (2012a), i.e.

1. At the surface
 - a resting
 - b performing shallow dives
2. Deep diving
 - a silent descent
 - b vocal
 - i descent-vocal
 - ii foraging
 - iii ascent-vocal
 - c silent ascent

Note that, for simulation, it is not simple to define changes in sub-states within state 2b.

Further we currently lump states 1a and 1b, just because there seems to be little gain in not doing so, and doing so would in fact require we manage to divide them based on the current data, which is not that simple.

Here we would like to look at the distribution of relevant variables (and their differences, i.e. displacements), namely 2D and 3D displacement, depth, pitch, heading, as a function of the state the animal is in. However, we do not have direct access to those related to x, y coordinates outside of the periods for which the animals was geo-referenced, i.e., outside the clicking periods.

First, we begin by defining the exact second each one the phases begins (and ends). This information is depicted visually in figure 5. We can then use that information to plot depth, heading and pitch as a function of the phase of the dive (Figure 6). We can clearly see that the deepest locations are recorded during phase 2b, and the shallowest in phase 1, a direct consequence of the way one distinguishes the phases of a dive. As expected, heading seems to be the variable less dependent on the phase. And extreme pitch is clearly associated with the descent and ascent phases, with mean pitch close to 0 in the surface (stage 1) and foraging stages (stage 2b).

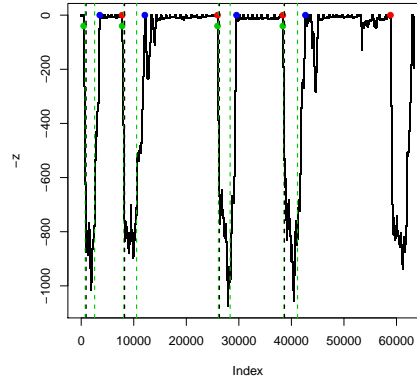


Figure 4: The dive profile for whale 248b. Note the green dots represent the start of a dive cycle, the red dots the end of a dive cycle, the blue dots the arrival back at the surface after a deep dive, and the green dashed vertical lines represent the first and last click in each dive (i.e. the start and end of phase 2b).

Unfortunately, at this stage, we do not have “reliable” data on x, y coordinates when the animal is not on the foraging (i.e. vocal) phase 2b. But nonetheless we can try to look at the coordinates from the dead-reckoning track, to see if that contains useful information.

We can look at histograms of the information about horizontal displacement and displacement in depth (Figures 8 and 9). Modeling these distributions, coupled with a uniform distribution for heading, might allow the simulation of dives. However, the problem is that these plots completely ignore potential temporal correlation in the data, which is actually severe, as can be seen from the next plots, showing the temporal autocorrelation in these variables as a function of dive phase (Figure 10). Note in particular that for heading, while a uniform might be adequate, there is also strong temporal autocorrelation (Figure 11), and hence sampling independent values from a uniform would lead to totally unrealistic simulated dives. Note that clearly these 4 dives from a single whale do not contain the amount of information one might expect, as the expected uniform distribution of headings, irrespective of the dive phase, is not really observed here.

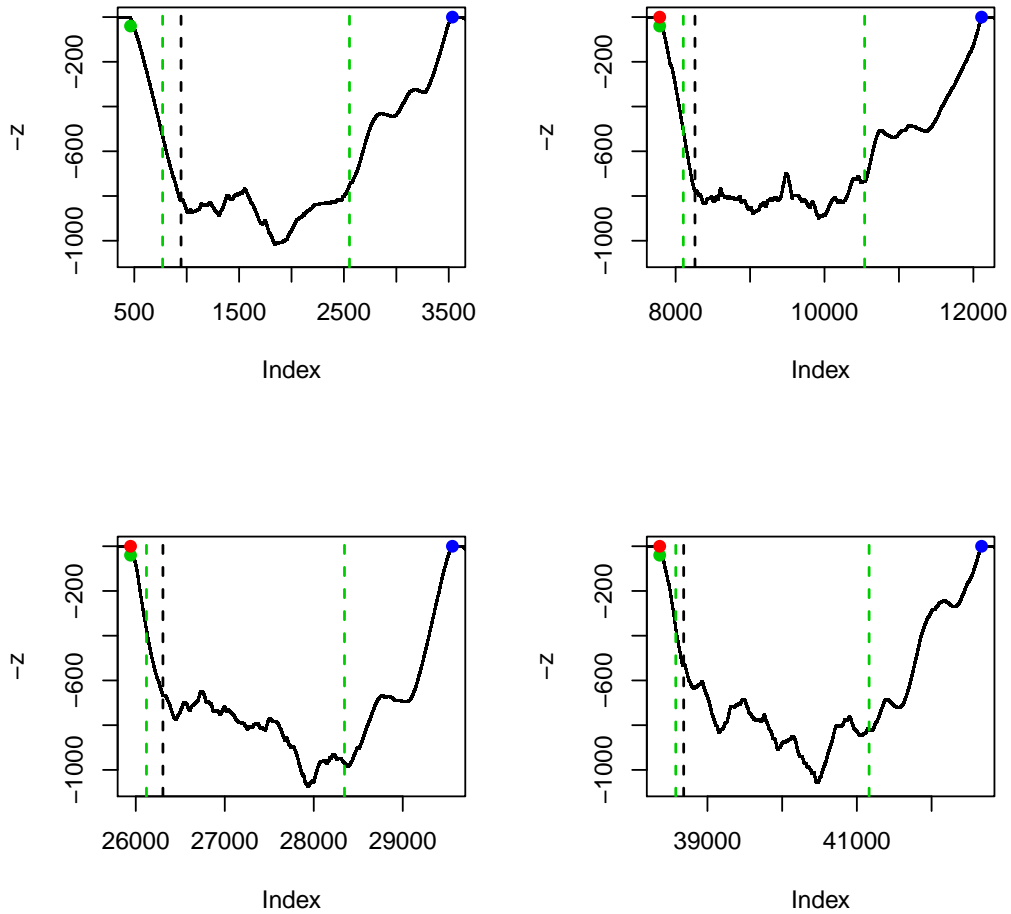


Figure 5: Individual deep dives profiles. Note the green dots represent the start of a dive cycle, the red dots the end of a dive cycle, the blue dots the arrival back at the surface after a deep dive, and the green dashed vertical lines represent the first and last click in each dive (i.e. the start and end of phase 2b). The black dashed line represents the start of the “foraging phase”.

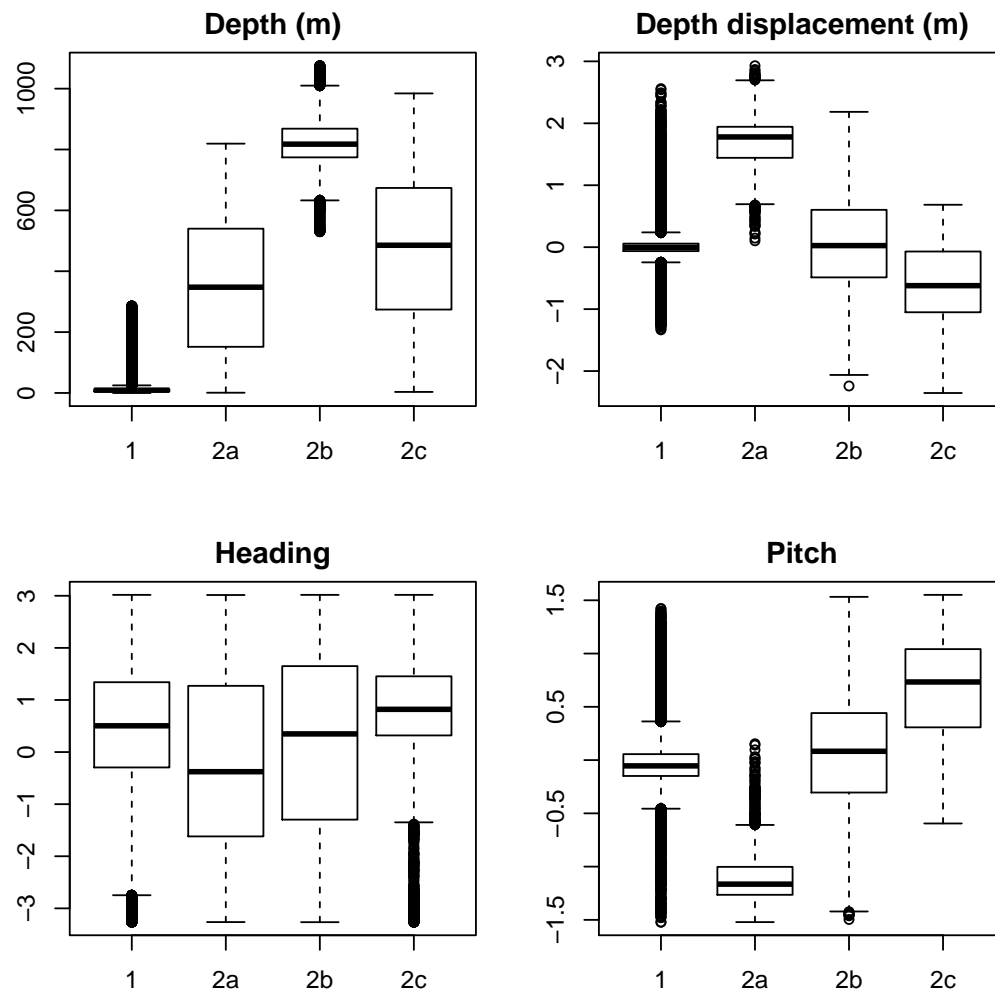


Figura 6: The distribution of depth, heading and pitch as a function of the phase of the dive.

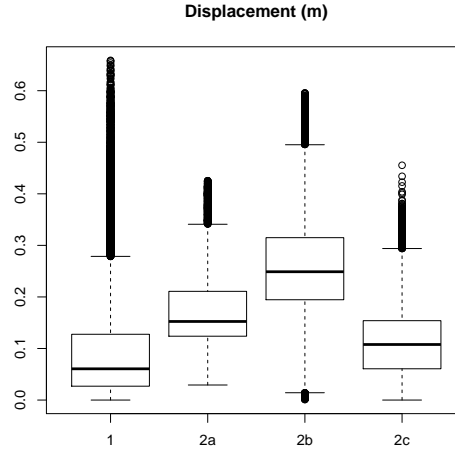


Figure 7: The distribution of 2D displacement as a function of the phase of the dive.

4 Dead-reckoning

Here we present two attempts at dead-reckoning the whale track. In section 4.1 we consider a quick-and-dirty approach, based on a single average speed, obtained from the initial section of the tagging period. Then in section 4.2 we build on that using a state space model fitted using a Kalman filter to estimate a vector of whale speeds using depth and pitch recorded from the DTag, and then use these speed estimates in a similar way to that presented in section 4.1 to predict the whale position over time.

4.1 Dead-reckoning using a naive speed estimate

We can calculate a mean (horizontal) velocity by dividing the distance between the tag-on position and the first click location by the elapsed time interval. This leads to an average speed of 3.61 km per hour. This can be used with the information in the prh file, coupled with the tag on location, to estimate the animal track via dead-reckoning.

The dead-reckoning track is shown in figure 12. It seems like the speed of the whale in the x, y plane was considerably overestimated, as in this

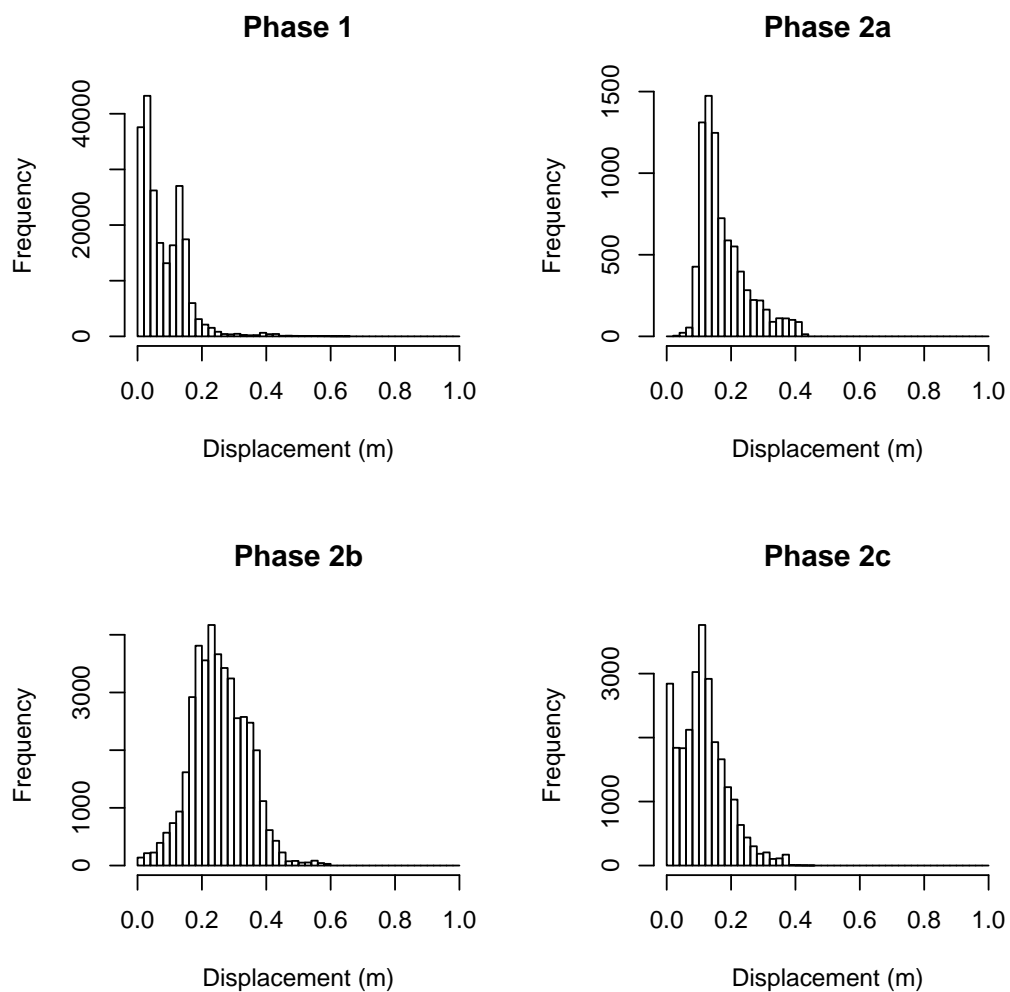


Figure 8: Histograms of 2D displacement as a function of the phase of the dive.

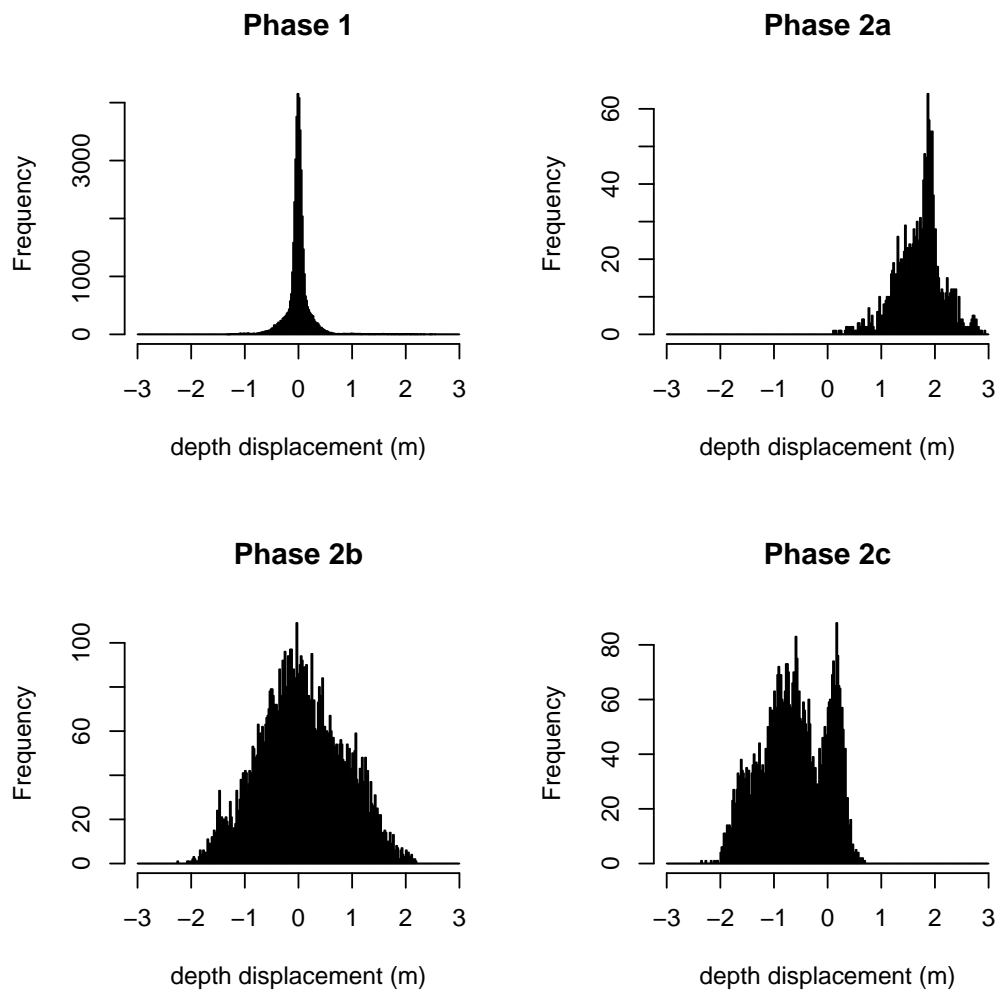


Figure 9: Histograms of depth displacement as a function of the phase of the dive.

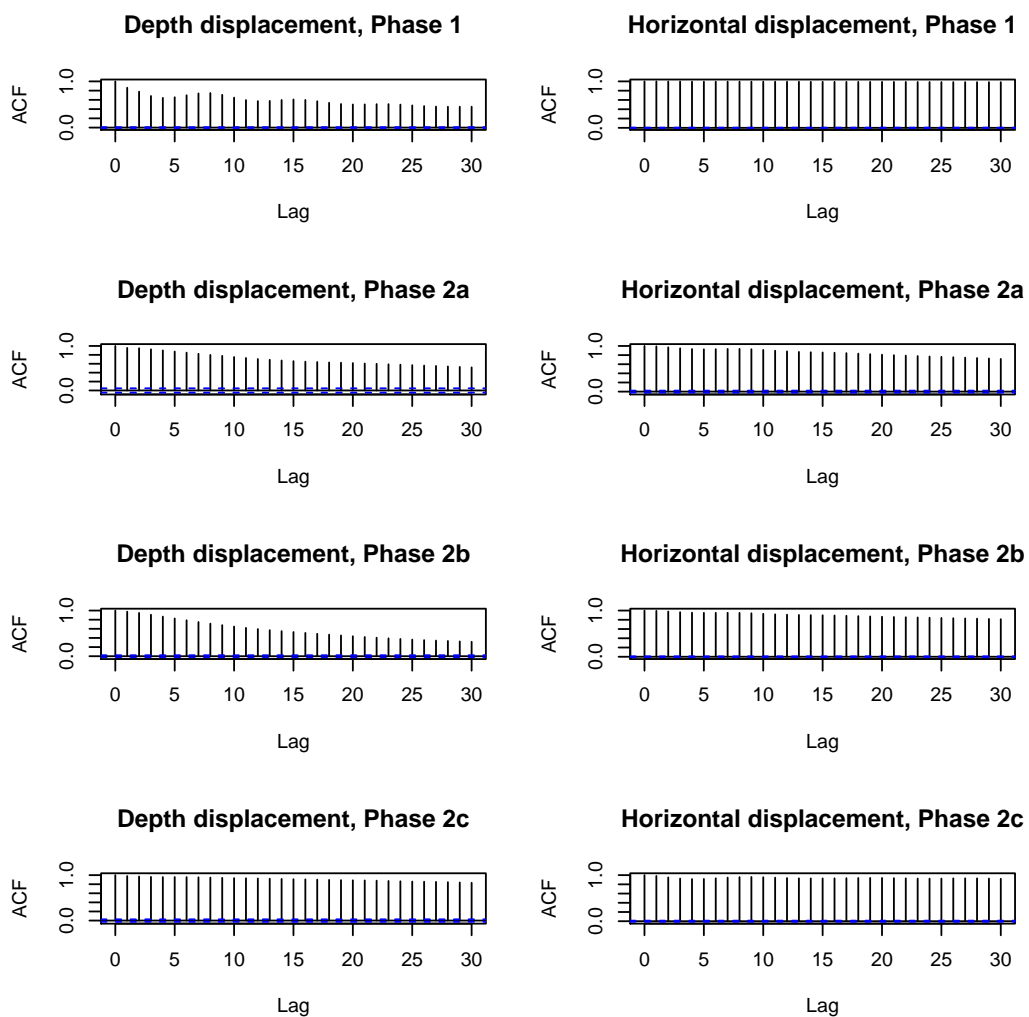


Figure 10: Autocorrelation functions for depth and horizontal displacement as a function of dive phase.

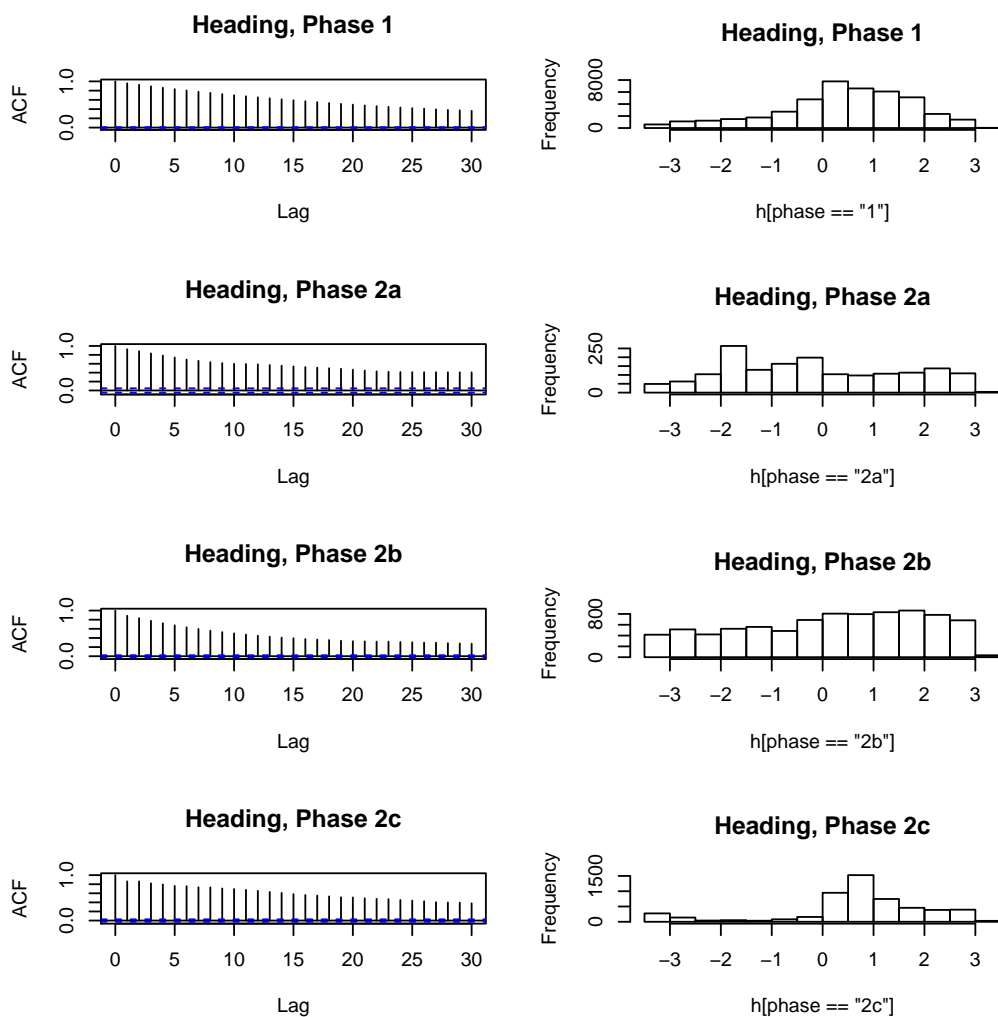


Figure 11: Distribution and autocorrelation functions for heading as a function of dive phase.

track (black line, green while deep diving below 300m) the whale shoots off the range before reaching the third deep dive. Nonetheless, the overall shape of the first two dives look reasonable, even if weirdly enough the whale apparently moves north instead of south after the first deep dive. One must remember that the velocity on the x, y plane, the one used for dead-reckoning, from the initial period, where it is likely that the animal is moving (much) faster in x, y plane than when it is coming up in its ascent phase, hence the ascent phase actually presents a much lesser displacement in x, y than what is "inferred" from the dead-reckoning.

On the bottom plot of figure 12 we can see that the initial speed is probably underestimated. This would be expected, given we obtained the above speed by using the initial part of the track, so after dividing it by 5, it is bound to underestimate the speed in that part of the track. On the other hand, the speed in several points after the first dive is probably still overestimated.

This poor performance leads naturally to the need to obtain a better vector of speed estimates to improve track prediction.

4.2 Dead-reckoning using Kalman filter speed estimates

So now we are going to try to use Mark Johnson's (MJ) code to obtain whale speeds via the Kalman Filter in order to implement dead-reckoning using better estimates of whale speed.

4.2.1 Using MJ code

We consider here the use of MJ MATLAB code, namely the function `kalmanspeedest.m`. To implement the Kalman filter ⁴ we used the code below in MATLAB on top of the data set "md07_248bprh.mat",

```
[speed fits] = kalmanspeedest(p,pitch,fs)
```

followed by code to export the vector of speeds as a txt

```
save('md07_248bspeed.txt', 'speed', '-ascii', '-double', '-tabs')
```

which is then read back into R.

⁴Something which I am failing to understand is that from what I can tell the code should not produce estimated negative speeds, and yet it currently does so. This gives me the opposite of a warm fuzzy feeling...

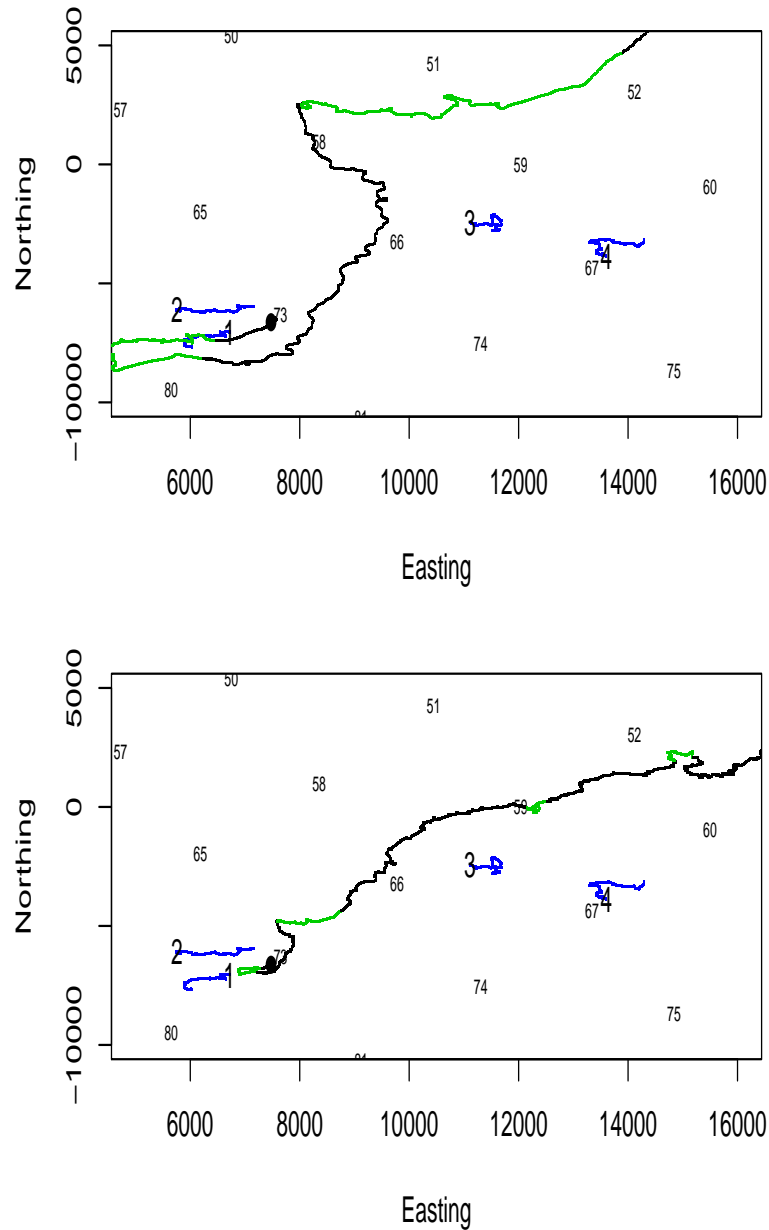


Figure 12: The location of the georeferenced clicks for each of the first 4 dives of whale md07_248b (in blue). The numbers 1,2,3,4 represent the first click of the 1st,2nd,3rd, and 4th dive respectively, and in black and green, the locations obtained by dead-reckoning of the prh file combined with an average speed for the whale (green portions of the track correspond to times at which depth was below 300 m, i.e. ¹⁷deep dives). The average speed on the top plot was derived by the animal speed between the tag on location and the first localized click, while on the bottom plot that value was divided by 5.

We can see that using this KF estimated vector of speeds we end up with a track much closer to the geo-referenced locations (cf. Figure 13 with figure 12), as should be expected given this was the procedure that JW/MJ have used to get those.

The original results obtained by MJ are presented in figure 15. We can zoom in each dive to compare it better with these (Figure 14). Note here he use the exact times to define what is the georeferenced bit of the track, rather than the portion of the dive below 300 m as was the case in (Figure 13). The pseudo-track dives look about the same as the georeferenced dives, just in the wrong absolute position, which is not unexpected due to drift errors. If one compares our results with those from MJ, it is interesting to note that while the third dive is placed to the NW of the true location by MJ, it is placed to the SW by us, and then for the fourth dive it is even further North to MJ than for us.

So the inconsistencies between ours and JW/MJ results might be due to differences between now and when they implemented this, namely at the level of:

1. the data: the data might have been updated/corrected since it was used by MJ/JW;
2. the actual code: the code might have suffered minor tweaks since it was used by MJ/JW;
3. code parameters: there are a number of tweaking parameters which might have been responsible for the differences which are still present between our results and those obtained by MJ, including the measurement error variance (which is taken as given in MJ code) as well as the state process variances (again, assumed fixed rather than estimated). From the original MJ code it seems clear that some manual fine tuning of these happened.

It is worth noting in particular that for us the first dive seems to cover a longer distance in the geo-referenced file (the blue line in figure's 14 top left panel) compared to the portion of the pseudo-track that would correspond to that period (the green line in figure's 14 top left panel). It is unclear at this point what this might mean, but it should not be an error in timing, because otherwise such pattern would propagate through to the subsequent dives, which apparently it does not.

It would be great if we managed to implement the Kalman filter in R, because that would avoid the going back and forth between MATLAB and R, and would allow for a quick assessment of how changing parameters might affect the track estimation process. This will be the subject of the next section.

4.2.2 Migrating MJ code to R

In this section we try to implement the fitting of the Kalman filter directly in R. The pitch and depth data required as inputs are in objects “md07_248bpitch” and “md07_248bdepth”, respectively. These contain 316980 records each, corresponding to a 5 Hz sampling scheme. We can use the same tag on position as used in the previous section, i.e. $x=7475.6$ and $y=-6630.1$.

Function `kalmanspeedest.m` was converted into the function `Kalman.Filter`:

```
> ##implementing MJ Kalman Filter in R
>
> Kalman.Filter=function(z,phi,sf,r=0.001,q1p=0.02,q2p=0.08){
+ #this function was implemented by Tiago A. Marques on the
+ #01-06-20012 to mimic function kalmanspeedest.m
+ # tiago@mcs.st-and.ac.uk
+ #-----
+ #-----
+ # kalmanspeedest.m originally developed in MATLAB by Mark Johnson (MJ)
+ # kalmanspeedest.m preamble reproduced here
+ #-----
+ # % Estimate the swim speed of a whale with given depth profile, p, in m,
+ # % pitch in radians, sampled at rate fs, Hz. Process is a 2-state Kalman
+ # % filter estimating speed and depth, followed by a Rauch smoother.
+ # % Output:
+ # % s is the swim speed estimate in m/s
+ # % fit is a structure of results including:
+ # % fit.ks = kalman filtered speed
+ # % fit.kd = kalman depth estimate
+ # % fit.rd = rauch depth estimate
+ # % fit.kp = kalman a posteriori state covariance (2x2xn)
+ # %
+ # % mark johnson, WHOI
```

```

+ # %      majohnson@whoi.edu
+ # %      November 2004
+ #-----
+ #-----
+ # The underlying state space model being fiited t the data is described in
+ # "Estimating speed using the Kalman filter... and beyond", equations 5 and 6
+ # a LATTE internal report available from TAM
+ #-----
+ #-----
+ #inputs:
+ #   z (was p in MJ code) is a vector of depths
+ #   phi (was pitch in MJ code) is a vector of pitches
+ #   sf (was fs in MJ code) is the sampling frequency, in Hz
+ #-----
+ #-----
+ #number of times each observation was observed
+ n=length(z)
+ #defining some required quantities
+ #note currently these are constants
+ #measument error in depth
+ r = r
+ #state error in speed
+ q1 = (q1p/sf)^2
+ #state error in depth
+ q2 = (q2p/sf)^2
+ #sampling period
+ SP = 1/sf
+ #state transition matrix entry (2,1) - see equation 6
+ a = -sin(phi)/sf
+ #initial states, pitch = 1, and depth = initial observed depth
+ #TAM?: why start pitch at 1? why the different "conceptual" choice
+ # for pitch and depth?
+ shatm=matrix(c(1,z[1]),2,1)
+ # state noise matrix
+ Q=matrix(c(q1,0,0,q2),2,2,byrow=T)
+ #observation matrix (a vector here)
+ H=matrix(c(0,1),1,2)
+ # initial state covariance matrix

```

```

+ # says how much we trust initial values of s and p?
+ Pm=matrix(c(0.01,0,0,r),2,2,byrow=T)
+ # place to store state predictions
+ skal = matrix(0,nrow=2,ncol=n)
+ # object for storing the kalman a posteriori state covariance (2x2xn)
+ Ps = array(data = 0, dim = c(2,2,n))
+ #TAM?: WHAT IS THIS OBJECT ???
+ Pms=Ps
+ #implementing the kalman Filter
+ for (i in 1:n){
+   # make state transition matrix
+   Ak=matrix(c(1,0,a[i],1),2,2,byrow=T)
+   #after the initial state only
+   #(hence this bit is ONLY not evaluated for the inital state)
+   if (i>1) {
+     # update a priori state cov
+     Pm = Ak%%P%%t(Ak) + Q
+     #a priori state estimate
+     shatm = Ak%%shat
+   }
+   # compute kalman gain
+   K = Pm%%t(H)%%solve(H%%Pm%%t(H)+r)
+   # a posteriori state estimates
+   shat = shatm + K%%(z[i]-H%%shatm)
+   # forcing speed and depth always to be positive
+   #TAM?: must be a smarter way to do this ???
+   shat = ifelse(shat<0,0,shat)
+   # a posteriori state cov
+   P = (diag(2)-K%%H)%%Pm ;
+   #store results of iteration
+   skal[,i] = shat
+   Pms[,i] = Pm
+   Ps[,i] = P
+ }
+ #object to hold the states smoothed by the Rauch smoother
+ srau = matrix(0,nrow=2,ncol=n)
+ #the last time point does not require any smoothing, it's the point itself
+ srau[,n] = shat

```

```

+ # Kalman/Rauch smoother
+ for (i in n:2){
+   # make state transition matrix
+   Ak=matrix(c(1,0,a[i-1],1),2,2,byrow=T)
+   # smoother gain
+   K=Ps[, ,i-1]%*%t(Ak)%*%solve(Pms[, ,i])
+   # smooth state
+   srau[,i-1] = skal[,i-1]+K%*%(srau[,i]-Ak%*%skal[,i-1])
+ }
+ #returning:
+ #a list containing
+ # speeds : the smoothed speeds
+ # fit.ks : the fitted speeds
+ # fit.kd : the fitted depths
+ # fit.rd : the smoothed depths
+ # fit.kp : the kalman a posteriori state covariance
+ return(list(speeds=srau[1,],fit.ks=skal[1,],fit.kd = skal[2,],fit.rd = srau[2,
+ ]

```

We can give it a test, by redoing the analysis as implemented in MATLAB:

This is presented in figure 16. Note this is exactly the same as figure 13, as would be expected⁵ given that implementing this in MATLAB and R should be the same thing.

Small changes to the values of input parameters leads to minor changes in the obtained track. As an example, we change the measurement error in depth from 0.001 to 0.01 below, and also change the state noise variances, and plot the 3 sets of tracks on top of each other (Figure 17).

So finally, we have been able to migrate Mark Johnson's Kalman Filter code to R, and we can now think about ways to improve the simulated annealing component of the process to georeferencing dives.

4.3 Including latitude and longitude as states

The key difference now is that we are going to include latitude (x) and longitude (y) as states in the SMM, therefore leading to an integrated procedure rather than a plug-in approach (i.e. a speed estimate plugged into a

⁵It provides the kind of warm fuzzy feeling that one always aims for in these situations!

dead-reckoning algorithm). Amongst other things, this provides in a straightforward manner error bounds on the predictions of localization.

The results of the fitting can be seen in figure 18. As expected, the depth profile is very well estimated (remember we actually observe depth, and with relatively small error). It is interesting to see the increasing variance in x, y , illustrating how drift errors add up over time.

One can take a closer look at the estimated speeds (Figure 19). It can be seen that the CV on the speed estimates sometimes “explodes”, especially when the animal is at the surface, which reflects that it is easier to estimate speed at the deepest parts of the deep dives. Note also the effect of the *ad hoc* rule to keep filtered speeds (and depths, not shown) strictly positive, and how smoothed speeds sometimes (but not often) get negative. The current implementation is not elegant nor theoretically justifiable, but seems to do the job. But I wonder what else might we try to enforce this in a way that essentially does not mean all the nice theoretical properties of the Kalman Filter are gone to waste.

We implemented another version of the KF in which neither depth nor speed were constrained (cf. green and black lines with blue and red lines in top left plot of figure 20).

We can use the variance-covariance matrix on the estimated states to construct 95% confidence ellipsoids for the location of the whale in space (Figure 21). We can easily see that the predictions drift away and quite fast they are completely in the wrong place (cf. green and black lines with blue lines).

Another quick attempt was made to evaluate the impact of increasing the measurement error in the depth observations.

Naturally, if one compares these (Figure 23) with the previous predictions (cf. Figure 21), we have more error in the predictions, but that is still far from being enough to overlap with the true known locations.

The above results of KF implementations suggest that we include in the process the available observations about animal location from the acoustic localizations on the AUTECH hydrophones. We do that in the next section.

5 Georeferentiation of dives

The key difference now is that we are going to include some observations about x, y location in the SSM formulation. This means we are now considering

a state space model along the lines of equations 7 and 8/9 in Marques and Thomas (2012b). So now we have the same 4 states, but every now and then, on top of a depth observation, we also have an x, y observation.

To do this, we create a new function to implement the Kalman Filter under this context. In essence, this just means that when we have an observation from a state, we predict and update, but if there is no observation, we just predict, but do not update the unobserved state components.

In order to do so, the first thing we must do is to be able to associate with the prh file the corresponding x, y locations⁶. This requires some careful thinking because of the way the different files are time indexed. We begin by binding all the georeferenced information in a single object

We begin by testing the new function a couple of times. Once we include the localizations, the results look just as one might expect (Figure 24), with the predictions bang on the localizations when we have them.

We can take a look at predictions from this latest formulation (Figure 25). As expected, we see that the variance in x, y vanishes every time we actually have x, y observations. Additionally, as might be expected, the variance in the other state predictions also decreases.

The next step in this process is an obvious one, and corresponds to including the pitch and heading as states. At the moment these are being taken as covariates observed without error, which despite practical, is inconsistent with the current implemented SSM framework.

6 Improving the entire process

We have now obtained a new state space model that allows us to estimate the animal position as well as to quantify the uncertainty in the position estimates. This material was the bulk of what was presented at ISEC 2012. Nonetheless, there are still a number of possible improvements and potential work ahead:

⁶A heads up: as implemented for the ISEC 2012 talk, the data used as localizations was the data after georeferencing, rather than the data coming out of the interpolation of TDOA's. This needs to be looked into, as it's totally circular, although of expected little practical consequences, as the localizations and the georeferencing are supposedly close enough. Additionally, only around 27000 locations, rather than 41230 were being used, due to an error in the code. Similarly, now corrected and of negligible practical consequences

- improve current mechanistic model, which is clearly not adequate (very biased outcome in the absence of acoustic localizations); e.g. water current (velocity and direction) might need to be accounted for
- improve ad hoc (and previously unmentioned) procedure to keep speed and depth estimates admissible (i.e. speed positive, depth below surface)
- look into the interpolating TDOA's algorithm to quantify measurement error in the (x, y) observation process
- include pitch and heading as states; extend to non-linear, possibly non-Gaussian, model
- and then look into the orientation algorithm to quantify measurement error in the observation process of pitch and heading

Referências

- Marques, T. A. and Thomas, L. (2012a). Modeling beaked whales movement, sound production and detection at AUTECH. Technical report, LATTE WORKING DOCUMENT.
- Marques, T. A. and Thomas, L. (2012b). Obtaining pseudo-tracks and georeferenced locations from DTAG data. Technical report, LATTE WORKING DOCUMENT.
- Marques, T. A., Thomas, L., Ward, J., DiMarzio, N., and Tyack, P. L. (2009). Estimating cetacean population density using fixed passive acoustic sensors: an example with Blainville's beaked whales. *The Journal of the Acoustical Society of America*, **125**, 1982–1994.

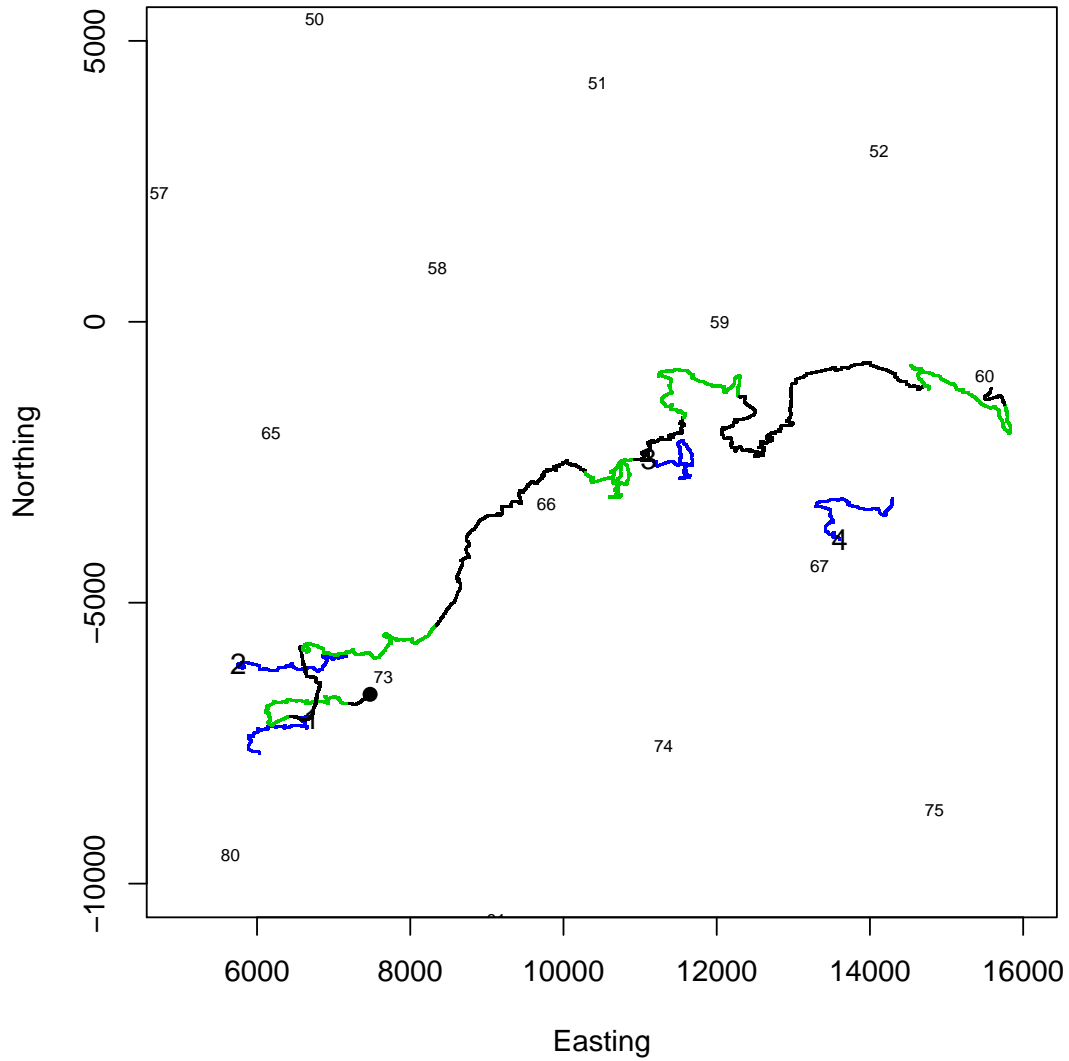


Figure 13: The location of the georeferenced clicks for each of the first 4 dives of whale md07_248b (in blue). The numbers 1,2,3,4 represent the first click of the 1st,2nd,3rd, and 4th dive respectively, and in black and green, the locations obtained by dead-reckoning of the prh file combined with a vector of speeds obtained via MJ Kalman Filter for the whale (green portions of the track correspond to times at which depth was below 300 m, i.e. deep dives).

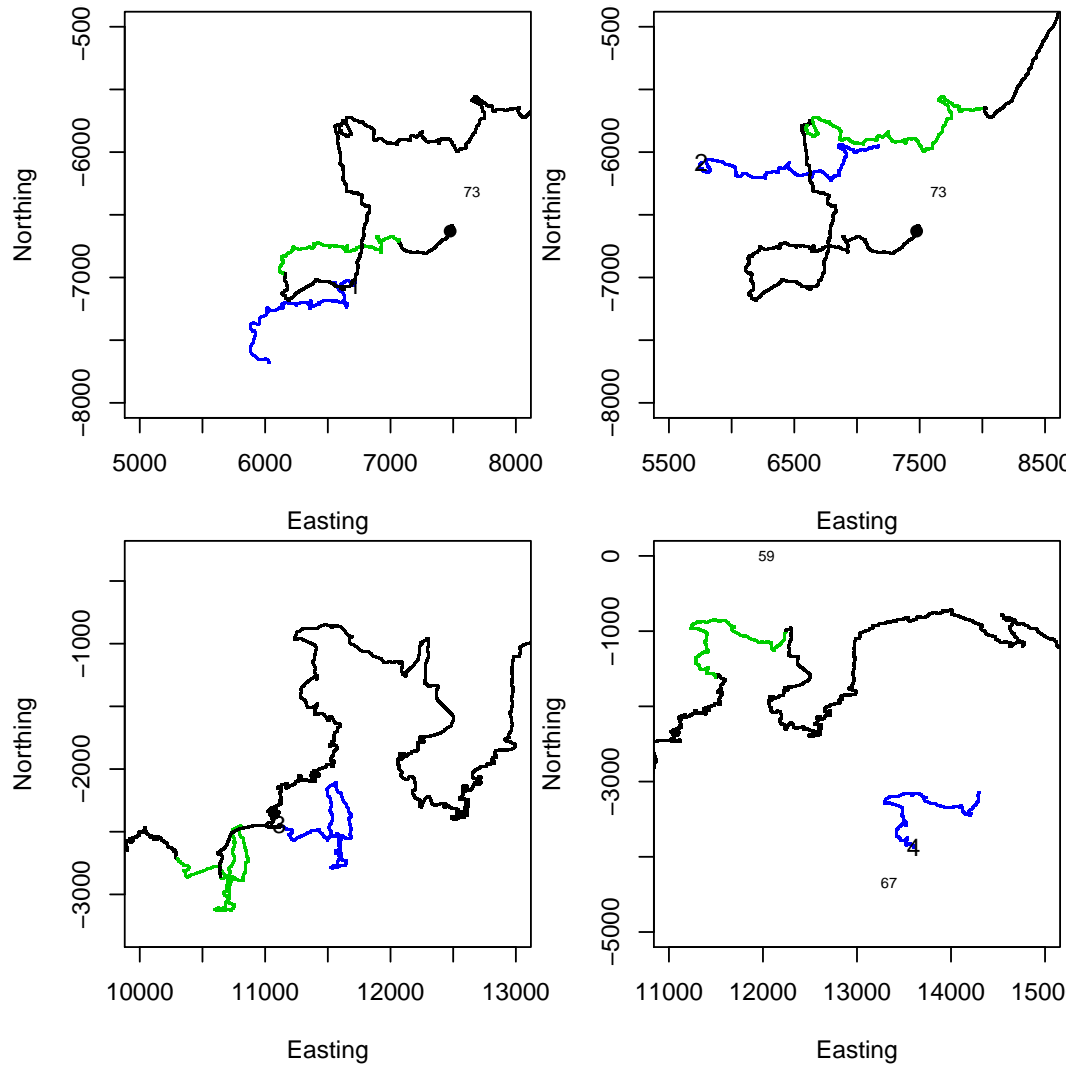


Figure 14: The location of the georeferenced clicks for each of the first 4 dives of whale md07_248b (in blue), with one dive per plot. The numbers 1,2,3,4 represent the first click of the 1st,2nd,3rd, and 4th dive respectively, and in black and green, the locations obtained by dead-reckoning of the prh file combined with a vector of speeds obtained via MJ Kalman Filter for the whale (green portions of the track correspond to times for which deep dives were georeferenced).

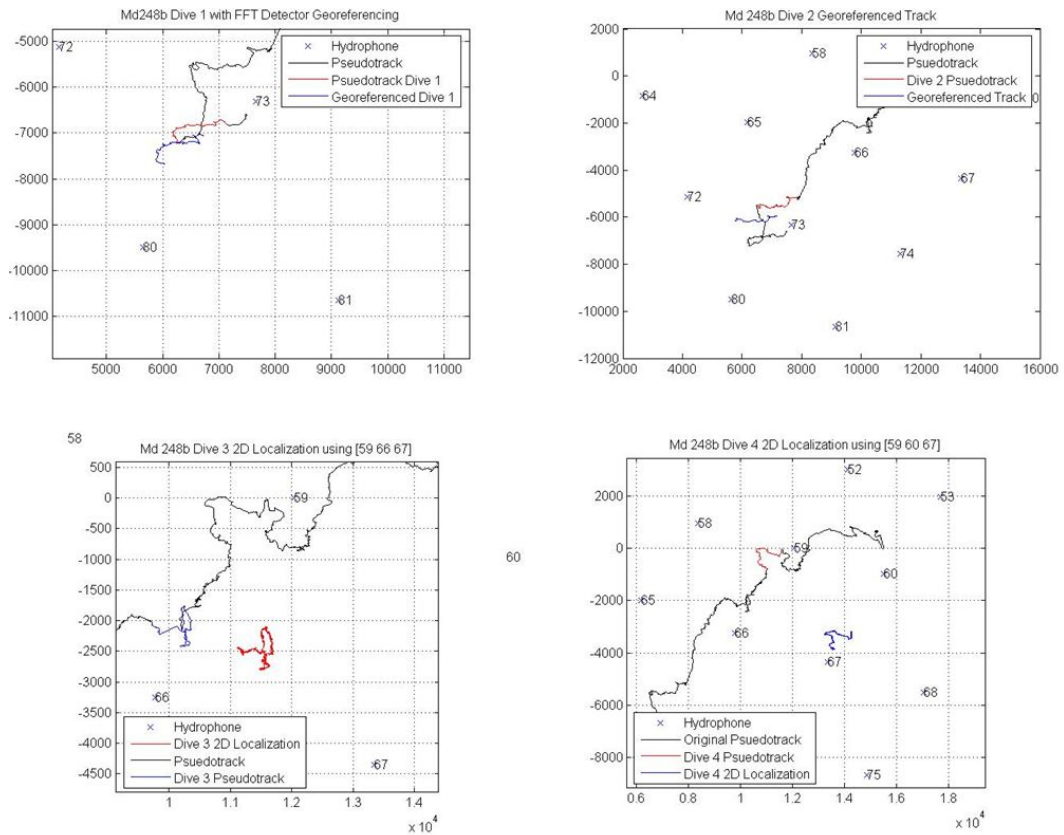


Figura 15: The same information as in figure 14, but as obtained directly by MJ. This was sent to us by JW.

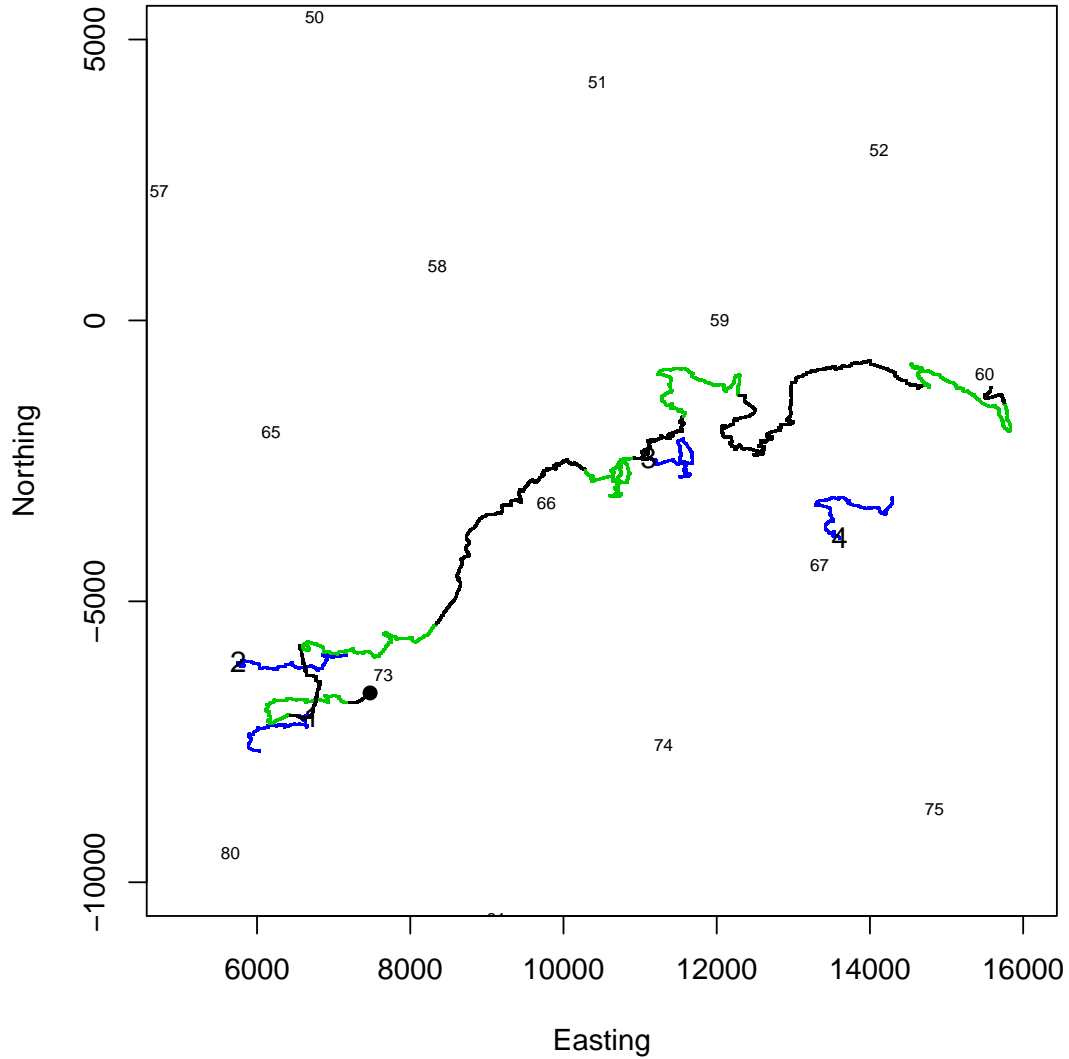


Figure 16: The location of the georeferenced clicks for each of the first 4 dives of whale md07_248b (in blue). The numbers 1,2,3,4 represent the first click of the 1st,2nd,3rd, and 4th dive respectively, and in black and green, the locations obtained by dead-reckoning of the prh file combined with a vector of speeds obtained via MJ Kalman Filter for the whale (green portions of the track correspond to times at which depth was below 300 m, i.e. deep dives), both directly in MATLAB and via our R implementation.

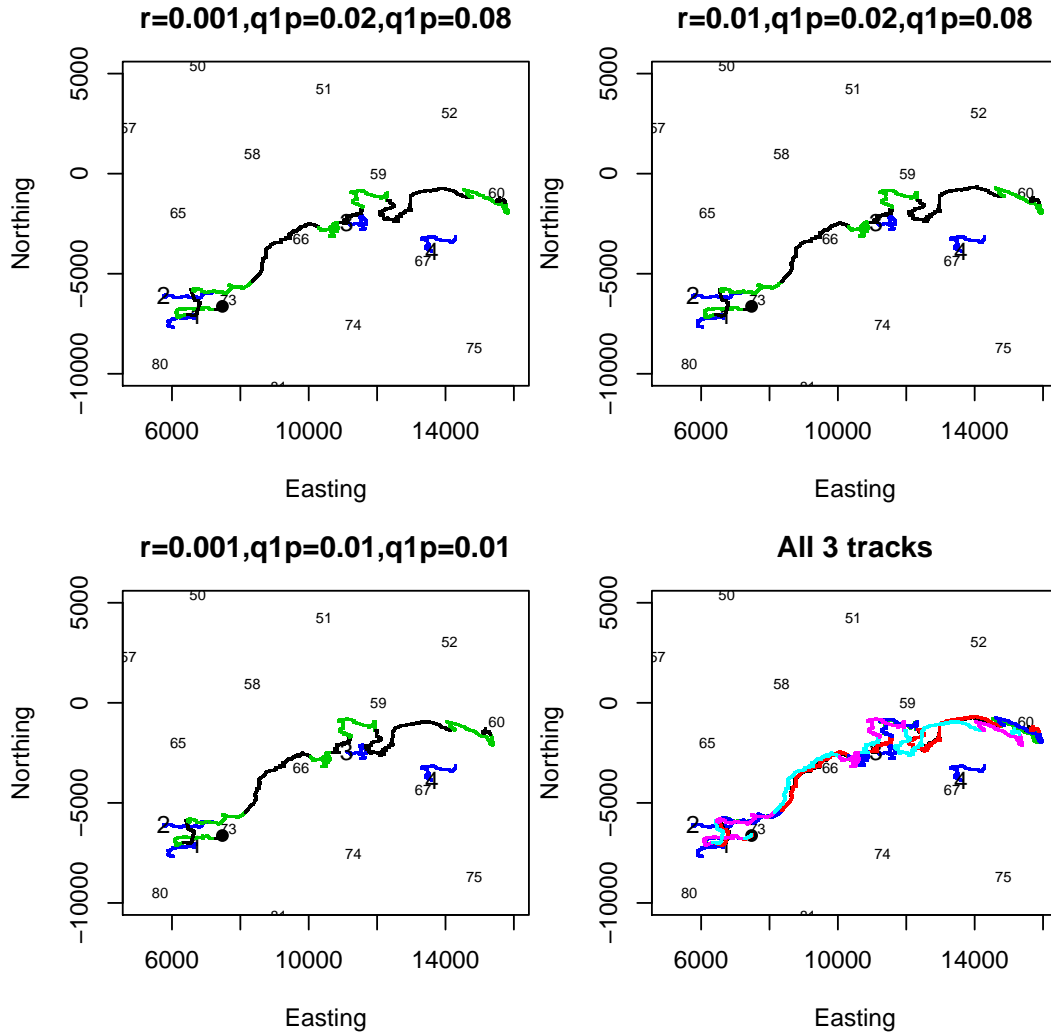


Figure 17: The location of the georeferenced clicks for each of the first 4 dives of whale md07_248b (in blue). The numbers 1,2,3,4 represent the first click of the 1st,2nd,3rd, and 4th dive respectively, and in black and green, the locations obtained by dead-reckoning of the prh file combined with a vector of speeds obtained via MJ Kalman Filter for the whale (green portions of the track correspond to times at which depth was below 300 m, i.e. deep dives), using 3 sets of slightly different input parameters.

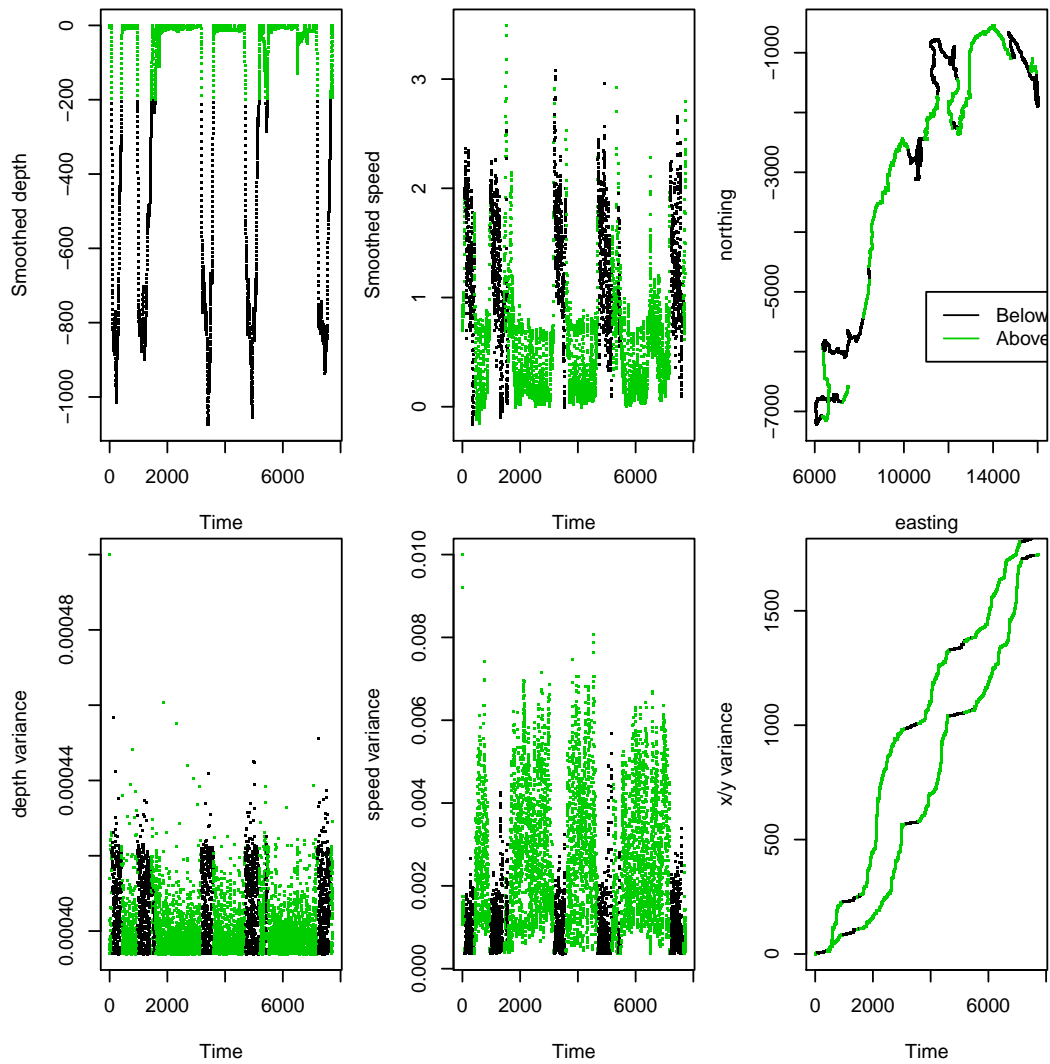


Figure 18: Results of fitting the SSM with 4 states and 1 observation to the data. Top row: estimates. Bottom row: corresponding variances. Left: Depth; Center: speed; Right: x, y coordinates.

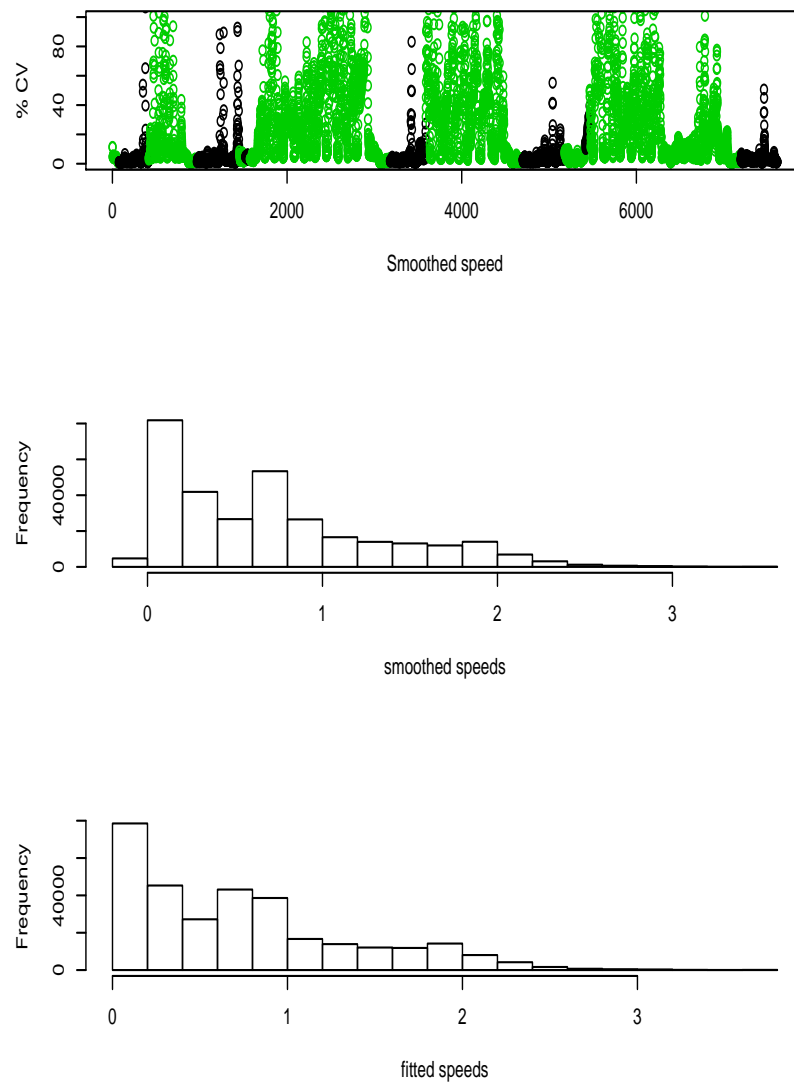
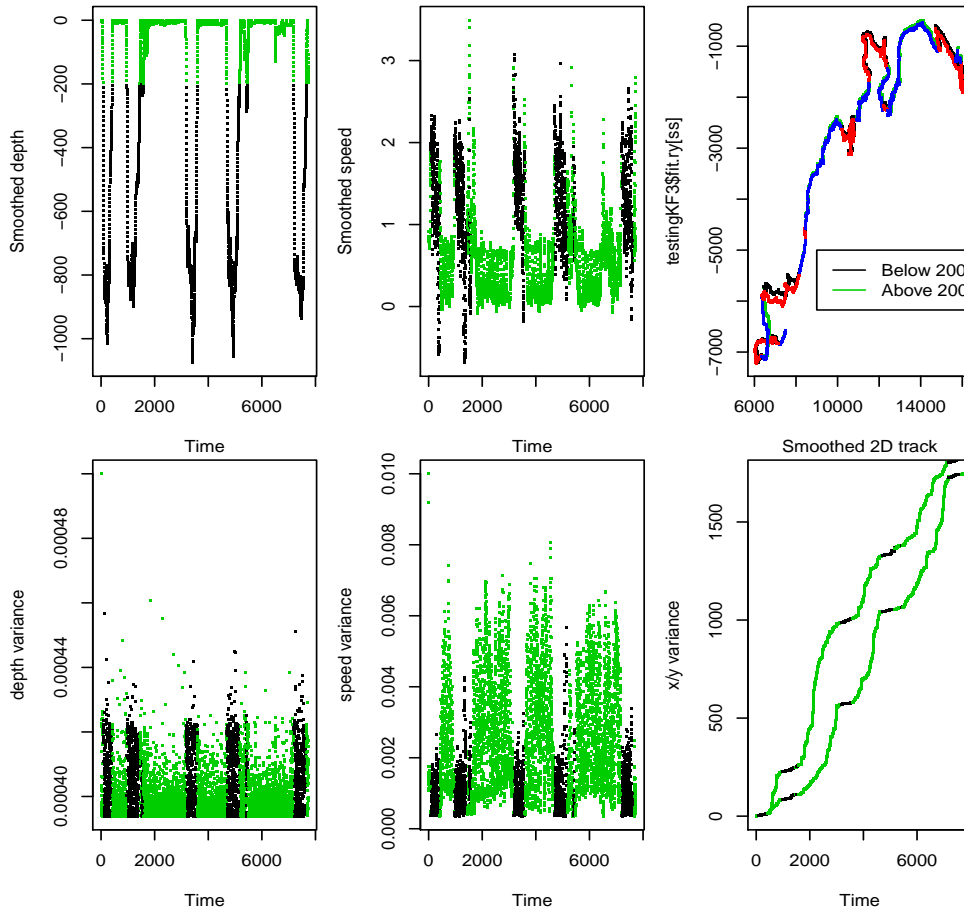


Figura 19: Additional results regarding the speeds. Top: speed CV. Center: histogram of fitted speeds. Bottom: histogram of smoothed speeds.



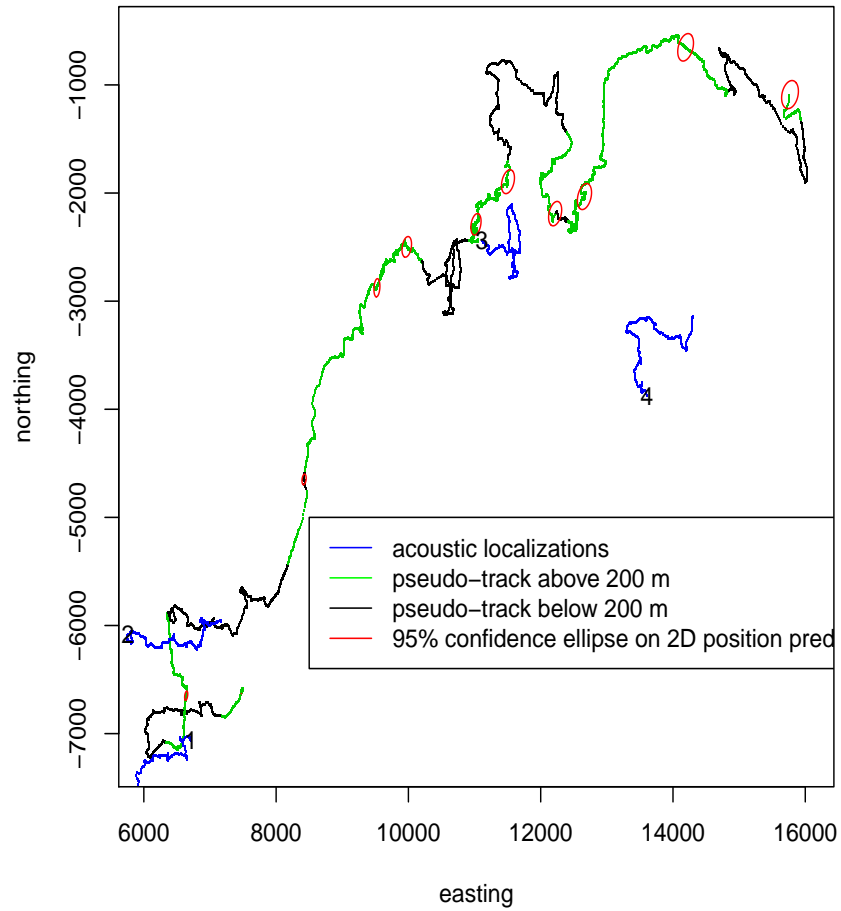


Figura 21: Track prediction and associated 95% confidence ellipsoids.

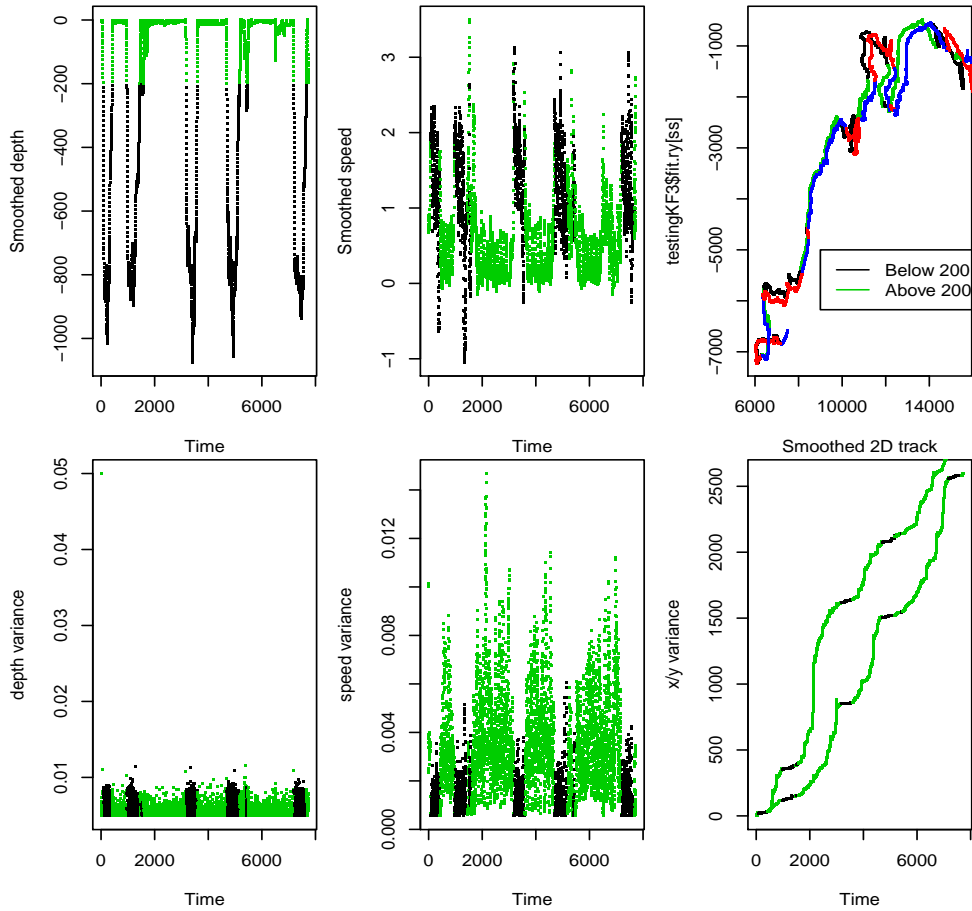


Figure 22: Results of fitting the SSM with 4 states and 1 observation to the data,, but increasing the amount of error allowable in the depth observations. Top row: estimates. Bottom row: corresponding variances. Left: Depth; Center: speed; Right: x, y coordinates. The third top plot shows original and added error track, and one can see the differences are minor, but there is drifting with time.

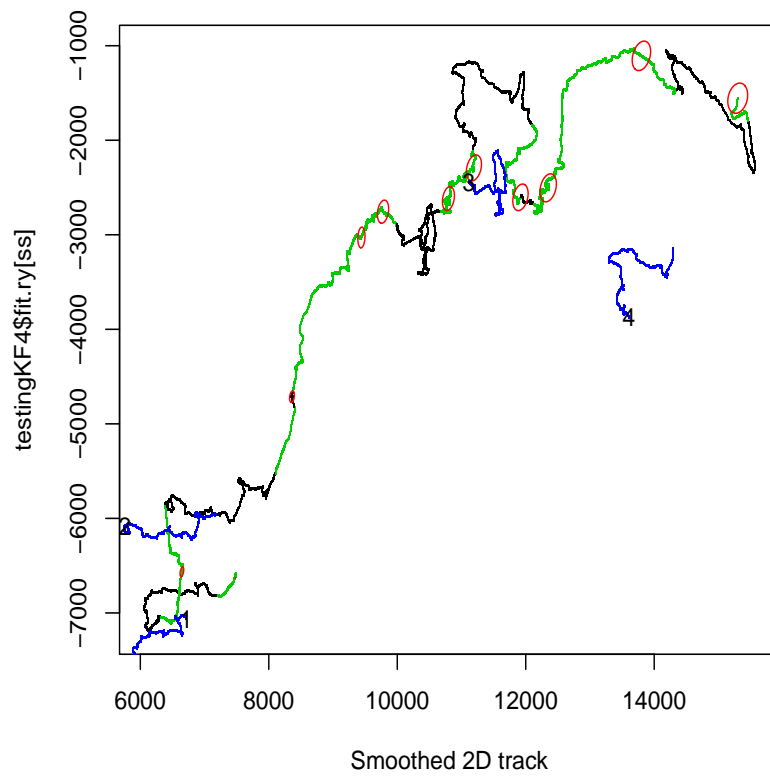


Figure 23: Track prediction and associated 95% confidence ellipsoids, now considering additional error in the depth observations.

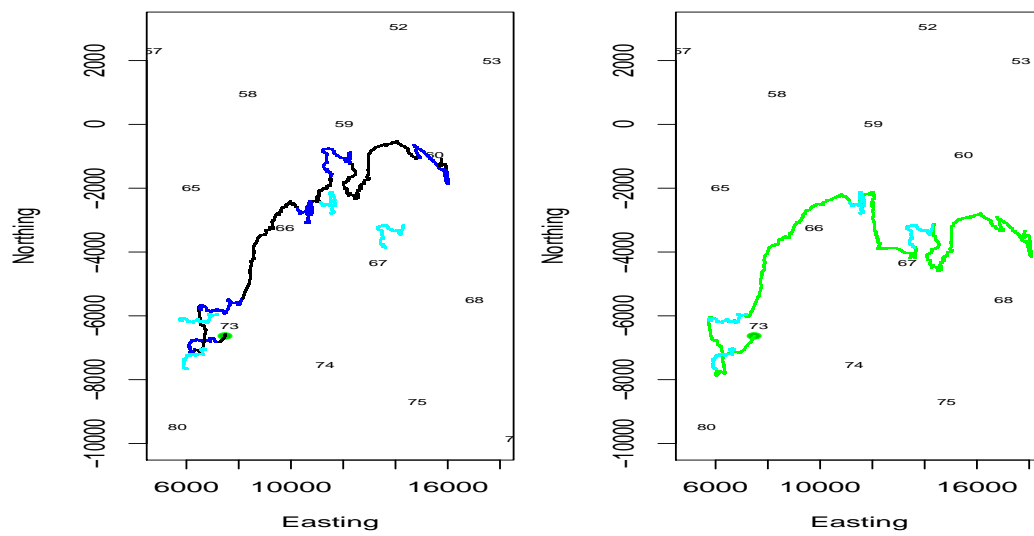


Figura 24: Track prediction before using x, y observations (left) and after using x, y observations. Note the predicted smoothed track is bang on the known localizations.

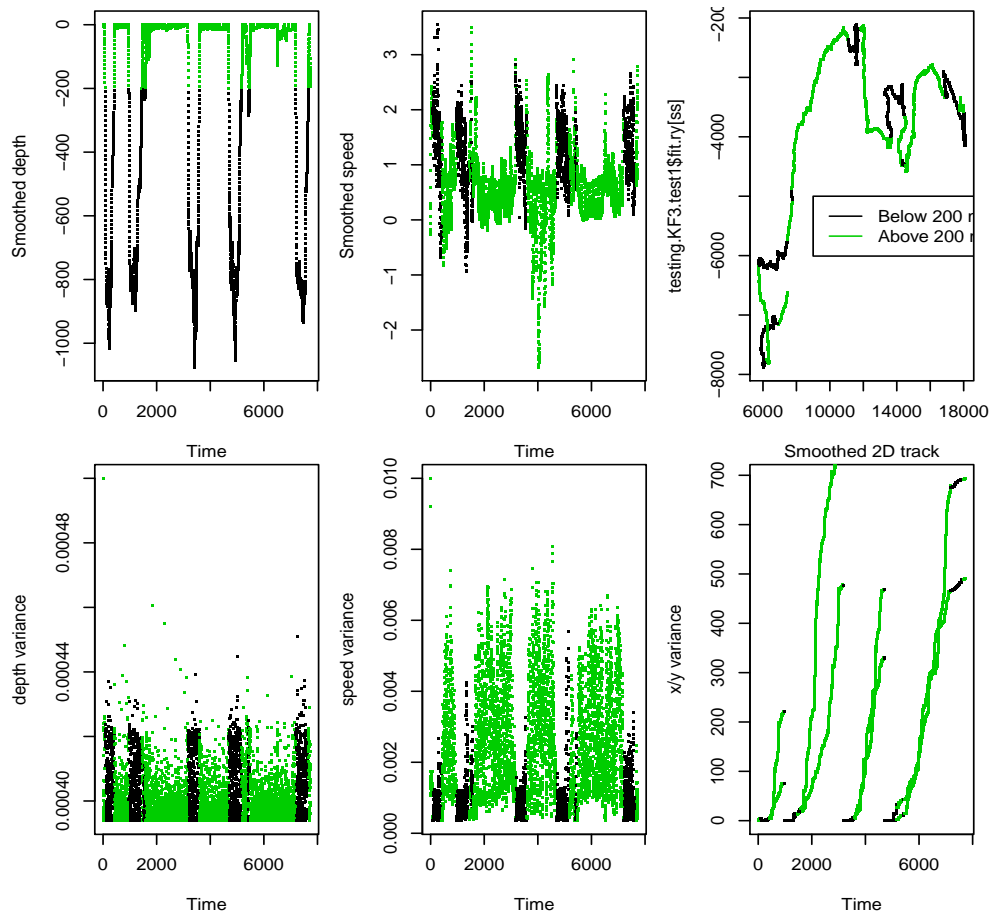


Figure 25: Results of fitting the SSM with 4 states and 3 observations to the data. Top row: estimates. Bottom row: corresponding variances. Left: Depth; Center: speed; Right: x, y coordinates.

Using animal-borne tags to estimate whale tracks in 3-dimensional space using state space models

Tiago A. Marques^{1,2}, Mark Johnson³, Jessica Shaffer⁴, Charlie White⁴ and Len Thomas¹

1 Centre for Research into Ecological and Environmental Modeling, University of St Andrews; 2 Centro de Estatística e Aplicações da Universidade de Lisboa; 3 Scottish Oceans Institute, University of St. Andrews; 4 Naval Undersea Warfare Center

03-07-2012



Version with appendices



Page 12 of 466

Overview of the talk

Introduction

Proposed Model

First results

Discussion and Open Questions

Thanks and References

Version with appendices

Page 121 of 466

LATTE

This work is developed within LATTE - Linking Acoustic Tests and Tagging using statistical Estimation: Modeling the Behavior of Beaked Whales in Response to Medium Frequency Active Sonar.

LATTE's end game:

1. develop movement models which integrate information at multiple scales (DTAG data, AUTECH hydrophone data, satellite tags)
2. fit models to baseline data from periods when sonar activity is absent
3. fit models to periods when sonar is actively being used
4. compare parameter estimates from 2 and 3 to infer behavioral changes

Version 1.0 with appendices

Page 122 of 466

DTAGs

DTAG's (Johnson & Tyack 2003) are digital recording tags used on marine mammals:

- ▶ The tag contains a large array of solid-state memory and records continuously from a built-in hydrophone and suite of sensors;
- ▶ The sensors sample the orientation of the animal in three dimensions with sufficient speed and resolution to capture individual fluke strokes;
- ▶ Orientation is deduced from the three-axis accelerometer and magnetometer signals and is expressed in terms of pitch, roll, and heading (PRH);

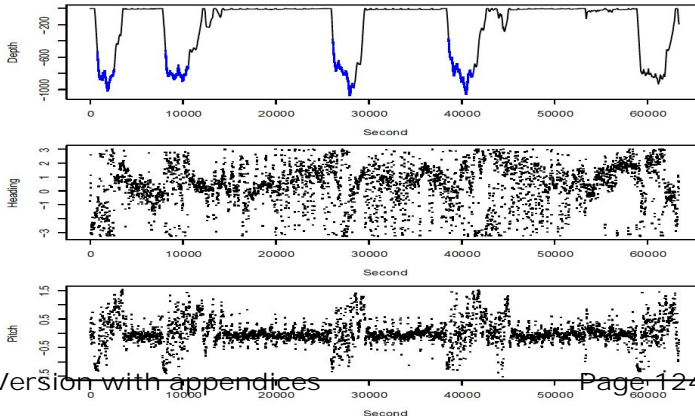
▶ the DTAG was **NOT** meant to be used to estimate a whale track from it!

Version with appendices

Page 123 of 466

Example DTAG data: pitch roll and heading (PRH)

1 whale, 5 deep dives, around 18 hours, sampled 5 times per second: a multivariate time series with over 300000 time points



Version with appendices Page 124 of 466

Existing procedure to estimate track from DTAG data

1. calculate 3D orientation (PRH) from three-axis accelerometer and magnetometer signals
2. estimate whale speed using a bivariate state space model with speed and depth as states and (noisy) depth observations (pitch assumed a known covariate)
3. use this speed estimate, jointly with tag-on position, pitch and heading in a dead-reckoning procedure to produce a “*pseudo-track*”
4. use the DTAG sound file to identify clicks produced by tagged whale
5. cross correlate these clicks with AUTECH hydrophones to find clicks time difference of arrival (TDOA) pairs
6. interpolate TDOA lines to get multiple TDOA's for each click
7. use multiple TDOA's to localize click (hence whale) in 3D space
8. join output of step 7 with that of step 3 to arrive at a “*georeferenced*” track, via a simulated annealing procedure

State space models

A simple state-space model (SSM) can be thought of a couple of equations, describing two “parallel” time series, the state and the observation processes. The states are the underlying true quantities we often want to make inferences about, while the observations are some observable quantities which can be related to the states by some known process:

$$o_t = F_t \theta_t + v_t, \quad v_t \sim N(0, V_t)$$

$$\theta_t = G_t \theta_{t-1} + \omega_t, \quad \omega_t \sim N(0, W_t)$$

where θ_t represents the state in time t and vector o_t represents the observations at time t , and V_t and W_t represent respectively the observations and states variance-covariance matrices.

Kalman Filter: a useful tool to fit linear state space models

Initialize the Kalman filter and then, at each *filtering* iteration:

- ▶ prediction stage
 - ▶ uses the mechanistic movement model (state equations) to predict what the next value of the state(s) ought to be
- ▶ update stage
 - ▶ compares predicted state(s) value(s) with observed value(s)
 - ▶ predicts filtered value as a weighted version of what it ought to be and what it was observed to be
 - ▶ weight known as *Kalman gain*, a compromise between how much faith we have in the model, and how much error we have in the observation process

A useful by-product is the variance-covariance matrix describing the uncertainty around the state estimates. After filtering, we go backwards in time, *smoothing* the estimates, obtaining the best estimate for each time point given all the data available.

Our initial approach

Consider a SSM to integrate¹ the dead-reckoning (predicting x, y) stage with the speed (s) estimation using noisy depth (z) observations²

$$\begin{pmatrix} s_t \\ z_t \\ x_t \\ y_t \end{pmatrix} = \begin{pmatrix} 1 & 0 & 0 & 0 \\ -\sin(\phi_{t-1})\Delta T & 1 & 0 & 0 \\ \Delta T \cos(\phi_{t-1}) \sin(\psi_{t-1}) & 0 & 1 & 0 \\ \Delta T \cos(\phi_{t-1}) \cos(\psi_{t-1}) & 0 & 0 & 1 \end{pmatrix} \begin{pmatrix} s_{t-1} \\ z_{t-1} \\ x_{t-1} \\ y_{t-1} \end{pmatrix} + \begin{pmatrix} \omega_{s_t} \\ \omega_{z_t} \\ \omega_{x_t} \\ \omega_{y_t} \end{pmatrix}$$

$$o_{z_t} = [0 \ 1 \ 0 \ 0] \begin{pmatrix} s_t \\ z_t \\ x_t \\ y_t \end{pmatrix} + v_{z_t}$$

¹i.e. integrate steps 2 and 3
²note also the use of heading (ψ) and pitch (ϕ) as known covariates

Our current approach

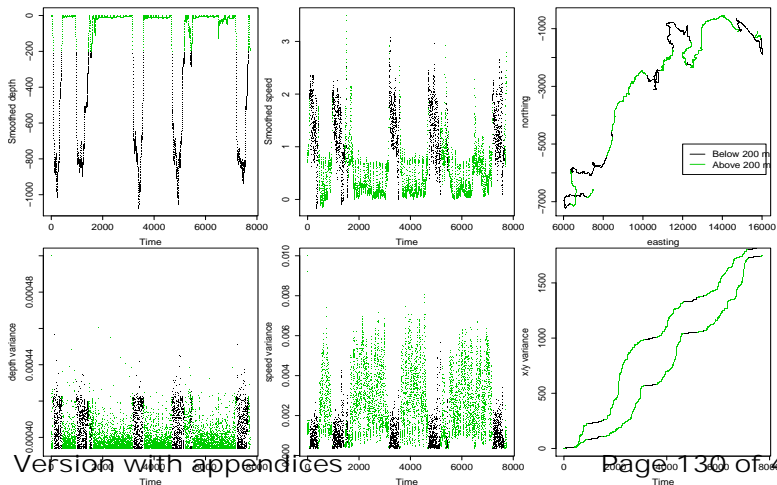
Integrate³ the dead-reckoning, the speed estimation, and the information from acoustic localizations⁴ within the SSM

$$\begin{pmatrix} s_t \\ z_t \\ x_t \\ y_t \end{pmatrix} = \begin{pmatrix} 1 & 0 & 0 & 0 \\ -\sin(\phi_{t-1})\Delta T & 1 & 0 & 0 \\ \Delta T \cos(\phi_{t-1}) \sin(\psi_{t-1}) & 0 & 1 & 0 \\ \Delta T \cos(\phi_{t-1}) \cos(\psi_{t-1}) & 0 & 0 & 1 \end{pmatrix} \begin{pmatrix} s_{t-1} \\ z_{t-1} \\ x_{t-1} \\ y_{t-1} \end{pmatrix} + \begin{pmatrix} \omega_{s_t} \\ \omega_{z_t} \\ \omega_{x_t} \\ \omega_{y_t} \end{pmatrix}$$

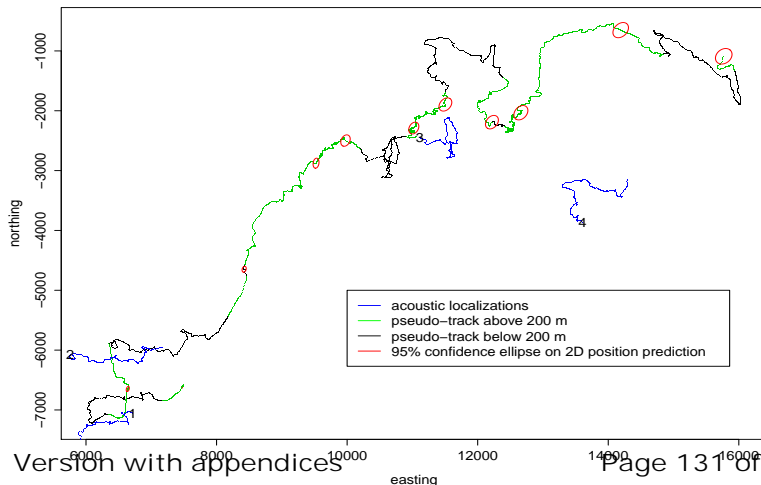
$$\begin{pmatrix} o_{z_t} \\ o_{x_t} \\ o_{y_t} \end{pmatrix} = \begin{pmatrix} 0 & 1 & 0 & 0 \\ 0 & 0 & 1 & 0 \\ 0 & 0 & 0 & 1 \end{pmatrix} \begin{pmatrix} s_t \\ z_t \\ x_t \\ y_t \end{pmatrix} + \begin{pmatrix} v_{z_t} \\ v_{x_t} \\ v_{y_t} \end{pmatrix}$$

³i.e. integrate steps 2, 3 and 8
⁴but note now we often have missing values in o_{x_t} and o_{y_t} .

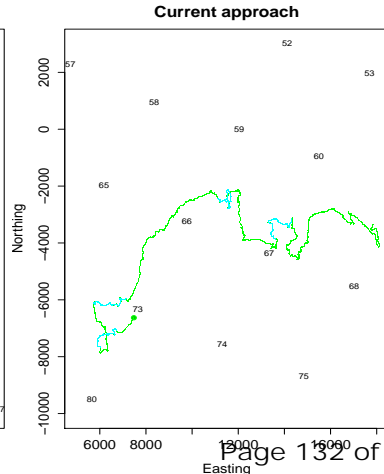
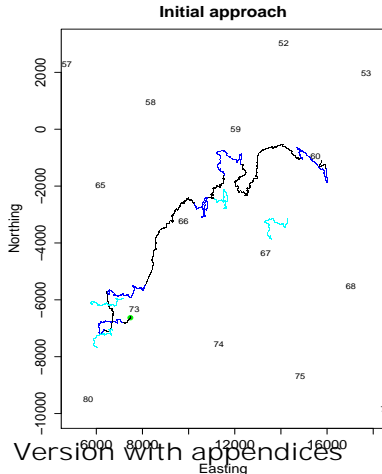
Predicting animal location - initial approach I



Predicting animal location - initial approach II



Predicting animal location - current approach



Existing procedure to estimate track from DTAG data

1. calculate 3D orientation (PRH) from three-axis accelerometer and magnetometer signals
 2. estimate whale speed using a 4-variate SSM with speed, depth, x and y as states and (noisy) depth and occasional x,y observations (pitch and heading still assumed as known covariates)
 3. use this speed estimate, jointly with tag-on position, pitch and heading in a dead-reckoning procedure embedded in the SSM to produce a "pseudo-track"
 4. use the DTAG sound file to identify clicks produced by tagged whale
 5. cross correlate these clicks with AUTECH hydrophones to find clicks time difference of arrival (TDOA) pairs
 6. interpolate TDOA lines to get multiple TDOA's for each click
 7. use multiple TDOA's to localize click (hence whale) in 3D space
 8. join output of step 7 with that of step 3 to arrive at a "georeferenced" track
- Version with appendices

Discussion

- ▶ integration of data seems possible and in particular provides error bounds for 3D whale location prediction over time
- ▶ initial model is (as expected!) biased and likely underestimates variance
- ▶ information on localization is fundamental to tie down track to a reasonable location
- ▶ improve current mechanistic model, which is clearly not adequate (very biased outcome in the absence of acoustic localizations); e.g. water current (velocity and direction) might need to be accounted for
- ▶ improve *ad hoc* (and previously unmentioned) procedure to keep speed and depth estimates admissible (i.e. speed positive, depth below surface) - any thoughts?
- ▶ look into the interpolating TDOA's algorithm to quantify measurement error in the x, y observation process

Version with appendices

Page 134 of 466

Our future approach

- ▶ include pitch and heading as states
- ▶ extend this to non-linear, possibly non-Gaussian, model: fancy, but still frightening!

$$\begin{pmatrix} s_t \\ z_t \\ x_t \\ y_t \\ \phi_t \\ \psi_t \end{pmatrix} = \begin{pmatrix} 1 & 0 & 0 & 0 & 0 & 0 \\ -\sin(\phi_{t-1})\Delta T & 1 & 0 & 0 & 0 & 0 \\ \Delta T \cos(\phi_{t-1}) \sin(\psi_{t-1}) & 0 & 1 & 0 & 0 & 0 \\ \Delta T \cos(\phi_{t-1}) \cos(\psi_{t-1}) & 0 & 0 & 1 & 0 & 0 \\ 0 & 0 & 0 & 0 & 1 & 0 \\ 0 & 0 & 0 & 0 & 0 & 1 \end{pmatrix} \begin{pmatrix} s_{t-1} \\ z_{t-1} \\ x_{t-1} \\ y_{t-1} \\ \phi_{t-1} \\ \psi_{t-1} \end{pmatrix} + \begin{pmatrix} \omega_{s_t} \\ \omega_{z_t} \\ \omega_{x_t} \\ \omega_{y_t} \\ \omega_{\phi_t} \\ \omega_{\psi_t} \end{pmatrix}$$

- ▶ look into the orientation algorithm to quantify measurement error in the observation process of pitch and heading

Thanks

- ▶ LATTE is funded by the US Office of Naval Research
- ▶ TAM partially funded by CEAUL
- ▶ I would like to thank Len Thomas, for not having fired me when he should have had, hence allowing me to return to an ISEC! It feels damn good to be here again.



Version with appendices

Page 136 of 466

References



Johnson, M. P. and Tyack, P. L. (2003).

A digital acoustic recording tag for measuring the response of wild marine mammals to sound.
IEEE Journal Of Oceanic Engineering, 28, 3–12.

Modeling beaked whale DTag data and simulating 3D movement via a latent-variable approach with feedback and semi-Markovian components

LATTE WORKING DOCUMENT

Tiago A. Marques, Roland Langrock & Len Thomas

Centre for Research into Ecological and Environmental Modelling
The Observatory, University of St Andrews, St Andrews, KY16 9LZ, Scotland

Version's date: October 22, 2015

Contents

1	Preliminary note	2
2	Introduction	2
3	The DTag data	4
3.1	Reading data in	4
3.2	Initial data processing	5
4	One dimensional modelling of depth profiles	7
4.1	Model and data details	7
4.2	The code	9
4.3	Implementing the code	9
4.3.1	Original run	9
4.3.2	Refitting model to JABES data	21
4.3.3	Excluding quadratic terms from deep diving transition probabilities	26
4.3.4	Fitting to multiple whales	26
4.4	Simulating from the model	28
4.5	Can we predict vocal state from depth profiles alone	35
5	Modelling displacement projected onto the sea surface	35
5.1	Unconstrained movement	35
5.2	Pros and cons of a conditional on depth approach	42

6	WIP: Modelling three dimensional dive tracks	43
7	placeholder: Modelling animal movement within a group	43
8	placeholder: Modelling 3D animal movement within a group	44
9	placeholder: Constraining movement models by 3D barriers	44
10	placeholder: Discussion and conclusions	44
	References	44
	Appendix	46
A	Estimating parameter variance	46

1 Preliminary note

This report was supposed to be about all that the introduction mentions it should be. However, we hit a wall regarding the estimation of depth profile model parameters based on DTag data, and therefore this report is essentially halted while we try to understand what is going on.

2 Introduction

In this report we attempt to fit a multitude of hidden Markov models (and extensions) to DTag data. The initial goal is to parameterize a model from which we can simulate realistic movement tracks for individual beaked whales.

This is a pre-requirement to a follow on objective not addressed here, which includes incorporating external factors (e.g. depth, home range, sonar exposure) in the movement model and adding the movement of whales within a group.

This report constitutes a support document for another document which describes the building blocks for setting up a simulation engine of beaked

whales at AUTECH (Marques and Thomas, 2012a), which includes details regarding the non-movement parts of said engine. A preliminary and deprecated report which might be relevant from an historical perspective to understand this document is Marques *et al.* (2013), dating back from before Langrock *et al.* (2013) and containing thoughts about using HMM to simulate dives.

We start by using the DTag data previously analysed in Marques and Thomas (2012b) to obtain georeferenced tracks for whale Md248b.

The goal of this report is ambitious: to obtain, within AUTECH, a realistic model to simulate beaked whale three dimensional dive tracks, both for groups and individuals within groups. This can be subdivided into 6 successive objectives which follow a natural order:

1. build on material from Langrock *et al.* (2013) to “warm up” and to get acquainted with the implementation of a fHsMM. This is also useful as it might provide insights and initial parameter values for objective 3 below. Because we have the acoustic data for Md248b we can actually use that data to evaluate when the whale was vocal, and hence to see how reasonable was the state assignment from the Viterbi algorithm, in particular regarding the 3rd behavioural state being interpreted as a foraging state. Note also this ties in with a point raised recently by McClintock *et al.* (2013) about the potential problems in identifying behavioral states with partial information (in his case, just x, y vs x, y combined with partial information on depth). Here the comparison would be from using just depth profiles vs depth and acoustic data.
2. build on material from Langrock *et al.* (2012) to fit a model to the whale’s 2D (x, y) data. Compare results with those obtained above, especially also in terms of state assignment in view of the point raised by McClintock *et al.* (2013).
3. build on the first two objectives output to fit a 3D model for movement, at first assuming conditional independence given the state on horizontal (i.e. in x, y) and depth (z) displacements.
4. build on the material in Langrock *et al.* (2014) to create a model for the movement of animals in a group. Since we can only get feedback from data when the animals are vocalizing, it seems adequate to do this

only for the periods when the animals are vocal. This corresponds to state 3 in the 7 behavioral states described in Langrock *et al.* (2013).

5. combine material from objectives 3 and 4 to get a way to simulate complete 3D tracks for all animals within a group.
6. Ideally, all the above will then have to be somewhat constrained such that the simulated movement also:
 - respects obvious x, y (i.e. land) and z (i.e. bottom depth) boundaries
 - preserves an existing density surface over a reasonable spatial and temporal scale.

This report is divided in to a number of sections. Following a section on the DTag data used, the above six objectives are addressed in turn in separate sections below.

3 The DTag data

3.1 Reading data in

We begin by reading in the available DTag data, which corresponds to whale Md248b, tagged at AUTECH in 2007. This whale DTag data has been analysed in detail in Marques and Thomas (2012b), and was the basis of the ISEC 2012 talk. Some of this data was taken directly from the R workspace used to implement the georeferencing procedure, other corresponds to outputs from that procedure.

We shortly describe the 3 objects read in:

- `md07_248b` - referenced to time since the tag-on event, a time indexed data frame with 316980 rows. Sampling occurs at 5 Hz and includes four variables: heading, pitch, roll and depth.
- `cli248b` - observed time, pitch, heading, roll and depth when each of the 22869 clicks the whale was produced, in the first 4 dives (for the 5th dive there was no longer an acoustic record - see Marques and Thomas (2012b) for details)

- `testing.KF3.test1` - the output of a Kalman filter to georeference the track building on independent localizations provided by AUTECH hydrophones, as described in Marques and Thomas (2012b). We focus here on the x, y estimated locations for each of the 316980 times in `md07_248b`.

An additional data set corresponds to object `interpxyz`, which contains the time indexed 3D localizations obtained from AUTECH's TDOA data.

This data can be summarized in figure 1, where the horizontal displacement and depth profiles are shown. Note we have data for 5 dives, but there are only DTag acoustic records for the first 4 dives. Further, there are only interpolation files for dives 2, 3 and 4. Dive 1 was harder to get georeferenced because not enough AUTECH localizations could be obtained. However, Jessica Shaffer did produce georeferenced files because the tag-on position was available and drift from that was assumed negligible, so we also had a georeferenced track based on said initial position.

3.2 Initial data processing

Because it might be interesting to compare the capability of the fHsMM used in assigning states (see section 4.5 for details), especially the foraging state, we also create a vocalization indicator variable (`voc`) inside `md07_248b`, such that `voc` is 1 if there was a click in the 1 second vicinity of the current period, and 0 otherwise¹.

Additionally, given the feedback mechanism involved, we also need to create a variable which represents the “time since the last deep dive”. As defined in Langrock *et al.* (2013), this corresponds to “the time since the whale last was more than 500 metres deep”.

Finally, as shown in the middle panel of figure 1, small scale measurement error means that some depths very close to the surface are sometimes registered as being above the water². This would not be a problem in general, but because we are using a gamma random variable to model depth we

¹Might a different variable be useful? As an example, could consider a `voc2` such that `voc2` is 1 between all `voc=1` previously defined within a deep dive. i.e., once vocal, the animals will only be non vocal when switching to the ascent state. See figure 1 bottom panel for details.

²Depth was never recorded to be more than 30cm above the sea level, which is reassuring and consistent with small scale measurement error.

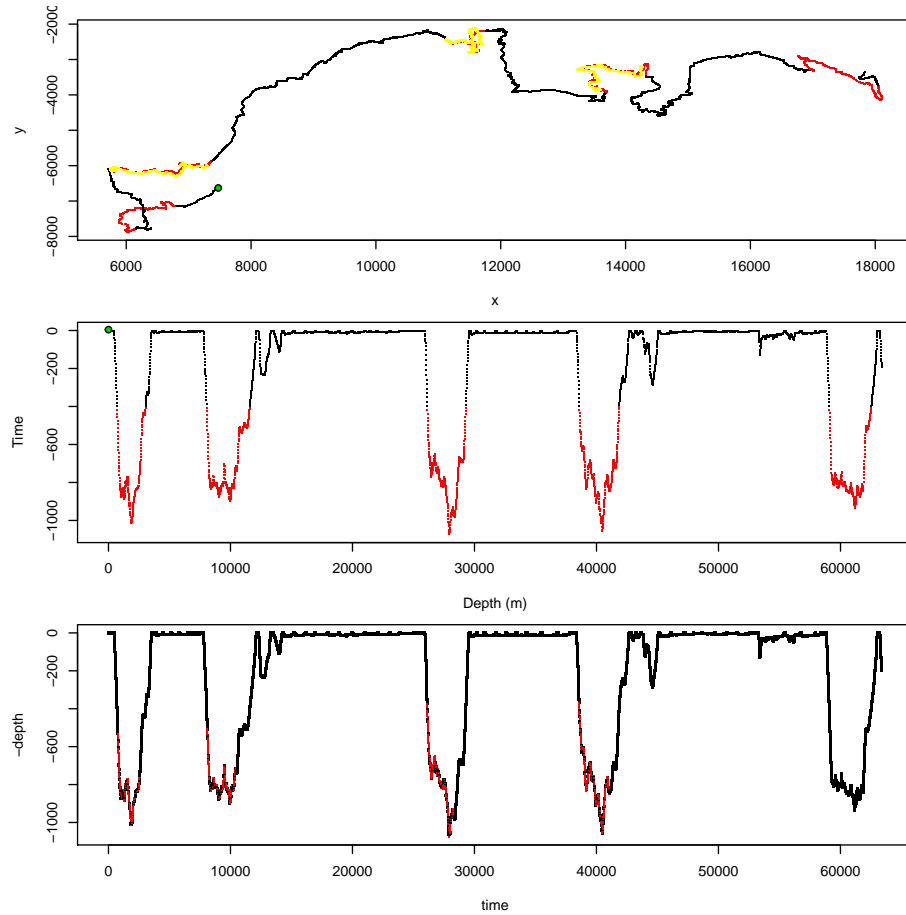


Figure 1: DTag data. Top panel: two dimensional view of the DTag data after georeferencing. Yellow represents locations from the interpolation TDOAs. Middle panel: depth profile. Green dot represents the first available position. Small red dots represent depths above the surface (i.e. errors). Red represents data below 400m depth. Bottom panel: the non vocal state seconds are shown in black. See many of these occur during the vocal state.

need a minor tweak of the data, with negligible consequences yet allowing implementation of the gamma likelihood. Because the gamma cannot cope with negative values (as the support of the gamma is strictly \mathbb{R}^+), we convert all depths to their absolute value, therefore forcing depths to be below the sea surface. Another perhaps more elegant alternative would be to consider modelling a transformation of depth (e.g. exponential) such that when transformed back to the original scale the response is necessarily positive.

4 One dimensional modelling of depth profiles

4.1 Model and data details

Langrock *et al.* (2013) presented a framework to model the depth profiles of beaked whales using a feedback hidden semi Markov model (FHSMM). The two extensions to the traditional HMM formulation were required for different reasons:

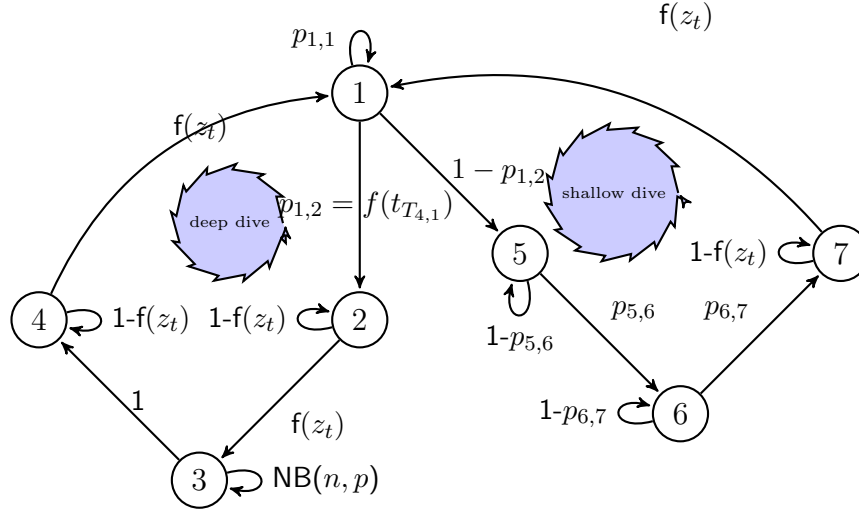
- the feedback component was used to make transition probabilities depend on the depth and time since specific events;
- the “semi”-Markovian component was used to allow non-geometric sojourn times in some of the states, which would otherwise be necessarily geometric due to the Markov model state transition formulation.

A gamma random variable was assumed for depth, with means and standard errors being conditional on one of 7 (hidden) behavioural states, which a priori were considered to correspond to:

1. at the surface
2. descent phase of a deep dive
3. foraging
4. ascent phase of a deep dive
5. descent phase of a shallow dive
6. bottom phase of a shallow dive

7. ascent phase of a shallow dive

A schematic representation of the model follows:



It should be noted upfront that the gamma mean was parameterized in such a way that the parameter to be estimated correspond to displacements rather than depths themselves, i.e. in state k the depth at time t , z_t , is given by a gamma with mean $\mu_t = z_{t-1} - \theta_k$, so we estimate the depth displacement rather than depth itself. Therefore, the parameter associated with the mean depth, conditional on state, should be positive on a descent state and negative in an ascent state, being approximately 0 in states for which there is no overall depth change.

The full model as presented in Langrock *et al.* (2013) encompasses 27 parameters:

- 14 of which are associated with state dependent probabilities (one mean and one standard deviation for each state)
- 13 are involved in transition probabilities, including those for the feedback and semi-Markovian components

Here we fit a similar model to data from Md248b. We overtly did not look into model selection issues, including changing the number of series terms used in the feedback mechanisms of some states. The input data corresponds to depths obtained directly from the DTag.

4.2 The code

A number of functions are required (and hence present in the underlying .Rnw file that this report is build upon), and are essentially those presented in the supplementary material to Langrock *et al.* (2013), upgraded with comments and some minor changes. These include functions to implement:

- the transformation and back-transformation of parameters
- generation of matrices of transition probabilities
- the evaluation of the log-likelihood, `mllk`, given parameter values
- the log-likelihood maximization routine itself, `mle`, which calls within it all the other functions
- a decoding function, `viterbi`, based on the Viterbi algorithm, which is used to predict the most likely state-sequence given observations

4.3 Implementing the code

We present in this section results from a variety of fitting exercises. However we leverage directly on analysis which have their own code and R workspaces living in subfolders under this report’s folder “RunInOctopus”. There are a couple of reasons why we proceed in this way:

1. this would be too much clutter to be all kept in the same .Rnw
2. these take so much time to run that they had to be run remotely in other machines any way, namely flipper and octopus

Hence here we just use results from those remote runs.

4.3.1 Original run

For implementation we start by defining the initial values for the 27 parameters in our model. An initial state distribution is also required. We begin by using for both of these sets of initial values those considered by Langrock *et al.* (2013). The initial state distribution is currently hardwired in the code

and as Langrock *et al.* (2013) we considered that the animal was certainly in state 2 (descent on a deep dive) when the recording started³.

```
## initial parameter values used in the numerical maximization
#(several different sets of initial values should be tried
#in order to ensure hitting the global maximum)
theta0    <- c(-5,15,0,-8,4,0,-4)
sigma0    <- c(1,5,8,4,4,1,4)
omega0    <- c(0.93,0.97)
sm0       <- c(150,20)
zeta0     <- c(-0.4,0.03)
alpha0    <- c(-2,0.5,-0.03)
gamma0    <- c(0.5,-8)
beta0     <- c(-0.15,-0.2,0.05)

# size of the state aggregate in the HMM-based approximation of the model
#with semi-Markovian state 3 (needs to be sufficiently large,
#but not excessively large, as the HSMM component substantially
#increases the computational effort)
m <- 250
```

Finally, we can run the code to maximize the likelihood and obtain the maximum likelihood parameter estimates.

```
#Note this would take tens of hours to run.
#Hence we rely on reading in data
#from other folders rather than using the code here.
#The original code is here for completeness

Sys.time()->s
# run numerical maximization of the likelihood
mle(dat4fhsmm,theta0,sigma0,omega0,sm0,zeta0,alpha0,gamma0,beta0) -> fHSMM
# display computing time
Sys.time()-s
# display results
```

³As described below, this will lead to problems as while it was reasonable for Langrock *et al.* (2013), that was clearly not the case for Md248b

We represent the gamma state conditional mean and standard deviation parameter estimates and the corresponding starting values in Figure 2. To put these in context we also present the values from Langrock *et al.* (2013). These were estimated for another whale, with a much longer depth time series. There are a couple of striking differences, related to the means of the gamma distribution for states 1 and 2. For both of these the values observed for Md248b are, compared to those from Langrock *et al.* (2013), more in line with what might be expected a priori:

- state 1 should have a mean value close to 0, although the interpretation of this parameter is far from straightforward, due to the technicality⁴ described in equation 1 of Langrock *et al.* (2013). As $\mu_t = \max(z_{t-1} + \theta_n, 1)$, the **max** operator enforces that, for this state, the mean depth in time t , μ_t , is actually 1 rather than any value that the estimated parameter θ itself might lead to. This occurs if $z_{t-1} + \theta_n$ was below 1 meter, which is very frequent for the 1st state (at the surface).
- the mean in state 2 seems too big in Langrock *et al.* (2013), while for Md248b it is similar in absolute value to the mean in state 4. There are two possible alternatives:
 1. our result would make sense if the ascent and descent phases from a deep dive took the same time at the same speed
 2. but ascent and descent speeds have been reported to be different elsewhere Tyack *et al.* (2006), implicitly leading to different time lengths for ascent and descent, which would mean that the values reported in Langrock *et al.* (2013) would be probably more adequate.

In section 4.3.2 we fit again the model to the data from Langrock *et al.* (2013), with other starting values for these two mean related parameters, to check whether the parameter estimates obtained for these two states might have been unduly influenced by starting parameters, which is a priori unlikely as that was extensively investigated by RL before.

⁴Some code to look at the effect of this technicality is embedded as comments in the .Rnw file

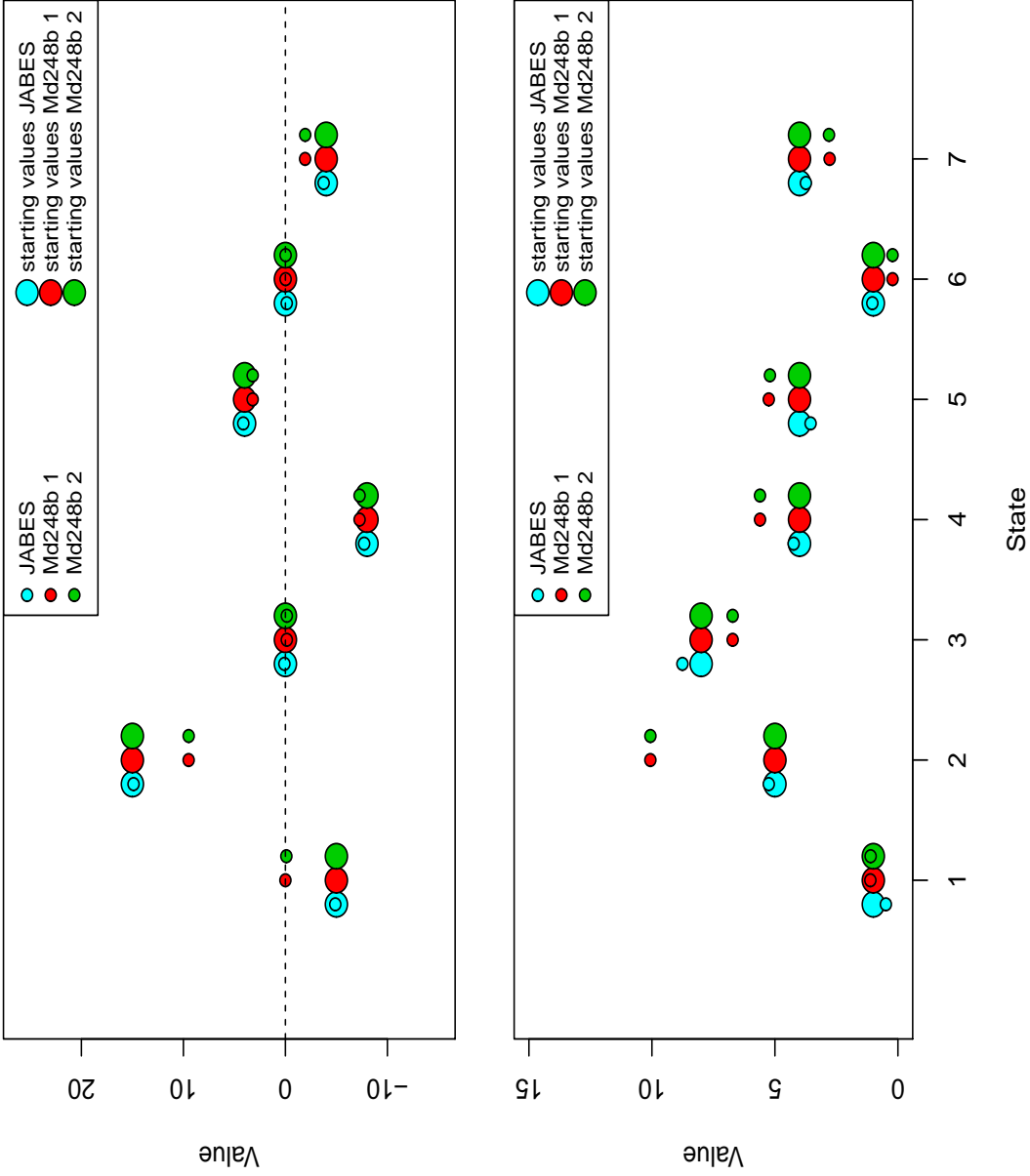


Figure 2: Starting values and parameter estimates for the state dependent gamma distribution parameters, both for the JABES paper as well as for two runs of d248b (with slightly different starting values of some parameters associated with the transition probabilities).

No clear patterns became apparent when looking at the parameter estimates associated with transition probabilities (Figure 3).

Note that there are considerable differences in the time spent foraging in a deep dive between the two whales considered, as can be seen in figure 4. Nonetheless, given what is known about the diving behaviour of these whales (e.g. Tyack *et al.*, 2006, refer 26.6 minutes on average for the vocal phase), the values obtained here for Md248b seem way too long for being adequate, the average time spent in state 3 being beyond the observed maximum (33.1 minutes) for the vocal phase by Tyack *et al.* (2006).

We then used the Viterbi algorithm to decode the states, i.e., provide an estimate of the most likely state at each time period given the available observations. The outcome is in figure 5.

A possible source for the problems noted above might be the fact that the animal seems to be at the surface when the recording starts, yet we have assigned it to be in the descending state, given the initial state distribution used. Zooming in the data we see that is certainly not adequate for Md248b (figure 6). Based on this fact, and because it is convenient that the whale is in state 2 when the analysis starts (because this does not require the time since last deep dive covariate to be available), we opted by removing the first 48 data points (corresponding to 480 seconds) and refitting the model.

The state assignment results are shown in figure 7.

We can look at the impact on the time spent in state 3 (cf. figure 8), which we had seen to be likely badly estimated before (cf. figure 4).

In a similar way, we can look again at the parameter estimates for this final model.

```
#load up the results run in octopus,  
#initial values same as JABES, but now with  
#the first 48 data points removed  
load("RunInOctopus/F2/F2.0/fHSMM6.Rdata")
```

What becomes apparent is that while the mean displacement in state 1 is indeed again estimated as essentially 0, the mean in state 2 becomes even larger than before and similar to what Langrock *et al.* (2013) had obtained, which given Tyack *et al.* (2006) is not implausible.

The likelihood surface is highly dimensional and hence one should attempt to rerun the model with different starting values to assess the possibility that we might have hit a relative maximum, rather than the absolute maximum

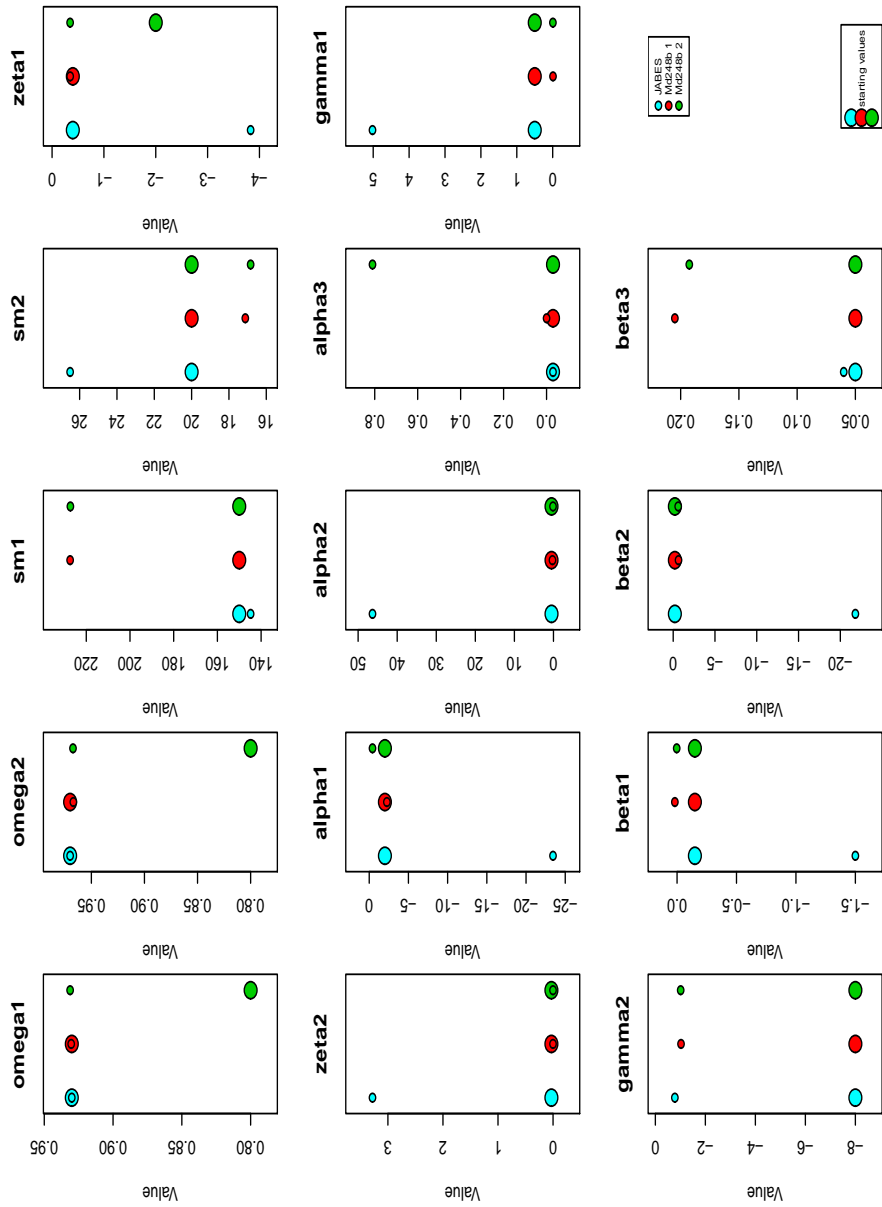


Figure 3: Starting values and estimates for parameters associated with transition probabilities, both for the JABES paper as well as for two runs of d248b (with slightly different starting values of some parameters associated with the transition probabilities).

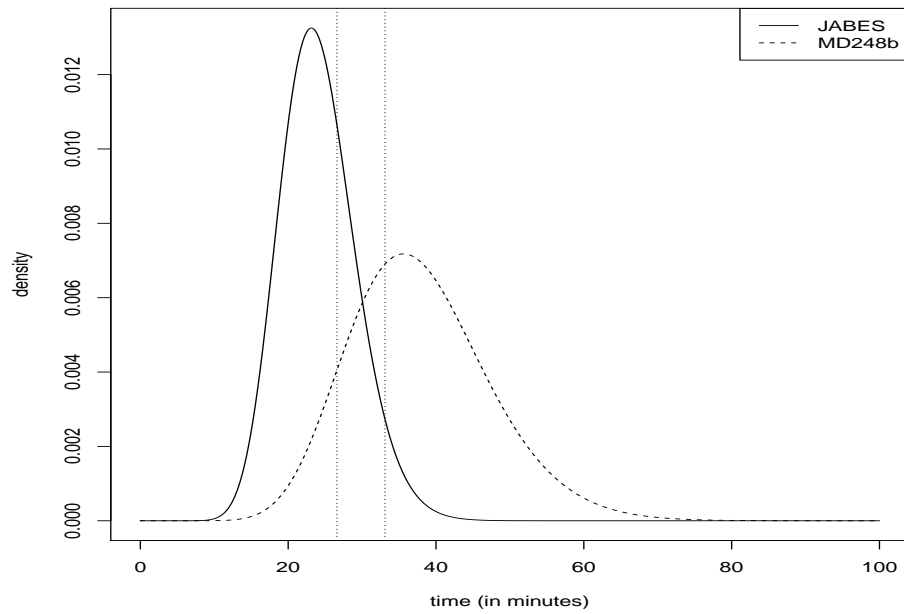


Figure 4: Distribution of the estimated time spent in state 3 for Md248b and the whale analysed in JABES. The dotted vertical lines represent the mean and maximum duration of the vocal period reported by Tyack *et al.* (2006), which should exceed slightly the time spent in state 3 (as some clicks are known to be produced while on what would be the descent phase - state 2).

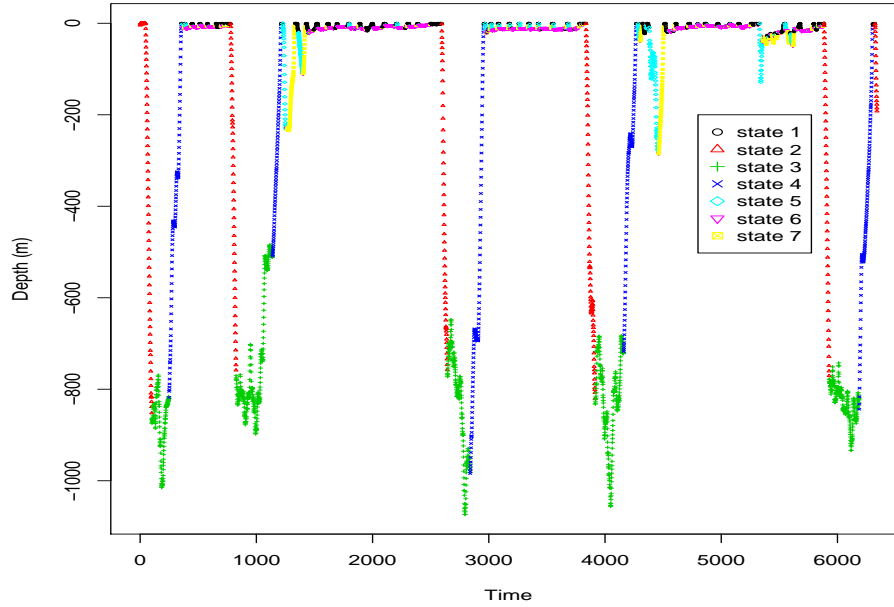


Figure 5: State decoding using the Viterbi algorithm for Md248b.

of this surface. Having run a number of different starting values we never obtained a value lower⁵ than 1.01591×10^4 , and hence we assume that this is a reasonable approximation to the desired MLE.

Note that, as stated upfront, the data set used contains a small number of transitions between each state (especially for deep diving states, as there are only 5 deep dives), and hence it is not clear at this point whether parameters associated with these are robustly estimated. In figure 10 we can take a look at the estimated relationships between the transition probabilities and the feedback covariates (depth and time). The functions are somewhat different from those in Langrock *et al.* (2013), though the functional form is at least similar, except for $\gamma_{2,3}$, for which parameter estimates are meaningless. Additionally, it should be noted that the probability associated to transitioning into a deep dive is so low compared to Langrock *et al.* (2013) that simulations from such a model would not lead to reasonable dive profiles. In the next section we continue to investigate why this might be the case by refitting the

⁵The numerical routine used works as a minimization routine on the negative log-likelihood

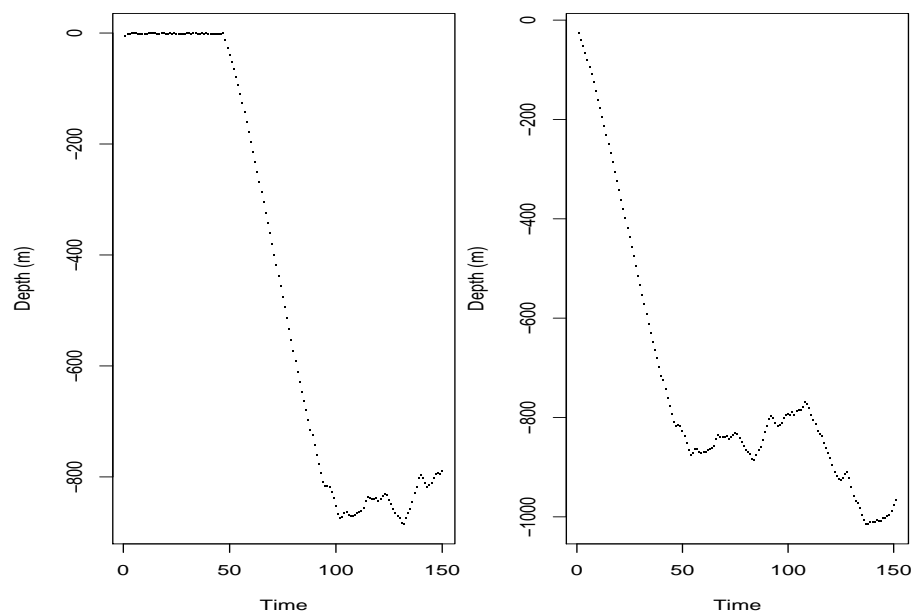


Figure 6: Zooming in the first few data points for Md248b. Left: the original data, where clearly the animal is not in the descent phase when the recording starts. Right: the same data deleting the first 48 time steps.

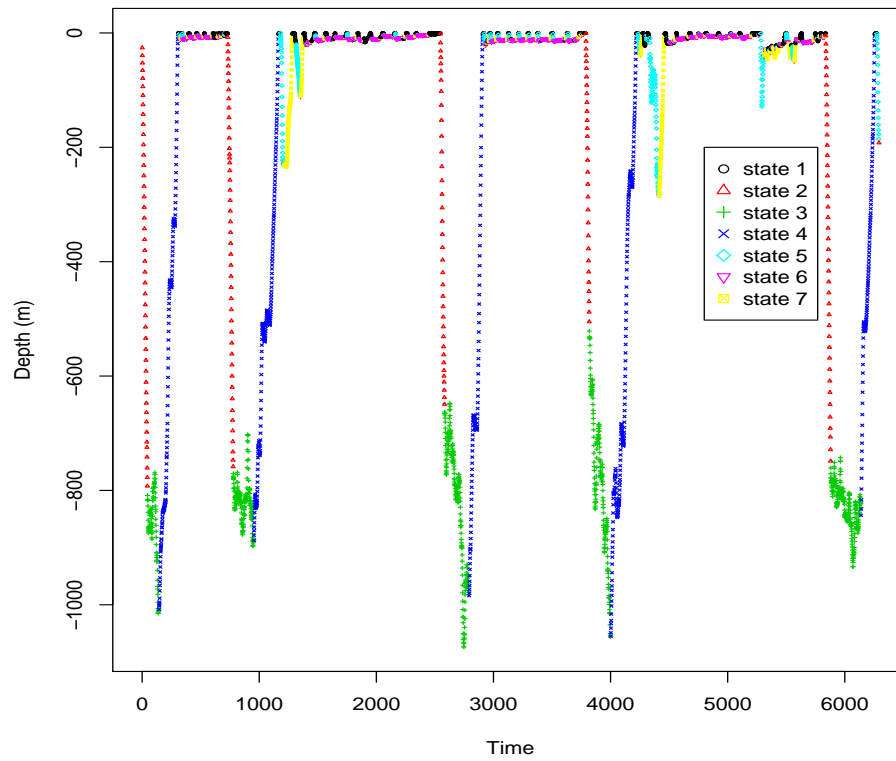


Figure 7: State decoding using the Viterbi algorithm for Md248b after removing the first 48 data points.

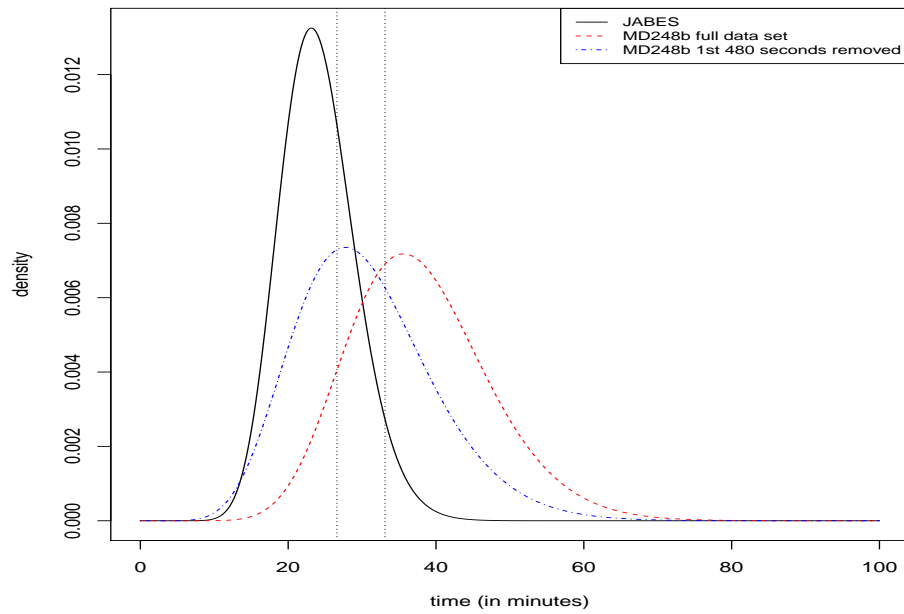


Figure 8: Distribution of the estimated time spent in state 3 for Md248b and the whale analysed in JABES. The dotted vertical lines represent the mean and maximum duration of the vocal period reported by Tyack *et al.* (2006), which should exceed slightly the time spent in state 3 (as some clicks are known to be produced while on what would be the descent phase - state 2).

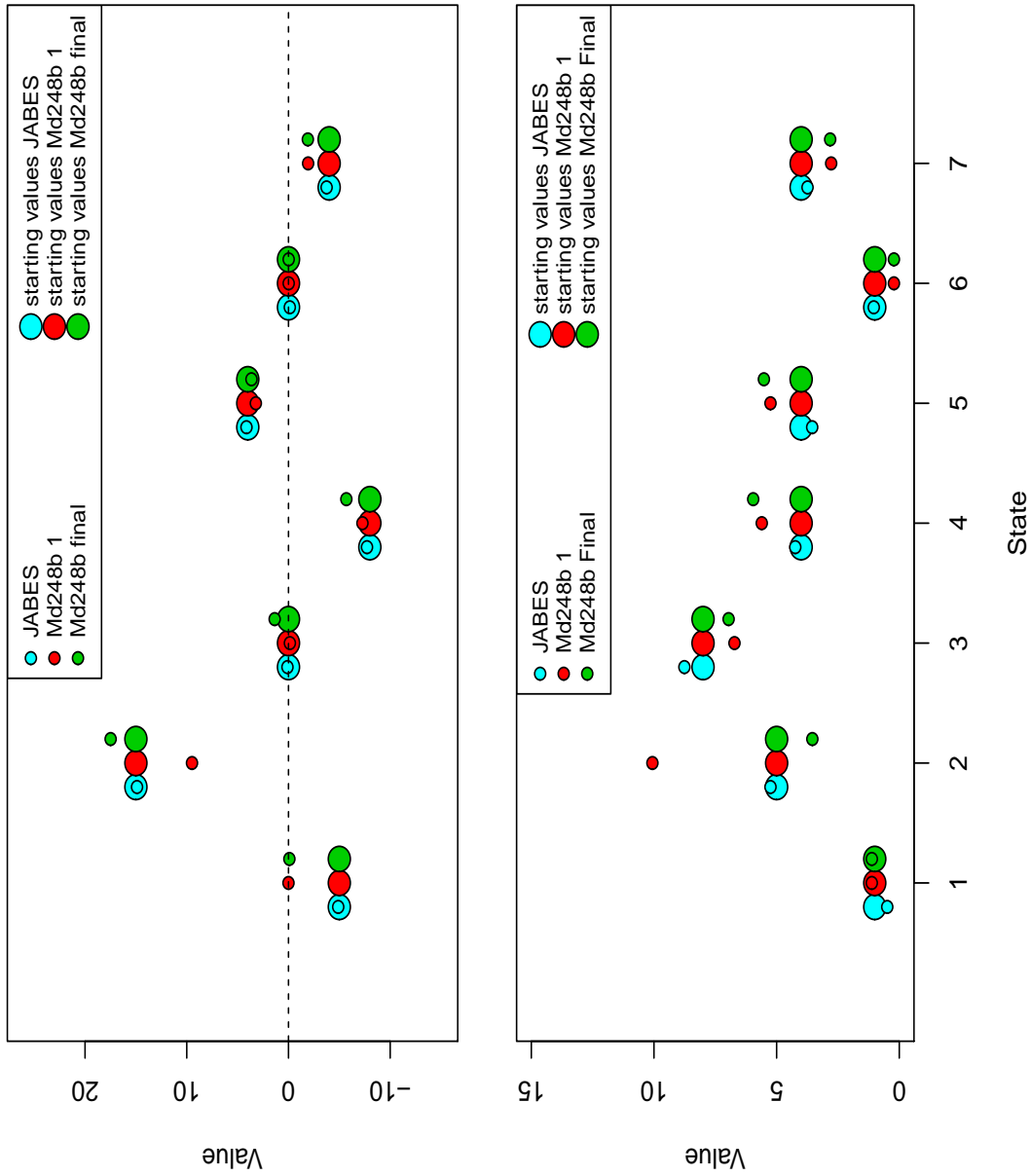


Figure 9: Starting values and parameter estimates for the state dependent gamma distribution parameters, both for the JABES paper as well as for the initial (all data) and final (first 48 data points removed) runs of Md248b.

model to the data from Langrock *et al.* (2013).

4.3.2 Refitting model to JABES data

We refitted the model of Langrock *et al.* (2013) with different starting values, in particular with the mean for the 1st two states conditional means close to 0, and yet in fact the submitted parameter estimates were obtained, which means that this is likely the maximum likelihood estimate of the parameters involved. As previously stated, in particular the mean of state 1 is hard to interpret due to the `max` operator.

The parameter values reported in Langrock *et al.* (2013) could not be matched exactly, which was unexpected. Just using slightly different versions of R could cause us to observe small differences, and so the values are nonetheless OK-ish for most parameters. The functional forms obtained from these parameters are close to those reported in the paper (cf. figure 11, estimated here, with figure 12, reproducing JABES results).

```
load("RunInOctopus/JABES again/hessian true/fHSMM.HT.Rdata")
#reproducing the parameter estimate values in table 3
#workspace with object fHSMM.HT object is attached
#OK-ish
round(fHSMM.HT$theta,2)

## [1] -4.94 14.90  0.10 -7.72  4.22 -0.12 -3.67

#OK-ish
round(fHSMM.HT$sigma,2)

## [1] 0.49 5.27 8.75 4.24 3.60 1.04 3.76

#ok-ish
round(fHSMM.HT$omega,2)

## [1] 0.93 0.97

#ok-ish
round(fHSMM.HT$sm,2)

## [1] 135.50 27.05
```

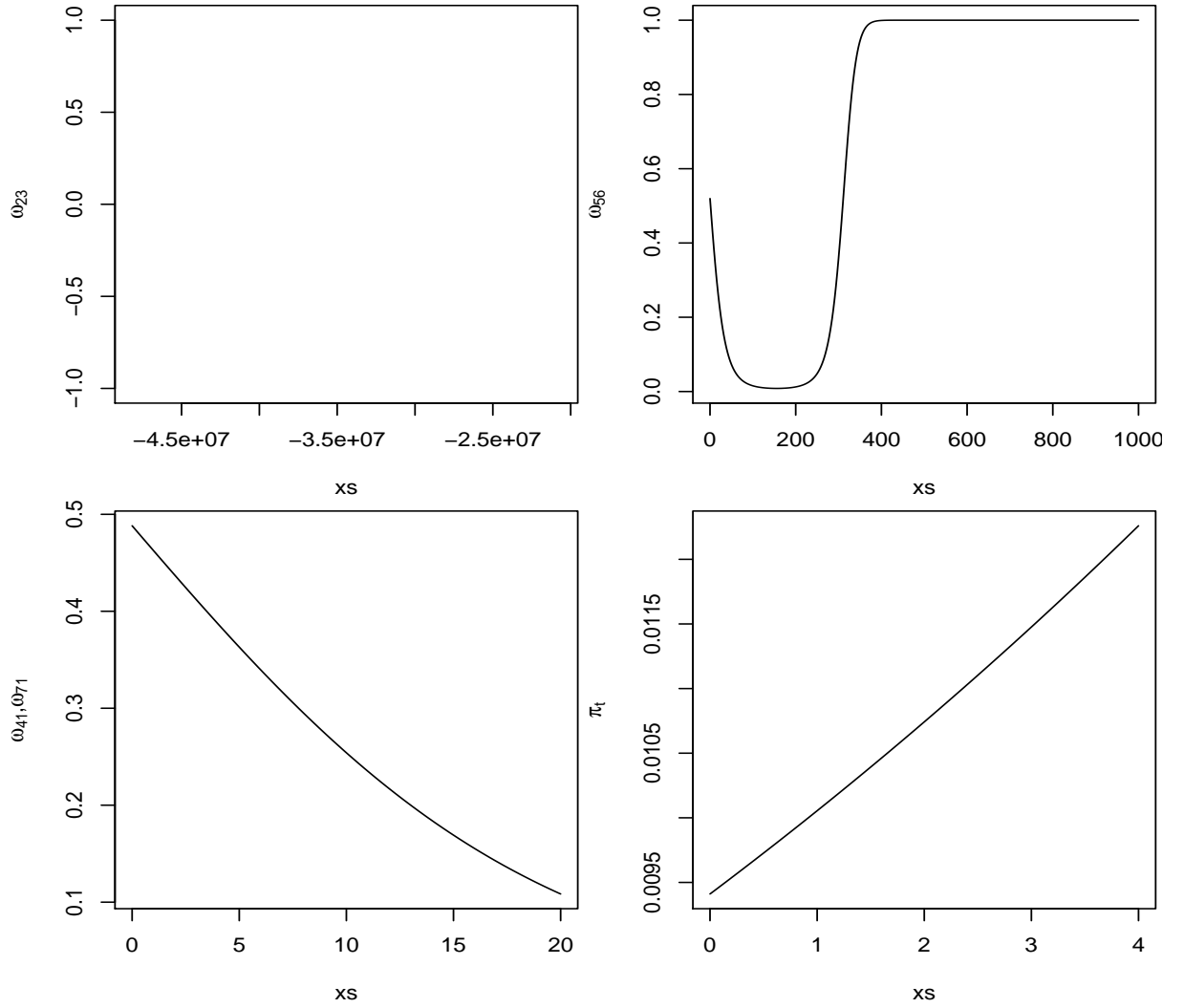


Figure 10: Transition probabilities as a function of feedback covariates for Md248b.

```

#ok-ish
round(fHSMM.HT$zeta*c(1,10^3)*c(10,1/10),2)

## [1] -3.83  3.28

#####
#                               nonsense
round(fHSMM.HT$alpha*c(1,10^3,10^3)*c(10,1/10,1/1000),2)

## [1] -4.39 -135.10 -12.25

#####
#ok-ish
round(fHSMM.HT$gamma*c(10,1/10),2)

## [1]  4.86 -0.80

#ok-ish
round(fHSMM.HT$beta*c(1,10^3,10^3)*c(10,1/10,1/1000),2)

## [1] -1.35 -24.57  0.07

```

However, for the α parameters in particular we now get nonsense estimates, namely -4.386 , -135.099 and -12.248 , which are far from those reported in the paper's table 1, namely $(-23.5, 46.46/10^3, -0.03/10^3)$.

There were actually a couple of reasons for these differences:

- differences in data and code used: in the paper we had used data with some missing observations (and the code that deals with them), while here we were using data with those missing observations imputed (and hence simpler code not having to deal with these)
- numerical instability: despite having managed to get adequate estimates given some particular starting values (and these being apparently a true maximum in the likelihood function), RL also found the same nonsense estimates for other starting values, associated with local maxima. So these methods seem to be very sensitive to numerical maximization problems⁶. This is hardly surprising given the high number

⁶As an aside, we had noted that minor differences in parameter estimates associated

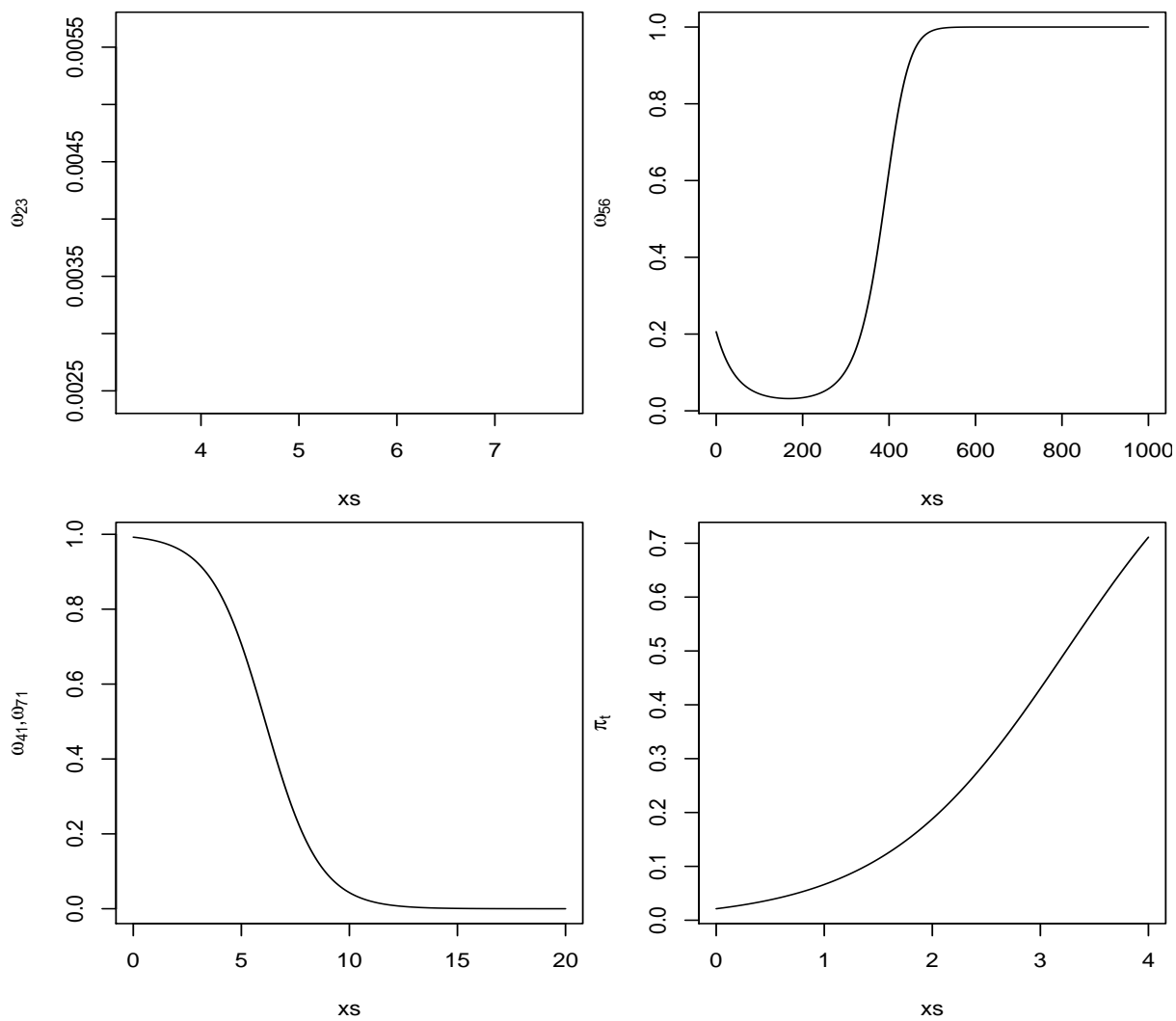


Figure 11: Transition probabilities as a function of feedback covariates for JABES data, re-estimated here

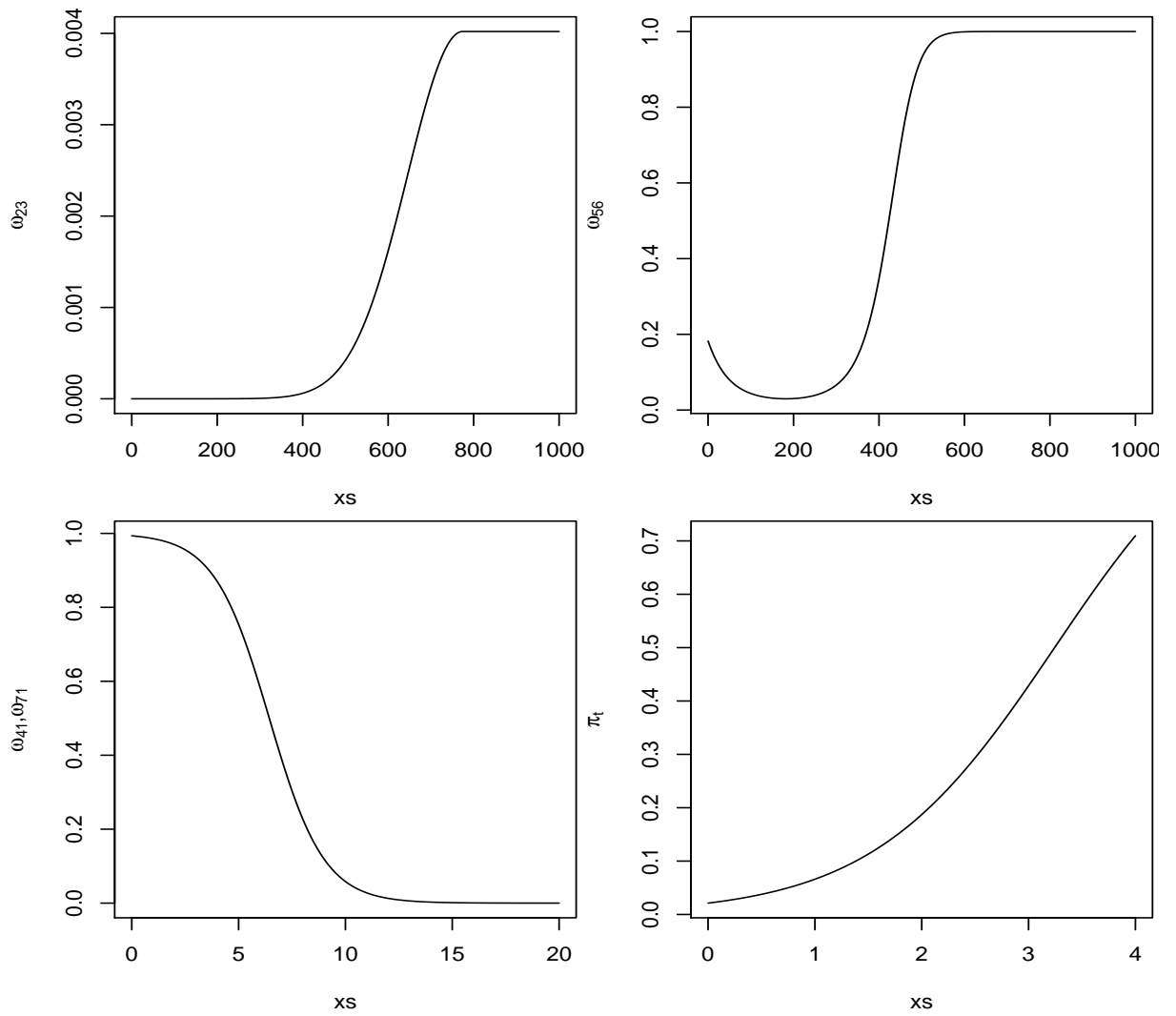


Figure 12: Transition probabilities as a function of feedback covariates for JABES data, based on the paper's table 1 values.

of parameters to be estimated.

It seems that in particular parameters associated with the quadratic terms are very unstable, and so one might consider

- not using them, if a linear term seems enough, or
- explore alternative functional forms in the predictors, e.g., using I-splines, as a reviewer pointed out and then suggested in Langrock *et al.* (2013).

The current problem is whether we can actually estimate the quadratic term associated with transition from state 2 to 3 ($\omega_{2,3}$) with our Md248b (or any similar sized) data set. While we have many non-transitions, i.e. state 2 at time $t-1$ and state 2 at time t , we actually only have five deep dives, i.e. 5 transitions where state 2 at time $t-1$ was followed by state 3 at time t . So it is not surprising that we have trouble estimating this transition probability. In the next section we attempt a fit removing the quadratic term, to see if we get a sensible functional form for $\omega_{2,3}$.

4.3.3 Excluding quadratic terms from deep diving transition probabilities

Because of the lack of information in deep dive transition probabilities noted above, we decided to exclude quadratic terms from the deep diving transition probabilities.

While the differences on estimated parameter values for the (state conditional) gamma distributions was negligible, the estimated transition probability forms became nonsensical (figure 13). In particular, the probability of entering a deep dive is still so small (bottom right) that simulating from this model would lead to essentially no deep dives arising. This is clearly at odds with the data, and must mean something is wrong.

4.3.4 Fitting to multiple whales

The work developed up to this point was fundamental but of little practical consequence, because what we require is a model from which to simulate from.

with these quadratic terms led to considerable differences in the actual shape of the resulting function, which in itself was a hint that numerical problems could occur

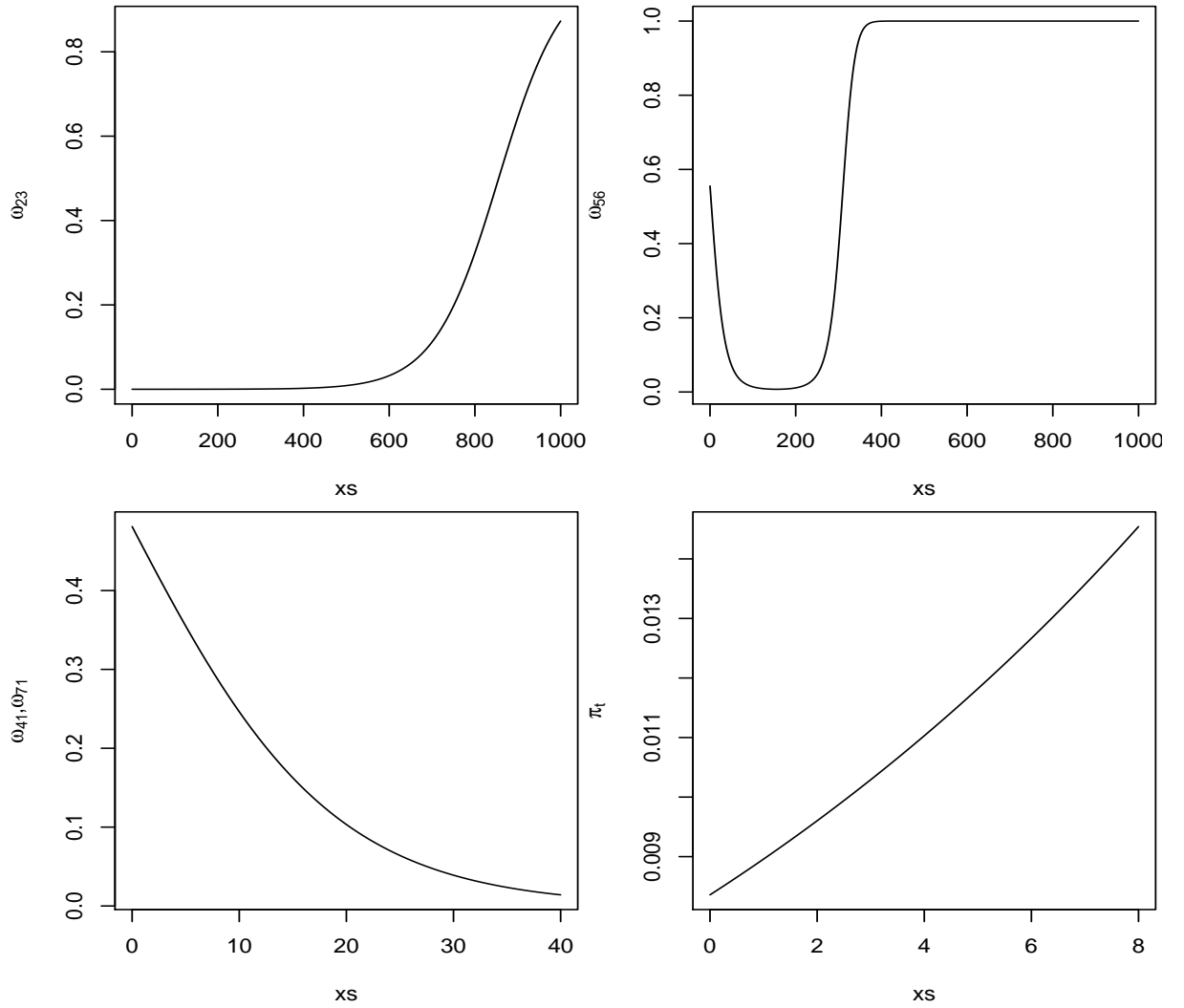


Figure 13: Transition probabilities as a function of feedback covariates for Md248b, considering a model without quadratic terms.

Having parameter estimates based on a single data set will not account for variability in parameter estimates across different animals, which would be certainly desirable to, if not necessarily to trust⁷, to justify and explain to others the inputs and outputs of such simulation.

A possible option might be to construct a likelihood using data from multiple animals, hence ending up with a parameter estimate which would include in its variance estimate the variability across different individuals. Given the time it takes to fit the models to a single whale, this seems quite demanding computationally. Further, this is not the conceptually best way to include variance in the parameter estimates, as presumably what we would want is to get estimates across multiple animals and then estimate the variance in parameter estimates (and their covariances across parameters) to simulate from. Assuming that parameter estimates are distributed as a multivariate gaussian and simulating from it might be a possible approach (e.g. using something like `mvrnorm` in package `MASS`).

To begin with we consider an additional data set, corresponding to whale Md07_248a.

To allow the use of the same likelihood and in particular the same initial distribution we consider truncating the data from Md07_248a, such that the data used for fitting starts on state 2. Despite losing some data, this is convenient because, as stated before, it means the time since the last deep dive, otherwise unknown, is not needed. On the other hand, the initial bouncing dives observed after the Tag was deployed might be atypical anyway. The truncated data used for both whales is shown in figure 14. While the amount of time is similar, the second whale considered has 2.5 additional dives than our original whale.

This has already run, but the results from this have not yet been analysed or reported here. However, these results were still producing nonsensical parameter estimates, and are therefore on hold until I can solve the issues with a single whale analysis.

4.4 Simulating from the model

Given that we have a fitted model, we can simulate depth profiles from that model. To begin with we simulate from the model fitted to the data used in

⁷As the fine scale differences obtained by adequately accounting for variability on parameter estimates across animals might represent a level of tuning with little practical influence on results, which will mostly be driven by the type of overall model considered.

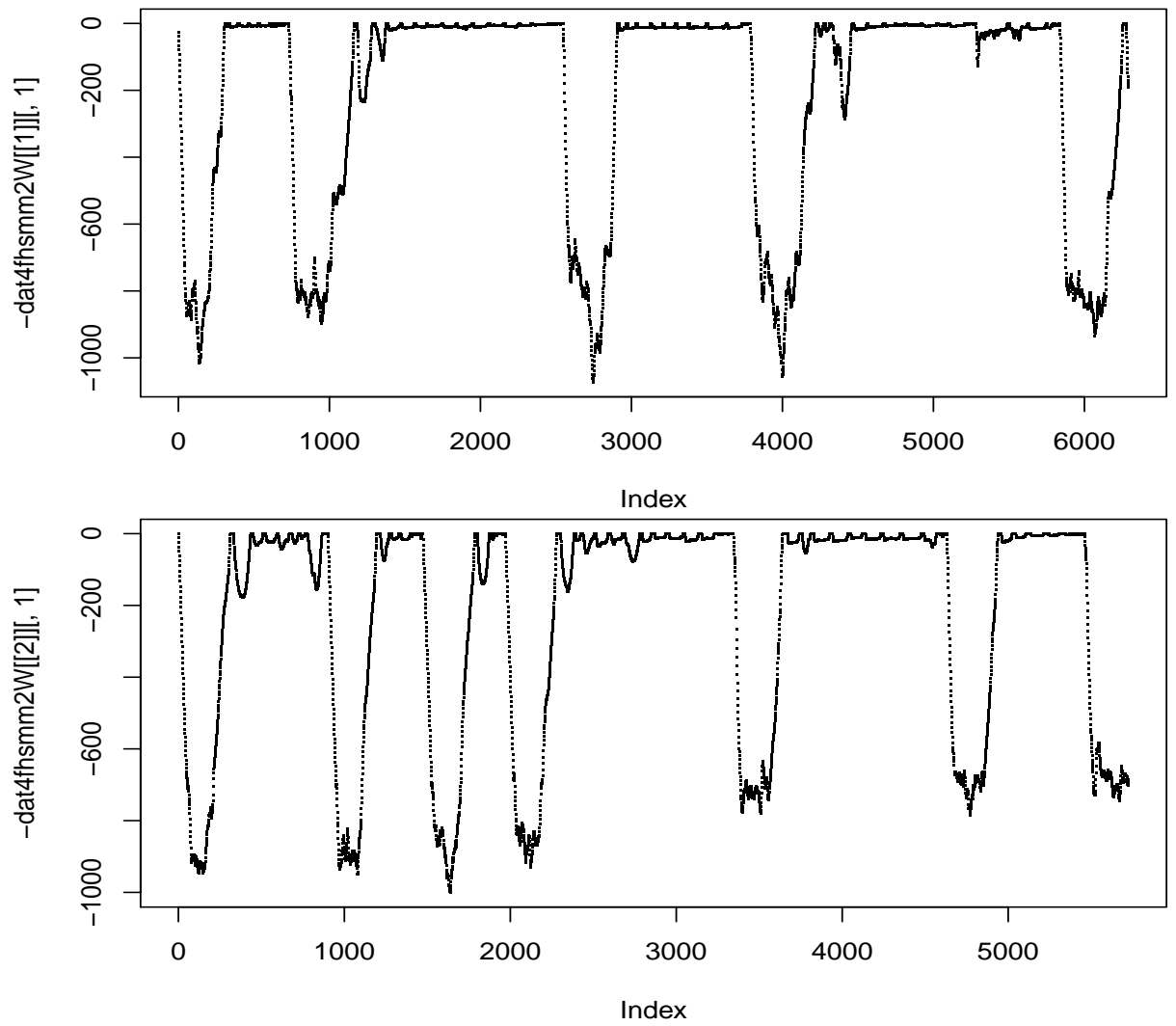


Figure 14: Depth profiles of the two whales used for jointly fitting the model.

Langrock *et al.* (2013). An example realization is shown in figure 15. There is nothing obviously wrong with this depth profile. We can take a look at the autocorrelation function for depth displacements pooled across states and within states (Figure 16).

Notice how depth differences conditional on state are independent when we simulate from the model, yet these have significant autocorrelation functions (acf) at lag larger than 1 in the original data (Figure 17). A couple of remarks on these figures:

- the pattern in acf plot of depth displacements (top middle plot) is an artifact created by an induced correlation structure in the differences because within different states these tend to occur in different areas of the 2D state space for the pooled successive differences, as shown in the top left plot.
- for the data itself, some of the patterns in the state-conditional acf plots might be artifacts as dwell time in some states is small. Therefore, one should not just pool across successive state runs to get the autocorrelation function, as we have done here assuming that the consequence of doing so would be minor, which would be the case if there were no frequent state transitions. If the mean dwell time in a state is q time units, the acf function can only be calculated up to lag $q - 1$, and likely just reliably estimated up to lag $q - d$, where d is some integer. Therefore, acf functions are presumably more reliable for states 2-4 than for states 1 and 4-7. **TO DO: obtain the observed distributions of dwell times per state.**

In conclusion, we now have a way to simulate depth profiles for beaked whales, but it is possible that our model does not capture all the correlation structure present in the actual animal movement. We proceed under the assumption that these are features which, at the level of detail we are interested, can be considered negligible.

Unfortunately, and not surprisingly given the values for some of the estimated transition probabilities, when we simulate from the model fitted to our Md248b, we just get a nonsense outcome (Figure 18), with simulated depth profiles being nowhere close to what we observed. **Which leaves us wondering what we can do next...?**

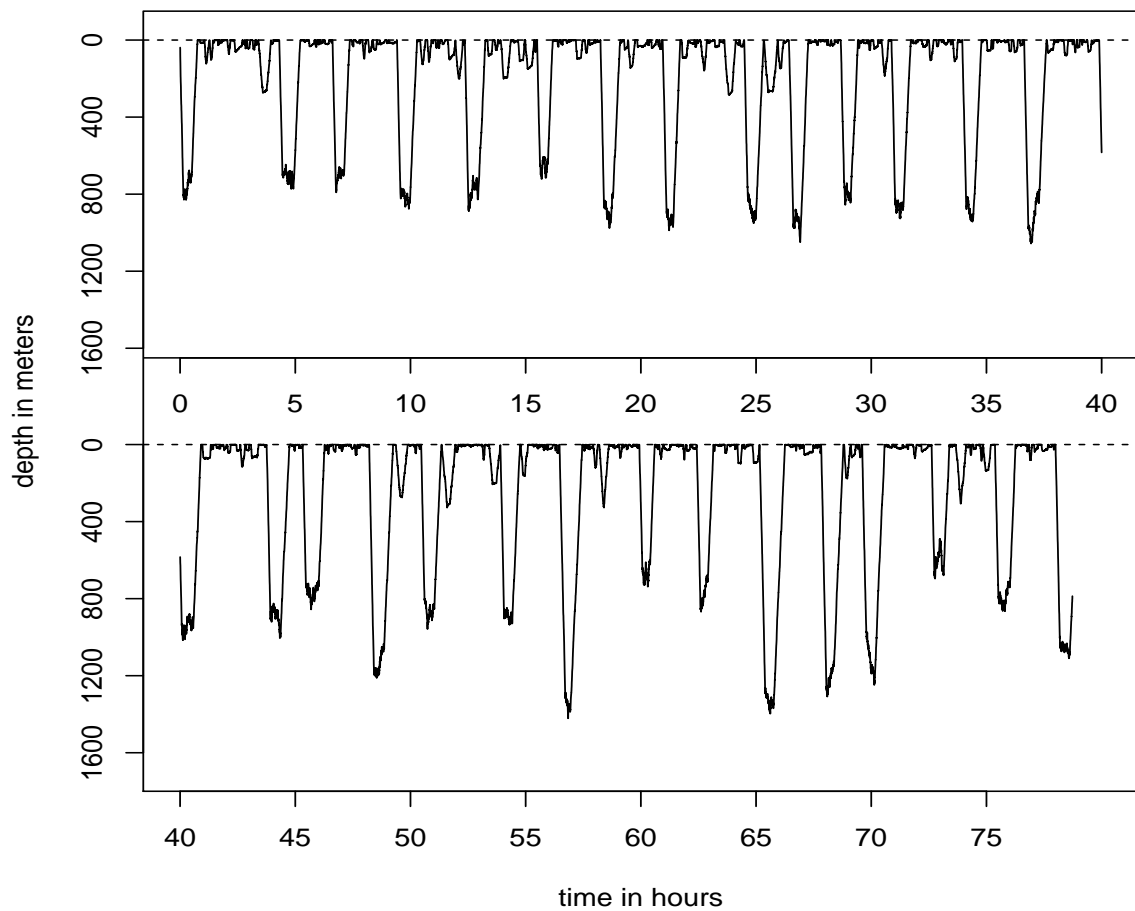


Figure 15: A realization of a depth profile simulated from the model fitted to data from Langrock *et al.* (2013).

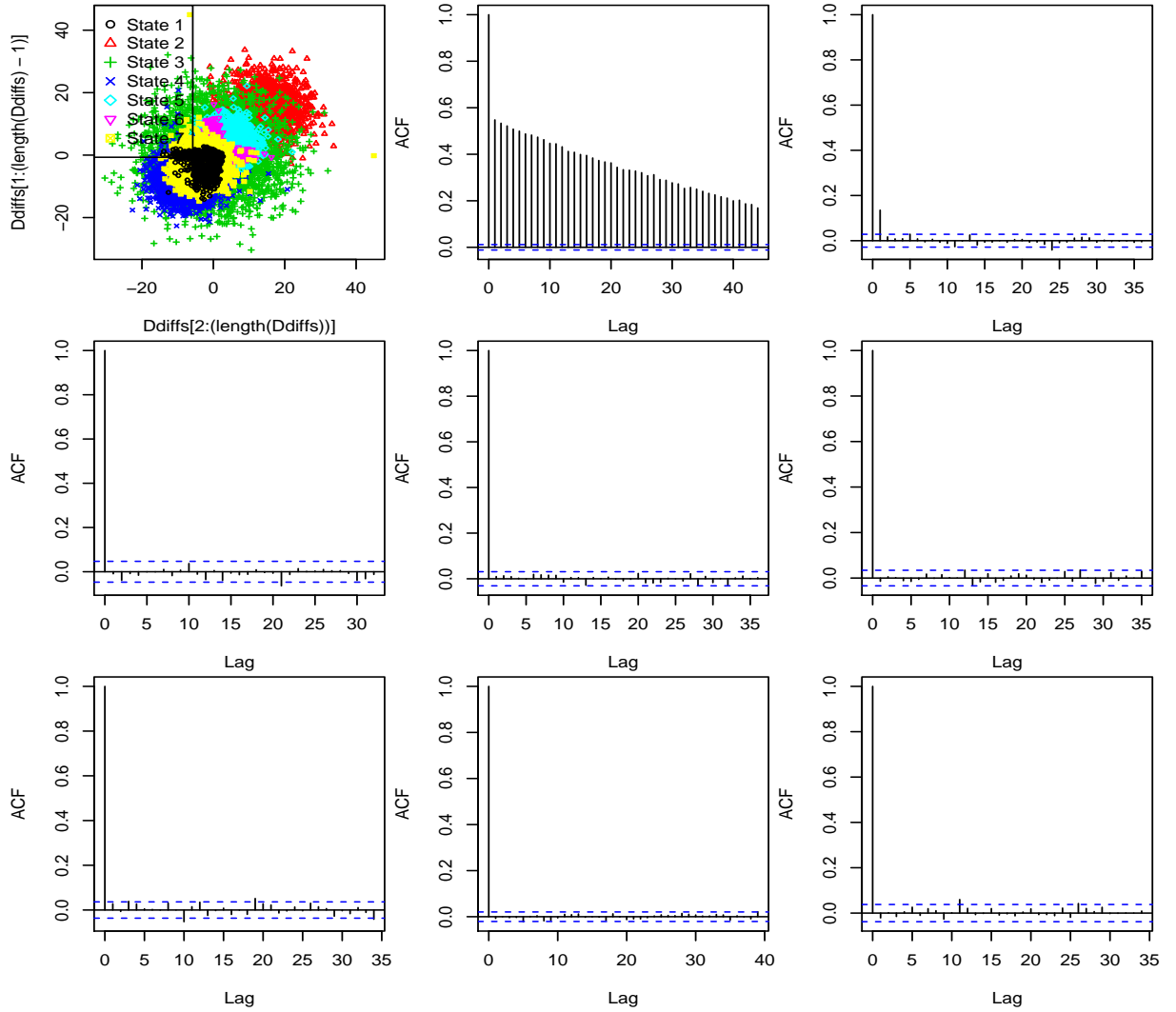


Figure 16: Autocorrelation within depth differences conditional on state assignment for the simulated data. Top left plot is the differences, with state represented by a different color. Top center is the autocorrelation function ignoring states. Other plots are autocorrelation functions within states.

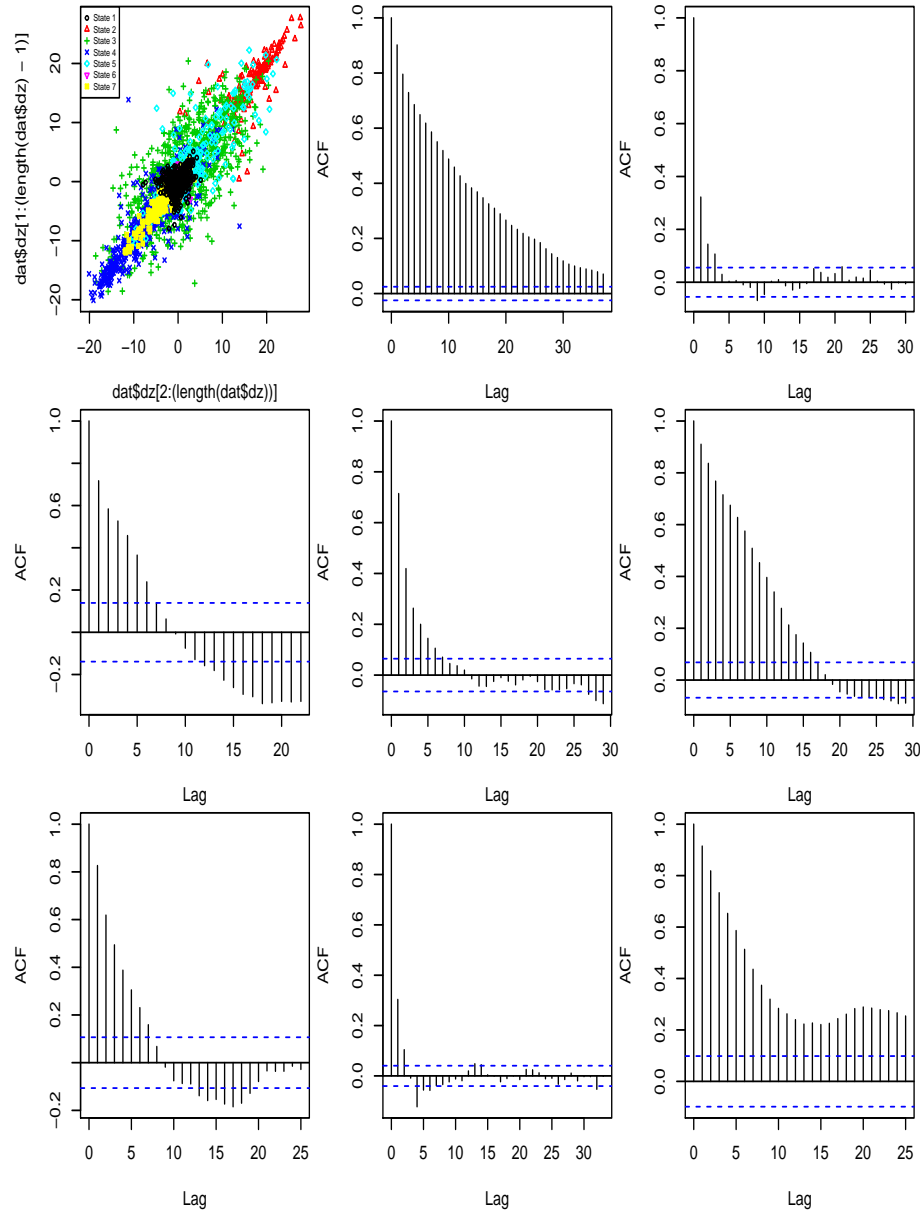


Figure 17: Autocorrelation within depth differences conditional on state assignment. Top left plot is the differences, with state represented by a different color. Top center is the autocorrelation function ignoring states. Other plots are autocorrelation functions within states.

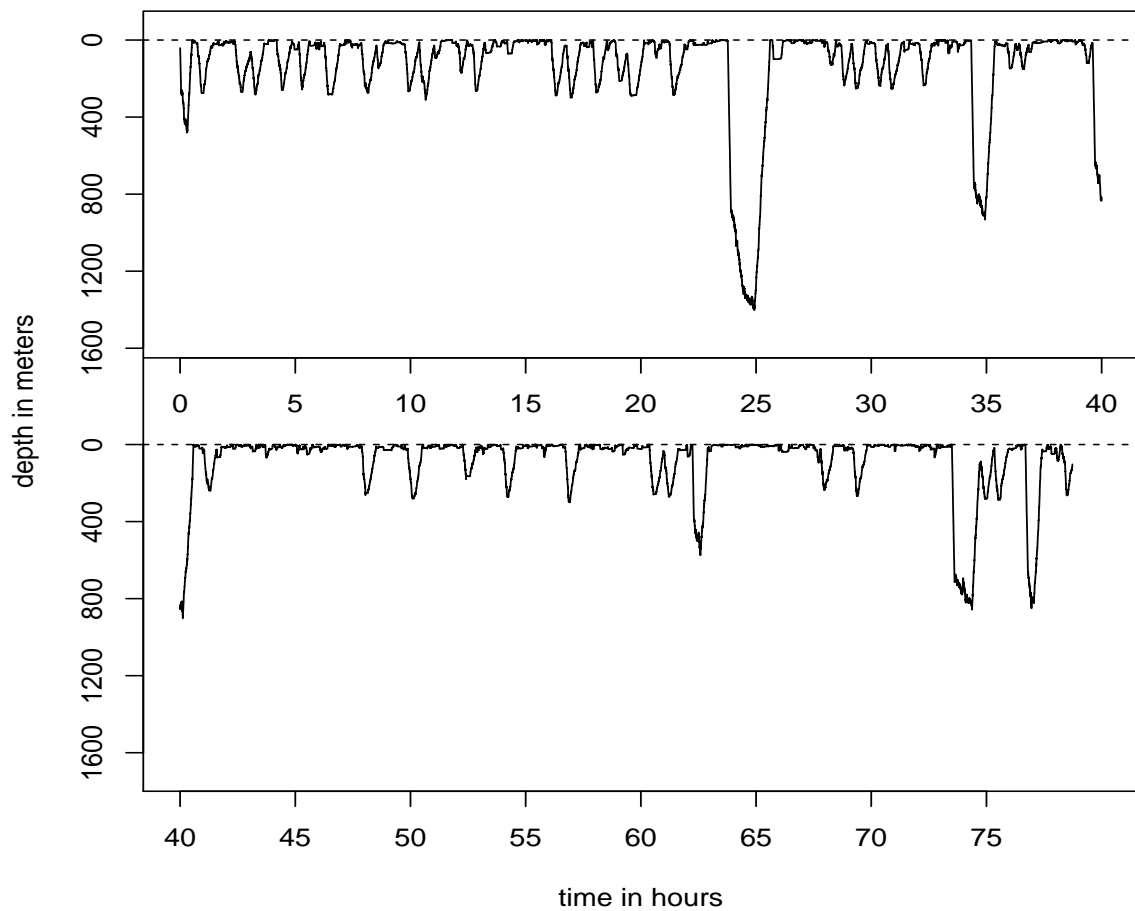


Figure 18: A realization of a depth profile simulated from the model fitted to Md248b data.

4.5 Can we predict vocal state from depth profiles alone

There are many available data sets with depth profiles out there, and vocal state is fundamental to understand cue rates and acoustic availability, two key parameters for density estimation of beaked whales from passive acoustic data. Therefore, it would be useful to be able to predict vocal state from depth profiles. In figure 19 we present the outcome of such a preliminary exercise. It seems clear that the whale typically starts vocalizing while still on the descent phase of a deep dive (state 2), which adds up with what is known already. So when the state is decoded as 3 we are almost sure the whale is in a vocal state, but the converse is not true, so a whale might be vocalizing and decoded as being in state 2.

5 Modelling displacement projected onto the sea surface

A number of efforts concerning animal movement have chosen to model step lengths and turning angles rather than x and y displacements (e.g. McClintock *et al.*, 2012; Morales *et al.*, 2004). This is appealing for a number of reasons, not the least because one might have clear expectations about these over time and space. As an example, displacement should be higher and turning angle variance lower in a migratory state, while the opposite might be expected in a foraging state. On the other hand, displacements in x and y are harder to interpret and should average 0 across animals with no directional movement. Here too we choose to work with step length d and turning angles φ .

5.1 Unconstrained movement

In this sub-section we address the modeling of unconstrained movement, i.e. movement that ignores avoiding shallow depths and home ranges. A plausible movement model might include state dependent step lengths and turning angles.

A couple of functions are required a priori, to obtain turning angles from the sequence of x, y locations. Here we actually leveraged on a very useful

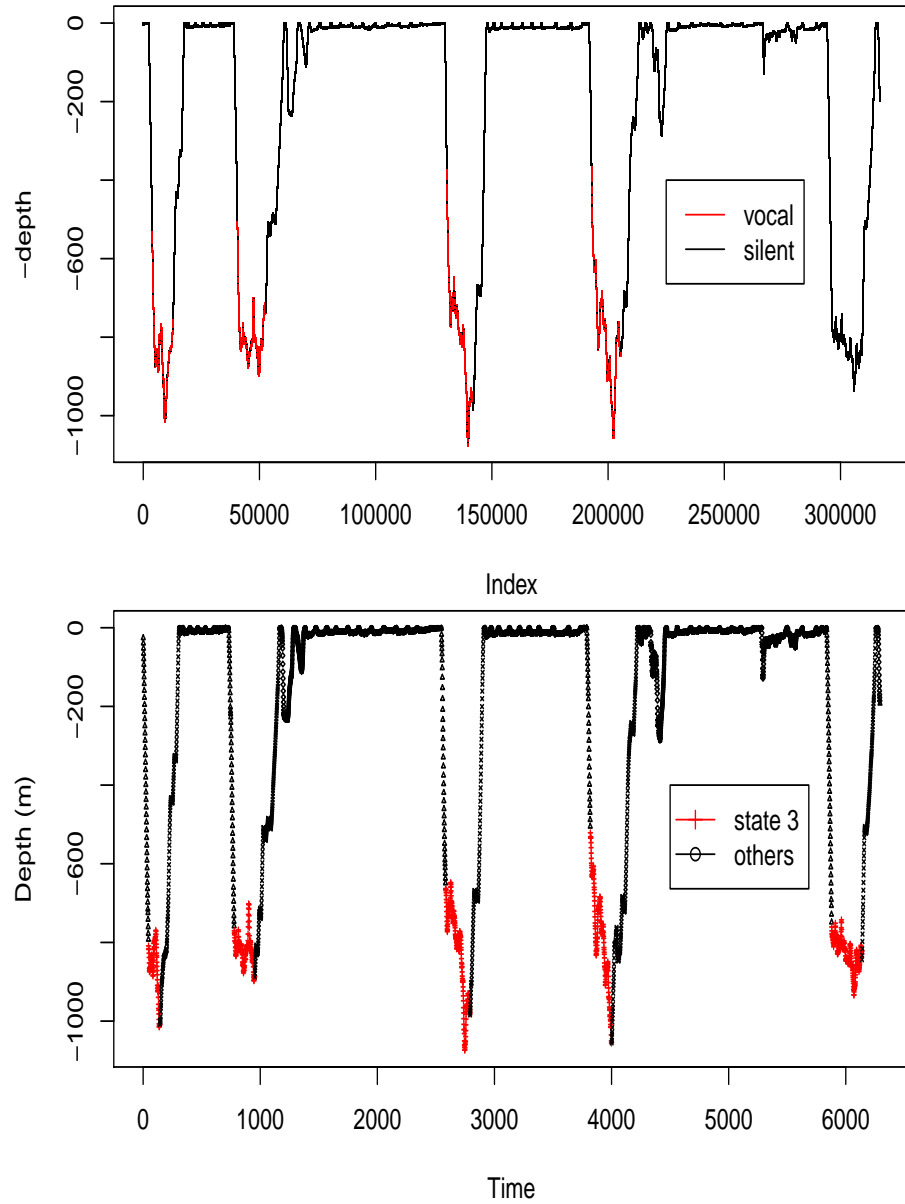


Figure 19: Predicting vocal state from depth profile. Top panel represents the vocal and silent periods, obtained directly from the acoustic data on the DTag. Bottom panel represents state assignment (state 3 vs. all other states).

post on a Quantitative Ecology blog which happened to include relevant code to do so. The functions were tested and they are working well.

Given our requirement to keep the animals in a relatively small area, due to the observed behavior of these whales which seem to be fairly consistently sighted in the same place, one possible model would be to consider random walks (e.g. Langrock *et al.*, 2012; McClintock *et al.*, 2012), such that turning angle is unbiased when near the animal’s home range center, but potentially biased towards this home range center when further away. Additionally, the unbiased random walk could be correlated or not, and, if existing, said correlation might be state dependent or not. It seems fair to assume that the DTAG data available allows us to parameterize these potentially state dependent distributions. A quick and dirty look into the step length and turning angle distributions of Md248b shows clear signs of persistence, most pronounced in step length, anticipating some correlation mechanism (figure 20).

We need now to extend the 1D depth model to a 2D horizontal displacement model. As a first step, we look into descriptive statistics for step length d and turning angles φ conditional⁸ on the state assignment obtained in the previous section, i.e. using depth alone.

A key point is that we have fitted the depth profile data at time steps of 10 seconds. This means that when later simulating depth profiles we will simulate depths as 10 second time steps. However, for the simulation exercise itself we opted by considering simulations at 1 second time steps. This creates an inconsistency which we decided to solve pragmatically: linear interpolation of simulated depths will be considered. Therefore, hereafter we look at turning angles and step lengths at 1 second resolution, rather than 10 second resolution.

Conceivably, the states decoded using depth alone are not only different in terms of depths: in fact, it is quite likely that they are different also in terms of the horizontal displacement characteristics.

Histograms of step length and turning angle conditional on state are shown in figure 22 and corresponding summary statistics are presented in table 1. General considerations from this data are not easy to make, but it seems clear that as expected mean turning angles are close to 0. Further, as might be expected, it seems like the behavior is more “calm”, perhaps

⁸In the next subsection we present a discussion of potential advantages and disadvantages of using a conditional on depth approach.

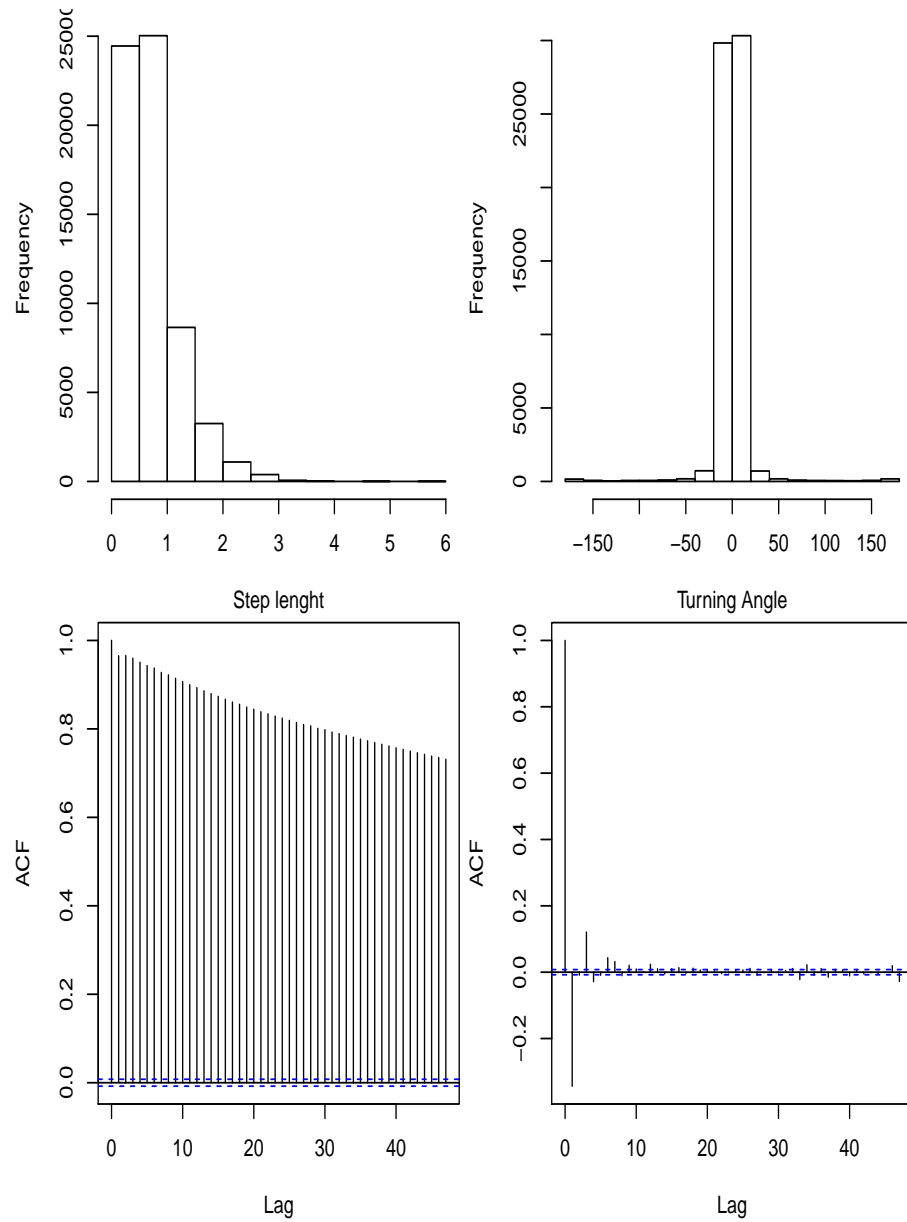


Figure 20: The distribution of step length and turning angles (top panels), with the corresponding autocorrelation functions (bottom pannels).

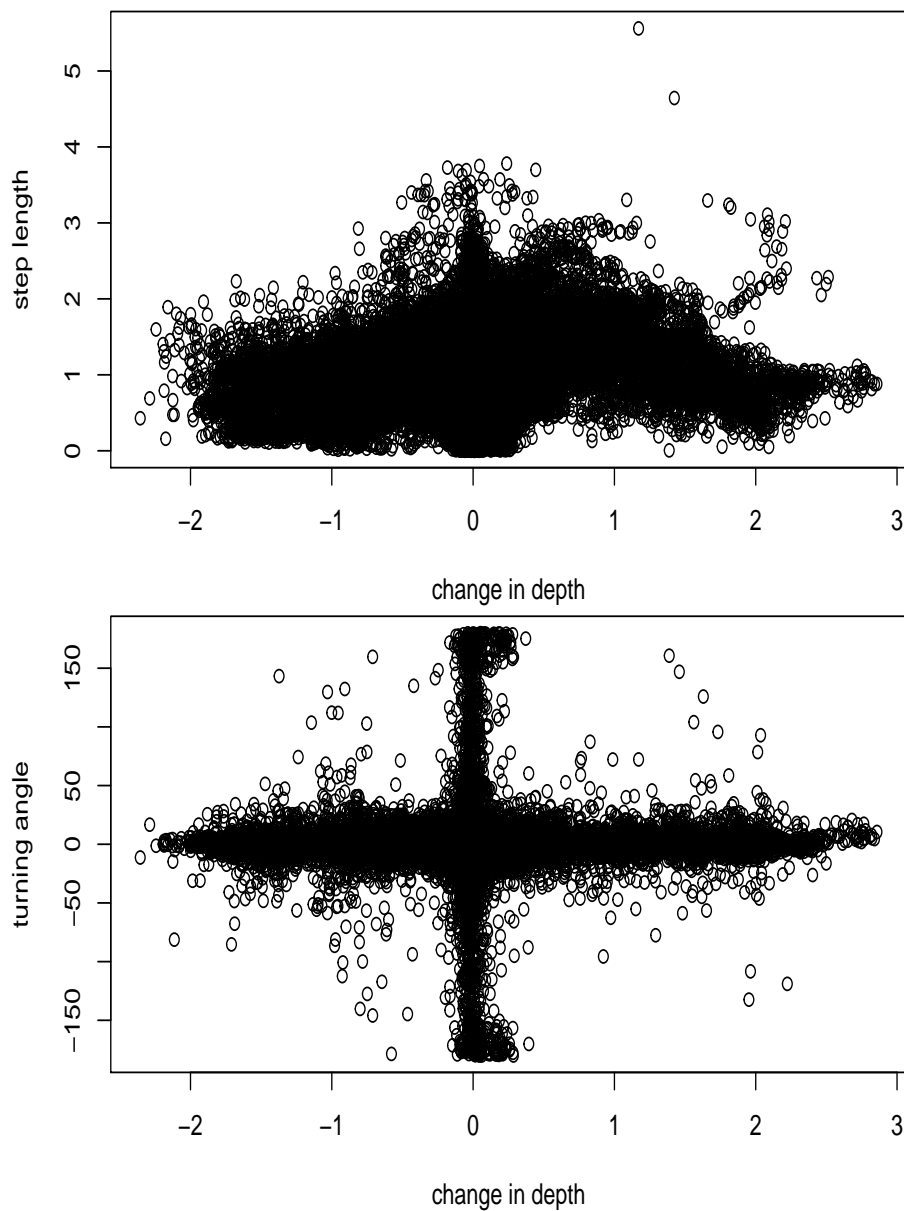


Figure 21: Relationship between turning angle and step length as a function of change in depth.

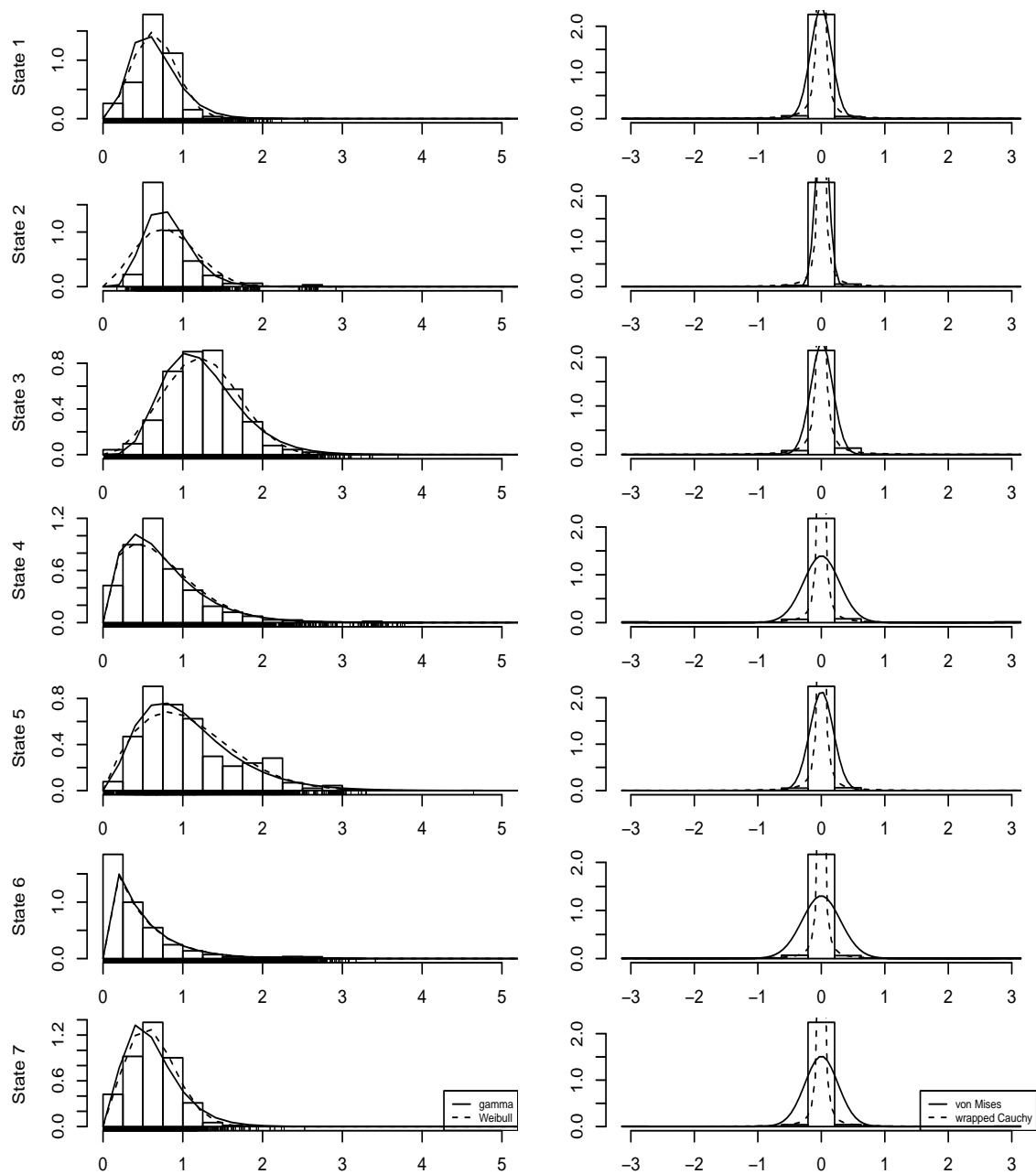


Figure 22: Observed step length and turning angle by state, with gamma and weibull distribution fits added to the step length data and von Mises and wrapped Cauchy added to the turning angle data

	1	2	3	4	5	6	7
mean d	0.66	0.82	1.24	0.74	1.07	0.43	0.63
sd d	0.25	0.34	0.43	0.50	0.60	0.47	0.29
mean ta	-0.26	0.78	0.45	0.17	0.26	-0.02	0.27
sd ta	11.11	5.62	10.66	22.61	13.21	22.70	19.90

Table 1: The mean and standard deviation of displacement (d) and turning angle (ta) for each of the seven states as decoded based on depth alone

less environmental but more physiologically driven (recovering from a deep dive and preparing for the next one), in shallow dives than in deep dives, where the animal is perhaps more focused and with clear behavioural objectives (finding prey). The horizontal displacement is higher in the foraging stage, which might be expected as that probably maximizes the encounter rate with prey given an optimal depth was achieved. The large variance in turning angles during foraging might also be related to the directed searching behavior and the detection of new prey leading to a directional change. The biological reason for why the horizontal displacement is relatively large for the shallow descent phase is unclear. The low standard deviation of the turning angle at the surface state might represent the fact that these animals are not reacting much to the environment in shallow waters. The same happens for the shallow dive states, which is consistent with the same explanation. In the same way, these standard deviations are larger for the deep diving states, which might correspond to the animal's need to adjust behaviour as a function of environmental cues, either to find prey while going down or to avoid predators when coming up. This seems to indicate that using 3D information might have additional advantages over 1D information alone for state assignment.

Despite the presence of correlation structure as evidenced in figure 20 as a first approach we model turning angles and step lengths assuming independence.

In table 2 we present the values of the estimated parameters for step length, considering both gamma and Weibull distributions. Likewise, table 3 we present the values of the estimated parameters for turning angles, considering both von Mises and Wrapped Cauchy distributions. Note that for the estimated mean of the Wrapped Cauchy the values around 6.3 are just approximations of $2 \times \pi$, i.e., approximately 0 too as expected.

	state	gdsh	gdr	gdm	gdsd	wd1	wd2	AICg	AICw	sldAICdiff
1	1.00	4.85	7.36	0.66	0.30	2.73	0.73	3523.86	1457.58	2066.28
2	2.00	7.84	9.55	0.82	0.29	2.44	0.92	601.88	1192.55	-590.66
3	3.00	6.80	5.47	1.25	0.48	3.01	1.39	11613.32	11000.21	613.11
4	4.00	2.21	3.00	0.74	0.50	1.56	0.82	9074.90	9199.86	-124.96
5	5.00	3.12	2.91	1.07	0.61	1.89	1.21	5455.14	5533.71	-78.57
6	6.00	1.07	2.51	0.43	0.41	1.01	0.43	6968.88	7040.40	-71.53
7	7.00	3.35	5.33	0.63	0.34	2.20	0.70	1928.40	1510.04	418.36

Table 2: Conditional on state (1 to 7) parameter estimates for the step length, considering the gamma (g) and weibull (w) distributions. sh=shape, r=rate, m= mean, sd= standard deviation. AIC values are also shown, as well as AIC differences.

	state	vmm	vmd	wcm	wcd	AICvm	AICwc	tadAICdiff
1	1.00	-0.00	36.93	6.28	0.96	-9485.93	-21902.30	12416.38
2	2.00	0.01	105.48	0.01	0.96	-3647.76	-4186.90	539.14
3	3.00	0.01	33.48	6.28	0.95	-6075.27	-12616.17	6540.90
4	4.00	0.00	12.52	6.28	0.96	2921.12	-14774.68	17695.80
5	5.00	0.00	28.87	0.00	0.96	-1715.53	-6390.59	4675.06
6	6.00	-0.00	10.96	0.00	0.97	11601.92	-46039.00	57640.91
7	7.00	0.00	14.66	0.00	0.97	753.78	-8212.92	8966.70

Table 3: Conditional on state (1 to 7) parameter estimates for the turning angle, considering the von Mises (vm) and wrapped Cauchy (wc) distributions. bm= mean, d= dispersion. AIC values are also shown, as well as AIC differences.

5.2 Pros and cons of a conditional on depth approach

This is also very useful because from a pragmatic point of view one might model directly these distributions conditional on a depth derived state. This will naturally be much simpler than actually extending the 1D model to 2D (x, y) or 3D (x, y, z) . However, this means that turning angle and step length are only dependent on state, but there is certainly a correlation structure between the actual z displacement and step length and turning angle.

This is clear from figure 21, showing that despite eventually being a good pragmatic solution capable of capturing overall movement patterns for simulation within LATTE, small scale movement correlations in 3D will be lost.

However, it should be noted that this same issue arose when modeling 1D depths with our fHSM (cf. figures 16 and 17).

Despite a 3D model for state assignment being more appealing conceptually, it might be considerably harder to implement, as can be anticipated because on average, compared to the 1D model, a 3D model will have 28 additional parameters: 7 means and 7 standard deviations for each of x and y (or equivalently turning angle and step lengths). Given there is no a priori reason to expect that each animal, over the long run, tends to turn always preferentially left or right, it seems plausible to simplify this model such that turning angle means are all 0, but that still corresponds to 21 extra parameters.

An additional advantage of this step length and turning angle formulation is that, within the simulation framework, using the turning angle mean to avoid boundaries might be a reasonable way to keep the animals from going out of the simulation range. Therefore, for animals that are close to boundaries, the mean turning angle would be such that they would avoid these.

6 WIP: Modelling three dimensional dive tracks

Extending the displacement in 2D to 3D is conceptually simple, because in 3D movement can still be represented by the same 2 components, a (now in a sphere) angle and a 3D displacement (Marques and Thomas, 2012c, for additional details).

In the .Rnw file there is code which will allow one to simulate spherical angles using `dmovMF` from package `movMF`. If we manage to get a way to estimate the parameters of such distributions conditional on state assignments from our 1D model we have a relatively simple way to simulate 3D movement assuming that, given the state, depth and horizontal displacements are independent.

7 placeholder: Modelling animal movement within a group

Just a placeholder

8 placeholder: Modelling 3D animal movement within a group

Just a placeholder

9 placeholder: Constraining movement models by 3D barriers

Just a placeholder

10 placeholder: Discussion and conclusions

As described in section 4.5, investigating further whether estimating cue rates from depth profiles by linking inferences based on acoustic data + depth profiles to depth profiles only is likely to be a useful research avenue.

References

- Langrock, R., King, R., Matthiopoulos, J., Thomas, L., Fortin, D., and Morales, J. M. (2012). Flexible and practical modeling of animal telemetry data: hidden Markov models and extensions. *Ecology*, **93**, 2336–2342.
- Langrock, R., Marques, T. A., Thomas, L., and Baird, R. W. (2013). Modeling the diving behavior of whales: a latent-variable approach with feedback and semi-Markovian components. *Journal of Agricultural, Biological, and Environmental Statistics*, **19**, 82–100.
- Langrock, R., Hopcraft, J. G. C., Blackwell, P. G., Goodall, V., King, R., Niu, M., Patterson, T. A., Pedersen, M. W., Skarin, A., and Schick, R. S. (2014). A model for group dynamic animal movement. *Methods in Ecology & Evolution*, **5**, 190–199.
- Marques, T. A. and Thomas, L. (2012a). Combining building blocks for simulating beaked whales at autec. Technical report, LATTE WORKING DOCUMENT.

- Marques, T. A. and Thomas, L. (2012b). Implementing a SSM to obtain pseudo-tracks and georeferenced track from DTAG data: an application to Md248b. Technical report, LATTE WORKING DOCUMENT.
- Marques, T. A. and Thomas, L. (2012c). Modeling beaked whales movement, sound production and detection at AUTEK. Technical report, LATTE WORKING DOCUMENT.
- Marques, T. A., Langrock, R., and Thomas, L. (2013). Modeling and simulating 3d beaked whale movement based on DTag data. Technical report, LATTE WORKING DOCUMENT.
- McClintock, B. T., King, R., Thomas, L., Matthiopoulos, J., McConnell, B. J., and Morales, J. M. (2012). A general modeling framework for animal movement and migration using multi-state random walks. *Ecological Monographs*, **82**, 335–349.
- McClintock, B. T., Russell, D. J. F., Matthiopoulos, J., and King, R. (2013). Combining individual animal movement and ancillary biotelemetry data to investigate population-level activity budgets. *Ecology*, **94**, 838–849.
- Morales, J. M., Haydon, D. T., Frair, J., Holsinger, K. E., and Fryxell, J. M. (2004). Extracting more out of relocation data: building movement models as mixtures of random walks. *Ecology*, **85**, 2436–2445.
- Tyack, P. L., Johnson, M., Soto, N. A., Sturlese, A., and Madsen, P. T. (2006). Extreme diving of beaked whales. *Journal of Experimental Biology*, **209**(21), 4238–4253.

A Estimating parameter variance

Being based on maximum likelihood estimation (MLE), we can use the properties of MLE to obtain the variances on the parameters. When called with the argument `hessian=TRUE`, `nlm` provides an estimate of the Hessian. In general the Hessian is a square matrix of second-order partial derivatives of a function, in this context the likelihood function with the derivatives evaluated at the maximum likelihood estimates of the parameters of interest. Being second-order derivatives, it intuitively conveys the notion that the larger the value of the Hessian the steeper the likelihood function is, and hence the lower the variance associated with the corresponding parameter estimate. If we invert the Hessian - in R that is implemented by `solve` - we obtain an estimate of the variance-covariance matrix associated with the maximum likelihood parameters.

There is an additional complication for some of the parameters involved, because these have been transformed prior to the numerical optimization, to respect some obvious parameter constraints (e.g. variances must be positive).

As an illustrative example, consider θ_2 , the parameter of the gamma distribution associated with mean depth in state 2. In state 2 the animal tends to get deeper at each time step, therefore *a priori* we know that this parameter should be positive. Hence, a transformation of the parameter was used prior to the maximization, $\log(\theta_2) = \theta_2^u$, such that $\theta_2 = \exp(\theta_2^u)$, which is always positive irrespectively of the actual values of θ_2^u . This means that the numerical optimization itself is over θ_2^u . Therefore, the variance obtained from `nlm`'s Hessian applies to this transformed parameter only, i.e. it corresponds to $\text{var}(\theta_2^u)$. To approximate the variance of the parameter of interest, which is naturally θ_2 , requires the back-transformation, here \exp , and hence we use the delta method as

$$\text{var}(\theta_2) = \text{var}(\exp(\theta_2^u)) = \text{var}(\theta_2^u) \frac{d \exp(\theta_2^u)}{d \theta_2^u} = \text{var}(\theta_2^u) \exp(\theta_2^u) = \text{var}(\theta_2^u) \theta_2 \quad (1)$$

so in this case the variance would be obtained by multiplying the parameters of interest by the variance of the parameter that the maximization occurred over. An implementation in R for the variance for θ_2 is shown here

```

#get the variance covariance matrix
varscovars=solve(fHSMM.HT$H)
#now get a vector with the variances
vars=diag(varscovars)
#for depth dependent mean in state 1
c(fHSMM.HT$theta[1]-1.96*sqrt(vars[1]*fHSMM.HT$theta[1]^2),
fHSMM.HT$theta[1]+1.96*sqrt(vars[1]*fHSMM.HT$theta[1]^2))

## [1] -5.147669 -4.741786

```

and a further example with γ parameters is shown here

```

#####
#                                looking into variances and 95% CI
#####

#example for
#for gamma parameters, positions 24 and 25
c(10*fHSMM.HT$gamma[1]-1.96*sqrt(10^2*vars[24]),
10*fHSMM.HT$gamma[1]+1.96*sqrt(10^2*vars[24]))

## [1] 3.766404 5.961713

c((1/10)*fHSMM.HT$gamma[2]-1.96*sqrt(vars[25]/100),
(1/10)*fHSMM.HT$gamma[2]+1.96*sqrt(vars[25]/100))

## [1] -0.9694756 -0.6236350

#example for beta_0, position 26
#c(10*fHSMM.HT$beta[1]-1.96*sqrt(10^2*vars[26]),
#10*fHSMM.HT$beta[1]+1.96*sqrt(10^2*vars[26]))
#using the delta method
#example for the sm parameters (negative binomial)
#c(fHSMM.HT$sm[1]-1.96*sqrt(vars[17]*fHSMM.HT$sm[1]^2),
#fHSMM.HT$sm[1]+1.96*sqrt(vars[17]*fHSMM.HT$sm[1]^2))
#c(fHSMM.HT$sm[2]-1.96*sqrt(vars[18]*fHSMM.HT$sm[2]^2),
#fHSMM.HT$sm[2]+1.96*sqrt(vars[18]*fHSMM.HT$sm[2]^2))

```

Analysis of the 2009 Submarine Commander Course data

LATTE WORKING DOCUMENT

Tiago A. Marques & Len Thomas

Centre for Research into Ecological and Environmental Modelling
The Observatory, University of St Andrews, St Andrews, KY16 9LZ, Scotland

Version's date: April 9, 2012

Contents

1	Introduction	2
2	Data details	2
3	Preliminary data analysis	4
3.1	Hydrophone data	4
3.2	Vocal groups	4
3.2.1	Initial data processing	4
3.2.2	Exploratory data analysis	6
3.2.3	Diel activity patterns	9
3.3	Military activity	14
3.3.1	Initial data processing	14
3.3.2	Exploratory data analysis	14
3.4	Sound exposure levels	15
4	Analysis strategy	15
5	Modelling BBW activity as a function of level 3 noise	22
5.1	Activity as a function of time since level 3 emission	23
5.2	Activity as a function of distance from and time since level 3 emission	23
6	Combining vocal groups and military activity data	24

7	Playing VG data as a video	27
	References	27

1 Introduction

This document contains the analysis of the data collected during the 2009 Submarine Commander Course at AUTECH, regarding beaked whale *vocal group* (VG) detections before, during and after military activities, as well as some details regarding the sound sources produced during those military activities. A VG is recorded for each detection of the vocal part of a beaked whale deep dive. Hence associated with each VG there is a group with an unknown number of animals in it. Given the beaked whale click and AUTECH's range characteristics (e.g. Marques *et al.*, 2009; Ward *et al.*, 2011; Kusel *et al.*, 2011) it is safe to assume that all deep dives are detected. Hence the number of recorded VG should match the number of deep foraging dives on the range during the recorded period.

Data sets from 2007 and 2008, with similar structure but shorter temporal coverage, served as the basis for the analysis presented in McCarthy *et al.* (2011) and Tyack *et al.* (2011) to evaluate the impact of military activities on beaked whale behavior. Both these references pointed to a clear influence of range operations on animal distribution and activity patterns.

2 Data details

We assume here that recorded VG correspond to foraging deep dives of Blainville's beaked whale (*Mesoplodon densirostris*). It is possible that a minor number of these might belong to other beaked whale species, but apart from that, false positives are not expected and are assumed absent from this data set.

As stated above, we assume that a VG vocalizing on the range is detected, which is reasonable given the AUTECH-beaked whale system characteristics. The main problems might be related to:

- groups which dove close together and are classified as a single group (a false negative)
- single group dive that is classified as two VG (a false positive) because the animals are lighting up hydrophones in different parts of the range, a possibility given the highly directional beam pattern of the beaked whale clicks.

In some sense, it seems like the former is more likely than the latter, but the truth is we have no data to perform an independent assessment of these.

Details about the key six data sets considered in this report, namely file names, file sizes, period that the files cover, etc. are given in table 1. Most of these data sets relate to vocal groups (VG), the exception being the one in the last row in table 1 (D6), which lists all the military noise produced in the AUTECH range during the analysis period. Some of the files information relates to periods which overlap in time: the first data set, D1, is a temporal subset of D2, which in turn is a temporal subset of the concatenation of (the “BDA”) files: D3 (Before the Mini Wars), D4 (During the Mini Wars) and D5 (After the Mini Wars).

The first two files were manually processed: D1 contains VG simultaneous to sonar, D2 contains VG simultaneous to some sort of noise producing military operation. Both of these files have most of their records from the Mini Wars period, but there are also occasional records from outside that period. The remaining 3 files (D3, D4 and D5) were processed automatically and contain all the VG detected during the entire period under consideration (18 April to 20 Jun 2009). The reason why D1 and D2 are kept separated is two fold, as these:

- also have additional information regarding the sound sources, and
- were processed manually, while the BDA files were processed in an automated fashion.

Considering the during period (D4), the difference between manual and automated processing is around 4% in terms of VG duration, and about 10% in the number of VG (Elena McCarthy, pers. comm., 15 June 2011). While considered small differences, it is important to be aware that these exist. The advantage of the automated procedure is essentially speed ¹ but

¹Say 5 minutes vs. 1 year of human time to process say 3 months of data!

also repeatability: different human experts will have different results, because their heuristic algorithms differ, but all computers will report the same result.

We also consider here a couple of additional data sets:

- exercise durations, a data set “manually harvested” by DM while we met at Mt. Hood. This contains the time start and end of periods of major activity during the mini wars. These were manually added into R using code that can be found in the .Rnw file.
- sound exposure levels and maximum sound levels during each of the exercises of the mini wars (see details in section 3.4).

3 Preliminary data analysis

Here we consider separate sections to explore the data in the vocal groups BDA files (section 3.2), the military activity data (section 3.3, work in progress), and the RMS and SEL data (section 3.4). Then in section 4 (not really started yet, see details below) we combine the information of these data sets.

The information regarding the manually processed data files is currently not used, but might be used later.

3.1 Hydrophone data

We begin by reading in the required hydrophone location data. Note that while these were originally in easting and northing arbitrary coordinates (as used in say Marques *et al.*, 2009), we have now been provided a table by EM via e-mail on the 20th June 2011 that contains locations in latitude and longitude, which is convenient here as the VG data uses latitude and longitude for hydrophone and source locations.

3.2 Vocal groups

3.2.1 Initial data processing

We create a single .xls file containing the result of stacking D3,D4 and D5 on top of each other, named “vaBDA.txt”. Finally the information is collected in a data frame which contains the following columns:

1. **group** - the number of the vocal group
2. **date** - the date the vocal group started vocalizing (deleted in the file subsequently analyzed, see details below)
3. **start** - the time vocalization started (reformatted in the file subsequently analyzed, see details below)
4. **stop** - the time vocal group went silent (reformatted in the file subsequently analyzed, see details below)
5. **duration** - the duration of the vocal period ² (reformatted in the file analyzed, see details below)
6. **HNcdtct** - information regarding the vocal group click counts at each hydrophone (will require a bespoke reading function to use, as the data is in a very specific format/convention, but there is potentially very interesting information in here).
7. **edge** - Whether all the hydrophones were edge hydrophones (reformatted in the file subsequently analyzed, see details below)
8. **nk** - The number of hydrophones at which the vocal group was detected
9. **center** - The center hydrophone (i.e. hydrophone with largest number of clicks detected) where the vocal group was detected
10. **lat** - The latitude of the vocal group (note this is weighted by activity on each hydrophone in the group)
11. **lon** - The longitude of the vocal group (note this is weighted by activity on each hydrophone in the group)
12. **overlap** - this field is empty unless the corresponding group overlaps in time and space with another group, in which case it contains the ID of the overlapping VG, e.g. [2-6] means that the vocal groups 2 and 6 overlap, and hence VG discrimination is not straightforward.

²What are the exact rules that go into defining the start and stop times, which directly lead to a duration?

13. **BDA** - a 3 level covariate created in the data subsequently analyzed which indicates whether the date and time corresponds to before (B), during (D) or after (A) the mini wars.
14. **Comments** - Any other relevant comments (deleted in the file subsequently analyzed, see details below)

Some of the information was slightly reformatted. For simplicity, we converted the 3 fields **date**, **start** and **stop** times to a date format like “2009-04-18 17:34:44”, which means that we only need to use two columns for obtaining the information in the current 3, and also it means that we can get the duration using **difftime**. This automatically corrects for a few incorrect duration values due to a misbehavior of an Excel function.

We also create a time indexing variable (time in days since the recording started, **tfs**), as well as the time difference between successive VG (Inter vocal group interval, **IVGI**, which provides an indication of activity, i.e. the lower the animal activity (and density of course!) the higher these time differences should be). Note that this IVGI is not group specific, i.e. the VG start and previous VG end might not be (and most likely are not) from the same original group.

3.2.2 Exploratory data analysis

We can start by looking at the duration of the vocal periods (Figure 1). In fact, the mean (29.2) and median (28.1) vocal group durations reported here are just above the deep dive average vocal period of 26 minutes value reported in Tyack *et al.* (2006). Given the latter is for individual animals, and here we deal with groups, these are remarkably consistent results.

We can also take a look at the number of hydrophones that vocal groups are detected in. Intuitively, we would expect that number to be smaller for VG defined as edge groups, which is clearly shown by the data (Figure 2). Note this is simply a data collection artifact, in the sense that the way a VG is defined as edge leads to this pattern.

An histogram of the number of times each hydrophone was the center hydrophone of a vocal group reveals an atypical distribution (Figure 3). In the left tail, there are clearly 4 hydrophones which are “problematic”, and these are hydrophones 21, 86, 87 (no VG detected) and 40 (2 VG detected). While hydrophones 86 and 87 were not operating, and hence this is an expected result, this seems to clearly indicate problems with the hardware in

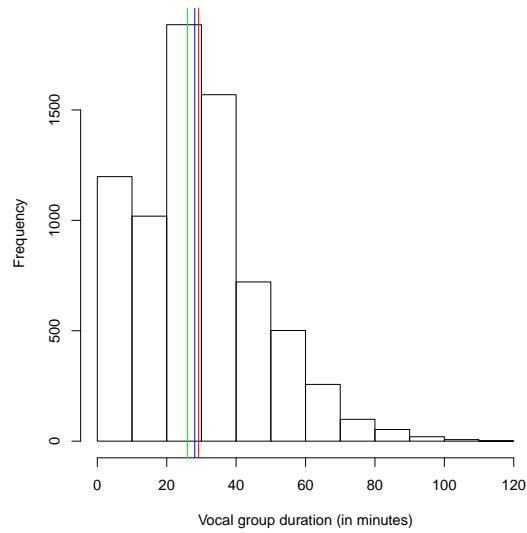


Figure 1: Histogram of the duration of vocal groups. The mean (red line) and median (blue line) vocal group durations are comparable to the values reported in Tyack *et al.* (2006) (green line).

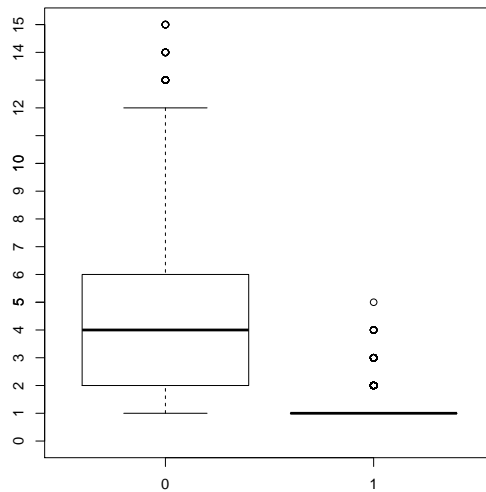


Figure 2: Box-plots of at how many hydrophones a vocal group was detected, as a function of the hydrophone location (edge=1 versus non-edge=0 hydrophones).

hydrophones 21 and 40. It was confirmed that a similar pattern was already present (but went unnoticed) in the files analyzed in McCarthy *et al.* (2011) and Tyack *et al.* (2011) (David Moretti, pers. comm.). This will be the subject of further investigation, but for now it seems simpler to just ignore these hydrophones in the analysis. On the right tail, there are a number of hydrophones with counts above 150 VG which also look suspicious. Note that these could result from slight differences in detectability of neighboring hydrophones, more than problems with these hydrophones per se.

For a better spatial perspective, the hydrophones and respective counts are presented in space (Figure 4), with the atypical hydrophones shown in color. Curiously enough, all high count hydrophones are edge hydrophones. This might indicate that this pattern is a data collection artifact. Edge hydrophones pick up VG which were actually on range, close to them, but also off range (because there are no other hydrophones closer to VG outside the range), and hence have a wider survey area, than inner hydrophones. But one must also not forget that when there is noise production on the range, edge hydrophones are more likely to pick up VGs, as shown in McCarthy *et al.* (2011) and Tyack *et al.* (2011), and so this might be the joint result of these two effects.

The results of a spatial smooth GAM model (e.g. Wood, 2006) show “hot spots” at the north and south western extremes of the AUTEK range, and “cold spots” at the Wiskey 2 and south central AUTEK areas (Figure 5). This is actually in contrast with an “old” beaked whale data set analyzed for Marques *et al.* (2009), as shown in figure 5 and 6 in Marques and Thomas (2008), where the northern eastern part of the range had the largest number of beaked whale click counts³.

Regarding the duration of the vocal groups, there seems to be a minor decrease of these during (D) the military operation period, as compared with the before (B) and after (A) periods (Figure 6, top). Further, the IVGI is clearly higher during the Mini Wars, which is consistent with a decrease in animal vocal activity (likely also in foraging dive behavior) with military activity (Figure 6, bottom).

The IVGI is shown as a function of time in figure 7. It seems clear that the number of vocal groups is smaller, and the IVGI is higher, during the

³But remember the previously analyzed data set had a much larger amount of false positives than what we are dealing with now, which can be a substantial cause for the differences.

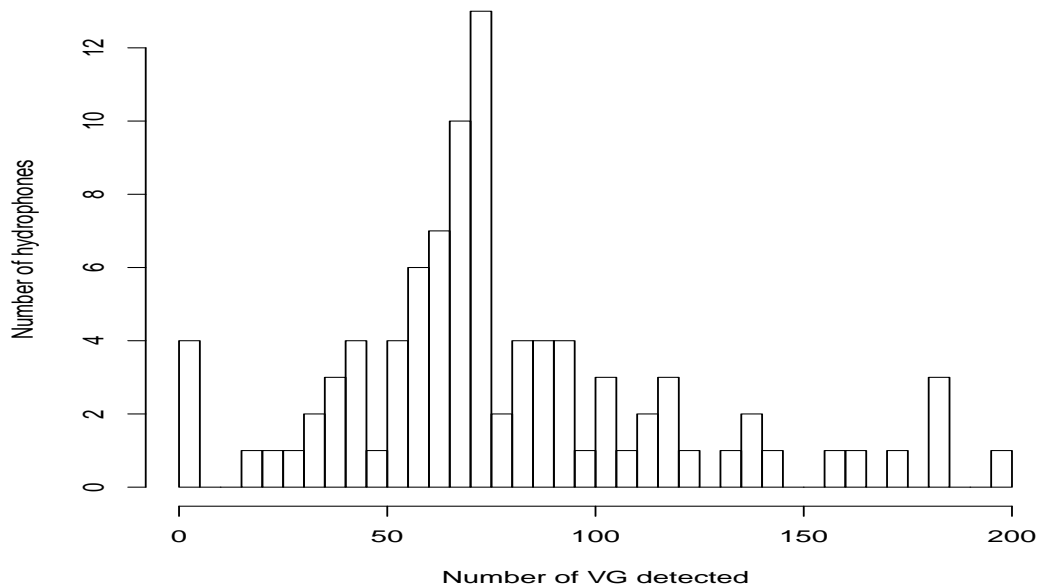


Figure 3: Histogram of the counts per hydrophone.

military operations. The mean IVGI in minutes before and after the military operations was respectively 11.4 and 12.6 minutes, while during the military operations that increased to 28.9 minutes, showing clearly that there is an impact of military activity in the frequency of VG.

We can also take a look at the pattern of the data in the latitude and longitude fields. These represent weighted averages of hydrophones locations, with weights being the number of click detections of a given vocal group in each hydrophone. If we separate the data by the BDA period, there is a clear pattern (figure 8). Note how this image reinforces the idea that animals are brought in towards edge hydrophones, as no animals can be "placed" outside the bounding hull around the hydrophones.

3.2.3 Diel activity patterns

An interesting exploratory analysis relates to the diel patterns of beaked whale activity, based on the VG. Plotting the number of VG as a function of time of day (figure 9), it seems like the activity patterns are constant over day and night, with the notable exception of the periods just before sunrise

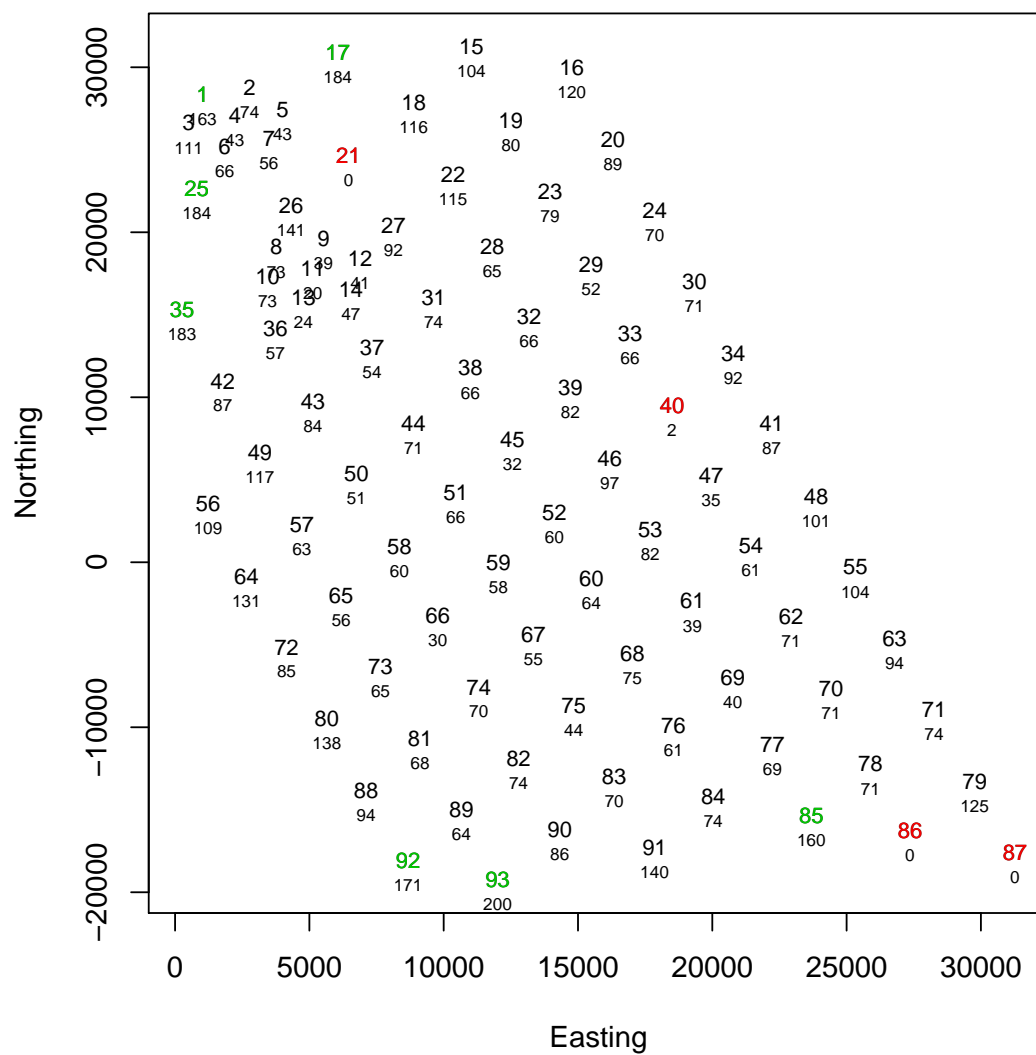


Figure 4: The number of vocal groups per hydrophone. Hydrophones with atypically low VG counts are represented in red, and hydrophones with atypical high VG counts are represented in blue.

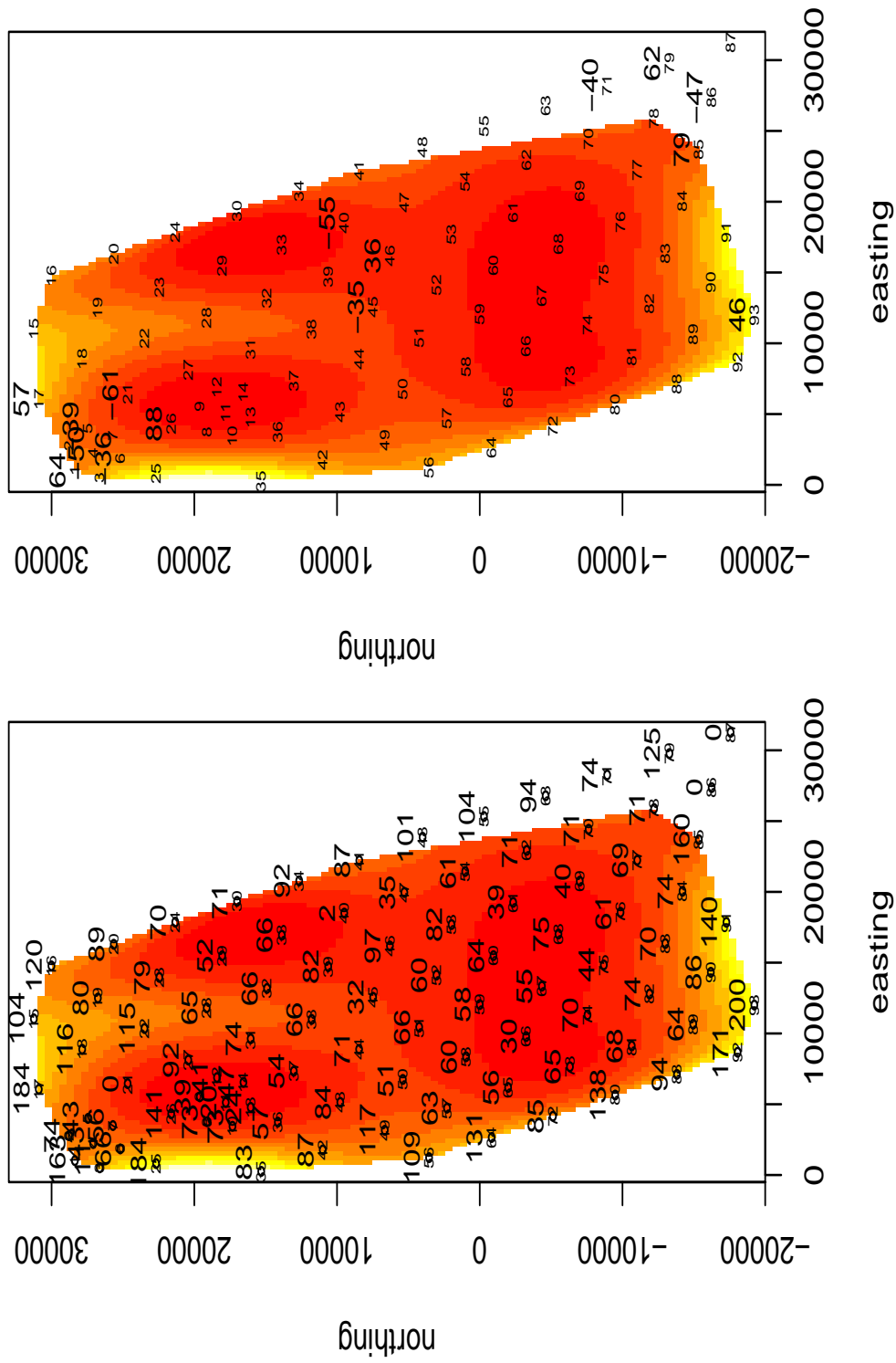


Figure 5: Number of VG as a gam smooth of latitude and longitude. Shown are both the observed counts and the fitted model (left) and the most extreme residuals in the response scale (right).

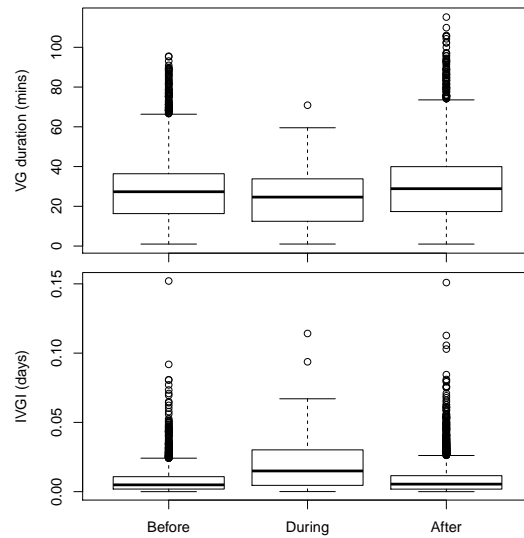


Figure 6: Box-plots of the duration of the vocal groups (top) and the IVGI (bottom) with respect to military activities (Mini Wars): before (B), during (D) and after (A)

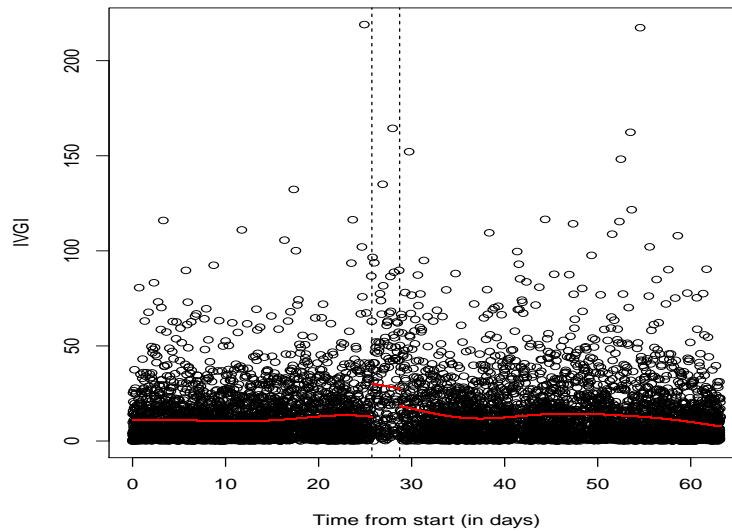


Figure 7: Inter vocal group interval (IVGI) for each click. Vertical dashed lines represent the start and end of the military operations. Red lines represent the fitted GAM model.

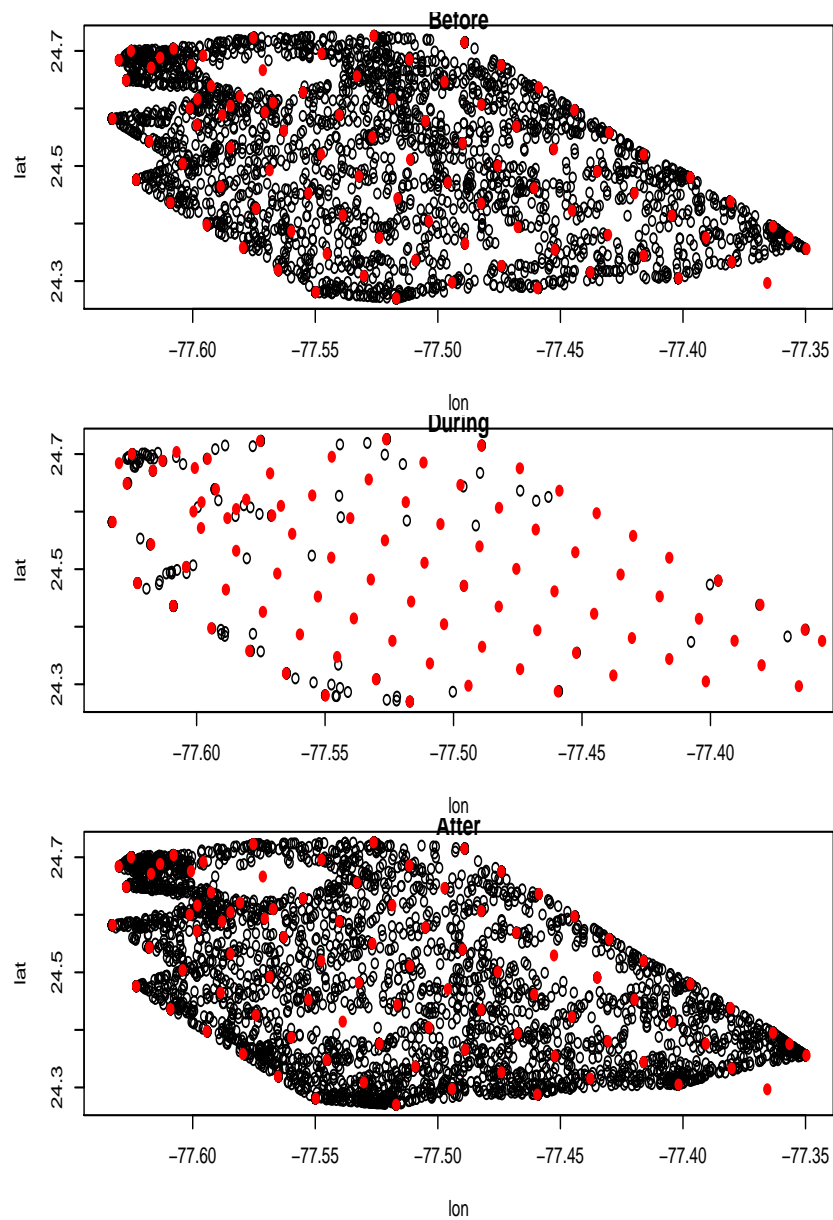


Figure 8: The “estimated” locations of vocal groups as a function of BDA period.

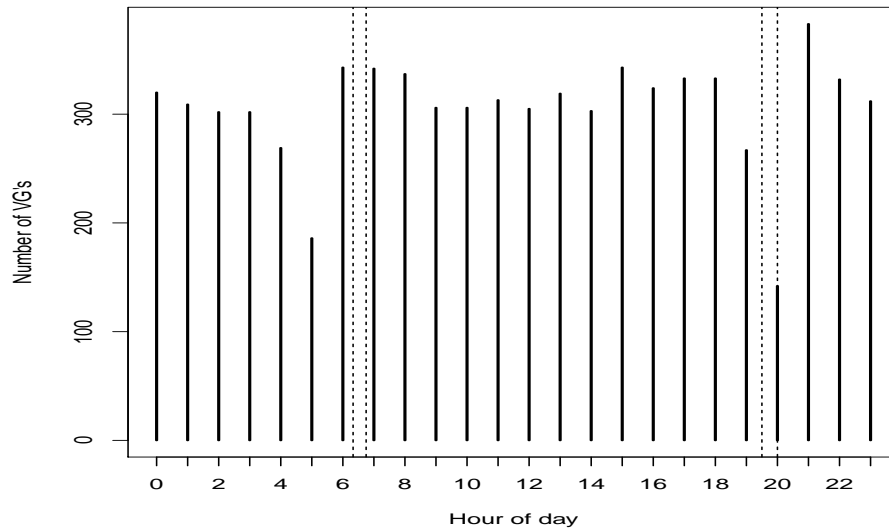


Figure 9: Number of vocal groups as a function of hour of day, pooled over the entire recording time. Dashed lines represent the range of sunset and sunrise hours during the surveyed period.

and during sunset, when the activity is lower. A GAM model considering this data set retrieves a uniform pattern, but of course that would not be the case if the data was properly analyzed using data accounting for the time component, rather than pooled over time.

3.3 Military activity

3.3.1 Initial data processing

Finally, we also read in the data corresponding to D6, dealing with the military activity data. Look in the .Rnw file the minor tweaking needed to get the data into a workable format.

3.3.2 Exploratory data analysis

This data set contains the record of 266 sound production events. However, the available information regarding each of these can vary considerably. Therefore, while for the 174 sources of level 3 we have the exact time the sound was produced (but not location, at least in this file), for courses from

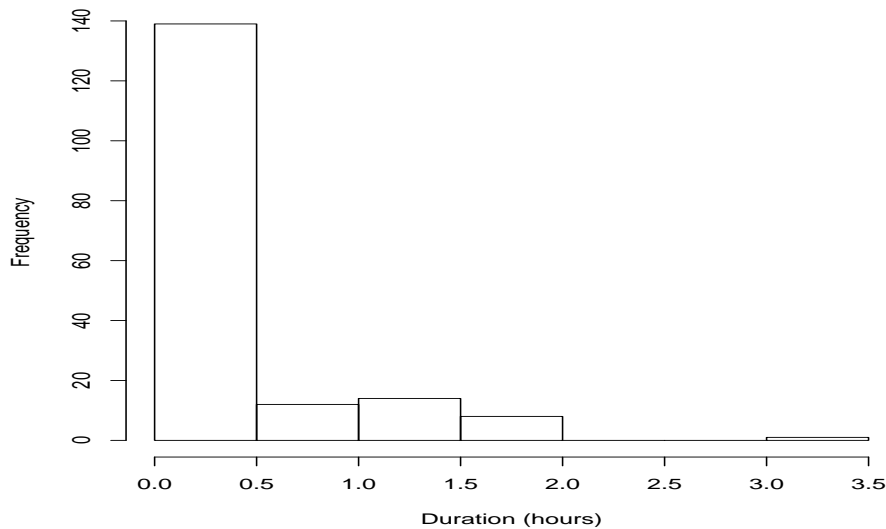


Figure 10: Histogram of the duration of level 3 sounds.

level 2 and 1 the information is often very sparse, ranging from a sound might have been produced somewhere sometime (mostly level 0 and 1 sounds), to somewhere at a given time or in a given place sometime (mostly level 2 sounds). For the time being it seems like it might be a good idea to concentrate on level 3 sounds, which correspond loosely to MFA sonar.

We can take a look at the duration of sonar emissions for each of the sound producing events (Figure 10). While most of the events only last for a few minutes, there are instances of up to 3.5 hour emissions.

3.4 Sound exposure levels

We also have available, for each one of the 6 periods over which scenarios were being run, the root mean square maximum sound level (RMS) and the accumulated sound exposure level (SEL) evaluated at each hydrophone, and at 4 depths (10, 100, 1000, 1500 m). These were sent to us by DM on the 26th March 2012. We can read all this data into R.

We can produce plots of spatial smooths for the RMS and SEL for each scenario (Figures 11-16).

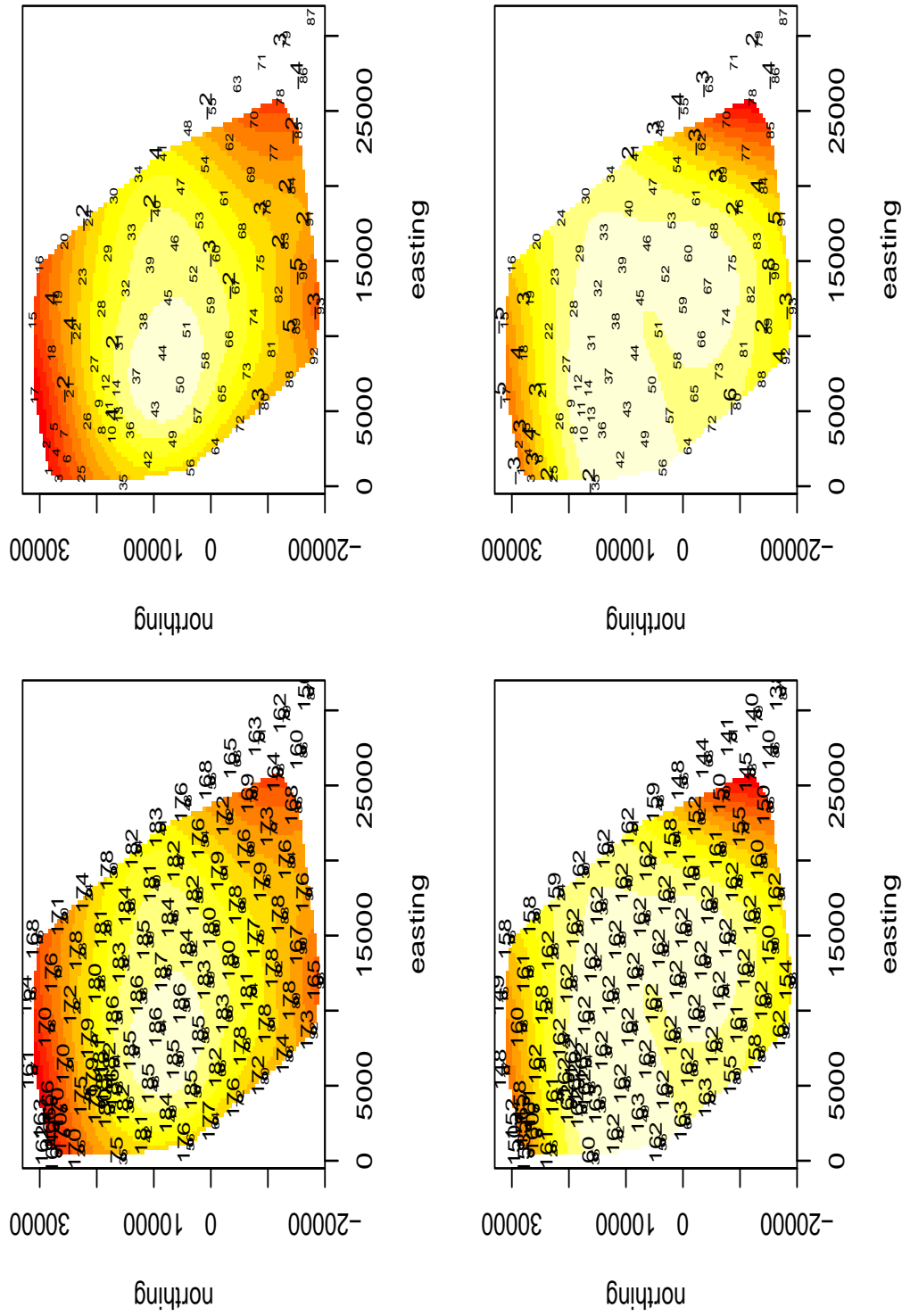


Figure 11: SEL (top plots) and RMS (bottom plots) for exercise 1401 as a gam smooth of latitude and longitude. Shown are both the observed values and the fitted model (left) and the largest residuals in the response scale (right)

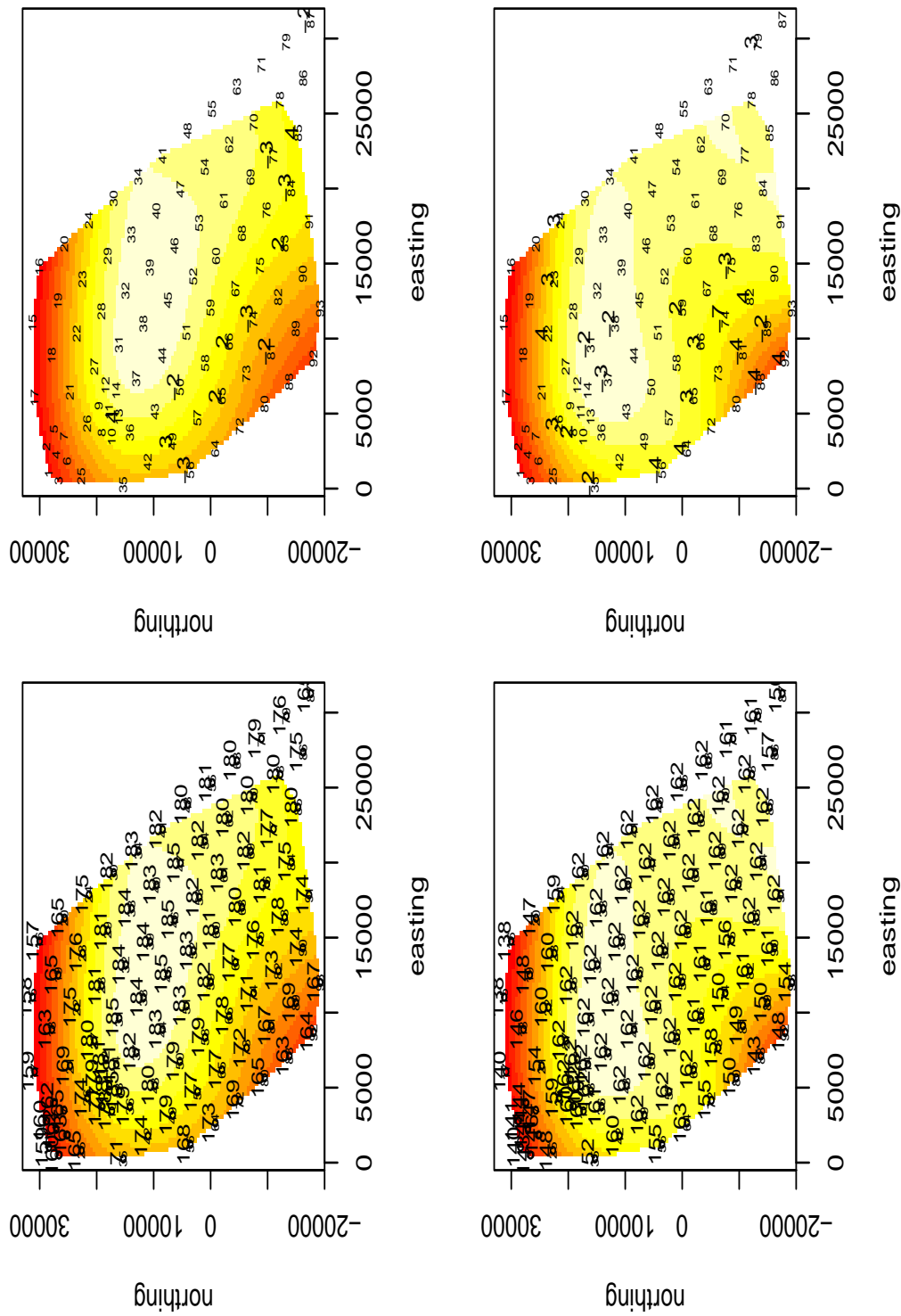


Figure 12: SEL (top plots) and RMS (bottom plots) for exercise 1501 as a gam smooth of latitude and longitude. Shown are both the observed values and the fitted model (left) and the largest residuals in the response scale (right)

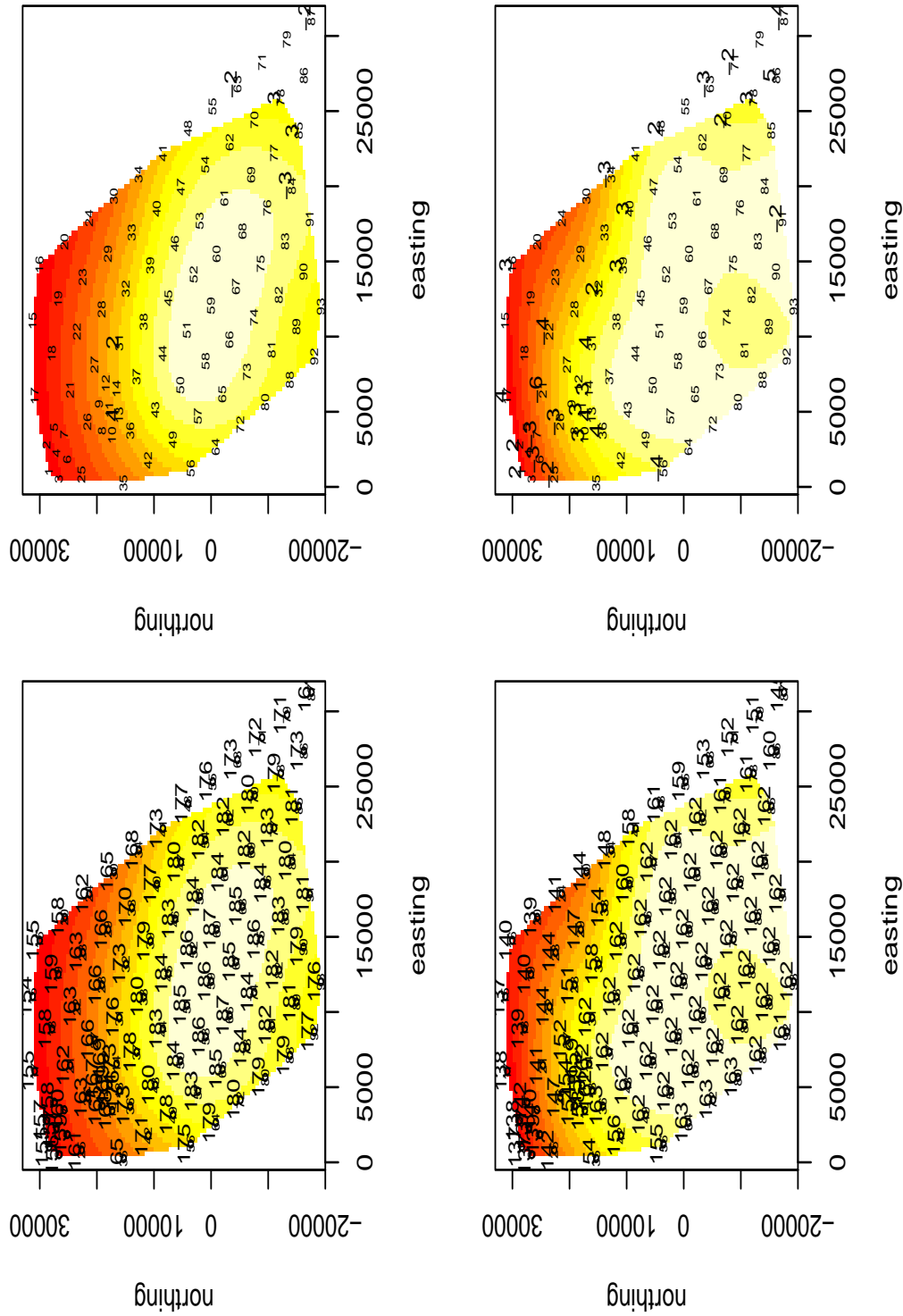


Figure 13: SEL (top plots) and RMS (bottom plots) for exercise 1504 as a gam smooth of latitude and longitude. Shown are both the observed values and the fitted model (left) and the largest residuals in the response scale (right)

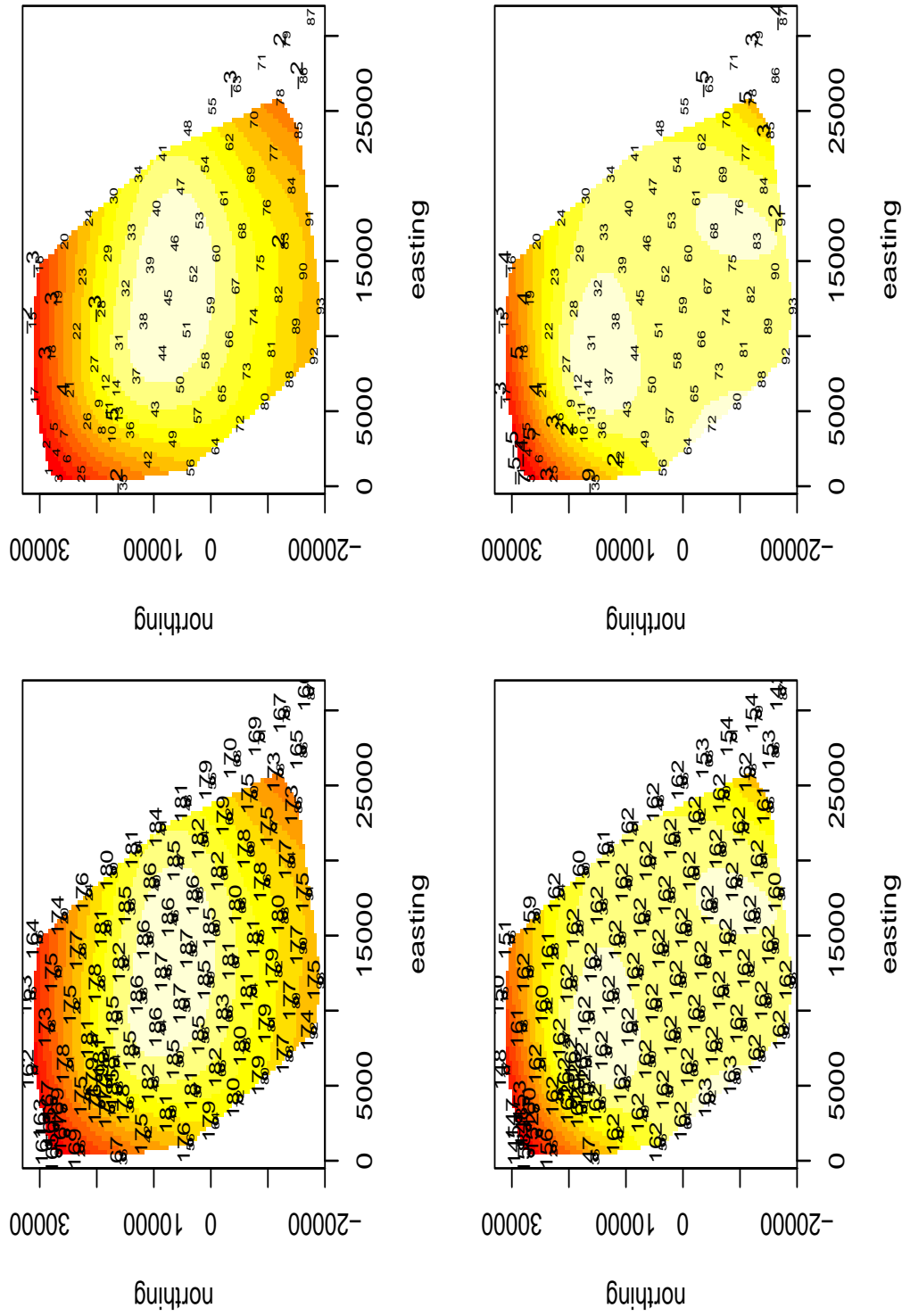


Figure 15: SEL (top plots) and RMS (bottom plots) for exercise 1604 as a gam smooth of latitude and longitude. Shown are both the observed values and the fitted model (left) and the largest residuals in the response scale (right)

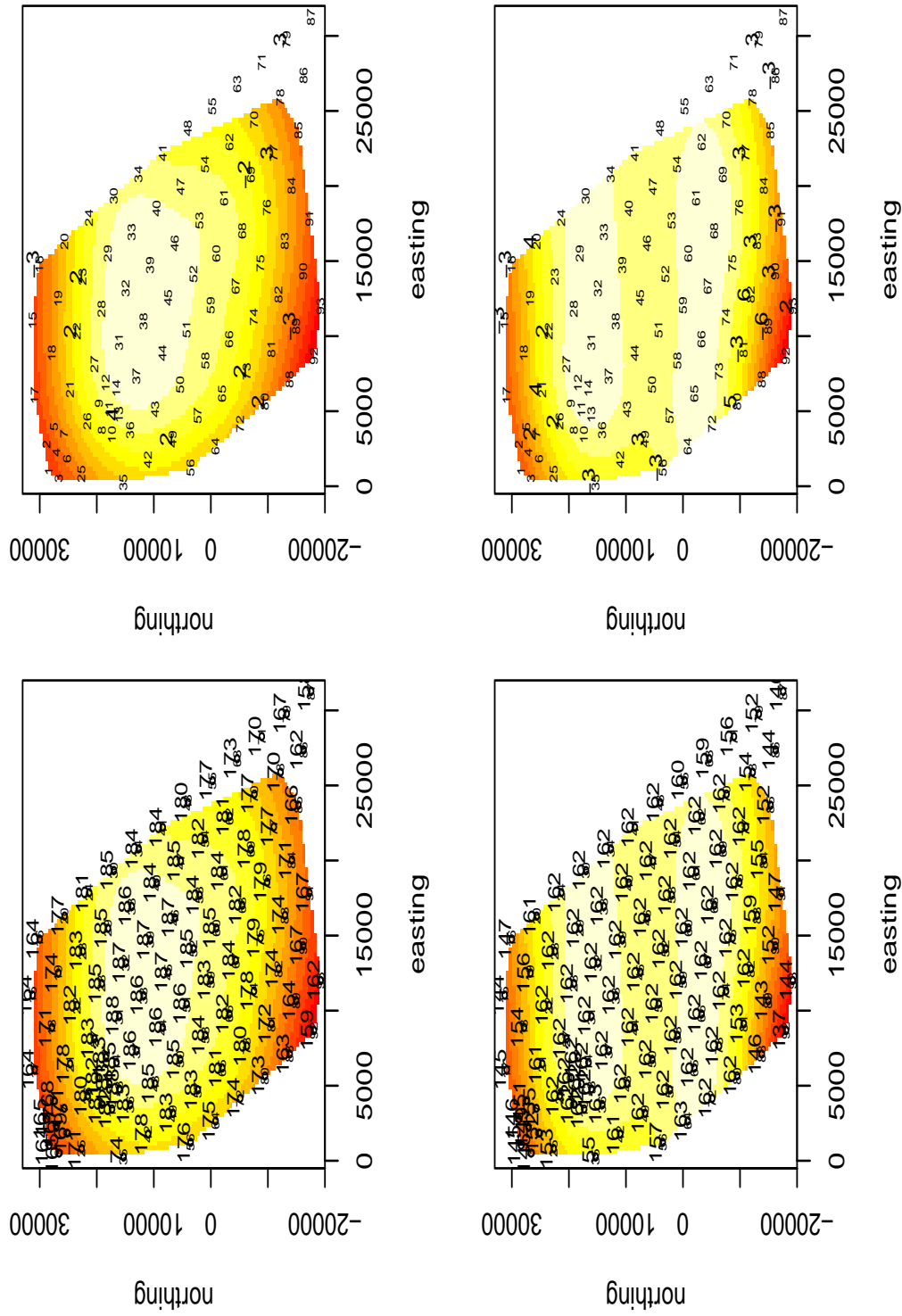


Figure 16: SEL (top plots) and RMS (bottom plots) for exercise 1702 as a gam smooth of latitude and longitude. Shown are both the observed values and the fitted model (left) and the largest residuals in the response scale (right)

4 Analysis strategy

After the EDAs, we have to cross the information in the BDA files (D3, D4 and D5 in table 1) with the information regarding the military sound activity (D6 in table 1). This will allow an analysis of some VG derived variables like

- IVGI or number of VG in short time periods ⁴,
- VG duration
- number of clicks per VG
- probability of a VG starting in a given time period (and area) - this is the idea on the basis of the dose response curve we have been discussing about and might be submitted to the MMB conference in Tampa, Florida.

as a function of potential covariates like

- latitude and longitude (needs careful thinking about what this might be, and depends on the dependent variable used too)
- time since last sound source
- distance from last sound source
- last sound source type
- last sound source level
- modeled sound exposure
- etc

⁴ Note these two are somewhat equivalent analysis, if you think of counts and waiting times in the context of a Poisson process, though here we have an over dispersed Poisson process

5 Modelling BBW activity as a function of level 3 noise

Level 3 noise is the one likely to have a major impact on animal activity, and also the one type of sound for which time and location of source is known in detail. Hence, we start by creating an analysis in which potential measures of activity (as VG length or IVGI) are modeled as a function of source distance (to estimated VG location) and time since last level 3 source.

5.1 Activity as a function of time since level 3 emission

A simple approach might be to compare the number of vocal groups initiated on the range during an hour before sonar emission, and one hour after (the start of) sonar emission. While this ignores the spatial component and arbitrarily considers a 1 hour time interval, it should provide a first indication if there is any strong effect present. For that one needs to create an appropriate data set that crosses information on vocal groups and level 3 sound emission. The results of said analysis are presented in figure 17. Perhaps surprisingly, there seems to be no effect, with very similar number of VG starting in the period before and after the start of a level 3 sound emission. While at first we thought that pattern would change once the spatial component was also included, we concluded that most likely what is happening is that, after the first level 3 event, i.e., when the Mini Wars start, the animals are no longer in an undisturbed setting, and until the operations stop and enough time is allowed for animals to resume their “normal” behavior, one can not interpret the results of any sonar event on range without accounting for the fact that the environment is no longer pristine (if ever AUTEK can be considered pristine with all the activity that goes on in it, but any way!).

For this reason, and after discussions at LATTE meeting in Mt. Hood (present: DM, DH, EM, LT, ND, RM and TM), we agreed that it might be better to divide the time into 3 different periods:

- before Mini Wars started (the control) (and maybe also include the data after the Mini Wars ended, allowing for some time for the system to recover - McCarthy *et al.* (2011) and Tyack *et al.* (2011) will be useful to define what said period might be.
- after mini wars started (the impact), within which

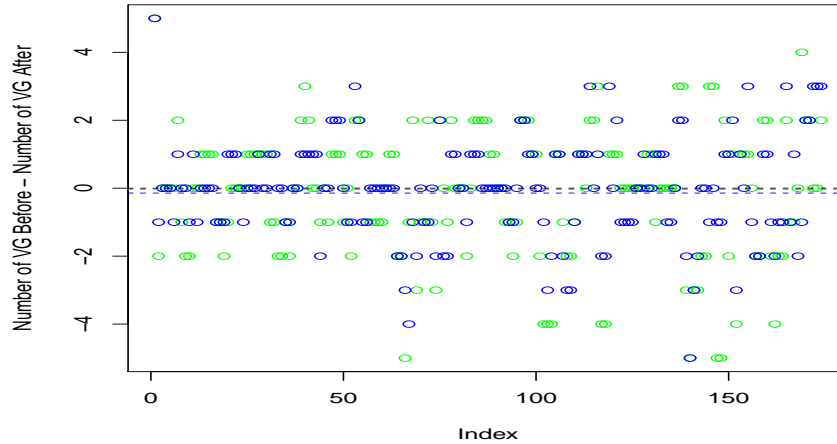


Figure 17: Difference in the number of vocal groups starting 30 (blue) and 60 (green) minutes before and after a level 3 sonar started emitting. Horizontal lines represent the mean of the differences, black line is at 0 (no effect).

- scenarios are being run (high impact)
- redeployment periods (low impact)

5.2 Activity as a function of distance from and time since level 3 emission

A simple way to include the spatial component might be to repeat this analysis but concentrating on VG before and after the source in a circle of say 10 km around the source. For that we need to know the source location for all sources. Given that we currently do not have that information, but also due to the fact that, as described above, it is likely that this analysis will not produce reasonable results as the entire Mini Wars period is impacted, this section is not further implemented here.

6 Combining vocal groups and military activity data

As explained above in section 5, our initial attempt to infer an impact of noise was unsuccessful, likely due to the fact that we concentrated on level 3 events, which occur all (but the very first one) during highly “impacted” times.

In figure 18 we represent the number of vocal groups starting in each of successive 5 hour periods, for the entire duration of the recordings. From this figure it seems to be obvious why the analysis illustrated by figure 17 failed to produce any significant results. All level 3 events (thin red dashed lines in figure 18) occur during highly impacted periods. At least visually it seems that the number of VG increases when there is nothing going on on the range, but that even a series of level 2 or 1 events (thin orange dashed lines in figure 18) seem to have an effect on VG counts. A time series model might help to clarify if these effects are real.

A model of the number of VG in a given time interval as a function of

- whether or not the time period is during the mini wars
- whether or not the time period is between mini wars end and last level 3 event
- time since last event
- level of last event
- an interaction term between time since last event and level of last event

might be useful here. A possible confounding factor is that really say a level 0 event occurring just after a level 2 event might seem to have a bigger impact than it really has (as one is just observing the effect from the level 2 event, just in the same way as when looking into the mini wars period one cannot really observe the effect of particular level 3 events, it is just that the animals are probably essentially all behaving as if “all hell has break loose”). This will be easier to address when an analysis considering the (modeled) cumulative sound field is implemented.

Another interesting idea is to take a look at the data within the mini wars period, using the start and end times provided by DM for the actual

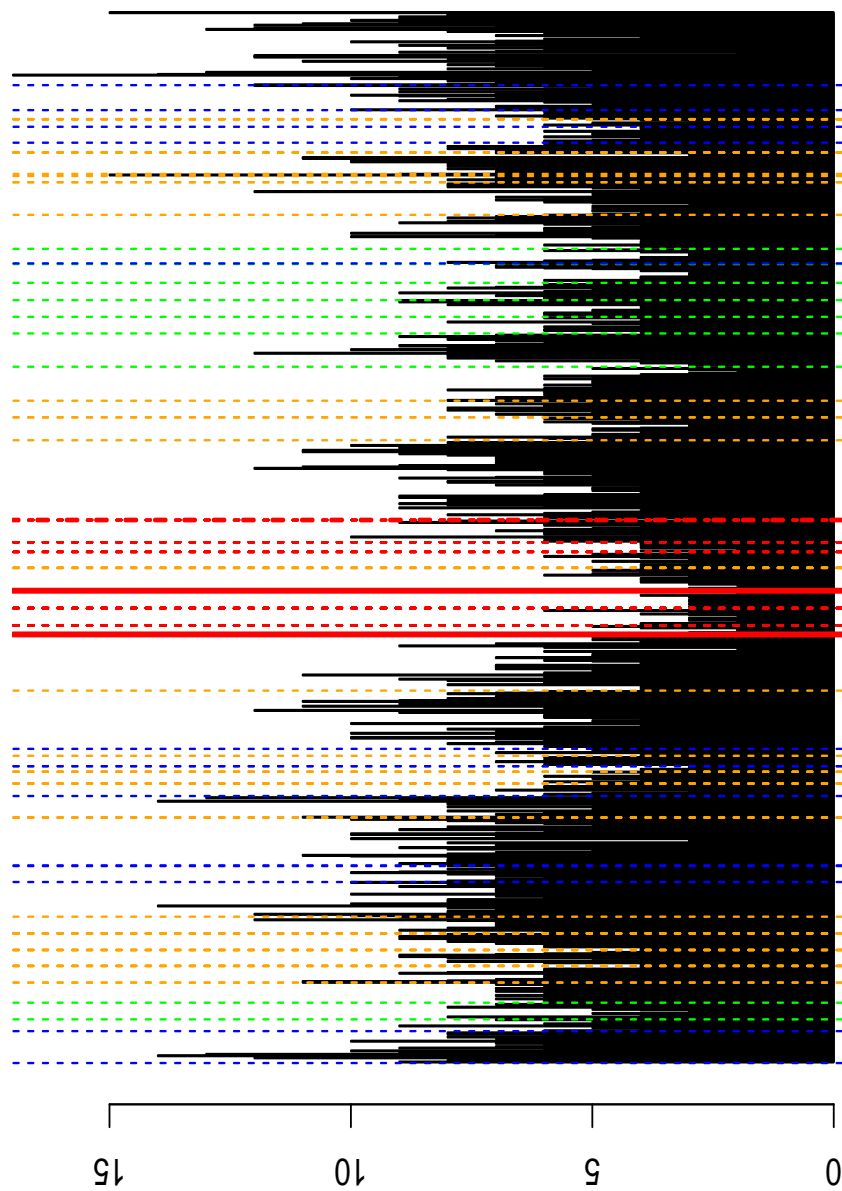


Figure 18: The number of vocal groups starting in 5 hour periods. The mini wars period is delimited by two vertical wide red lines, the last level 3 event is the wide dashed vertical red line, and events of level 0,1,2,3 are coded as blue, green, orange and red vertical dashed lines.

exercises, to see if we manage to spot an effect of the exercises even during this highly impacted period. The result of that analysis is shown in figure 20, and that effect is clearly visible.

The only counter intuitive fact on this plot is that the 4th exercise, which at least in terms of the duration (shortest exercise) and number of level 3 events (=16, minimum was 16, maximum was over 40) was quite small, seems to have had a large impact on the animals, without any sign of recovery after it. After the 5th and 6th exercises there were again signs of recovery, so we wonder whether there was more to it during the exercise, i.e. if something abnormal happened during what we call the "recovery period". Note that there is something that differs for the 5th exercise that might explain an atypical "recovery period". While for all the other exercises the exercise always started from the south, the 5th exercise started in the north part of the range, which necessarily means that something different happened during the redeployment phase. It is hard to know if this might be a hint of something real or whether this is just another "so... so... story".

we can also look at the effect of the first exercise sound exposure levels, and see if the counts per hydrophone within that period are dependent on the observed hydrophone specific SEL.

7 Playing VG data as a video

This section is just a place holder for R code. The underlying .Rnw file contains the code for implementing a tool that allows one to "replay" the SCC vocal group data in real (or probably preferably, in fast forward) time.

References

- Kusel, E. T., Mellinger, D. K., Thomas, L., Marques, T. A., Moretti, D., and Ward, J. (2011). Cetacean population density estimation from single fixed sensors using passive acoustics. *The Journal of the Acoustical Society of America*, **129**, 3610–3622.
- Marques, T. A. and Thomas, L. (2008). Click count EDA report with NUWC feedback. Technical report, DECAF internal report.
- Marques, T. A., Thomas, L., Ward, J., DiMarzio, N., and Tyack, P. L.

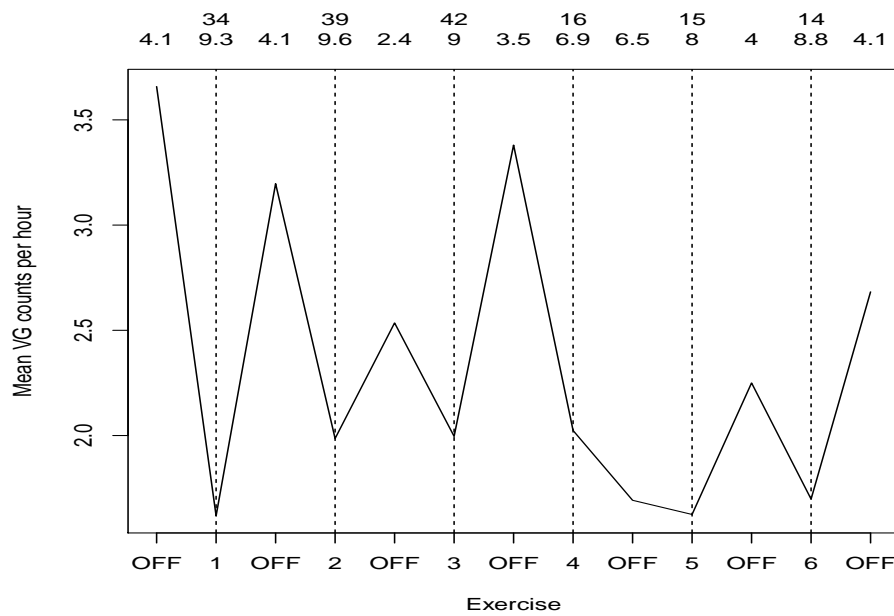


Figure 19: The mean number of vocal groups starting per hour, during the mini wars period, as a function of whether or not an actual exercise is going on. The first and second row of numbers on top of the plot correspond respectively to the number of level 3 events in each exercise and the period length (in hours)

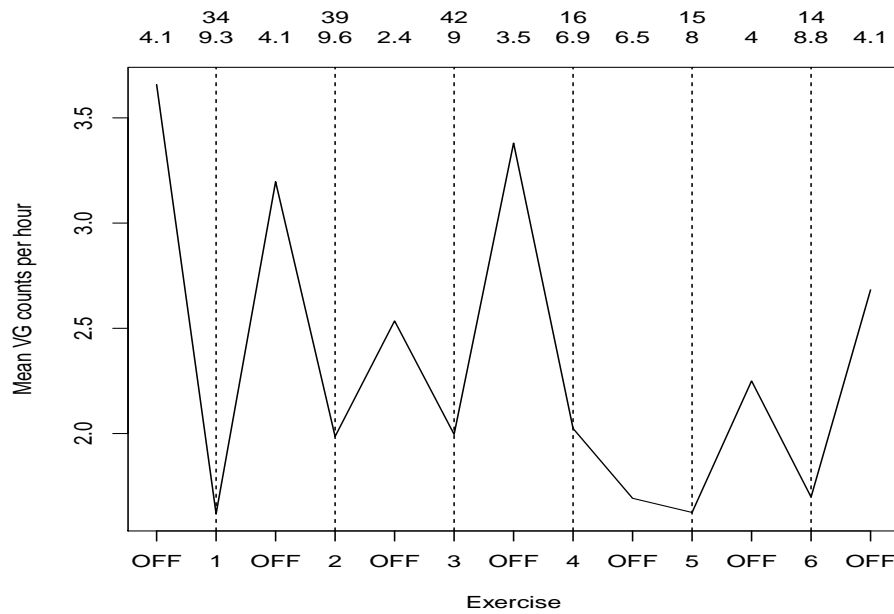


Figure 20: The mean number of vocal groups starting per hour, during the mini wars period, as a function of whether or not an actual exercise is going on. The first and second row of numbers on top of the plot correspond respectively to the number of level 3 events in each exercise and the period length (in hours)

- (2009). Estimating cetacean population density using fixed passive acoustic sensors: an example with Blainville's beaked whales. *The Journal of the Acoustical Society of America*, **125**, 1982–1994.
- McCarthy, E., Moretti, D., Thomas, L., DiMarzio, N., Morrissey, R., Jarvis, S., Ward, J., Izzi, A., and Dilley, A. (2011). Changes in spatial and temporal distribution and vocal behavior of blainville's beaked whales (*Mesoplodon densirostris*) during multiship exercises with mid-frequency sonar. *Marine Mammal Science*, **27**, E206–E226.
- Tyack, P. L., Johnson, M., Soto, N. A., Sturlese, A., and Madsen, P. T. (2006). Extreme diving of beaked whales. *Journal of Experimental Biology*, **209**(21), 4238–4253.
- Tyack, P. L., Zimmer, W. M. X., Moretti, D., Southall, B. L., Claridge, D. E., Durban, J. W., Clark, C. W., D'Amico, A., DiMarzio, N., Jarvis, S., McCarthy, E., Morrissey, R., Ward, J., and Boyd, I. L. (2011). Beaked whales respond to simulated and actual navy sonar. *PLoS ONE*, **6**, e17009.
- Ward, J., Jarvis, S., Moretti, D., Morrissey, R., DiMarzio, N., Thomas, L., and Marques, T. (2011). Beaked whale (*Mesoplodon densirostris*) passive acoustic detection with increasing ambient noise. *The Journal of the Acoustical Society of America*, **129**, 662–669.
- Wood, S. N. (2006). *Generalized Additive Models: an introduction with R*. CRC/Chapman & Hall.

File	Code	Sent by (on)	From	$R \times C$
2009MaySCC_sonar_and_whales_forLen_27June2011.xlsx	D1	EMcC (28-06-11)	3 May - 14 Jun	103,96
Tiago_vocal_groups_on_range_during_military_activities.xls	D2	EMcC (24-03-11)	23 Apr - 17 Jun	1202,24
Tiago_vocal_activity_BEFORE_Sonar.xls	D3	EMcC (18-03-11)	18 Apr - 14 May	3239,13
Tiago_vocal_activity_DURING_Sonar.xls	D4	EMcC (18-03-11)	14 - 17 May	150,13
Tiago_vocal_activity_AFTER_Sonar.xls	D5	EMcC (18-03-11)	17 May to - Jun	3950,13
Tiago_Activity_on_AUTEC_April-June2009_v2.xls	D6	DA (20-04-11)	17 Apr - 20 Jun	292,15

Table 1: Details for the files analyzed in this report. All the files are from the 2009 Submarine Commander Course at AUTEC. $R \times C$ is the number of rows and columns in the original data file.

Exploratory analysis of available DTAG data

Tiago A. Marques & Len Thomas

Centre for Research into Ecological and Environmental Modelling
The Observatory, University of St Andrews, St Andrews, KY16 9LZ, Scotland

Version's date: July 18, 2011

Contents

1	Introduction	1
2	Data details	2
3	Exploratory Data analysis	3
4	Depth profile data	8
	References	11

1 Introduction

In this document we present the available DTAG data. This is essentially the same data which was used to estimate the detection function in Marques *et al.* (2009), the corresponding internal DECAF report where analysis are presented being Marques and Thomas (2008b)

Currently we DTag data available for 13 (3+3+3+4) dives from 4 whales - Md296, Md245a, Md248a and Md248b, used for the detection function estimation in Marques *et al.* (2009).

We also have some additional DTag data from 1 dive for Md245a, 1 dive for Md248b and 6 dives from a fifth whale (Md227a). While these data were not associated with the hydrophone data due to several reasons (animal off the range, hydrophones not recording, etc.) and hence not used for the detection function estimation, here we can use them in the same way as we are not interested in the hydrophone information.

2 Data details

After discussion with Jessica Ward, we agreed on an adequate data format which would be easily updated as/if additional dives became available. This would be a flat txt file, with as many rows as relevant hydrophone-click combinations and the following 21 columns (the code in brackets represents the name of the variable within the R workspace):

1. Tag - a code for the tag (**tag**);
2. Dive # - a code for the dive (**dive**);
3. Year - the year the data was collected in (**year**);
4. Julian Day - the Julian day (**jd**);
5. GMT (seconds) - the number of seconds since the start of the year (**gmts**);
6. Hyd - the hydrophone number (**hyd**);
7. Detection - 0 if click was detected at hydrophone, 0 otherwise (**det**);
8. Whale X (m) - the x coordinate of the whale (**x**)
9. Whale Y (m) - the y coordinate of the whale (**y**)
10. Whale Z (m) - the z (depth) coordinate of the whale (**z**)
11. Slant range (m) - the 3D distance from the whale to the hydrophone (**slant**)
12. Horizontal Range (m) - the 2D distance (as projected on the sea surface) from the whale to the hydrophone (**dist**)
13. Elevation Angle (rad) - the off-axis elevation angle, in $(-\pi/2, \pi/2)$, also named vertical aspect angle in previous reports (**vaa**). This is measured on the frame of the whale
14. Azimuth Angle (rad) - the off-axis horizontal angle, in $(-\pi, \pi)$, also named horizontal aspect angle in previous reports (**haa**). This is measured on the frame of the whale

15. Winds speed (m/s) - the winds speed in meters per second (**wind**)
16. Noise1 (5-ms rms dB - uncorrected direct measurement from wav file) (**noise1**)
17. Noise2 (500-ms rms dB - uncorrected direct measurement from wav file) (**noise2**)
18. Hydrophone Calibration constant (Db) $N = N_{rms} - HydCal + 20$ (allies to wav gain)(**hc**)
19. Heading (**heading**)
20. Pitch (**pitch**)
21. Roll (**roll**)

Note we also require the location of the hydrophones, which is in a separate file. Details about reading the data in and preliminary data manipulation are in the source.Rnw file.

A dive indicator was added (**dvid**) to the data, as well as a variable containing the vertical aspect angle in the full circle (**vaa2**). For some details about *vaa2*, which we ended up not really using here (as well as for the reasons for that choice), see Marques and Thomas (2008a).

3 Exploratory Data analysis

As a first step, we can compute how many inter click intervals we have (equals to number of clicks -1) per dive, and what these look like (Table 1 and Figures 1-4). We can see that the reported mean

For direct comparison with Johnson *et al.* (2006), we removed anomalously long and short ICIs. We can see that the reported mean of the mean ICIs was 0.324 seconds, a value just slightly lower than that reported by Johnson *et al.* (2006) (0.37 seconds, 1 whale, 4 dives, Canary Islands). Note however that the mean ICI for no dive was as high as that reported value.

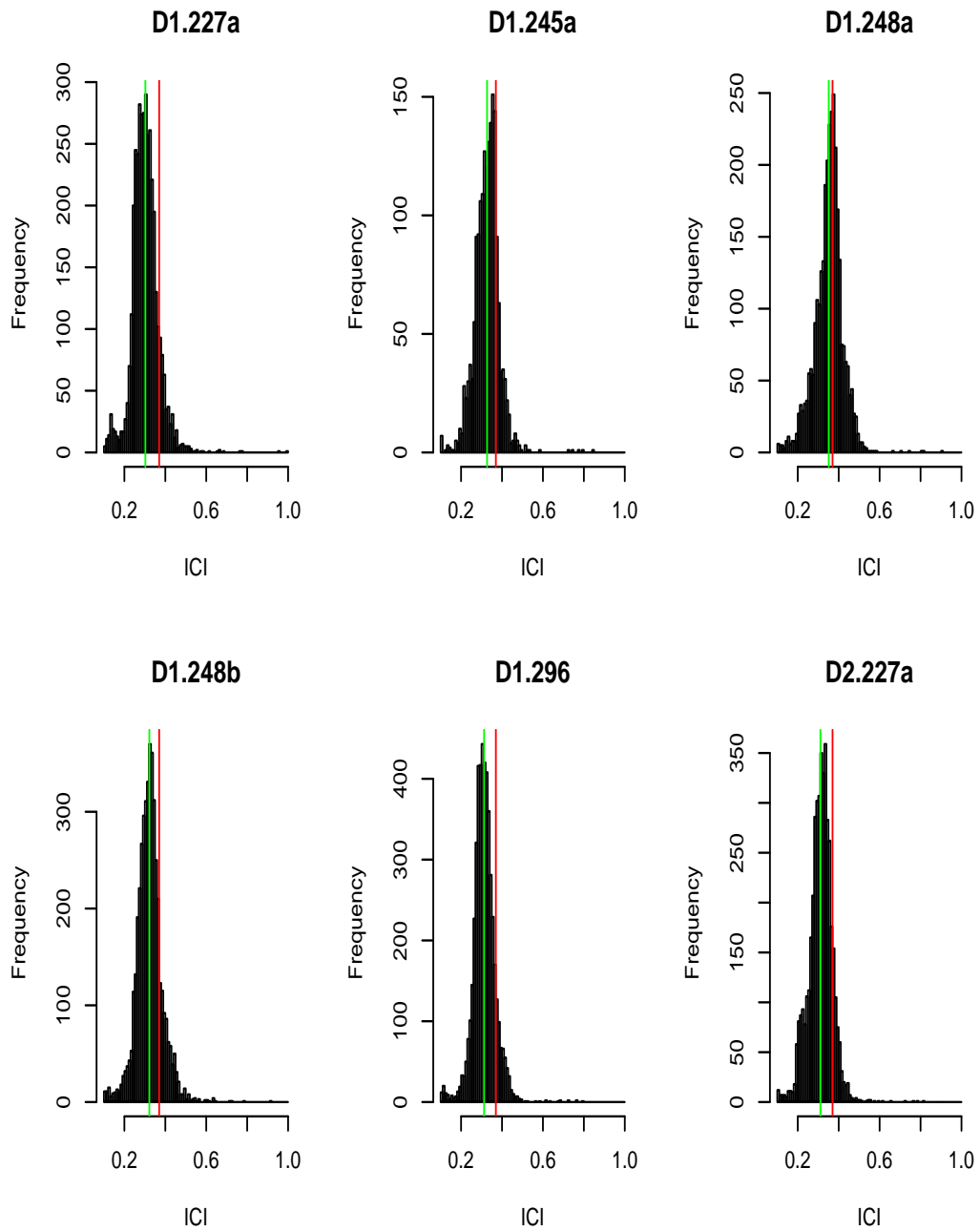


Figure 1: ICI histograms for ICS's above 0.1 second and below 1 second, discriminated by dive.

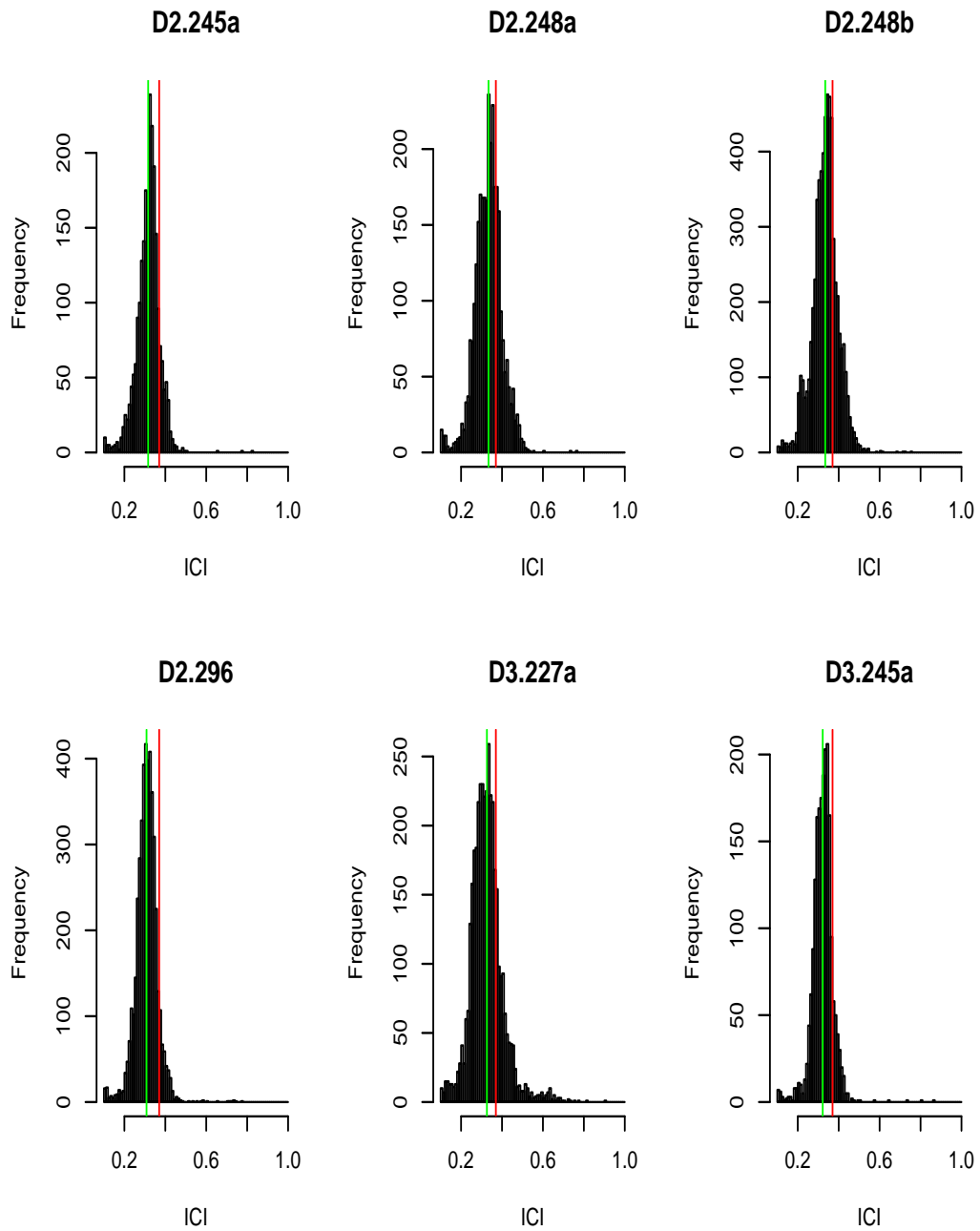


Figure 2: ICI histograms for ICS's above 0.1 second and below 1 second, discriminated by dive.

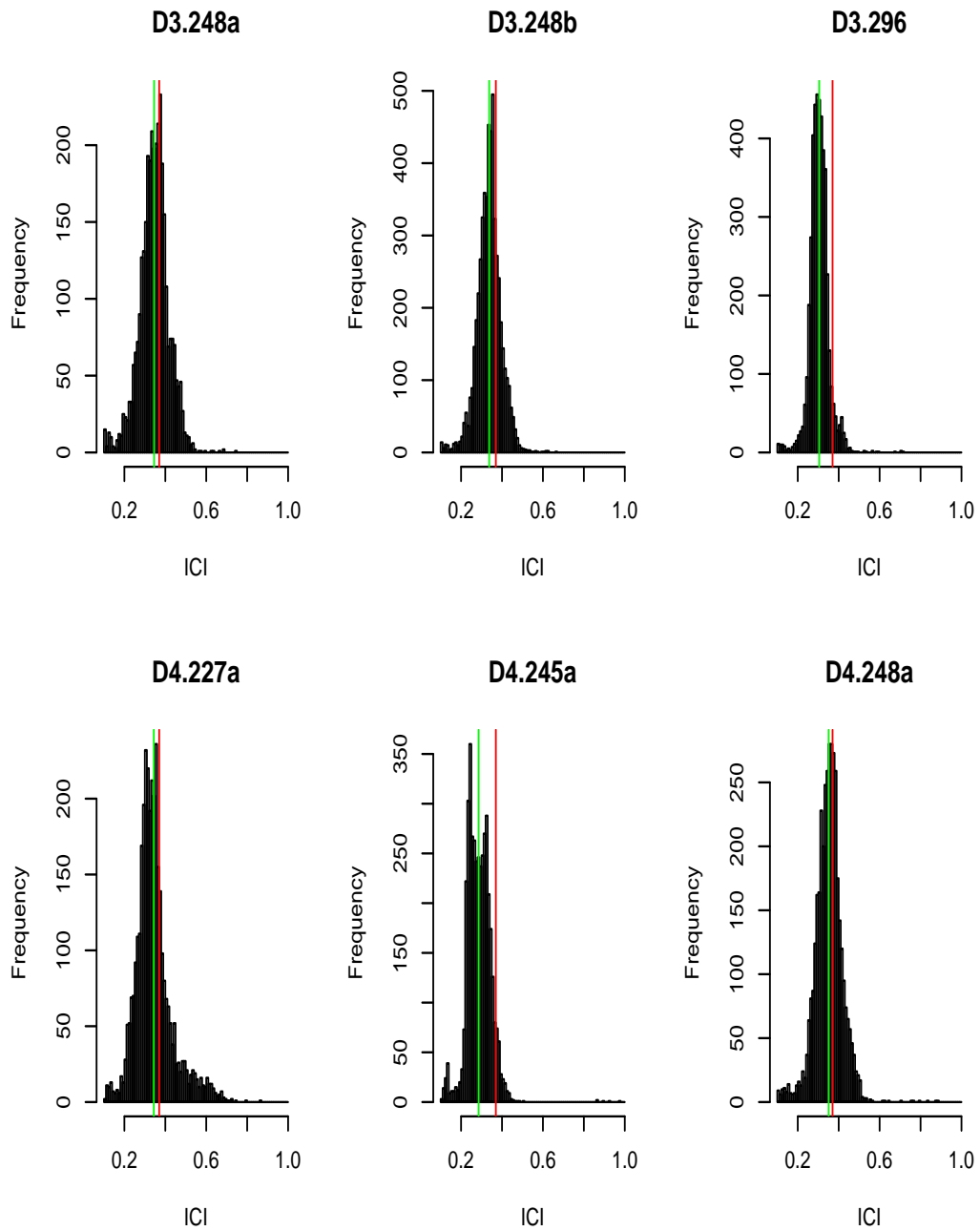


Figure 3: ICI histograms for ICS's above 0.1 second and below 1 second, discriminated by dive.

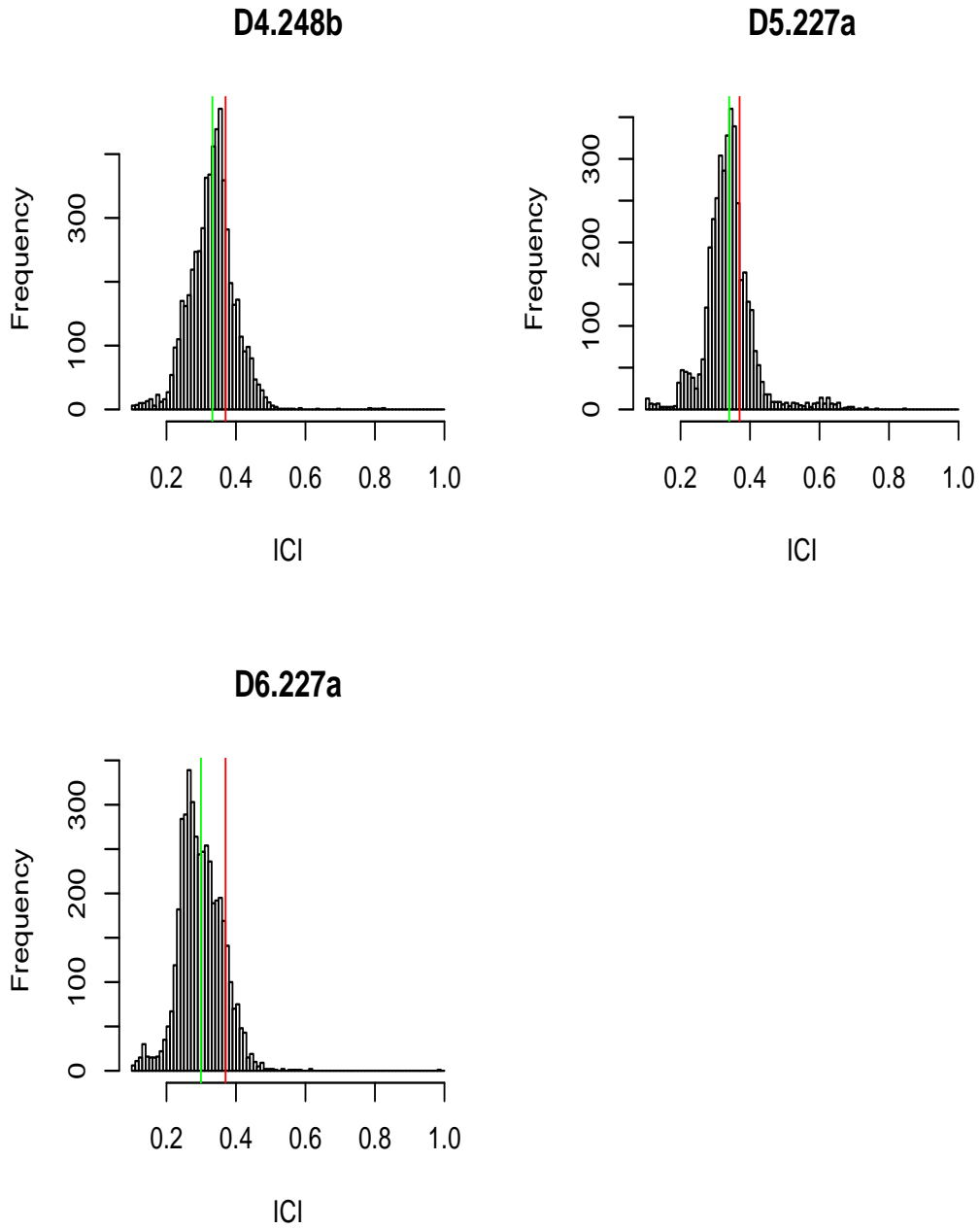


Figure 4: ICI histograms for ICS's above 0.1 second and below 1 second, discriminated by dive.

4 Depth profile data

In this document we present a simple EDA of the data kindly sent to us by Robin Baird on the 19th May 2008. This data corresponds to a time-depth tag data deployed on a *Mesoplodon densirostris* in 2006. An exhaustive analysis of this data (and several other whales) is in Baird *et al.* (2008).

```
> file <- "datfiles/CLEAN Md 2006Nov22 female 0390674 TM.csv"
> BWdat <- read.table(file = file, header = F, skip = 4,
+   sep = ",", na.strings = "", colClasses = "numeric")
> names(BWdat) <- c("Tday", "D", "D1")
> BWdat <- BWdat[BWdat$Tday < 39046.7275, ]
> BWdat <- within(BWdat, TdayS <- (Tday - Tday[1]))
> BWdat <- within(BWdat, ThourS <- TdayS * 24)
> BWdat <- within(BWdat, TminS <- TdayS * 24 * 60)
> BWdat <- within(BWdat, TsecS <- TdayS * 24 * 60 * 60)
> BWdat <- within(BWdat, TsecSr <- round(TdayS * 24 * 60 *
+   60))
```

The continuous deep diving pattern is almost tiring just from watching (Figure 5). If we zoom in in a couple of dives, it is simple to see why these whales are rarely detected by visual observers (Figure 6). Because the DTag data we have, as used in say Marques *et al.* (2009), corresponds to data recorded at each click event, we do not have information regarding all non deep dive parts of the track, but this would be useful to have and we have already requested it to NUWC. In some sense, modeling explicitly what happens or not outside the vocal parts of the dives might be unnecessary (even if less interesting and realistic.). Treating this part of the movement as a black-box, and just having a distribution to go from the point where the whale goes silent (on the ascent phase) to the point where it starts vocalizing again (in the descent phase of the next deep dice) might just be enough.

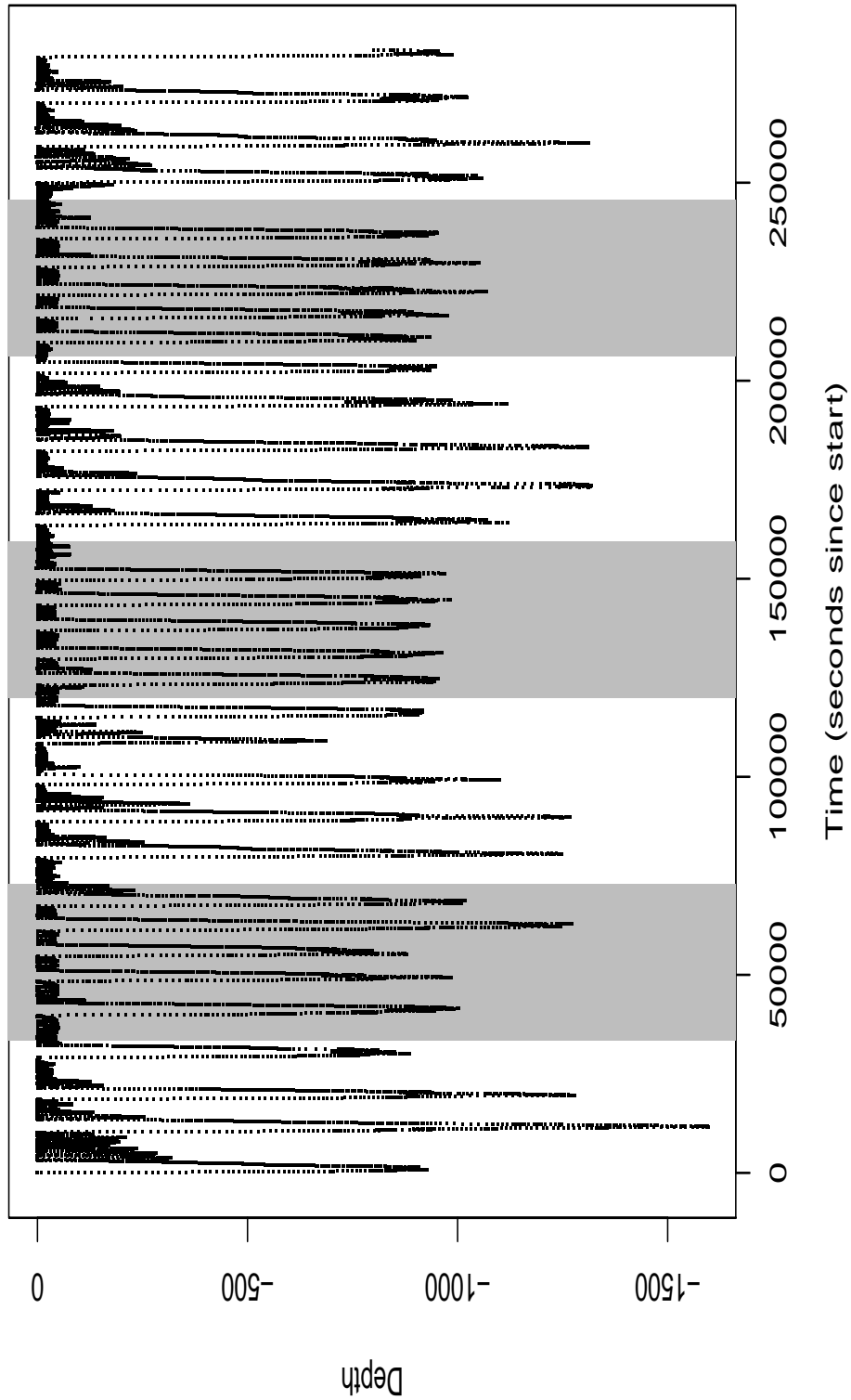


Figure 5: The depth profile of the 80 hour dive. Shaded periods correspond to “night” periods, 20:00 to 07:00, although the best would be to have sunset and sunrise hours.

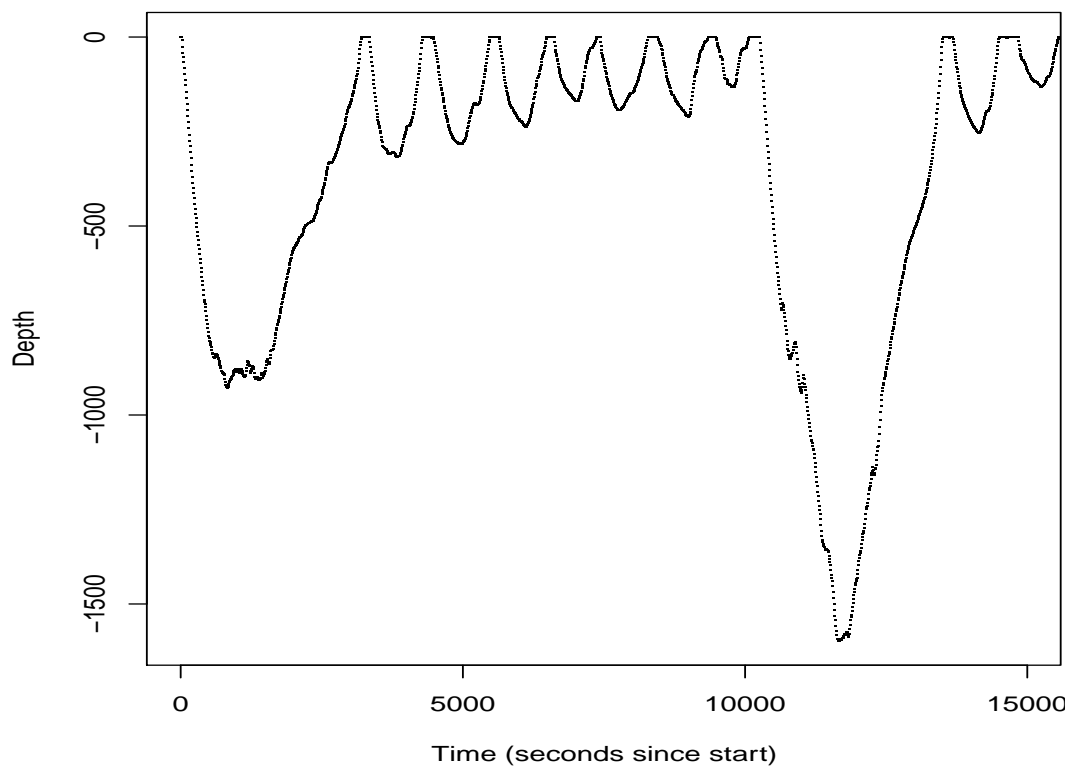


Figure 6: Zooming in the first dive.

References

- Baird, R. W., Webster, D. L., Schorr, G. S., Mcsweeney, D. J., and Barlow, J. (2008). Diel variation in beaked whale diving behavior. *Marine Mammal Science*, **24**, 630–642.
- Johnson, M., Madsen, P. T., Zimmer, W. M. X., de Soto, N. A., and Tyack, P. L. (2006). Foraging Blainville’s beaked whales (*Mesoplodon densirostris*) produce distinct click types matched to different phases of echolocation. *The Journal of Experimental Biology*, **209**, 5038–5050.
- Marques, T. A. and Thomas, L. (2008a). A closer look at vaa. Technical report, DECAF internal report.
- Marques, T. A. and Thomas, L. (2008b). Estimating the mean probability of detection of a beaked whale click at AUTECH. Technical report, DECAF internal report.
- Marques, T. A., Thomas, L., Ward, J., DiMarzio, N., and Tyack, P. L. (2009). Estimating cetacean population density using fixed passive acoustic sensors: an example with Blainville’s beaked whales. *The Journal of the Acoustical Society of America*, **125**, 1982–1994.

	Nall	Nlow	Nreg	Nhigh	meanall	meanreg
D1.227a	4006	92	3818	96	0.362	0.303
D1.245a	1822	4	1785	33	0.387	0.327
D1.248a	3107	9	3028	70	0.448	0.351
D1.248b	4508	4	4406	98	0.393	0.322
D1.296	4905	8	4788	109	0.376	0.313
D2.227a	4336	19	4246	71	0.356	0.311
D2.245a	2365	16	2298	51	0.361	0.316
D2.248a	3124	10	3041	73	0.403	0.334
D2.248b	6166	11	6044	111	0.386	0.334
D2.296	4603	11	4486	106	0.374	0.308
D3.227a	3932	23	3828	81	0.389	0.326
D3.245a	2077	9	2022	46	0.365	0.322
D3.248a	3393	9	3302	82	0.417	0.346
D3.248b	5447	11	5343	93	0.386	0.337
D3.296	4517	4	4436	77	0.349	0.304
D4.227a	3514	10	3440	64	0.396	0.344
D4.245a	4162	6	4038	118	0.357	0.286
D4.248a	3896	6	3805	85	0.431	0.351
D4.248b	5815	9	5699	107	0.403	0.332
D5.227a	4051	19	3966	66	0.383	0.340
D6.227a	4473	13	4355	105	0.364	0.299
mean	4010	14	3913	83	0.385	0.324

Table 1: The columns represent, for each dive, respectively the Number of ICIs available (Nall), the number of those less than 0.1 seconds (Nlow), the ones between 0.1 and 1 second (Nreg), and those above 1 second (Nhigh), as well as the means for all (meanall) and the regular (meanreg) ICIs.

Obtaining pseudo-tracks and georeferenced locations from DTAG data

Tiago A. Marques & Len Thomas

Centre for Research into Ecological and Environmental Modelling
The Observatory, University of St Andrews, St Andrews, KY16 9LZ, Scotland

Version's date: November 14, 2013

Contents

1	Introduction	2
1.1	State-space model notation	3
2	A state-space model to obtain pseudo-tracks	3
2.1	The geometry of the problem	4
2.1.1	Obtaining the depth state transition equation	4
2.1.2	Dead-reckoning given speed, prh and initial position	5
2.2	Estimating speed via the Kalman Filter	7
2.2.1	Zooming in Mark's tool	7
3	Current georeferencing procedure	13
3.1	Including behavioral states	14
4	Improving the current SSM formulation	15
4.1	Considering location as states	15
4.2	Including observations from acoustic localization	16
4.3	Considering heading and pitch as states	17
5	So now what?	18
	References	19

1 Introduction

In this document we describe the procedures involved in going from DTAG data, in the form of “prh” files (time indexed files of pitch, heading and roll), to pseudotracks and from those and acoustic localizations, to georeferenced locations.

The document is structured as follows. Building on a brief description of state-space models notation, in section 2 we address the current approach to process DTAG data to obtain a pseudo-track over time. This is divided in two parts: in section 2.1 we present the basic trigonometry involved, and how locations can be updated based on this via dead-reckoning. In section 2.2 we present a state-space model¹ to estimate states depth and speed from depth observations (and where pitch is taken as a known covariate, i.e. pitch is assumed to be observed without error). This is essentially what, to date, has been fitted to DTAG data using a Kalman filter, based heavily on Mark Johnson’s work (and code). We look in close detail to the Kalman filter code created by Mark Johnson to estimate speed as a function of depth and pitch collected from DTAG data. We refer to the use of this “best” speed estimate together with depth, pitch, heading and tag on position to obtain a track, as “pseudo-tracking”.

Including acoustic localizations (details of how these are obtained are available in (Marques *et al.*, 2012)) in this process to provide tracks which are combined with locations assumed to be known with negligible error, and hence counterbalancing the drift from dead-reckoning, leads to a process referred to as “geo-referencing”. A brief description of how this has been done to date, namely a simulated annealing algorithm implemented to process the data used in Marques *et al.* (2009), is presented in section 3. This lays the ground for possible improvements, as described in section 3.1, namely by including behavioral states.

In section 4 we build on the existing model, namely to consider additional states in the formulation, like actual location, heading and pitch. We lay down such models in some detail because that will be the basis for subsequent work, namely a state-space model which includes the acoustic localizations of animals to improve on track estimation.

The implementation of these models is the subject of a separate LATTE

¹Strictly speaking, we present it as a dynamic linear model, along the lines of Petris *et al.* (2009)

internal report Marques and Thomas (2012).

1.1 State-space model notation

A simple state-space model can be thought of a couple of equations, describing two “parallel” time series, the state and the observation processes. The states are the underlying true quantities we often want to make inferences about, while the observations are some observable quantities which can be related to the states by some known process. Borrowing the notation from Petris (2010) we have

$$o_t = F_t \theta_t + v_t, \quad v_t \sim N(0, V_t) \quad (1)$$

$$\theta_t = G_t \theta_{t-1} + \omega_t, \quad \omega_t \sim N(0, W_t) \quad (2)$$

where θ_t represents the state in time t and vector o_t represents the observations at time t , and V_t and W_t represent respectively the observations and states variance-covariance matrices. For simplicity in the above we have assumed the observation and state process errors to be Gaussian, but in general they do not need to be so.

2 A state-space model to obtain pseudo-tracks

In this section we describe a possible state-space model to estimate whale speed and depth from DTAG data, where the input observed data comprises depth. Pitch is also a necessary input, but is taken as an external covariate, not as part of the observation vector, and hence assumed to be known without error. The reason this was implemented in this way was purely pragmatic: at the time this was just a first stab at the problem (Mark Johnson, pers. comm.).

The DTAG comprises a number of sensors which allow us to measure variables including depth, magnetic fields and acceleration (Johnson and Tyack, 2003). From these we can obtain, coupled with calibration information, estimates of whale pitch, heading and roll (in the following we refer to these as prh data, or prh files). Here we do not investigate further the methods/details required for obtaining these files. Instead, we build on these files to try to obtain a spatially indexed track. We note however that if one wants to delve

deeper into the process, then this would be a good place to start: there is a lot of complex 3D trigonometry involved in converting acceleration and magnetometer data measured on the frame of the DTAG into pitch, heading, and roll on the hearth frame (see Johnson and Tyack, 2003, for details).

Given an initial tag-on position, the prh data over time, and a reasonable constant speed, simple 3D trigonometry leads to a track in 3D space through dead-reckoning. Section 2.1.2 describes how this is implemented in detail. However, this 3D track is affected by additive drift errors over time. An example is shown in figure 5 in Mitani *et al.* (2003).

Here we concentrate on obtaining the best possible estimate of speed, so that we can also obtain the best possible estimate for the track path, at least without any additional information. We build on this in section 4.2), by adding acoustic localization information to the process.

We present a state-space model which provides an estimate of speed (s) and depth (z) as a function of pitch (ϕ) and depth (z) inputs. We explicitly note a particularity of the proposed model: while depth is assumed to be an observation made with error, pitch is taken as a known covariate. This was a pragmatism-derived implementation decision, not really based on any theoretical consideration. Note in particular that, from figure 5 in Johnson and Tyack (2003), it seems clear that there is non negligible measurement error associated with pitch.

Below we describe two processes:

1. The relation between depth, pitch and speed, as well as how to use speed (and a starting location) to update an animal position over time (section 2.1), considering a dead-reckoning process.
2. How to obtain an estimate of speed from the DTAG data (section 2.2), using the Kalman filter (as previously stated, heavily based on MJ code);

2.1 The geometry of the problem

2.1.1 Obtaining the depth state transition equation

We consider here that the animal moves in a straight line between successive time points. Consider a depth difference $\Delta z_t = z_t - z_{t-1}$ between the animal's position at two successive time points t and $t-1$, such that $\Delta T_t = T_t - T_{t-1}$ (We assume for notation simplicity that $\Delta T_t = \Delta T$, for all t). Let h_t represent

the slant distance between the animal location at time t and time $t - 1$. Then by simple trigonometry² we have that

$$\Delta z_t = h_t \sin(\phi_t)$$

which can be rearranged to

$$h_t = \frac{\Delta z_t}{\sin(\phi_t)}$$

Assuming that the mean animal speed between time point t and $t - 1$ is given by s_t , then

$$s_t = \frac{h_t}{\Delta T}$$

we can write that

$$s_t = \frac{\frac{\Delta z_t}{\sin(\phi_t)}}{\Delta T} = \frac{\Delta z_t}{\Delta T \sin(\phi_t)} \quad (3)$$

We can therefore explicitly connect the depth observation (z) to the pitch state (s), as well as writing down the depth state updating process, by rearranging this expression, leading to

$$z_t = \sin(\phi_t) s_t \Delta T + z_{t-1}$$

We could also write pitch as a function of the depth (or speed) as

$$\phi_t = \arcsin\left\{\frac{\Delta z_t}{s_t \Delta T}\right\}$$

but this is not used here.

2.1.2 Dead-reckoning given speed, prh and initial position

Given a reasonable estimate of the whale initial x, y, z location, as well as speed (s), depth (z), heading (ψ) and pitch (ϕ) over time, we can build a pseudo-track by dead-reckoning.

²Note that as $-\sin(\phi) = \sin(-\phi)$ depending on whether we define pitch angle positive when pointing upwards or downwards one needs to change the sign associated with this sin expression.

We can estimate the (two dimensional, i.e. as projected on the sea surface) easting (v_x) and the northing (v_y) velocity components as ³:

$$\begin{pmatrix} v_x \\ v_y \end{pmatrix} = s \cos(\phi) \begin{pmatrix} \sin(\psi) \\ \cos(\psi) \end{pmatrix} + s_c \begin{pmatrix} \sin(\rho) \\ \cos(\rho) \end{pmatrix}$$

The term $\cos(\phi)$ accounts for the pitch of the whale (i.e., while the whale displaces itself at a given speed s along the straight line that goes through (x_t, y_t, z_t) and $(x_{t+1}, y_{t+1}, z_{t+1})$, that is reduced in the x and y dimensions by a factor that depends on the pitch; the higher the pitch, the higher the reduction factor; this seems intuitive enough, but a plot would help visualizing this effect.). The second term of this sum accounts for the water current, assumed to have heading ρ and velocity s_c . If $s_c = 0$, i.e., if we assume the influence of the current is negligible, the second part disappears. Note that is the case presented by Wilson *et al.* (2007). We will assume this is a valid assumption in our case, although presumably part of the problems we encountered in drifting stem from this being an unreasonable, despite clearly simplifying, assumption. However, lacking information on the currents at AUTECH at the time the data was collected, it is hard to improve on this at this point.

So now, to update the position in time we just need to update the x and y positions by adding the previous coordinate to the product of velocity (in each dimension) and elapsed time (note this product corresponds to displacement for the corresponding x or y dimension), i.e.

$$\begin{pmatrix} x_{t+1} \\ y_{t+1} \end{pmatrix} = \begin{pmatrix} x_t + \Delta T v_x \\ y_t + \Delta T v_y \end{pmatrix} \quad (4)$$

Note that this formulation hints towards the fact that x and y could also be treated as states we want to estimate. This would mean we have it all defined as a single procedure, rather than the current plug-in approach in which we first estimate speed, and then use this estimated speed to propagate the path, without accounting for the associated variance in this process. Including location as states will in fact be the approach presented in section 4.1.

³this is equation 7 from Johnson and Tyack (2003), but TAM only really understood this after reading Wilson *et al.* (2007), in particular around equations 1-3, and seeing these are the same if one considers $v = \frac{h}{\Delta T}$; Mitani *et al.* (2003) and Shiomi *et al.* (2008) also helped in this process.

2.2 Estimating speed via the Kalman Filter

2.2.1 Zooming in Mark's tool

The Kalman Filter is a tool that can be used to estimate unknowns in a system specified as a dynamic linear model (as in equations 1 and 2 above). Intuitively, the filter proceeds by sequentially updating the current position of the system states by a weighted average of (1) the next position given the expected system evolution and (2) the observation (which is related to the state value by some observation model), in which the weight depends on how much relative faith we have (1) on the knowledge of the system vs (2) the measurement error in the observation process.

Here we take a look into a couple of MATLAB .m files referred to as “Mark’s tool”, which were developed by Mark Johnson and sent to us by Jessica Ward. The reason to do so is because these two files should be an implementation of the pseudo-track procedure, and hence understanding these will help understand the entire process.

The two MATLAB files correspond to:

- **ptrack.m** - this script calculates the pseudo-track by dead-reckoning (see section 2.1 for more details on this), given as inputs (vectors of) pitch, heading and speed⁴; the input parameter p can be either be a scalar, and then it is interpreted as a mean speed to be used for dead-reckoning, or it can be a vector of depths, which then gets used with the pitch vector in the next function, which implements a Kalman-Filter to estimate speeds over time. These speeds then get used to implement the dead reckoning. Within **ptrack.m** there is an optional low-pass filter⁵ to be implemented over the track (x, y or x, y, z) and speeds.
- **kalmanspeedest.m** - this function is called inside **ptrack.m**, if (and only if) p is a vector of depths. This implements the Kalman filtering and smoothing to obtain speed and depth estimates which then get used inside **ptrack.m** for dead-reckoning. From what we can tell,

⁴note other inputs are required by the function, but not relevant here so we ignore them

⁵Quoting MJ: The LPF is a bag on a dog. It is not the right way to do it but was a quick hack to overcome problems at sharp pitch changes. Contrary to the very simple dynamic model that I used in the kf, animals are not rigid and do not move without slip or lift. this leads to awkward data at turning points in the dive where the animal can be pitched upwards but still moving downwards. ideally the model should include inertia but there is a limit to how much we can sophisticate it without courting unobservability again.

only the estimated speeds, not the estimated depths, are used in the `ptrack.m` function, but there is no reason to do so, and in fact, given that these are supposedly a better estimate of depth, we should use these for consistency. In practice, observed and estimated depths are very similar.

We look below in closer detail to `kalmanspeedest.m`, to understand how the Kalman Filter is implemented and to check the underlying state-space model formulation.

The input parameters in `kalmanspeedest.m` are vectors with depth (`p`) and pitch (`pitch`) (over time), as well as `fs`, the sampling frequency in Hz.

The first relevant chunk of code is:

```
% measurement noise cov. : this should be set equal to the noise power
% in the depth estimate, p, e.g.,  $0.05\text{ m}^2$ . was 0.005
%TAM - strictly, this is not a covariance, but a variance %TAM - this
corresponds to the matrix  $V_t$  in equation 1
r = 0.001 ;
% speed state noise cov. : accounts for variations in speed, was 0.05
q1 = (0.02/fs)^2 ;
% depth state noise cov. : accounts for errors in pitch angle, was 0.05
q2 = (0.08/fs)^2 ;
% T is the time interval between successive measurements
T = 1/fs ;
```

This seems to imply that these variances are being fixed rather than estimated. The comments in the code (e.g. “was 0.05”) probably mean that there was some initial tuning to find variance values which provided reasonable results.

Then the following code chunk follows:

```
% vector Kalman filter with 2 states: s and p
% transition matrix entry (2,1)
a = -sin(pitch)/fs ;
% starting state estimate
shatm = [1;p(1)] ;
% state noise matrix
%TAM: note this is matrix  $W_t$  in equation 2
```

```

Q = [q1 0;0 q2] ;
% observation vector
%TAM: note this is matrix  $F_t$  in equation 1
H = [0 1] ;
% initializing the state covariance matrix:
% says how much we trust initial values of  $s$  and  $p$ 
Pm = [0.01 0;0 r] ;

```

In the current implementation, Q , which corresponds to W_t in equation 2, is assumed known, i.e. we assume we know the process error (a.k.a. process noise). Similarly, the variance in the observations, r , is also cast in stone, and does not get updated. There are Kalman Filter variants in which these variances can also be estimated, but we do not consider them for now.

In the above the line stating “initial state covariance matrix:” is initializing the estimation error covariance matrix (quantifies our precision around the state predictions), which would correspond to P_0 in Simon (2001) and $P_{0|0}$ in Gannot and Yeredor (2008). Further r should be the measurement error variance in depth⁶.

Note also that Pm gets updated at each iteration, and hence hopefully the initial values we use for the variances in the predictions of speed and depth will not have a big influence in the final outcome.

Given this, we can write the observation and state equations respectively as

$$o_t = [0 \ 1] \begin{pmatrix} s_t \\ z_t \end{pmatrix} + v_{z_t} \quad (5)$$

and (note $1/fs = \Delta T$)

$$\begin{pmatrix} s_t \\ z_t \end{pmatrix} = \begin{pmatrix} 1 & 0 \\ -\sin(\phi_t)\Delta T & 1 \end{pmatrix} \begin{pmatrix} s_{t-1} \\ z_{t-1} \end{pmatrix} + \begin{pmatrix} \omega_{s_t} \\ \omega_{z_t} \end{pmatrix} \quad (6)$$

where we recall that here v and ω are assumed to be Gaussian unbiased errors (with some variance covariance matrix; here also so far we assume covariances in the errors are 0). We then have a set of lines which initiates

⁶Apparently it is just a non-ideal coding shortcut that r is used twice, one for the variance in the observation of depth, and another for the initial estimate of variance in depth in the state process

the objects used to store state estimates and state smoothed estimates (as well as to store covariance matrices)

```
% place to store states
skal = zeros(2,length(p)) ;
% TAM: place to store smoothed state estimates
srau = skal ;
%TAM: place to store the Kalman
%a posteriori state predictions covariance matrix (2x2xn)
Ps = zeros(2,2,length(p)) ;
Pms = Ps ;
```

The next chunk of code is the beginning of the implementation of the Kalman filter itself, defining for each observation

```
for k=1:length(p),
```

the actual state transition matrix, i.e. G_t in equation 2 and expression Φ_n in (Gannot and Yeredor, 2008, equation 8.20)

```
Ak = [1 0;a(k) 1] ;
```

After this comes an expression⁷ that updates the state covariance matrix.

```
if k>1,
```

```
% update a priori state variance-covariance matrix
```

```
Pm = Ak*P*Ak' + Q ;
```

Note this is expression 8.33 in Gannot and Yeredor (2008), followed by the deterministic part of equation 6 above:

```
% a priori state estimate
```

⁷It must be noted this expression is not evaluated for $k = 1$; this confused me for a while because I could not understand where P or $shat$ was obtained from, but then I realized these are defined as the next chunk of code is evaluated when $k = 1$ and produces the first instances of these objects

```
% i.e. expression p1 in page 141 in Gannot and Yeredor (2008)
shatm = Ak*shat ;
end
```

Note that here *shat* is a 2 by 1 matrix with the current state estimates (see how it gets defined below). Now finally we compute the Kalman gain

```
K = Pm*H'/(H*Pm*H'+r) ;
```

which corresponds to expression 8.32 in Gannot and Yeredor (2008) or to the first equation on the top right corner of page 74 in Simon (2001) (although in this case one needs that Mark's Pm = Simon's AP_k = Gannot's $P_{n|n-1}$). Then we finally compute the current state estimate

```
% a posteriori state estimate
shat = shatm + K*(p(k)-H*shatm) ;
% speed and depth must always be positive
% shat = max([shat'; [0 0]])' ;
```

which is at the very essence of the Kalman filter, corresponding to equation 8.21 in Gannot and Yeredor (2008) or the second equation on the top right corner of page 74 in Simon (2001). Note also there is a commented line of code which, if evaluated (i.e. uncommented), enforces both speed and depth to be strictly non negative.

Next there is the expression which computes the state covariance, which is expression 8.35 in Gannot and Yeredor (2008). I suspect that this also corresponds to the third equation on the top right corner of page 74 in Simon (2001) (which might be a variation the form of equation 8.34 in Gannot and Yeredor (2008)). Note that this matrix corresponds to the mean square error of our prediction, and hence is of the uttermost importance to evaluate our predictions quality (Gannot and Yeredor, 2008, ,cf. pag. 141).

```
% a posteriori state variance-covariance matrix
%TAM: note eye(2) returns the 2 x 2 identity matrix, [1 0; 0 1]
P = (eye(2)-K*H)*Pm ;
```

Finally we place current iteration results in the appropriate places, respectively the current state estimates in *skal*, the a priori state variance-

covariance matrix in `Pms`, and the a posteriori state variance-covariance matrix in `Ps`:

```
skal(:,k) = shat ;
Pms(:,:,k) = Pm ;
Ps(:,:,k) = P ;
end
```

By now the filtering has been completed, and we move on to the smoothing part of the algorithm (strictly, the Kalman filter is over at this point, but the smoothing is such a common objective that it is sometimes treated as part of the Kalman filter itself). Here the code starts with

```
%Vh is P(T) - TAM: not sure what this comment refers to (neither does MJ!)
srau(:,length(p)) = shat ;
```

which just stores the last state as the smoothed estimate (as there is nothing to smooth here “in the present”, we can only smooth “into the past”). Then, for each of the remaining $(p - 1)$ states, go backwards and compute

```
% Kalman/Rauch smoother
for k=length(p):-1:2,
% make state transition matrix
Ak = [1 0;a(k-1) 1] ;
% smoother gain TAM.
K = Ps(:,:,k-1)*Ak'*inv(Pms(:,:,k));
% smooth state
srau(:,k-1) = skal(:,k-1)+K*(srau(:,k)-Ak*skal(:,k-1)) ;
end
```

These equations are represented in Gannot and Yeredor (2008) by equations 8.68 and 8.69. We can see that the previous⁸ smoothed estimate is obtained by the filtered estimate “updated” by an amount proportional to the difference between the current smoothed estimate and the previous (a

⁸i.e next, as we are now going backwards in time... that is the definition of confusing wording!

priori) filtered estimate, where the constant of proportionality K is known as the smoothed gain matrix (expression 8.69).

This is called a fixed-interval smoother, in which all previous filtered estimates have a corresponding smoothed estimate. Note there are other possible types of smoothers: we could also have a fixed-lag smoother (sequentially smooth an estimate m time steps into the past, based on all $n > m$ data points) or a fixed-point smoother (smooth a specific, fixed, time estimate).

This code was implemented elsewhere using the original MATLAB files, and is then migrated into R for further developments.

3 Current georeferencing procedure

After obtaining a pseudo-track, one might want to improve on this track by including independent information collected on the surrounding hydrophones. This will actually be the focus of section 4.2.

To date, the process that tried to improve on the pseudo-track estimation was based on code from Charlie White. Here we lay down the procedure:

1. a track is obtained by dead-reckoning, as described in section 2.1.2, using a reasonable mean speed constant over time
2. the clicks emitted by the DTagged whale are cross-correlated with surrounding hydrophone data. For all clicks detected at more than 1 hydrophone, we have a time-difference of arrival (TDOA). Given 2 or more TDOA's for a single click we can localize the animal in 3D space using hyperbolic localization. Due to its acoustic characteristics, most often a click is not detected at more than 2 hydrophones. However, by interpolating the "TDOA lines" (over the entire dive) we can obtain TDOA's enough (some measured, some extrapolated) to localize the animals. There might be some room for improvement at this extrapolation step. See more details about this in section 4.2.
3. given these localizations, a geo-referencing procedure is implemented. This uses a simulated-annealing (SA) optimization procedure (for more details on his SA procedure, see Marques (2011)) to iteratively obtain tracks which are closer and closer to the whale acoustics-based localizations (assumed known without error). This SA procedure goes in a loop:

- (a) use current vector of speeds to obtain pseudo-track by dead reckoning
- (b) calculate distance to known locations
- (c) check if convergence is achieved (i.e. sum of distances is already small enough, given some criteria) and if not
- (d) change the previous vector of speeds by a random amount and go back to step 3a

In step 3c above, if convergence is achieved, then we use the current track as the geo-referenced track.

From what we can tell, this SA based procedure is complemented with some manual tweaking which is hard to describe in a quantitative way. The entire procedure seems currently a bit convoluted, because it is equivalent to use a relatively complex optimization routine that converges when the track goes close enough through the points assumed known. But the procedure is not any better than just joining the points assumed known using a speed equal to the mean speed required to join those points. In the current approach you can have the animal backtracking in a random way, which might be more realistic, but on average, the end result would be the same. We only improve on “joining the dots” if we bring in additional information about animal movement into the process.

3.1 Including behavioral states

The above formulation does not consider changes in animal behavior modes, i.e., attempts no mechanistic description of the dive itself. An alternative approach might be to consider that a whale dive is made up of a number of different behavioral states, e.g. deep diving (descent, feeding, ascent) and at the surface. It is likely that speed (and other relevant variables) present different distributions depending on the behavioral state of the animal. Hence accounting for that in the process might lead to improved inferences. An option would be to have behavioral mode as a state. Depending of the current state, other states are updated using different schemes.

It might make sense to include both heading and pitch as observations, at least to include measurement error in the process. Potentially these might also be included as states, if we want to introduce some Markovian dependency over consecutive values of these variables, which would again probably

make sense. For example pitch is likely correlated over time, and measurement error in pitch is not constant over time either (see e.g. figure 5, bottom panel, in Johnson and Tyack (2003)).

Also, as introduced in section 4.1, here we would want to move away from the above formulation because we actually want the states to be (at least) s , x , y and z . And every now and then we will have observations about some of these states (with some error), namely about x, y coming from the localizations on the AUTECH range hydrophones. This is easily incorporated in the modelling framework, being simple to implement even within the Kalman Filter framework. As a separate example, McClintock *et al.* (2012) considered a discrete time state switching model, with movement dependent on behavioral state, for which often, but not always, there were observations of the animals locations.

4 Improving the current SSM formulation

Here we build on the original SSM framework developed by MJ in several aspects:

1. considering x and y as states in the SMM, in section 4.1;
2. including observations from acoustic localization, in section 4.2;
3. considering heading and pitch as states, in section 4.3.

4.1 Considering location as states

Given that the (first!) end game is actually to predict animal locations, it makes sense to include these as states in the model, rather than the current plug-in approach, in which a vector of speeds is estimated using the Kalman filter, and then dead-reckoning based on the initial location and speed, pitch and heading information is implemented.

We could consider x, y locations as additional states, and use equation 4 combined with 6 to come up with a different state transition matrix as

$$\begin{pmatrix} s_t \\ z_t \\ x_t \\ y_t \end{pmatrix} = \begin{pmatrix} 1 & 0 & 0 & 0 \\ -\sin(\phi_t)\Delta T & 1 & 0 & 0 \\ \Delta T \cos(\phi_t) \sin(\psi_t) & 0 & 1 & 0 \\ \Delta T \cos(\phi_t) \cos(\psi_t) & 0 & 0 & 1 \end{pmatrix} \begin{pmatrix} s_{t-1} \\ z_{t-1} \\ x_{t-1} \\ y_{t-1} \end{pmatrix} + \begin{pmatrix} \omega_{s_t} \\ \omega_{z_t} \\ \omega_{x_t} \\ \omega_{y_t} \end{pmatrix} \quad (7)$$

and considering a very similar observation process:

$$o_{z_t} = [0 \ 1 \ 0 \ 0] \begin{pmatrix} s_t \\ z_t \\ x_t \\ y_t \end{pmatrix} + v_{z_t} \quad (8)$$

Note that this formulation exacerbates the approach inadequacy, as we are trying to make inferences about 4 states using as inputs just observations about one of the states (depth).

Note that, just as pitch was being considered before a covariate observed without error, here we would require both pitch and heading to be included as such.

4.2 Including observations from acoustic localization

Here we assume that every so often we might actually observe some x, y coordinates from acoustic localizations. What this means is that the observation equation becomes

$$\begin{pmatrix} o_{z_t} \\ o_{x_t} \\ o_{y_t} \end{pmatrix} = \begin{pmatrix} 0 & 1 & 0 & 0 \\ 0 & 0 & 1 & 0 \\ 0 & 0 & 0 & 1 \end{pmatrix} \begin{pmatrix} s_t \\ z_t \\ x_t \\ y_t \end{pmatrix} + \begin{pmatrix} v_{z_t} \\ v_{x_t} \\ v_{y_t} \end{pmatrix} \quad (9)$$

but that we often have missing values in o_{x_t} and o_{y_t} .

Note that, regarding the localization data itself, there is actually more to it than meets the eye. The data actually available to us are time-of-arrival (TOA) of clicks at individual hydrophones. However, we have an advantage over a traditional localization procedure: because we can use the DTAG sound record as a template, we can use some sort of comb⁹ filter to evaluate, of the clicks produced by the whale, which and when were these detected at surrounding hydrophones. For each click detected at least at a

⁹This equates to sliding back and forth the sound record of an hydrophone against the DTAG template sound record. For a fixed object, the TDOA corresponds the time delay that maximizes the correlation between the two sound records, and naturally this should be proportional to the distance between whale and hydrophone, with the speed of sound in the water being the proportionality constant. What confuses me is the fact that the whale moves over time, hence over the course of a dive this TDOA is changing.

pair of hydrophones, this information can be used to get a time-difference-of-arrival (TDOA, the difference in time between the arrival of a click at two hydrophones). This TDOA instead leads to a location along an hyperbola. Several TDOAs for the same click would hence allow to resolve the click's position. Because the clicks are highly directional, seldom a click is detected at more than a couple of hydrophones, in fact more often than not it is detected in a single hydrophone. Hence, we do not get enough TDOA's for each individual click to get reliable localizations. But successive TDOA's can in turn be used to produce, by interpolation, TDOA lines (effectively, a set of points forming a line on a plot where TDOA is plotted against time). These are then used in an hyperbolic algorithm to get localizations for each individual click, even if not detected at a sufficient number of hydrophones per se to provide a localization. We can see potential for improvement of this process, in particular at the level of:

- the comb filter and the cleaning up of the TDOA plots
- the interpolation procedure and ways to improve it
- using the TDOAs to get the location. Would in not be smarter to get the location from the TOAs? If so, should one not compare localization from TDOAs with TOAs, to see what happens in the absence of the DTAG data?

4.3 Considering heading and pitch as states

A natural extension given the above is to include both heading and pitch at least in the state vector (and also as observations). This would lead to the following observation equation

$$o_t = \begin{pmatrix} 0 & 1 & 0 & 0 & 0 & 0 \\ 0 & 0 & 1 & 0 & 0 & 0 \\ 0 & 0 & 0 & 1 & 0 & 0 \\ 0 & 0 & 0 & 0 & 1 & 0 \\ 0 & 0 & 0 & 0 & 0 & 1 \end{pmatrix} \begin{pmatrix} s_t \\ z_t \\ x_t \\ y_t \\ \phi_t \\ \psi_t \end{pmatrix} + v_z \quad (10)$$

where as before handling missing values, in particular in x, y , is straightforward, and state equation

$$\begin{pmatrix} s_t \\ z_t \\ x_t \\ y_t \\ \phi_t \\ \psi_t \end{pmatrix} = \begin{pmatrix} 1 & 0 & 0 & 0 & 0 & 0 \\ -\sin(\phi_{t-1})\Delta T & 1 & 0 & 0 & 0 & 0 \\ \Delta T \cos(\phi_{t-1}) \sin(\psi_{t-1}) & 0 & 1 & 0 & 0 & 0 \\ \Delta T \cos(\phi_{t-1}) \cos(\psi_{t-1}) & 0 & 0 & 1 & 0 & 0 \\ 0 & 0 & 0 & 0 & 1 & 0 \\ 0 & 0 & 0 & 0 & 0 & 1 \end{pmatrix} \begin{pmatrix} s_{t-1} \\ z_{t-1} \\ x_{t-1} \\ y_{t-1} \\ \phi_{t-1} \\ \psi_{t-1} \end{pmatrix} + \begin{pmatrix} \omega_{s_t} \\ \omega_{z_t} \\ \omega_{x_t} \\ \omega_{y_t} \\ \omega_{\phi_t} \\ \omega_{\psi_t} \end{pmatrix} \quad (11)$$

at the cost of loosing the ability to use a “simple” tool like the Kalman filter for fitting, because now inside the transition matrix G_t we have not only constants but also the states at previous time points.

Instead of using matrices, it helps if we write down explicitly the state transition equations:

$$\begin{aligned} s_t &= s_{t-1} + \omega_{s_t} \\ z_t &= z_{t-1} - s_{t-1} \sin(\phi_{t-1})\Delta T + \omega_{z_t} \\ x_t &= x_{t-1} + s_{t-1} \cos(\phi_{t-1}) \sin(\psi_{t-1})\Delta T + \omega_{x_t} \\ y_t &= y_{t-1} + s_{t-1} \cos(\phi_{t-1}) \cos(\psi_{t-1})\Delta T + \omega_{y_t} \\ \phi_t &= \phi_{t-1} + \omega_{\phi_t} \\ \psi_t &= \psi_{t-1} + \omega_{\psi_t} \end{aligned} \quad (12)$$

as clearly we cannot write these equations as linear combinations of the states. **And the question here is, so now what?**

5 So now what?

From the above material, it seems like there are a number of places to improve upon, and these include, in a random order, things as general as:

1. deal with the ad hoc way of keeping speed and depth with the proper sign
2. delve into the procedure that creates the prh files to evaluate error in pitch and heading
3. estimate one of rather than assume both process and observation errors known

4. delve into the data that exists prior to localizations (i.e. TOAs and TDOAs)
5. include information on water current (and hence modify SSM accordingly?)
6. fit the latest non linear state space model
7. other thoughts to come?

References

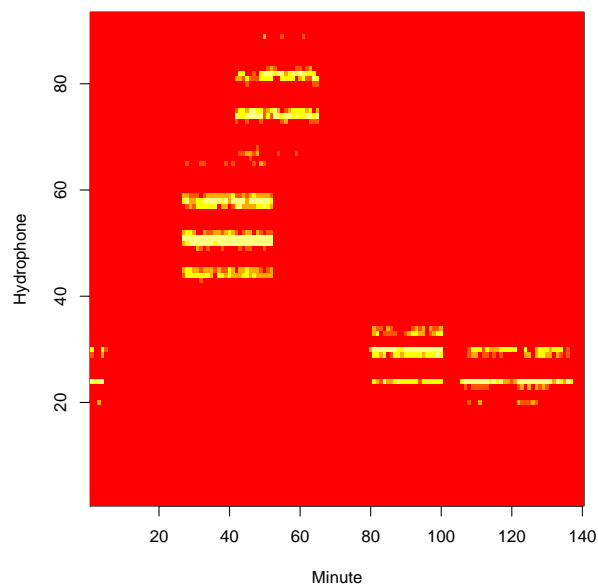
- Gannot, S. and Yeredor, A. (2008). *Springer Handbook of Speech Processing*, chapter The Kalman Filter, pages 135–159. Springer.
- Johnson, M. P. and Tyack, P. L. (2003). A digital acoustic recording tag for measuring the response of wild marine mammals to sound. *IEEE Journal Of Oceanic Engineering*, **28**, 3–12.
- Marques, T. A. (2011). A tutorial on simulated annealing. Internal LATTE report.
- Marques, T. A. and Thomas, L. (2012). Using dedicated kalman filter r packages to fit the georeferencing ssm. Technical report, LATTE WORKING DOCUMENT.
- Marques, T. A., Thomas, L., Ward, J., DiMarzio, N., and Tyack, P. L. (2009). Estimating cetacean population density using fixed passive acoustic sensors: an example with Blainville’s beaked whales. *The Journal of the Acoustical Society of America*, **125**, 1982–1994.
- Marques, T. A., Shaeffer, J., and Thomas, L. (2012). Procedure description: using AUTECH’s hydrophones surrounding a DTAGed whale to obtain localizations. Technical report, LATTE WORKING DOCUMENT.
- McClintock, B. T., King, R., Thomas, L., Matthiopoulos, J., McConnell, B. J., and Morales, J. M. (2012). A general modeling framework for animal movement and migration using multi-state random walks. *Ecological Monographs*, **82**, 335–349.

- Mitani, Y., Sato, K., Ito, S., Cameron, M. F., Siniff, D. B., and Naito, Y. (2003). A method for reconstructing three-dimensional dive profiles of marine mammals using geomagnetic intensity data: results from two lactating weddell seals. *Polar Biology*, **26**, 311–317.
- Petris, G. (2010). An R package for dynamic linear models. *Journal of Statistical Software*, **36**, 1–16.
- Petris, G., Petrone, S., and Campagnoli, P. (2009). *Dynamic Linear Models with R*. Springer.
- Shiomi, K., Sato, K., Mitamura, H., Arai, N., Naito, Y., and Ponganis, P. J. (2008). Effect of ocean current on the dead-reckoning estimation of 3-d dive paths of emperor penguins. *Aquatic Biology*, **3**, 265–270.
- Simon, D. (2001). Kalman filtering. *Embedded Systems Programming*, pages 72–79.
- Wilson, R. P., Liebsch, N., Davies, I. M., Quintana, F., Weimerskirch, H., Storch, S., Lucke, K., Siebert, U., Zankl, S., Muller, G., Zimmer, I., Scolaro, A., Campagna, C., Plotz, J., Bornemann, H., Teilmann, J., and McMahon, C. R. (2007). All at sea with animal tracks; methodological and analytical solutions for the resolution of movement. *Deep Sea Research Part II: Topical Studies in Oceanography*, **54**, 193 – 210.

Explaining the code for the simulation of click count vectors

Tiago A. Marques & Len Thomas

Centre for Research into Ecological and Environmental Modelling
The Observatory, University of St Andrews, St Andrews, KY16 9LZ, Scotland



Version's date: April 12, 2012

Contents

1	Introduction	3
1.1	Additional reading	3
2	The code	4
2.1	Some preliminaries	4
2.2	Simulating groups of whales: location and size	8
2.2.1	Simulating individual animal coordinates through time	13
2.3	Simulating the state of a group: vocalizing or not	21
2.3.1	Creating objects with relevant information	25
2.4	Simulating click times	29
2.5	Simulating click characteristics	32
2.5.1	Simulating correlated values through time around a given mean	32
2.5.2	Simulating depth	33
2.5.3	Simulating heading	41
2.5.4	Simulating pitch	42
2.6	Obtaining relevant variables for each hydrophone-click combi- nation	43
2.6.1	Filtering out whale-hydrophone combinations	45
2.6.2	Obtaining <i>haa</i>	46
2.6.3	Obtaining <i>vaa</i>	48
2.6.4	Detection function	49
2.6.5	Obtaining all the relevant variables	50
2.7	Wrapper function for full simulation exercise	54
2.8	Reading binary files back in	59
3	Overview	62
4	Known issues, shortcomings, work to do, etc.	65
	References	69

1 Introduction

This document was built over a document produced within the realms of DECAF. In the corresponding DECAF folder there might be additional useful information to understand this document. However, we have tried to make this document self contained. The idea is to use this material within LATTE.

In this document we present, illustrated with examples, the code used for the simulation of vectors of click counts per minute. Note that despite this being its key objective, this code could be easily generalized to simulate a general population of whales through time and many of the details regarding their dives. This would naturally require that the appropriate information regarding the corresponding whale species was available.

The objective of the original DECAF simulation exercise was to produce click count vectors as close as possible to observed click counts. A fundamental problem with this approach is that some of the information that would be required to parameterize some of the functions used was either lacking or potentially misleading (e.g. the click count data, especially while it is based in the FFT detector, has large number of false positives and false negatives).

This work builds on the rationale previously described in the report “Rationale for the simulation of plausible vectors of detected click counts.pdf” (Marques and Thomas, 2008c). In addition to this, some of the parameters and assumptions used were obtained in the analysis described in the report “Further analysis of the hydrophone+DTag data.pdf” (Marques and Thomas, 2008a).

The next section (section 2) presents the code, and a running example is used throughout to illustrate it. Due to the extent of section 2, which makes its reading difficult, this is followed by an overview of the code which might be useful for reference (section 3), and we finish we some avenues for pending work (section 4).

1.1 Additional reading

This document included originally extra material regarding sections 2.5.1 and 2.5.2, which was moved into separate documents as it was somewhat peripheral to the key goal of this document, which is simply to describe the simulation code. Hence for initial attempts, alternatives and further details regarding section 2.5.1 the reader is referred to Marques and Thomas (2008d) and regarding section 2.5.2 to Marques and Thomas (2008e).

2 The code

2.1 Some preliminaries

As we are working over a specific area (the AUTECH range), we first need some relevant information, namely the hydrophones location

```
> #reading the hydrophone data in
> hyd<-read.table(file="datfiles/HYDtable.txt")
> names(hyd)<-c("hydID", "on", "x", "y", "z", "dunno")
> #adding the fact that some hydrophones were actually off
> #during the period for which we have data - this is
> #actually not used in the simulation
> hyd$off<-0;hyd$off[c(47,48,54,55,62,63,70,71,79,86,87)]<-1
```

as well as to define a working area. For simplicity we define said area here as the convex hull around the recording hydrophones, extended by 4 km.

```
> #selecting a work area for simulating the animals in
> #setting the work area as the convex hull around the hydrophones
> work.area<-convexhull.xy(x=hyd$x[hyd$off==0],y=hyd$y[hyd$off==0])
> #and extend it 4000 m out of this convex hull
> work.area<-dilation.owin(w=work.area,r=4000)
> #plot(work.area)
> #points(hyd$x,hyd$y)
> #points(hyd$x[hyd$off==0],y=hyd$y[hyd$off==0],col="green",pch=21,bg="green")
```

We can now generate animals within said working area, as in figure 1.

Because it is more interesting to generate animals according to a model that represents what is observed at AUTECH, we use here a density surface model estimated in a previous analysis (see figure 5 in the report “Click Count EDA Report with NUWC feedback.pdf”). In order to do this, we first need to read in:

- data regarding the respective model;
- an adequately sized prediction grid over which the model results can be evaluated.

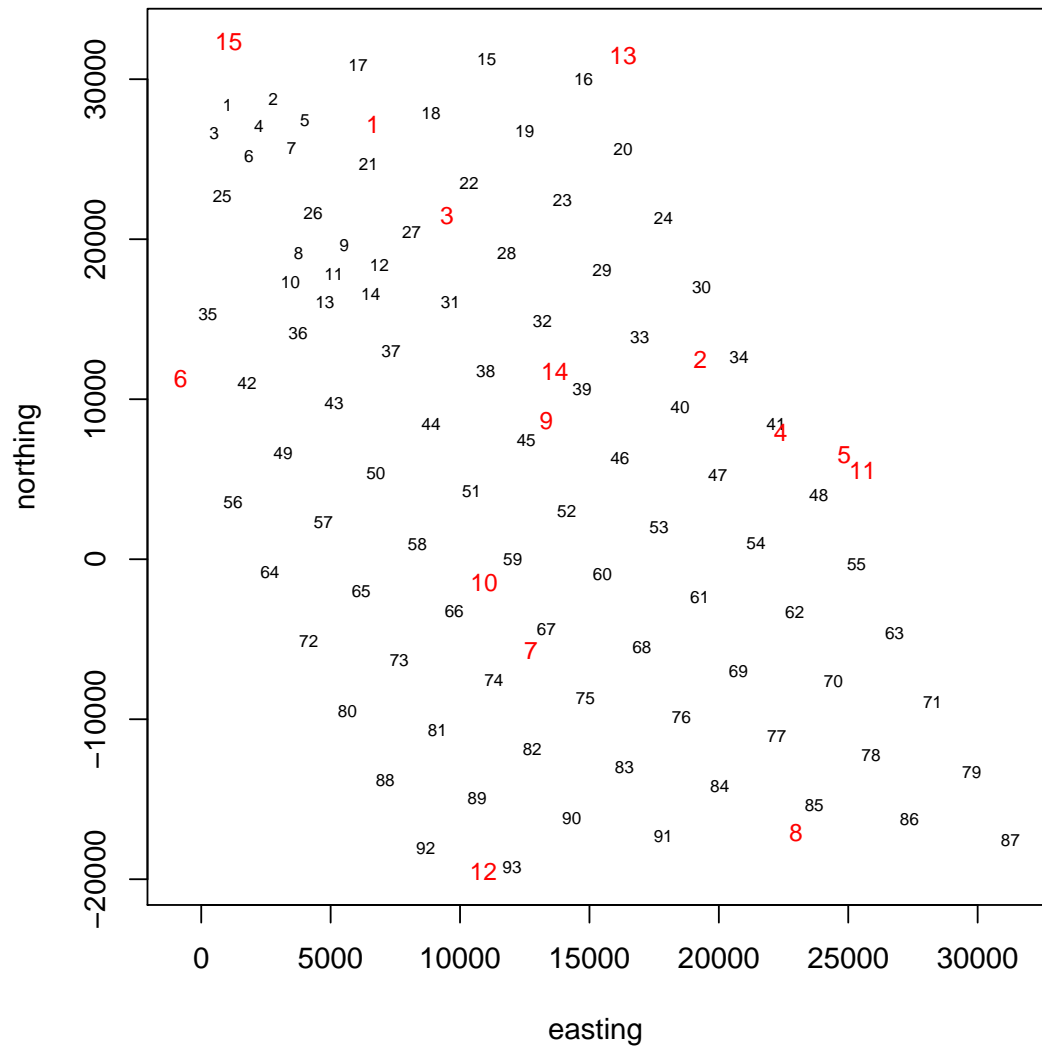


Figure 1: An example of a simulated location of animals within the chosen work area. Red numbers are the locations of 15 animals, while the black small numbers are the AUTECH hydrophones numbers and locations.

```

> #read the data created in EDA click counts that can be used to create a sur
> fn<-"datfiles/allSets.cc.per.hydrophone.txt"
> allSets.cc.per.hydrophone<-read.table(file=fn,header=T)
> #reading a 100 by 100 prediction grid
> fn<-"datfiles/AUTEC100by100predictiongrid.txt"
> pred.grid<-read.table(file=fn,header=T)
> rm(fn)

```

The Poisson model used is shown in Figure 2, top panel. We have not used what might be the best model for this data, which would be a gamma model (rather than the Poisson model used here, see Marques and Thomas (2008b), figure 1 + text for details), because the gamma model produces unreasonable estimates just outside the areas for which data was available. The bottom panel in Figure 2 is the Poisson model with predictions over the entire working area (i.e. extending 4km outside the recording hydrophones). This confirms that no wild results are produced by using the predictions outside the range of the data. Because the estimated surface is quite tame, everything seems to work well. This will likely be one of the least influent aspects of this simulation exercise.

Because we want to use the above gam model as a basis for the density surface, we will also need a wrapper function that allows its use within the appropriate function `rpoint` (which creates points from a given spatial point pattern, defined using a fitted model object), something like

```

> #Written by Tiago Marques on 13th May 2008 and last updated on 13th May 2008
> #Purpose: creating a wrapper for predict.gam to use in rpoint
> pred.gam.for.rpoint<-function(x,y){
+   preds<-predict.gam(object=some.gam.object,newdata=data.frame(x=x,y=y),type=
+   return(preds)}

```

We are now ready to start simulating animals. Note that despite the fact that we will base all subsequent work in the above model for animal distribution at AUTEC, this could be easily generalized, or updated if a new model becomes available, by changing `pred.gam.for.rpoint` accordingly. In particular the user could define manually the positions of each of the animals/groups to be considered.

2.2 Simulating groups of whales: location and size

The following function allows to generate the groups locations (as is, within an area of 4000 *m* around the hydrophones, see previous section for details):

```
> generate.group.coordinates<-function(n,dens,dens.type="gam",within){
+ #Written by: Tiago Marques on 10th March 2008 and last updated on 13th May 20
+ #Purpose: this function returns the x,y coordinates for n simulated groups
+ #given a specific density surface in a given area
+ #Inputs:
+ #          n          a scalar, the number of groups in the area
+ #          dens.type   if "gam", then dens should be a gam object resulting
+ #                      nothing else is currently implemented, except using
+ #                      poisson (in space) model
+ #          dens        a model object or a number; if a number, generates a
+ #                      if a model object, model must be a function of x,y
+ #                      proportionally to the model value evaluated at x,y
+ #          within      an object of type window, as defined in library spatstat
+ #                      which animal locations are to be generated within
+ #Returns:
+ #          an object of class ppp (see spatstat) which most important attributes
+ #          are x and y, the location of each group
+ #Warnings: spatstat needs to have been installed
+ require(spatstat)
+ if(dens.type=="gam") {
+   pred.gam.for.rpoint<-function(x,y){
+     preds<-predict.gam(object=dens,newdata=data.frame(x=x,y=y),type="response")
+     return(preds)}
+   ggc<-rpoint(n=n,f=pred.gam.for.rpoint,win=within,giveup=1000)}
+ else {
+   print("Warning: Locations generated by Poisson process")
+   ggc<-rpoint(n=n,f=1,win=within,giveup=1000)}
+ return(ggc)}
```

Given the object created by this function, we can use the following function to add group sizes to each of the groups

```
> add.group.sizes<-function(pop,mean.cs=4.1){
+ #Written by: Tiago Marques on 10th March 2008 and last updated on 13th May 20
```

```

+ #Purpose: this function adds group sizes to an object with the groups locat.
+ #Details: given a population pop (currently a ppp class object)
+ #          this function generates group sizes for each group in
+ #          pop from a 1+Poisson(mean.cs-1) (see document "Adding
+ #          variance to Moretti et al.doc" for further details)
+ #Inputs:
+ #          pop - an object of class ppp containing the x,y group locations
+ #          mean.cs - the mean group size
+ #Returns: a ppp class object with $marks = the group sizes
+ css<-1+rpois(pop$n,mean.cs-1)      #get group sizes given number of groups
+ pop<-setmarks(pop,css)             #add them to the pop object
+ return(pop)
+ }

```

Note the default mean group size used here is 4.1, as this was the mean cluster size reported by Claridge (2006), and also used by Moretti *et al.* (2006) to estimate beaked whale density at AUTECH.

We create here an example population with 4 groups, which location is shown in figure 3. In the remainder of this section we continue to use this 4 group example for illustration, treating it as a running example from the creation of the number of clusters till the last stage of the simulation process.

Up to this point we have assumed that all the animals in a given group are at the same position in space, but that is not realistic. It is not clear how one should model the individual animal's locations in space. However, it seems convenient to generate animal coordinates, because we need to associate each simulated click with a given coordinate, and too much clumping in space might be obtained if all animals are at exactly the same location.

Hence a new function that generates individual animal coordinates given the group location is required. Here I have assumed that the individual animal locations can be approximated by a bivariate normal distribution (with 0 covariance). As a first approach, and purely arbitrary lacking data for a better parameter value, a value of 150 (meters) for the standard deviation of each normal random deviate was used. At the AUTECH scale, this puts animals within a reasonable distance from each other so that they would likely be a single group.

```

> generate.animal.coordinates<-function(animais,stdv=150){
+ #Written by: Tiago Marques on 15th April 2008 and last updated on 13th May 20

```

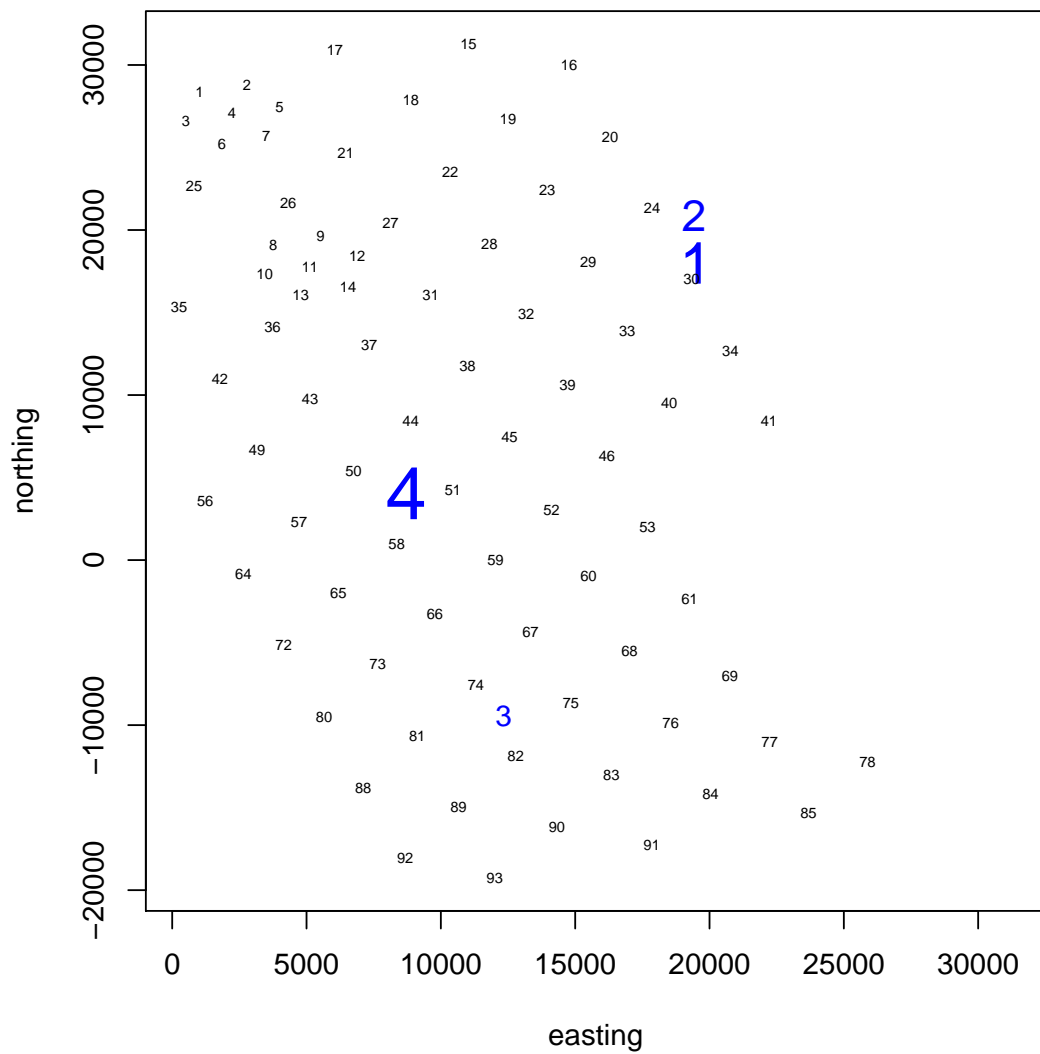


Figure 3: An example of 4 simulated groups. The size of the group indicator, used to represent the group initial location, is proportional to the group size.

```

+ #Purpose: This function returns the initial animals locations
+ #          assuming that animais is an object of class ppp created
+ #          by "generate.group.coordinates", to which marks (i.e.
+ #          group sizes) were added by function "add.group.sizes"
+ #Details: We assume a bivariate normal distribution in space given the cent
+ #Input:
+ #  animais - the object of class ppp with group coordinates and group size
+ #  stdv -    the standard deviation of the multivariate normal used for g
+ #           the individual animal's coordinates
+ #Returns:
+ #  a data.frame with individual animals coordinates and group index
+ if (animais$markformat=="none") Print("The group has no group size yet!")
+ #defining the variance covariance matrix
+ varcovar<-matrix(c(stdv^2, 0, 0, stdv^2),2,2)
+ #creating the object to hold individual animal coordinates
+ #by getting the first groups coordinates
+ coords<-with(animais,mvrnorm(marks[1],c(x[1],y[1]),Sigma=varcovar))
+ #and a group indicator
+ sindex<-with(animais,rep(1,marks[1]))
+ #then for the remaning groups
+ for(i in 2:animais$n) {
+   temp<-with(animais,mvrnorm(marks[i],c(x[i],y[i]),Sigma=varcovar))
+   coords<-rbind(coords,temp)
+   sindex<-c(sindex,with(animais,rep(i,marks[i])))
+ }
+ res<-data.frame(x=coords[,1],y=coords[,2],sindex=sindex)
+ return(res)}

```

An example of the implementation of said function over the previously created groups is shown in figure 4. While on the top panel we put the locations in perspective to the entire range, on the 4 bottom panels we zoom in each of the groups, to gain a better feel for how far apart animals in a group might be of each other. Again, note that we have no relevant information to define this spacing in any better way than the arbitrary standard deviation (=150) used above in `generate.animal.coordinates`.

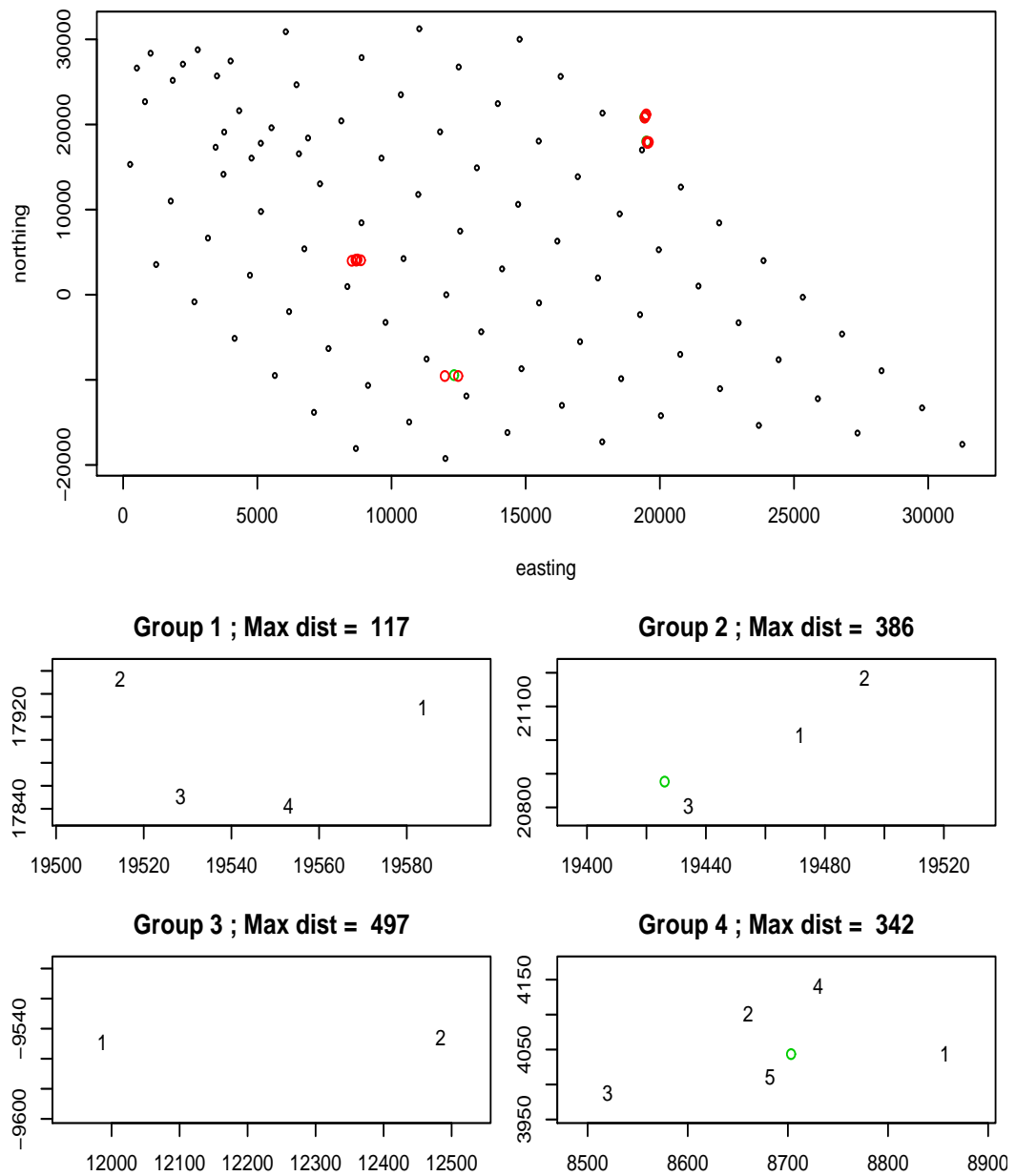


Figure 4: The location of the animals (in red) of each of 4 simulated groups (center of each group location is shown in green). The 4 smaller plots zoom in each of the groups, to gain a better feel for the relative position of the animals. The maximum distance in meters between animals in a group is shown on top of each group plot.

2.2.1 Simulating individual animal coordinates through time

Initially, we had not considered to simulate x, y coordinates over time, i.e. the animal would be considered not to move much during the period analyzed. This was justified because:

1. It is likely that, for the probability of detecting a click, the actual distance is much less relevant than haa and vaa , hence changing x, y at a local scale would have negligible influence in detection probabilities;
2. There is little or no information about the necessary parameters to simulate such variables, especially given that x, y locations within a group have a strong yet unknown correlation through time;
3. From a purely pragmatic point of view, it would keep simulations simpler and faster.

However, it seems like this might not be the best approach because:

1. It is really implausible from a biological point of view and hence not defensible and hard to explain to others.
2. At least from dive to dive the animals should change position, hence we might as well change their position within a dive too.

However, as stated above, there is no information available providing plausible parameter estimates to simulate the x, y positions of animals within a group through time. Additionally, it is not simple to simulate these things directly. Hence, a possible simplistic approach might be: For each group

1. Simulate a Brownian movement in space through the time interval considered, which will represent the position of the center of the group over time, starting at the coordinate obtained with function `generate.group.coordinates`. This Brownian movement will have a “large” dispersion parameter, say σ_g .
2. For each animal, create a Brownian motion in space, over the time interval considered. This Brownian motion will have a “small” dispersion parameter, say σ_a , such that $\sigma_a \ll \sigma_g$.

3. The Brownian movement of each animal is now normalized such that its geometric center is exactly at the animal's original simulated position, which was obtained as described above using `generate.animal.coordinates`, but with such original position being updated at each time point according to the previously simulated group's Brownian movement.

This should mean that we simulate movement through time that is strongly correlated across animals within a group (the larger the difference between σ_a and σ_g the larger the correlation should be). This does impose implicit assumptions on the animal's movements that we have no data to either support or refute.

It seems clear that, due to the way in which movement is simulated, it should not be adequate to simulate over long time periods, as it is unlikely that over such periods an animal's movement pattern might be modelled by purely random movement, as it must at the very least to interact with all the surrounding environment (i.e. not into shore for example).

At this stage we have no information to say if the animals have different average displacements over the x, y space while at the surface vs. while deep diving¹, and hence no differentiation is made between the two states. If at a later stage this is shown to be the case, we might need to implement changes to the simulation code. The reason being that now we can simulate x, y displacement independently of knowing the state of the animal, which will not be the case then.

At this point, it seems like it makes life easier if we simulate x, y positions changing each minute, at the middle of an analyzed minute (i.e., all clicks produced within the same minute have the same x, y coordinates). Refinements are possible, for example (1) to keep this spacing in time and use a finer scale for x, y values based on interpolation or (2) use a finer time scale for x, y simulation from the start. However, given that some discretization will be necessary, choosing 1 minute intervals makes life much easier and likely has no (or negligible) impact in any relevant outcome.

The first function one needs is one that simulates Brownian motion through time, as a building block for other functions. This is also a reasonable way to do it because if a more complex way of simulation movement (and most importantly one way for which parameters are data driven rather than obtained by educated guessing) becomes available then one just needs to update this

¹ Which is not unlikely, as these represent different overall animal activities, say feeding vs. breathing/socializing.

function and the remaining code should work on top of it. Such a function is shown below:

```
> get.xy<-function(minutes,sd=20,xy.start=NA){
+ #Written by: Tiago Marques on 20th April 2008 and last updated on 13th May 20
+ #Purpose: this function returns a brownian motion over the a given number o
+ #Inputs:
+ #      minutes - the number of minutes over which positions are to be simu
+ #      sd      - the standard deviation of the updates in x and y dimentio
+ #      xy.start- a used defined initial x,y position (NA by default)
+ #Details: note that sd is in meters and represents the sd of change in mete
+ #      in the x and y dimention (no differences across dimentions are c
+ #      a common sd is used. Note that this is not the change in distanc
+ #      each coordinate; need to check later what this sd should be, by
+ #Returns: an array with dimentions (minutes,2), with the x,y position by mi
+ #####
+ #if a start point is not provided use an arbitrary one
+ if(is.na(xy.start[1])) {
+   group.x<-10000;group.y<-10000
+ }
+ else { #use the one given
+   group.x<-xy.start[1];group.y<-xy.start[2]
+ }
+ #for each time period, update the x,y position
+ for(j in 2:minutes) {
+   group.x[j]<-group.x[j-1]+rnorm(1,sd=sd)
+   group.y[j]<-group.y[j-1]+rnorm(1,sd=sd)
+ }
+ #return the x,y positions in an array with as many lines as time intervals
+ res<-array(c(group.x,group.y),dim=c(minutes,2))
+ return(res)
+ }
```

We can now simulate the movement through time of the center of each one of our groups. We just need an appropriate wrapper for `get.xy`, namely

```
> get.xy.per.group<-function(groups,minutes,sd){
+ #Written by: Tiago Marques on 20th April 2008 and last updated on 13th May 20
```

```

+ #Purpose: create the x,y position for each whale over the time period consid
+ #Inputs:
+ #          groups - an object of class ppp with the initial location of gro
+ #          minutes - the number of minutes over which positions are to be s
+ #          sd      - the standard deviation of the updates in x and y dimentio
+ #Returns:
+ #          an array with dimentions (minutes,2,n.s), with the x,y position by
+ #          (where n.s is the number of groups)
+ #Details: the actual generation of new x,y locations is done by function "g
+ #####
+ #how many groups are there
+ n.s<-groups$n
+ #set up an appropriate object to hold the results: creates an array to keep
+ xy.per.group<-array(0,dim=c(minutes,2,n.s))
+ #get the coordinates for each group
+ for(j in 1:n.s) {
+   #simulates x,y locations, given brownian motion, over minutes
+   xy.per.group[,j]<-get.xy(minutes,sd,xy.start=c(groups$x[j],groups$y[j])
+ }
+ return(xy.per.group)
+ }

```

For simplicity, we can plot (Figure 5) the outcome of updating the position of the center of each one of our example groups over 5 minutes (note the arbitrary use of 20 for the standard deviation of the Brownian motion).

```
> test4.xy.per.group<-get.xy.per.group(test4,5,sd=20)
```

Now, we can update the individual animals position through time accordingly. We require a third function as

```

> get.xy.per.animal<-function(whales,xy.group,minutes,sd){
+ #Written by: Tiago Marques on 21st April 2008 and last updated on 13th May 20
+ #Purpose: creates the x,y position for each whale over the time period of m
+ #Inputs:
+ #          whales - the object containing the location of each animal
+ #          xy.group - the location of the animal over the time period required
+ #          minutes - REDUNDANT (this is nrow(xy.group))

```

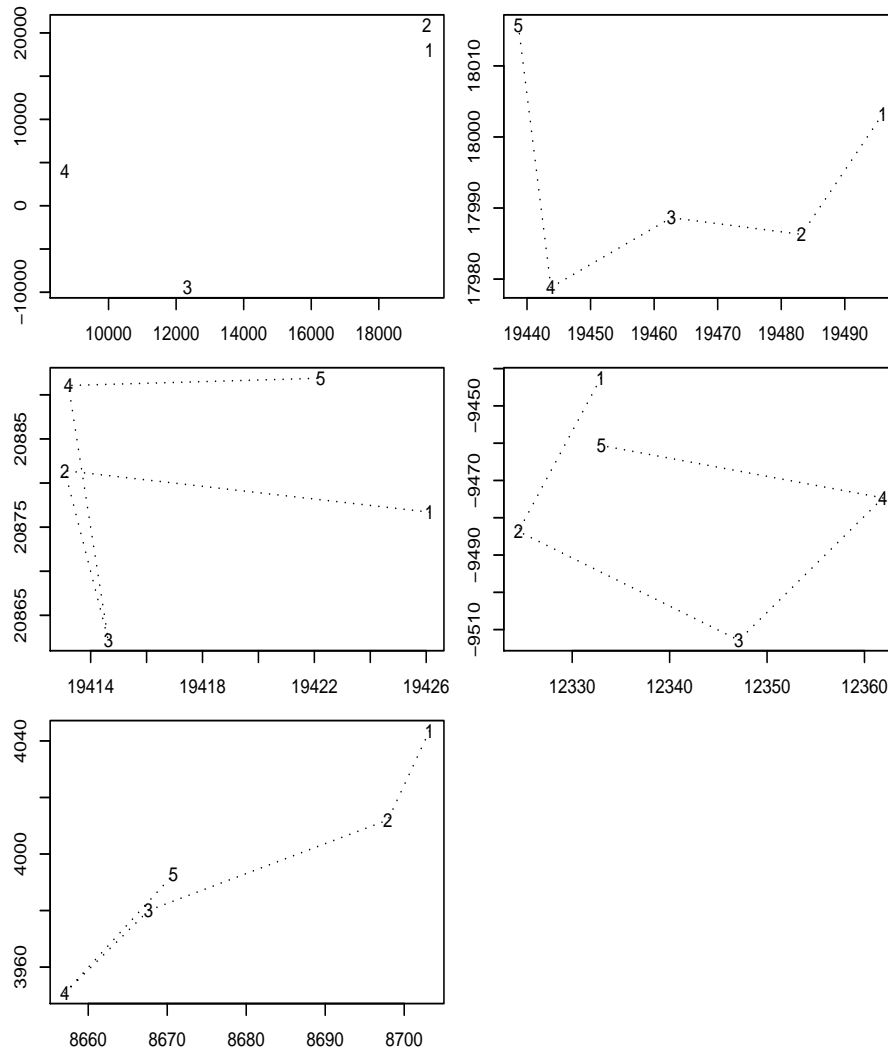


Figure 5: The position of the center of a group, in a five minute period (group changes position once every minute). The symbol used for each minute's position is the actual minute number. The top left plot is the overall initial position of the group within AUTECH.

```

+ #      sd -      the standard deviation of x,y movement (to use in get.xy)
+ #Details: this adds some variability to individual animal's locations using
+ #      the groups location over time and the relative position of the
+ #      with respect to the center of the group
+ #Returns: an object of class array with dimensions (number of minutes,2, number of animals)
+ #      first dimension is the corresponding minute, the second dimension is the
+ #      corresponding coordinate (x or y) and the third is the animal index
+ #####
+ #the number of animals involved
+ n<-nrow(whales)
+ #creates an array to keep the coordinates through time
+ xy.per.animal<-array(0,dim=c(minutes,2,n))
+ #for each individual whale
+ for(j in 1:n) {
+   #update it's mean position through time using the group movement as reference
+   group<-whales$sindex[j]
+   diff.x<-xy.group[1,1,group]-xy.group[1:minutes,1,group]
+   diff.y<-xy.group[1,2,group]-xy.group[1:minutes,2,group]
+   xy.per.animal[,1,j]<-whales[j,1]-diff.x
+   xy.per.animal[,2,j]<-whales[j,2]-diff.y
+   #now jitter a bit around said position using the individual animal movement
+   animal.movement<-get.xy(minutes,sd,xy.start=c(0,0))
+   xy.per.animal[, ,j]<-xy.per.animal[, ,j]+animal.movement
+ }
+ return(xy.per.animal)
+ }
> test4.xy.per.animal<-get.xy.per.animal(test4.animals,test4.xy.per.group,5,sd=20)

```

We can look at the outcome of this, for the first five minutes, say for groups 1 and 3 (Figure 6).

As stated above, by changing σ_a and σ_g we can change the way that the individual animals behave with respect to each other and with respect to the mean position of the group.

Finally, to keep with our example, we create the positions through time (over 140 minutes) for all the animals in every cluster using:

```

> test4.xy.per.group<-get.xy.per.group(test4,140,sd=20)
> test4.xy.per.animal<-get.xy.per.animal(test4.animals,test4.xy.per.group,140,sd=20)

```

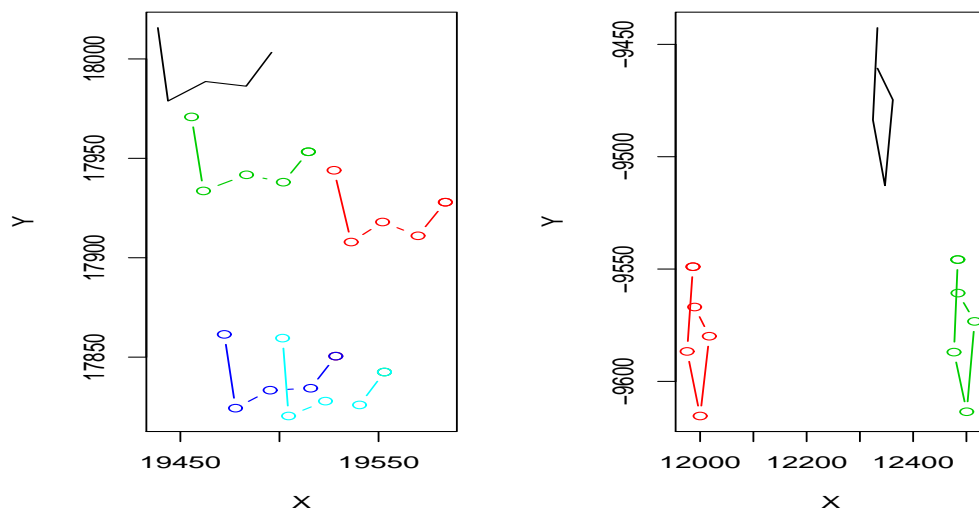


Figure 6: Groups 1 and 3. The position of the center of the group, in a five minute period (black; group changes position once every minute), along with the position of each animal of the 2 groups. Changing the parameters of the movement models (namely increasing σ_a with respect to σ_g) would change how similar the tracks within a given group look like.

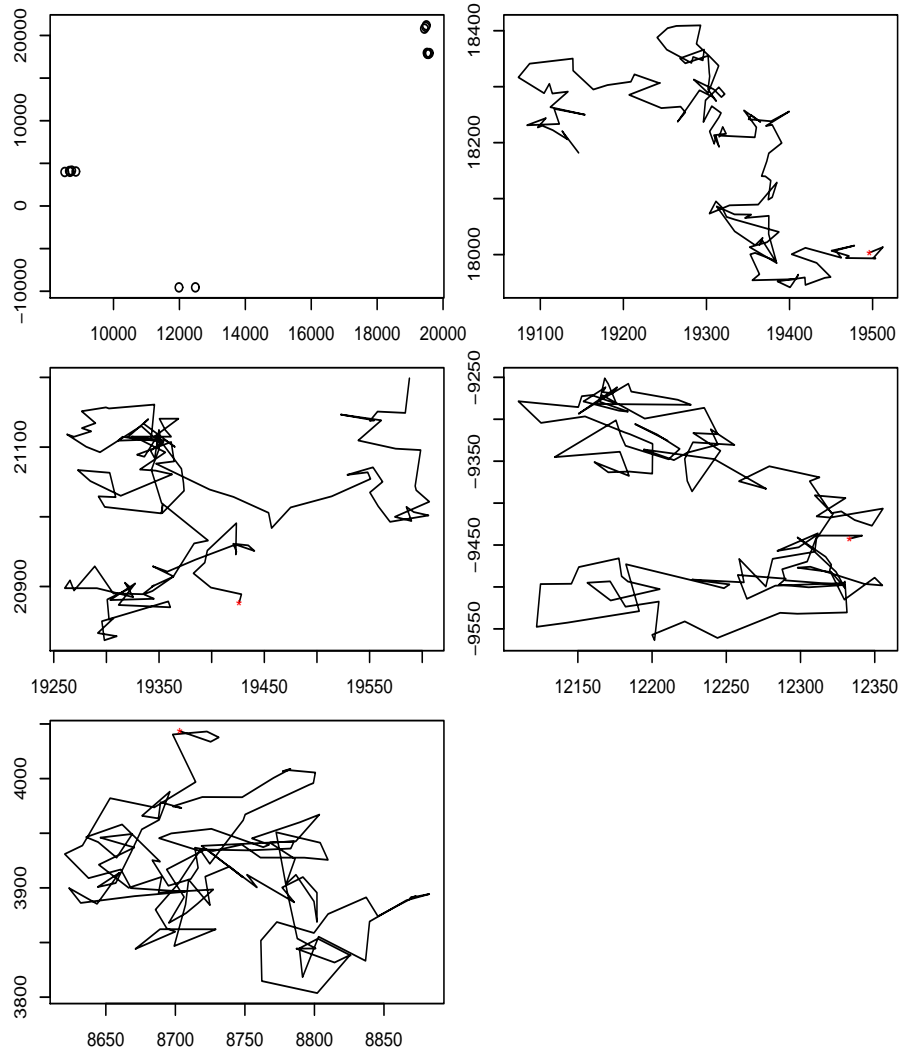


Figure 7: The position of the center of a group over a 140 minute period (group changes position once every minute). The initial position of each group is shown in red. The top left plot is the initial overall position of the group within AUTEK.

We can plot the mean position of the group through time, for each group (Figure 7). For illustration, the complete track of the animals of group 2 is shown in Figure 8.

2.3 Simulating the state of a group: vocalizing or not

Given the location of a group, we can then simulate its state during the simulated period. In order to do so we need first to decide what said period is. For consistency with what was done in Moretti *et al.* (2006) we consider here that period to be 140 minutes.

Note that here we assume that the animals in a group are all in the same state. This is likely unrealistic as even if they dive synchronously, some animals in a group will start clicking before than others, and similarly some will stop before others. This is a point that we might want to further develop later. However, given that we are working on a minute by minute scale, it might be that most animals in a groups start and stop clicking in under a minute from the first animal that respectively starts and stops clicking. Again, there is no available information to develop any more complex behavior, despite the fact that this is certainly an over-simplification, which might actually lead to dive starts being better detected in the simulated dives than in real life dives.

Hence, for each group, we need to know when it was vocalizing or not. As described in the document “Rationale for the simulation of plausible vectors of detected click counts.pdf”, a possible approach might be to simulate periods of vocalization with mean 26.4 (standard deviation 4.1) and periods of non-vocalization with mean $92 + (46.5 - 26.4) = 112.1$ (standard deviation² $= \sqrt{(46^2 + 7.6^2 + 4.1^2)} = 46.8$), which corresponds to adding the inter-deep-dive interval (IDDI) to the difference between the deep dive (DD) length and the vocalizing length (cf. values reported in Tyack *et al.* (2006)).

We have assumed here for simplicity that all these variables have lognormal distributions (hence avoiding negative values for time). An example of simulated values for IDDI is shown in figure 9.

The simplest way to achieve this is to generate a vector of states (V:vocalizing or S:Silent) for each group (remember these animals dive synchronously), along with the times of state change. That can be done using the following

² This assumes that the 3 random variables are independent, which is unlikely true, but might work from a purely pragmatic perspective for the purposes at hand.

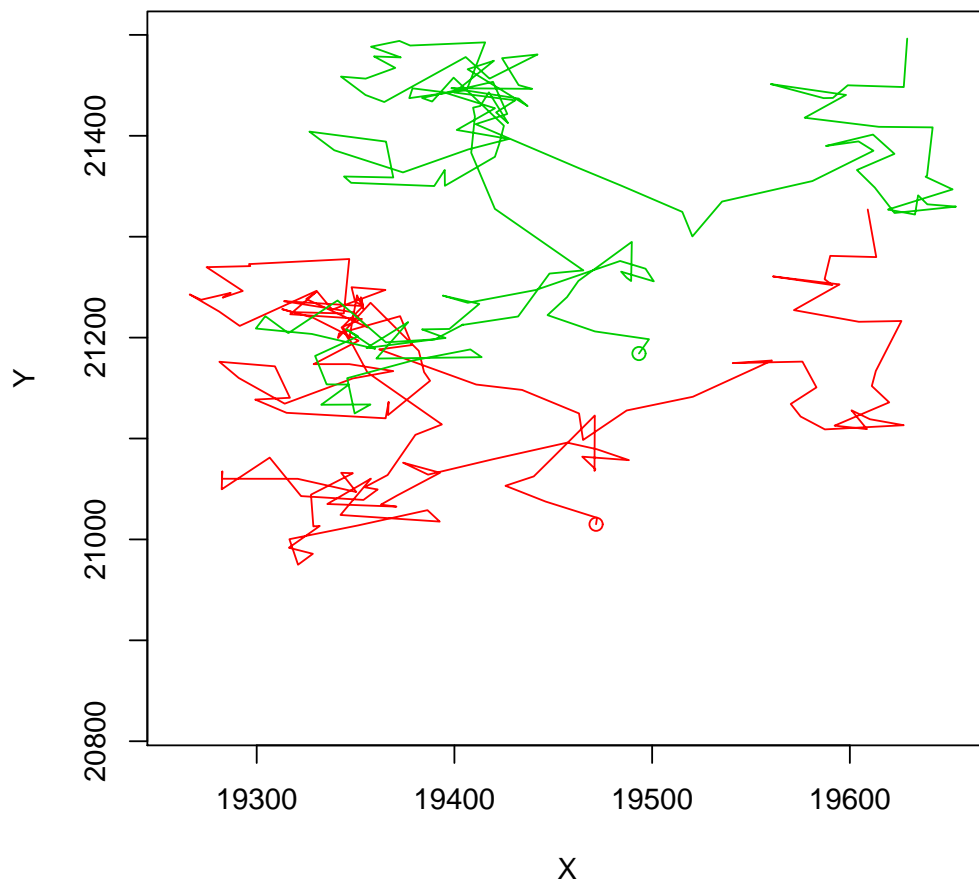


Figure 8: The position of the two animals from group 3 over 140 minutes.

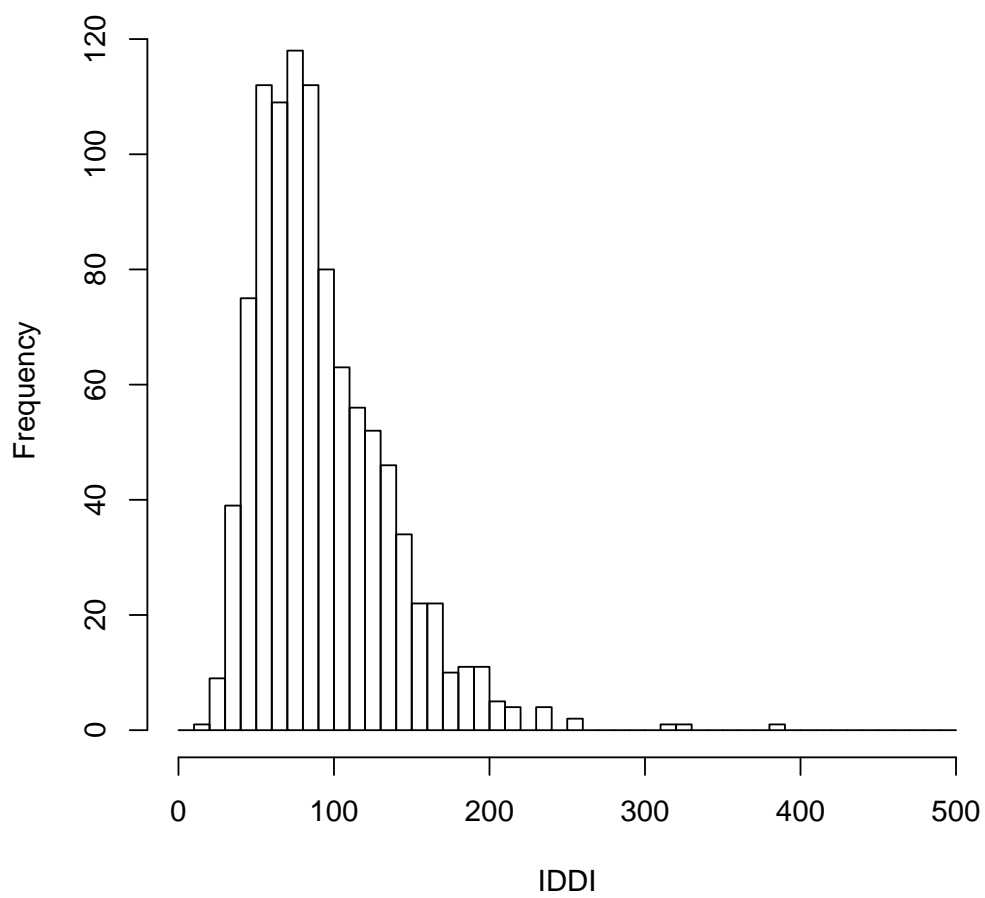


Figure 9: Simulated inter-deep-dive intervals.

function:

```
> get.state.vector<-function(animais,Smean=112.8,Ssd=46.8,Vmean=26.4,Vsd=4.1,
+ #Written by: Tiago Marques on 20th April 2008 and last updated on 13th May 20
+ #Purpose: simulate states (vocalizing or not) and respective end times
+ #Inputs:
+ #   animais      - a ppp object that contains the number of groups
+ #   Smean        - the mean length (in minutes) of the inter-deep-dive interval
+ #   Ssd          - the sd (in minutes) of the inter-deep-dive interval
+ #   Vmean        - the mean length (in minutes) of the deep-dives
+ #   Vsd          - the sd (in minutes) of the deep-dives
+ #   lim.time     - the interval of time, in minutes, for which we want the s
+ #Returns:
+ # an object of class list which element j is the states and times at which
+ #Details: The input parameters all have default values obtained from Tyack (
+ #####
+ #S parameters in terms of the lognormal
+ muS<-log(Smean)-(1/2)*log(1+Ssd^2/Smean^2)
+ sigmaS<-sqrt(log(1+Ssd^2/Smean^2))
+ #V parameters in terms of the lognormal
+ muV<-log(Vmean)-(1/2)*log(1+Vsd^2/Vmean^2)
+ sigmaV<-sqrt(log(1+Vsd^2/Vmean^2))
+ #getting the initial states
+ P.V<-Vmean/(Vmean+Smean)
+ init.state<-sample(c("V","S"),animais$n,prob=c(P.V,1-P.V),replace=T)
+ #and the initial (censored) corresponding time
+ Ds<-ifelse(init.state=="V",
+ rlnorm(n=animais$n,meanlog=muV,sdlog=sigmaV),
+ rlnorm(n=animais$n,meanlog=muS,sdlog=sigmaS))
+ Us<-runif(n=animais$n,0,Ds)
+ Dcens<-Ds-Us
+ #create an object to hold all relevant info
+ state.vector<-vector("list",animais$n)
+ #for each group
+ for(j in 1:animais$n) {
+   #record the initial state and time at which said state ends
+   states<-init.state[j]
+   times<-Dcens[j]
```

```

+   #set auxiliary variables for the while loop
+   state.i<-init.state[j]
+   Time.i<-Dcens[j]
+   counter<-2
+   #while the time is smaller than the wanted interval
+   while (Time.i<lim.time) {
+     #get the time at which this state ends
+     new.Time<-ifelse(state.i=="V",
+ rlnorm(n=animais$n,meanlog=muS,sdlog=sigmaS),
+ rlnorm(n=animais$n,meanlog=muV,sdlog=sigmaV))
+     Time.i<-Time.i+new.Time
+     #and get the state
+     state.i<-ifelse(state.i=="V","S","V")
+     states[counter]<-state.i
+     times[counter]<-Time.i
+     #update counter
+     counter<-counter+1
+   }
+   #times[counter-1]<-lim.time
+   #The preceeding line would be used instead of the following line
+   #if I did not need to know when a dive has ended outside the
+   #recording period
+   times[counter-1]<-Time.i
+   #record all the info in the appropriate place
+   state.vector[[j]]<-data.frame(State=states,Time=times)
+   }
+   return(state.vector)
+   }
> state.vector.test4<-get.state.vector(test4)

```

One can see an example of the simulated states for each of the 4 groups of our example in figure 10.

2.3.1 Creating objects with relevant information

Next we want to simulate clicks for each of the animals in each group, for the periods in which the animals are vocalizing. The first thing to do is to obtain an object containing the start and stop times of all vocalizing periods,

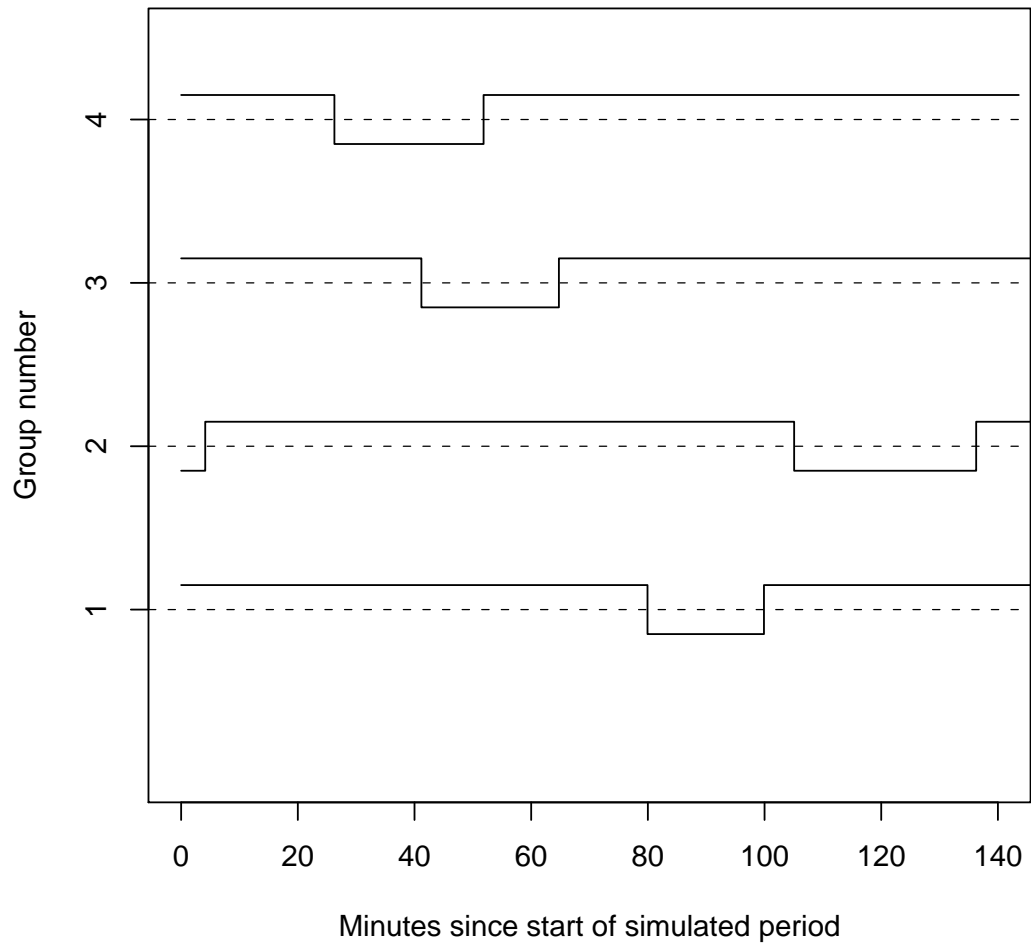


Figure 10: An example of silent (line slightly above group number) and vocalizing states (line slightly below group number) for the simulated groups.

as well as an indicator of which group those periods correspond to, which can be done using

```
> get.Vstate<-function(state.vector){
+ #Written by: Tiago Marques on 24th April 2008 and last updated on 19th May 2008
+ #Purpose: rearranges the information in an object created by get.state.vector
+ #Inputs:
+ #      state.vector - a state.vector, created by function "get.state.vector"
+ #Returns: an object of class data.frame with a row for each vocalizing period
+ #      and respective start/end times of each state and a group indicator
+ #####
+ n<-length(state.vector)
+ dados<-unlist(state.vector[[1]])
+ #set appropriate objects
+ start.times<-end.times<-groups<-states<-c()
+ #for each group, get
+ for(i in 1:n) {
+   dados<-state.vector[[i]]
+   start.times<-c(start.times,c(0,dados$Time[-nrow(dados)]))
+   end.times<-c(end.times,c(dados$Time))
+   states<-c(states,dados$State)
+   groups<-c(groups,rep(i,nrow(dados)))}
+ #select the vocalizing states
+ #note a 2 means a vocalizing period as V is the second level of the factor
+ index<-states==2
+ times<-data.frame(group=groups[index],t.start=start.times[index],t.end=end.times[index])
+ return(times)
+ }
> Vstate.test4<-get.Vstate(state.vector.test4)
```

Note that we will need to generate click times for each animal (rather than for each group), and hence it is convenient to modify the object that contains the periods that each group is vocalizing, so that it has more than a row for each group (depending on the number of animals and dives in each group). In addition to that we also add an extra column that contains the length of each vocalizing period. This can easily be done by

```
> get.Vstate.per.animal<-function(Vstate,animals){
+ #Written by: Tiago Marques on 24th April 2008 and last updated on 13th May 2008
```



```

+ #Purpose:
+ #Inputs:
+ #      Vstate - the vocal times for each group, created by function "get."
+ #      animals - an object as created by "generate.animal.coordinates"
+ #Details:
+ #Returns: an object of class data.frame with with one row for each differen
+ #with a group and animal indicator , the respective start and end times and
+ #####
+ #count how many animals are there
+ animals$animal<-1:nrow(animals)
+ #and get the appropriate information for each using the group indicator for
+ res<-merge(animals,Vstate,by.x="sindex",by.y="group")
+ res<-within(res,V<-t.end-t.start)
+ return(res)}
> V.per.animal.test4<-get.Vstate.per.animal(Vstate.test4,test4.animals)

```

The advantage of having created this object is that we can now easily assign clicks to each row, with each row corresponding to a single dive, with an indicator of which cluster and respective animal the dive corresponds to. Therefore, if at some point the vocal phase is slightly different for each animal, an object of the same structure can be created, hence all functions that are built on top of it should still work.

On the other hand, if we want to introduce some heterogeneity in vocal start and stop times within a group, modifying this object

```
> round(V.per.animal.test4,2)
```

	sindex	x	y	animal	t.start	t.end	V
1	1	19659.42	18166.54	1	24.93	48.02	23.09
2	1	19659.42	18166.54	1	125.77	152.65	26.89
3	1	19639.22	18007.92	2	24.93	48.02	23.09
4	1	19639.22	18007.92	2	125.77	152.65	26.89
5	1	19546.84	18523.07	3	24.93	48.02	23.09
6	1	19546.84	18523.07	3	125.77	152.65	26.89
7	1	19510.23	18378.92	4	24.93	48.02	23.09
8	1	19510.23	18378.92	4	125.77	152.65	26.89
9	1	19499.06	18029.26	5	24.93	48.02	23.09
10	1	19499.06	18029.26	5	125.77	152.65	26.89

11	1	19451.92	18137.29	6	24.93	48.02	23.09
12	1	19451.92	18137.29	6	125.77	152.65	26.89
13	2	12256.00	-9487.54	7	27.89	54.89	27.00
14	2	12443.00	-9726.69	8	27.89	54.89	27.00
15	2	12313.50	-9465.36	9	27.89	54.89	27.00
16	2	12364.00	-9925.14	10	27.89	54.89	27.00
17	2	12321.72	-9605.13	11	27.89	54.89	27.00
18	2	12319.57	-9674.25	12	27.89	54.89	27.00
19	3	959.07	26768.23	13	0.00	26.39	26.39
20	3	983.62	26974.53	14	0.00	26.39	26.39
21	3	851.33	26996.23	15	0.00	26.39	26.39
22	3	876.70	26936.95	16	0.00	26.39	26.39
23	3	773.89	27067.34	17	0.00	26.39	26.39
24	4	3511.61	-1445.75	18	109.82	143.39	33.57
25	4	3130.44	-1442.57	19	109.82	143.39	33.57
26	4	2857.72	-1185.53	20	109.82	143.39	33.57
27	4	3354.96	-1382.09	21	109.82	143.39	33.57

with some random noise might be the simplest way to do it ³.

2.4 Simulating click times

We can now generate times of click events for each of these periods, as well as the relevant characteristics which might influence their detection function, like whale pitch, heading and depth. Because we only require these different variables (pitch, heading and depth) at click times we generate the click times first and the variables afterwards (see next section).

The reported inter-click-interval in vocalizing periods is reported in Madsen *et al.* (2005) as being between 200 to 500 ms, with mean 400 ms (see their figure 3). A possible way to simulate similar ICI's is using a beta random variable with adequate parameter values, as shown in figure 11, e.g. using

```
> par(mfrow=c(1,1),mar=c(4.5,4.5,3,0.5))
> hist(0.2+0.3*rbeta(1000,3,1.5),main="Simulated ICI's",xlab="ICI")
```

For each vocalizing period, we want to obtain the times of the produced clicks, which can be done using something like

³Actually, due to implementation issues it might be best to do it after the function `split.V` is used - see section 2.5.2 below.

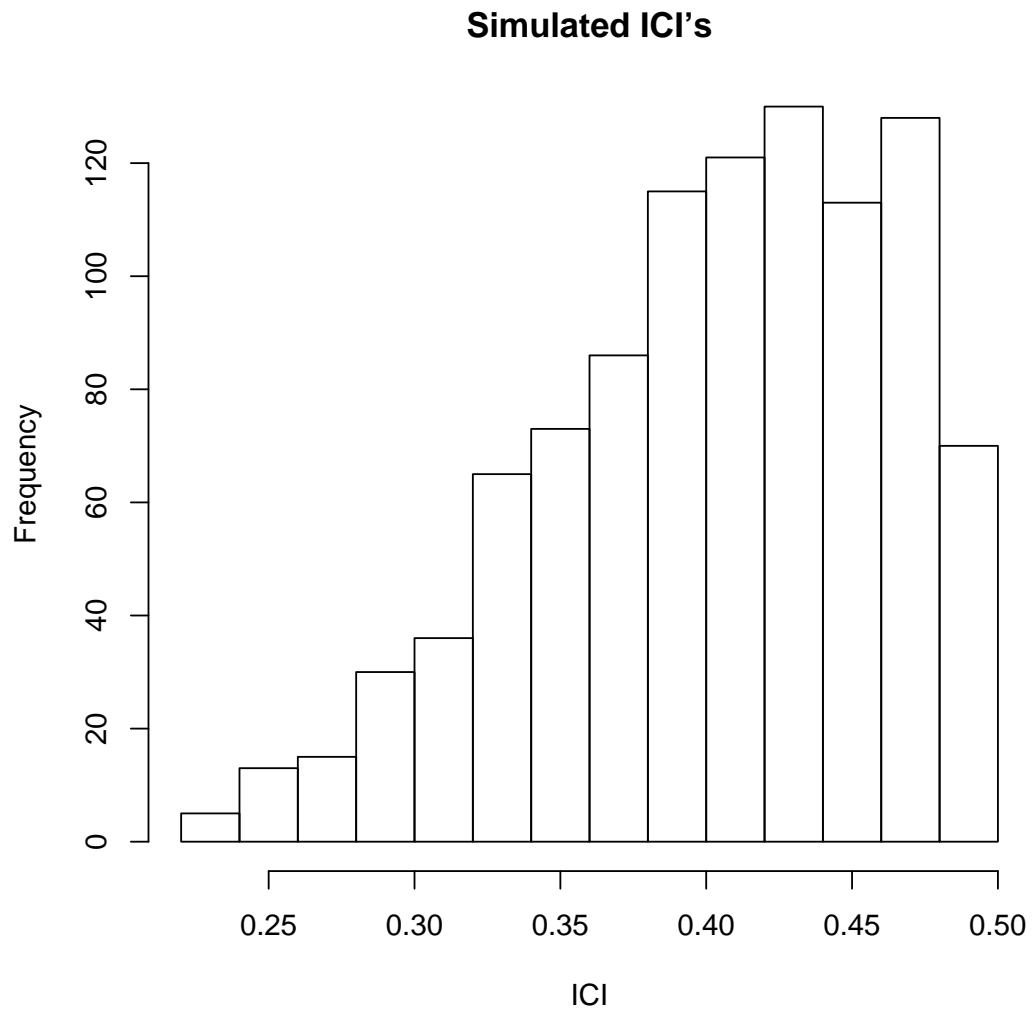


Figure 11: Simulated ICI considering a beta distribution with parameters $(3,1.5)$, which has a mean value of 0.4 seconds. Note this corresponds to the 4 parameter beta distribution to avoid the usual $(0,1)$ support of the beta.

```

> get.click.times<-function(Vstate,ICIpars=c(0.2,0.3,3,1.5),rec.period=140){
+ #Written by: Tiago Marques on 27th April 2008 and last updated on 19th May 20
+ #Purpose: simulates the click times for each dive per animal combination
+ #Inputs: Vstate - an object produced by function "get.Vstate"
+ #          or preferably by function "get.Vstate.per.animal".
+ #          ICIpars - the 4 parameters of the beta defining the ICI distrib
+ #          rec.period - the length of the simulation period
+ #Details:
+ #Returns: an object of class list with length = number of dives-animal comb
+ #          the last 3 components are the group, animal, and dive-per-anima
+ #          Element i (i=1,2,...,dv) contains the click times for the ith d
+ #####
+ #create an appropriate object to hold the click times
+ times<-vector("list",nrow(Vstate))
+ #for each dive-animal
+ for(j in 1:nrow(Vstate)) {
+   #get the vocalizing start time
+   all.times<-Vstate$t.start[j]
+   #start a counter
+   counter<-1
+   #and while the end time is not reached
+   while (all.times[counter]<Vstate$t.end[j]) {
+     #keep generating new ICI's
+     #note ICI's are in seconds while the times in minutes, so we need to di
+     new.ICI<-ICIpars[1]+ICIpars[2]*rbeta(1,ICIpars[3],ICIpars[4])
+     #and updating the object with click times
+     all.times[counter+1]<-all.times[counter]+new.ICI/60
+     counter<-counter+1}
+   #remove the first click (its just a pragmatic measure)
+   # and the last click as it was already outside the vocalizing period
+   times[[j]]<-all.times[-c(1,counter)]]}
+ #add the group index
+ times[[j+1]]<-Vstate$sindex
+ #add the animal index
+ times[[j+2]]<-Vstate$animal
+ #add the dive-animal index
+ times[[j+3]]<-1:nrow(Vstate)
+ return(times)

```

```
+ }
> click.times.test4<-get.click.times(V.per.animal.test4)
```

In order to adequately model the detection probability of each click we would need the animal position and at least the horizontal aspect angle *haa* and vertical aspect angle *vaa*, which were found to be important predictors of detection probability for beaked whale clicks, as described in “Further analysis of the hydrophone+DTag data.pdf” (Marques and Thomas, 2008a).

Hence, what we need is to simulate values for *haa* and *vaa* for each click produced. These *haa* and *vaa* need to be strongly correlated through time, as was observed in Marques and Thomas (2008a). Note that, before obtaining *vaa* and *haa*, we need depth, heading and pitch through time. Given these, *vaa* and *haa* are obtained by simple trigonometry.

2.5 Simulating click characteristics

Given the click times, we can now generate the relevant variables which will influence the detection probability of each click.

Before this we need to look at how one could simulate values around a given mean, correlated through time. This is relevant for simulating for example pitch around 0 or large negative pitch, and depth around a given mean depth say.

2.5.1 Simulating correlated values through time around a given mean

The function used here for simulating correlated values through time around a given mean is shown below.

```
> satbucl<-function(st=0,target=0,period=1:(25*60),pars=c(10,0.8),simple="Y",l
+ #This function Simulates values Around a given Target, starting at st
+ #over a period of length equal to length(period), using the parameters
+ #as defined in pars according to a given method
+ #pars is defined as:      pars[1]: sd of the updating Gaussian distribution
+ #                          pars[2]: weight given to the previous variable value
+ #                          in the weighed average
+ #If simple is not "Y", then one must provide the argument bounds, and the f
+ #only returns values within those bounds
```

```

+ #Returns: a vector of length = length(period) with the simulated values
+ #Note: this was suggested by S. Buckland
+ #Note2: the code could be simpler, with the if statement inside the 4 look,
+ #I do not want to evaluate the if statement at each iteration if no bounds
+ #Note3: presumably we could make the simulated values assymmetric
+ #(once collapsed over time) by using
+ #an assymmetric distribution instead of the Gaussian, but I have not looked
+ p.n<-length(period)
+ if(simple=="Y") {
+   for(j in 2:p.n){
+     mean.j<-weighted.mean(x=c(st[j-1],target),w=c(pars[2],1-pars[2]))
+     st[j]<-rnorm(1,mean=mean.j,sd=pars[1])
+   }
+ }
+ else {
+   for(j in 2:p.n){
+     mean.j<-weighted.mean(x=c(st[j-1],target),w=c(pars[2],1-pars[2]))
+     st[j]<-rnorm(1,mean=mean.j,sd=pars[1])
+     while (st[j]<bounds[1] | st[j]>bounds[2]) {st[j]<-rnorm(1,mean=mean.j,sd=pars[1])}
+   }
+ }
+ return(st)}

```

where if the argument `simple` is not "Y" then the argument `bounds` defines the range of possible values, and values outside that range are discarded and new candidate values obtained.

This is a modification of a previous function `satbuc`, which does not include the possibility to define constraints in the values that it can simulate. For further details about this function see Marques and Thomas (2008d).

2.5.2 Simulating depth

A separate document (Marques and Thomas, 2008e) describes in more detail some of the intermediate steps involved in the simulation of depth over time. Said document also describes some previous attempts at it, less successful but yet worth looking at if one is thinking about improving this code. That document presents some overlap with this one.

There is some limited knowledge about beaked whale distribution with depth, although some DTag data is available, some of it being from within

AUTEC. Using DTag data from the Canary Islands, Tyack *et al.* (2006) reported *Mesoplodon* buzzes recorded in the range 244-1244 m deep⁴, with a mean of 724 m, while 95% of these buzzes occurred at depths between 463 and 1196 m. It seems therefore not unlikely that in some of the areas at AUTEC beaked whales might dive almost all the way down close to the bottom, as the minimum hydrophone depth is 1294m and the average hydrophone depth is 1652m (see Figure 12).

However, for the single beaked whale dive for which we currently have DTag data at AUTEC (Dive 1 on 23 Oct 06), the whale clicked between depths of 582 and 1049m, while the bottom was around 1600m deep, which means that for this dive the whale foraged quite far from the bottom.

The analysis described in Marques and Thomas (2008a) considers the detection probability to be a function of the 2D distance as projected onto the sea surface (rather than a 3D slant distance), hence one might be tempted to ignore depth in the simulations. This (if possible, which is not - see below) could actually have a small impact in the simulations for 2 reasons:

1. The whales seem to produce most of their clicks in a “relatively narrow” depth band (i.e. clicks are only produced at the deep part of their dives), which tends to be quite close to the bottom, hence the 2D and 3D distances are highly correlated;
2. As mentioned before, *vaa* and *haa* seem to be the major sources of heterogeneity in click detection probability, hence the 2D vs. 3D distance might not be that relevant any way.

However, we need to know the actual depth in order to calculate *vaa* from pitch (see below), and hence we need to simulate depth too. One would like to simulate profiles like the one in figure 2 in Marques and Thomas (2008a), which is rather complicated having only 1 dive. Additionally, note that depth is related to pitch in several ways:

1. Depth decreases fast until the time that pitch stabilizes around 0, i.e. once the animal is just swimming up and down, foraging, rather than actively going down to reach a given depth;

⁴ Note that, given that sample size was 3 whales, these is most likely an underestimate of the true maximum depth and an overestimate of true minimum depth for a buzz.

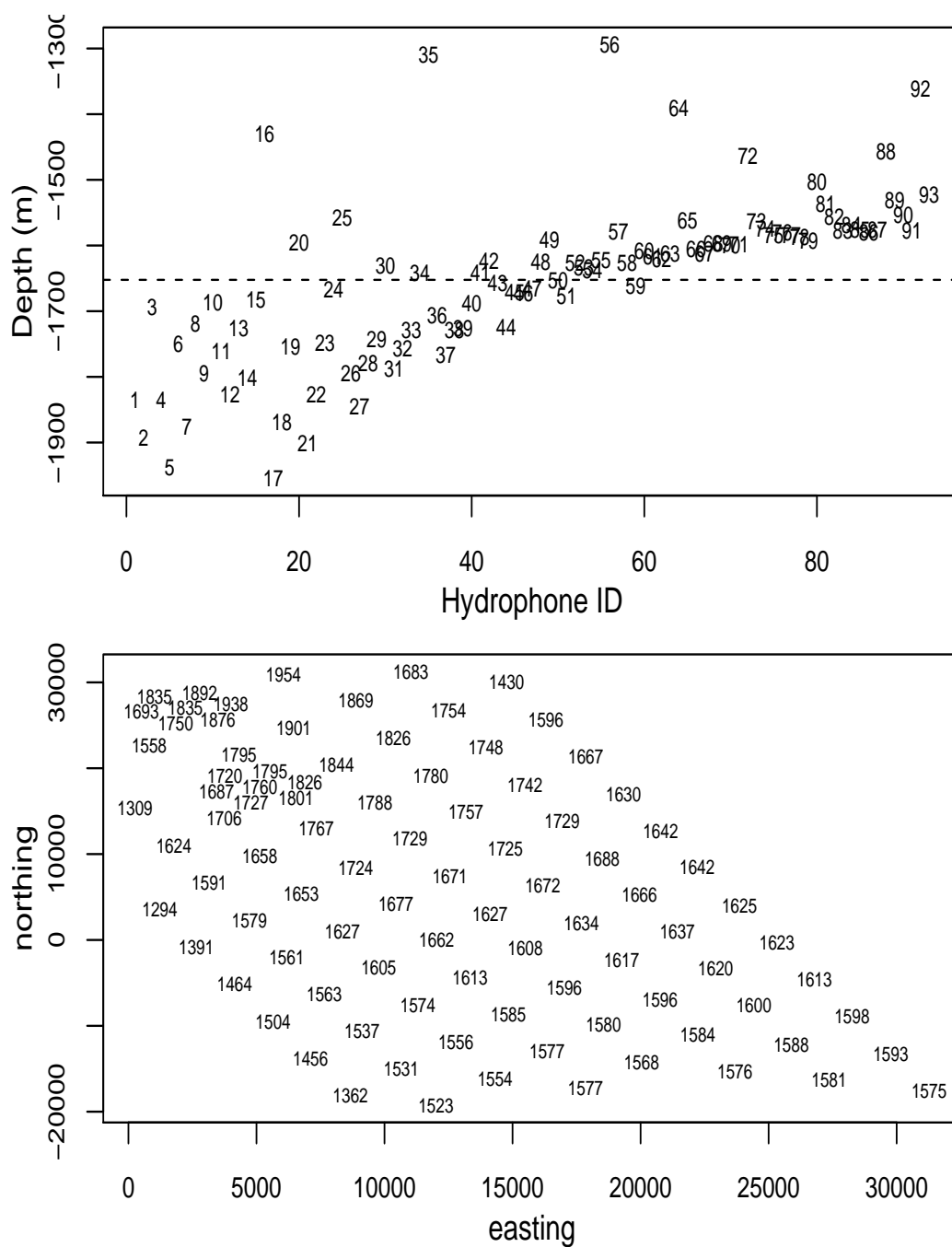


Figure 12: The depths of the AUTECH hydrophones. The dashed line on the top panel is at 1652m, the mean depth over all hydrophones.

2. One should be able to calculate change in depth given pitch and speed (although conceivably an animal might go up and down in the water column while keeping its pitch equal to 0).

Additionally, and to complicate things further, depth is also related to the state of the animal, and hence there's a relation between the time that an animal is silent or vocalizing and the corresponding changes in depth, which in turn must have a correspondence to changes in pitch. All these interdependencies across different variables turn this into a complicated problem to solve.

A possible way forward would be to divide the vocalizing period in 3 sub-periods. The first one would be designated as vocal descent period (*VDP*), and the second designated as vocal constant depth period (*VCDP*), the third as the vocal ascent period (*VAP*) (might be absent, i.e. the whale goes silent as it starts to go up). Under this conceptual setting, we could have the whale going mostly down, steadily decreasing depth and with a large negative pitch during the *VDP*, and the whale would be moving randomly around a given depth (here referred to as the mean depth of the *VCDP*, $VCDP_z$), with pitch varying randomly around 0, during the *VCDP*, and finally moving up with large positive pitches during the (if present) *VAP*. Depth will decrease from a randomly generated depth for the start of the vocal phase till a randomly generated $VCDP_z$, and then if *VAP* is present it will increase till a randomly generated depth for the end of the vocal phase. Further define VDP_{zs} and VAP_{ze} respectively as the depth at which the *VDP* starts and the *VAP* ends. Figure 13 illustrates all these for an hypothetical dive with a *VAP*.

Currently, there is no data from which to model the length of these sub-periods or some of the corresponding depths, except that Tyack *et al.* (2006) report (all depths in meters, standard deviations in brackets):

- average pitch is between 60° and 83° degrees during *VDP*;
- mean maximum dive depth is 835 (143) (from which one can simulate a mean maximum dive depth Z_{max});
- vocal phase mean depth start is 426 (125) (from which one can simulate VDP_{zs});
- vocal phase mean depth end is 738 (98) (from which one can simulate VAP_{ze}).

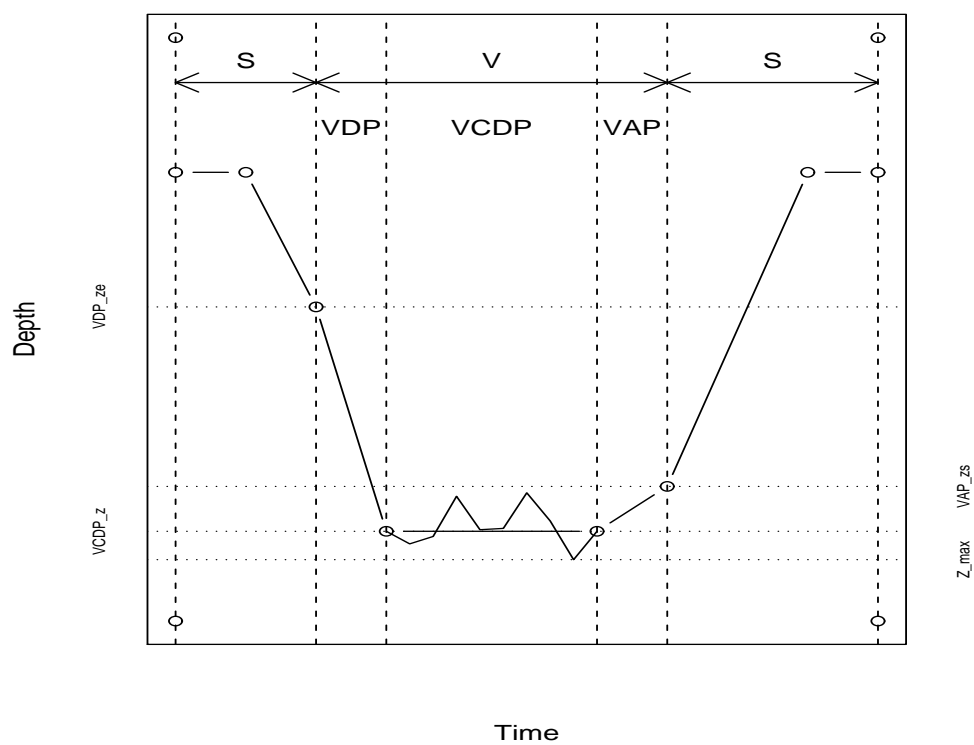


Figure 13: An hypothetical dive with a vocal ascent period, with all the acronyms used in the text. See text for further details.

Hence we are missing the information required to generate $VCDP_{\bar{z}}$, as well as to sub divide the vocalizing period. In the following (see Marques and Thomas (2008e) for details) we decided to simplify the current approach and consider simply two vocalizing sub-periods. Under this setting, whales are assumed to:

1. start vocalizing at a depth of VDP_{zs} and go down till a depth VDP_{ze} ; this is the VDP as above;
2. then move from VDP_{ze} ($\equiv VCDP_{zs}$) to a $VCDP_{ze}$, and at the end of the vocalizing period move up; this is the $VCDP$ as above.

A way to implement this (agai, see Marques and Thomas (2008e) for an alternative) might be to first generate relevant depths, and then subdivide VDP and $VCDP$ according to the depth difference that the whale must travel while going down and clicking. We must assume that the descent speed in the non vocal phase is the same as in the vocal phase as Tyack *et al.* (2006) state that “For deep dives, we considered the descent to extend from the surface until the whale began to produce regular echolocation clicks. Likewise, the ascent was considered to start at the last regular click and end at the surface.”. The reported mean descent rate is 1.6 m/s (sd=0.21). We actually used a descent rate of 1.5 m/s based on data from Baird *et al.* (2008).

Although this might be unrealistic and changed later if further information is obtained, it seems unfeasible to simulate depth through time in any more complicated way. Note in this case we assume that the animals dives from VDP_{zs} to VDP_{ze} , and we generate

- VDP_{zs} from a $N(426,125)$;
- and VDP_{ze} from a $N(787,121)$

Note that VDP_{ze} mean and standard deviation are the respective means of the means and standard deviations of the mean maximum dive depth and of vocal phase mean depth end $((835+738)/2$ and $(143+98)/2$). There is no justification for the use of these values, they just seem plausible values at this point, and they allow us to move forward.

So now we have these we can simulate depth during $VCDP$ using what was described in section 2.5.1, and obtain a depth reading for the VDP for any desired click time.

This can be done using a function like `get.depth.per.click` below, which is applied to our running example for illustration.

```

> get.depth.per.click<-function(Vstate,clicks,Vs,rec.period=140,smooth="No",spli
+ #this function returns a list with the depth associate with each click
+ #for each vocalizing period
+ #Inputs: Vstate - an object produced by function "get.Vstate"
+ #or preferably by function "get.Vstate.per.animal".
+ #      clicks - an object with the time of each click
+ #      VS      - an object with the length of each vocalizing sub-period (V
+ #      rec.period - the length in minutes of the recording period
+ #      smooth - If yes, lowess smooths of the simulated depths are returned
+ #      spar - the lowess smoother span (large spar, more smooth)
+ depths<-vector("list",nrow(Vstate))
+ for(j in 1:nrow(Vstate)) {
+   #select those clicks made in the VDP
+   inVDP<-clicks[[j]]<Vstate$t.start[j]+Vs[[j]][1]
+   inVCDP<-clicks[[j]]>Vstate$t.start[j]+Vs[[j]][1]
+   #for these, depth is given by initial depth + deltaT * descent speed (=
+   depths[[j]]<-Vs[[j]][3]+(clicks[[j]][inVDP]-Vstate$t.start[j])*(1.5*60)
+   depths[[j]]<-c(depths[[j]],satbucl(st=Vs[[j]][4],target=Vs[[j]][4],peri
+   if (smooth=="Yes") {depths[[j]]<-lowess(depths[[j]],f=spar)$y}
+   depths[[j]]<-depths[[j]][clicks[[j]]<rec.period]
+ }
+ return(depths)
+ }
> #
> depths.test4<-get.depth.per.click(V.per.animal.test4,click.times.test4,spli

```

We can take a look at the change in depth for the vocal period of some of the animals from our example (Figure 15). The lack of reality is currently evident, but this might be good enough for the purposes at hand.

A few points in the process remain unrealistic and could be addressed later:

- There is no randomness in depth during *VDP*;
- There is no variability across animals within group in the length of the 2 sub-periods (*VDP* and *VCDP*) as well as the depth at which the animal begun to click (VDP_{zs}) and the mean depth at which it foraged (VDP_{ze});

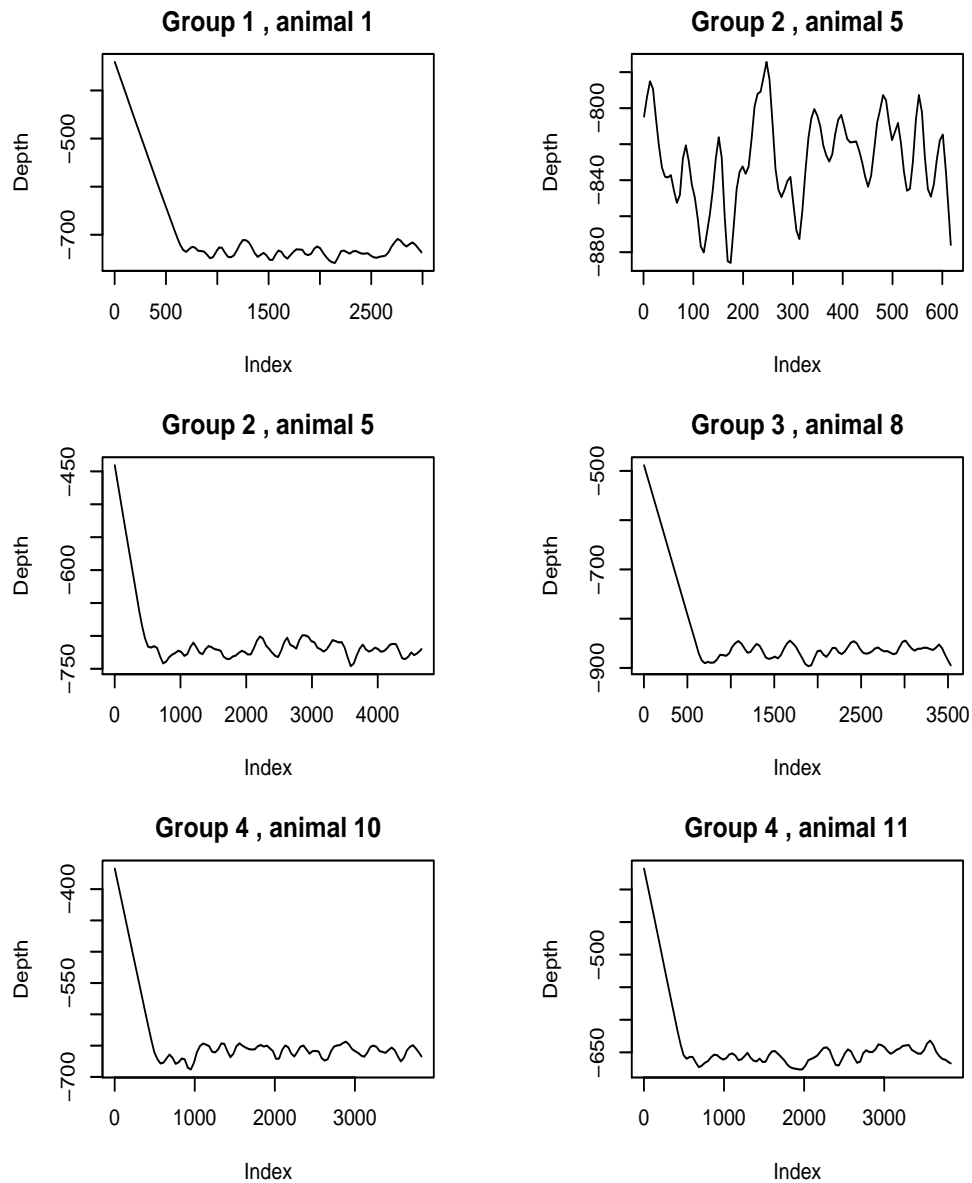


Figure 14: The simulated dive for the 1 animal in each group/dive combination (except the two bottom plots which are for 2 animals from group 4). Note that only the end of the 1st dive was recorded for group 2. The lack of reality is currently evident (cf. with say Figure 2 in Marques and Thomas (2008a)), but this might be good enough for the purposes at hand.

- For *VCDP* there is no relation between the elapsed time between clicks and change in depth. At the time-space scale we are currently working this is likely irrelevant, but change in depth might be made a function of time between clicks. This would require changes in `satbucl`;
- The smoother was added just because things look better, but adds to the arbitrariness involved;
- The variance in depth during *VCDP* is currently arbitrary and not data based.

Before proceeding any further, we need to clean the object containing the click times (`click.times.test4`). For dives which were not finished before the end of the simulation period, this object still has those click times happening after the end of the simulation period. The reason for these not having been removed from the start was because we needed all the click times of a dive to get the depths in `get.depth.per.click`. But for the rest of the simulation exercise, these are actually not needed.

```
> clean.click.times<-function(times,minutes){
+ #this function just removes all click times which happened after
+ #the simulation period is over
+ n.dives<-length(times)-3
+ for(j in 1:n.dives) {
+   ind<-times[[j]]<minutes
+   times[[j]]<-times[[j]][ind]
+ }
+ return(times)
+ }
> click.times.test4<-clean.click.times(click.times.test4,140)
```

2.5.3 Simulating heading

We can simply use the models described in Marques and Thomas (2008a) to generate heading for the time of each click produced in the previous section.

This can be done using the function `get.headings` below. This function calls another function `get.dive.headings`⁵, which uses the geometric and

⁵ Which is not shown in this report for brevity, but is documented in the corresponding sweave .Rnw file.

weibull models as described in Marques and Thomas (2008a) to simulate heading through time.

```
> get.headings<-function(Vstate.per.animal){
+ #this function returns the heading for all the clicks that are present
+ #in each of the dives recorded in the object "Vstate.per.animal"
+ #get the total number of dives
+ dives<-length(Vstate.per.animal)-3
+ #an object to store the headings
+ headings<-Vstate.per.animal
+ #for each dive
+ for(j in 1:dives) {
+ headings[[j]]<-get.dive.headings(Vstate.per.animal[[j]])
+ }
+ return(headings)}
> #by default there's eval=F as anchor
> #use eval = T to run again
> headings.test4<-get.headings(click.times.test4)
```

2.5.4 Simulating pitch

As above, we can use what was described in Marques and Thomas (2008a) for pitch simulation. This can certainly be improved at a later stage, but currently, it seems like proceeding further with some reasonable simulations is more useful than to stop to look for an optimized process.

Hence, currently, the function `get.pitches` calls function `get.dive.pitches`⁶, which is based on material found on Gillespie (2006). This was not based on models like those for heading, but rather more ad hoc. The advantage of setting it this way is that if a better way of simulating pitch through time is obtained, then we can just update `get.dive.pitches` and the rest of the code should not have to be changed.

```
> get.pitches<-function(Vstate.per.animal){
+ #this function returns the pitch for all the clicks that are present
+ #in each of the dives recorded in the object "Vstate.per.animal"
+ #get the total number of dives
```

⁶ Which is not shown in this report for brevity, but is documented in the corresponding sweave .Rnw file.

```

+ dives<-length(Vstate.per.animal)-3
+ #an object to store the headings
+ pitches<-Vstate.per.animal
+ #for each dive
+ for(j in 1:dives) {
+ pitches[[j]]<-get.dive.pitches(Vstate.per.animal[[j]])
+ }
+ return(pitches)}
> #
> #executing the code - commented for faster report production
> #uncomment to run again
> pitches.test4<-get.pitches(click.times.test4)

```

2.6 Obtaining relevant variables for each hydrophone-click combination

Now that we have simulated the characteristics of each click, we want to estimate the probability that a click is detected in a given hydrophone. From the analysis presented in Marques and Thomas (2008a), there are at least 3 relevant variables influencing said detection probability:

1. Dh - whale to hydrophone horizontal (2D) distance;
2. vaa - vertical aspect angle;
3. haa - horizontal aspect angle.

Note that to obtain vaa and haa we need first to obtain, for each click-hydrophone combination, the relevant hydrophone-whale angles,

1. $hw_{v\theta}$ - hydrophone-whale vertical angle;
2. $hw_{h\theta}$ - hydrophone-whale horizontal angle.

In figure ?? there is a representation of distances and angles considered.

For any given click, given the whale's position (x, y, z) and its corresponding heading and pitch, as obtained in the previous sections, one can calculate Dh , vaa and haa for any hydrophone. In other words, while a given click has a heading, pitch and depth (independent of hydrophone location), Dh , vaa

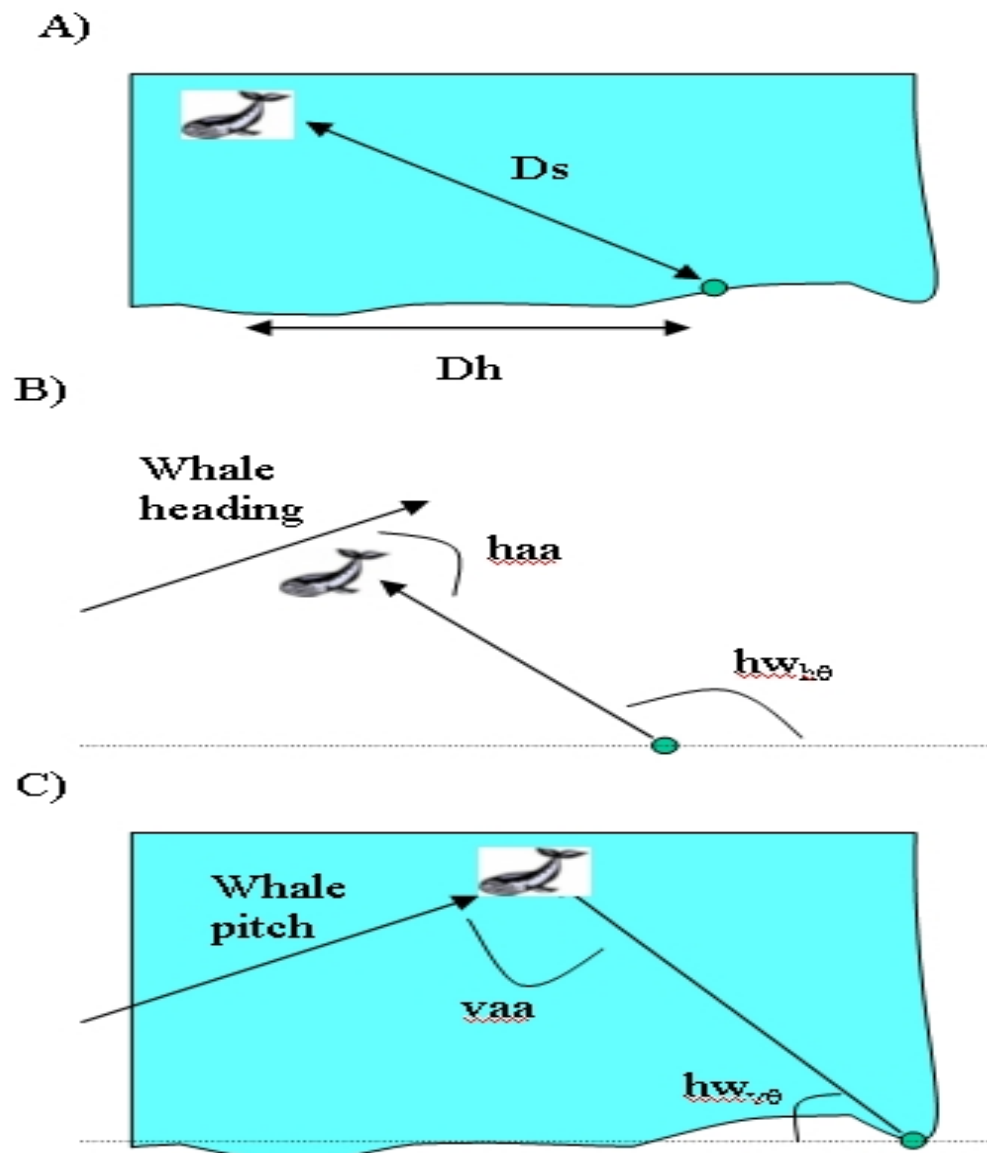


Figure 15: The simulated dive for the 1 animal in each group/dive combination (except the two bottom plots which are for 2 animals from group 4). Note that only the end of the 1st dive was recorded for group 2. The lack of reality is currently evident (cf. with say Figure 2 in Marques and Thomas (2008a)), but this might be good enough for the purposes at hand.

and *haa* are a function of a combination of these click characteristics and the hydrophone location relative to the whale location at the time of the click.

In the following we start by reducing the time that the code takes to run by filtering out whale-hydrophone combinations which are too far apart, and hence for which no detections are expected any way. Then we present in turn some simple functions required to calculate *vaa* and *haa*, and we finish by integrating all these to obtain the relevant click properties for all whale-hydrophone combinations.

2.6.1 Filtering out whale-hydrophone combinations

It is likely simpler to define, for each simulated whale, which are the hydrophones at which clicks are potentially detected with non negligible probabilities. All the other hydrophones can be ignored. At this point we assume that no clicks will be heard at hydrophones more than 7km away from the click (This is likely overly optimistic any way, as this distance is likely to be smaller).

We create a matrix with as many rows as hydrophones and as many columns as animals, in which each element is true if the corresponding animal hydrophone are within some distance of each other (here we used 7km as a default). This is done using the code below:

```
> get.relevant.hyds<-function(xy.anim.pos,hyds.pos,radius=7000){
+   #This function returns a matrix with as many columns as animals
+   #and as many rows as hydrophones, filled with 0's and 1's
+   #where a 1 corresponds to a hydrophone for which there is
+   #at least 1 click produced by the corresponding animal which
+   #is closer than the argument radius
+   #Inputs:
+   #xy.anim.pos      the x,y positions of the animals
+   #hyds.pos         the x,y positions of the hydrophones - defaults to AUTECH
+   #radius           the distance at which a click is considered impossible to
+   #                 defaults to 7 km
+   n.anim<-dim(xy.anim.pos)[3]           #how many animals are they
+   n.hyd<-nrow(hyds.pos)                 #and how many hydrophones
+   rel.hyd<-matrix(NA,nrow=n.hyd,ncol=n.anim)
+   for(j in 1:n.anim) {
+     xy<-xy.anim.pos[,j]
```

```

+      #a distance matrix with as many rows as xy pos and as many columns as l
+      pair.dists<-crossdist(X=xy[,1],Y=xy[,2],x2=hyds.pos$x,y2=hyds.pos$y)
+      #the minimum distance per hydrophone
+      min.dist<-apply(pair.dists,2,min)
+      #now get an indicator of which are less than the radius
+      rel.hyd[,j]<-min.dist<radius
+    }
+    return(rel.hyd)
+  }
> test4.rel.hyds<-get.relevant.hyds(test4.xy.per.animal,hyd)

```

The object created will be useful later to skip loop cycles for hydrophone-whale combinations that are not close enough in space (see section 2.6.5).

2.6.2 Obtaining *haa*

We begin by creating a function which returns $hw_{h\theta}$, the horizontal angle between a whale and a hydrophone (see ?? for details).

We define here that, assuming a whale to be in the center of a compass rose, a $hw_{h\theta}$ of 0° corresponds to a hydrophone to east of the whale, and 90° to the north of the whale. Remember that whale heading varied between -180° and 180° . For consistency with this definition, we add 180 to all headings and assume that a heading of 90° is a whale moving north⁷.

To get *haa* we need two quantities, the heading of the whale and $hw_{h\theta}$, the angle between the hydrophone and the whale. The heading of the whale was obtained in section 2.5.3, and the whale-hydrophone angle can be obtained by a function like

```

> get.angles<-function(whale,hyds){
+ #Given the x,y location of the whale and the hydrophones this function retu
+ #the angle from the whale to the hydrophone
+ #An angle of 0 corresponds to a hydrophone with the same y cordinate and a
+ #i.e. exactly to the right of the whale
+ #Inputs:
+ #      whale - x,y location of the whale
+ #      hyds  - x,y location of the hydrophones

```

⁷ This is a detail, but it assumes that if heading north at AUTECH a whale does not change its x coordinate.

```

+ #get the difference in x
+ whale<-as.numeric(whale)
+ xs<-whale[1]-hyds[,1]
+ #get the distances
+ rs<-sqrt((whale[1]-hyds[,1])^2+(whale[2]-hyds[,2])^2)
+ #get the angle in -90,90: with 0 being a vertical line going through the wh
+ teta<-asin(xs/rs)*180/pi
+ #get the quadrants
+ quad<-ifelse(whale[1]<=hyds[,1] & whale[2]<=hyds[,2],1,ifelse(whale[1]>hyds
+ #given the quadrant, get the angle (0 is straight up)
+ angles<-ifelse(quad==1,90+teta,ifelse(quad==2,teta+90,270-teta))
+ return(angles)
+ }

```

Note that we have a different whale-hydrophone angle by hydrophone for each whale position. As we have simulated one x, y position per minute, over 140 minutes, we have those many angles to calculate. This can be done using the following function

```

> get.angle.per.animal.hyd.min<-function(minutes=140,anim.xy,hyd.xy){
+ #number of animals involved
+ nanim<-dim(anim.xy)[3]
+ #set up an object to hold angles
+ angle.per.animal.hyd.min<-array(0,dim=c(minutes,nanim,nrow(hyd.xy)))
+ for(an in 1:nanim) {
+   for(mi in 1:minutes) {
+     angle.per.animal.hyd.min[mi,an,]<-get.angles(anim.xy[mi,1:2,an],hyd
+   }}
+ return(angle.per.animal.hyd.min)
+ }
> test4.angle.per.animal.hyd.min<-get.angle.per.animal.hyd.min(140,test4.xy.p

```

Note that while this was implemented over all hydrophones, in practice we only care about those that are “close” to the animals. Also, although we did it for all x, y positions over time, we only require those corresponding to minutes in which the animal was vocally active. Implementing these restrictions should speed up things, but requires that one keeps track of the valid combinations of relevant hydrophone/minutes per animal. And because

there is only one x, y position per minute, this code is fast to run any way, so we keep it as is for the time being.

Finally, the following function allows us to get haa from vectors of angles and headings.

```
> get.haa<-function(angles,headings){
+ #This function returns the horizontal aspect angle (haa)
+ #of the whale with respect to the hydrophone
+ #Note it assumes that headings come in the -180,180 range
+ #Inputs:
+ #          angles      the angle between whale and hydrophone (0 means hyd
+ #          headings    the heading of a whale (0 means facing east - after
+ #          hence if angle=heading then haa=0
+ #if angle > heading returns a positive haa, and a negative otherwise
+ #get the headings in the 0,360 range
+ headings<-headings+180
+ #now get the difference
+ haa<-angles-headings
+ haa<-ifelse(haa>180,haa-360,ifelse(haa<(-180),haa+360,haa))
+ return(haa)
+ }
```

2.6.3 Obtaining vaa

We just require two simple functions to obtain vaa .

The first function allow us to calculate $hw_{v\theta}$, the vertical angle from hydrophone to the whale (see ?? for details; this was defined as a negative angle, as long as the hydrophone is deeper than the whale, for consistency with the fact that negative pitches correspond to a whale facing the bottom and positive pitches to a whale facing the surface). Said function is shown below:

```
> get.vawh<-function(zw,zh,dwh){
+ #this function calculates the vertical angle from whale to hydrophone
+ #Inputs:
+ #          zw          the depth of the whale
+ #          zh          the depth of the hydrophone
+ #          dwh         the horizontal distance between the whale and hydrophon
```

```
+ vawh<-atan((zw-zh)/dwh)#id depths are negative requires #vawh<--atan((zw-zh)
+ return(vawh)
+ }
```

and, given $hw_{v\theta}$ and pitch, the vaa is obtained by using a second function as

```
> get.vaa<-function(vawh,pitch){
+ #this function calculates the vaa
+ #Inputs:
+ #          vawh      the vertical angle from whale to hydrophone
+ #          pitch     the whale pitch
+ vaa<-pitch-vawh
+ return(vaa)
+ }
```

2.6.4 Detection function

In order to estimate a click detection probability we require a detection function. An example of said function was obtained in Marques and Thomas (2008a). Note however that it is unlikely that this function is a good representation of reality, as it was obtained using DTag data and such data is only available for optimal weather (=low noise) conditions. Nonetheless, lacking any better option, we use here the results obtained in Marques and Thomas (2008a). If at a later stage we obtain more realistic detection functions one can simply update this code.

For simplicity, we saved the glm model⁸ selected for the detection function in Marques and Thomas (2008a) using

```
save(list="pooledmod3.logistic", file = "detfun.R")
```

in the workspace *furtherDTagHyd.RData*, and then copy-pasted the file into the current working directory and read in to R using

```
> load("datfiles/detfun.R")
```

We can now predict detection probabilities for any click given the relevant variables, using a simple call to `predict.glm`. The following function is a wrapper for calculating the detection probability of each click and simulating its detection:

⁸A gam model was originally used, but then for pragmatic reasons due to failure to predict outside the range of the data with gam cc basis a standard logistic model was used. See Marques and Thomas (2008a) and comments in the .Rnw file for further details.

```

> simulate.detection<-function(new.data,model=pooledmod3.logistic){
+ #Inputs:
+ #           new.data - a data frame with the relevant variables
+ #           model - a glm/gam logistic type model
+ #create the data frame for predictions to be made for
+   ndat<-with(new.data,data.frame(poolednewdrange=dwh,pooledhaa=haa,po
+   #calculate the probability of detection
+   Pdet<-predict.glm(model,newdata=ndat,type="response")
+   #use rejection method to see which are detected
+   U<-runif(nrow(new.data),0,1)
+   detect<-ifelse(Pdet>U,1,0)
+ return(cbind(new.data,data.frame(Pdet=Pdet,det=detect)))
+ }

```

2.6.5 Obtaining all the relevant variables

Now, we use all the functions above to obtain click counts per hydrophone per minute.

There are multiple ways in which this information could be gathered and stored. Initially we organized this data in a data frame which included a row for each click-hydrophone (at which said click could be detected) combination, and then all the relevant variables. This was then used to compute *vaa*, *haa*, *Dh* (and later) detection probabilities) at once for all click events using the vectorization capabilities in R.

However, said data frame was too large for even small simulation exercises, and for that reason we opted by storing the information for all relevant variables for each click-hydrophone combination in a separate file (additionally, a separate file is created which indexes the larger file, i.e., lists at which rows are the clicks for a given hydrophone and animal-dive combination), but outputting in R directly a matrix with number of click counts detected by minute and hydrophone. This is not as fast as the previous option, as we need to perform some operations using for loops rather than using vectorization.

This is implemented in the function below

```

> get.cc<-function(xy.anim,angles,click.times,headings,depths,pitches,hyds,re
+ #Written by: Tiago Marques on 5th May 2008 and last updated on 19th May 2008
+ #Purpose:   given all the relevant variables, simulate click count vectors
+ #Inputs:

```

```

+ #      Per minute:
+ #      xy.anim - the x,y position for each animal
+ #      angles - the horizontal angles for each animal-hydrophone combination
+ #      Per click:
+ #      click.times - the click time
+ #      headings - the heading
+ #      depths - the depth
+ #      pitches - the pitch
+ #      hyds - the hydrophones
+ #      rel.hyds - a true/false matrix (a true means that hydrophone-animal
+ #      fname - a prefix for the names of produced files
+ #Details:
+ #Returns: an object of class matrix with dimensions (number of minutes) * (1
+ #          containing the click counts per minute per hydrophone
+ #          2 files are produced: 1 with the relevant click properties for a
+ #          1 with an indexing system (start and end
+ #          active hydrophone-dive combinations)
+ #####
+ n.anim.dive<-dim(xy.anim)[3]
+ n.dives<-length(click.times)-3
+ n.hyds<-nrow(hyds)
+ group.ind<-unlist(click.times[n.dives+1])
+ anim.ind<-unlist(click.times[n.dives+2])
+ minutes<-dim(xy.anim)[1]
+ #####
+ #create an object to hold the click counts
+ res<-matrix(0,nrow=minutes,ncol=n.hyds)
+ #plus an object to index the text file created
+ file.index<-data.frame(index=1,dive=1,animal=1,group=1,hyd=1,start.row=1,end
+ counter<-0
+ rows.counter<-1
+ #####
+ test.file<-file(description=fname,open="wb")
+ #####
+ #for each animal-dive combination
+ for(j in 1:n.dives) {
+   #get click times for the jth dive-animal combination
+   current.times<-unlist(click.times[j])

```



```

+   #count how many they were
+   n.clicks<-length(current.times)
+   #get the headings
+   current.headings<-unlist(headings[j])
+   #get the depths
+   current.depths<-unlist(depths[j])
+   #get the pitches
+   current.pitches<-unlist(pitches[j])
+   for(k in 1:n.hyds) {
+       #check if said animal was detectable from said hydrophone, if not g
+       if (rel.hyds[k,anim.ind[j]]==F) next
+       #add the counter for valid hyd-dive combination
+       counter<-counter+1
+       #get the group indicator
+       current.gr<-rep(group.ind[j],n.clicks)
+       #get the animal indicator
+       current.an<-rep(anim.ind[j],n.clicks)
+       #(for this animal-hydrophone combination)
+       #get the hydrophones characteristics
+       current.hyd<-rep(k,n.clicks)
+       current.hyd.x<-rep(hyds$x[k],n.clicks)
+       current.hyd.y<-rep(hyds$y[k],n.clicks)
+       current.hyd.z<-rep(-hyds$z[k],n.clicks)
+       #get the angle per minute, x per minute and y per minute, for the c
+       angle.per.min<-angles[,current.an,k]
+       x.per.min<-xy.anim[,1,current.an]
+       y.per.min<-xy.anim[,2,current.an]
+       #which minutes were there clicks in
+       mins.for.rep<-ceiling(current.times)
+       #how many clicks in each minute
+       reps<-as.data.frame(table(mins.for.rep))
+       #create the angles, xs and ys
+       current.angles<-rep(angle.per.min[reps[,1]],times=reps[,2])
+       current.xs<-rep(x.per.min[reps[,1]],times=reps[,2])
+       current.ys<-rep(y.per.min[reps[,1]],times=reps[,2])
+       #put it all as a data frame
+       all.click.vars<-data.frame(ctime=current.times,gr=current.gr,an=cur
+       x=current.xs,y=current.ys,z=current.depths,heading=current.headings

```

```

+       angle=current.angles,hyd=current.hyd,hx=current.hyd.x,hy=current.hyd.y)
+       #get the horizontal aspect angle
+       all.click.vars$haa<-get.haa(all.click.vars$angle,all.click.vars$headings)
+       #get the whale-hyd horizontal distance
+       all.click.vars$dwh<-sqrt((current.xs-current.hyd.x)^2+(current.ys-current.hyd.y)^2)
+       #get the vertical angle whale hyd
+       all.click.vars$vawh<-get.vawh(current.depths,current.hyd.z,all.click.vars$depths)
+       #get vaa
+       all.click.vars$vaa<-get.vaa(all.click.vars$vawh,current.pitches)
+       #now deal with the detection function
+       all.click.vars<-simulate.detection(all.click.vars,model=pooledmod3)
+       #now update the click count object with the corresponding click count
+       cc.per.minute.per.hyd<-with(all.click.vars,xtabs(det~ceiling(ctime)))
+       c.row<-as.numeric(names(cc.per.minute.per.hyd))
+       res[c.row,k]<-res[c.row,k]+as.numeric(cc.per.minute.per.hyd)
+       #write text file
+       #TF<-ifelse(counter==1,T,F)
+       #write.table(x=all.click.vars,file = paste(fname,".txt",sep=""),append=TRUE)
+       #create a binary file to store results
+       writeBin(as.numeric(as.matrix(all.click.vars)),test.file,size=4)
+       #update file.index object
+       file.index[counter,]<-c(counter,j,anim.ind[j],group.ind[j],k,rows.counter)
+       rows.counter<-rows.counter+n.clicks
+       }
+       write.table(x=file.index,file=paste(fname,".file.index.txt",sep=""),append=TRUE)
+       close(test.file)
+       return(res)
+ }

```

This function can be used over our running example⁹

```

> WD <- getwd()
> setwd("Rfiles")
> test4.cc.per.minute.per.hyd<-get.cc(test4.xy.per.animal,test4.angle.per.animal,
+ headings.test4,depths.test4,pitches.test4,hyd,test4.rel.hyds,"test4")
> setwd(WD);rm(WD)

```

⁹ In the code shown, the use of `getwd` and `setwd` is just for tidying up the folder where the R workspace is stored.

A good way to view a summary of a simulation exercise might be an image plot of the click counts per hydrophone per minute. The corresponding plot for the running example is shown in figure 16. Reassuringly, the individual dives (5 in total) can be easily identified (cf. with figure 3 and figure 10).

However, in order to create an object with the same structure as the original click counts, used for gam analysis and video production, one needs to go through all the minutes and hydrophones in turn, as in

```
> get.cc.for.model<-function(cc.per.minute.per.hyd){
+ minutes<-nrow(cc.per.minute.per.hyd);hyds<-ncol(cc.per.minute.per.hyd)
+ res<-data.frame(TP=rep(1:minutes,each=hyds),HYD=rep(1:hyds,minutes),CC=0)
+ CC<-c()
+ for(m in 1:minutes) {
+     CC<-c(CC,cc.per.minute.per.hyd[m,])
+ }
+ res$CC<-CC
+ return(res)
+ }
> test4.cc<-get.cc.for.model(test4.cc.per.minute.per.hyd)
```

Note that the function `get.cc` has, as side effect, the production of a binary file, and an auxiliary txt file that indexes the information in the binary file. See section 2.8 for details about getting the information in the binary file back into R.

2.7 Wrapper function for full simulation exercise

It is convenient to put all the relevant code inside a single function which produces as output the click count per minute per hydrophones. This function would have as input parameters the characteristics defining a given simulation scenario, like:

- Animal density
- Mean group size
- Number of hydrophones and respective location
- Number of minutes to simulate click counts over

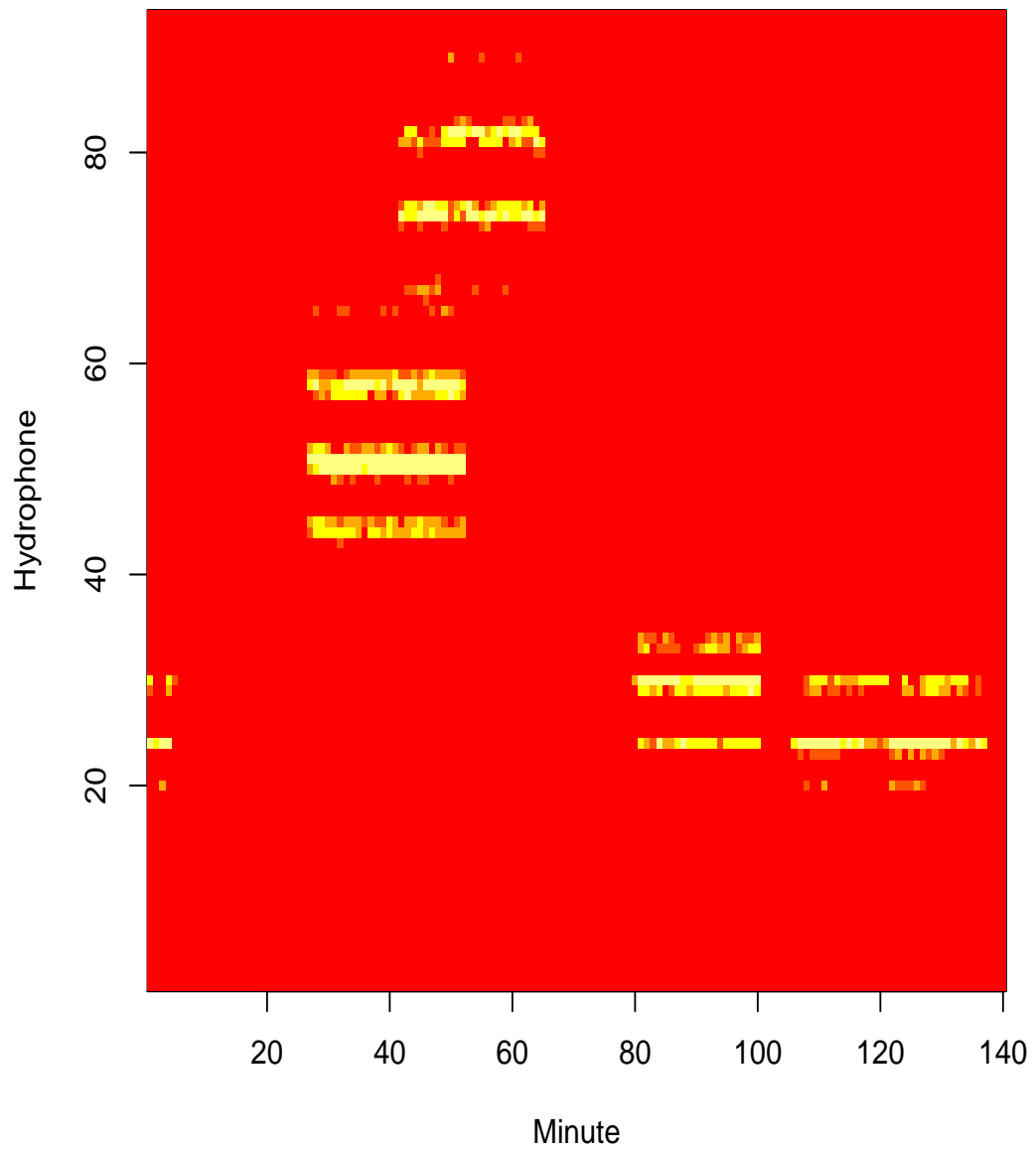


Figure 16: An image plot where the number of detected click counts per minute and hydrophone for the running example is shown.

- Any other variable that might be relevant

This function is shown below:

```
> simulate.cc<-function(grN=3,grS=4.1,dens=gam2.mean.cc.by.hyd,denstype="gam",
+ minutes=130,hyds=hyd,waR=4000,sA=150,sxyG=20,sxyA=4,
+ plot.type=3,relhyd.rad=7000,fname){
+ #Written by: Tiago Marques on 12th May 2008 and last updated on 19th May 2008
+ #Purpose: wrapper to run at once all the code required to simulate
+ #          click count vectors (per minute per hydrophone)
+ #INPUTS:
+ #grN:          number of groups
+ #grS:          mean group size (by default 4.1)
+ #dens:         a gam model defining a density surface. By default the estimation
+ #denstype:     if not "gam", uses a uniform density rather than the object
+ #minutes:      the number of minutes we want to simulate click counts for
+ #hyds:         an object with as many rows as hydrophones and at least a x and y
+ #              hydrophones coordinates
+ #waR:          the radius around the hydrophones over which animals are generated
+ #sA:           the standard deviation from the bivariate normal used to generate
+ #              coordinates
+ #sxyG:         the standard deviation for horizontal group displacement per minute
+ #sxyA:         the standard deviation for horizontal animal displacement
+ #              (around a mean animal coordinate) per minute
+ #plot.type:    if 0, no plot is produced, if 1, just the cc image plot, if 2,
+ #              if 3, also the group location and sizes plot
+ #relhyd.rad:   the maximum distance at which clicks are considered to be detected
+ #fname:        the output file names
+ #Returns: an object of class matrix with dimensions (number of minutes) * (number of
+ #          containing the click counts per minute per hydrophone
+ #          3 files are produced: 1 with the relevant click properties for each minute,
+ #          1 with an indexing system (start and end of the period of activity for each
+ #          active hydrophone-dive combinations)
+ #          1 R workspace with the state vector and the click count vectors
+ #          (useful for later plotting without running the function again)
+ #####
+ #DETAILS:
+ #  NOTE 1: currently, does not allow to change the default input parameters
```

```

+ #   fundamental functions related to dive details, namely:
+ #       1. get.state.vector
+ #       2. get.click.times
+ #       3. split.V
+ #       4. get.depth.per.click
+ #   NOTE 2 : the detection function used cannot be costumized
+ #####
+ #defining the working area
+ wa<-convexhull.xy(x=hyds$x,y=hyds$y)
+ #and extend it 4000 m out of this convex hull
+ work.area<-dilation.owin(w=wa,r=waR)
+ #creating the groups x,y coordinates
+ sim<-generate.group.coordinates(n=grN,dens=dens,dens.type=denstype,within=w)
+ #then assign group sizes to it
+ sim<-add.group.sizes(pop=sim,mean.cs=grS)
+ #generating the animals coordinates
+ sim.animals<-generate.animal.coordinates(sim,stdv=sA)
+ #get the xy coordinates, per group per minute
+ sim.xy.per.group<-get.xy.per.group(sim,minutes,sd=sxyG)
+ #get the xy coordinates, per animal per minute
+ sim.xy.per.animal<-get.xy.per.animal(sim.animals,sim.xy.per.group,minutes,s)
+ #obtain the state vector
+ state.vector.sim<-get.state.vector(sim,lim.time=minutes)
+ #rearrange state vector info
+ Vstate.sim<-get.Vstate(state.vector.sim)
+ #get state vector by animal
+ V.per.animal.sim<-get.Vstate.per.animal(Vstate.sim,sim.animals)
+ #get click times
+ click.times.sim<-get.click.times(V.per.animal.sim,rec.period=minutes)
+ #gets sub states within vocalizing state
+ split.V.sim<-split.V(V.per.animal.sim)
+ #gets depth per click
+ depths.sim<-get.depth.per.click(V.per.animal.sim,click.times.sim,split.V.sim)
+ #this cleans click times for dives outside the recording period
+ click.times.sim<-clean.click.times(click.times.sim,minutes)
+ #gets headings per click
+ headings.sim<-get.headings(click.times.sim)
+ #gets pitch per click

```

```

+ pitches.sim<-get.pitches(click.times.sim)
+ #get relevant hyds
+ sim.rel.hyds<-get.relevant.hyds(sim.xy.per.animal,hyds,radius=relhyd.rad)
+ #get horizontal angle per animal hyd and minute
+ sim.angle.per.animal.hyd.min<-get.angle.per.animal.hyd.min(minutes=minutes,
+ #get all relevant vars
+ #if folder for storage does not exist, create it
+ dirb<-"Rfiles"
+ dir.create(dirb,showWarnings=F)
+ dir.name<-paste(dirb,"/",fname,sep="")
+ dir.create(dir.name,showWarnings=F)
+ WD <- getwd()
+ setwd(dir.name)
+ sim.cc.per.minute.per.hyd<-get.cc(sim.xy.per.animal,sim.angle.per.animal.hyd,
+ headings.sim,depths.sim,pitches.sim,hyds,sim.rel.hyds,fname)
+ setwd(WD)
+ #plot the output
+ #if required, plot the state vector
+ if(plot.type>0) {
+ par(mfrow=c(plot.type,1),mar=c(4.5,4.5,1,1))
+ plot.cc(sim.cc.per.minute.per.hyd,breaks=c(0,5,10,20,50,max(sim.cc.per.minu
+ })
+ if(plot.type>1) plot.state.vector(state.vector.sim,minutes)
+ if(plot.type>2) plot.groups(sim,hyds)
+ #saving some relevant information
+
+ obj.names<-paste(c("groups.", "states."),fname,sep="")
+ assign(eval(obj.names[1]),sim)
+ assign(eval(obj.names[2]),state.vector.sim)
+ save(list=obj.names,file=paste(dir.name,"/",fname,".Rdata",sep=""))
+ #####
+ return(sim.cc.per.minute.per.hyd)
+ }

```

Which can be run as an example

```

> #
> set.seed(123)

```

```

> test.sim.123<-simulate.cc(plot.type=3,fname="seed123")
> #set.seed(123)
> #test.sim.123.grN6.min80<-simulate.cc(grN=6,plot.type=3,minutes=80,fname="s
> #set.seed(123)
> #test.sim.123.grN7.min180<-simulate.cc(grN=7,plot.type=3,minutes=180,fname=
> #set.seed(123)
> #test.sim.123.grN12.min140<-simulate.cc(plot.type=3,grN=12,minutes=140,fname

```

The click count per minute per hydrophone for this example is shown in figure 18 (this object, as produces by `simulate.cc`, can be plotted using `plot.cc`).

Note that the information in the groups and the `state.vector` from `test.sim.123` is available as a separate workspace, which can be loaded simply by using e.g. `load("Rfiles/seed123.Rdata")`. These objects can then be plotted easily using functions `plot.groups` and `plot.state.vector`.

2.8 Reading binary files back in

Function `get.cc` produces a binary file with all the click-hydrophone events, and all the corresponding relevant variables, in case one needs to check the original raw simulated data.

The following function allows one to read back into R the created file, or subsets of it matching some selection criteria

```

> read.res.file<-function(fname,index.file,hyd=0,an=0,gr=0,dv=0){
+ #Written by: Tiago Marques on 20th May 2008 and last updated on 20th May 2008
+ #Purpose: To read a file (or part of a file) created by function get.cc
+ #Inputs:
+ #       fname - the name of the file to read from
+ #       index.file - the text file that contains a description of which info
+ #                   which rows of file fname
+ #       hyd,an,gr,dv - the indexes of which hydrophone, animal, group and d
+ #                   (by default hyd=an=gr=dv=0 - the entire file is read)
+ #                   Currently one can select only 1 of each (hydrophone
+ #                   and omitting some of these but not all uses the non c
+ #Details: Function get.cc creates a binary file with all the hydrophone-click
+ #of a given simulation scenario, and the index.file describes which lines ha
+ #This function allows to retrieve that information

```

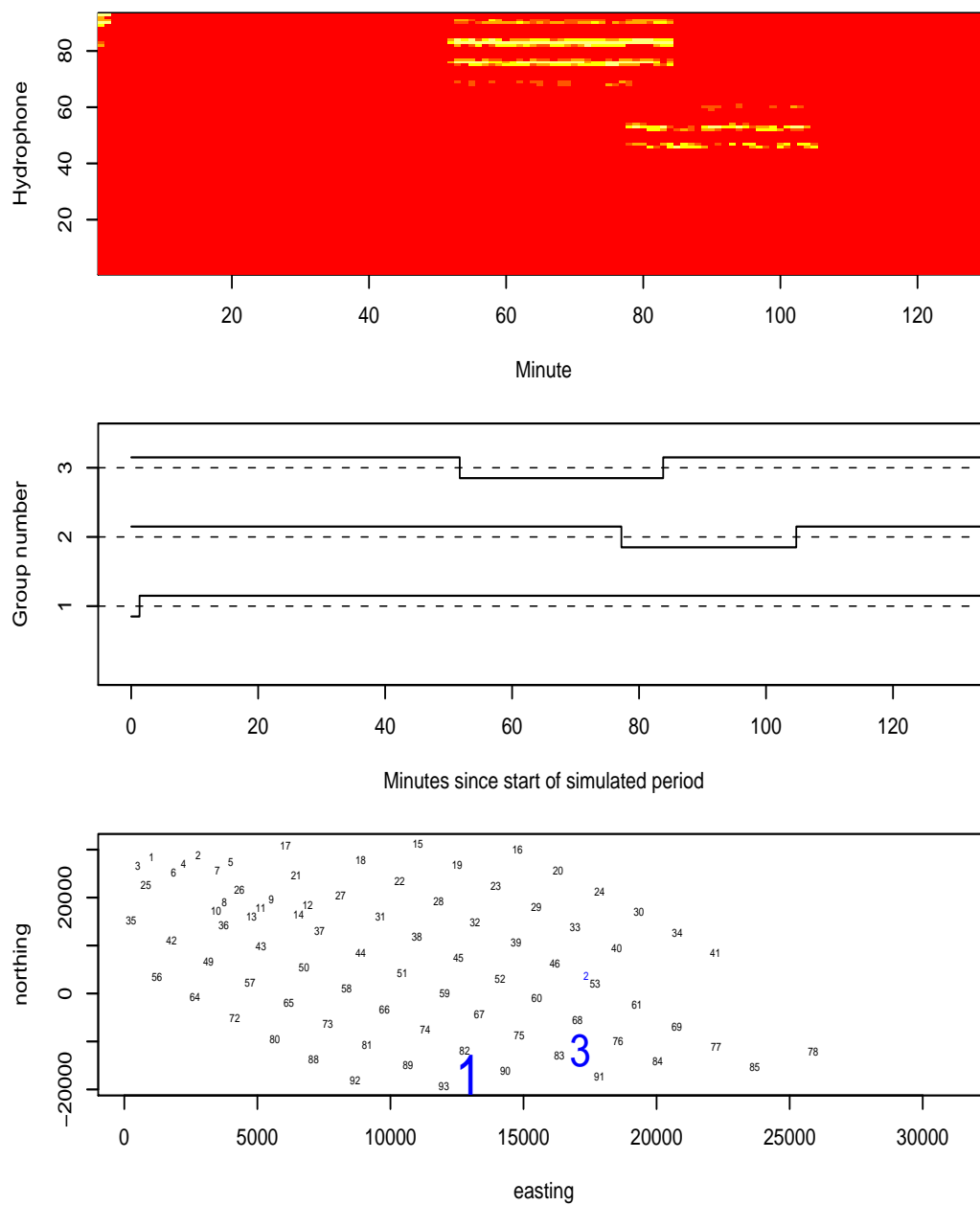



Figure 17: An image plot where the number of detected click counts per minute and hydrophone, for the example of running `simulate.cc` stored in `test.sim.123`.

```

+ #Returns: an object of class data.frame with variable dimensions, depending
+ #####
+ #Read the indexing information in
+ index<-read.table(index.file,header=T)
+ #opening the file to read
+ test.file<-file(description=fname,open="rb")
+ #creating the object to hold the data
+ alldata<-matrix(NA,nrow=1,ncol=19)
+ #if too many selection arguments are given
+ if(max(c(length(hyd),length(an),length(gr),length(dv)))>1) {
+   print("Warning: At most, only 1 hyd, 1 animal, 1 dive and 1 group can be
+   stop()})
+   #get selection indexes
+   #(i.e. T if row in index.file matches selection criteria or if crit
+   indhyd<-(index$hyd==hyd | hyd==0)
+   indan<-(index$animal==an | an==0)
+   indgr<-(index$group==gr | gr==0)
+   inddv<-(index$dive==dv | dv==0)
+   index<-index[indhyd & indan & indgr & inddv,]
+   if(nrow(index)==0) {
+     print("Warning: Selection criteria used returns no data")
+     stop()})
+   for(j in 1:nrow(index)) {#for each row in the indexing file
+     #position the reading position
+     seek(test.file,where=(4*(index$start.row[j]-1)*19))
+     #read the corresponding data
+     temp<-matrix(readBin(test.file,"numeric",n=index$clicks[j]*19,size=
+     #rbind it to previous data
+     alldata<-rbind(alldata,temp)})
+ close(test.file)
+ alldata<-as.data.frame(alldata[-1,])
+ name<-c("ctime","gr","an","x","y","z","heading","pitch","angle","hyd","hx",
+ names(alldata)<-name
+ return(alldata)
+ }

```

The following command would read back in all the information from the file “seed123” (using ”seed123.file.index.txt” as a guide for what to read back

in)

```
read.res.file("seed123","seed123.file.index.txt")
```

As an additional example, the following command would read only click-hydrophone events involving hydrophone 82 and animal 2.

```
read.res.file("seed123","seed123.file.index.txt",hyd=82,an=2)
```

3 Overview

Due to the large number of functions used and objects created, in this section we review (see also figure refoverview), through the running example, the key functions used and the objects created by them, object details, and brief explanations about the information contained in each object:

- function `generate.group.coordinates` was used to create `test4`, which was then modified by `add.group.sizes`. `test4` is an object of class `ppp` which contains the number of groups (`n`), the x (`x`) and y (`y`) coordinates of the center of the group (at minute 0) and the group sizes (`marks`).
- function `generate.animal.coordinates` was used to create `test4.animals`, which is an object of class `data.frame`. It contains the the x (`x`) and y (`y`) coordinates of the position of each animal (at minute 0) and a group indicator (`sindex`).
- function `get.xy.per.group` was used to create `test4.xy.per.group`, which is an object of class `array`. The subset `test4.xy.per.group[j,1:2,k]` contains the x, y coordinates for the center of group k in minute j (in the running example, $j=1,2,\dots,140$ and $k=1,2,3,4$).
- function `get.xy.per.animal` was used to create `test4.xy.per.animal`, which is an object of class `array`. The subset `test4.xy.per.animal[j,1:2,i]` contains the x, y coordinates for the center of animal i in minute j (in the running example, $j=1,2,\dots,140$ and $i=1,2,\dots,14$).
- function `get.state.vector` was used to create `state.vector.test4`, which is an object of class `list`. Its element k contains the vocal states and start times of each vocal state (V: vocalizing or S: silent). The function `plot.state.vector` is useful to plot this type of object.

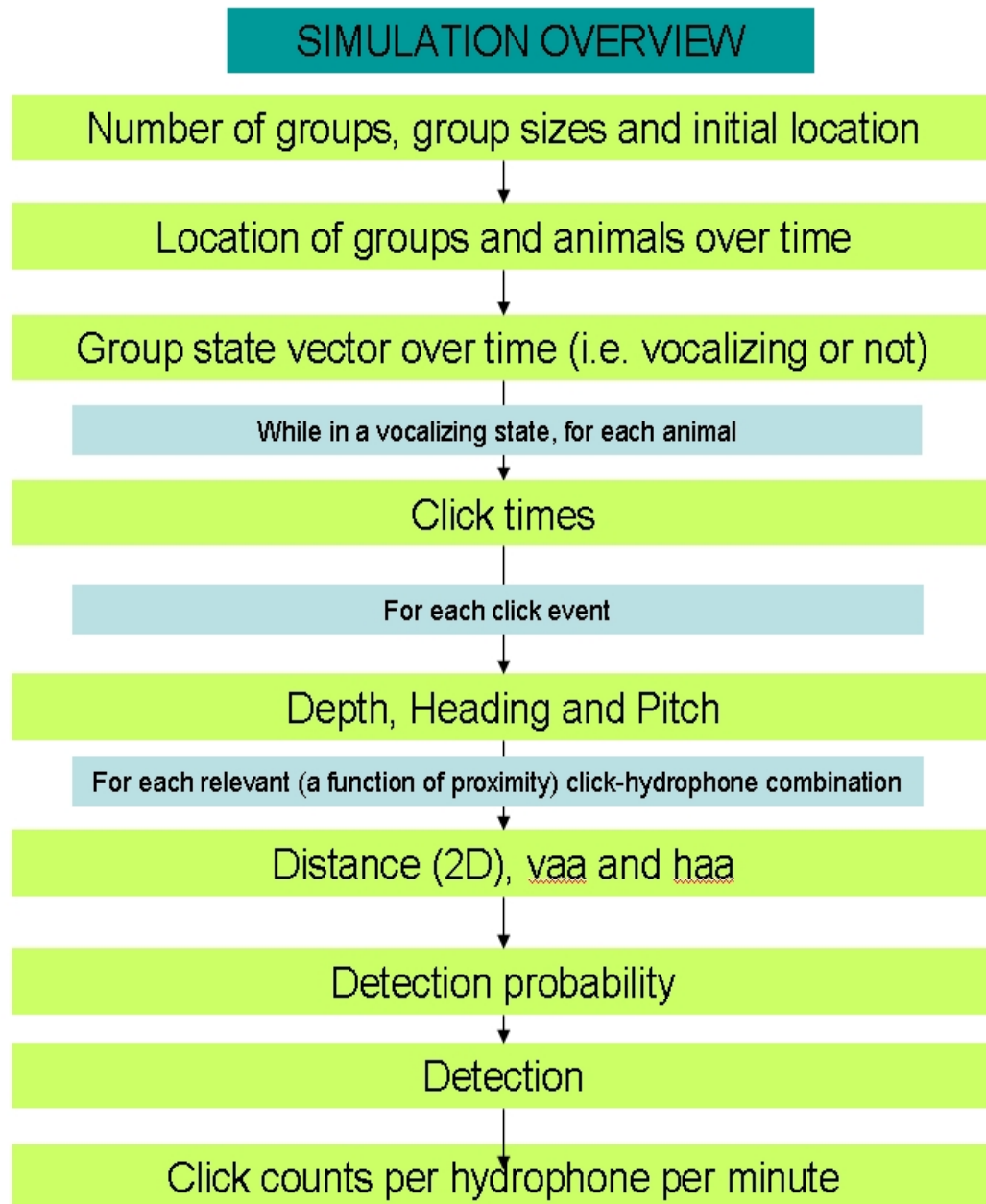


Figure 18: An overview of the simulation process.

- function `get.Vstate` was used to create `Vstate.test4`, using the information stored in `state.vector.test4`. This `Vstate.test4` is an object of class `data.frame`, which contains start (`t.start`) and end (`t.end`) times (in minutes since start) of the vocal states of each group (`group`).
- function `get.Vstate.per.animal` was used to create an object of class `data.frame` named `V.per.animal.test4`. It contains start (`t.start`) and end (`t.end`) times (in minutes since start) of the vocal states of each animal (`group`), the length of the vocalizing period (`V`), plus a number of relevant columns (`sindex,x,y,animal`) with self explanatory names.
- function `get.click.times` was used to create `click.times.test4`, which is an object of class `list`. It has length $L_1 = L_2 + 3$ (i.e. L_1 the number of dives and animals combinations plus 3; these last 3 elements are used for storage of indicator values, namely the group, animal and animal/dive indicator). Hence, element z ($z = 1, 2, \dots, L_1 - 3$) contains the click times for the animal-dive combination z . In the running example $L_1 = L_2 + 3 = 17 + 3 = 20$.
- function `split.V` was used to create `split.V.test4`, which is an object of class `list`. It has length L_2 equal to the number of dives and animals combinations. Element z ($z = 1, 2, \dots, L_2$) is a vector of size 4, which contains respectively (in position 1) the start and (in position 2) end time of the vocal period and (in position 3) the start depth of the vocal period, as well as (in position 4) the mean foraging depth, for the z^{th} dive-animal combination.
- function `get.depth.per.click` was used to create `depths.test4`, which is an object of class `list`. It has length L_2 equal to the number of dives and animals combinations (here, 17). Element z ($z = 1, 2, \dots, L_2$) is a vector of variable size, which contains the depth at which each click was produced for the z^{th} dive-animal combination.
- function `get.headings` was used to create `headings.test4`, which is an object of class `list`. It has length L_1 . Hence, element z ($z = 1, 2, \dots, L_2$) contains the headings for each click for the animal-dive combination z . As before the last 3 elements are used for storage of indicator values, namely the group, animal and animal/dive indicator.

- function `get.pitches` was used to create `pitches.test4`, which is an object of class `list`. It has length L_1 . Hence, element z ($z = 1, 2, \dots, L_2$) contains the pitches for each click for the animal-dive combination z . As before the last 3 elements are used for storage of indicator values, namely the group, animal and animal/dive indicator.
- function `get.relevant.hyds` was used to create `test4.rel.hyds`, which is an object of class `matrix`. It has as many columns as there are animals and as many rows as there are hydrophones, filled with T's and F's, where a T corresponds to a hydrophone for which there was at least 1 click produced by the corresponding animal which is closer than some radius (in the running example, 7km).
- function `get.angle.per.animal.hyd.min` was used to create an object of class `array` named `test4.angle.per.animal.hyd.min`. The subset `test4.angle.per.animal.hyd.min[j,i,h]` contains the hydrophone-animal angle for the animal i in minute j and hydrophone h (in the running example, $j=1,2,\dots,140$; $i=1,2,\dots,14$ and $h=1,2,\dots,93$).
- function `get.cc` was used to create an object of class `matrix` named `test4.cc.per.minute.per.hyd`. It contains the (detected) click counts per hydrophone per minute. This function also creates a file which contains all the relevant variables for all relevant click-hydrophone combinations (i.e. within a pre-defined radius, here 7km), as well as a second file which indexes the information in the previous file.

Finally, `simulate.cc` is wrapper function for all the above functions, executing a full simulation exercise given relevant input parameters. The output of this function is the same as from function `get.cc`: a matrix with click counts per hydrophone per minute, as well as the 2 previously mentioned files. Relevant plots can also be produced.

4 Known issues, shortcomings, work to do, etc.

There are a number of potential issues worth looking at. A non-exhaustive list is here for reference, so that we can work on it as time gets available (this

list is a living beast, that gets things added and removed (once done) as we go along):

- Code improvements
 - Properly comment all functions;
 - Run code checks;
 - The way the `gam` object that contains the detection function is added to the workspace is cumbersome;
 - Function `get.dive.pitches` always generates pitches as if a full dive is being simulated, but this is not the case for dives which had already started when the simulation starts.
- Making it closer to reality
 - Function `get.dive.pitches` is still based on the material found on Gillespie (2006), and the use of `satbuc1` might be desirable;
 - The simulation of *ICI* does not allow for silent periods, which sometimes happened for brief periods in the DTag data during *V*;
 - In general, the information in the DTag sent by Tyack has not been incorporated, and this could be done at multiple places; In particular, a better way to simulate dives, as well as movement in the horizontal dimension, would be desirable;
 - Try to add randomness in vocal periods of animals within groups and relevant depth limits, which are constant at the moment;
 - Further thinking about simulation of correlated values through time might be useful;
 - Need a detection function based on more data (more dives, wider range of predictors, etc).
 - The capacity to include other study areas (rather than sticking with AUTEK) would be a plus.
- Data visualization
 - In terms of data visualization, both for simulated data but also for analysis of real data, it would be helpful to have a tool that

would allow screening of click counts per hydrophone over time and space. In figure 19 we present an eventual way of visualizing such information, with the top panel focussing on the temporal component, and having a slider that determines which spatial component is shown in the bottom panel. This has not been implemented.

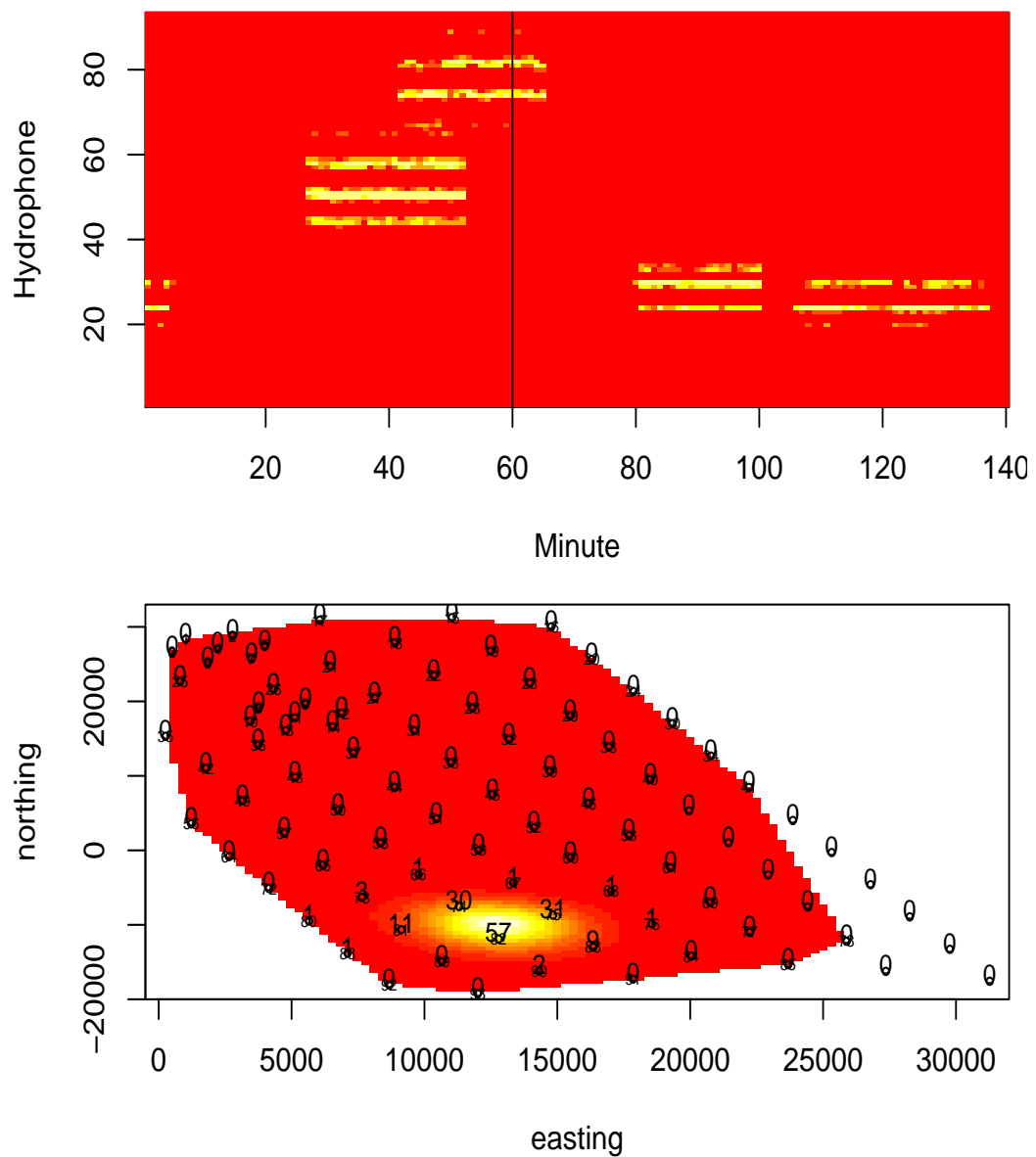


Figure 19: An hypothetical visualization tool. When the top panel (focussing on the time dimension) ruler is moved, the bottom panel shows the corresponding information in a spatially explicit way.

References

- Baird, R. W., Webster, D. L., Schorr, G. S., Mcsweeney, D. J., and Barlow, J. (2008). Diel variation in beaked whale diving behavior. *Marine Mammal Science*, **24**, 630–642.
- Claridge, D. E. (2006). *Fine-scale distribution and habitat selection of beaked whales*. Master’s thesis, University of Aberdeen, Scotland, U.K.
- Gillespie, D. (2006). Simulating sperm whale dives.
- Madsen, P. T., Johnson, M., de Soto, N. A., Zimmer, W. M. X., and Tyack, P. (2005). Biosonar performance of foraging beaked whales (*Mesoplodon densirostris*). *The Journal of Experimental Biology*, **208**, 181–194.
- Marques, T. A. and Thomas, L. (2008a). Further analysis of the hydrophone+DTag data. Technical report, DECAF internal report.
- Marques, T. A. and Thomas, L. (2008b). A further look at extreme residuals - building on “click count eda report”. Technical report, DECAF internal report.
- Marques, T. A. and Thomas, L. (2008c). Rationale for the simulation of plausible vectors of detected click counts. Technical report, DECAF internal report.
- Marques, T. A. and Thomas, L. (2008d). Simulating correlated values over time. Technical report, DECAF internal report.
- Marques, T. A. and Thomas, L. (2008e). Some ideas about simulating beaked whale dives. Technical report, DECAF internal report.
- Moretti, D., DiMarzio, N., Morrissey, R., Ward, J., and Jarvis, S. (2006). Estimating the density of Blainville’s beaked whale (*Mesoplodon densirostris*) in the Tongue of the Ocean (TOTO) using passive acoustics. In *Proceedings of the Oceans’06 MTS/IEEE-Boston*, Boston, MA.
- Tyack, P. L., Johnson, M., Soto, N. A., Sturlese, A., and Madsen, P. T. (2006). Extreme diving of beaked whales. *Journal of Experimental Biology*, **209**(21), 4238–4253.

Modelling group size as a function of autogrouper outputs

LATTE WORKING DOCUMENT

Tiago A. Marques, Jessica Shaffer & Len Thomas

Centre for Research into Ecological and Environmental Modelling
The Observatory, University of St Andrews, St Andrews, KY16 9LZ, Scotland

Version's date: September 25, 2013

Contents

1	Introduction	1
2	Modeling approach	2
3	Discussion	10
	References	13

1 Introduction

Autogrouper is a routine which works over timings of beaked whale click detection reports to associate clicks within hydrophones into click trains, and subsequently associates click trains across hydrophones to define vocal groups. Each vocal group detected corresponds to a beaked whale deep foraging dive. Associated with each of these automatically derived vocal groups a number of summary statistics can be readily obtained, as the total number of clicks or the total number of hydrophones. A full description of those statistics available here is in the next section.

The autogrouper is an automated way to implement the routine described in Moretti *et al.* (2010) to identify dives, and these dives have already been

used as the units of analysis in a number of reasearch efforts (e.g. McCarthy *et al.*, 2011). More details about autogrouper and its evaluation can be found in a couple of documents circulated by JS, namely “Autogrouper Evaluation LATTE rev1.docx” and “Correlation of Group Size to Click Counts at AUTECH.doc”.

Group size is an important factor in density estimation studies, and characterizing the group size distribution over space and time at AUTECH might bring additional insights into the effect of sonar use on these animals. It seems natural that the acoustical footprint of a group is dependent of its group size, and this has in fact been shown for a reduced number of groups of known size (DiMarzio *et al.*, 2008).

In this report we analyze a data set of dives associated with groups for which group size was assessed by visual observers, allowing one to model group size as a function of the acoustical footprint of the groups on the surrounding AUTECH hydrophones.

This might be used as a basis for parameterizing the simulation engine required for LATTE, by modeling the estimated group sizes over space and time. Additionally, if this modelling exercise is successful it might be used to estimate density at AUTECH by exhaustive counting of animals present on the range over time. As groups diving on the range are assumed to be detected with certainty, this allows one to know, in a probabilistic sense at least, in almost but not quite real time, how many animals are echolocating and present within the range at any moment in time.

2 Modeling approach

The data was imported into R directly from the .xls file “LATTEgroupclick-count_version2.xls”. A number of potential covariates to model group size are available:

1. the number of hydrophones at which group i was detected, K_i ($K_i = 1, 2, \dots$)
2. the number of clicks from group i detected at hydrophone k , $c_{i,k}$, from which the total number of clicks detected for group i (N_i) can be obtained summing over the K_i hydrophones, i.e. $N_i = \sum_{k=1}^{K_i} c_{i,k}$
3. the mean number of clicks detected per hydrophone for animal i , $\frac{N_i}{K_i}$

4. the duration of the clicking period per hydrophone, from which the total clicking duration, d_i can also be obtained
5. the maximum click count per hydrophone for group $i = \max(c_{i,1}, c_{i,2}, \dots, c_{i,K_i})$
6. a pooled click rate, $r_i = \frac{N_i}{d_i}$

The cluster size data available, as well as its relationship with potential covariates, is shown in figure 1. This is a small data set, with only 43 groups visually confirmed. Note in particular that for of these groups (tagged animals) were not necessarily independent, but correspond to successive dives of the same group, but we ignore that issue here for the moment. The independence assumption might actually not be unrealistic, as each group's deep dive is likely independent from the previous one in terms of its acoustical footprint, conditional on the group size.

The distribution of group sizes is, by definition of what is a group, discrete. Therefore a count model should be used, like the Poisson or negative binomial. However, with such a low mean as observed here (mean=2.7, sd=0.98) these models should have a considerable number of 0's, yet a group of zero is not a group! This might be addressed in at least one of two ways:

- consider a zero-truncated model. <http://www.ats.ucla.edu/stat/r/dae/ztp.htm> describes the use of a zero-truncated glm function using package `VGAM`, but apparently no significance values for terms, AIC's or other simple model selection tools seem to be available. On top of things, loading this packages causes unpredictable behaviour in `mgcv`;
- consider modeling $Y = X - 1$, where X is the actual group size, as a poisson or negative binomial.

Simply for pragmatic reasons, we opt for the latter here, but note that the former might be interesting to explore further. Using a manual stepwise backward approach with AIC and GVC as guidance we trim the model using all available covariates until only significant terms remain.

```
> library(mgcv)
> model1=gam(cs0~s(meancount)+s(cdur)+s(nhyd)+s(nclicks,k=4)+s(crate),
+ data=d4reg,family=poisson)
> #drop least important covariate
```

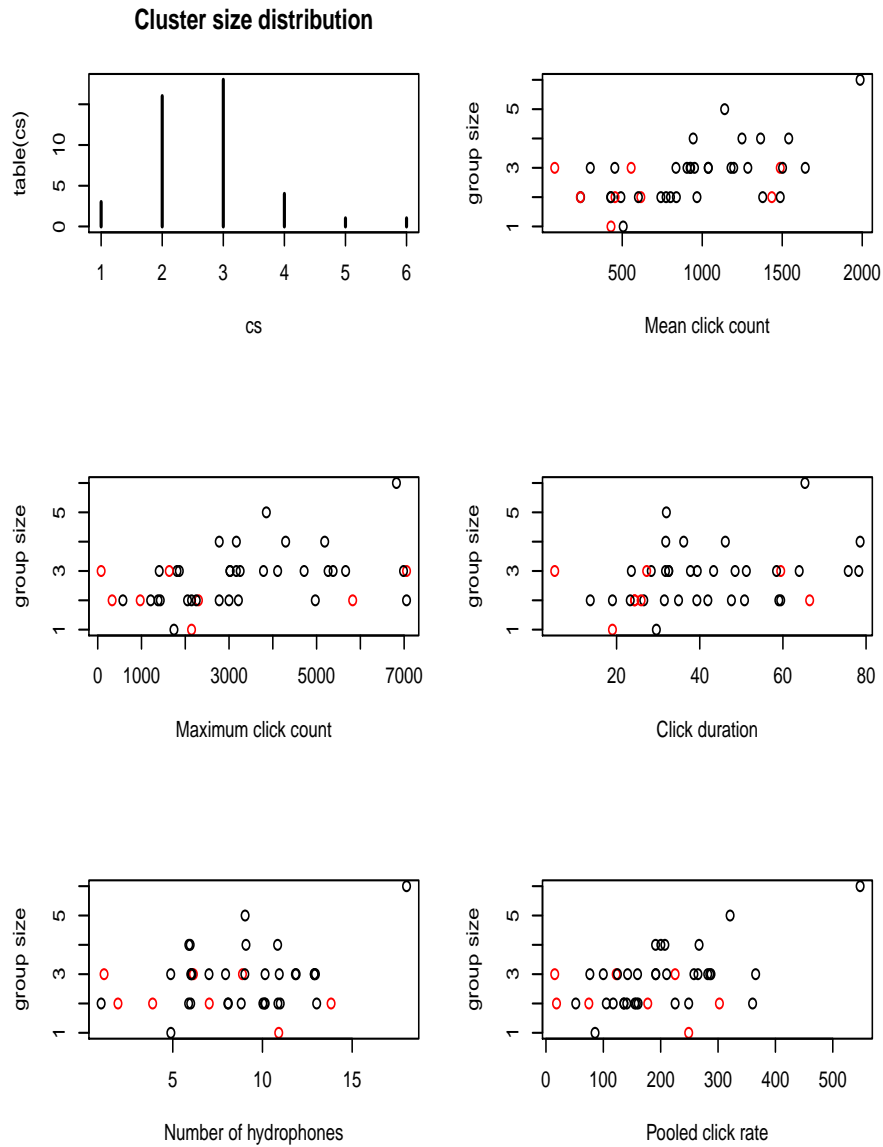


Figure 1: Cluster size distribution and scatter plots of group size as a function of 5 available explanatory covariates. Groups without maximum certainty in visual to acoustic matching are highlighted in red.

```

> model2=gam(cs0~s(meancount)+s(cdur)+s(nhyd)+s(crate),data=d4reg,family=poisson)
> #drop 2nd least important covariate
> model3=gam(cs0~s(cdur)+s(nhyd)+s(crate),data=d4reg,family=poisson)
> #drop 3rd least important covariate
> model4=gam(cs0~s(nhyd)+s(crate),data=d4reg,family=poisson)
> #if you redo the same procedure, without crate in the initial model,
> #you end up with a different best model, namely model5
> model5=gam(cs0~s(meancount),data=d4reg,family=poisson)
> #I tried to see what a GLM model can do
> #but the AIC is terrible here...
> model5g=gam(cs0~s(meancount),data=d4reg)
> model5g.glm=glm(cs0~meancount,data=d4reg)
> #hummm, curious, this is the same model as the gam model now
> #but this was not the case at all with a Gaussian response
> #where the gam was clearly favoured
> #I wonder why the big difference
> model5.glm=glm(cs0~meancount,family=poisson,data=d4reg)
> #and by lowering the degrees of freedom associated with the smoother
> #the AIC also becomes considerably worse
> model5.k4=gam(cs0~s(meancount,k=4),data=d4reg,family=poisson)
> #just to check a really bad model
> model6=gam(cs0~s(maxcount),data=d4reg,family=poisson)
> #nonsense model just for comparison
> model7=gam(cs0~s(rnorm(43)),data=d4reg,family=poisson)
> #
> #model8=gam(cs0~s(cdur)+s(crate),data=d4reg,family=poisson)

```

We can compare the AIC of all models (Table 1). Note in particular that the gam and glm provide exactly the same fit, i.e. the gam is not required¹

The best model of those tried according to AIC is `model5` the one where group size is predicted as a function of a single variable, the mean number

¹It is interesting to note that a previous run of this same model but with the response erroneously defined as Gaussian meant that the gam smooth term was deemed required. It is unclear why this would be the case, depending on the family used the gam being more or less likely to require the smooth terms. On the other hand, does it make any sense to use a measure as AIC to choose the distribution to use? Seems not sensible here (in fact the Gaussian would be selected, and yet we do that all the time when say choosing across candidate models for a detection function. Comes to justify once more the advice that one should not try models which are a priori known to be false... but still.

	df	AIC	UBRE	dev	R2
model1	6.00	124.86	-0.37	0.42	0.49
model2	5.00	122.90	-0.42	0.42	0.51
model3	4.00	121.46	-0.45	0.40	0.48
model4	3.00	122.39	-0.43	0.29	0.37
model5	2.00	120.62	-0.47	0.28	0.32
model5.k4	2.00	120.62	-0.47	0.28	0.32
model5.glm	2.00	120.62		0.28	
model5g	7.13	100.94	0.60	0.31	0.48
model6	2.00	124.00	-0.39	0.15	0.14
model7	2.43	127.42	-0.31	0.05	0.02

Table 1: AIC comparison for considered models.

of clicks per hydrophone. The model is shown in figure 2. We proceed inferences with this model, but note that the second best model was `model3`, which surprisingly does not include the single variable in `model5`. This model considers as explanatory variables the number of hydrophones, the click rate and the total click duration. The variables included in this model actually make some sense from an explanatory point of view, and it has a larger adjusted R^2 and a higher percentage of the deviance explained. However, the negative trend in group size associated with the increase in the number of hydrophones was unexpected.

```
> summary(model3)
```

```
Family: poisson
```

```
Link function: log
```

```
Formula:
```

```
cs0 ~ s(cdur) + s(nhyd) + s(crate)
```

```
Parametric coefficients:
```

```
              Estimate Std. Error z value Pr(>|z|)
(Intercept)   0.4595      0.1248   3.682 0.000231 ***
```

```
---
```

```
Signif. codes:  0 '***' 0.001 '**' 0.01 '*' 0.05 '.' 0.1 ' ' 1
```



```

Approximate significance of smooth terms:
              edf Ref.df Chi.sq p-value
s(cdur)      1      1  2.898 0.08868 .
s(nhyd)      1      1  3.916 0.04784 *
s(crate)     1      1  7.537 0.00604 **
---
Signif. codes:  0 '***' 0.001 '**' 0.01 '*' 0.05 '.' 0.1 ' ' 1

R-sq.(adj) =  0.484   Deviance explained =   40%
UBRE score = -0.44885   Scale est. = 1         n = 43

> summary(model5)

Family: poisson
Link function: log

Formula:
cs0 ~ s(meancount)

Parametric coefficients:
              Estimate Std. Error z value Pr(>|z|)
(Intercept)   0.4799      0.1226   3.913 9.11e-05 ***
---
Signif. codes:  0 '***' 0.001 '**' 0.01 '*' 0.05 '.' 0.1 ' ' 1

Approximate significance of smooth terms:
              edf Ref.df Chi.sq p-value
s(meancount)  1      1  7.404 0.00651 **
---
Signif. codes:  0 '***' 0.001 '**' 0.01 '*' 0.05 '.' 0.1 ' ' 1

R-sq.(adj) =  0.324   Deviance explained =   28%
UBRE score = -0.46847   Scale est. = 1         n = 43

```

The model explains of 27.99 % of the deviance. We can compare the predicted group sizes² with the observed group sizes (Figure 3). We can get

²Because group sizes have to be integers, we are using as ‘predicted’ the rounded value of the group size, rather than the real (positive) value obtained when predicting from the model

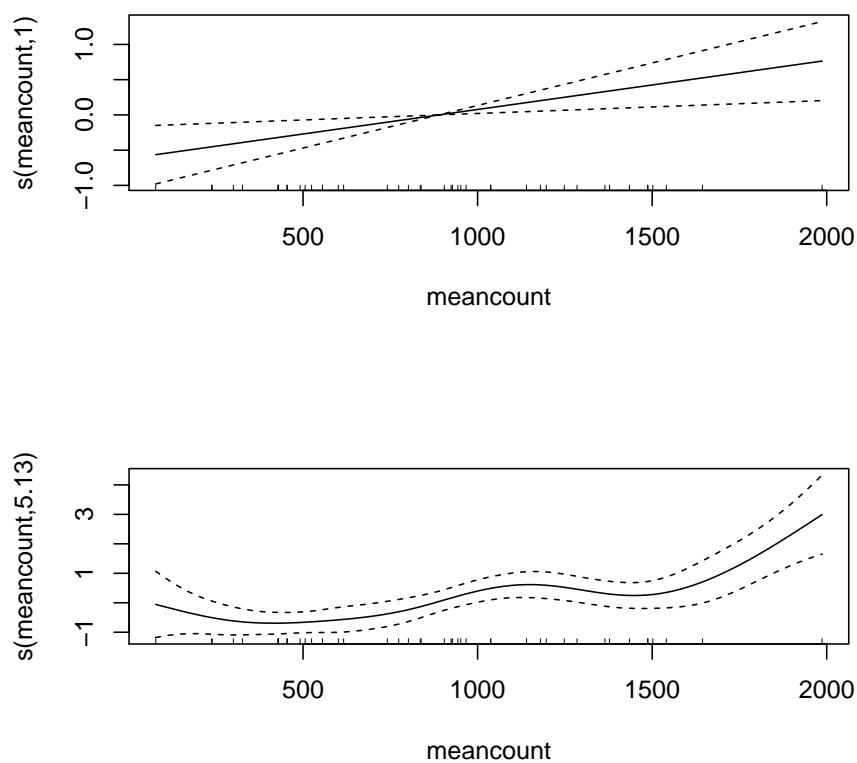


Figure 2: Cluster size as a function of the mean number of clicks per hydrophone. Top row is a model with a poisson response, bottom a gaussian response, for comparison.

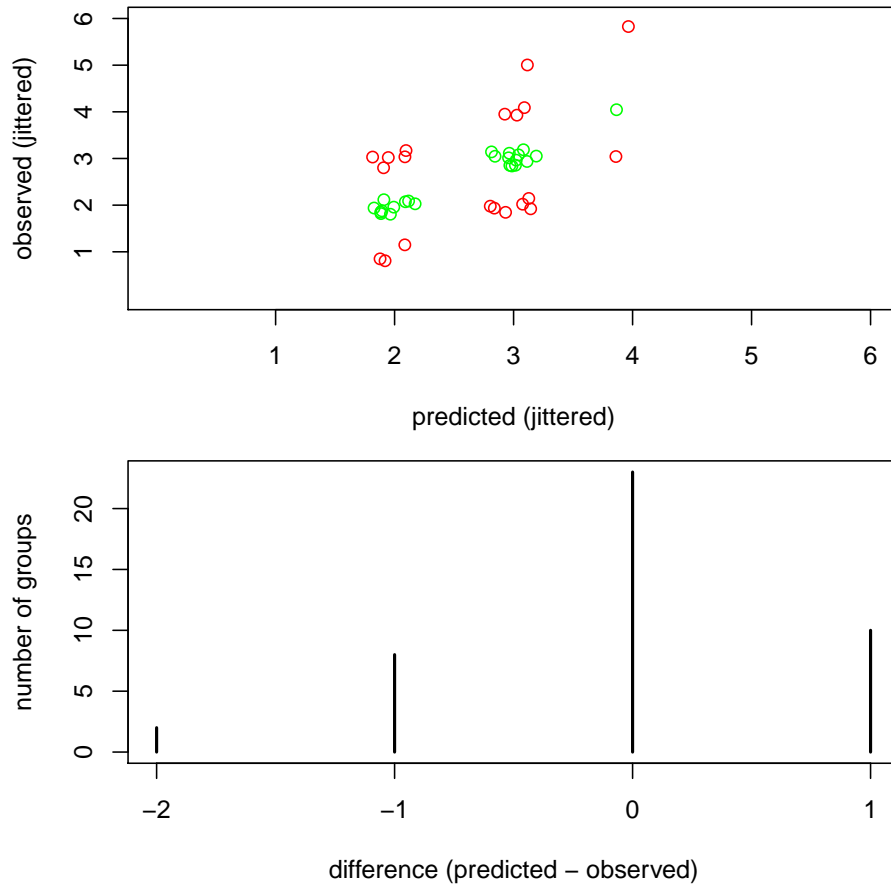


Figure 3: Cluster size as a function of the mean number of clicks per hydrophone. Top row is a model with a poisson response, bottom a gaussian response, for comparison.

the right group size for 23 groups, i.e. 53.49 % of the groups, while only 4.65 % are more than 1 individual off. Note for comparison that using `model3` we obtain the same group size predictions to be more than 1 individual off (4.65 %) as well as the same number of exact group size matches (23).

The residuals of `model5` are shown in figure. There are no major reasons to worry, although large group sizes tend to be underestimated and small group sizes overestimated. This is not unusual with Poisson glms.

We investigated also if a dummy covariate for whether the detection occurred over the whiskey hydrophones, and in particular an interaction of this dummy with the number of hydrophones, help in any way. This could be expected as the number of hydrophones might be related with group size if all hydrophones are equally separated, but this relation might be masked if for animals detected around the whiskey phones that number doubles because hydrophones are more densely distributed³. One can see that, as expected, the number of hydrophones at which a clicks are detected is somewhat higher if whiskey hydrophones are involved (Figure 5). However, the interaction term was not significant and the model not favoured by AIC.

3 Discussion

The best model was `model5`, a gam (note this is essentially a glm, only 1 df used for the smooth) Poisson with mean number of detected clicks as explanatory variables. While even this model can only explain 27.99 % of the deviance, only 4.65 % of the groups have been incorrectly estimated by more than 1 animal. The mean predicted group size using the model was 2.69767441860465, not surprisingly exactly the same as the observed group size. The results of this model might be used as inputs for a number of additional analysis:

- spatio-temporal modelling of group sizes at AUTECH; this can then be used as an input on LATTE's simulation engine;

³An aside regarding modelling: the notion that one should not use interactions without the main effects being present in the model is often reported. Is this an example where it makes sense to have just the interaction term and the number of hydrophones, but not the dummy, as we do not expect that groups on whiskey hydrophones are by themselves any larger or smaller than those elsewhere?

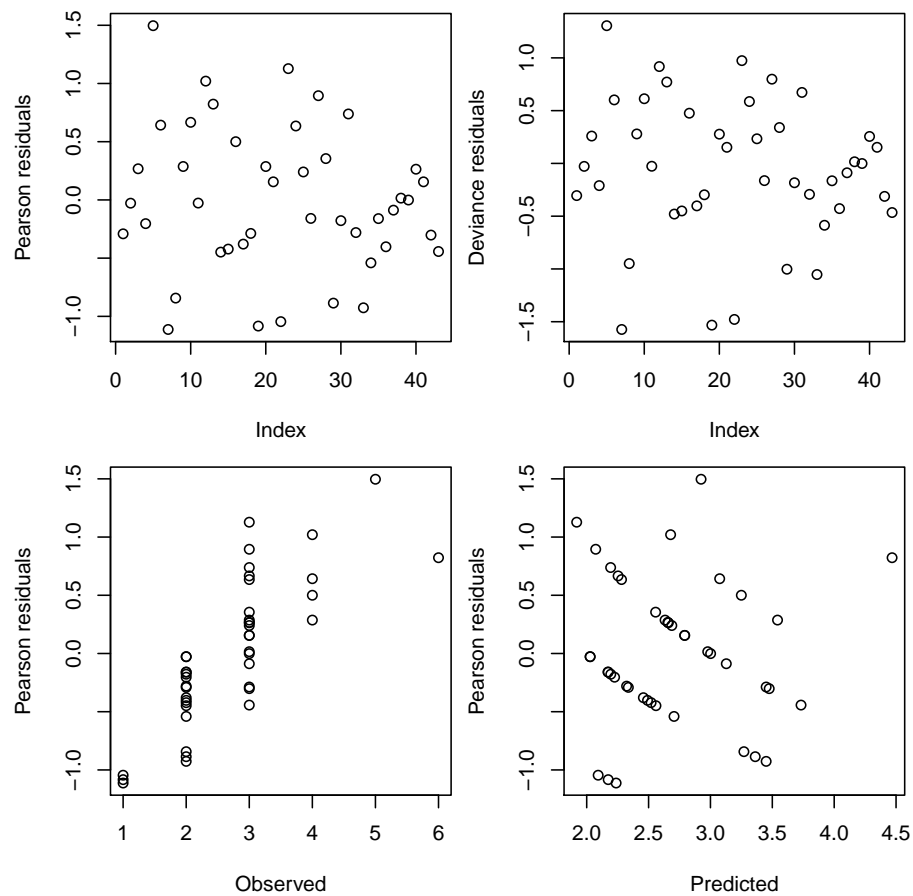


Figure 4: Residuals for the best model (includes only the mean number of clicks detected).

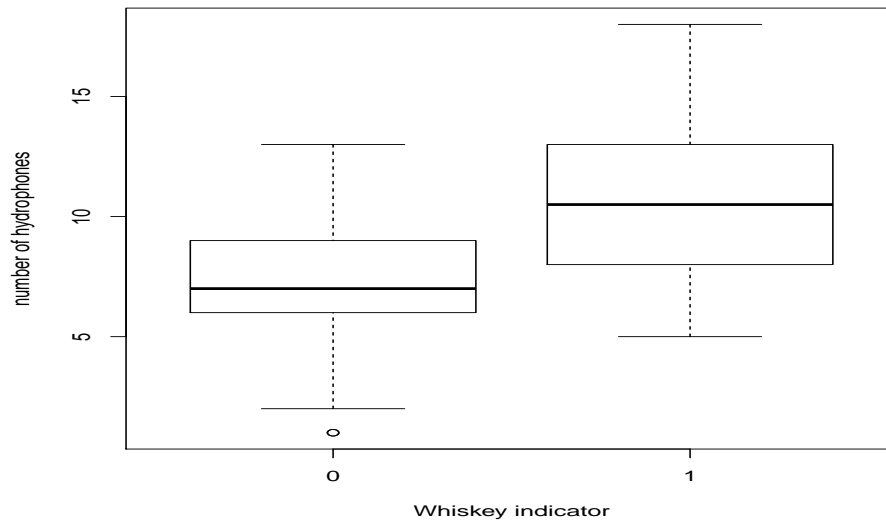


Figure 5: Number of hydrophones as a function of whether whiskey hydrophones were involved (1) or not (0) in the detection.

- automatic density estimation by counting groups on the range at each moment in time. The only multiplier required is the proportion of time a group is vocally active, which we do not have yet. Identifying “quiet” instances on the AUTECH range, when groups can be tracked over multiple dives, to start addressing this multiplier, seems a useful way forward. Tracking groups across dives might be useful regardless as it helps in operations, eg. where to direct a boat to find the group given the acoustical footprint of a dive.

A number of open questions:

- perhaps unexpectedly the number of hydrophones or the total duration of the dive were not strongly related to group size (at least using the best model)
- how much of (1) the unexplained variance or (2) some variables not being considered significant in explaining group size might be related to erroneous visual group size estimation and/or vocal group to visual group incorrect matching?

- are there any more similar data to increase the robustness of this analysis? in particular, what about more groups of single animals? this might also help with model selection.

References

- DiMarzio, N., Moretti, D., Ward, J., Morrissey, R., Jarvis, S., Izzi, A. M., Johnson, M., Tyack, P., and Hansen, A. (2008). Passive acoustic measurement of dive vocal behavior and group size of Blainville’s beaked whale (*Mesoplodon densirostris*) in the Tongue of the Ocean (TOTO). *Canadian Acoustics*, **36**, 166–173.
- McCarthy, E., Moretti, D., Thomas, L., DiMarzio, N., Morrissey, R., Jarvis, S., Ward, J., Izzi, A., and Dilley, A. (2011). Changes in spatial and temporal distribution and vocal behavior of blainville’s beaked whales (*Mesoplodon densirostris*) during multiship exercises with mid-frequency sonar. *Marine Mammal Science*, **27**, E206–E226.
- Moretti, D., Marques, T., Thomas, L., DiMarzio, N., Dilley, A., Morrissey, R., McCarthy, E., Ward, J., and Jarvis, S. (2010). A dive counting density estimation method for blainville’s beaked whale (*Mesoplodon densirostris*) using a bottom-mounted hydrophone field as applied to a mid-frequency active (mfa) sonar operation. *Applied Acoustics*, **71**, 1036–1042.

Mesoplodon densirostris cluster sizes in the Bahamas

Tiago A. Marques & Len Thomas

Centre for Research into Ecological and Environmental Modelling
The Observatory, University of St Andrews, St Andrews, KY16 9LZ, Scotland

Version's date: June 27, 2013

Contents

1	Introduction	2
2	Exploratory data analysis	2
3	Important output for simulating groups at AUTECH	10
	References	13

1 Introduction

In this document we describe an exploratory data analysis performed over a data set containing *Mesoplodon densirostris* group sizes sent to us by Diane Claridge via e-mail on the 10th June 2013. While there are a number of reports of cluster size estimates in the literature (e.g. Claridge, 2006; Moretti *et al.*, 2010), these all use portions of this larger data set, so it was decided that a first hand look at the data set would be useful.

The data were in an excel worksheet, along with a second excel worksheet with some description about each of the columns. For each group detected a number of variables are available:

- Date, recoded to **date**: the date the sighting occurred
- Sequence, recoded to **seq**: a categorical variable, "S" means sighting; "E" means encounter or when we made close enough approach on group to get ID photos
- Group size, recoded to **cs**: the observed cluster (i.e. group i.e. pod) size
- Project, recoded to **project**: the project under which data was collected. Categorical variable: BBES & SERDP = large vessel platform; all others = small vessel platform
- Elapsed time, recoded to **time**: encounter duration, in minutes; the longer we spend with a group, the more confident we are of group size. Sightings don't have elapsed times.
- Latitude, recoded to **lat**
- Longitude, recoded to **long**

2 Exploratory data analysis

We begin by reading the cluster size data in. We also read in the data regarding hydrophone locations and depths ¹.

¹Heavily based on code and data being used in folder ABM, which contains LATTE's AUTECH simulation exercise.

```

> #-----
> #                                GROUP SIZE DATA
> #-----
> csdata=read.table(file="datfiles/Bahamas_MdGroups_Tiago2.txt",sep="\t",header=
> #recoding date field to read in properly as date
> csdata$date=strptime(csdata$date,"%d-%b-%y")
> #adding fields with year and month, for temporal analysis
> csdata$mon=csdata$date$mon+1
> csdata$year=csdata$date$year+1900
> #-----
>
> #-----
> #                                HYDROPHONE DATA
> #-----
> #reading the hydrophone data in
> hyd<-read.table(file="datfiles/HYDtable.txt")
> names(hyd)<-c("hydID","on","x","y","z","dunno")
> #adding the fact that some hydrophones were actually off
> #during the period for which we have data - this is
> #actually not used in the simulation
> hyd$off<-0;hyd$off[c(47,48,54,55,62,63,70,71,79,86,87)]<-1
> #reading the hydrophone data in
> seamap678<-read.csv("datfiles/seamap678.csv")
> seamap678<-seamap678[,c(3,5,6)]
> names(seamap678)=c("hyd","long","lat")
> #note we only have info for the active hyds
> # so, proving this will work
> #cor(unique(hyd$hydID[hyd$off==0]),as.numeric(names(with(seamap678,tapply(lat,
> #adding lat and long
> hyd$lat[hyd$off==0]=with(seamap678,tapply(lat,INDEX=hyd,FUN=mean))
> hyd$long[hyd$off==0]=with(seamap678,tapply(long,INDEX=hyd,FUN=mean))
> #-----
>
> #-----
> #                                DEPTH DATA
> #-----
> etopo1 <- read.table("datfiles/etopo1.xyz", quote="\")
> #summary(etopo1)

```

```

> #adding adequate names
> names(etopo1)=c("X","Y","Z")
> #creating a sequence of bins such that all places on land
> # i.e such that depth is between 0 and max(Z)=93
> # are in the initial bin
> depths=seq(max(etopo1$Z),min(etopo1$Z),by=-max(etopo1$Z))
> #note the minor tweak such that the last class is a bit bigger
> #to include all depths
> depths[length(depths)]=min(etopo1$Z)-0.01
> # coding up the depth class that each point belongs to
> #note this becomes a number, from 1 to 53=max(etopo1$colZ)
> #(53 levels of depth, where the 1 corresponds to above 0)
> etopo1$colZ=cut(x=etopo1$Z,breaks=depths,labels=F)
> #a pallete to color water in blue tones
> blues = shade.col(max(etopo1$colZ), acol=as.vector(col2rgb("darkblue")/255), b
> #making sure that land is black
> blues[max(etopo1$colZ)]= "black"
> #creating a matrix which can be plotted using say image or contours
> Zforplot=matrix(etopo1$Z,ncol=sqrt(length(etopo1$Y)),nrow=sqrt(length(etopo1$Y
> Zforplot=Zforplot[180:1,]
> Zforplot=t(Zforplot)
> #-----

```

There are 413 records, for which 412 actually have a record for cluster size. A first step is to visualize the data, by plotting group size locations in space with respect to the AUTEK range (Figure 1). We can see that there are many sightings near Abaco and at AUTEK, which might correspond to different projects. Given the sparsity of records south of 25.5N outside AUTEK, and given that we were thinking about using that as the northern limit for our simulations, it might be simpler to use a simple model to draw samples from, rather than a complex spatial-temporal model of group sizes.

We can see that typical cluster sizes are below 5, with the largest observed cluster size being 11 (figure 2). South of 25.5N the largest cluster size was 5 animals, which is clearly reflected on the south (2.82) vs. north (3.64) mean cluster size. The confidence intervals for mean group size south (2.5,3.14) and north (3.46,3.83) of 25.5N do not overlap, which indicates clearly that higher groups seem to avoid (or maybe “dissolve”?) in the south.

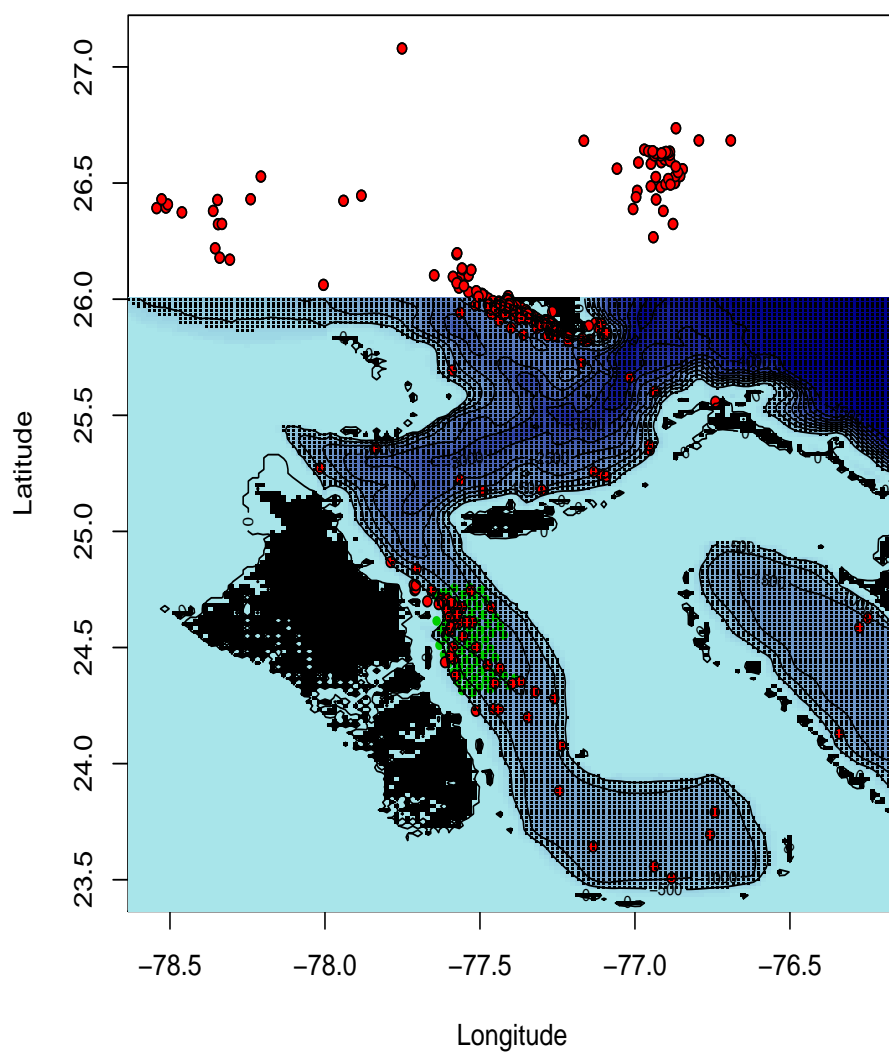


Figure 1: Group locations within the AUTECH range location and the wider Bahamas region.

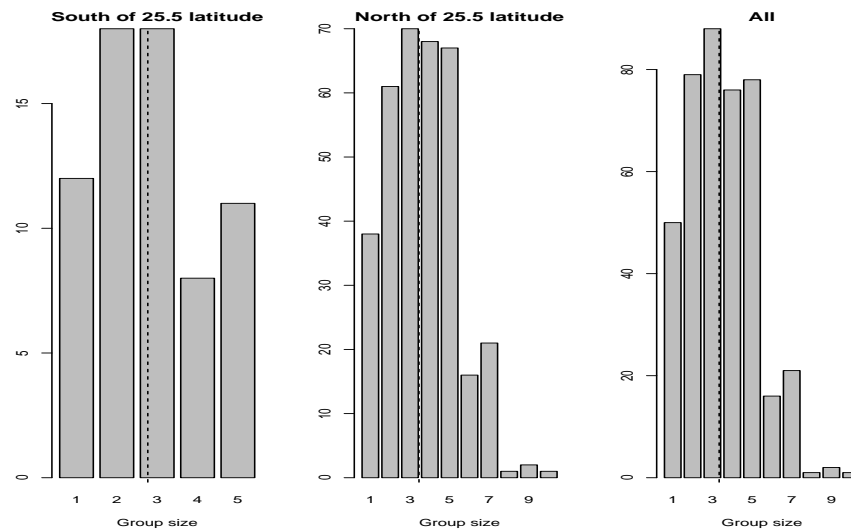


Figure 2: Histogram of cluster sizes.

We can also take a look at cluster sizes per project (figure 3), which show that groups above 5 members were only encountered in BBES, NEA Feacal and mostly BMMR0. There seems to be a slight increase in group size as a function of the time spent with a group (Figure 4), but likely the causal relation happens in the opposite direction, i.e. larger groups lead investigators to spend more time with them, and vice versa.

Finally, we can check whether there are interesting patterns in cluster size with respect to time (figure 5), both over the years and within the years (i.e. a season effect say). While over the years group sizes seem relatively constant, with maybe a slight decreasing trend (or more likely I may just be over-interpreting the data!) in the last decade or so, over the year it seems like the lower group sizes are found over spring months. I wonder why this is and whether it adds up with Diane's feelings / knowledge about their biology.

To finish, we just looked at a gam model of cluster size as a function of month and latitude and longitude (Figure 6). At the scale considered it is difficult to distinguish latitude from longitude, as these are correlated due to the shape of the study area and where most of the data lies.

Family: gaussian
Link function: identity

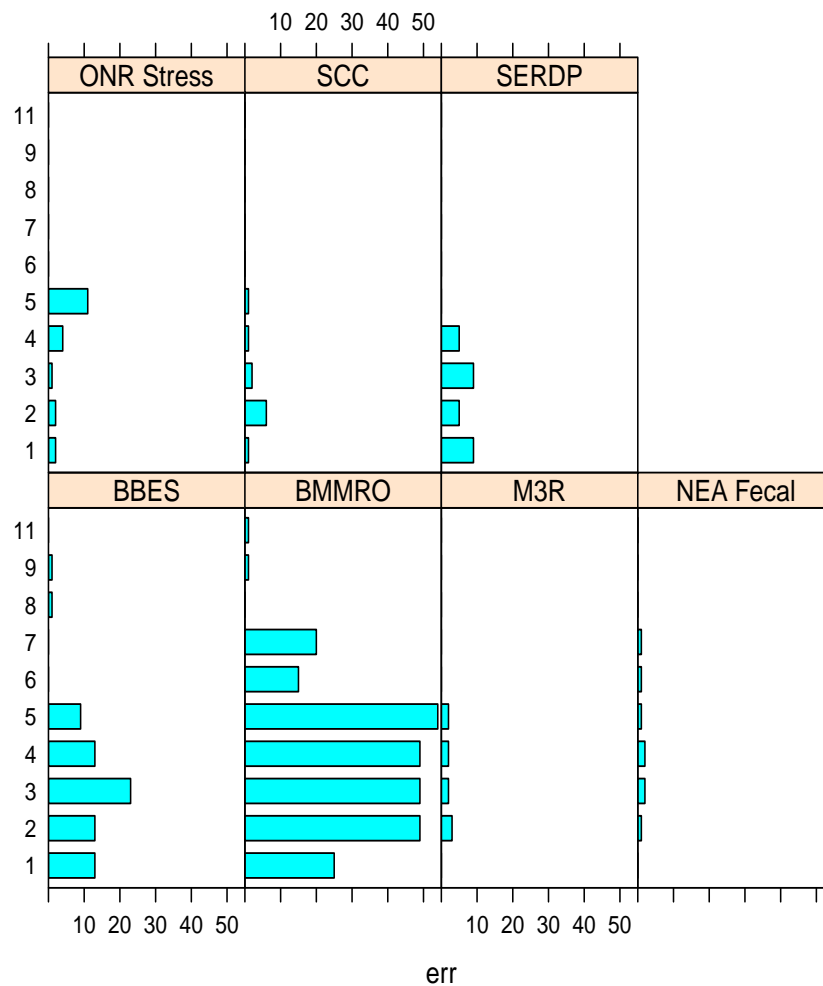


Figure 3: Group sizes by project.

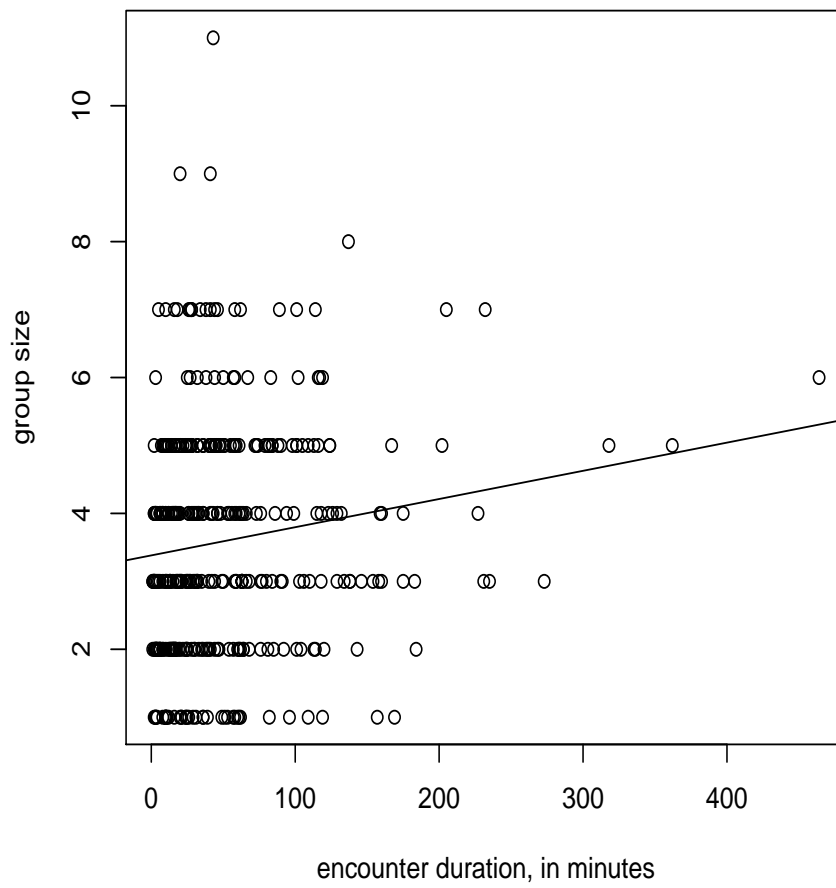


Figure 4: Group size as a function of time spent with group

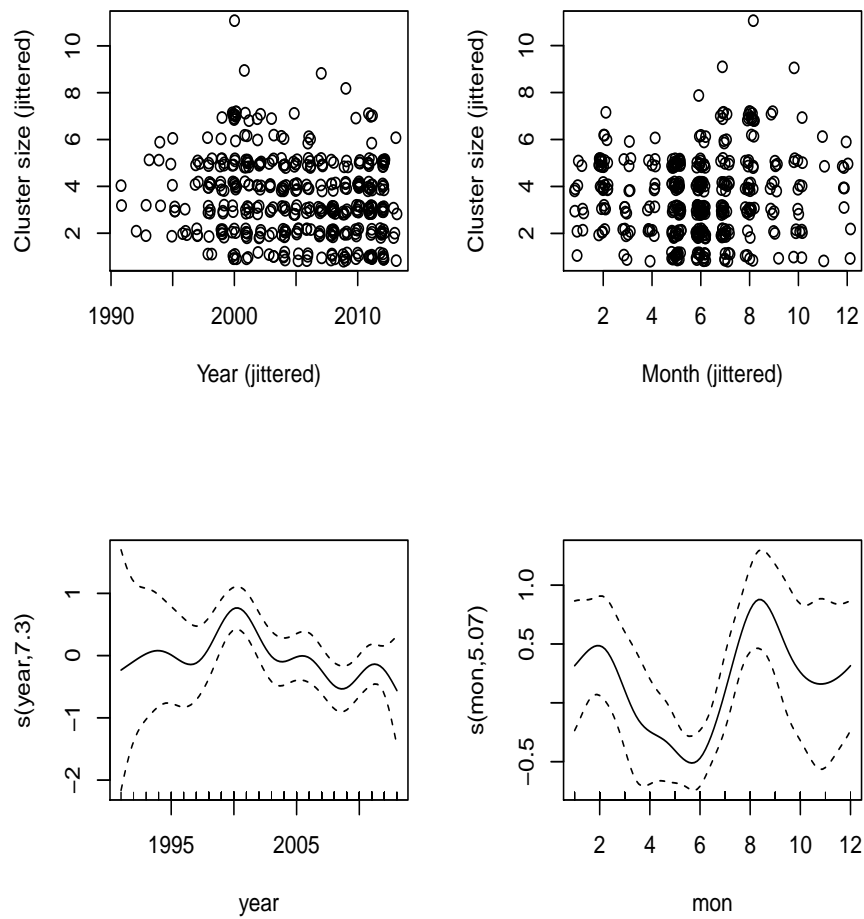


Figure 5: Group size as a function of year and month


```

Formula:
cs ~ s(mon, bs = "cc") + s(lat) + s(long)

Parametric coefficients:
              Estimate Std. Error t value Pr(>|t|)
(Intercept)  3.50971    0.08017   43.78  <2e-16 ***
---
Signif. codes:  0 '***' 0.001 '**' 0.01 '*' 0.05 '.' 0.1 ' ' 1

Approximate significance of smooth terms:
              edf Ref.df      F  p-value
s(mon)    4.561   5.649  5.532 2.92e-05 ***
s(lat)    2.556   3.149  2.585  0.0502  .
s(long)   1.117   1.217  3.311  0.0605  .
---
Signif. codes:  0 '***' 0.001 '**' 0.01 '*' 0.05 '.' 0.1 ' ' 1

R-sq.(adj) =  0.0937   Deviance explained = 11.2%
GCV score =  2.709   Scale est. = 2.6483    n = 412

```

3 Important output for simulating groups at AUTECH

Given all the above, and at the spatio-temporal scale our simulations are likely to occur, the best option to simulate cluster sizes from might be to sample from a multinomial distribution with parameters estimated empirically from the left panel in figure 2, reproduced in figure 7 left panel. These probabilities are shown in table 1. This seems more adequate than say to draw random deviates from a Poisson distribution ², which would be far over-dispersed and presenting way too often group sizes larger than 5. An example of 1000 simulated values from the later is presented in figure 7, right panel.

²with a tweak to avoid cluster sizes of zero, e.g. $Y=1+X$, where X is Poisson with mean equal to the observed cluster size - 1

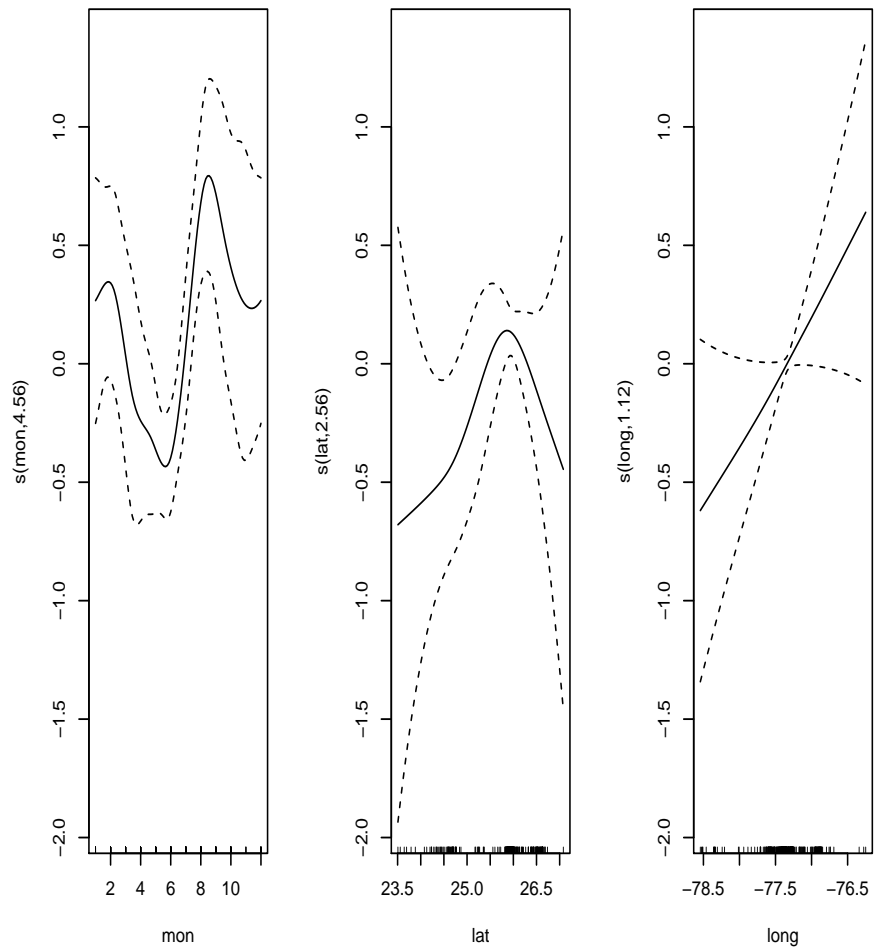


Figure 6: A quick gam model of cluster size as a function of month, latitude and longitude.

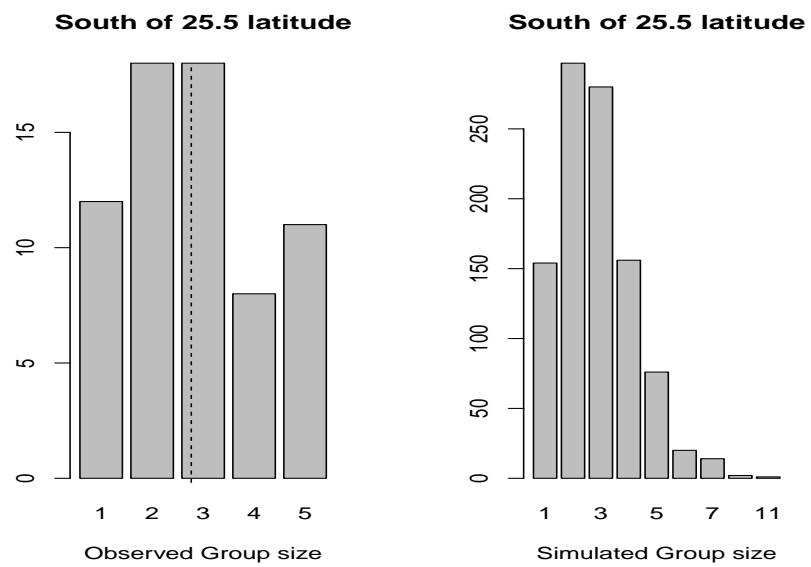


Figure 7: A quick gam model of cluster size as a function of month, latitude and longitude.

	1	2	3	4	5
Probability	0.179	0.269	0.269	0.119	0.164

Table 1: Empirical probabilities associated with each group size.

References

- Claridge, D. E. (2006). *Fine-scale distribution and habitat selection of beaked whales*. Master’s thesis, University of Aberdeen, Scotland, U.K.
- Moretti, D., Marques, T., Thomas, L., DiMarzio, N., Dilley, A., Morrissey, R., McCarthy, E., Ward, J., and Jarvis, S. (2010). A dive counting density estimation method for blainville’s beaked whale (*Mesoplodon densirostris*) using a bottom-mounted hydrophone field as applied to a mid-frequency active (mfa) sonar operation. *Applied Acoustics*, **71**, 1036–1042.

Modeling the number of clicks as a function of depth

Tiago A. Marques & Len Thomas

Centre for Research into Ecological and Environmental Modelling
The Observatory, University of St Andrews, St Andrews, KY16 9LZ, Scotland

Version's date: February 19, 2015¹

Contents

1	Introduction	2
1.1	Data details	2
2	Exploratory Data analysis	3
2.1	Dive data	3
2.2	Click times	3
2.3	Inter-click-interval	8
2.4	Vocal and silent period duration	9
2.5	Estimating a mean using observations repeated over individuals	9
3	Data and estimates required for density estimate	12
3.1	Estimating click rate	12
3.1.1	Using clicks per second	12
3.1.2	Using a weighted mean	15
	References	16

¹ This document was created using Sweave, using on a platform.

1 Introduction

In this document we present an analysis of DTag data for 4 beaked whales, with multiple dives for each whale. The data was sent as txt files. The data was compiled by Walter Zimmer and sent by Peter Tyack to us on the 28th of April 2008. These data were previously analysed in a separate report "A closer look at click rates as reported in the 2009 JASA paper for DWH".

Each of the received files contains 4 columns, with time, depth, pitch, and heading.

The DTag information for each whale is separated in two files:

- A file with the variables by second (time indexing variable starts at second 1);
- A file with the variables at each click time (starts at time of first click).

1.1 Data details

The data files were read into R:

```
#note this code chunk is not evaluated to speed up report generation  
#reading the data in  
cli227a<-read.table("datfiles/md07_227a_click_data.txt")  
sec227a<-read.table("datfiles/md07_227a_sec_data.txt")  
cli245a<-read.table("datfiles/md07_245a_click_data.txt")  
sec245a<-read.table("datfiles/md07_245a_sec_data.txt")  
cli248a<-read.table("datfiles/md07_248a_click_data.txt")  
sec248a<-read.table("datfiles/md07_248a_sec_data.txt")  
cli248b<-read.table("datfiles/md07_248b_click_data.txt")  
sec248b<-read.table("datfiles/md07_248b_sec_data.txt")
```

We can check what they look like (after appropriate headers were added: sec - second; cli - click; z - depth; h - heading; p - pitch). These are the first few lines of a data set by second

```
head(sec227a)  
  
##      sec      z      h      p  
## 1      0 11.77 1.551 -0.1319
```

```
## 2    1 12.08 1.524 -0.1358
## 3    2 12.49 1.536 -0.1504
## 4    3 12.76 1.564 -0.1388
## 5    4 13.06 1.595 -0.1281
## 6    5 13.36 1.612 -0.1179
```

and this is the first few lines of a data set by click

```
head(cli227a)

##      cli      z      h      p
## 1 1458 474.8 -0.4150 -1.193
## 2 1458 474.8 -0.4111 -1.192
## 3 1458 474.9 -0.4076 -1.191
## 4 1458 474.9 -0.4044 -1.191
## 5 1459 476.5 -0.3622 -1.188
## 6 1459 476.6 -0.3627 -1.188
```

2 Exploratory Data analysis

2.1 Dive data

To get a first feel for the data we plotted the dive profiles (with click events), the heading and pitch through time, for each of the 4 whales (Figures ?? to ??).

The first thing that worth noting is that the sound data is not as long as the positional data ², which covers more dives (for all whales) than the sound data. This is clear from the presence of deep dives for which click events are not available (see figures ?? to ??). While we have click data for respectively 6, 4, 4, and 4 dives for whales 227a, 245a, 248a and 248b, there are respectively 8, 5, 7, 5 dives with Dtag data.

2.2 Click times

We can look closer at the data for click times, because here we hope to obtain a way to simulate clicks over time, and we propose to do so as a function of

² Presumably due to lack of memory on the Tag

Figure 1: The dive profile (top), heading per second (center) and pitch per second (bottom) for whale 227a. On the top panel blue indicates depth at click event. Note that sound recording is only available for part of the total DTag period.

Figure 2: The dive profile (top), heading per second (center) and pitch per second (bottom) for whale 245a. On the top panel blue indicates depth at click event. Note that sound recording is only available for part of the total DTag period.

57

Figure 3: The dive profile (top), heading per second (center) and pitch per second (bottom) for whale 248a. On the top panel blue indicates depth at click event. Note that sound recording is only available for part of the total DTag period.

Figure 4: The dive profile (top), heading per second (center) and pitch per second (bottom) for whale 248b. On the top panel blue indicates depth at click event. Note that sound recording is only available for part of the total DTag period.

Figure 5: The number of clicks per dive (the dashed lines represent separation between whales), and an histogram of the same data, pooled across whales and dives.

depth.

For simplicity, we build a single data frame which contains the information per click from the 4 whales, named `calldata`.

```
CT<-rbind(cli227a,cli245a,cli248a,cli248b)
W<-rep(c(1,2,3,4),times=c(length(cli227a[,1]),length(cli245a[,1]),length(cli248a[,1]),length(cli248b[,1])))
calldata<-data.frame(CT=CT,W=W);names(calldata)<-c("CT","z","h","p","W")
rm(CT,W)
```

In total we have 79405 clicks, respectively 24318, 15854, 16364 and 22869 for each whale.

One can now look at the time differences between successive clicks, adding a code to uniquely identify each dive. The number of clicks per dive is shown in Figure ??, top panel.

The mean number of clicks per dive is 4411, which is almost at the center of the 4000-5000 range reported for the number of clicks per deep dive in ?. An histogram of the number of clicks per dive is shown in Figure ??, bottom panel.

These numbers reflect the fact that these data sets only contain regular clicks, while buzz clicks are not included (P. Tyack has already confirmed this).

2.3 Inter-click-interval

The shortest time between the last click in a dive and the first click in the next dive was 3070 seconds.

The maximum inter-click-interval (ICI) within a deep dive was 46.4 seconds, while the mean ICI was 0.39 seconds. Note that if the mean is calculated over those ICI under a second, it is only 0.328. Of the 79401 ICI, 97.937% were under a second, and 98.966% under 3 seconds. We can take a look at the ICIs distribution (Figure ??). It seems like the ICI are a mixture

Figure 6: Distribution of ICI, focusing on different ICI ranges in each panel.

of two distributions, namely a prevalent one with a mean under a second and a second one, far less common, with a mean around 3 seconds.

2.4 Vocal and silent period duration

The mean duration of the vocalization period³ (V, sample size 18) and silent period (S, sample size 5+3+3+3=14) was respectively 28.8 ($se=1.8$) and 137.9 ($se=21.1$) minutes, which corresponds to about 17.266 % of the time vocally active. Remember that the values reported in (and derived based on) ? were respectively 26.4 and 112.1, which is remarkably consistent.

2.5 Estimating a mean using observations repeated over individuals

All the numbers reported above assume that each event is independent. However, this might not be the case, as we expect measures from a single animal to be less variable than measures across animals.

Consider the estimation of the mean duration of the vocalizing period as an example. The previous sentence means it was considered that we had a sample of 18 vocalizing periods, but arguably what we have is a sample of 4 individuals, each providing repeated measures about vocalizing periods.

Note that if one fits a model with whale as a (fixed) factor, there seem to be differences across whales in the length of the vocalizing period in particular whale 4 seems to present longer vocalizing periods.

Hence, instead of using a simple mean to estimate the mean vocalizing period, essentially the intercept parameter estimate of a linear model like

we could fit a random effect model (essentially because whale is not a fixed factor, but a random sample of a much larger number of possible whales) that accounts for this fact.

³ We consider here said period to be from the first to the last click within a deep dive.

Although the point estimate might not be too different⁴, changing from 28.8 to 29.1, the uncertainty (here the standard error) around that estimate increases from 1.81 to 2.97 (reflecting the fact that we do not have 18 independent observations, but 4 sets of independent observations).

Note we could formally test for the need of the random effects as

```
lm.model3.null<-lm(Vmin~1,data=V.dat)
#Likelihood ratio test statistic
LRTS<-as.numeric(2*(logLik(lm.model3)-logLik(lm.model3.null)))
LRTS;pchisq(LRTS,1,lower=F)

## [1] 5.972
## [1] 0.01453
```

Hence, at the 5% significance level the model including the random effect seems to be required. However, it is argued that the approximation to the chi-square is not adequate, and a parametric bootstrap procedure described in ?, p. 160 might provide more reliable results. This is implemented below

```
y <- simulate(lm.model3.null)
lrstat <- numeric(1000)
for(i in 1:1000){
y <- unlist(simulate(lm.model3.null))
bnull <- lm(y ~ 1)
balt <- lme(y~1,random=~1|V.whale,data=V.dat,method="ML")
lrstat[i] <- as.numeric(2*(logLik(balt)-logLik(bnull)))
}
rm(balt,bnull,y)
```

We can see that the actual distribution for the test statistic is far from what would be expected for a chi-square (e.g. we observe a large proportion of very small values (say < 0.0001), here 0.721). The p-value of this test is given by⁵

⁴ But note this is not necessarily the case in general, especially if there were differences across whales in length of vocalizing period and markedly different number of repeated measurements for each whale.

⁵ The second line of code is the standard error for this estimate of the p-value assuming a binomial distribution.

```
mean(lrstat > LRTS)

## [1] 0.003

sqrt(mean(lrstat > LRTS)*(1-mean(lrstat > LRTS))/1000)

## [1] 0.001729
```

which just reinforces the above result that the random effect is required for adequately modelling this data. Note we could estimate predicted random effects for each whale using the command (see ?, p. 161 for details)

```
ranef(lm.model3)

## (Intercept)
## 1 -3.101
## 2 -3.359
## 3 0.214
## 4 6.246
```

(note how as expected the sum of the random effects is ≈ 0). Note that these are smaller than the corresponding fixed effects

```
cc[[1]]$V.whale

## V.whale
## 1 2 3 4
## -3.505 -4.231 0.636 8.853
```

and if we wanted to predict a new value for a given whale, instead of using the fixed effect model, i.e.

```
as.numeric(mean(V.dat$Vmin)+cc[[1]]$V.whale)

## [1] 25.27 24.55 29.41 37.63
```

we should use the random effect model

```
fixef(lm.model3)+ranef(lm.model3)[[1]]  
## [1] 26.02 25.76 29.33 35.37
```

3 Data and estimates required for density estimate

In this section we look into two data components required in the process of estimating beaked whale abundance at AUTECH for the 6 day trial data set. These components are:

1. the estimated click rate
2. a distribution for the relevant variables needed (as depth, pitch, heading) to calculate the required distributions (say distance, vaa and haa) of the variables to integrate out in the model of detection probability.

3.1 Estimating click rate

To estimate abundance using cue (click) count based methods we require a click rate (and the corresponding variance). We want an unbiased estimate for this rate, averaged over a long time period. This is because we do not want either to obtain the click rate corresponding the vocalizing period of a deep dive (very high click rate) nor the click rate of a non vocal period (click rate = 0), but a representative average of the two periods, so that we can scale up the number of clicks detected over a long time period (in this case, 6 days).

As described in the previous subsection, we need to account for the hierarchical nature of the data available (namely dives within whales).

There are multiple alternatives to estimate said click rate. Here we consider counting the number of clicks per some time interval (say a second), and compute the appropriate average.

3.1.1 Using clicks per second

From figure ?? it is obvious that we need to remove the data for which sound was not available. We assume that an animal's time can be subdivided in

dive cycles, and a dive cycle lasts from the moment a deep dive starts till the moment the next deep dive starts. Therefore, considering full dive cycles for which sound data was available seems a straightforward way to be unbiased. In figure ?? the periods considered are between the dashed lines ⁶.

We begin by obtaining the number of clicks for each second (code omitted for brevity).

```
## [1] 199911      2
## 101 102 103 104 105 106 201 202 203 204 301 302 303 304
## 4007 4337 3933 3515 4052 4474 6392 2847 2432 4183 3809 3907 4364 4284
## 401 402 403 404
## 4540 6279 5746 6304
##
## 1 2 3 4 5 6 7 8 9 10 11 12 13 14
## 4007 4337 3933 3515 4052 4474 6392 2847 2432 4183 3809 3907 4364 4284
## 15 16 17 18
## 4540 6279 5746 6304
```

Given this, we can build a model for the number of clicks per second as:

```
m.cps<-lme(n~1,random=~1|W,data=clicks.per.second,method="ML")
sum.m.cps<-summary(m.cps)
```

We therefore estimate the mean number of clicks per second as 0.41 with a corresponding standard error of 0.04.

Naturally, some sort of ZIP or “hurdle” model, with a distribution appropriate to counts, like a negative binomial, might be better given the large number of seconds ($\approx 86\%$) with zero clicks.

Another relevant issue is the fact that this model does not account for the autocorrelation in click numbers with time, so we might be underestimating the true variance.

This model uses data from 4 whales tagged in 2007, yet we could add a fifth whale which was tagged in 2006. The data for this comes from the workspace “gxestimate”, as described in ?.

⁶ Although this is not ideal, we manually selected the seconds that correspond to the start of each dive cycle. Details about how this was done can be found in file “obtaining dive cycles.R”.

Figure 7: The dive profiles of the 4 whales. A green cross indicates the first click in each deep dive, and a red cross a ICI larger than 15 seconds. A blue dot (perceived as blue lines during the deeper part of deep dives) represents a click. Dashed lines represent start and end of each dive cycle.

Figure 8: The click rate per deep-dive cycle, separated by whale. Data points are represented by actual dive number.

```
load(file="datfiles/Md296.clik.s.per.second.Rdata")
clicks.per.second2<-rbind(clicks.per.second,clicks.per.secondMd296)
m.cps2<-lme(n~1,random=~1|W,data=clicks.per.second2,method="ML")
sum.m.cps2<-summary(m.cps2)
```

We now estimate the mean number of clicks per second as 0.422 with a corresponding standard error of 0.04.

Note that, as expected, this corresponds to an average of the click rates per whale, 0.422.

3.1.2 Using a weighted mean

It was felt that it might be more adequate to use a weighted mean to estimate the mean click rate. To do so, we calculate a weighted mean of click rate per deep-dive cycle, weighted per deep-dive cycle time length.

The deep-dive cycles click rates present a considerable variation per whale, as can be seen in figure ?? . It can be seen that there are no clear differences in clicks per dives across whales, so maybe the use of dives as independent sampling units (rather than nested within whales) is not unrealistic.

Obtaining the variance of a weighted mean is done using ⁷

```
var.wtd.mean.cochran <- function(x,w)
# Computes the variance of a weighted mean following Cochran 1977 definition
{
  n = length(w)
  xWbar = weighted.mean(x,w)
  wbar = mean(w)
  out = n/((n-1)*sum(w)^2)*(sum((w*x-wbar*xWbar)^2)-2*xWbar*sum((w-
wbar)*(w*x-wbar*xWbar))+xWbar^2*sum((w-wbar)^2))
  return(out)}
```

The estimated click rate is 0.407 with a CV of 0.098 %.

⁷ see Problem with Weighted Variance in Hmisc.pdf for this formula.

References

- Faraway, J. J. (2006). *Extending the Linear Model with R*. Chapman & Hall / CRC.
- Madsen, P. T., Johnson, M., de Soto, N. A., Zimmer, W. M. X., and Tyack, P. (2005). Biosonar performance of foraging beaked whales (*Mesoplodon densirostris*). *The Journal of Experimental Biology*, **208**, 181–194.
- Marques, T. A. and Thomas, L. (2008). Estimating the mean probability of detection of a beaked whale click at AUTECH. Technical report, DECAF internal report.
- Tyack, P. L., Johnson, M., Soto, N. A., Sturlese, A., and Madsen, P. T. (2006). Extreme diving of beaked whales. *Journal of Experimental Biology*, **209**(21), 4238–4253.

An exploratory look over John Durban's satellite tag data

Tiago A. Marques & Len Thomas

Centre for Research into Ecological and Environmental Modelling
The Observatory, University of St Andrews, St Andrews, KY16 9LZ, Scotland

Version's date: October 6, 2015¹

Contents

1	Introduction	1
1.1	Data details	2
2	Location data	5
3	Estimating home ranges	9
3.1	Minimum convex polygon	9
3.2	Kernel estimator	11
3.3	Tags to consider further	12
4	Further analysis of selected tags	14

1 Introduction

In this document we present an exploratory analysis of the satellite tag sent to us by John Durban via e-mail on 21/04/2014 at 12:13. The objective of this analysis would be to try to parametrize some movement models which would convey the notion of home range to our LATTE simulations, i.e., instead of animals wandering off as simulations extend over time, animals would tend to return to their home range.

¹ This document was created using Sweave, using on a platform.

John Durban (JD), jointly with Devin Johnson, is making progress with hierarchical models linking movement and diving changes to received sonar levels based also on these data sets (see e-mail 09/05/2014 16:50). JD also said that PTT's 93232 (May 2009), 111664, 111670 (May 2012), 129715 (Nov 2013) are close to mini wars (from D. Moretti = 14-17 May 2009; 14-16 May 2012; 16-19 November 2012). PTT's 93232, 52627, 111675, 111682, (112032 not much data) correspond to adult males, others are adult females.

The initial file provided had some problems due to ARGOS reusing PTT numbers, but the file "Md data for Tiago.2.csv" should be ready to use.

1.1 Data details

The data file was read into R:

```
path1="C:/Users/Tiago Marques/Dropbox/"
path2="LATTE/stuff from others/John Durban/datfiles/"
file="Md data for Tiago_2.csv"
data <- read.csv(paste0(path1,path2,file))
```

In total we have 1488 locations for 12 whales, ranging from just 2 to 397 positions per whale.

We can check what the data looks like

```
head(data)
```

##	PTT	Date	Lat	Lon	Error	Semi.major.axis
## 1	93222	5/6/2009 22:17	25.95403	-77.33416	3404	24985
## 2	93222	5/7/2009 7:29	25.93503	-77.34785	1662	51770
## 3	93222	5/7/2009 10:11	25.81120	-77.34227	6877	43800
## 4	93222	5/7/2009 11:43	25.78868	-77.33188	10836	29273
## 5	93222	5/7/2009 14:20	25.78831	-77.27233	3073	12577
## 6	93222	5/7/2009 15:07	25.86723	-77.19825	2419	25492
##	Semi.minor.axis	Ellipse.orientation				
## 1	463			82		
## 2	53			128		
## 3	1079			118		
## 4	4011			118		
## 5	751			27		
## 6	229			113		

The columns represent:

- PTT : a unique tag identifier
- Date : the time/date of each location measurement
- Lat : latitude
- Lon : longitude
- Error : a quantification of the measurement error; errors are not isotropic, leading to the next 3 quantities
- Semi.major.axis : major axis of the error ellipse
- Semi.minor.axis : minor axis of the error ellipse
- Ellipse.orientation : direction of the error ellipse major axis

We can see the last 4 columns refer to measurement error quantification. ARGOS satellite tag localizations are known to be affected by errors. It seems like here these are represented as error ellipsis.

Some of the locations have large errors in them. As an example, 59 have errors of more than 10000 (assuming these are meters?). An exploratory analysis of the errors is shown in figure 1.

Trying to understand what the error numbers actually mean we also plotted how the actual error relates to the product of the axis of the error, and as expected there is a relationship between these. The relationship is so evident that it is likely that the error value is actually a value derived deterministically from the error axis (Figure 1, bottom left).

It seems like the errors tend to be higher in some directions than others, with a mean around 89^2 , a possible consequence of the typical satellites available for this area (Figure 1, bottom right).

The large majority of observations has errors below 5 km. At the scale we are interested in making inferences here (the beaked whales home range scale) these seem potentially negligible. Hence, for the purpose of this analysis we will essentially ignore this, concentrating on obtaining some statistics assuming these positions were error free. Later we could repeat any analysis presented here with positions obtained from processing the current data with methods which account for location errors.

²We are not sure about what the units are, probably a heading but not sure what 0 might represent.

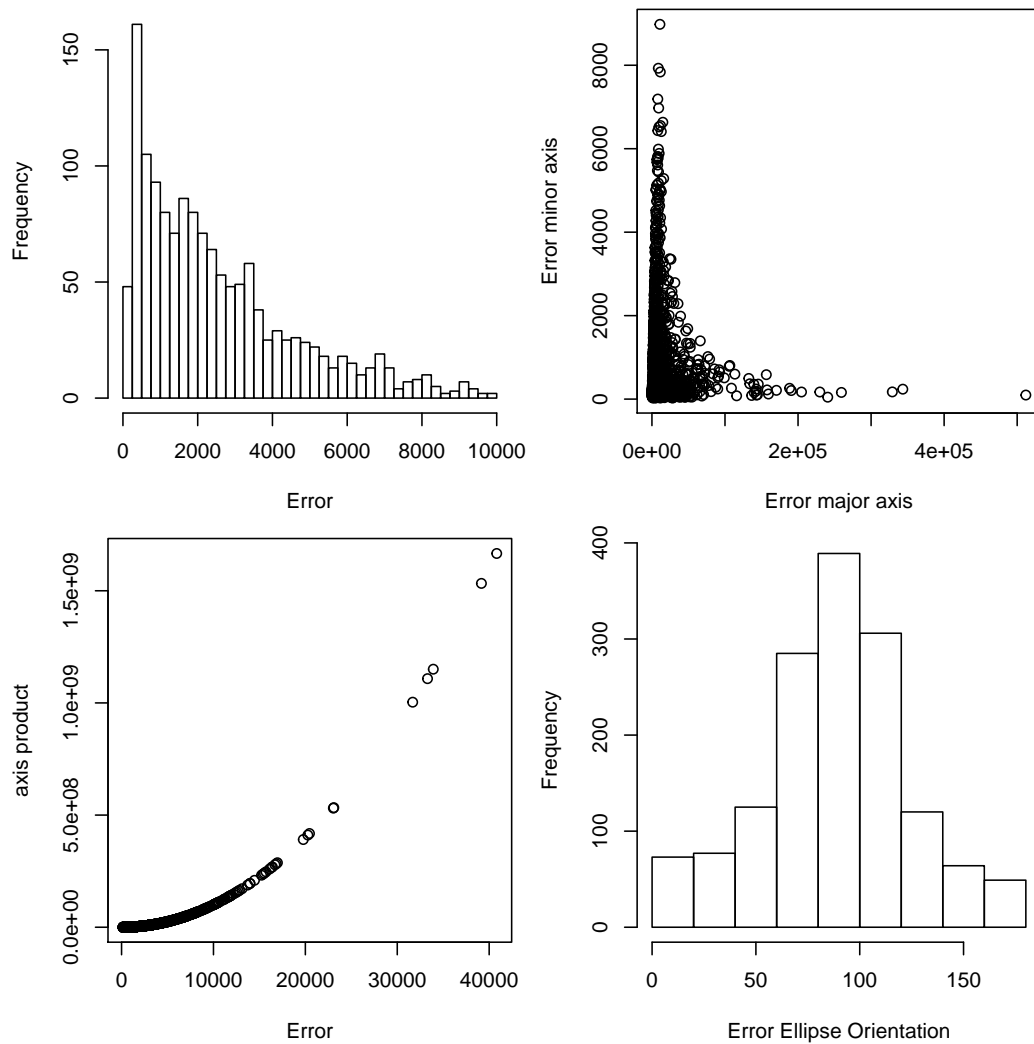


Figure 1: Measurement errors associated with the satellite tag localizations. Top left: measurement error (error ≤ 10000). Top right: relation between major and minor axis errors. Bottom left: Relation between error and minor and major axis product. Bottom right: direction of the orientation of error ellipse.

2 Location data

We begin by plotting the location data in space (Figure 2). This is actually not an easy figure to interpret because of the spatial scale, but some obvious measurement error problems are evident for some whales.

We can zoom in each of the whales (Figure 3). Clearly some whales provide reasonable information (e.g. PTT 108419) while others provide very little information (e.g. PTT 112032). It might be useful to see all these plots with a common spatial scale. This is shown in figure 4.

It is also fundamental to understand the duration of the time periods considered, as we are interested in movements at a coarse scale. To do so we need to convert the field "Date" to dates that R can actually process.

	PTT	sex	cmw	posits	smonth	syear	dur
1	93222	F	0	35	5	2009	5.15
2	93232	M	1	171	5	2009	25.96
3	52627	M	0	62	10	2010	14.31
4	108419	F	0	397	6	2011	45.64
5	111664	F	1	144	5	2012	16.74
6	111670	F	1	227	5	2012	26.84
7	111682	M	0	194	6	2012	23.90
8	111680	F	0	74	6	2012	5.19
9	112032	M	0	2	6	2012	0.01
10	111676	F	0	55	6	2012	7.35
11	111675	M	0	84	7	2012	8.60
12	129715	F	1	43	11	2013	17.24

Table 1: Summary statistics per whale, including sex, whether the tag was close to an SCC exercise (cmw), number of positions (posits), month (smonth) and year (syear) of first position and duration in days (dur).

As expected, the number of positions available per animal increases linearly with the deployment duration (Figure 5).

We want to parametrize the displacement of animals at the home range scale. Conceivably, we can only do this based on data which would allow us to reasonably estimate an animal's home range. Therefore we begin by investigation whether estimates of home range sizes using this data set seem to be sensitive to the amount of data available.

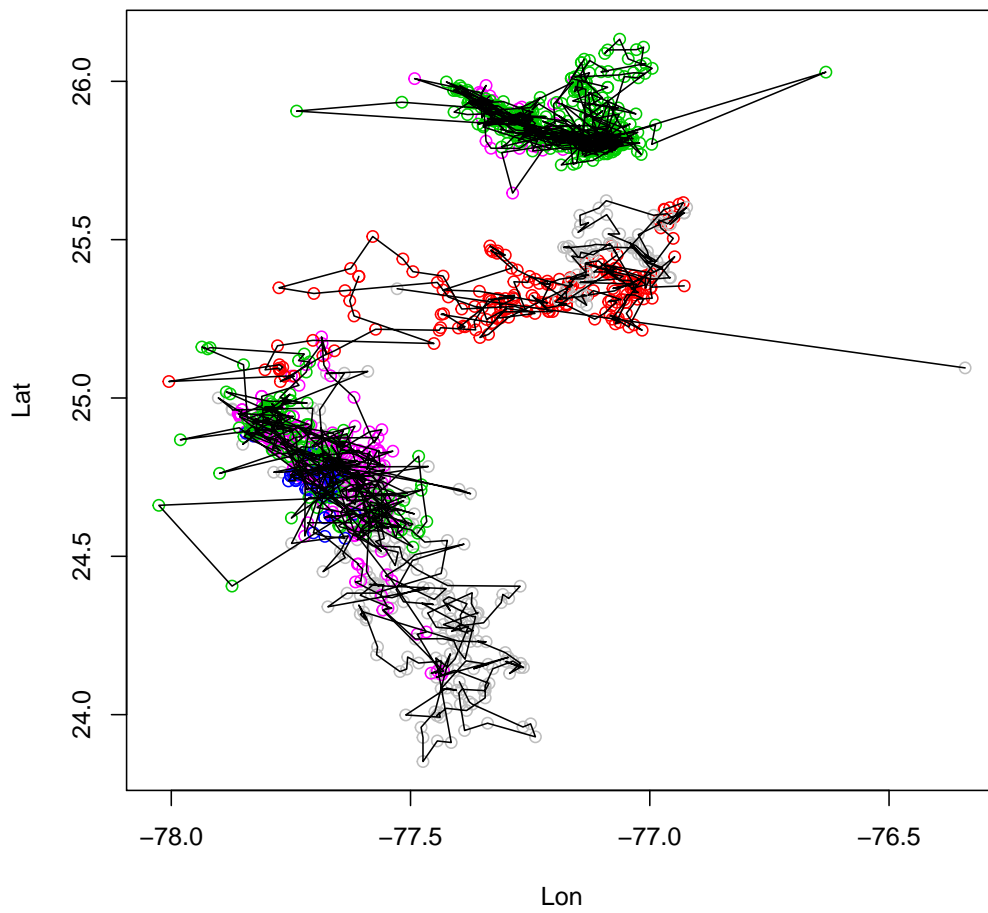


Figure 2: Locations of 12 satellite tagged whales in space.

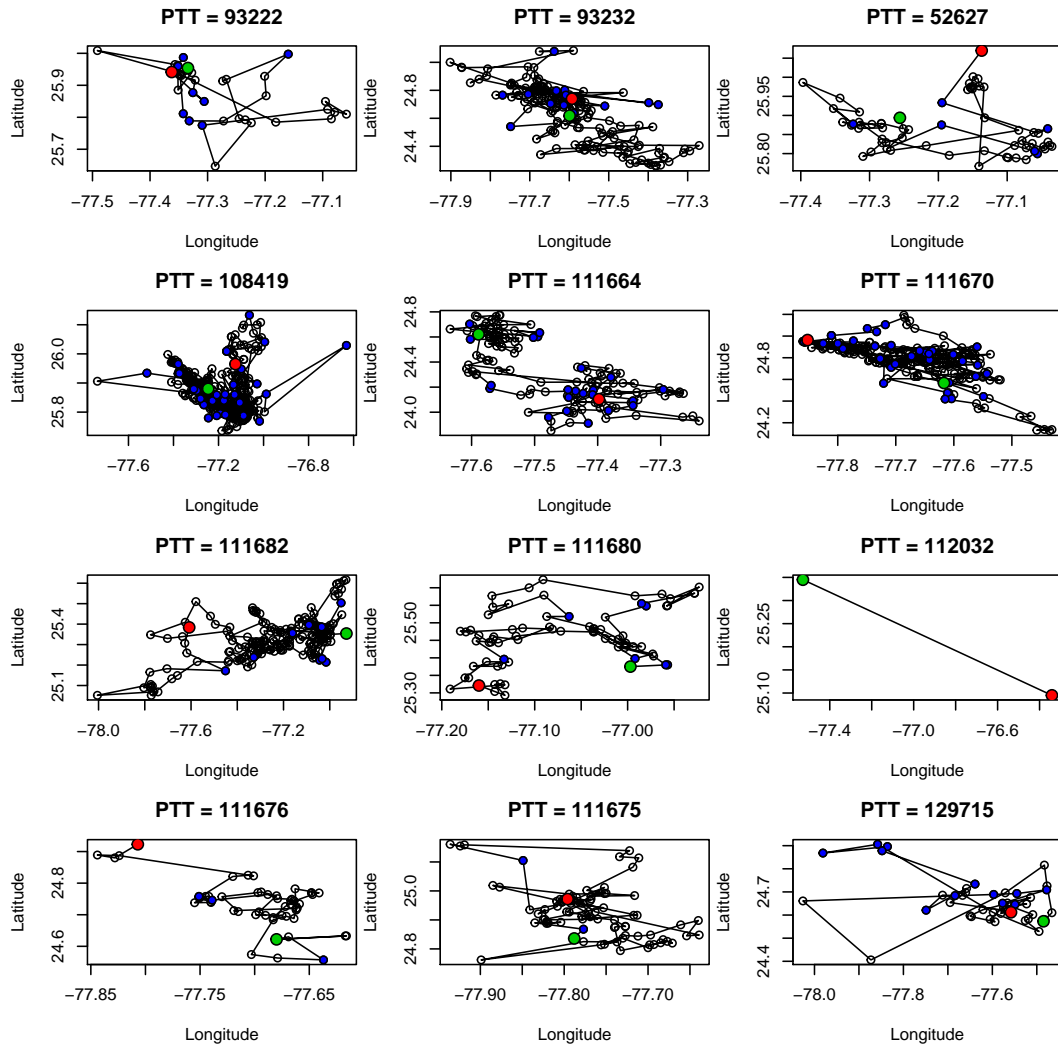


Figure 3: Locations of 12 satellite tagged whales in space, with one panel per whale

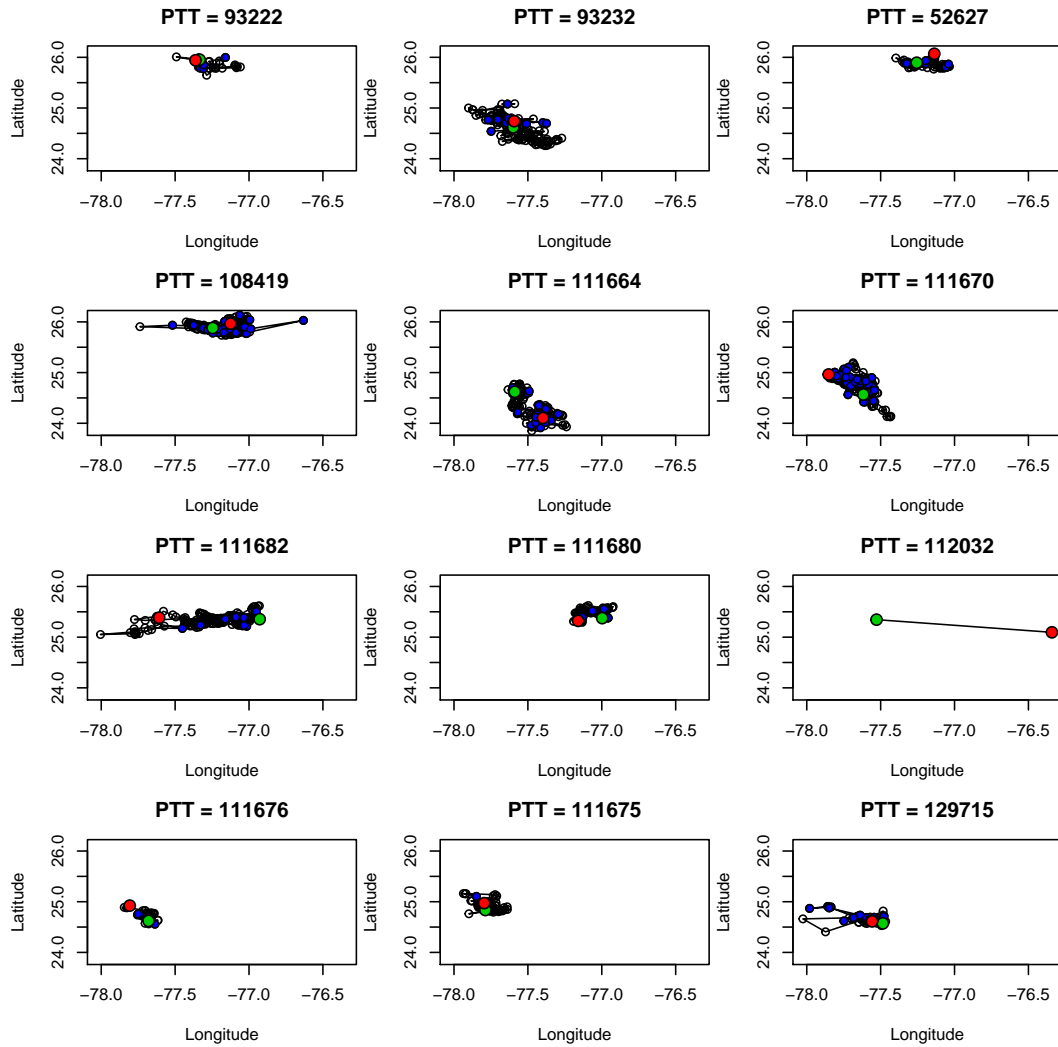


Figure 4: Locations of 12 satellite tagged whales in space, with one panel per whale, at the same spatial scale.

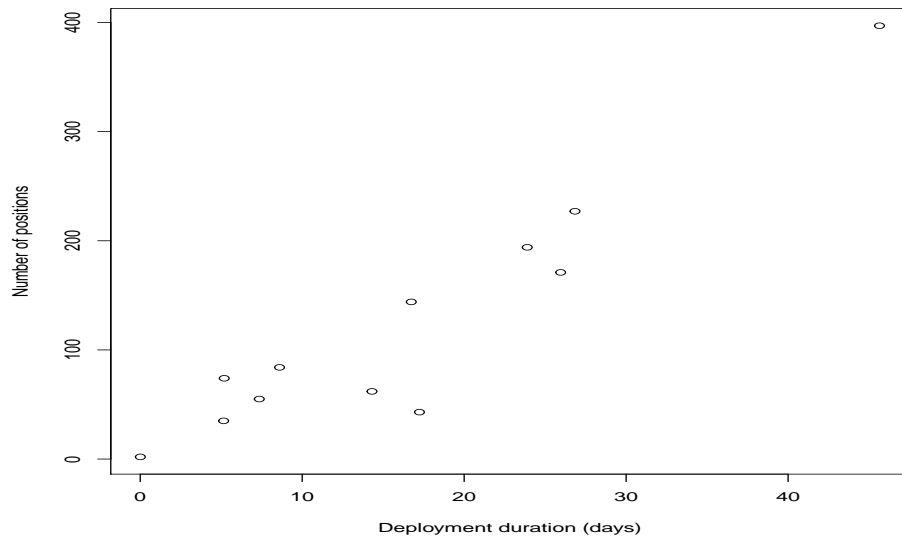


Figure 5: The number of available positions as a function of deployment duration.

3 Estimating home ranges

This is implemented using bespoke functions from package `adehabitatHR`.

We begin by noting that, for the time being, this package assumes that the units are projected units (m, km, ha) but we have the animal's locations in latitude and longitude. We considered the input units to be km and the output units to be ha, but in order for the areas to make sense one would have to project the latitude and longitude first. Because here we are only interested in the relative size of the home range we ignore it for now.

3.1 Minimum convex polygon

We begin by using the minimum convex polygon approach, removing 5 % of the most extreme observations.

As we can see in figure 6, all the deployments under 2 weeks have considerably small home ranges. After two weeks, the home range estimated from deployments tends to be much larger (even if the variance associated with these is also much larger). One can only postulate that said variance might be reflective of true differences in home range sizes, despite the fact

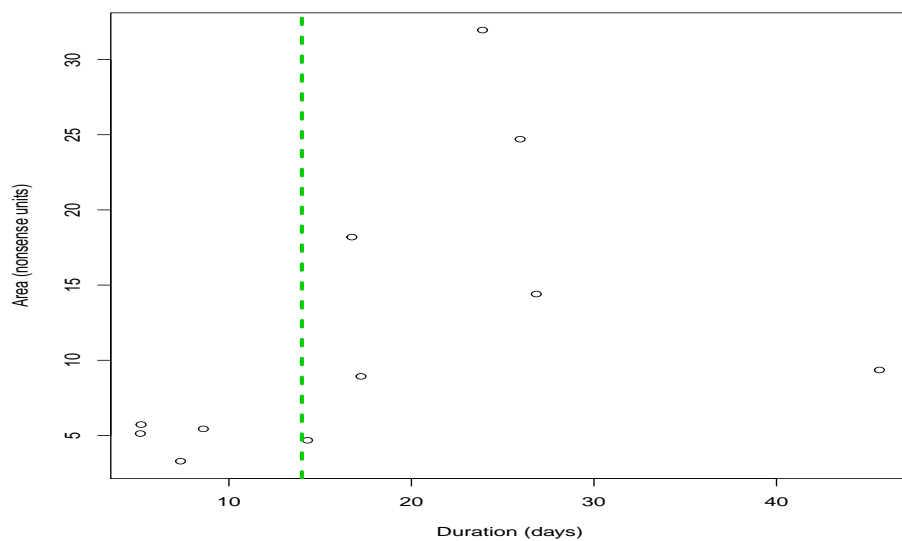


Figure 6: Relationship between the estimated area of the home range size as a function of the deployment duration, with an arbitrary line separating “low” duration deployments from “reasonable” (more than 2 weeks) duration deployments.

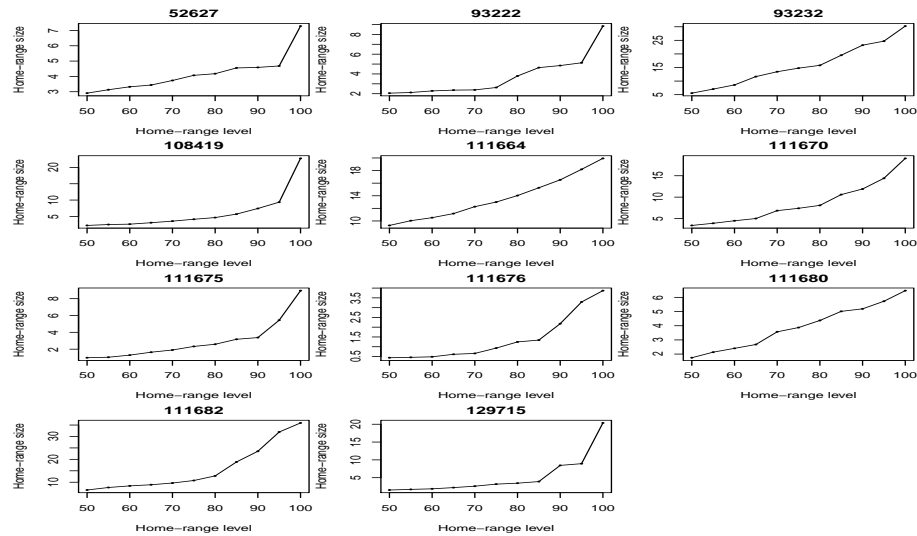


Figure 7: Relationship between the estimated area of the home range size as a function of the amount of data discarded, per animal.

that there is no strong evidence to do so.

Figure 7 displays the relationship between the percentage of points included in the calculation of the minimum convex polygon and the home range size. Ideally one would hope to observe an asymptote and a jump from say 95% to 100%, hence justifying the 5% cut off, but while that is observed for some animals (e.g. 52627 or 108419) it certainly does not happen even for some animals with longer durations (e.g. 93232 and 111670), which render this analysis somewhat inconclusive.

3.2 Kernel estimator

Another approach to estimate the home range size of animals is to consider an utilization distribution (a measure of how the animal uses space). The use of kernels to estimate this distribution was a natural development. Here we use such kernel methods to compare with the results obtained for the mcp approach.

In figure 8 we present such estimated utilization function for each of the animals, while in figure 9 we represent the values of the estimated home ranges using this kernel approach compared to those from the mcp approach.

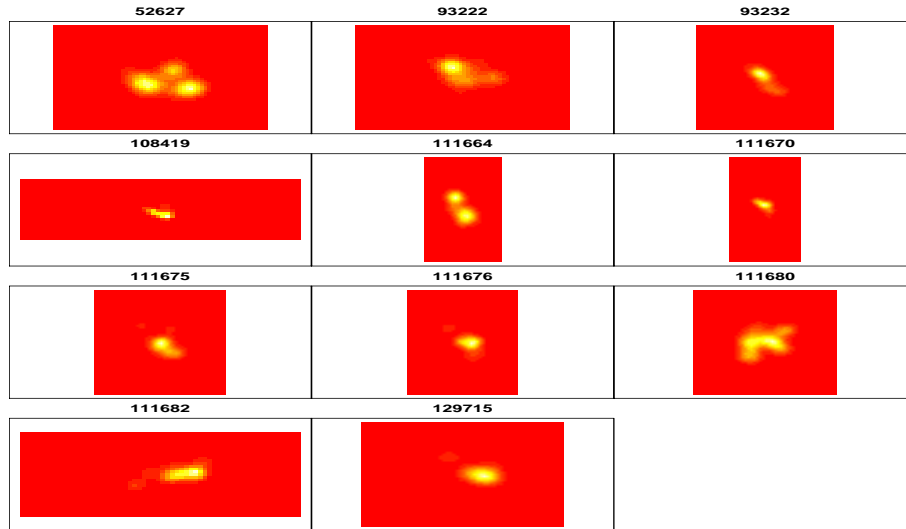


Figure 8: Estimated area utilization function using the kernel estimator.

As we can see the kernel approach tends to estimate a larger home range, but since we are only interested in the relative size of the home ranges this should not be a major problem for us.

3.3 Tags to consider further

We need to use the satellite tag data to parametrize the strength of attraction towards an hypothetical home range centre.

We will assume that the 7 animals with deployment durations above 15 days correspond to animals for which the home range can be adequately characterized, while inferences based on information available for animals with shorter deployment durations probably would be underestimating their true home range size. If we used these in the next step of the analysis would therefore overestimate the strength of attraction towards an home range centre.

We note however this was a very simple analysis with a pragmatic objective: decide which data to use at a the later stage of estimating such strength of attraction towards an home range centre. Because this will be implemented assuming that the localizations available provide a representative sample of how the animals explore typically its home range , excluding

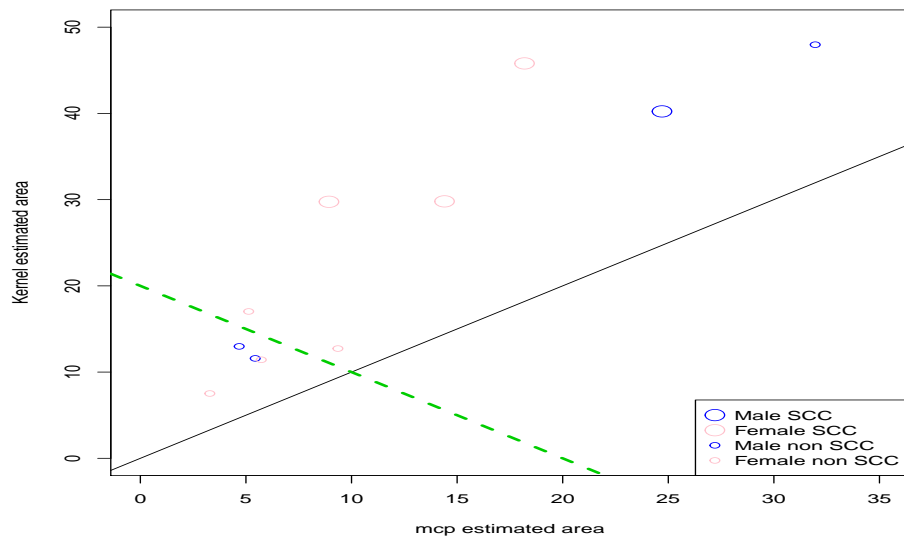


Figure 9: Relation between the estimated home range area per animal using the kernel estimator and the minimum convex polygon (mcp) methods, with a green line separating long (more than 14 days) and short deployments. Sex and closeness to a mini war SCC exercise also shown.

short deployments leading to small estimate home ranges makes sense, as these will likely correspond to animals that were not allowed to fully explore their home range (during the small temporal observation window available).

If there was a clear ecological question being asked about the home range size of these animals one would probably require considerably more data to answer the question adequately.

4 Further analysis of selected tags

Based on the previous section, we selected a number of tags for further processing. These will be used as a basis to estimate parameters of movement models via an Approximate Bayesian Computation (ABC). The rationale of ABC is to simulate according to a model and a set of distributions for the parameters of interest. Then for each simulation keep the parameter values used in said simulation if some measure of “distance” between the observed tracks is lower than a threshold. As an example, keep all the tracks such that the distance to the home range center is never larger than k kilometers (where k is obtained from the available data). Reading about ABC is a must.

Here we begin by creating a list such that each component of said list will contain the locations for each animal, such that we can the apply functions over these array elements to get the statistics of interest.

A current problem is that we need to have all these measurements in compatible units. While we have the coordinates in Latitude and Longitude, we want distances in km and bottom depths (which will also be required as we want the movement at the home range scale to be such that shallow depths are avoided, as this is a clear feature of the data) are available in a grid of different units.

We can project these data into km using the function `latlong2km` in package `dsm`; only after after that we can calculate the geometric centroid associated with each tag.

```
#converting the Lat Long coordinates to unit system  
#being used for the overall simulation exercise  
#-----  
#reference point used for the coordinate system in meters  
#from "simulation.R"  
library(dsm)
```

```

ref=c(-78.4133,23.1383)
for (i in 1:ntags){
  coordtemp=latlong2km(tags[[i]]$Lon,tags[[i]]$Lat,ref[1],ref[2])
  tags[[i]]$x=coordtemp$km.e
  tags[[i]]$y=coordtemp$km.n
}
rm(coordtemp)
#an example of an animal just to see all seems OK
#par(mfrow=c(1,2))
#plot(tags[[2]]$Lon,tags[[2]]$Lat)
#plot(tags[[2]]$x,tags[[2]]$y)
#exporting the information on the tags
#to read in the simulation folder
#to be able to plot these in that context
save(tags,file="tags.Rdata")
#looking at the data
#for (i in 1:ntags){
#points(tags[[i]]$x,tags[[i]]$y,type="l",col=i)
#}

```

One of the key features we want our movement model to reproduce is the home range property, i.e. animals will present some site fidelity instead of wandering off to infinity.

It is sensible to assume that for these tags, the geographic centroid of the available positions is an estimate of the center of such home range (here loosely defined as the position around which one could typically find the animals). Therefore we calculated the centroid for each animal's positions. Figure 10 presents the location data for these 5 animals as well as the corresponding centroids. While as mentioned above, for the sake of pragmatism, we are ignoring location measurement errors at this stage, it seems clear that for animal PTT=129715 there are at least a couple locations which are impossible (as these happen to be on land). We remove these from further analysis.

We can now evaluate, for each animal, how far away it typically is from its centroid. Also, a measure of the maximum distance one is likely to observe might be useful. These are both features that our movement model should be able to reproduce. In figure 11 we present the mean, 90th percentile and

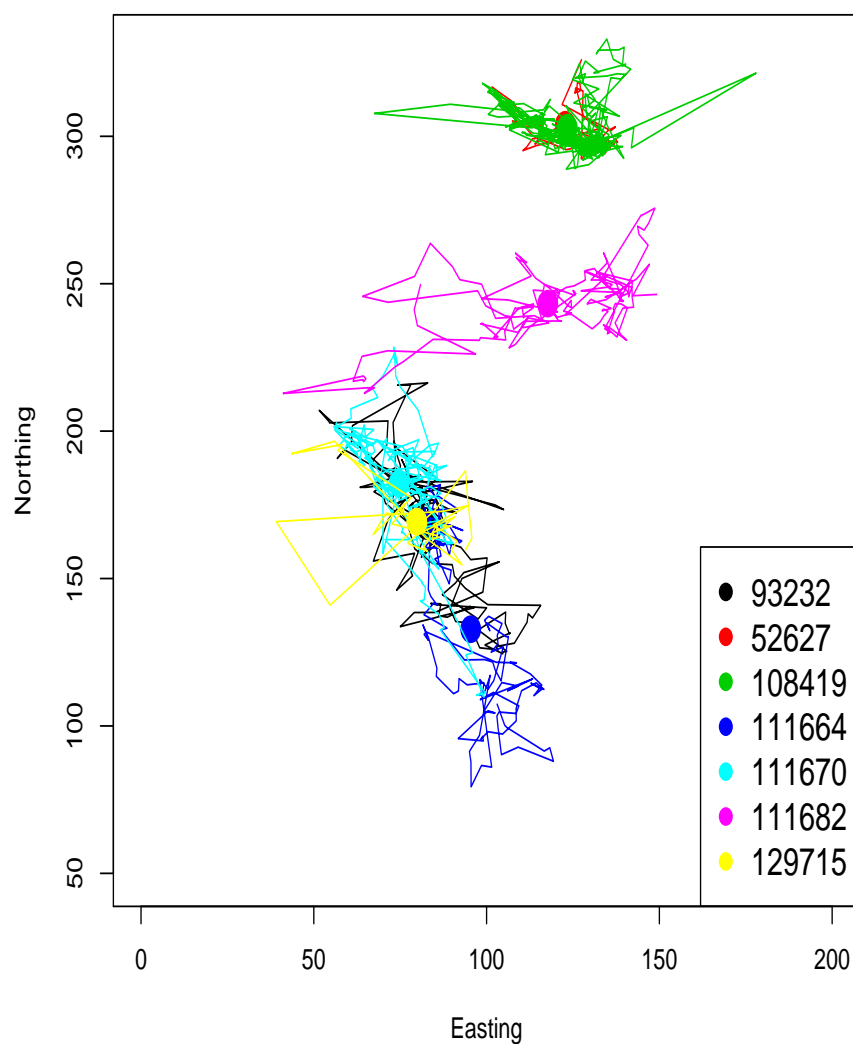


Figure 10: The locations of the animals selected for further analysis, with the respective centroids shown.

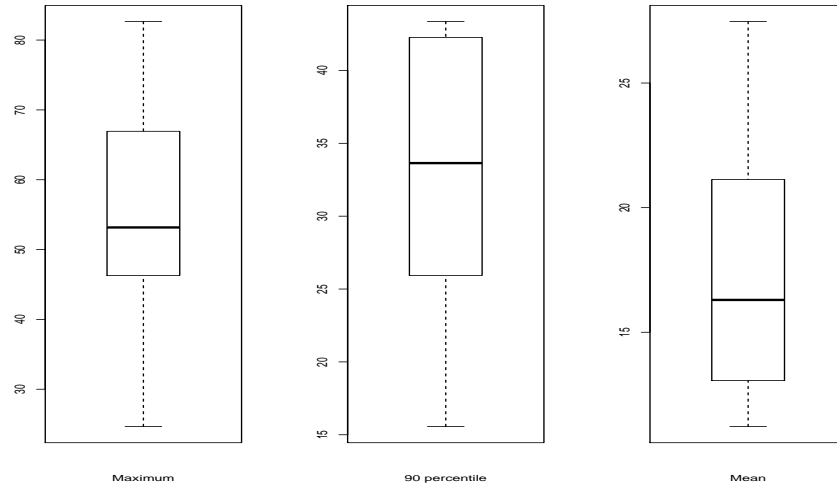


Figure 11: The maximum, 90th percentile and mean distance in kilometers between locations and the centroid for each of the animals with longer deployments.

maximum distance of animal’s position for their respective centroids.

We can look at the distance from the centroid for all positions pooled across animals (Figure 12). While there is a lack of distances in the first 5 km, the remainder of the distribution seems a decreasing function of distance. The absence of locations at the center is actually likely an artifact due to the area available (there is a clear analogy with point transect data). This seems to hint for a ”home range” mechanism of attraction which starts to occur at around 20 km and is really strong beyond say 40-60 km.

We can summarize the information in these distributions in order to try to get a feeling for what kind of statistics one might hope to aim for within an ABC context.

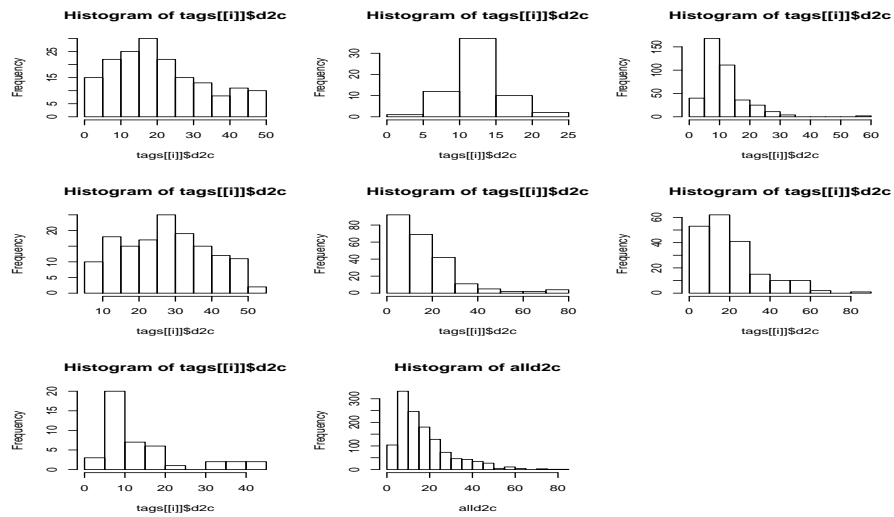


Figure 12: Histogram of distances from the centroid for all positions pooled across animals.

Exploratory analysis of a simultaneous multi animal DTAG data

Tiago A. Marques & Len Thomas

Centre for Research into Ecological and Environmental Modelling
The Observatory, University of St Andrews, St Andrews, KY16 9LZ, Scotland

Version's date: June 28, 2011¹

Contents

1	Introduction	1
2	Data details	1
3	Exploratory Data analysis	2
	References	5

1 Introduction

In this document we present an analysis of a DTag data set in which 3 sperm whales were simultaneously tagged.

2 Data details

Data was sent as a .csv file by Mark Johnson on the 11th October 2010. The .csv file has columns (identified by a header line):

1. time in seconds (referred to tag B);

¹ This document was created using Sweave, using R version 2.12.0 (2010-10-15) on a i386-pc-mingw32 platform.

2. depth of whale A, B, C in meters, adjusted to the same time clock;
3. distance between pairs of whales A-B, A-C and B-C in meters

Depth accuracy is better than 1 m and distance accuracy is better than 10 m. Empty cells indicate times when the distance could not be measured.

The header of this file was manually edited and the blank fields manually changed to "NA". This file was then read into R.

3 Exploratory Data analysis

A summary of the data is presented in table 1. A data point is provided every 3 seconds. The data spans a 11.46 hours period. We can see that there are a considerable number of seconds points for which the inter-animal distances are not available. These essentially correspond to times when the corresponding pair of animals was not at depth producing clicks (distance between whales is presumably obtained by considering that you know when a click was produced by whale A, you know when it was received by whale B, and you know the speed of sound in the water, so you can get the distance by the difference in those times).

If we plot the 3 whales depth over time the synchronicity of the animals is remarkable (Figure 1). While at the start of the data one of the whales is coming up while the others are going down, they sort of get in sync at around second 6000, and then for most of the time the whales dive synchronously (6 deep dives non-stop), then just A and C do the 7th deep dive, then just A does the 8th deep dive. They then spend a while at the surface, and resume deep diving at about the same time (37000 seconds in), performing two (and a half, when the tag data stops) additionally almost perfectly synchronized dives.

We can plot the average distance between whales i ($i = A, B, C$) as a function of whale's i depth (Figure 2). While we were expecting to see some pattern, like say whales being closer at the surface and more spread out while deep diving, the plots display an otherwise apparent lack of discernible pattern. Would this make more sense if one would look at it within dives?

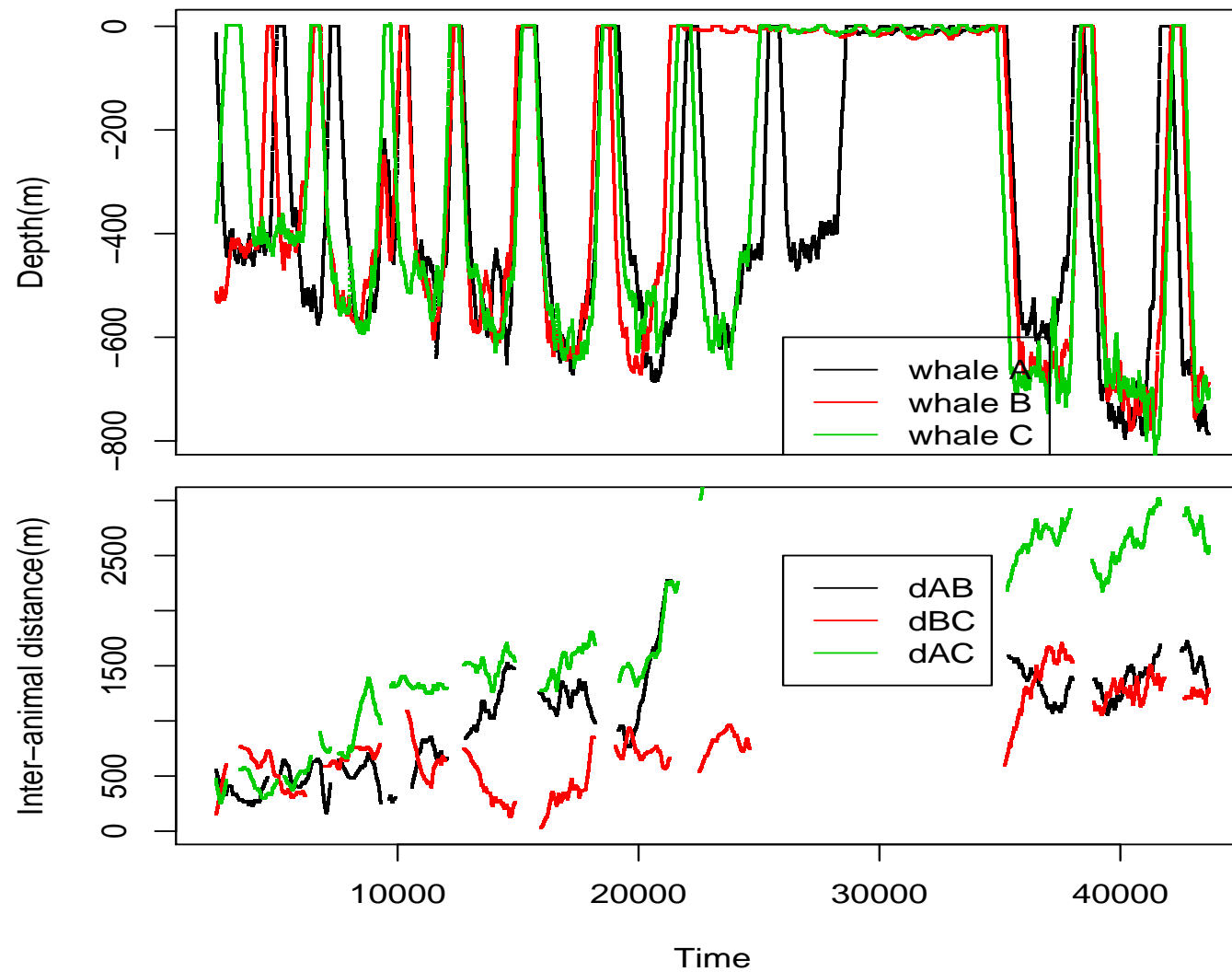


Figure 1: Depth profiles for the 3 sperm whales simultaneously tagged (top panel). The synchrony is remarkable. Distances between animals (bottom panel)

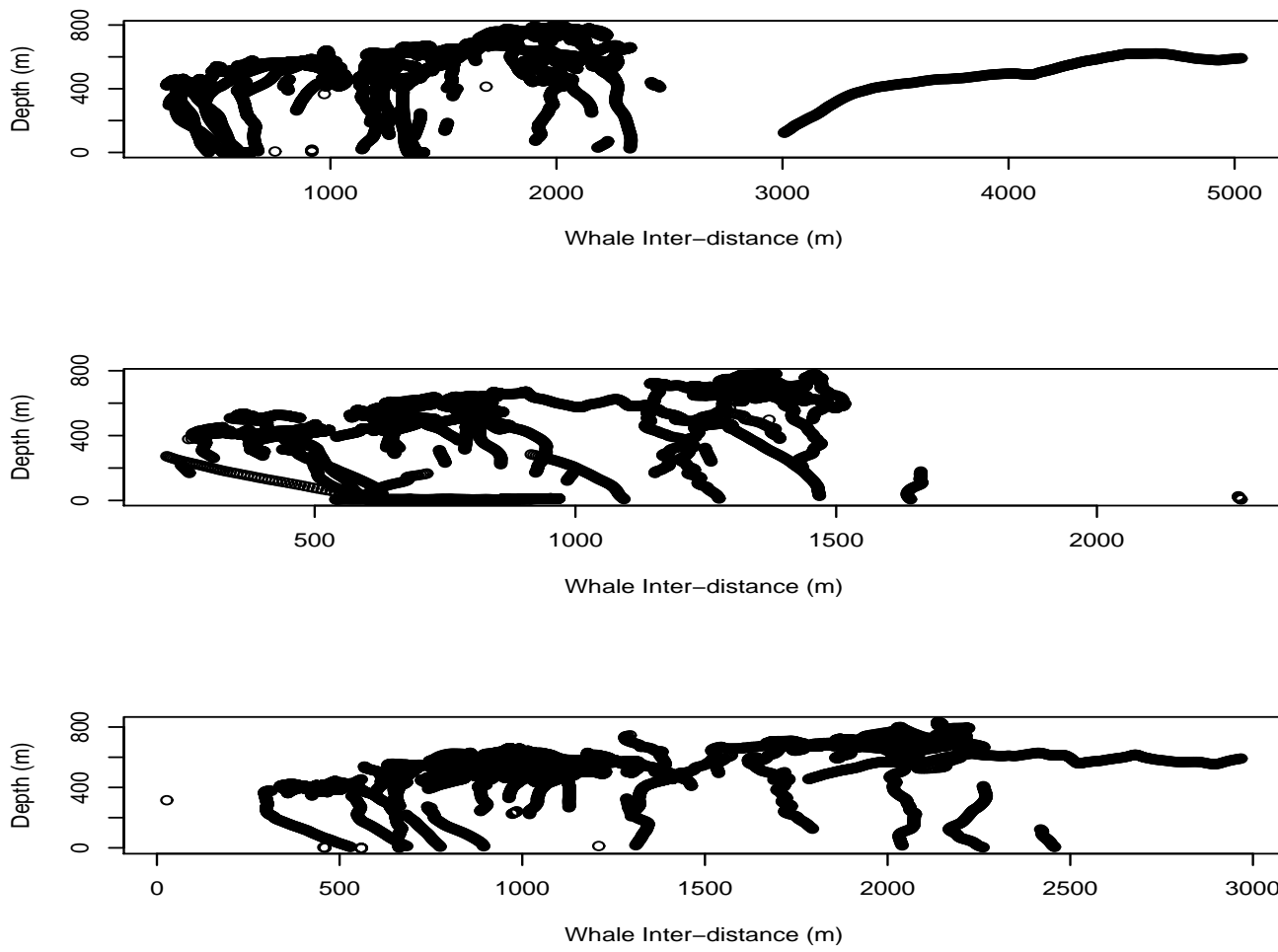


Figure 2: Mean distance of whale i ($i = A, B, C$) to the remaining two whales as a function of whale depth (A - top, B - middle, C - bottom).

References

time		zA			zB			zC			dAB			dAC			dBC		
1	Min. : 2450	Min. : -0.05865	Min. : -0.5139	Min. : -5.352	Min. : 167.2	Min. : 257.2	Min. : 27.1	Min. : 538.7	Min. : 727.0	Min. : 796.7	Min. : 1141.7	Min. : 1706.2	Min. : 6222.0	Min. : 1275.3	Min. : 1525.5	Min. : 1749.3	Min. : 2558.9	Min. : 5028.8	Min. : 6406.0
2	1st Qu.:12761	1st Qu.: 12.13690	1st Qu.: 8.0675	1st Qu.: 8.447	1st Qu.: 594.5	1st Qu.:1275.3	1st Qu.: 538.7	1st Qu.: 727.0	1st Qu.: 796.7	1st Qu.: 1141.7	1st Qu.: 1706.2	1st Qu.: 6222.0	1st Qu.: 1275.3	1st Qu.: 1525.5	1st Qu.: 1749.3	1st Qu.: 2558.9	1st Qu.: 5028.8	1st Qu.: 6406.0	1st Qu.: 796.7
3	Median :23072	Median :413.38500	Median :266.7980	Median :392.560	Median :1113.7	Median :1525.5	Median : 727.0	Median : 796.7	Median : 1141.7	Median : 1706.2	Median : 6222.0	Median : 1275.3	Median : 1525.5	Median : 1749.3	Median : 2558.9	Median : 5028.8	Median : 6406.0	Median : 796.7	Median : 1141.7
4	Mean :23072	Mean :336.10399	Mean :283.8964	Mean :318.948	Mean :1008.8	Mean :1749.3	Mean : 796.7	Mean : 1141.7	Mean : 1706.2	Mean : 6222.0	Mean : 1275.3	Mean : 1525.5	Mean : 1749.3	Mean : 2558.9	Mean : 5028.8	Mean : 6406.0	Mean : 796.7	Mean : 1141.7	Mean : 1706.2
5	3rd Qu.:33383	3rd Qu.:545.86250	3rd Qu.:542.9640	3rd Qu.:565.738	3rd Qu.:1371.2	3rd Qu.:2558.9	3rd Qu.:1141.7	3rd Qu.: 1706.2	3rd Qu.: 6222.0	3rd Qu.: 1275.3	3rd Qu.: 1525.5	3rd Qu.: 1749.3	3rd Qu.: 2558.9	3rd Qu.: 5028.8	3rd Qu.: 6406.0	3rd Qu.: 796.7	3rd Qu.: 1141.7	3rd Qu.: 1706.2	3rd Qu.: 6222.0
6	Max. :43694	Max. :794.81200	Max. :780.2400	Max. :833.044	Max. :2276.5	Max. :5028.8	Max. :1706.2	Max. : 6222.0	Max. : 1275.3	Max. : 1525.5	Max. : 1749.3	Max. : 2558.9	Max. : 5028.8	Max. : 6406.0	Max. : 796.7	Max. : 1141.7	Max. : 1706.2	Max. : 6222.0	Max. : 1275.3
7		NA's : 10.00000	NA's : 1.000	NA's : 1.000	NA's :6791.0	NA's :6406.0	NA's :6222.0	NA's :6222.0	NA's :6222.0	NA's :6222.0	NA's :6222.0	NA's :6222.0	NA's :6222.0	NA's :6222.0	NA's :6222.0	NA's :6222.0	NA's :6222.0	NA's :6222.0	NA's :6222.0

Table 1: Summary of the available data.

Modeling beaked whale density in the Bahamas

Tiago A. Marques & Len Thomas

Centre for Research into Ecological and Environmental Modelling
The Observatory, University of St Andrews, St Andrews, KY16 9LZ, Scotland

Version's date: December 9, 2013

Contents

1	Introduction	2
2	Region of inference	2
2.1	Hydrophone location	2
2.2	Bottom depth	4
3	The line transect survey data	4
3.1	Reading and formatting data	4
3.2	Data preparation for spatial modelling	9
3.3	A note regarding off effort sightings	9
3.4	Unit definition for the spatial model	11
3.5	A summary of the issues needing sorting	12
4	Density modelling and prediction grid	13
4.1	Density modelling covariates	13
4.2	Relevant covariates for prediction	13
4.3	Obtaining Additional covariates	13
	References	19

1 Introduction

In this document we present the steps required to model a spatial density surface of beaked whales in the Bahamas.

The visual line transect survey data itself was from Diane Claridge. Currently in this report we use 2011 and 2012 data, but 2013 data in a similar format is available and designed line transect surveys from previous years is also available, but requires additional formatting before use. There is also some additional acoustic line transect data which is not being accounted for at this point.

Bathymetry data was provided by Diane Claridge and Jessica Shaffer.

2 Region of inference

The region we want to make inferences over corresponds to the Tongue of the Ocean and the NE and NW Providence Channel (Figure 1), in the Bahamas. This is the area in broad vicinity of the AUTECH range. We begin by reading in the information about the AUTECH hydrophone location and bathymetry.

2.1 Hydrophone location

We begin by reading in the hydrophone data from a file that has been around since DECAF. Note that in this file the coordinates are in an arbitrary coordinate system, and here it might be better to have them in latitude and longitude, despite these having been shifted and jittered for security reasons. For that reason, we considered using the information archived on OBIS Seemap (available within the DECAF case studies data sets), as that has already been approved for public release. We consider here the data in file “seamap678.csv”, which had to be tweaked to filter the adequate information. Details are given in the .Rnw file. We see the hydrophones range between 1200 to 2000 meters deep, with a mean depth of -1652 m. Note that we corrected the hydrophone locations using depth information as described in Marques *et al.* (2012).



Figure 1: The AUTECH range location within the Bahamas region, with key islands and regions.

2.2 Bottom depth

The data set containing depths for the TOTO and Cul de Sac areas was provided by Jessica Shaffer via the file “Autec_Weapons_Range_0.2min_bathy.txt”. The resolution of depths available in this file is 0.0033 decimal degrees. Assuming roughly that 1 degree corresponds to 111km, this means that each grid cell corresponds to an area of 0.3663^2 km^2 . Note that this bathymetry data is actually hosted in another document’s folder. See Marques *et al.* (2012) for details. The bathymetry and hydrophone locations is shown in figure 2.

Additional bathymetry data was provided by Diane Claridge covering the NE and NW Providence channel. The full bathymetry coverage is presented in figure 4, which also includes the survey effort (see next section). Note that the bathymetry for the providence Channel has a resolution approximately 3^2 times higher than that for the TOTO, and for this reason we actually only use one out of every 3 values in each direction when creating a consolidated depth file (section 4.2).

Naturally we will only predict over a region which makes sense. In particular, that means that we should make sure that we do not predict into shallow waters not surveyed. It is expected that beaked whale density in these areas is negligible any way. For the time being we conservatively restrict ourselves to areas deeper than 50 meters, but arguably even at depths considerably deeper than this (say 200m or so) density might be negligible.

It might be more convenient to work with projected coordinates into an appropriate x, y system. We do so by leveraging on a function from package `dsm (latlong2km)`.

3 The line transect survey data

3.1 Reading and formatting data

The visual line transect survey data was contained in Access databases provided by Diane Claridge. These consisted of the following self-explanatory named files:

- Bahamas_June_2011_editted.mdb
- Bahamas_June_2012_editted.mdb

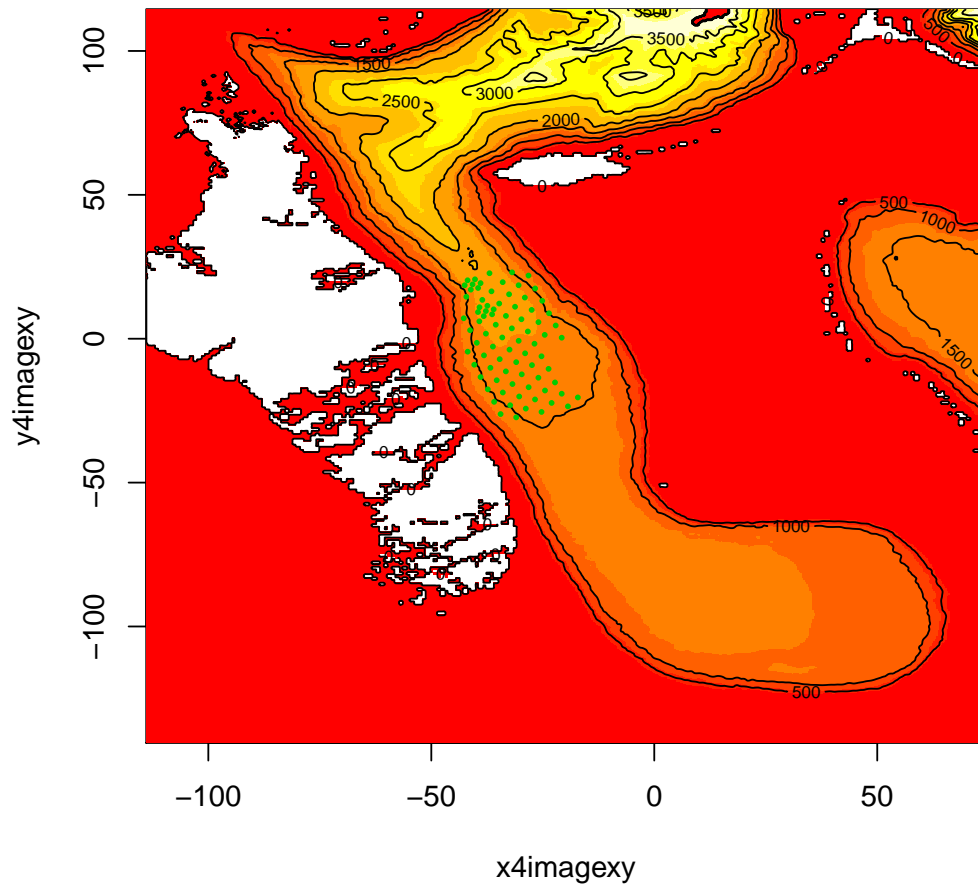


Figure 2: The AUTECH range within the Tongue of the Ocean. Green dots represent best available hydrophone locations. Yellow is deep and red is shallow, while white represents land. Note projected coordinates into a arbitrary x,y system with 1 km side units.

The relevant information for each database was present in 4 tables (note many more are present in the original Access files):

1. GpsData - the spatial location information. Allows spatial indexing of information in the other tables via the field index, which has a corresponding field GPSIndex in those tables.
2. effort - effort description; links to GpsData's index field via GPSIndex. We assumed the GPSIndex in an effort table row represents the first waypoint of that transect leg, and all the subsequent GPS records in GpsData up till the next GPSIndex in the next effort row correspond to waypoints in the previous leg¹.
3. Primarysighting - detection data; links to GpsData index field via GPSIndex.
4. LookUp - descriptions for the abbreviations/terms used

We can take a first look at the actual survey data, effort and sightings, as that will be helpful in defining the width and length of the segments to be used for the spatial model. The first step was to combine the information between the different tables, taking care to exclude the off effort periods. This actually proved much harder than expected, because there were a number of issues creating artifacts in the data (extra long transects, ghost transects, etc). In particular there were also a number of problems in associating effort legs with GPS records. These were solved in a pragmatic way to allow implementation of the analysis. A full description of the problems and how they were dealt with is provided in a separate document ("problems and proposed solutions.docx"). These problems were solved in close collaboration with Diane Claridge. Additional problems relating mostly to coordinates recorded as 0 leading to extremely long transects or ghost transects were also addressed in "problemchecks".

The detection distances and length of on effort transect legs are shown in figure 3. The survey effort is shown in figure 4. To make sure that nothing felt out of place, the detections and on-effort transect legs from which detections were made are presented in figure 6.

¹As it will become apparent later, this created problems, because sometimes the boat would go off effort, logging data in the GPS table, but not logging that as off effort in the effort table, creating ghost transects.

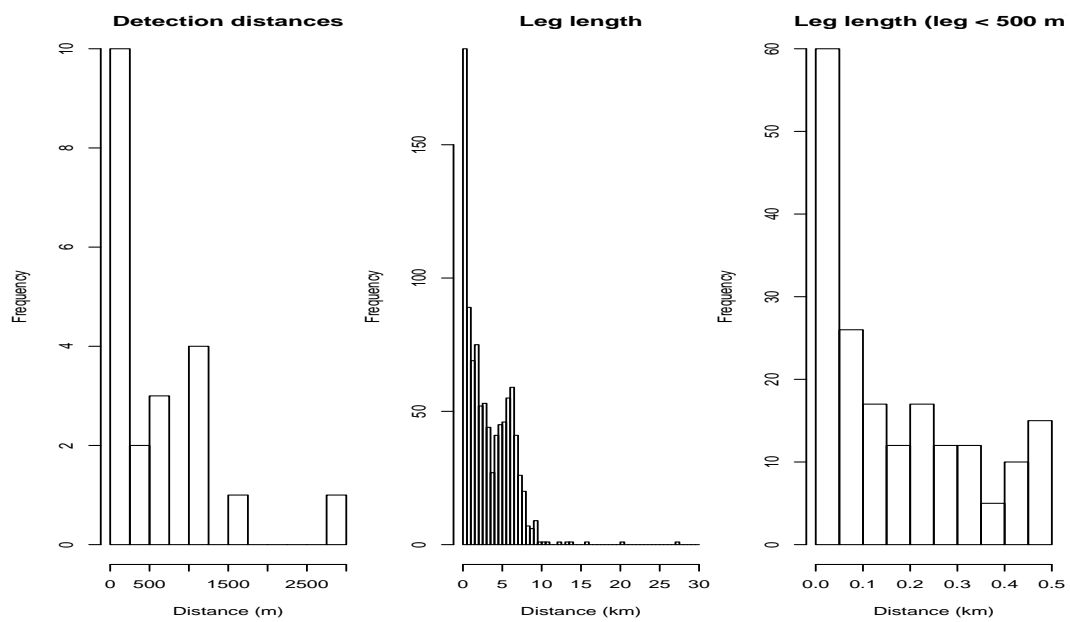


Figure 3: The detection distances to *Mesoplodon* sightings (left panel) and the effort legs (right panel zooms in the first bar of middle panel).

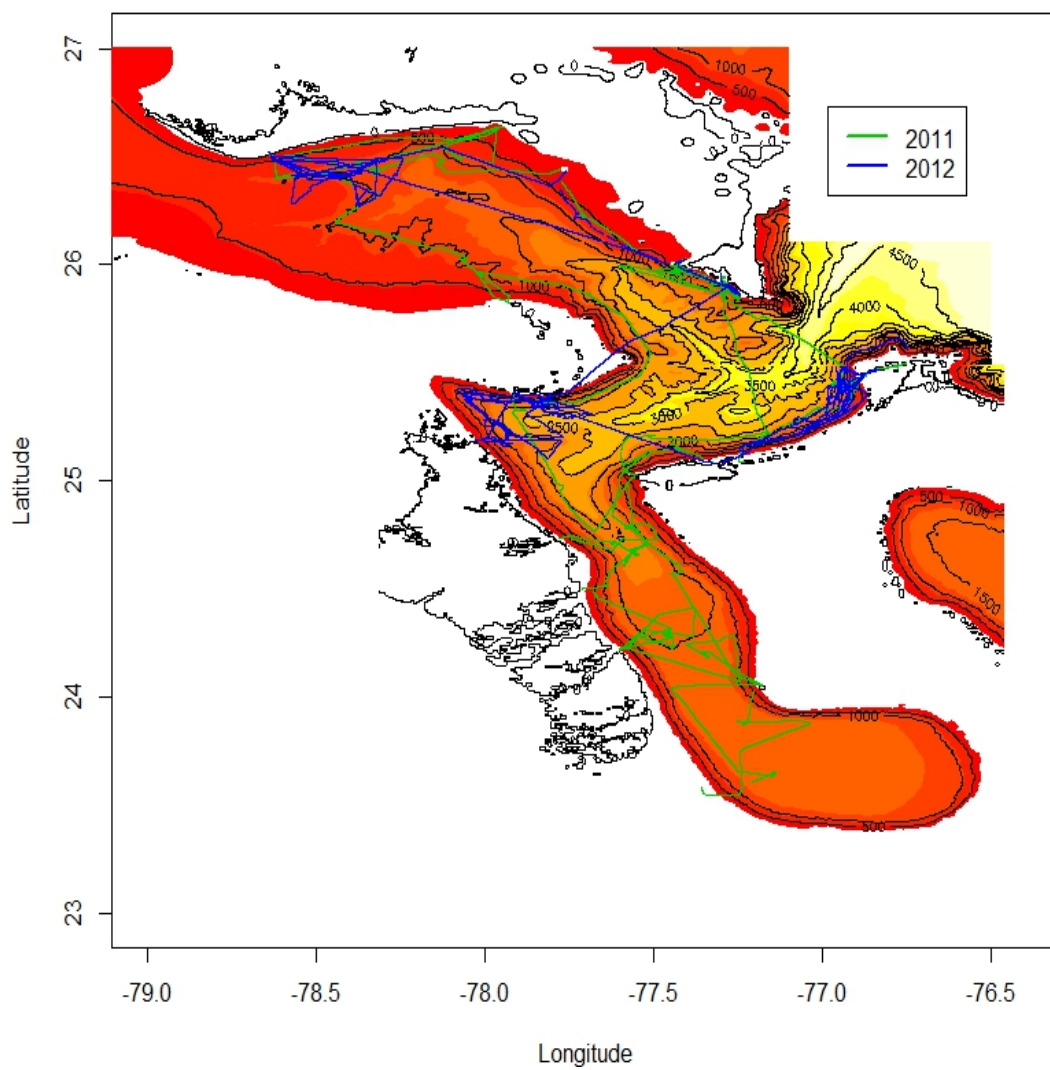


Figure 4: The entire area for which predictions are required, with the survey effort overlaid.

3.2 Data preparation for spatial modelling

The data adequately formatted to implement the distance sampling analysis is included in 3 separate objects:

1. **data4p**: includes just the distance data, used for the modelling of the detection function
2. **dataDlike**: includes just the effort data as usually formatted in distance
3. **data4sdm**: obtained by merging the above two objects, includes the observations associated with the adequate effort leg. Note that merging only worked adequately because there was at most 1 sighting per leg. Otherwise, merging would have to be replaced by a procedure that actually counted the number of sightings per transect length, as otherwise legs with k sightings would appear repeated k times in this object, rather than a single line with an associated count of k .

We have 24 detections for beaked whale groups, of which 22 are Blainville's beaked whales and 2 are Gervais' beaked whales. We have distances for 21 of these sightings. An histogram of the distance data is present in figure 3. It seems clear that we currently do not have a reasonable large enough sample to model a detection function.

3.3 A note regarding off effort sightings

We have 24 detections, but only 16 actually correspond to available distances on effort, as 7 were off effort and 1 on effort sighting distance was unavailable. It seems like it could be possible to use these observations in the analysis:

1. for those recorded as off effort, if the standard survey protocol was being implemented these can be actually used both for the detection function modelling and the sdm (unlike what happens for design based approaches, as here we do not rely on design but on a model for predicting density outside the covered areas). This requires however that all line length which was associated with these off effort periods is accounted for, which is not the case at the moment (at the moment we just have here transect legs in which the data was deemed fit for detection function (but not encounter rate) estimation in a design based approach).

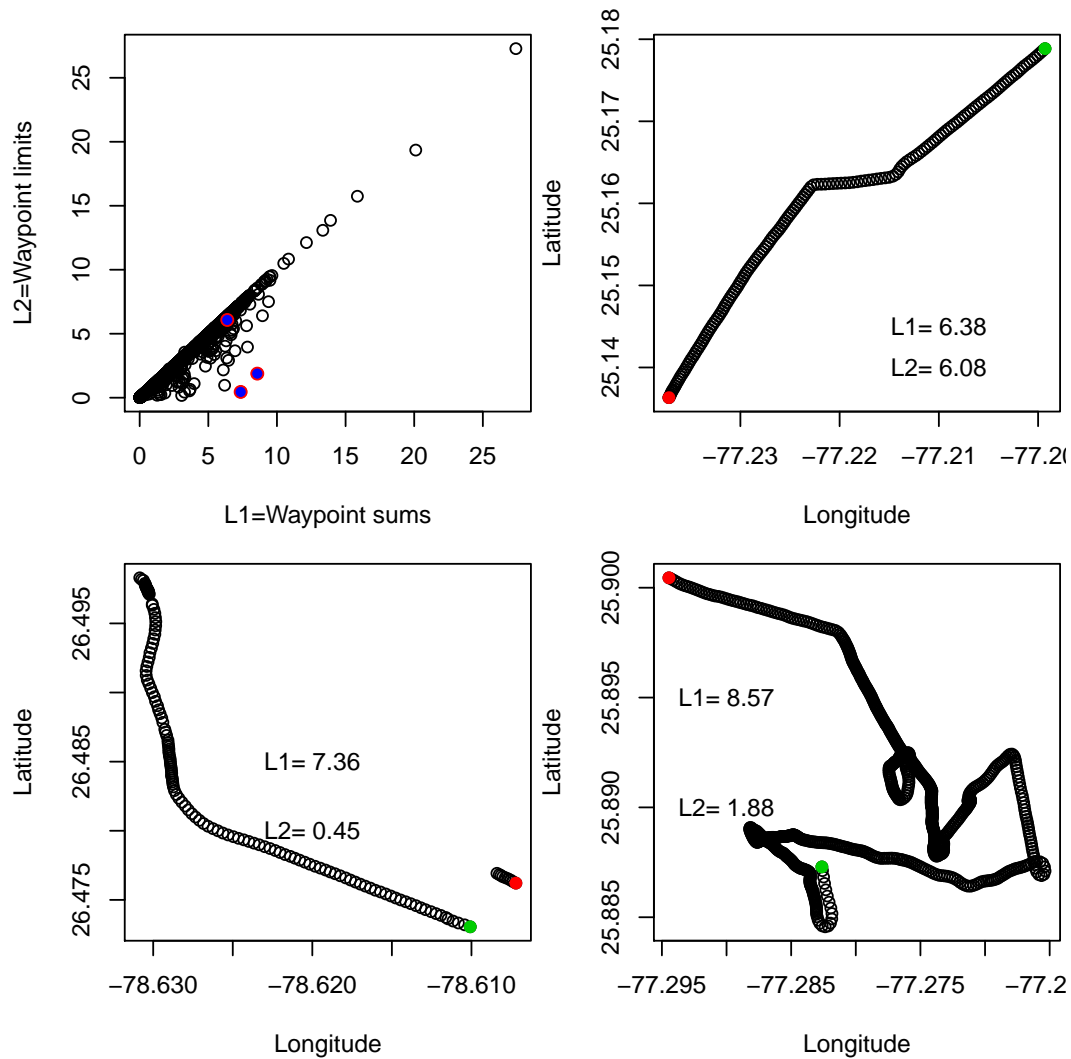


Figure 5: Leg distance depending on the measuring algorithm. Top left panel represents all legs, while remaining panels represent the 3 highlighted legs in the top left plot. For the detailed legs, the red and green dots representing the first and last point in the leg, respectively.

2. we can use in the sdm alone those recorded as on effort, but without a distance (i.e. these correspond to a segment with an animal on it, even if we do not have the corresponding distance).

3.4 Unit definition for the spatial model

For building the count model (sensu Hedley and Buckland (2004)) a preliminary segment definition of squared units of 3000 m side might seem appropriate. If we look at figure 3 it also seems like the actual legs themselves might be used as individual segments. However, actually zooming in the smaller legs reveals a potential problem (figure 3). There are many very small legs, say less than 100 meters long. It makes sense to concatenate these, as a boat transect of 100 meters is meaningless and it will lead to too many zeros for modelling (due to the small number of detections). A somewhat halfway house is to break down larger transects and concatenating smaller ones. **This is however not easy to do automatically, because by now it is not certain whether there are off effort legs between these on effort small legs.**

To obtain the length for each transect leg we assume that the sum of the distances between waypoints ($L1$) might be the easiest and more sensible implementation. Another option would be to calculate the distance between the start and end location of each transect ($L2$). While the later might be more adequate if the transects followed straight lines, with the former leading to overestimation of transect length being proportional to the number of GPS points between the extremes and the magnitude of GPS errors, we opted by the former because many legs were not linear, which would lead to underestimation of transect leg length if the distance between endpoints was then used. In figure 5 we explore the impact of using each of the approaches on survey effort. The top left plot presents the two ways of calculating the distances for all available legs. We zoom in 3 transect legs (highlighted in red in figure 5 top left panel) for further discussion:

- top right panel - the use of $L1$ seems reasonable, while $L2$ underestimates the line length.
- bottom left - a (perceived) transect leg which in fact corresponds to 2 different legs, with a gap of 15 hours between 2012-06-08 21:52:24 and 2012-06-09 10:12:42. **We do not know if the second leg, here**

corresponding to the large sub-leg, is on or off effort. But the key problem is that this actually means that many of the legs away from the 1:1 line in figure 5, left panel, corresponding to legs for which the distances are very different depending on how they get calculated, will require some dedicated human attention.

- bottom right - a leg which is essentially spaghetti; while $L1$ is the most reasonable line length, there are problems in terms of defining an offset area in the spatial model because we will tend to grossly overestimate the area covered.

Therefore, figure 5 reveals additional problems, which means that we are going to stop and think before moving forward. Together with the issues already detected before, this makes us think that it might be more productive to have someone cleaning up the original databases before this data is used any further.

3.5 A summary of the issues needing sorting

There are a number of data issues which require sorting:

- Issues described in word file “problems and proposed solutions.docx”;
- Issues described in the file “problemchecks.R”;
- Additional unidentified issues stemming from similar reasons as those above, namely due to incorrect GPS index associations, latitudes and or longitudes recording as 0’s and effort not logged in the effort tables but present in the GPS tables;
- Issues due to very small transects recorded which need to be glued together in a reasonable way (which can not be automated) - cf figure 3.

One should be careful because it is possible that some problems present were not identified above, and hence a general sanity check seems required at this point. Note in particular that these problems were only identified using the on effort legs. If we do decide to use off effort data as suggested in section, then making sure the off effort data is also adequate is fundamental.

4 Density modelling and prediction grid

In this section we describe the variables used for modelling density and the procedure of associating these to the transect legs (section 4.1) and how we obtained these in the prediction grid (section 4.2).

4.1 Density modelling covariates

We will create a density model based on the data frame `data4sdm`. For that reason we need to associate to each row of this object the corresponding variables potentially useful to model density. The available covariates include:

- x and y ; these are already included in `data4sdm`
- bottom depth
- distance to the edge
- distance to AUTECH
- bottom slope
- bottom aspect orientation

4.2 Relevant covariates for prediction

For the implementation of a density estimate over the wider area of inference we require an appropriate prediction grid. Details of how we obtain such a grid are in the `.Rnw`, but it involves consolidating the 3 bathymetry files into a single matrix, with resolution equaling the lower resolution available (i.e. TOTO/Cul de Sac data). The outcome, along with the survey effort and *Mesoplodon* detections, is presented in figure 7. We also need to obtain the value of each of the relevant variables mentioned in section 4.1 at the locations in the prediction grid.

4.3 Obtaining Additional covariates

We can obtain the distance to the boundary of the prediction area, as that corresponds to a potentially relevant ecological variable explaining density, as

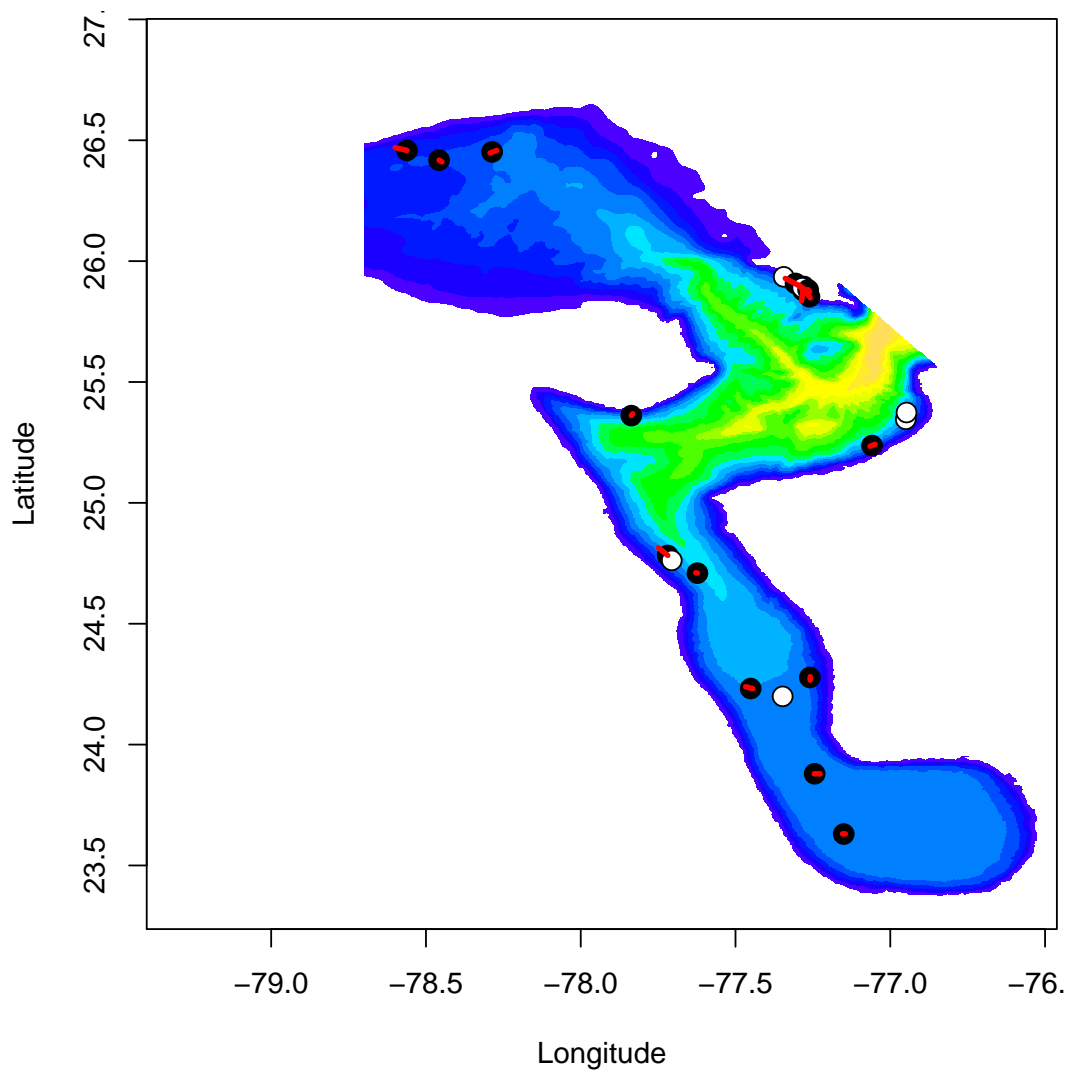


Figure 6: The locations of detected beaked whales (black dots, white dots are off effort detections), as well as the legs of on effort transects from which detections were made.

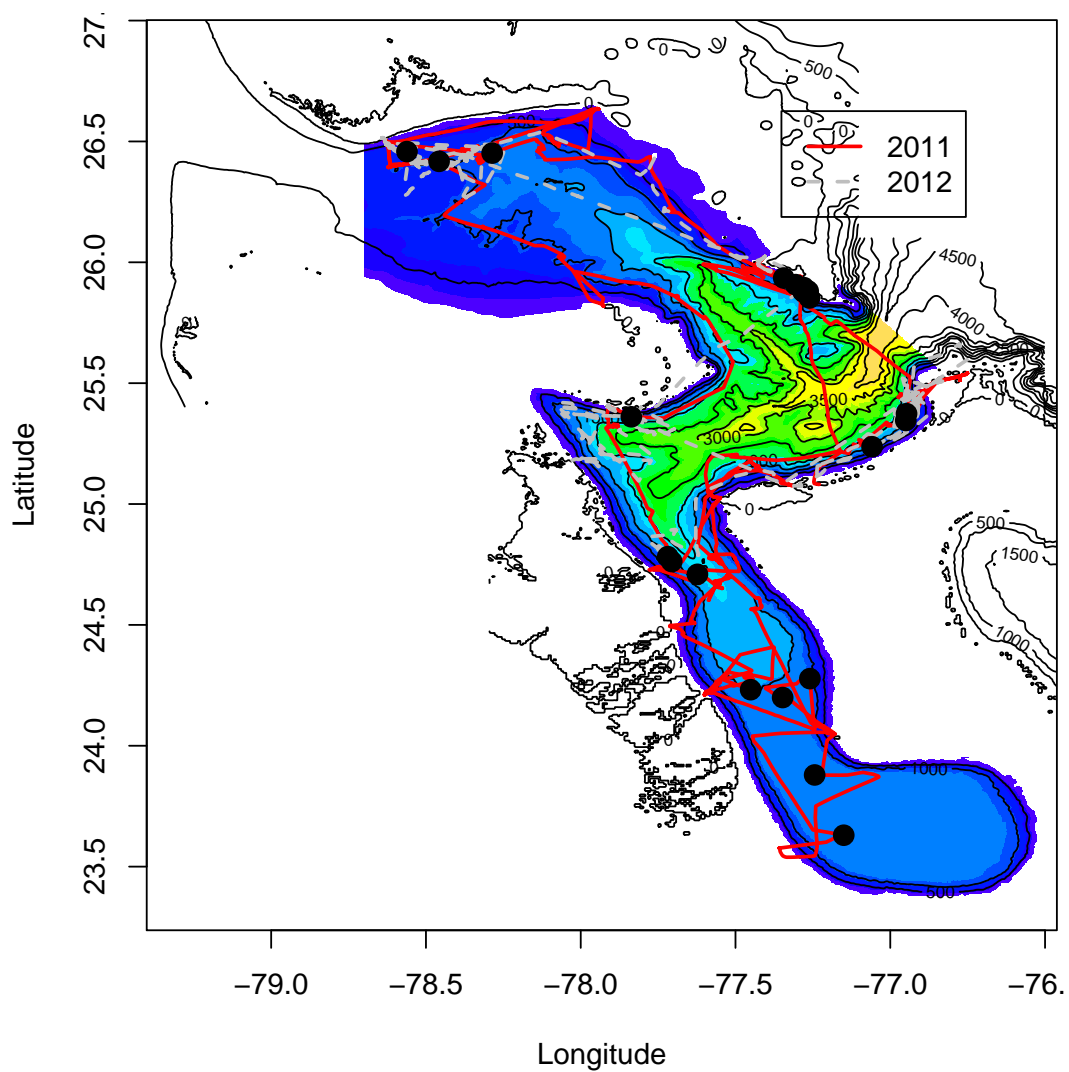


Figure 7: The grid to be used for prediction, with the survey effort superimposed on it. Black dots represent beaked whale detections.

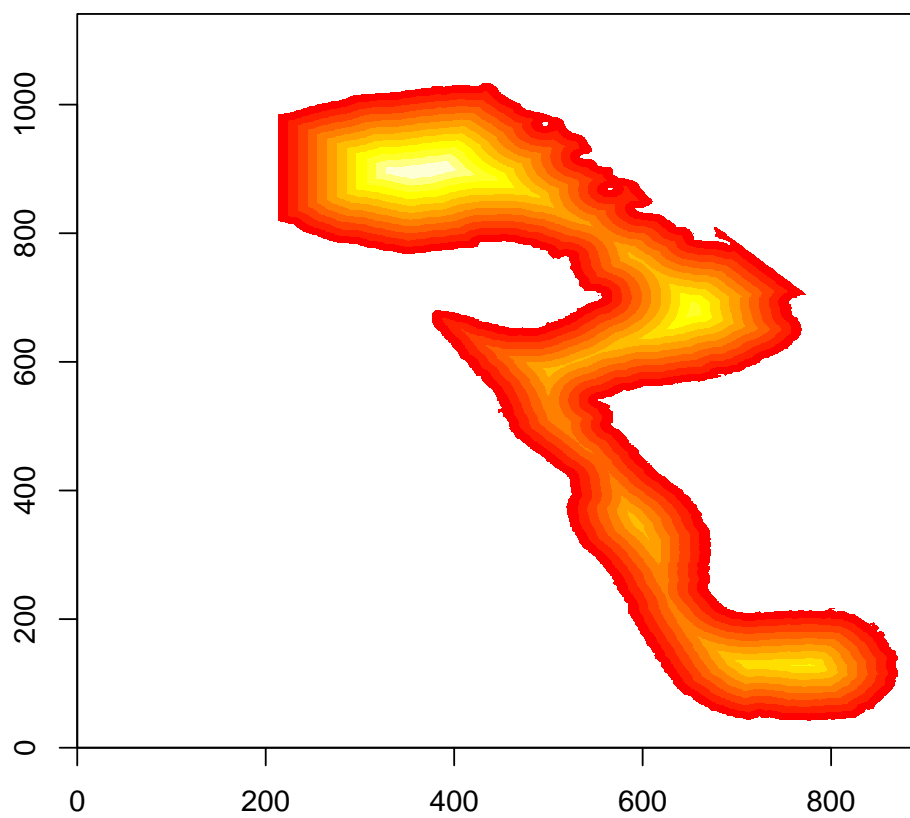


Figure 8: Distance to the boundary of the prediction grid.

the animals might have preferences to areas close to this (which corresponds to the 50m isodepth line). This is presented in figure 8.

We can also obtain a number of depth derived relevant variables like slope, aspect orientation, roughness. We leverage on package **raster** to do so, and the results are shown in figure 9. Note that slope and roughness seem highly collinear variables, so only one of these should be used in any given model.

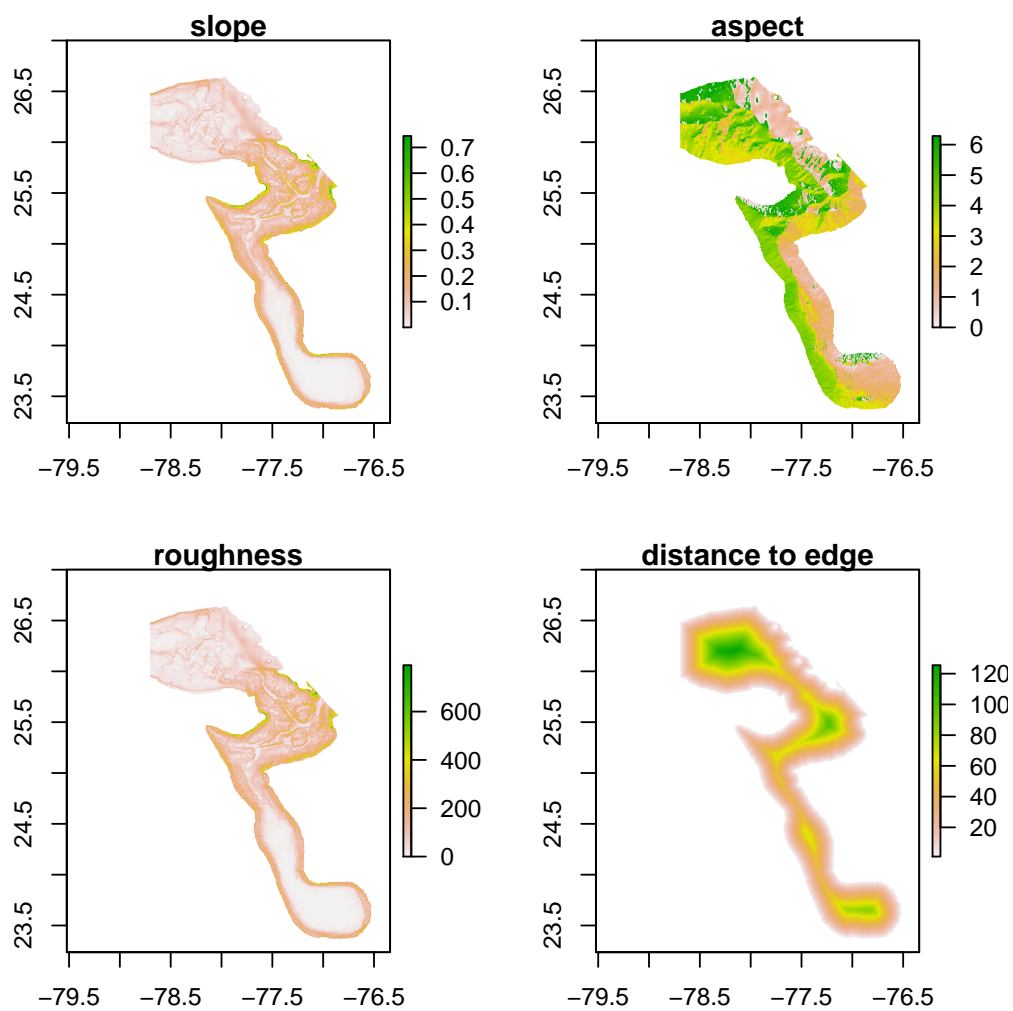


Figure 9: Slope, aspect orientation, roughness and distance to edge over the prediction grid.

References

- Hedley, S. L. and Buckland, S. T. (2004). Spatial models for line transect sampling. *Journal of Agricultural, Biological, and Environmental Statistics*, **9**(2), 181–199.
- Marques, T. A., Shaeffer, J., and Thomas, L. (2012). Procedure description: using AUTECH’s hydrophones surrounding a DTAGed whale to obtain localizations. Technical report, LATTE WORKING DOCUMENT.

Using dedicated Kalman Filter R packages to fit the georeferencing SSM

LATTE WORKING DOCUMENT

Tiago A. Marques & Len Thomas

Centre for Research into Ecological and Environmental Modelling
The Observatory, University of St Andrews, St Andrews, KY16 9LZ, Scotland

Version's date: 2 de Novembro de 2012

Conteúdo

1	Introduction	1
2	Previously fitted model	2
3	Fitting the SMM in KF specialized R packages	3
3.1	Fitting the SMM in MARSS	6
3.2	Fitting the SMM in KFAS	7
4	Aknowledgments	13
	References	13

1 Introduction

The current formulation for georeferencing the DTAG data considers a state space model with four states (speed, depth, x and y) and three observations (depth, x and y). Observations on x, y are only present when independent acoustic localizations are available.

Here we build directly on previous work where the SSM was fitted to DTAG data from Md248b. This is described in detail by Marques and Thomas (2012a). The reader is also referred to Marques *et al.* (2012) for details

about the process originating the localization data and to Marques and Thomas (2012b) for the description of the SSM considered, as well as a description of the rationale and previous steps leading to that.

This document contains the analysis of the data from the whale md07_248b. To set the scene, in section 2 we present the results obtained so far with the R implementation of Mark Johnson's MATLAB code.

Following this, in section 3.1 we try to reproduce these results using MARSS Holmes *et al.* (2012b,a), and in section 3.2 using KFAS Helske (2012).

2 Previously fitted model

As stated above, these results are taken from Marques and Thomas (2012a). In said report the state space model fitted to the data included 4 states

$$\begin{pmatrix} s_t \\ z_t \\ x_t \\ y_t \end{pmatrix} = \begin{pmatrix} 1 & 0 & 0 & 0 \\ -\sin(\phi_t)\Delta T & 1 & 0 & 0 \\ \Delta T \cos(\phi_t) \sin(\psi_t) & 0 & 1 & 0 \\ \Delta T \cos(\phi_t) \cos(\psi_t) & 0 & 0 & 1 \end{pmatrix} \begin{pmatrix} s_{t-1} \\ z_{t-1} \\ x_{t-1} \\ y_{t-1} \end{pmatrix} + \begin{pmatrix} \omega_{s_t} \\ \omega_{z_t} \\ \omega_{x_t} \\ \omega_{y_t} \end{pmatrix} \quad (1)$$

and we assume that at every time step there is a depth observation, but also that every so often, when the animals are deep diving, we might actually observe some x, y coordinates from acoustic localizations leading to the following observation equation:

$$\begin{pmatrix} o_{z_t} \\ o_{x_t} \\ o_{y_t} \end{pmatrix} = \begin{pmatrix} 0 & 1 & 0 & 0 \\ 0 & 0 & 1 & 0 \\ 0 & 0 & 0 & 1 \end{pmatrix} \begin{pmatrix} s_t \\ z_t \\ x_t \\ y_t \end{pmatrix} + \begin{pmatrix} v_{z_t} \\ v_{x_t} \\ v_{y_t} \end{pmatrix} \quad (2)$$

where we often have missing values in o_{x_t} and o_{y_t} .

To reproduce the results here we first need to read in a number of R objects. This is done silently in the pdf, but the .Rnw document contains all the required code to do so.

Figure 1 represents the track prediction both ignoring (left plot) and using (right plot) the acoustic localizations. In figure 2 we zoom in the right plot. Although virtually indistinguishable at the scale being plotted, note as expected there is not a complete overlap between the estimated georeferenced track and the acoustic localizations used. The extent to which these two

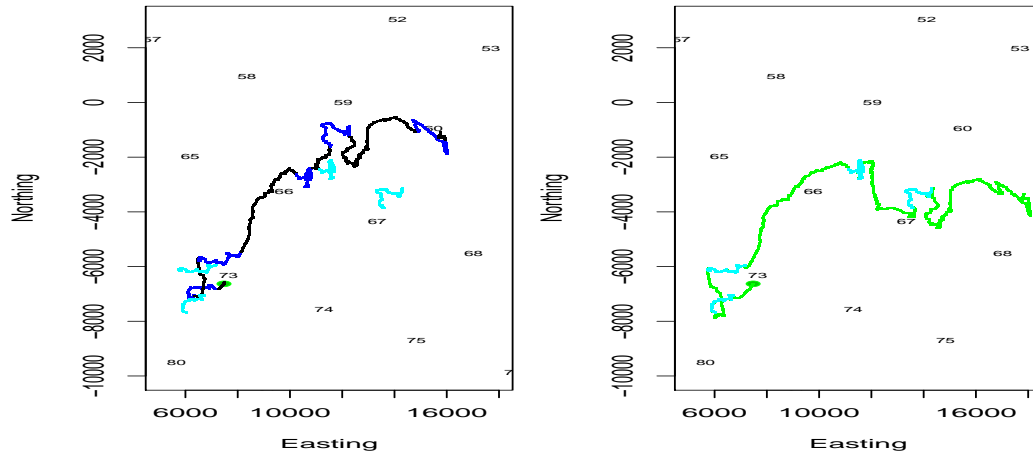


Figure 1: Track prediction before using x, y observations (left) and after using x, y observations. Note the predicted smoothed track is for the right plot very close to the acoustic localizations considered (virtually indistinguishable at the scale being plotted).

overlap depends on how much credit we give to the acoustic localizations themselves compared to the process model. These are influenced by the relative weights of measurement error on (x, y) and the state process itself.

We can take a look at predictions from this latest formulation (Figure 3). As expected, we see that the variance in x, y vanishes every time we actually have x, y observations, because we assume there to be little observation/measurement error in (x, y) . The extent over which this is reasonable still requires additional thinking.

The next step is to bring in the angles ϕ and ψ as states, hence leading to a 6 states and 5 observations SMM.

3 Fitting the SMM in KF specialized R packages

We now turn into trying to estimate the SSM described in the previous section using specialized R packages for Kalman Filter estimation. A description of possible packages to do so is available in Tusell (2011). This option seems

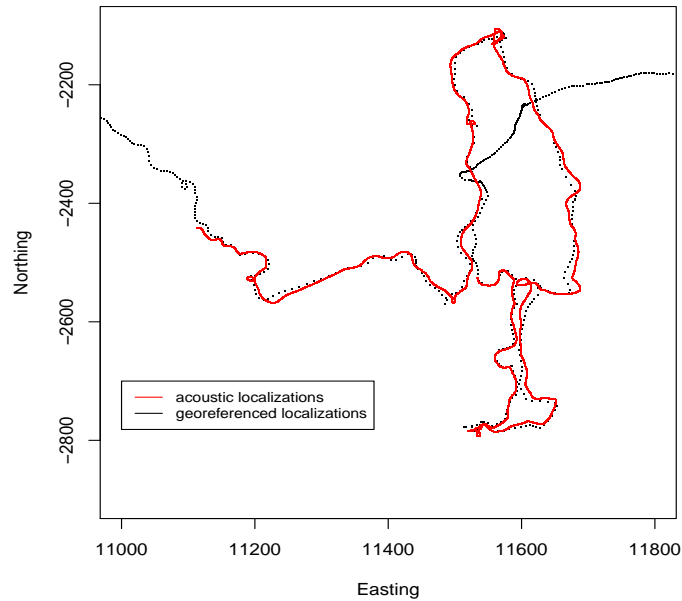


Figure 2: Zooming in on the 3rd dive of Md248b.

desirable for at least two reasons:

- it is reassuring if we obtain the same results, given that we coded our KF implementation ourselves, and these has been tested by others;
- it might be easier to generalize code to other models. In particular, Holmes *et al.* (2012b) mention that MARSS “... development will include Bayesian estimation and constructing non-linear time-series models.

In this section we attempt to fit the previously fitted model using specialized R packages. We consider two options

- MARSS (Holmes *et al.*, 2012b,a).
- KFAS (Helske, 2012)

The first required step is to build the time varying transition matrix. Note that this is varying over time not because there is any change in the way the state is updated, but because the transitions are dependent on time varying covariates. We do that below:

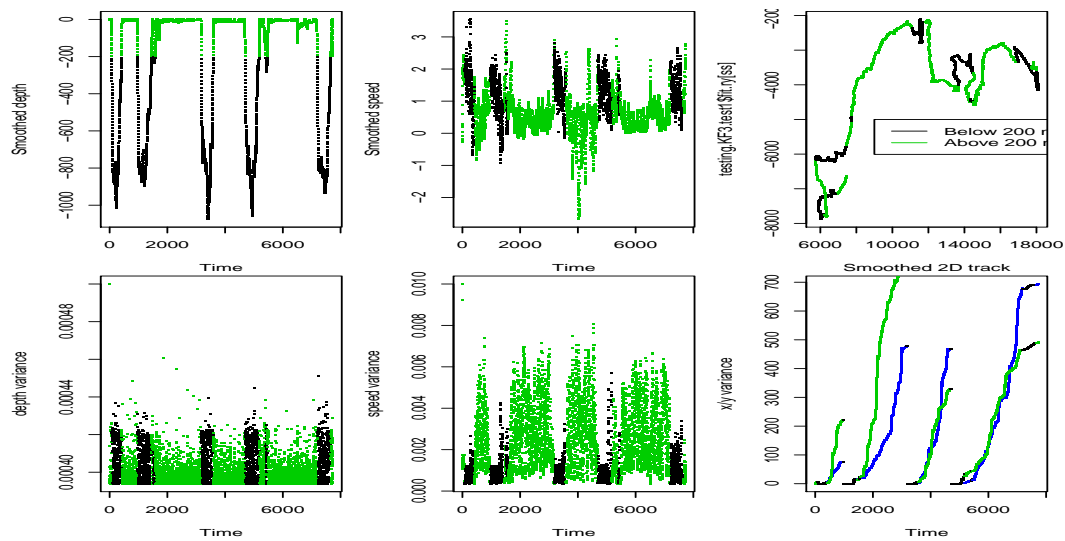


Figure 3: Results of fitting the SSM with 4 states and 3 observations to the data. Top row: estimates. Bottom row: corresponding variances. Left: Depth; Center: speed; Right: x, y coordinates. In the bottom right plot the blue corresponds to x and the green to y .

```

> #This is based heavily on code sent by Elizabeth Holmes via
> #e-mail on the 31/08/2012 19:45
> #the time between samples
> delT=0.2
> #T is the number of time steps
> nT=nrow(new.georef)
> #set up the base structure for Bt
> Bt=array(diag(4),dim=c(4,4,nT))
> #set the time dependent bits
> for(i in 1:nT){
+ Bt[2,1,i]= -sin(new.georef$pitch[i])*delT
+ Bt[3,1,i]= delT*cos(new.georef$pitch[i])*sin(new.georef$head[i])
+ Bt[4,1,i]= delT*cos(new.georef$pitch[i])*cos(new.georef$head[i])
+ }

```

Now, let's move on to fitting in the actual packages.

3.1 Fitting the SMM in MARSS

Despite contact with Elizabeth Holmes, the package lead author, we have not yet managed to get MARSS to work over our data. We are waiting for additional feedback from Elizabeth regarding a bunch of current error messages when we try to fit to our data set in MARSS.

```

> #Next, we use this object within the fitting. We also set up a model object th
>
> #set the model list
> model.list=list()
> model.list$B=Bt
> model.list$Z=cbind(matrix(0,3,1),diag(3))
> model.list$Q="diagonal and equal" #or something like that
> model.list$R="diagonal and equal" #or something like that
> model.list$U="zero" #because U doesn't appear in your eqn on slide 10
> model.list$A="zero" #because A doesn't appear in your eqn on slide 10
> #model.list$x0=c(0.1,0.1,new.georef$x[1],new.georef$y[1])
>
> data=t(new.georef[1:nT,5:7])
> ##construct the MLEobj; set fit=FALSE since you don't actually need to estima

```

```

> #MLEobj=MARSS(data,
> #inits=list(x0=matrix(c(0.1,0.1,new.georef$x[1],new.georef$y[1]),ncol=1,nrow=4)
> #model=model.list,fit=FALSE,control=list(trace=-1))
>
> #construct the MLEobj; set fit=FALSE since you don't actually need to estimate
> MLEobj=MARSS(data,inits=list(x0=matrix(c(0.1,0.1,TAGONx,TAGONy),ncol=1,nrow=4)
+           model=model.list,fit=FALSE)
> #get states from MARSSkf
> kf=MARSSkf(MLEobj)
> names(MLEobj)
> summary(MLEobj)

```

Elizabeth did said that “MARSS is meant for estimation of parameters. It does have a time-varying Kalman filter, but it’s rather slow. I’d try the KFAS package which also has a time-varying Kalman filter and is much faster than that used in MARSS.”and continued with “MARSS is not optimized for speed and it’ll take a long time to work with a big dataset. I think KFAS uses basically the same sort of model specification as MARSS, so if you build your Z and B as above, you’ll be well on your way to model specification for KFAS also.”

Therefore, for the time being, we move on to KFAS.

3.2 Fitting the SMM in KFAS

We begin by loading up library KFAS.

```

> library(KFAS)

```

As a first attempt at fitting, we fit the model to the first 15000 time points. Observations and state estimates are presented in figure 4. Depth is about OK, but the x, y are totally nonsense. I wonder why? I believe that this is not really working because KFAS did not use the start values provided by argument $a1=c(0.1,0.1,TAGONx,TAGONy)$ in `SSModel`.

```

> nT=15000
> data=new.georef[1:nT,5:7]
> a1s=c(0.1,0.1,TAGONx,TAGONy)
> ISECm=SSModel(y=data,Z=cbind(matrix(0,3,1),diag(3)),T=Bt[,1:nT],a1=)
> teste1=KFS(ISECm)
> rm(a1s)

```

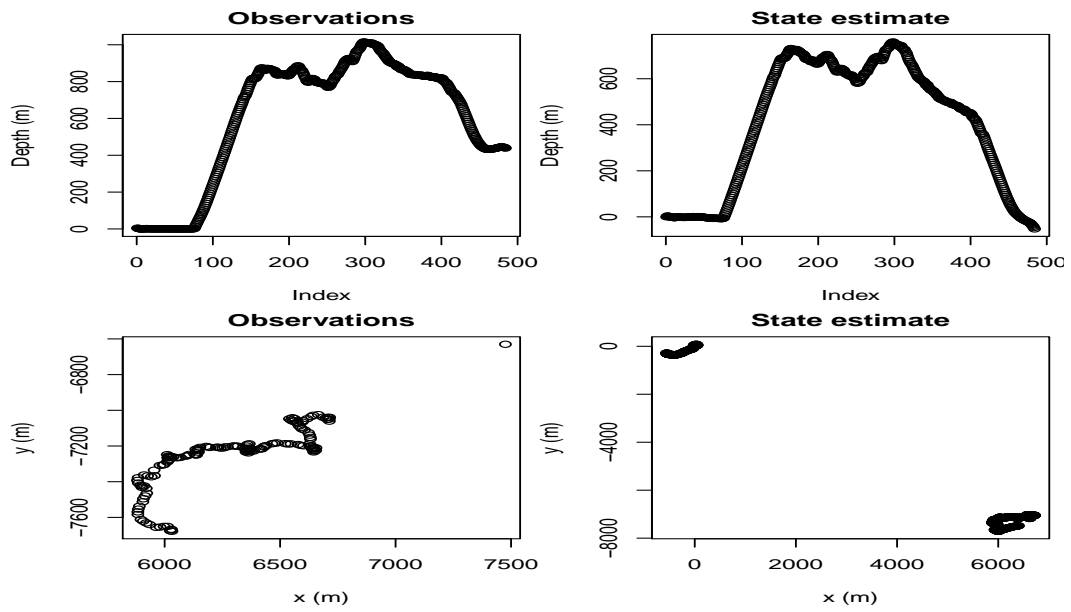


Figure 4: Observations and state estimates, for depth (left panel) and x, y locations (Right panel).

In fact, if one looks at the first few state estimates, inside object `ISECm$a`, one sees that these are 0 at step 1, and that they are only non zero at step 2 for depth, which is the state that had a direct observation

```
> teste1$a[,1:4]

      [,1]      [,2]      [,3]      [,4]
state1    0 0.00000  1.6382609  1.6382609
state2    0 4.46553  4.4302805  4.4128382
state3    0 0.00000 -0.3650823 -0.5447008
state4    0 0.00000  0.5430388  0.8165144
```

We can now repeat this same procedure by actually explicitly using the TAG on position as the first data point (Figure 5), still considering only the first 15000 data points. The output is now closer to what one might expect, but unlike what we had before for our own R code (cf. Figure 1), the predicted track still goes quite far from the actual x, y observations, and there seem to be some drifting with depth, that becomes “above the water surface” for the later period.

```
> nT=15000
> data=new.georef[1:nT,5:7]
> data[1,2:3]=c(TAGONx,TAGONy)
> ISECm2=SSModel(y=data,Z=cbind(matrix(0,3,1),diag(3)),T=Bt[,1:nT])
> teste2=KFS(ISECm2)
```

Considering the same procedure for the entire track (Figure 6), we can see that:

- the depth estimates suffer from some drifting phenomena, and becomes implausible before the end of the first deep dive;
- the x, y are not nearly as close to the observations as we had before (cf. Figure 1).

```
> nT=nrow(new.georef)
> data=new.georef[1:nT,5:7]
> data[1,2:3]=c(TAGONx,TAGONy)
> ISECm3=SSModel(y=data,Z=cbind(matrix(0,3,1),diag(3)),T=Bt[,1:nT])
> teste3=KFS(ISECm3)
> save(teste3,file="Routputs/teste3.Rdata")
> rm(teste3,ISECm3)
```

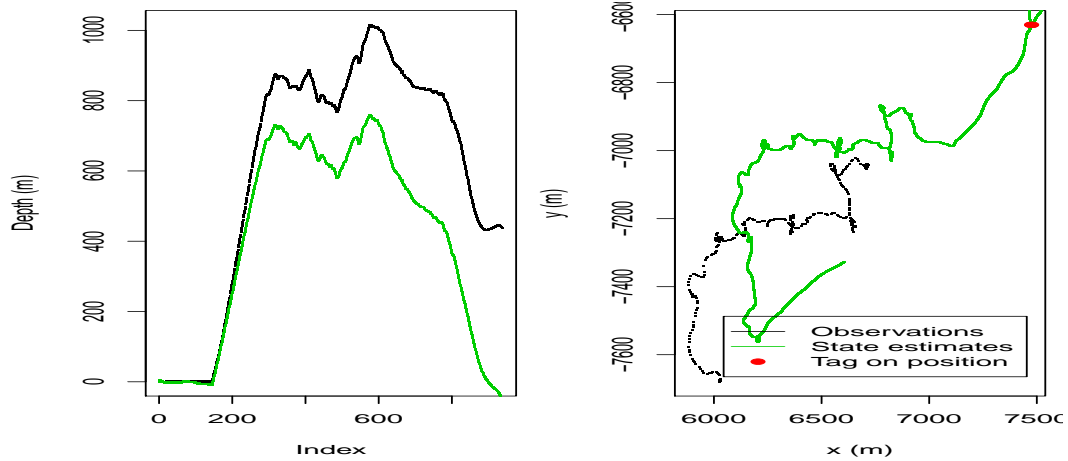



Figure 5: Observations and state estimates, for depth (left panel) and x, y locations (Right panel), for first 15000 time steps, using the Tag-on position as data

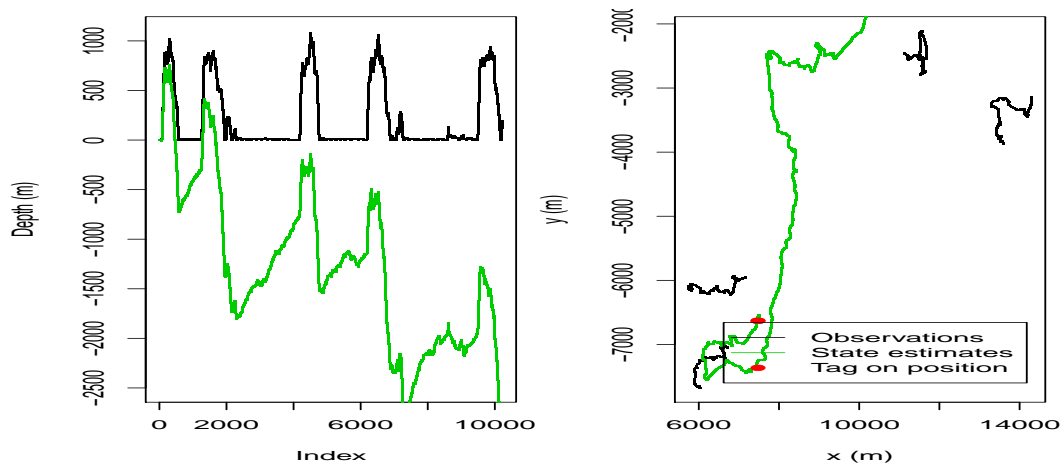


Figure 6: Observations and state estimates, for depth (left panel) and x, y locations (Right panel), for the full track, using the Tag-on position as data

This suggests (at least) one of 3 explanations, listed below from the a priori least to more plausible:

1. There is a problem with **KFAS** itself;
2. There is a problem with our implementation in **KFAS** (e.g. a bug in the code when defining the model);
3. There are some different settings in **KFAS** and in my native R implementation of the Kalman filter which explain the differences. In particular, it seems like the observations do not have a strong enough impact on the predictions. This might be the most parsimonious explanation. In particular, there were a number of values for the observation and state variances which were user defined in my R implementation but which are not being defined in **KFAS**.

Note however what I am outputting are filtered estimates, in object **\$a**, while the smoothed estimates are in object **\$alphahat**, but these two objects contain the exact same values (except for the first 2 and last two values).

Why would that be?

It is not clear what might be the default values used for the state and observation covariances in **KFAS**, but it seems clear that changing these might lead to an improvement. Therefore, we considered user-defined **Q** and **H** matrices (this is **KFAS** parlance) in the **SSModel** arguments.

```
> nT=nrow(new.georef)
> data=new.georef[1:nT,5:7]
> data[1,2:3]=c(TAGONx,TAGONy)
> #observation covariance matrix
> H=matrix(c(0.001,0,0,0,5,0,0,0,5),3,3,byrow=T)
> #state covariance matrix
> #state error in speed
> sf=5
> q1p=0.02;q2p=0.08;q3p=1.6e-05
> q1 = (q1p/sf)^2
> #state error in depth
> q2 = (q2p/sf)^2
> #state error in x
> #q3 = (q1p/sf)^2
```

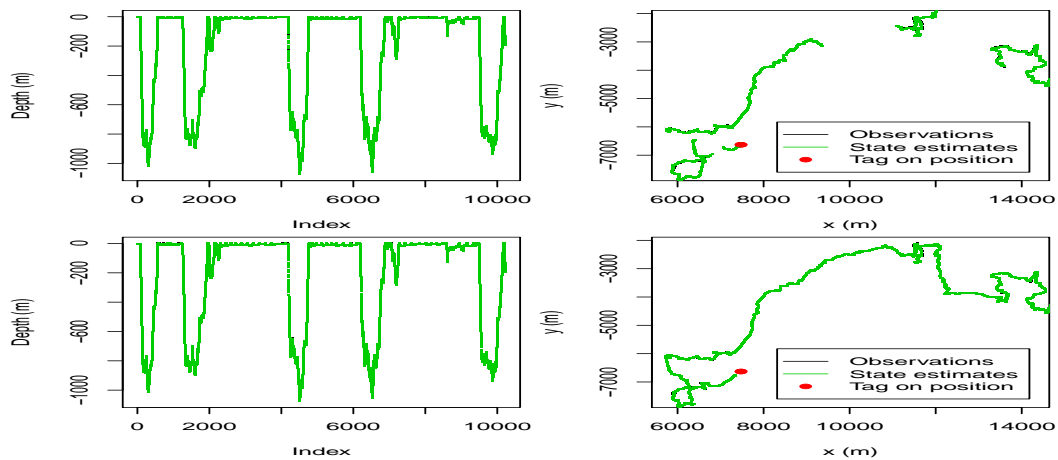


Figure 7: Observations and state estimates, for depth (left panel) and x, y locations (Right panel), for the full track, using the Tag-on position as data

```
> q3=q3p
> Q=matrix(c(q1,0,0,0,0,q2,0,0,0,0,q3,0,0,0,0,q3),4,4,byrow=T)
> #build up model
> ISECm4=SSModel(y=data,Z=cbind(matrix(0,3,1),diag(3)),T=Bt[,1:nT],H=H,Q=Q)
> teste4=KFS(ISECm4)
> save(teste4,file="Routputs/teste4.Rdata")
> rm(teste4,ISECm4)
```

This leads to the results shown in figure 7 (here we show both filtered and smoothed estimates). The results now look much more like what we had obtained before. Note that the black lines (data) are masked by smoothed predictions. However, there are two questions that get raised:

- Why is it that the smoothed estimates do not reach the tag on position¹?
- Clearly the default values in KFAS lead to state estimates way too far off the observations (and even inadmissible estimates for depth), but to what extent are we being over confident in the data when using

¹This is not easy to see from the plot itself, because the pdf loses resolution, but in the R plot that was clear

the values that lead to the results in Marques and Thomas (2012b) (essentially those reproduced here by the right plot of figure 1, and figure 7). Given that we can obtain such different results when using the default values for the state and observation covariance matrices and when using the values originally considered, what is the “right” thing to do?

4 Acknowledgments

We acknowledge here the kind input of the developers of the packages used. Jouni Helske provided useful feedback regarding the implementation of KFAS. Elizabeth Holmes provided feedback and code for the implementation in MARSS.

Referências

- Helske, J. (2012). *KFAS: Kalman Filter and Smoother for Exponential Family State Space Models*. R package version 0.9.11.
- Holmes, E. E., Ward, E. J., and Scheuerell, M. D. (2012a). *Analysis of multivariate timeseries using the MARSS package - version 3.0*.
- Holmes, E. E., Ward, E. J., and Wills, K. (2012b). State-space models for analyzing time-series data. *The R Journal*, **4**, 11–19.
- Marques, T. A. and Thomas, L. (2012a). Implementing a ssm to obtain pseudo-tracks and georeferenced track from dtag data: an application to md248b. Technical report, LATTE WORKING DOCUMENT.
- Marques, T. A. and Thomas, L. (2012b). Obtaining pseudo-tracks and georeferenced locations from dtag data. Technical report, LATTE WORKING DOCUMENT.
- Marques, T. A., Shaeffer, J., and Thomas, L. (2012). Procedure description: using AUTECH’s hydrophones surrounding a DTAGed whale to obtain localizations. Technical report, LATTE WORKING DOCUMENT.
- Tusell, F. (2011). Kalman filtering in r. *Journal of Statistical Software*, **39**, 1–27.

A note about the modelling and simulation of step lengths and turning angles

LATTE WORKING DOCUMENT

Tiago A. Marques & Len Thomas

Centre for Research into Ecological and Environmental Modelling
The Observatory, University of St Andrews, St Andrews, KY16 9LZ, Scotland

Version's date: October 26, 2015

Contents

1	Introduction	2
2	Data Reading	2
3	Required functions	3
4	Obtaining turning angles and step lengths	3
5	Exploratory data analysis	3
5.1	Step length	7
5.1.1	A gamma conditional on state	9
5.2	Turning angle	12
6	Open questions	12
	References	14

1 Introduction

In this report we briefly investigate the modelling of 2D horizontal movement based on the available DTag data.

An often used conceptual approach to the modelling of movement in continuous space and discrete time is the use of a step length (S) and turning angle (θ) formulation. This was the approach taken by say Morales *et al.* (2004) using mixtures of random walks conditional on behavioral states, further built on say by Langrock *et al.* (2012) or McClintock *et al.* (2012).

In all the above references, and several others for that matter (e.g. Codling *et al.*, 2008), the emphasis is on the turning angle component, for which persistence (through a correlated random walk CRW), bias (through a biased random walk BRW) or both persistence and bias (through a biased and correlated random walk BCRW) has been investigated.

In this report we look in closer detail at the turning angles and step lengths observed for DTag data and investigate their correlation structure, noting implications for simulation.

We conclude by focusing on the second component of movement, i.e. at the modelling of step lengths, because we observed that for our data set of beaked whale movement persistence was in fact far more pervasive in step length than in turning angle, something which is quite sensible given an animal inertia.

2 Data Reading

This report builds directly over an .Rdata workspace that is populated by the .Rnw of a different LATTE internal report, “Modeling beaked whale DTag data and simulating 3D movement via a latent-variable approach with feedback and semi-Markovian components” Marques *et al.* (2013). Therefore the usual raw data reading component is lacking and replaced by a load workspace statement¹. This uses the DTag data of Blainville’s beaked whale Md248b used in the above mentioned report.

¹To keep this report fully working a copy of the required workspace is present in the local folder.

3 Required functions

A couple of functions are required a priori, to obtain turning angles from the sequence of x, y locations. Here we actually leveraged on a very useful post on a Quantitative Ecology blog which happened to include relevant code to do so. The functions were tested and they are working well.

4 Obtaining turning angles and step lengths

We computed turning angles and step lengths at two different temporal scales, one considering data every second (the simulation time scale), the other considering data every ten seconds (the time step scale at which states were estimated/generated).

5 Exploratory data analysis

We start by describing the observed distribution of turning angles and step lengths, as well as its correlation structure, at each one of the temporal scales considered. These are represented in figures 1 and 2.

The observed distributions are consistent with typical distributions used in these cases, namely Gamma or Weibull distributions for step length and Wrapped Cauchy or von Mises for the turning angle.

We can also explore the potential autocorrelation between turning angles and step lengths (Figure 3). Only the 1 second time scale is shown, but the 10 second time scale patterns are very similar.

A few interesting remarks are possible regarding the observed temporal autocorrelation patterns:

- There is a much stronger temporal auto-correlation in step length when compared to turning angle, clear in figure 1. This should not be mistaken with what happens at the heading level, where correlation is much stronger (cf. figure 9).
- The auto-correlation pattern in turning angles is reversed when we move from the 1s to the 10 second time scale, changing from a negative correlation to a positive correlation at lag 1 (cf. top right panels in figs 1 and 2). This is an unexpected feature and is quite interesting in

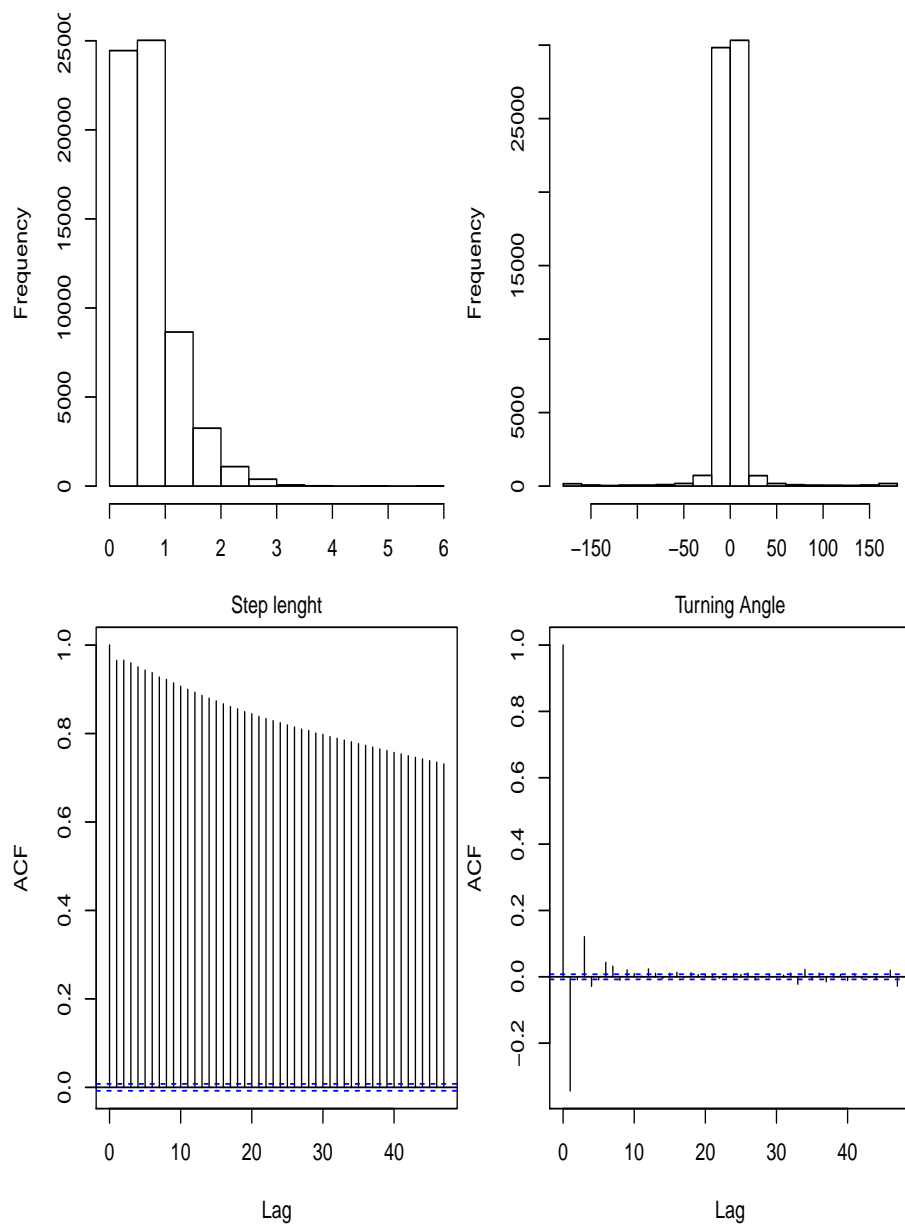


Figure 1: The distribution of step length and turning angles (top panels), with the corresponding correlograms below (bottom panels), at a 1 second temporal scale.

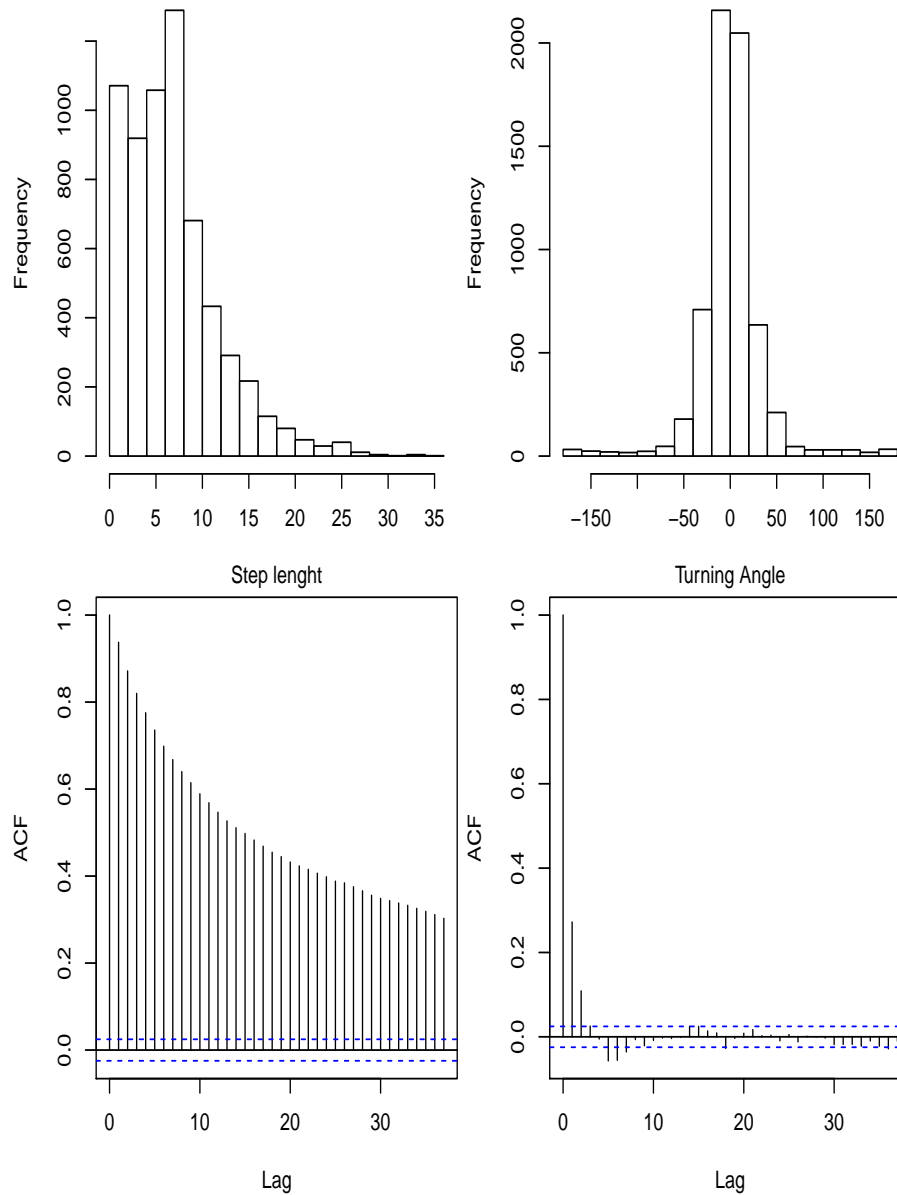


Figure 2: The distribution of step length and turning angles (top panels), with the corresponding correlograms below (bottom panels), at a 10 second temporal scale.

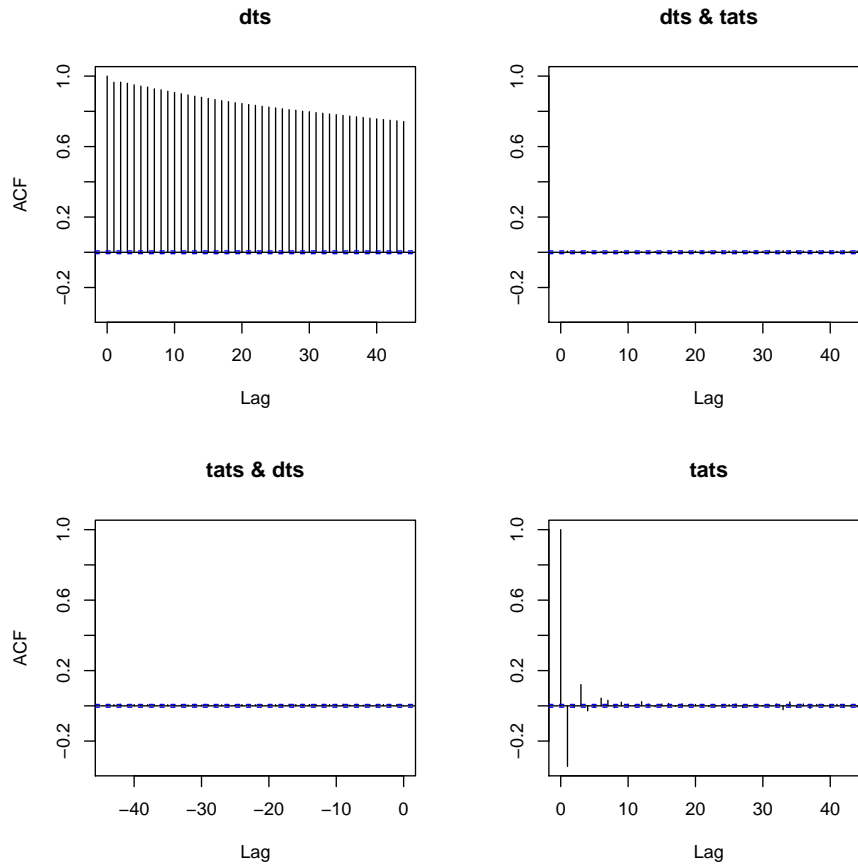


Figure 3: Correlograms and cross correlograms for step length (dts) and turning angle (tats), at the 1 second time scale.

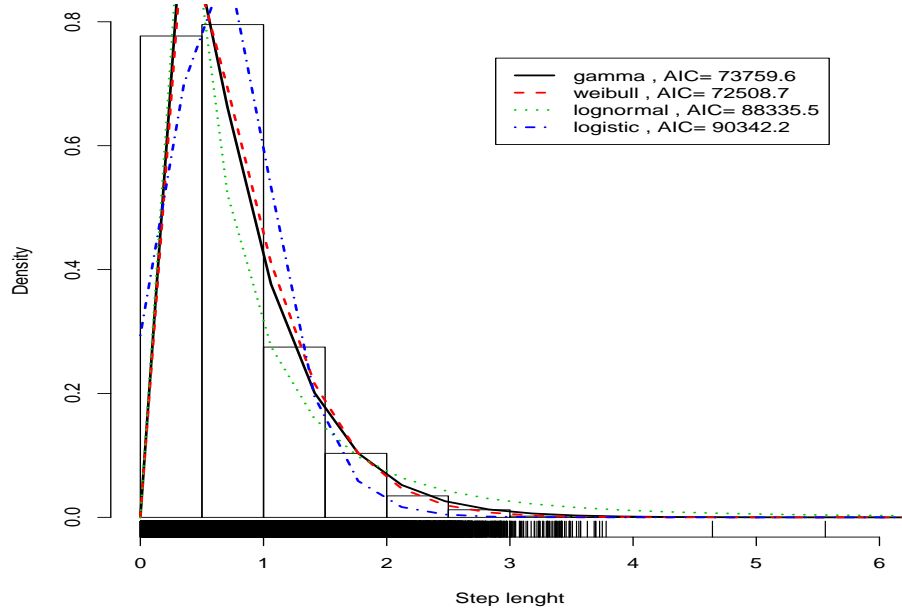


Figure 4: The distribution of step lengths with multiple distributions fit to the data. The Weibull seems the best fit of those tried.

general as it implies that some inferences might be conditional on the time scale used for observing the process.

- The lack of correlation between step lengths and turning angles (cf. figure 3) implies that we can simulate these independently, which is good news.

5.1 Step length

We now look in more detail at the distribution of step lengths observed for Md248b. We consider here only the analysis at the 1 second scale, since this is what we will be interested in simulating at.

We can fit a number of reasonable distributions (i.e. for strictly positive values) to the observed step length data, ignoring the temporal autocorrelation structure of the data (Figure 4). Of those tried, the Weibull seems to be by far the best option. Note this was the same model found to best fit step length data by Langrock *et al.* (2012).

Despite an obvious place to start given its simplicity, the clear autocorrelation shown in figure 1 implies that if realistic tracks are required we might not be able simply model step length as a heavy tailed distribution like the Weibull (e.g. McClintock *et al.*, 2012) or the gamma (e.g. Langrock *et al.*, 2012), i.e. as e.g.

$$S_t \sim Ga(\alpha, \beta) \quad (1)$$

where S_t represents the time length at time step t ($t = 1, 2, \dots, T$).

We need instead to consider some persistence for step length, such that this correlation structure is preserved. A typical autocorrelation structure can be defined as

$$S_t = \theta S_{t-1} + \epsilon_t \quad (2)$$

where ϵ_t represents a error with mean zero and some variance. The problem here is that under this context ϵ_t cannot be a gamma since the mean value of a gamma is strictly > 0 .

We could consider a model respecting the relation

$$E(S_t) = E(S_{t-1}) \quad (3)$$

where we use a different mean and variance parametrization for the gamma².

To implement this kind of model we need some bespoke likelihood functions, because now the mean value of step length depends on the previous time step length. We consider here 3 additional scenarios:

1. S_{t+1} is a gamma random variable with mean value equal to S_t (and some variance, which actually also depends on S_t);
2. S_{t+1} is a Gaussian random variable with mean value equal to S_t and a constant variance;

²Note this uses a non-standard parametrization of the gamma distribution as a function of the mean and variance. This is actually harder to implement for the Weibull as it is not simple to algebraically express the shape and scale parameters of a Weibull as a function of its mean and variance. Also, unlike what the notation suggests, the variance is now a function of the mean value, so this formulation implies a clear restriction on the subjacent distribution.

3. S_{t+1} is a Gaussian random variable with mean value equal to S_t and variance proportional to S_t .

Note in particular that the Gaussian-based models are simpler (as the Gaussian has the property of independence between the mean and the variance) but can lead to negative step lengths, hence the Gamma-based model is more realistic.

When we implement this we see that the AIC for the gamma model is 2.94742×10^4 , which means that this model is more parsimonious than any of the models shown in figure 4 which ignored the temporal autocorrelation. Somewhat surprisingly the Gaussian models AIC's are -7.28582×10^4 and -1.94208×10^4 , respectively ³.

The Gaussian model fit overlaid on the data actually looks considerably off, and this seems to be caused by the extremely heavy tails associated with the differences in step length, which tend to be small (99.79 % of the values are smaller than 1) (Figure 5).

However, when we tried to simulate from the gamma model model, a perhaps obvious after the fact consequence of the model used became clear. If one successively simulates from a Gamma with the mean value being the same as the previous observation the simulated step length values quickly tends to 0 (Figure 6). While this is a natural consequence of most of the mass being below the mean in a gamma distribution, it does mean that we need to find an alternative way of simulating correlated step lengths.

However, as noted above, simulation from the Gaussian model would potentially lead to negative step lengths, which is not a possible outcome. Irrespectively, when we simulate from the estimated model we end up with a distribution for step lengths that is inconsistent with the observed data (Figure 7, cf. figure 4). This happens as a natural consequence of modeling differences rather than step lengths themselves: by doing so we loose the distributional properties of the original observations.

5.1.1 A gamma conditional on state

While in the previous section we modeled the step length irrespective of the behavioral state, we can actually consider a model conditional on state.

³This does not add up, why would the AIC values change from negative to positive. This is being ignored for the time being as these models are inadequate any way since they can lead to negative step lengths.

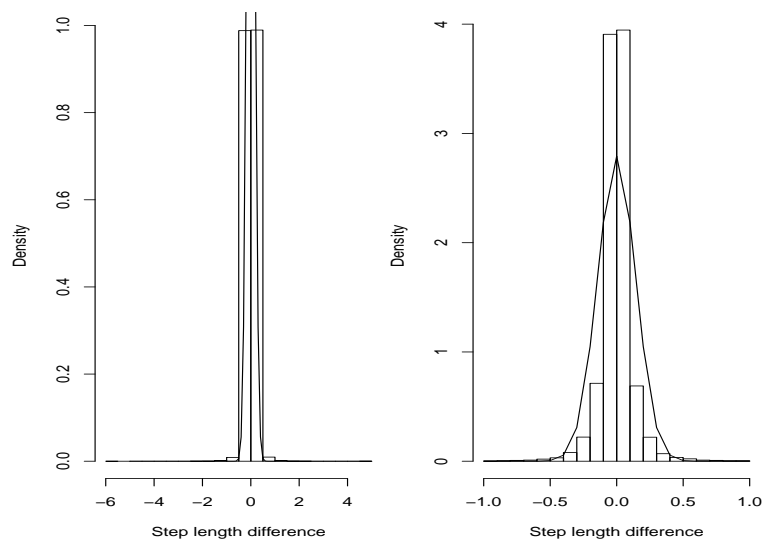


Figure 5: The observed differences in step length and the Gaussian model fitted to these (corresponds to the Gaussian model with a constant variance). Left plot encompasses all data, right plot zooms in in the area of higher density.

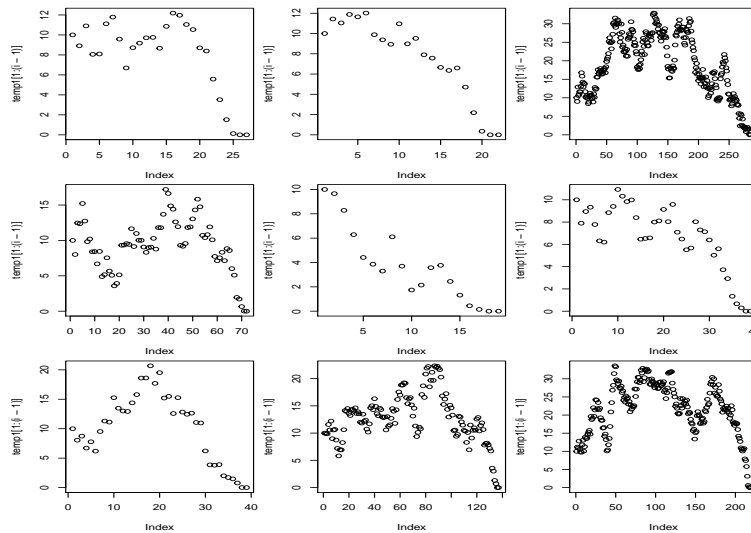


Figure 6: Nine examples of simulated step lengths such that the current step length is a gamma with the same mean value as the previous step length. Arbitrary (yet realistic given our scale) variance and starting step lengths were used.

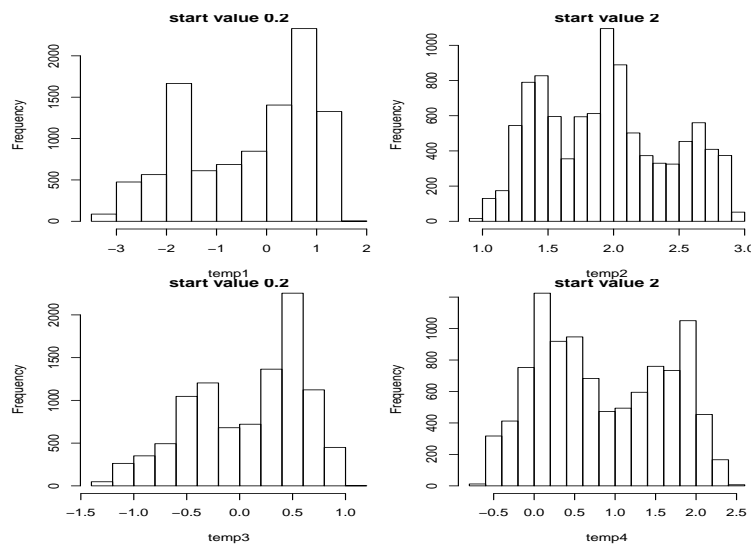


Figure 7: A couple of examples of simulated values from the simulation of Gaussian differences.

We tried to fit such a model but did not manage to make it converge. We have not pursued this further because the same problem remains regarding the simulation from this model.

As for the unconditional-on-state model from the previous section it will lead to step lengths that quickly tend to zero.

5.2 Turning angle

We are focusing on step lengths here, but this section could be populated with turning angle results analogous to those for step length from the previous section.

A distinct feature worth noting is the fact that there is an excess of turning angles around -180 and 180 degrees, which was visible at the tail of turning angle at the 1 second time scale (cf. figure 1). These seem to correspond to times when the animals suddenly change direction almost 180 degrees. An example is presented in figure 8, where the net outcome for the animal of 3 quick succession U-turns leading to a 180 degree U-turn back on its own track.

This type of behavior is not possible to capture with a single distribution. To do so one would probably require a mixture of two distributions, one with most of the mass and average around 0, the other with average around 180.

We note that while correlation in step length is stronger than in turning angle, the autocorrelation in heading (Figure 9) is much stronger than that in any of these two quantities. The subtleties of modeling turning angles (mean 0, negligible autocorrelation) or headings (mean = previous heading, strong autocorrelation) might deserve further investigation.

6 Open questions

From a purely pragmatic point of view we will carry on simulating step length considering gammas with mean values and variances conditional on state, i.e. ignoring the correlation structure in step lengths in the movement (i.e. persistence in the amount of 2D displacement).

Nonetheless, we identified a number of issues that would deserve further investigation. In particular:

- How can one implement a correlated Weibull model similar to the gamma CRW, given that the Weibull was much preferred (when the

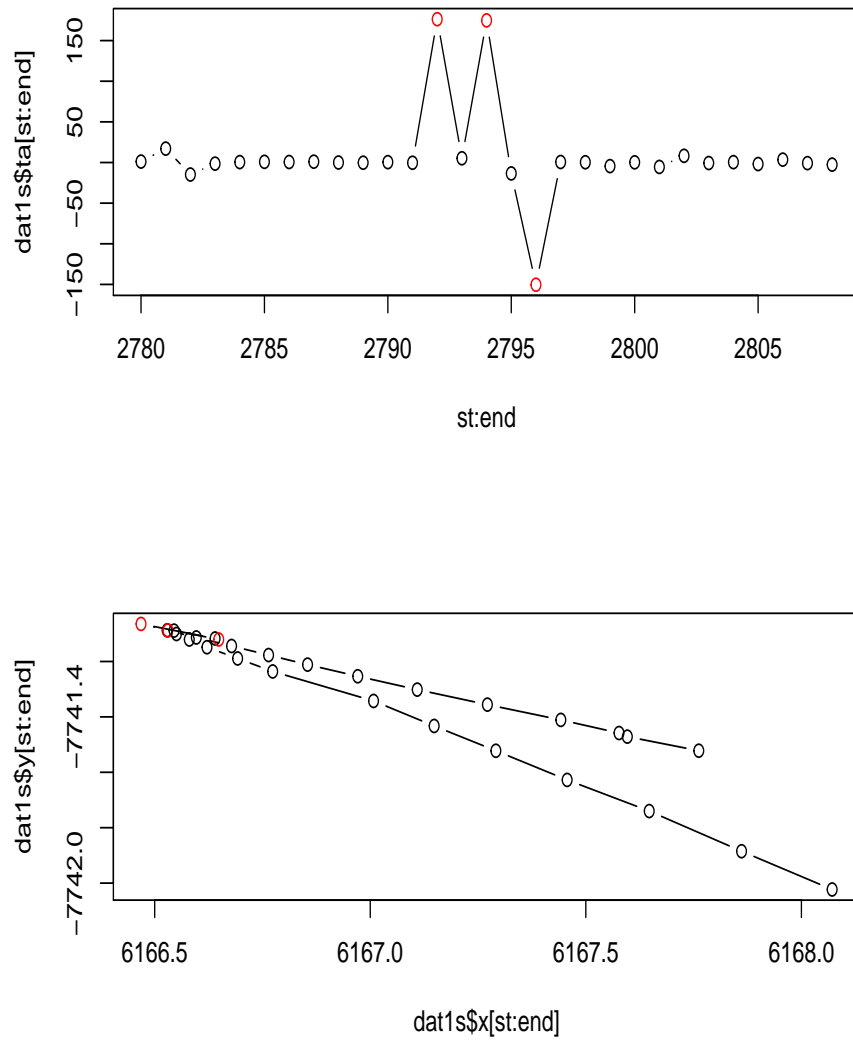


Figure 8: Zooming in on a portion of the track in which a succession of 3 closely spaced 180 U-turns occur. The highlighted points correspond to time steps in which an almost 180 degree turn occurs.

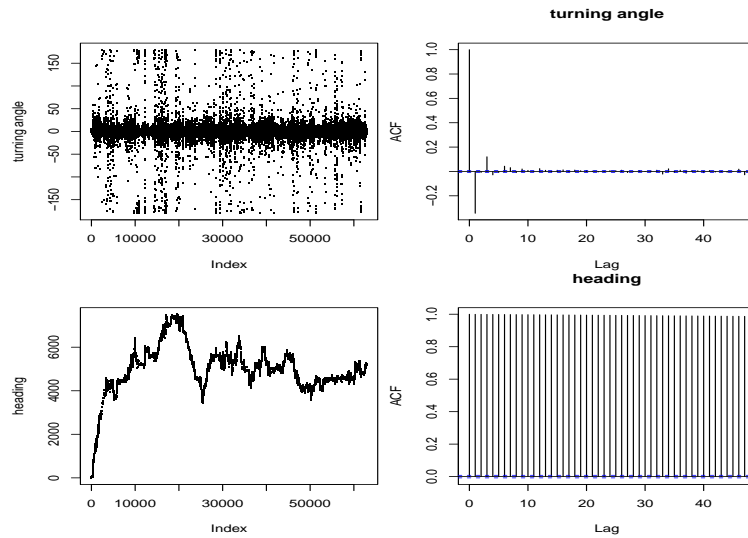


Figure 9: Comparison of autocorrelation in heading and turning angle.

autocorrelation was ignored)? This requires being able to express scale and shape parameters as a function of means and variances, but is perhaps not really useful unless we solve the gamma-tends-to-zero issue mentioned above, as this will be the case with the Weibull too.

- Intuitively it seems odd that a model that is actually implausible like the Gaussian (and hence which has areas of support which never get any data) or the tend-to-0 gamma is preferred by AIC?
- Preliminary analysis of step length conditional on state revealed there seemed to be differences in mean step length by state. If one considers the gamma CRW this cannot be imposed (is this right?), as we only control the variance, not the mean in each state (as the mean is conditional on the previous time step). This is again perhaps a non issue if this gamma formulation cannot be used given the the gamma-tends-to-zero issue mentioned above.
- Simulating gamma correlated random variables seems to be a non-trivial task. How can we simulate correlated gamma variables without these tending to 0 as shown in figure 6?

References

- Codling, E. A., Plank, M. J., and Benhamou, S. (2008). Random walk models in biology. *Journal of The Royal Society Interface*, **5**, 813–834.
- Langrock, R., King, R., Matthiopoulos, J., Thomas, L., Fortin, D., and Morales, J. M. (2012). Flexible and practical modeling of animal telemetry data: hidden Markov models and extensions. *Ecology*, **93**, 2336–2342.
- Marques, T. A., Langrock, R., and Thomas, L. (2013). Modeling beaked whale dtag data and simulating 3d movement via a latent-variable approach with feedback and semi-markovian components. Technical report, LATTE WORKING DOCUMENT.
- McClintock, B. T., King, R., Thomas, L., Matthiopoulos, J., McConnell, B. J., and Morales, J. M. (2012). A general modeling framework for animal movement and migration using multi-state random walks. *Ecological Monographs*, **82**, 335–349.
- Morales, J. M., Haydon, D. T., Frair, J., Holsinger, K. E., and Fryxell, J. M. (2004). Extracting more out of relocation data: building movement models as mixtures of random walks. *Ecology*, **85**, 2436–2445.

A tutorial on simulated annealing

Tiago A. Marques

Centre for Research into Ecological and Environmental Modelling
The Observatory, University of St Andrews, St Andrews, KY16 9LZ, Scotland

Version's date: September 21, 2011¹

Contents

1	Introduction	1
2	Optimization routines	2
2.1	Newton-Raphson approximation	2
2.2	Stochastic gradient method	6
3	Simulated Annealing	7
3.1	Introduction	7
3.2	The basics	7
3.3	Extensions and modifications	11
4	Conclusion	15
	References	15

1 Introduction

Charlie White used Simulated Annealing (SA) to implement the process of “geo-referencing” the DTAG data, by finding a vector of optimal whale speeds while “forcing” pseudo-tracks to go through the positions obtained by

¹ This document was created using Sweave, using R version 2.13.1 (2011-07-08) on a i386-pc-mingw32 platform.

localizing clicks ² on the AUTECH range hydrophones. Here we start by describing simple forms of numerical optimization all the way up to simulated annealing. We build heavily on material and code presented by Robert and Casella (2010).

Simulated annealing is a popular way to solve an optimization problem. Here we focus specifically on estimating the minimum or the maximum of a function f , with most examples relating to maximization (as maximizing f is equivalent to minimizing $-f$ or $1/f$). If one has a function $f(x)$, and needs to estimate its maximum say, the fool proof way to do it is to evaluate that function at all possible values³ of the argument x . The solution is then x_{max} , for which the function takes the value y_{max} , i.e.

$$\max(f(x)) = f(x_{max}) = y_{max}. \quad (1)$$

However, for many but the most simple problems, in particular for continuous multi-dimensional problems, it quickly becomes virtually impossible to cover adequately the entire space of the arguments of f , and hence some other, cleverer, approach is required.

In section 2 we present some general results regarding optimization procedures, leading naturally to simulated annealing in section 3.

2 Optimization routines

2.1 Newton-Raphson approximation

One of the simplest numerical optimization methods for minimizing or maximizing a function is the Newton-Raphson approximation. This procedure can be used to find the root of a function. Starting from an initial guess x_0 , the root is iteratively approximated by

$$x_{k+1} = x_k - \frac{f(x_k)}{f'(x_k)}$$

until the algorithm converges (hence a tolerance parameter to define convergence is also necessary). Note that x_{k+1} corresponds to the intersection with

²The localized positions of the clicks are assumed to be known without error. This is unrealistic and likely a step of the process which can also be improved.

³Note naturally this is only valid for functions with discrete arguments.

the x -axis of a line tangent to f at $f(x_k)$. One can easily derive this considering the equation for a straight line that passes on point $(x_0, f(x_0))$. Since the slope of that line is by definition the first derivative of $f(x)$, i.e. $f'(x)$, x_{k+1} corresponds to solving the line equation to find its root, i.e. where the tangent line intersects the x axis.

In figure 1 an example of the algorithm is presented, based on function `newton.method` from package `animation`.

Note that Newton-Raphson can be easily extended to find maxima or minima, as that corresponds to finding roots for the first derivative of the function one hopes to minimize or maximize, now considering

$$x_{k+1} = x_k - \frac{f'(x_k)}{f''(x_k)} = x_k - \frac{\frac{\partial f(X_i)}{\partial X}}{\frac{\partial^2 f(X_i)}{\partial X \partial X^T}}$$

where $\frac{\partial f(X_i)}{\partial X}$ and $\frac{\partial^2 f(X_i)}{\partial X \partial X^T}$ are often referred to as the gradient and the Hessian, respectively. Sometimes the gradient is also represented by ∇f .

If the surface of the function to be maximized is complex, say multi-modal, then the result of the maximization will depend on the starting point. An illustrative example of the implementation of `nlm` (which is based on Newton-Raphson) is shown in Figure 2, from where it is clear that the outcome depends on the starting values. Note that the we consider here a function which is the $-(\log\text{-likelihood})$, as `nlm`, by default, minimizes a function rather than maximizing it. In this case, 4 out of 9 starting value sets ended in the wrong mode. In scenario 4, the procedure failed to converge because the starting point was in a region where the gradient is very steep. Curiously, there were two other possible outcomes starting from quite close to that region, leading to either the right (scenario 3) or the wrong (scenario 2) mode being selected. This should warn us to the influence of starting values in this type of numerical maximization algorithms.

An improvement over a conventional Newton-Raphson approach is to use the (deterministic) gradient method, which in essence uses the gradient of the function near the current point X_t to obtain the next point at which f is evaluated, X_{t+1} , using a recurrence expression like

$$X_{t+1} = X_t + \alpha_t \nabla f(X_t), \quad \alpha_t > 0$$

in which α_t is a decreasing sequence of t , and $\nabla f(X_t)$ is (the vector of) first derivative(s) or gradient. Accounting for the gradient is standard using R's

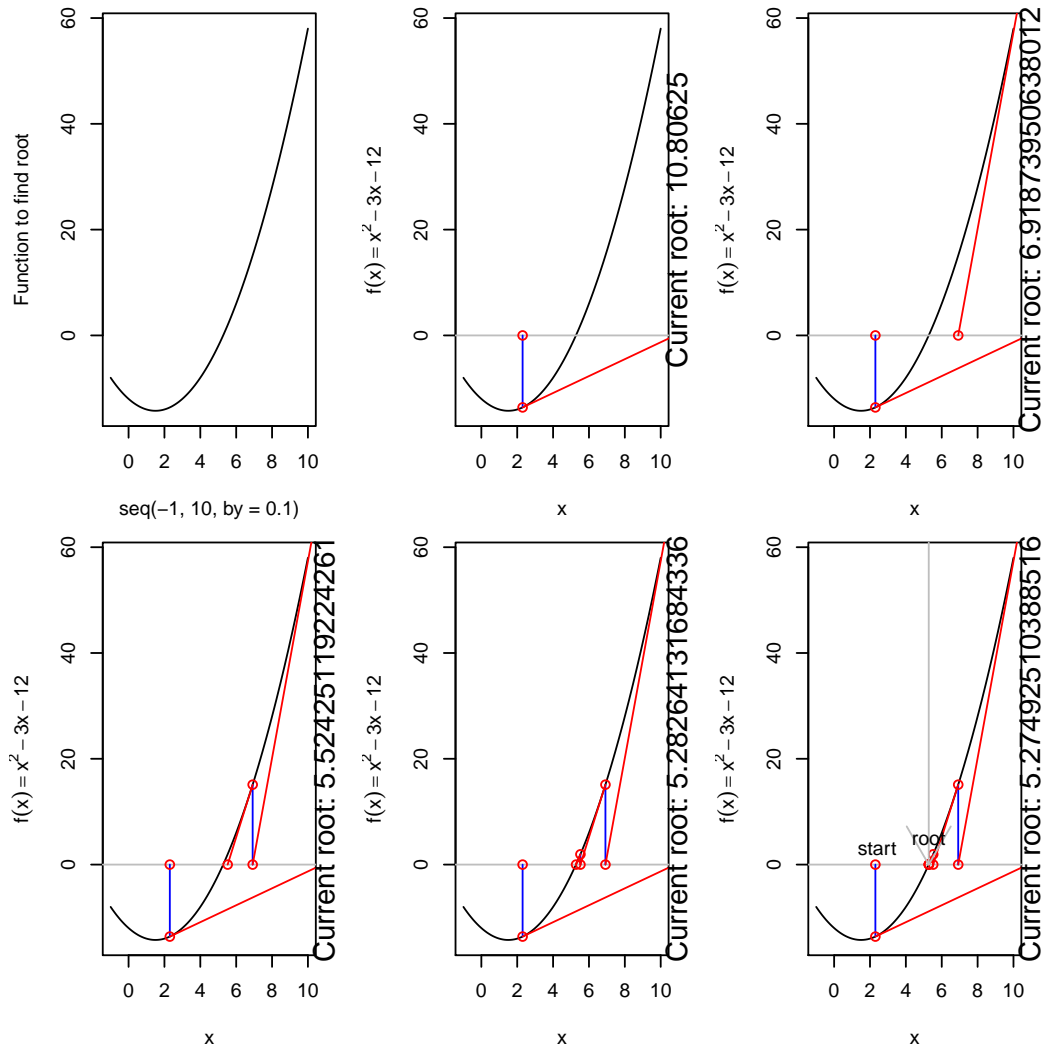


Figure 1: Example of finding a root of a function using the Newton-Raphson algorithm.

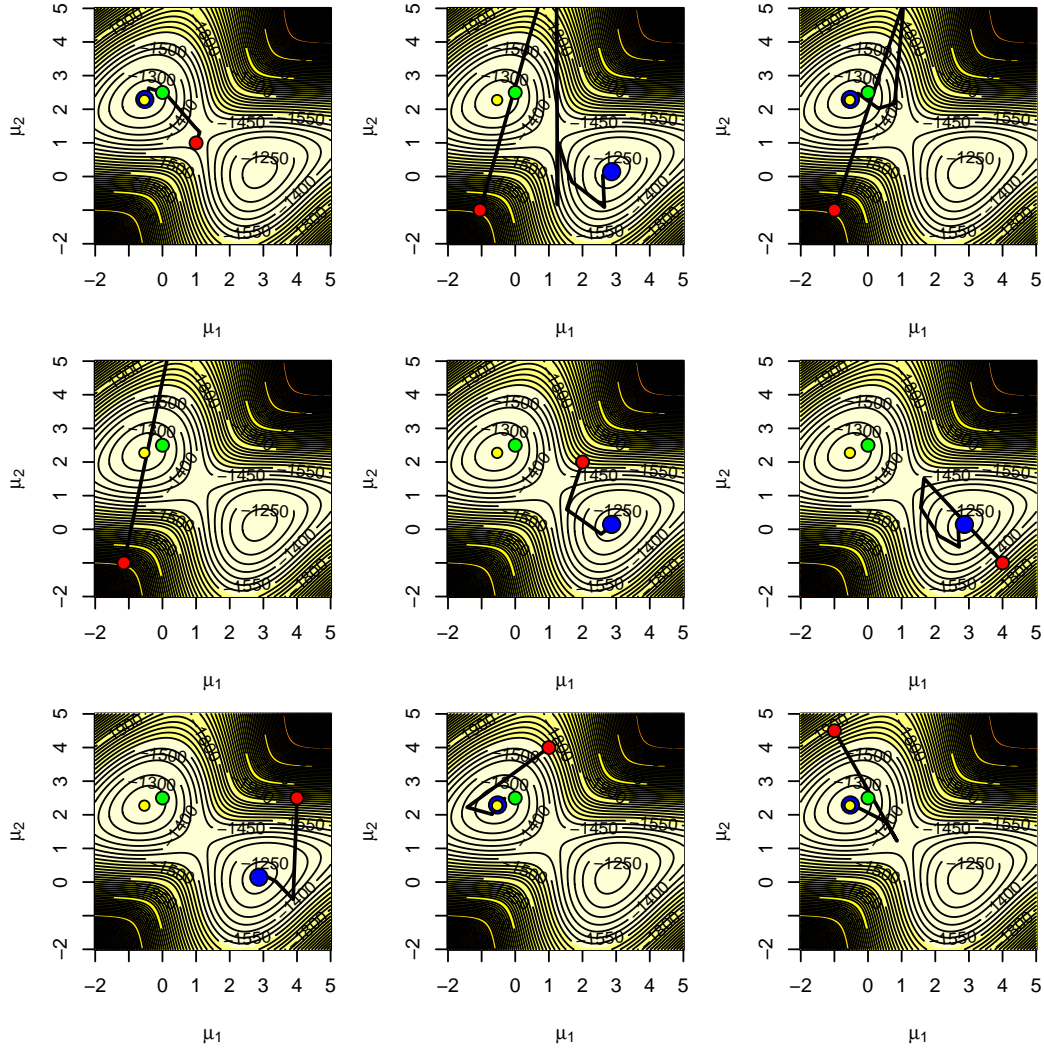


Figure 2: Nine examples of Newton-Raphson algorithm attempting to find the maximum likelihood estimate of the location parameters of a Gaussian mixture, based on a sample of size 101. Contour lines represent the $-\log$ -likelihood. The green dot is at the true parameter values, the smaller yellow dot is at the maximum of the likelihood surface, the red dot is at the starting point and the blue dot is at the minimum estimate (the function used in `nlm` is $-\log$ -likelihood, hence the minimum corresponds to the maximum of the \log -likelihood).

`nlm`, by explicitly providing the arguments `gradient` and `hessian` associated with the function that the optimization is being applied to. Otherwise `nlm` uses numerical derivatives to approximate the gradient.

2.2 Stochastic gradient method

Instead of using numerical optimization methods, one might try to evaluate f at a set of points drawn from a distribution which support is the same as the possible values the function argument can take, let's say X . In such case, a simple, yet non-efficient, way to sample from the parameter space to evaluate the function at is to use a Uniform distribution, e.g. if the function argument can only take values in the interval $(0,1)$, one might sample from the standard Uniform.

However, under this setting, ideally one would choose points from X using information about f itself, using more points near the maximum value of f . This is not easy, as we do not know f , if we did, we would not need an optimization routine to begin with! A possible approach is to use a stochastic gradient method, in which the new proposal is obtained by choosing a random direction and a decreasing step (depending on the gradient) from the current one. Hence, we could consider something like

$$\nabla f(X_t) \approx \frac{f(X + \beta_t \epsilon_t) - f(X - \beta_t \epsilon_t)}{2\beta_t} \epsilon_t \quad (2)$$

in which β_t represents a second decreasing sequence (which should converge slower than α_t), and ϵ_t is uniformly distributed in the unit sphere $\|\epsilon_t\|=1$. (Note that for equation 2 to make sense, in terms of it being an approximation to the gradient, the denominator should be $2\beta_t \epsilon_t$.) In this way, rather than the update moving in the direction of maximum change in f (steepest gradient), the update moves in a random direction, which is actually useful if one is trying to move away from relative maxima or minima.

In figure 3 there is a (highly contrived and yet useful for illustration) function of two arguments, (x, y) . The extreme multimodal surface would be extremely hard to minimize (and even harder to maximize!) using a standard numerical optimization routine. Here we consider a stochastic gradient method to find the minimum of this function, which we know is 0, obtained when evaluating the function at $(0,0)$. An example is shown in figure 4, in which $\alpha_t = (1/(t+1))$ and $\beta_t = (1/(t+1))^{0.5}$. We can see that a reasonable

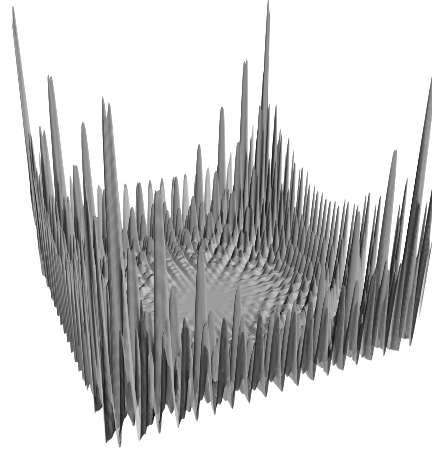


Figure 3: A highly complex function of two arguments, (x,y) .

estimate of the minimum is easily obtained, but as before, the success of this approach depended closely on the α_t and β_t (decreasing) sequences chosen.

3 Simulated Annealing

3.1 Introduction

Simulated annealing (SA) was introduced by Kirkpatrick *et al.* (1983), and apparently essentially independently reinvented by Cerny (1985) (though this later author did not re-coin the term). The idea behind simulated annealing relates to the stochastic gradient method. The difference is that in SA the new candidate point X_t at which f is evaluated is chosen from a sequence of densities π_t . As the algorithm progresses, these densities tend to be more and more concentrated around the maximum of $f(X)$ which we want to estimate.

3.2 The basics

A first fundamental step in SA is to obtain an efficient sequence of densities π_t . A standard choice are the Boltzman-Gibbs transforms of f

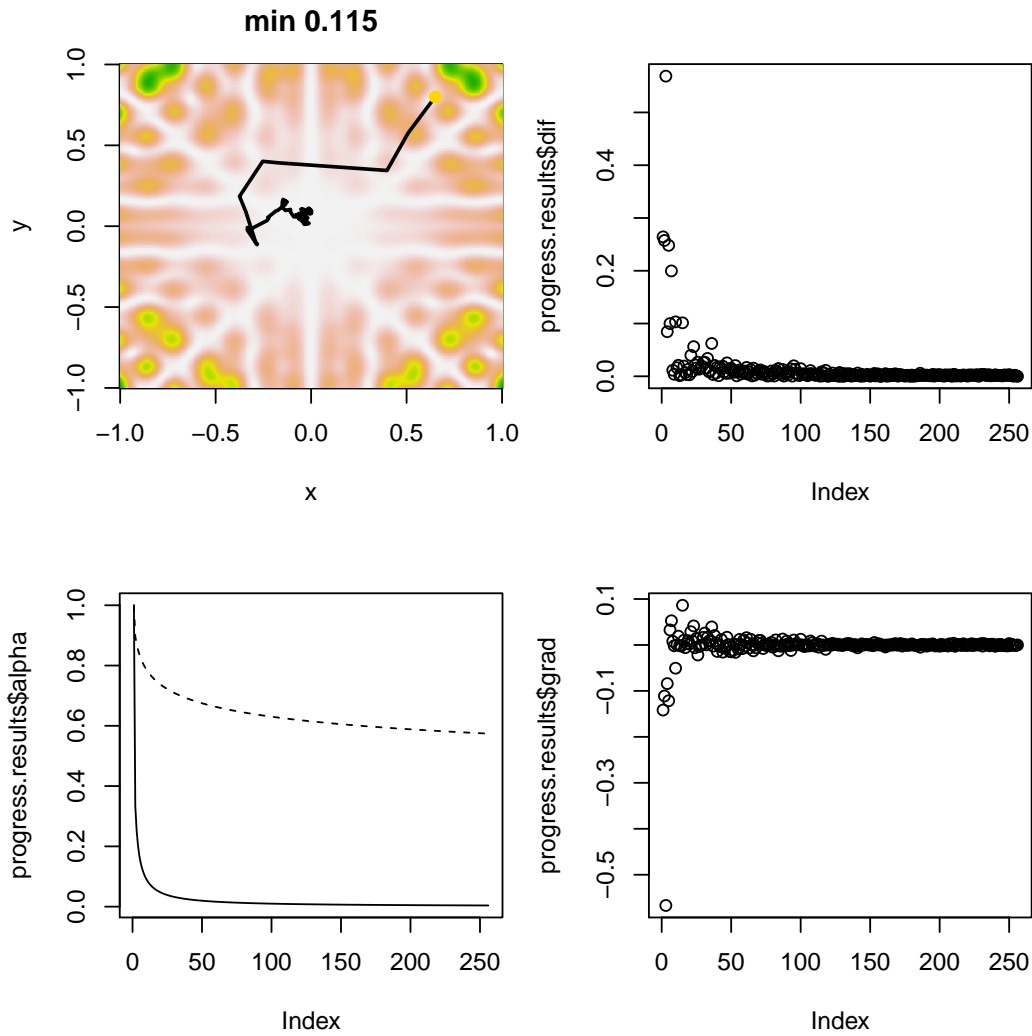


Figure 4: Function maximization using a stochastic gradient method. Top left represents the function and the “path” taken by the algorithm, starting at the yellow dot at $(.65, .8)$; top right represents the stopping threshold; bottom left the α_j (solid line) and β_j (dashed line) sequences; and bottom right the gradient.

$$\pi_t(X) = \exp \left\{ \frac{f(X)}{T_t} \right\} \quad (3)$$

where T_t is a decreasing sequence of “temperatures”. If $\lim_{t \rightarrow \infty} T_t = 0$, T_t is said to be a cooling schedule. The choice of T_t is the second fundamental part of the implementation of SA. Here we consider for illustration a sequence of the form

$$T_t = \frac{1}{(1+t)^p} \quad (4)$$

where p is a power parameter that controls the rate at which T_t decreases to 0. From equation 3 it is clear that as T_t tends to 0, the density $\pi_t(X)$ becomes more and more concentrated around the maximum of f .

For SA, a usual way to update X_t is based on the Metropolis-Hastings algorithm. ϵ is generated from a distribution with symmetric density g , and the new value $X_{t+1} = X_t + \epsilon$ is accepted with probability ρ , where

$$\rho = \exp \left\{ \frac{h(X_t + \epsilon) - h(X_t)}{T_t} \right\} = \exp \left\{ \frac{\Delta h}{T_t} \right\}.$$

If the proposed value is not accepted, which happens with probability $(1 - \rho)$, then the proposed value is rejected, i.e. $X_{t+1} = X_t$.

Note that there might be a scale parameter associated with g , which controls how far from the current position the candidate position might be. Rather than a scalar, the scale could also be a sequence of values, changing as the algorithm progresses. In particular, the scale could also be a function of the temperature. Carefully choosing the function used for the perturbation g becomes quite important.

So, in essence, instead of following a stochastic or deterministic gradient, the algorithm tries a random perturbation of the previous position at which the function was evaluated. If the perturbation increases f , it is accepted (as then $\rho=1$, as given $T_t > 0$, $\frac{\Delta h}{T_t} > 0$). If the perturbation decreases f , it can still be accepted with probability $\rho > 0$. Hence, the random moves make it so that one can get away from relative maximum or minima with some non-null probability. Because of the exponential term, the odd movement when temperature is already considerably cold is still possible, despite being associated with a low probability.

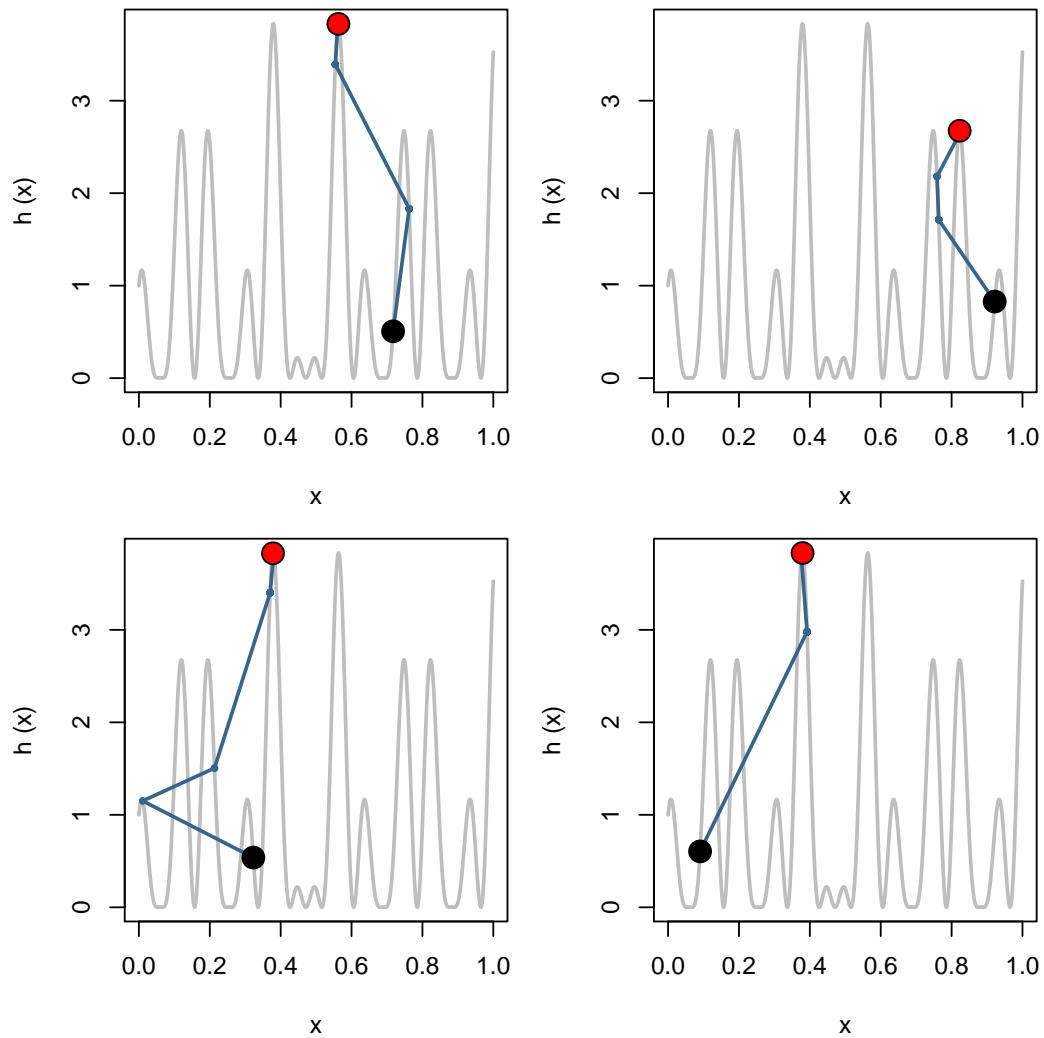


Figure 5: Simulated annealing with 4 different random starting point to maximize a function of a single argument (taking possible values in the interval $(0,1)$). Black dot represents the function evaluated at the starting point, red dot represents the function evaluated at the estimated maximum, black line represents the path taken.

An example of SA over a function with a single argument taking values in the interval $(0,1)$ is shown in figure 5. It can be seen that the result is clearly dependent of the starting point used. In figure 6 we display another example of the maximization, considering different powers in the expression that defines the sequence T_t (cf. equation 4). Considering starting points systematically spaced in the $(0,1)$ interval, we can see that with very low values of p , and hence a slow decrease in temperature over time, the algorithm is inefficient, because too many iterations are required. At the other extreme, for large p , temperature decreases abruptly at the start of the algorithm, and hence avoiding local maxima near the starting point is difficult. Intermediate values of p provide the best results, but even then finding the maximum is not guaranteed. This hints towards potential problems in complex and highly dimensional problems, where choice of p might be difficult.

A second example of SA based on code from Robert and Casella (2010)⁴ is presented in figure 7. Here, we consider a Gaussian perturbation with scale dependent on the temperature, and we considered temperature sequences of the form $1/\{K \times \log(1+t)\}$. We can see that the best results seem to be found for intermediate/large values of K .

A third SA example from Robert and Casella (2010), regarding minimization of a function, is obtained using similar settings but for the function introduced in figure 3. The results are presented in figure 8, but we failed to obtain the best combination possible of temperature and scale to mimic the results presented obtained in figure 5.10 of Robert and Casella (2010). We note there were multiple typos in the code provided.

3.3 Extensions and modifications

As described here, and strictly speaking in a pure SA approach, the algorithm reports as the outcome the state of the system in its last iteration. However, it might be possible that this is actually not the maximum value at which the function was evaluated. A simple addition to an SA procedure is to keep a track of what the maximum (in a maximization problem) value for the function being maximized was, and keep moving forward until at least that

⁴There is something strange regarding the code provided, as the results in their figure 5.9 suggest much better performance than those reported here (although they also mention the use of a function named `SA`, while they provided only `SAmix`. Note that in `SAmix` there is a typo in the code provided, where the temperature sequence is being defined, which causes the problems.)

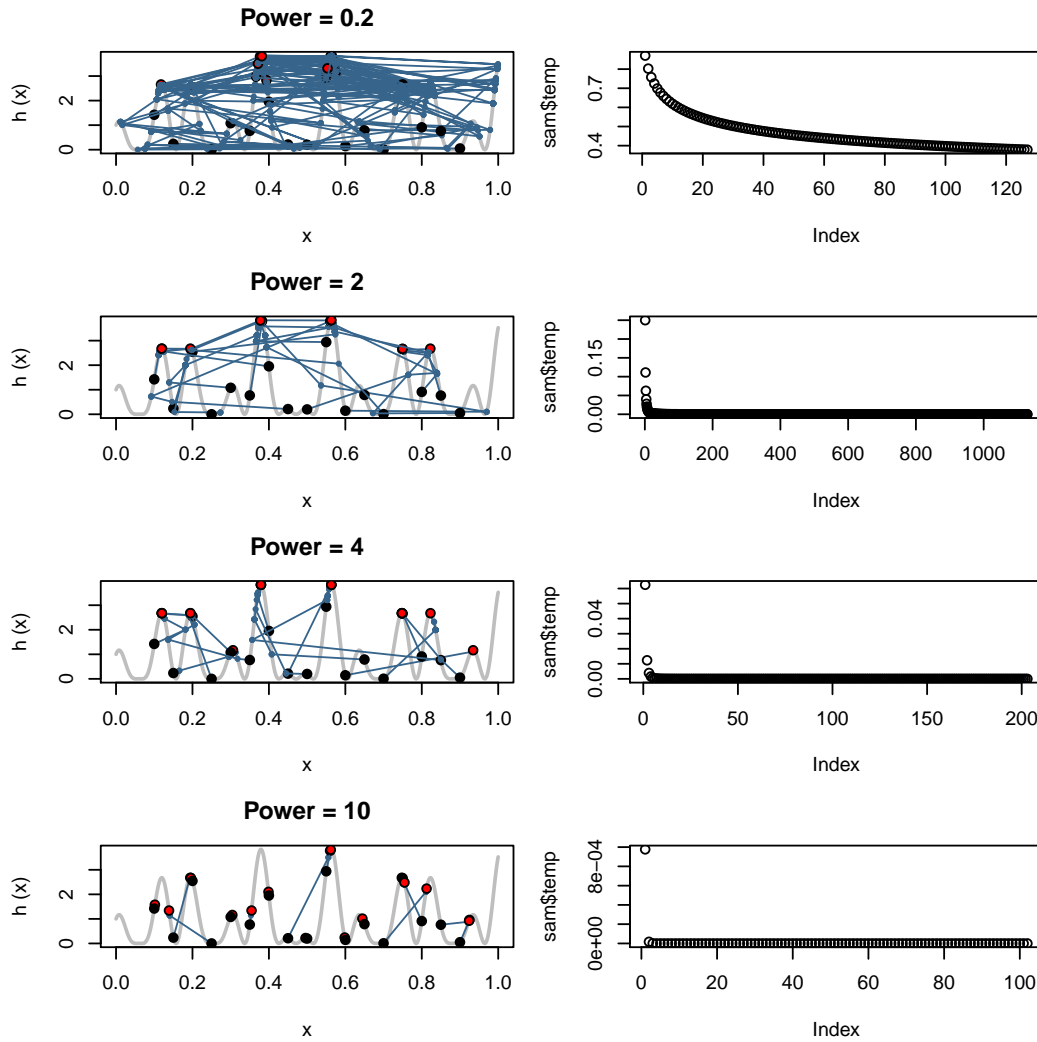


Figure 6: Simulated annealing with 4 different rates of decreasing temperature, considering systematically placed starting points. Left column plots correspond to the the value of the function evaluated at the algorithm's start and end points (respectively in black and red), and the path taken by the algorithm as black lines, and the right column plots represent the temperature sequences.

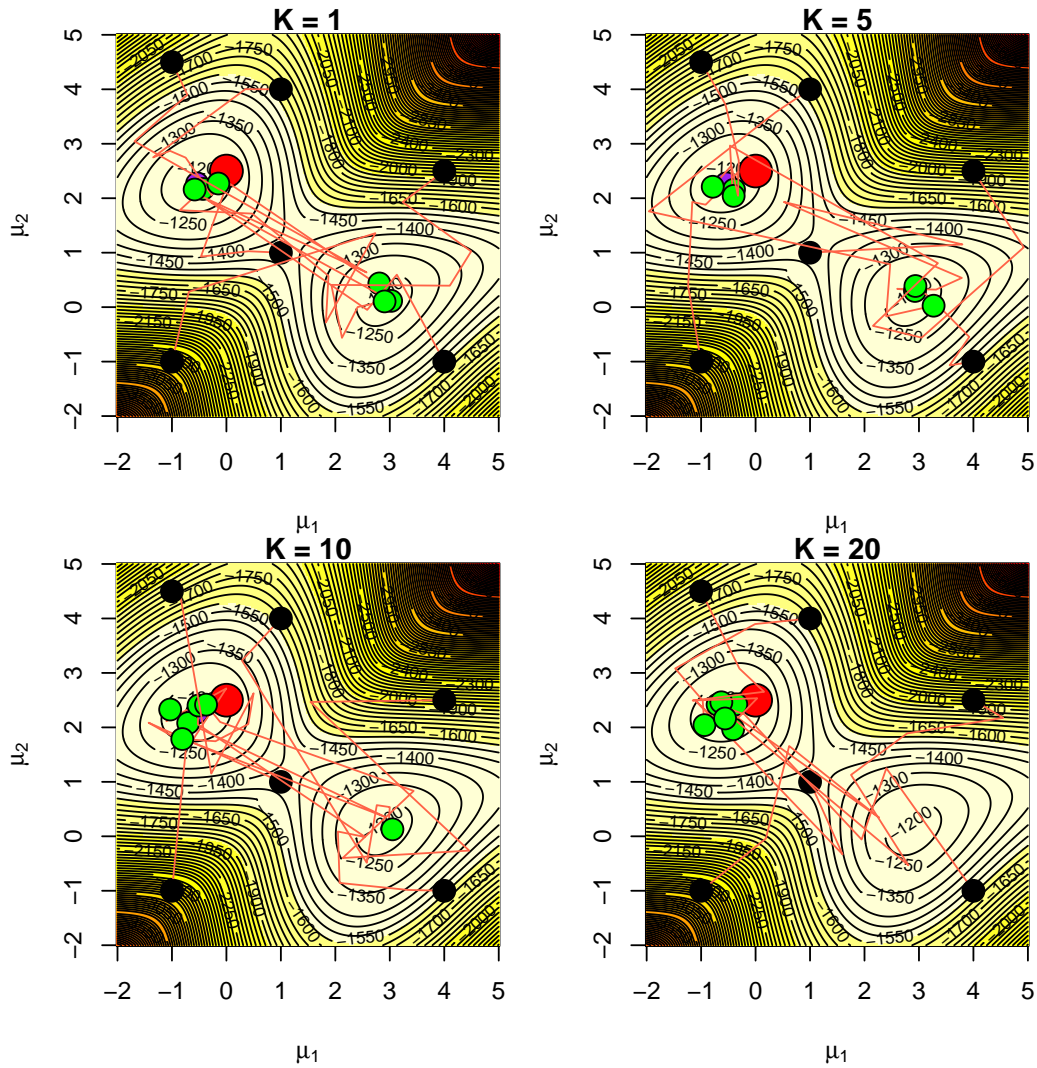


Figure 7: Simulated annealing with 4 different rates of decreasing temperature, considering 6 arbitrary starting points in each, for the example of estimating the localization parameters of a two point gaussian mixture.

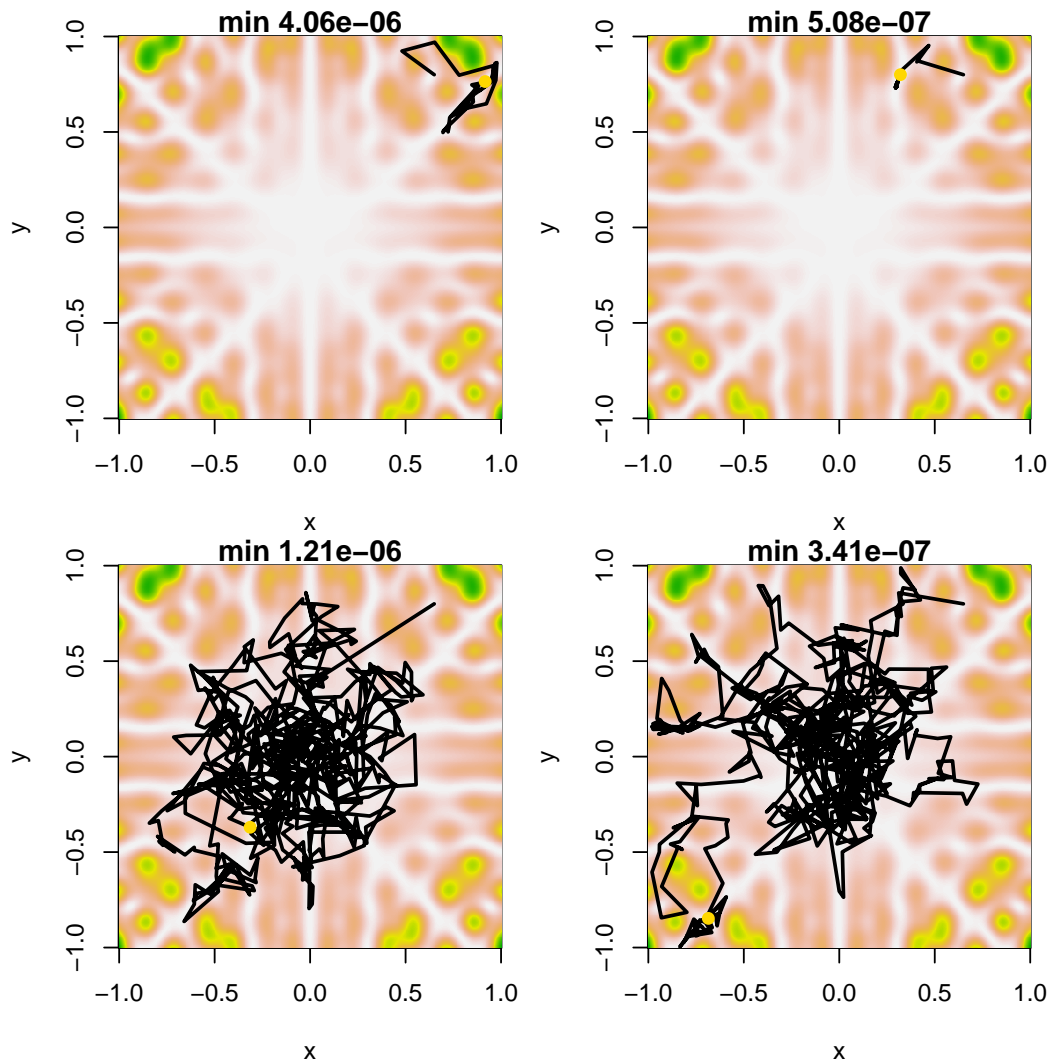


Figure 8: Simulated annealing with 4 different rates of decreasing temperature, considering 1 arbitrary starting point in each, for the example of estimating the minimum of an highly complex function.

same value is obtained again; if that takes long, one might “restart” the SA algorithm at that position.

We note that extensions to conventional SA exist in which adaptive procedures are used regarding the choice of temperature and scale. For these, after a few (hundreds or thousands maybe!) iterations of an adaptive period, the initial values of temperature and scale are updated, depending on the acceptance rates and changes in evaluated values of f given the initial argument values considered.

“Simulated Tempering” (ST) is a variant of SA which considers a sequence of temperatures which are not deterministic, but random, and hence, the algorithm can move away from local minima or maxima even when the “average” temperature has cooled considerably⁵. ST was introduced by Marinari and Parisi (1992). The idea is that while the convergence might actually be (slightly) slower when using SA, it might potentially be exponentially faster, hence for complicated problems, the gamble might be worth it.

4 Conclusion

Simulated annealing can be used to maximize or minimize a function, but there is no way to guarantee that the result is a reasonable approximation to the real maximum or minimum, as the algorithm might be trapped in local extremes, in particular if the function at hand is complex and multi-dimensional. Controlling the procedure by changing the function to sample updates from, as well considering different scale and temperature sequences, can lead to considerably different results, and therefore one should be careful in checking the results and evaluating their sensitivity to these parameters.

References

Cerny, V. (1985). Thermodynamical approach to the traveling salesman problem: An efficient simulation algorithm. *Journal of Optimization Theory and Applications*, **45**, 41–51. 10.1007/BF00940812.

⁵An historical footnote: the wording simulated annealing and simulated tempering comes from terms used in the metallurgy industry. In annealing, a metal is heated and then is let to cool down, so that defects in the material tend to disappear. In tempering, the temperature is increased and decreased successively, to obtain for the material involved the configuration of least energy (and hence more stable).

- Kirkpatrick, S., Gelatt, C. D., and Vecchi, M. P. (1983). Optimization by simulated annealing. *Science*, **220**, 671–680.
- Marinari, E. and Parisi, G. (1992). Simulated tempering: A new monte carlo scheme. *EPL (Europhysics Letters)*, **19**(6), 451.
- Robert, C. P. and Casella, G. (2010). *Introducing Monte Carlo Methods with R*. Springer.

A maximum likelihood localization procedure based on arrival times at multiple sensors

Tiago A. Marques & Len Thomas

Centre for Research into Ecological and Environmental Modelling
The Observatory, University of St Andrews, St Andrews, KY16 9LZ, Scotland

Version's date: November 13, 2012

Contents

1	Introduction	1
1.1	TOA based likelihood	2
1.2	TDOA based likelihood	3
1.3	Some random questions/remarks	3
2	The localization algorithm, assuming TOE known to be 0	4
2.1	A simple application	6
2.1.1	Do not forget though...	8

1 Introduction

In this document we describe a localization algorithm based on maximum likelihood. We assume that we have been able to associate some sound across a number of hydrophones, and given the times of arrival (TOA) of the sound, we estimate the most likely position of the sound source.

Consider the following notation. We have a source at $p = (x, y, z)$, and we wish to estimate its position based on the arrival times at K sensors, located at $p_k = (x_k, y_k, z_k)$, $k = 1, 2, \dots, K$.

The Euclidian distance between sensor k and the source, d_k , is given by

$$d_k = \sqrt{\{(x - x_k)^2 + (y - y_k)^2 + (z - z_k)^2\}}. \quad (1)$$

On the other hand, the distance d_k can also be expressed as a function of the speed of sound (c), the time-of-emission (TOE) of the sound t and the time-of-arrival (TOA) at sensor k , t_k as

$$d_k = c(t_k - t). \quad (2)$$

Equating these two expressions leads to

$$c(t_k - t) = \sqrt{\{(x - x_k)^2 + (y - y_k)^2 + (z - z_k)^2\}}. \quad (3)$$

This represents an equation with 4 unknowns (x, y, z and t), which intuitively tells us that if we have 4 arrival times, we can solve the system of 4 equations with respect to the 4 unknowns.

But what happens if we have 5 TOA's? We say the solution is over-parameterized. In the absence of measurement error any 4 TOA's should provide the same solution (i.e. same estimate) for p . However, this is never the case in practice due to a variety of reasons. This means that it might be more sensible to move to a method that explicitly incorporates the measurement error.

1.1 TOA based likelihood

If one assumes that the observed TOA have a Gaussian distribution, with mean value equal to the true TOA and a standard deviation driven by the (essentially unknown and random) measurement error, we can build a maximum likelihood estimation procedure.

Under such a setting, we have that TOA_k is a Gaussian with mean given by rearranging equation 3, namely

$$t_k = \frac{\sqrt{\{(x - x_k)^2 + (y - y_k)^2 + (z - z_k)^2\}}}{c} - t \quad (4)$$

which leads to the following likelihood

$$L(x, y, z, t, \sigma | TOAs) = \prod_{k=1}^K \frac{1}{\sigma \sqrt{2\pi}} \exp\left\{-\frac{(t_k - t_{k,p})^2}{2\sigma^2}\right\} \quad (5)$$

where $t_{k,p}$ and t_k (given by equation 4) represent, respectively, the observed TOA at hydrophone k , and the expected TOA at hydrophone k , given the

animal is at p , and where σ represents the standard deviation of the measurement error in TOA's. Note that we have a likelihood for 5 parameters, and hence we need at least 5 TOA's to maximize it.

1.2 TDOA based likelihood

Another possible approach is to consider the data to be time-difference-of-arrival ($TDOA_{ki}$) at pairs of hydrophones k and i . This means that when we look at the TDOA's, the TOE actually cancels out and can not be estimated, as

$$d_k - d_i = c(t_k - t) - c(t_i - t) = ct_k - ct - ct_i + ct = c(t_k - t_i) = cTDOA_{ki} \quad (6)$$

which rearranged leads to equations like

$$TDOA_{ki} = \frac{\sqrt{\{(x - x_k)^2 + (y - y_k)^2 + (z - z_k)^2\}} - \sqrt{\{(x - x_i)^2 + (y - y_i)^2 + (z - z_i)^2\}}}{c} \quad (7)$$

So now, considering the observed TDOA data to have a Gaussian distribution, we have a likelihood of the form

$$L(x, y, z, \sigma | TDOAs) = \prod_{k=1}^K \frac{1}{\sigma \sqrt{2\pi}} \exp\left\{-\frac{(TDOA_{ki} - TDOA_{ki,p})^2}{2\sigma^2}\right\} \quad (8)$$

where the $TDOA_{ki}$ are the observed TDOA's and $TDOA_{ki,p}$, the expected TDOA's, are given by equation 7.

1.3 Some random questions/remarks

Note that if one has say detections at 4 sensors, one can get 4 TOA's, and hence estimate location and TOE for the set of equations, but one really needs 5 sensors if is to use the likelihood approach (as there is an additional parameter to be estimated, corresponding to the variance on the TOA measurements). On the other hand, with only 4 sensors one gets 6 TDOA's, and hence can easily get the localization (and the variance on the TDOA measurements), but not the TOE.

Here are some questions that arose from this, divided in two groups, including:

1. questions to someone who knows about localization
 - This seems relatively simple, but I wonder if I am doing something wrong?
 - Why haven't I found these likelihood equations in the literature (maybe didn't look hard enough?)
 - Is there anywhere at all where this is described more or less like this?
 - If so, where?
 - If not, why not?
2. questions about further implementation within LATTE
 - For multiple clicks, the variance in the measurement of the TOA's would be a common parameter across all clicks, where individual click likelihoods would multiply up (I wonder if one gains much though?)
 - Does it make sense to think about a procedure in which a likelihood like this could be used, assuming independent detection of clicks, such that in one go one would estimate the animal track, based jointly on
 - the likelihood from the Kalman filter used for the georeferencing
 - and this type of localization likelihood?

I'm a bit lost here, as the data would be then x, y, z (pitch and heading as covariates) for the first likelihood, and the TOA 's for the second, which makes no sense, as x, y are data in the first bit and parameters in the second... Needs more thinking... clearly...

2 The localization algorithm, assuming TOE known to be 0

NOTE: (this is currently deprecated, and only kept here for historical reasons)

Only in hindsight it became obvious that in real life situation we do not really have the fundamental piece of information used below, which is the time of emission (TOE), required to calculate the expected TOA given the corresponding object-hydrophone distance. Hence, this is not useful in general. Assuming a given sound is received at K hydrophones, and that the observed TOA is a Gaussian random variable, with mean value equal with the expected TOA (which is approximately the true time of emission plus the distance between source and receiver divided the sound speed), and standard deviation σ (unknown, which we also estimate within the procedure), we can write down the likelihood of a position $p_i = (x_i, y_i, z_i)$ as a function of the data (K TOAs)

$$L(p, \sigma | TOAs) = \prod_{k=1}^K \frac{1}{\sigma \sqrt{2\pi}} \exp\left\{-\frac{(TOA_k - TOA_{k,p})^2}{2\sigma^2}\right\} \quad (9)$$

where TOA_k and $TOA_{k,p}$ represent, respectively, the observed TOA at hydrophone k , and the expected TOA at hydrophone k , given the animal is at p . This likelihood can be easily coded in R as:

```
> LOCATION.LIK=function(par.vect,obsTOAs){
+   #this function computes the likelihood associated with a given location,
+   #given the observed TOAs
+   x=par.vect[1]
+   y=par.vect[2]
+   z=par.vect[3]
+   sigma=par.vect[4]
+   n.hyds=length(obsTOAs)
+   estimatedTOAs=numeric(n.hyds)
+   #estimate the TOAs, given current location
+   for (i in 1:n.hyds) {
+     estimatedTOAs[i]=get3Ddist(xsyszs[i,],c(x,y,z))/ss}
+   #calculate the likelihood of that location
+   LIK=sum(dnorm(obsTOAs-estimatedTOAs,0,sd=sigma,log=T))
+   #cat("dnorm log:",dnorm(obsTOAs-estimatedTOAs,0,sd=sigma,log=T),"\n")
+   #cat("dnorm:",dnorm(obsTOAs-estimatedTOAs,0,sd=sigma),"\n")
+   #cat("deltaTOA:",obsTOAs-estimatedTOAs,"\n")
+   #cat("estimatedTOAs:",estimatedTOAs,"\n")
+   #cat("obsTOAs:",obsTOAs,"\n")
+ }
```



```
+   return(LIK)
+ }
```

2.1 A simple application

We consider here we have 9 hydrophones, placed in a 3 by 3 regular grid, 100 meters apart, and at depths around 1000 m. The hydrophone coordinates are listed in table 1 and are represented in 2D in figure 1. We are further assuming a whale at (50,50,600) m.

	x	y	z
1	0.00	0.00	900.00
2	100.00	0.00	912.50
3	200.00	0.00	925.00
4	0.00	100.00	937.50
5	100.00	100.00	950.00
6	200.00	100.00	962.50
7	0.00	200.00	975.00
8	100.00	200.00	987.50
9	200.00	200.00	1000.00

Table 1: Hydrophone x,y,z coordinates.

Given the whale and hydrophone locations, we can calculate the exact TOA (assume sound emitted at time 0) as each of the K hydrophones:

```
> #object to hold the true TOA given hyds and whale location and sound speed ss
> TOA=numeric(nhyds)
> for (i in 1:nhyds) {
+   TOA[i]=get3Ddist(xsyszs[i,],whale)/ss}
> #assuming that the TOA is a Gaussian random variable with expected value
> #given by get3Ddist/ss, and given some observed TOA values, we can estimate
> #the location of the sound source
> TOA

[1] 0.2054805 0.2136001 0.2409472 0.2298852 0.2380476 0.2636549
[7] 0.2713137 0.2790112 0.3018462
```

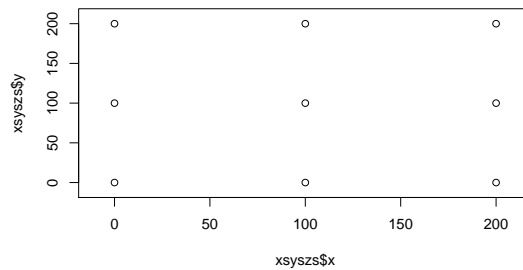


Figure 1: Hydrophone 2D location.

```
> #fabricate some observed TOA by adding some error to the true TOA
> obsTOA=TOA+rnorm(nhyds,0,sd=0.01)
```

We can also add some measurement error to the TOAs,

```
> obsTOA
```

```
[1] 0.2081731 0.2039143 0.2428538 0.2112255 0.2351362 0.2747080
[7] 0.2672302 0.2857076 0.3224991
```

and estimate the location from said data:

```
> start.par=c(75,25,500,0.02)
> est.pars=optim(par=start.par,fn=LOCATION.LIK,method="BFGS",obsTOAs=obsTOA,cont
> round(est.pars$par,3)
```

We can repeat this process 100 times, to see if we get unbiased answers, leading to estimates of $x=54.27$, $y=47.25$, $z=600.81$, $\sigma=0.01$. This is not too bad...

2.1.1 Do not forget though...

Nonetheless, it was not reassuring to see that (cf. Figure 2):

- `optim` fails to get the right maximum even when starting from not-so-weird values
- the maximum likelihood estimate of the position can be quite far off even with what was supposed to be relatively good data
- `optim` seems sensitive to the starting values used
- `optim` was going crazy with the default `method`
- this does not even make sense as in the true procedure we do not really have the TOE, that has to be estimated as part of the process too!

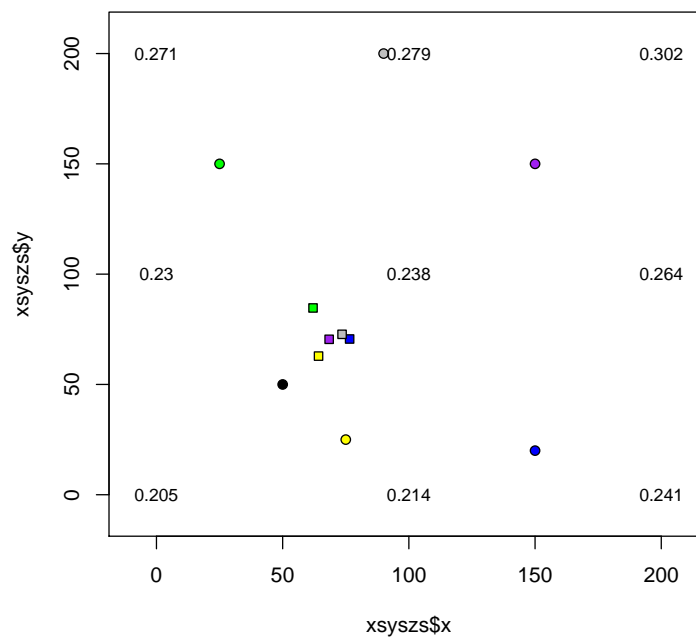


Figure 2: Hydrophone 2D location (black circles), whale location (black dot), and MLE estimates (squares) given 5 corresponding different starting value vectors (see text and code for details).

Thoughts about a conceptual model for sonar avoidance reaction by beaked whales

Tiago A. Marques & Len Thomas

Centre for Research into Ecological and Environmental Modelling
The Observatory, University of St Andrews, St Andrews, KY16 9LZ, Scotland

Version's date: November 1, 2015

Contents

1	Introduction	1
2	Reaction to sonar	3
3	Proposed model	5
3.1	Reaction initiation	6
3.2	Avoidance reaction	7
3.3	In short	9
4	Final notes	9
	References	9

1 Introduction

Within LATTE we have developed a way to simulate beaked whale movements under baseline scenarios preserving a few characteristics, namely:

- movements are similar to what we know from DTag data
- animals avoid shallow areas and hence do not strand

- animals have embedded the notion of home range size that keeps them from drifting away towards infinity

The details of such a model are the subject of other internal LATTE reports (e.g. Marques and Thomas, 2012). Here we concentrate on the simulation of beaked whale movement in the presence of sonar operations and hence potentially disturbing the animals.

To simulate the behaviour of beaked whales in the presence of sonar we need to find a reasonable way to model such behaviour. This is a difficult task because despite all the effort that has been put into this problem, there is still not much data - i.e. satellite tag data with corresponding sonar context data - allowing to robustly formalize and parametrize such a model.

Our rationale is to separate such a model into 2 different components. In the first component an animal either enters or not a disturbed state as a function of the received sound level. In the second component, given that the animal is disturbed, we need to model its behaviour, and in particular, how long it takes for the animal to resume its normal behaviour, assuming that changes are temporary. There is, to some extent, considerably more information available to implement the first component than the second.

In Moretti *et al.* (2014) we have been able to characterize a dose-response curve describing beaked whale reaction to sonar, measured by the amount of detected deep dives on AUTECH hydrophones, as a function of the received sound level. To use this information we need to be able to either (1) convert it into reaction as a function of distance, or equivalently, (2) to be able to simulate and propagate over space the sonar emission. Given that the remaining simulation components themselves involve considerably complex processes, it seems desirable to approximate the problem using the former option. Then, given that source position is known, we can predict sound levels everywhere around it as a function of distance alone. Of course this makes a number of assumptions which might not be realistic, like that the attenuation process is isotropic and constant over space, so this component might be updated at a later development stage. However such simplifying assumptions are common in similar settings (e.g. Von Benda-Beckmann *et al.*, 2014).

The lower number of detected dives as a function of sonar noise level reported in Moretti *et al.* (2014) could be explained both by either, or a combination of, (1) animals stop producing sound or (2) animals flee away (irrespective of their sound production patterns). This represents a funda-

mental distinction in this context, since what we want is to simulate animal movement given sonar use, and that is necessarily very different depending on which of these responses occurs (or is stronger, in the case both occur to some extent).

In this document, focussing on beaked whales, we begin by reviewing existing references and data sets which might contain information about sonar reactions and then propose a mathematical way of describing such reaction behaviour. The underlying objective is not necessarily to create a behavioural model that represents the way animals effectively act upon in reality but simply to conceptualize a model which leads to movements with characteristics that might approximate well enough the existing data. Hopefully such a model will be robust and versatile, meaning that as more data is collected and becomes available it can be updated by changing parameters.

2 Reaction to sonar

The papers listed below contain information relevant about marine mammal reactions to sonar:

- Tyack *et al.* (2011) demonstrated a clear reaction of beaked whales to sonar during operations, with significantly less detections during operations compared to before and after control periods. From this data alone it was not clear whether animals remain in the area but silent or whether animals flee away, although the return of sound detections in the after operations period started at the south west of the AUTECH range, perhaps indicating that temporarily displaced animals were returning.
- Miller *et al.* (2012) described reactions of different species, namely killer (*Orcinus orca*), long-finned pilot (*Globicephala melas*), and sperm (*Physeter macrocephalus*) whales to sonar and killer whale experimental playbacks. A key conclusion was that different species seem to present different reactions to sonar and that the reaction was unrelated to taxonomic distance, explicitly stating that this could represent a problem when trying to extrapolate results across species even for closely related species.

- Von Benda-Beckmann *et al.* (2014) used simulations to see the effect of ramp up procedures as a mitigation tool within Navy sonar operations, and for that matter they considered a model of behaviour such that whales would, after responding to the sonar use, move away perpendicularly with respect to the ship's track. This was based on prior knowledge based mostly on pilot whales (Paul Wensveen, pers. comm., as described by Miller *et al.* (2012)). Note that these authors mention that other reactions might be possible, like moving directly away from the source, and noted a reference to Kvadsheim *et al.* (2011), but we could not find explicit descriptions of this behaviour in said report.
- DeRuiter *et al.* (2013) identify disturbance in behaviour of Cuvier's beaked whales as a function of simulated sonar exposures. They use the Mahalanobis distance to identify changes in behaviour in a multi-variate space. Interestingly, a quite similar (in terms of received level at the whale position) coincidental real sonar did not produce the same reaction as the simulated sonar. This calls for the notion of considering context when disturbance is being assessed. The sonar response intensity¹ was modelled as a function of accumulated sonar levels. There was also a decay component such that the longer the time since the disturbance the smaller its effect seems to be on the whale's behaviour.
- Stimpert *et al.* (2014) describe the reaction of a Baird's beaked whale to simulated sonar. The simulated sonar exposure started at about 2.7 km from the last whale sighting, but the movement of whale with respect to the source was not described. Some changes are shown to occur after the exposure, but these are mostly interpreted in a depth context and associated with Mahalanobis distance point change analysis (as in DeRuiter *et al.*, 2013), which is to some extent uninformative in terms of parametrizing animal behaviour post exposure, especially given the most important component of such behaviour for LATTE is at the x, y rather than z displacement.
- Miller *et al.* (2015) looked at the movement of a northern bottlenose whale after exposure to sonar. Taken verbatim from their abstract: "At a received sound pressure level (SPL) of 98 dB re 1 μ Pa, the whale

¹Described as the expected Mahalanobis distance between a given dive and dives in a control period.

turned to approach the sound source, but at a received SPL of 107 dB re 1 μ Pa, the whale began moving in an unusually straight course and then made a near 180° turn away from the source, and performed the longest and deepest dive (94 min, 2339 m) recorded for this species. Animal movement parameters differed significantly from baseline for more than 7 h until the tag fell off 33–36 km away. No clicks were emitted during the response period, indicating cessation of normal echolocation-based foraging. A sharp decline in both acoustic and visual detections of conspecifics after exposure suggests other whales in the area responded similarly.”. Kvadsheim *et al.* (2014) report additional information about the collection of this data set.

- Wensveen *et al.* (2015) present information about how the observed movement in long-finned pilot whales might reduce sound exposure from naval sonar. Being simulation based it contains some interesting ideas about how to simulate whale movement in reaction to sonar.
- Ellison *et al.* (tted), although in a context of oil development / seismic surveys, presented a simulation to look at the effect of the cumulative exposure to multiple sound sources. As part of that work the authors looked at the consequences of whales averting the sound sources, and to do so a model to simulate aversion was put forward. The authors mention that ”The values of aversion parameters for bowhead whales that we selected were speculative, but plausible. They were intended to represent a possible behavioral response to sound exposure, not to predict response behavior explicitly.”. Not surprisingly the authors conclude that ”Altering the aversion parameters would result in substantial changes in the results, which emphasizes the need for sensitivity analysis and more extensive empirical data on avoidance behaviors.”

3 Proposed model

The model proposed here, as mentioned above, is separated into 2 components:

1. an avoidance reaction is initiated (or not)
2. conditional on that reaction being initiated, what that reaction is and how long it lasts.

We address these in separate subsections below.

3.1 Reaction initiation

This will be a stochastic process. The reaction will be triggered as a function of the distance to the source and source level. This seems a reasonable intuitive approximation and is akin to DeRuiter *et al.* (2013) who considered “two possible metrics for exposure intensity or ”dose”: sound level and distance between the whale and the sound source.”

Many other factors might actually influence whether a reaction is triggered or not (e.g. Ellison *et al.*, 2012), like context (e.g. source moving away or towards the animal), behavioural state (e.g. resting versus migrating, say), or reproductive status of the animals (e.g. mother with calves might be more sensitive than lone males). These will be ignored since we are not including them as part of the simulation of animal movement in the absence of sonar, so there is no real way one could easily include them in the process, even if reliable data were available (which there are not).

To be able to determine whether a reaction is initiated one can consider either, or both, (1) instantaneous disturbance or (2) accumulated disturbance. For the former the animal reacts because the sound level has such an intensity that it triggers an immediate response, while for the latter the sound itself might be not enough to trigger a reaction if it were of a short duration, but when accumulated over time enough energy reaches the animal such that such a behaviour is triggered. While if only one is implemented the latter would be preferable, it seems like ideally one would need to have both: it does not seem sensible to have a really loud sound and the animal only reacting to it up to half hour later say, once it has accumulated over time. Further, Moretti *et al.* (2014) only modelled the probability of observing a dive as a function to the maximum received sound level during the half hour period before, so we do not have solid information to parametrize the accumulation component. This means that actually maybe we can only implement this using maximum RL in a given interval rather than accumulated RLs over said interval.

Note that the accumulation component requires necessarily either (1) some discretization of the process or (2) to embed a notion of hazard (using survival analysis jargon, an animal would be considered to be at risk of reacting) and integrating over said hazard. The former will be used as is much simpler to implement.

From a pragmatic point of view the easiest way to implement this within a simulation context is to trigger a behaviour as a function of maximum or accumulated received levels in the half hour period prior to the start of a deep dive (an approximation shared with say Moretti *et al.*, 2014). For simplicity this could coincide to the period prior to the start of a deep dive, and then the animal either initiates said deep dive or aborts it and starts an avoidance behavior, leading us to the next section. A number of simplifications to consider include:

- the animal position during the half hour previous to the deep dive initiation could be considered to be fixed; this could be e.g. (1) the geometric centroid of its positions during that period or, an even courser approximation, (2) the point of the start of the deep dive itself; this greatly reduces the computational burden as otherwise one would have to consider the received sound level at each position the animal has been through during that half hour period.
- the animal “decides” whether it gets disturbed or not at the moment it is about to initiate a deep dive. This again saves the intensive computational resources required to otherwise evaluate at each time point whether the animal has or not reached a threshold level. Not doing so would further mean that a tab of the received sound level would have to be kept at each time point, and then this would become inconsistent with the previous approximation if we were adding the presumably received level over time but at a fixed location that the animal was assumed to be at.

3.2 Avoidance reaction

This is a key component in the process for which unfortunately we have almost no information available to parametrize. Therefore, we propose a model that can be used for pragmatic reasons but which might be updated as more information becomes available. We consider as for other components movement to be conceptualized as a mixture of random walks with specific distributions for step length and turning angles conditional on behavioural states (as in e.g. Morales *et al.*, 2004; McClintock *et al.*, 2012).

Conceptually, one could imagine that once a disturbance avoidance behavior starts the animal (or group) will initiate a movement away from the

disturbing sound source. This could be achieved via a biased random walk towards a position that will represent a temporary home range center away from the original home range center. A key aspect would be therefore to determine where such new home range center would be. Note this is certainly not how the animal will truly behave, but it might approximate well the behaviour in a way that we can parametrize it using a small number of parameters, e.g. a distance and a direction (each with distributions rather than fixed values). The strength of attraction to such new and temporary home range center would be stronger at first, and then potentially start to become fainter and fainter until the animal gets back to undisturbed movement patterns and, we assume, drifts back to its original movement around its original home range center.

Therefore, to implement this behaviour one might conceptualize three different components: first (1) obtain the location of the new temporary home range center, then (2) define how the animal approaches this location, and finally (3) how the animal returns to its original home range center. We consider these in turn below

1. For the location of the temporary displacement home range center one might define
 - a distribution for the direction the animal new home range centre is with respect to its current position. This could be a distribution which mean is the direction to increase the fastest its distance with respect to the source, and variance proportional to the sound level, making the animal more and more likely to flee away in a direction moving away from the source as the sound increases;
 - a distribution for the distance the animal will be displaced, this could again have a mean of X km, but a variance dependent on the original sound level, such that the animal could potentially move much further out as the sound increases.
2. Regarding the movement towards the new location, this could be more and more directed as the original sound was more intense. This could be incorporated via the strength of the bias in a biased random walk, in other words, on the variance of the turning angles involved.
3. Regarding the movement towards the original home range center, it could actually be similar to what is the usual movement of the animals

on the undisturbed state, or “faster” in the sense that once the animals “feel happy” to return they do it faster than they would normally approach their home range center, since by definition of their original home range center they tend to “like” that area.

The movement in the depth dimension while around the displaced home range center might be ignored at first, assuming that deep dives are temporary halted once the fleeing away movement is triggered, as described for a northern bottlenose whale, a species of beaked whale, in Miller *et al.* (2015). Deep dive occurrence would only resume after some time period. The length of that period would correspond to a component controlled by an additional distribution.

3.3 In short

Therefore, to simulate from such a model we need to define:

- a model for the initial reaction being initiated, and conditional on that initiation
- where the avoidance movement goes to, and conditional on that location
- what are the characteristics of that movement
- how long it lasts
- when deep dives are resumed
- if different than simply undisturbed movement, how animal returns to original home range center and when it restarts an undisturbed movement pattern

4 Final notes

This conceptual movement model assumes that animal disturbance occurs at the group level, and that animals do not change their group structure as a function of this disturbance. For the duration of the disturbed period we assume that only the group center (or a “leading” animal) is tracked.

References

- DeRuiter, S. L., Southall, B. L., Calambokidis, J., Zimmer, W. M. X., Sadykova, D., Falcone, E. A., Friedlaender, A. S., Joseph, J. E., Moretti, D., Schorr, G. S., Thomas, L., and Tyack, P. L. (2013). First direct measurements of behavioural responses by Cuvier's beaked whales to mid-frequency active sonar. *Biology Letters*, **9**, 20130223.
- Ellison, W. T., Southall, B. L., Clark, C. W., and Frankel, A. S. (2012). A new context-based approach to assess marine mammal behavioral responses to anthropogenic sounds. *Conservation Biology*, **26**, 21–38.
- Ellison, W. T., Racca, R., Clark, C., Streever, B., Frankel, A., Fleishman, E., Angliss, R., Berger, J., Ketten, D., Guerra, M., Leu, M., McKenna, M., Sformo, T., Southall, B., Suydam, R., and Thomas, L. (submitted). Assessing aggregated exposure and responses of marine mammals to multiple sources of anthropogenic underwater sound. *Arctic*.
- Kvadsheim, P., Lam, F.-P., Miller, P., Doksæter, L., Visser, F., Kleivane, L., van Ijsselmuide, S., Samarra, F., Wensveen, P., Curé, C., Hickmott, L., and Dekeling, R. (2011). Behavioural response studies of cetaceans to naval sonar signals in Norwegian waters - 3S-2011 cruise report. Technical report, Forsvarets forskningsinstitutt/Norwegian Defence Research Establishment.
- Kvadsheim, P., Lam, F.-P., Miller, P., Wensveen, P., Visser, F., Sivle, L. D., Oudejans, M., Kleivane, L., Curé, C., Ensor, P., van Ijsselmuide, S., and Dekeling, R. (2014). Behavioural responses of cetaceans to naval sonar signals – the 3s-2013 cruise report. Technical report, Forsvarets Forskningsinstitutt.
- Marques, T. A. and Thomas, L. (2012). Modeling beaked whales movement, sound production and detection at AUTECH. Technical report, LATTE WORKING DOCUMENT.
- McClintock, B. T., King, R., Thomas, L., Matthiopoulos, J., McConnell, B. J., and Morales, J. M. (2012). A general modeling framework for animal movement and migration using multi-state random walks. *Ecological Monographs*, **82**, 335–349.

- Miller, P., Kvadsheim, P., Lam, F.-P., Wensveen, P., Antunes, R., Alves, A., Visser, F., L., K., Tyack, P. L., and Sivle, L. D. (2012). The severity of behavioral changes observed during experimental exposures of killer (*Orcinus orca*), long-finned pilot (*Globicephala melas*), and sperm (*Physeter macrocephalus*) whales to naval sonar. *Aquatic Mammals*, **38**, 362–401.
- Miller, P. J. O., Kvadsheim, P. H., Lam, F. P. A., Tyack, P. L., Curé, C., DeRuiter, S. L., Kleivane, L., Sivle, L. D., van IJsselmuide, S. P., Visser, F., Wensveen, P. J., von Benda-Beckmann, A. M., Martín López, L. M., Narazaki, T., and Hooker, S. K. (2015). First indications that northern bottlenose whales are sensitive to behavioural disturbance from anthropogenic noise. *Royal Society Open Science*, **2**(6).
- Morales, J. M., Haydon, D. T., Frair, J., Holsinger, K. E., and Fryxell, J. M. (2004). Extracting more out of relocation data: building movement models as mixtures of random walks. *Ecology*, **85**, 2436–2445.
- Moretti, D., Thomas, L., Marques, T. A., Harwood, J., Dilley, A., Neales, B., Shaeffer, J., McCarthy, E., L., N., Jarvis, S., and Morrissey, R. (2014). A risk function for behavioral disruption of Blainville’s beaked whales (*Mesoplodon densirostris*) from mid-frequency active sonar. *PLOS One*, **9**, e85064.
- Stimpert, A. K., DeRuiter, S. L., Southall, B. L., Moretti, D. J., Falcone, E. A., Goldbogen, J. A., Friedlaender, A., Schorr, G. S., and Calambokidis, J. (2014). Acoustic and foraging behavior of a Baird’s beaked whale, *Berardius bairdii*, exposed to simulated sonar. *Scientific Reports*, **4**, 7031.
- Tyack, P. L., Zimmer, W. M. X., Moretti, D., Southall, B. L., Claridge, D. E., Durban, J. W., Clark, C. W., D’Amico, A., DiMarzio, N., Jarvis, S., McCarthy, E., Morrissey, R., Ward, J., and Boyd, I. L. (2011). Beaked whales respond to simulated and actual navy sonar. *PLoS ONE*, **6**, e17009.
- Von Benda-Beckmann, A. M., Wensveen, P. J., Kvadsheim, P. H., Lam, F.-p. A., Miller, P. J. O., Tyack, P. L., and Ainslie, M. A. (2014). Modeling effectiveness of gradual increases in source level to mitigate effects of sonar on marine mammals. *Conservation Biology*, **28**(1), 119–128.
- Wensveen, P. J., von Benda-Beckmann, A. M., Ainslie, M. A., Lam, F.-P. A., Kvadsheim, P. H., Tyack, P. L., and Miller, P. J. (2015). How effectively

do horizontal and vertical response strategies of long-finned pilot whales reduce sound exposure from naval sonar? *Marine Environmental Research*, **106**, 68 – 81.